OLD DOMINION UNIVERSITY RESEARCH FOUNDATION

DEPARTMENT OF MATHEMATICAL SCIENCES
SCHOOL OF SCIENCES AND HEALTH PROFESSIONS
OLD DOMINION UNIVERSITY
NORFOLK, VIRGINIA

PRELIMINARY INVESTIGATIONS INTO THE ACTIVE CONTROL OF LARGE SPACE STRUCTURES—SOLUTION OF THE TIMOSHENKO BEAM EQUATIONS BY THE METHOD OF CHARACTERISTICS

By

John Tweed

Final Report
For the period February 15, 1976 - August 15, 1980

Prepared for the
National Aeronautics and Space Administration
Langley Research Center
Hampton, Virginia

Under
Research Grant NSG 1279
Dr. Michael F. Card, Technical Monitor
Structures and Dynamics Division

August 1980

DEPARTMENT OF MATHEMATICAL SCIENCES
SCHOOL OF SCIENCES AND HEALTH PROFESSIONS
OLD DOMINION UNIVERSITY
NORFOLK, VIRGINIA

PRELIMINARY INVESTIGATIONS INTO THE ACTIVE CONTROL OF LARGE SPACE STRUCTURES—SOLUTION OF THE TIMOSHENKO BEAM EQUATIONS BY THE METHOD OF CHARACTERISTICS

By

John Tweed

Final Report
For the period February 15, 1976 - August 15, 1980

Prepared for the
National Aeronautics and Space Administration
Langley Research Center
Hampton, Virginia

Under
Research Grant NSG 1279
Dr. Michael F. Card, Technical Monitor
Structures and Dynamics Division

Submitted by the
Old Dominion University Research Foundation
P. O. Box 6369
Norfolk, Virginia 23508

August 1980

TABLE OF CONTENTS

LIST OF FIGURES

PRELIMINARY INVESTIGATIONS INTO THE ACTIVE CONTROL OF LARGE SPACE STRUCTURES -- SOLUTION OF THE TIMOSHENKO BEAM EQUATIONS BY THE METHOD OF CHARACTERISTICS

By

John Tweed*

ABSTRACT

In this report, the method of characteristics is used to develop an algorithm for solving the damped, Timoshenko beam equations with free-free boundary conditions and prescribed initial data. A number of special cases are considered and, where appropriate, comparisons are made with known results.

INTRODUCTION

The possibility of using large orbiting space structures to help meet future needs on Earth has prompted industries and government agencies to begin preliminary design studies on a number of such structures: for example, large communications antennae are proposed as a means of handling the ever-increasing quantities of information which are being transmitted around the world. High-resolution soil moisture radiometry techniques are being put forward as a method of accessing the world's food inventory, and, in an effort to relieve the energy shortage, large, orbiting, solar power stations are being considered which are designed to transmit the Sun's energy to Earth via microwaves. The cost of such structures is enormous and proportional to the amount of construction material used. Keeping material to a minimum will result in a considerable lack of stiffness and perhaps in dynamic behavior unlike any structure presently in existence. To function properly these structures must be kept free of unwanted motions such as those due to the docking of other spacecraft, solar

* Professor, Department of Mathematical Sciences, Old Dominion University, Norfolk, Virginia 23508

winds, and meteroid showers. An active structural control system integrated into the structural design is one method of solving this problem. Since the design of such a control system is a difficult and sophisticated problem, it is felt that simpler problems should be studied with a view to increasing the understanding of the dynamic behavior of large structures and giving direction to studies in the control of these structures.

A simple structure which retains many of the important features of a large, flexible structure is the Timoshenko beam, which admits shear deformation and rotary inertia effects. A previous study (ref. 1) shows that, in a Timoshenko beam of infinite length, it is possible for the displacement response to an initial disturbance to be a dispersive pulse moving along the beam. This type of response occurs if the beam is relatively soft in shear and if the wavelength of the disturbance is small compared to the length of the beam. Based on studies to date, this type of motion is possible within the range of stiffness and mass parameters associated with current proposed configurations of large space structures. Since the study on beams of infinite length was not entirely realistic, two subsequent studies (refs. 2, 3) were performed for beams of finite length. In the first of these studies (ref. 2), the modal method was used to examine the dynamic response of an undamped, uniform Timoshenko beam to an initial (1 + cos) lateral displacement, which was centrally located on the beam. Three types of motion were discerned: beamlike motion, a dispersive pulse motion, and wavelike motion. Since only the first few modes are necessary to fully understand beamlike motions, such motions in large space structures present no new problems and are easily controlled in the usual way. However, if the structure does not behave like a beam but exhibits the other two types of motion, the solution to the control problem is not clear: for example, to accurately describe a pulse, many modes are needed. If a controller is included for every mode, then an adaptive, active control system might be necessary since the frequencies and shapes of that many modes (200 or more) cannot be known accurately a priori. Because of the difficulty of determining the high modes accurately, it was felt

that alternative methods of solving the problem should be examined. Therefore, in the next study (ref. 3) a finite-difference program was developed. This program was designed to solve the Timoshenko beam equations with distributed loads, velocity damping, free-free boundary conditions and the same initial data as that discussed in reference 2. For large disturbances, the finite-difference solution agreed well with the modal solution but required more CPU time. When small wavelike disturbances were considered, a fine resolution in the spatial domain was required, and, since the wave speeds were fairly large, very small time steps had to be taken. The result was a significant increase in CPU time and also in buildup error. Consequently, the finite-difference study was abandoned in favor of the present study, which takes advantage of the hyperbolic nature of the Timoshenko beam equations by using the method of characteristics.

GOVERNING EQUATIONS

The equations governing the behavior of a Timoshenko beam may be written in the following form:

$$w = w_1 + w_2 \qquad \text{(total deflection)} \qquad (1)$$

$$\Psi = \frac{\partial w_1}{\partial x} \qquad \text{(bending rotation)} \qquad (2)$$

$$\frac{\partial V}{\partial x} + q = \rho A\left[b_1 \frac{\partial w}{\partial t} + \frac{\partial^2 w}{\partial t^2}\right] \qquad \text{(vertical motion)} \qquad (3)$$

$$\frac{\partial M}{\partial x} + V + r = \rho I\left[b_2 \frac{\partial \Psi}{\partial t} + \frac{\partial^2 \Psi}{\partial t^2}\right] \qquad \text{(rotational motion)} \qquad (4)$$

$$M = EI \frac{\partial^2 w_1}{\partial x^2} \qquad \text{(bending moment)} \qquad (5)$$

and

$$\frac{\partial w_2}{\partial x} = \frac{V}{sAG} \qquad \text{(shear)} \qquad (6)$$

where

$A = A(x)$	effective cross-sectional area
$b_1 = b_1(x,t)$	transverse damping force/unit mass/unit velocity
$b_2 = b_2(x,t)$	longitudinal damping force/unit mass/unit velocity
$E = E(x)$	Young's modulus
$G = G(x)$	shear modulus
g	acceleration due to gravity
$I = I(x)$	second moment of cross-sectional area
$k_g = k_g(x)$	radius of gyration of cross section
L	length of beam
$M = M(x,t)$	bending moment
$q = q(x,t)$	distributed force/unit length
$r = r(x,t)$	distributed torque/unit length
$s = s(x)$	shear correction factor
t	time
$V = V(x,t)$	shear force
$w = w(x,t)$	total deflection
$w_1 = w_1(x,t)$	bending deflection
$w_2 = w_2(x,t)$	shear deflection
x	distance measured along span
$\gamma = \gamma(x,t)$	shear strain
$\theta = \theta(x,t)$	total slope
$\psi = \psi(x,t)$	bending rotation
$\rho = \rho(x,t)$	mass of beam/unit volume

In the case of a free-free beam, we are required to solve equations (1) to (6) subject to boundary conditions of the type:

$$\left.\begin{aligned} M(0,t) = V(0,t) = 0 , \quad t > 0 \\ M(L,t) = V(L,t) = 0 , \quad t > 0 \end{aligned}\right\} \tag{7}$$

and to initial conditions such as

$$\left.\begin{aligned} w(x,0) &= w^{o}(x) && 0 < x < L \\ \psi(x,0) &= \psi^{o}(x) && 0 < x < L \\ \frac{\partial w}{\partial t}(x,0) &= \frac{\partial \psi}{\partial t}(x,0) = 0 , && 0 < x < L \end{aligned}\right\} \tag{8}$$

where $w^{o}(x)$ and $\psi^{o}(x)$ are prescribed functions of x.

For computational convenience, we describe the problem in terms of dimensionless variables as shown below.

After choosing a suitable unit of time, t_o, we may introduce a dimensionless time variable, $\tau = t/t_o$, and a dimensionless space variable, $\xi = x/L$. Furthermore, if we let $A_o = L^2$, $I_o = L^4$, and assume that $A(x) = A_o\bar{A}(\xi)$, $I(x) = I_oI(\xi)$, $G(x) = G_oG(\xi)$, $E(x) = E_oE(\xi)$, and $\rho(x) = \rho_o\rho(\xi)$, we may introduce the following dimensionless quantities:

$$\begin{aligned} \zeta(\xi,\tau) &= w(\xi L,\tau t_o)/L \\ \zeta_i(\xi,\tau) &= w_i(\xi L,\tau t_o)/L , \quad i = 1,2 \\ \phi(\xi,\tau) &= \psi(\xi L,\tau t_o) \\ \bar{M}(\xi,\tau) &= LM(\xi L,\tau t_o)/E_oI_o \\ \bar{V}(\xi,\tau) &= V(\xi L,\tau t_o)/A_oG_o \\ \bar{q}(\xi,\tau) &= q(\xi L,\tau t_o)t_o^2/\rho_oA_oL \\ \bar{r}(\xi,\tau) &= r(\xi L,\tau t_o)t_o/\rho_oI_o \\ \bar{s}(\xi) &= s(\xi L) \end{aligned}$$

$$\bar{b}_i(\xi,\tau) = b_i(\xi L, \tau t_o)t_o \ , \quad i = 1,2$$

$$\zeta^o(\xi) = w^o(\xi L)/L$$

$$\phi^o(\xi) = \psi^o(\xi L)$$

$$\alpha_1 = \frac{t_o}{L}\sqrt{\frac{G_o}{\rho_o}}$$

and

$$\alpha_2 = \frac{t_o}{L}\sqrt{\frac{E_o}{\rho_o}}$$

In terms of these dimensionless quantities, the equations (1) through (8) take the form

$$\zeta = \zeta_1 + \zeta_2 \tag{9}$$

$$\phi = \frac{\partial \zeta_1}{\partial \xi} \tag{10}$$

$$\alpha_1^2 \frac{\partial \bar{V}}{\partial \xi} + \bar{q} = \bar{\rho}\,\bar{A}\left[\bar{b}_1 \frac{\partial \zeta}{\partial \tau} + \frac{\partial^2 \zeta}{\partial \tau^2}\right] \tag{11}$$

$$\alpha_2^2 \frac{\partial \bar{M}}{\partial \xi} + \alpha_1^2 \bar{V} + \bar{r} = \bar{\rho}\,\bar{I}\left[\bar{b}_2 \frac{\partial \phi}{\partial \tau} + \frac{\partial^2 \phi}{\partial \tau^2}\right] \tag{12}$$

$$\bar{M} = \bar{E}\,\bar{I}\,\frac{\partial^2 \zeta_1}{\partial \xi^2} \tag{13}$$

$$\frac{\partial \zeta_2}{\partial \xi} = \frac{\bar{V}}{\bar{s}\,\bar{A}\,\bar{G}} \tag{14}$$

with boundary conditions

$$\left.\begin{aligned} \bar{M}(0,\tau) = \bar{V}(0,\tau) = 0 \ , \quad \tau > 0 \\ \bar{M}(1,\tau) = \bar{V}(1,\tau) = 0 \quad \tau > 0 \end{aligned}\right\} \tag{15}$$

and

initial conditions:

$$\left.\begin{aligned} \zeta(\xi,0) &= \zeta^{o}(\xi) && 0 < \xi < 1 \\ \phi(\xi,0) &= \phi^{o}(\xi) && 0 < \xi < 1 \\ \frac{\partial \zeta}{\partial \tau}(\xi,0) &= \frac{\partial \phi}{\partial \tau}(\xi,0) = 0 , && 0 < \xi < 1 \end{aligned}\right\} \tag{16}$$

If we now let $\dot{\phi} = \frac{\partial \phi}{\partial \tau}$, $\dot{\zeta} = \frac{\partial \zeta}{\partial \tau}$, and set

$$\vec{u} = \begin{pmatrix} \dot{\zeta} \\ \dot{\phi} \\ \overline{V} \\ \overline{M} \end{pmatrix} \tag{17}$$

we find that equations (9) through (14) can be written as a linear first order system

$$\frac{\partial \vec{u}}{\partial \tau} = D(\xi) \frac{\partial \vec{u}}{\partial \xi} + B(\xi,\tau)\vec{u} + \vec{f}(\xi,\tau), \quad 0 < \xi < 1, \quad \tau > 0 \tag{18}$$

with boundary conditions

$$\left.\begin{aligned} \overline{M}(0,\tau) &= \overline{V}(0,\tau) = 0 , && \tau > 0 \\ \overline{M}(1,\tau) &= \overline{V}(1,\tau) = 0 , && \tau > 0 \end{aligned}\right\} \tag{19}$$

and initial conditions

$$\left.\begin{aligned} \dot{\zeta}(\xi,0) &= \dot{\phi}(\xi,0) = 0 && 0 < \xi < 1 \\ \overline{V}(\xi,0) &= \overline{s}\ \overline{A}\ \overline{G} \left[\frac{\partial \zeta^{o}}{\partial \xi}(\xi) - \phi^{o}(\xi)\right] && 0 < \xi < 1 \\ &\text{and} \\ \overline{M}(\xi,0) &= \overline{E}\ \overline{I}\ \frac{\partial \phi^{o}}{\partial \xi}(\xi) && 0 < \xi < 1 \end{aligned}\right\} \tag{20}$$

where

$$D(\xi) = \begin{pmatrix} 0 & 0 & \alpha_1^2/\bar{\rho}\,\bar{A} & 0 \\ 0 & 0 & 0 & \alpha_2^2/\bar{\rho}\,\bar{I} \\ \bar{s}\,\bar{A}\,\bar{G} & 0 & 0 & 0 \\ 0 & \bar{E}\,\bar{I} & 0 & 0 \end{pmatrix} \tag{21}$$

$$B(\xi,\tau) = \begin{pmatrix} -\bar{b}_1 & 0 & 0 & 0 \\ 0 & -\bar{b}_2 & \alpha_1^2/\bar{\rho}\,\bar{I} & 0 \\ 0 & -\bar{s}\,\bar{A}\,\bar{G} & 0 & 0 \\ 0 & 0 & 0 & 0 \end{pmatrix} \tag{22}$$

and

$$\vec{f}(\xi,\tau) = \begin{pmatrix} \bar{q}/\bar{\rho}\,\bar{A} \\ \bar{r}/\bar{\rho}\,\bar{I} \\ 0 \\ 0 \end{pmatrix} \tag{23}$$

Since the D matrix has eigenvalues

$$\lambda_1 = \alpha_1\sqrt{\frac{\bar{s}\,\bar{G}}{\bar{\rho}}}, \quad \lambda_2 = -\alpha_1\sqrt{\frac{\bar{s}\,\bar{G}}{\bar{\rho}}}, \quad \lambda_3 = \alpha_2\sqrt{\frac{\bar{E}}{\bar{\rho}}}, \quad \lambda_4 = -\alpha_2\sqrt{\frac{\bar{E}}{\bar{\rho}}} \tag{24}$$

and corresponding eigenvectors

$$\vec{x}_1 = \begin{pmatrix} \alpha_1/\bar{A}\sqrt{\bar{s}\,\bar{\rho}\,\bar{G}} \\ 0 \\ 1 \\ 0 \end{pmatrix} \qquad \vec{x}_2 = \begin{pmatrix} -\alpha_1/\bar{A}\sqrt{\bar{s}\,\bar{\rho}\,\bar{G}} \\ 0 \\ 1 \\ 0 \end{pmatrix} \tag{25 (cont'd.)}$$

$$\vec{x}_3 = \begin{pmatrix} 0 \\ \alpha_2/\bar{I} \quad \bar{\rho}\ \bar{E} \\ 0 \\ 1 \end{pmatrix} \qquad \vec{x}_4 = \begin{pmatrix} 0 \\ -\alpha_2/\bar{I} \quad \bar{\rho}\ \bar{E} \\ 0 \\ 1 \end{pmatrix} \qquad (25)\ \text{(concl'd.)}$$

which are linearly independent, the system is seen to be hyperbolic. On solving this hyperbolic system for the vector $\vec{u}$ we calculate $\zeta(\xi,\tau)$ and $\phi(\xi,\tau)$ from the equations

$$\zeta(\xi,\tau) = \zeta^0(\xi) + \int_0^\tau \dot{\zeta}(\xi,y)\, dy \qquad (26)$$

and

$$\phi(\xi,\tau) = \phi^0(\xi) + \int_0^\tau \dot{\phi}(\xi,y)\, dy \qquad (27)$$

The matrix T whose columns are the eigenvectors $\vec{x}_1$, $\vec{x}_2$, $\vec{x}_3$, and $\vec{x}_4$ of D is nonsingular and such that

$$T^{-1} DT = \Lambda = \text{diag}(\lambda_1,\lambda_2,\lambda_3,\lambda_4) \qquad (28)$$

Therefore, if we introduce the new variable $\vec{v} = T^{-1}\vec{u}$ and let $B^* = T^{-1}BT$ and $f^* = T^{-1}\vec{f}$, we find that equation (10) may be written in the form

$$\frac{\partial \vec{v}}{\partial \tau} = \Lambda(\xi)\ \frac{\partial \vec{v}}{\partial \xi} + B^*(\xi,\tau)\vec{v} + \vec{f}^*(\xi,\tau) \qquad (29)$$

i.e.,

$$\frac{\partial v_i}{\partial \tau} - \lambda_i \frac{\partial v_i}{\partial \xi} = \sum_{j=1}^{4} b^*_{ij}\ v_j + f^*_i\ , \quad i = 1,2,3,4 \qquad (30)$$

while the boundary conditions become

$$\left.\begin{aligned} v_1(0,\tau) + v_2(0,\tau) &= 0 \\ v_3(0,\tau) + v_4(0,\tau) &= 0 \\ v_1(1,\tau) + v_2(1,\tau) &= 0 \\ v_3(1,\tau) + v_4(1,\tau) &= 0 \end{aligned}\right\} \qquad t > 0 \tag{31}$$

and the initial conditions become

$$\vec{v}(\xi,0) = \vec{v}^{\,o}(\xi) = \begin{pmatrix} \bar{s}\,\bar{A}\,\bar{G}\left[\frac{\partial \zeta}{\partial \xi}^{o}(\xi) - \phi^{o}(\xi)\right] \\ \bar{s}\,\bar{A}\,\bar{G}\left[\frac{\partial \zeta}{\partial \xi}^{o}(\xi) - \phi^{o}(\xi)\right] \\ \bar{E}\,\bar{I}\,\frac{\partial \phi}{\partial \xi}^{o}(\xi) \\ \bar{E}\,\bar{I}\,\frac{\partial \phi}{\partial \xi}^{o}(\xi) \end{pmatrix}, \quad 0 < \xi < 1 \tag{32}$$

THE ALGORITHM

On the characteristic curves C_i, which are defined by the differential equations $\frac{d\xi}{d\tau} = -\lambda_i$, $i = 1,2,3,4$, equation (30) takes the simple form

$$dv_i = \left(\sum_{j=1}^{4} b^{*}_{ij}\, v_j + f^{*}_{i}\right) d\tau \tag{33}$$

Equation (33) forms the basis of an algorithm for solving the system (30) numerically. This algorithm, which has been discussed by Leonard and Budiansky (refs. 4,5) for systems without damping, is described below in the case of a uniform, homogeneous beam with square section. In this case the eigenvalues reduce to $\pm a_1/\sqrt{s}$, $\pm a_2$, and hence the characteristics become straight lines.

On the strip $0 \leq \xi \leq 1$, $\tau > 0$, we construct a mesh of size $\Delta\xi$, $\Delta\tau$ where $\Delta\tau = \Delta\xi/\alpha_2$. We let $p = \alpha_1/\alpha_2\sqrt{5}$ and make use of the notation $\xi_i = i\Delta\xi$, $\tau_j = j\Delta\tau$, $f(\xi_i,\tau_j) = f_i^j$, etc. A typical cell in this mesh is shown in figure 1. If, for a fixed value of j, the solution is known at the mesh points (ξ_i,τ_j). it can be found at the points $(\xi_i \pm p,\tau_j)$ by using three-point Lagrange interpolation. The solution may then be advanced in time to the points $(\xi_i\ \tau_j + 1)$ by means of equation (34) below.

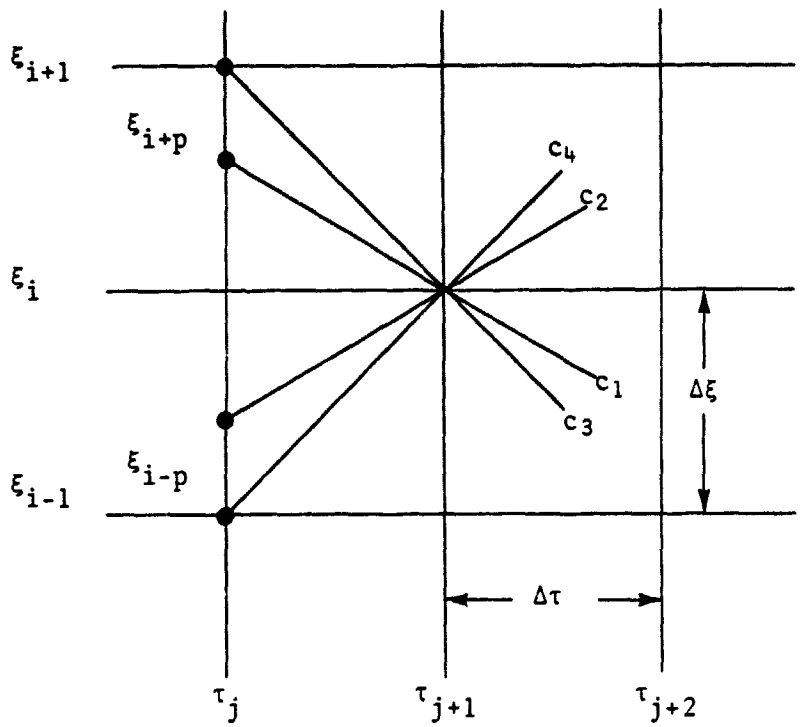

Figure 1. Finite-difference characteristic mesh.

$$\left(v_m - \frac{\Delta\tau}{2}\sum_{k=1}^{4} b^*_{mk} v_k\right)_i^{j+i} = \left(v_m + \frac{\Delta\tau}{2}\sum_{k=1}^{4} b^*_{mk} v_k\right)_{i+p_m}^{j} + \frac{\Delta\tau}{2}\left(f^{*j+i}_{m\ i} + f^{*j}_{m\ i+p_m}\right) \tag{34}$$

which is a finite-difference expression for equation (33) with p_m taking the values p, -p, 1, -1 as m takes the values 1, 2, 3, or 4, respectively. Subject to the boundary conditions

$$\left.\begin{aligned}\left(v_1 + v_2\right)_o^{j+1} &= \left(v_3 + v_4\right)_o^{j+1} = 0\\ \left(v_1 + v_2\right)_n^{j+1} &= \left(v_3 + v_4\right)_n^{j+1} = 0\end{aligned}\right\} \quad j \geq 0 \tag{35}$$

the solution of equation (34) may be written in the form

$$\vec{v}_i^{j+1} = C_i^{j+1}\,\vec{r}_i^{j+1},\ \vec{v}_i^{o} = \vec{v}^{o}(\xi_i),\ 0 < i < n,\ j \geq 0 \tag{36}$$

where the mth component of $\vec{r}_i^{j+i}$ is given by

$$\begin{aligned} r_{m\,i}^{j+1} = &\left\{1 - \delta_{i0}\left(\delta_{m_2} + \delta_{m_4}\right) - \delta_{in}\left(\delta_{m_1} + \delta_{m_3}\right)\right\} \\ &\times \left\{\left(v_m + \frac{\Delta\tau}{2}\sum_{k=1}^{4} b^*_{mk} v_k\right)_{i+p_m}^{j} + \frac{\Delta\tau}{2}\left(f^{*j+1}_{m\,i} + f^{*j}_{m\,i+p_m}\right)\right\} \end{aligned} \tag{37}$$

and the matrix C_i^{j+1} by

$$C_i^{j+1} = \begin{pmatrix} \frac{1+a}{h} - \frac{2bc}{k} & \frac{a}{h} - \frac{2bc}{k} & -\frac{c}{k} & \frac{c}{k} \\ \frac{a}{h} - \frac{2bc}{k} & \frac{1+a}{h} - \frac{2bc}{k} & -\frac{c}{k} & \frac{c}{k} \\ \frac{b}{k} & \frac{b}{k} & \frac{1 + d + 2bc}{k} & \frac{d + 2bc}{k} \\ -\frac{b}{k} & -\frac{b}{k} & \frac{d + 2bc}{k} & \frac{1 + d + 2bc}{k} \end{pmatrix} \tag{38}$$

if $0 < i < n$, by

$$C_0^{j+1} = \begin{pmatrix} \frac{1}{h} & \frac{a}{h} - \frac{2bc}{hk} & -\frac{2c}{hk} & \frac{c}{h} - \frac{2cd}{hk} \\ -\frac{1}{h} & 1 - \frac{a}{h} + \frac{2bc}{hk} & \frac{2c}{hk} & -\frac{c}{h} + \frac{2cd}{hk} \\ 0 & \frac{b}{k} & \frac{1}{k} & \frac{d}{k} \\ 0 & -\frac{b}{k} & -\frac{1}{k} & 1 - \frac{d}{k} \end{pmatrix} \tag{39}$$

if i = 0, and by

$$C_n^{j+1} = \begin{pmatrix} 1 - \frac{a}{h} + \frac{2bc}{hk} & -\frac{1}{h} & \frac{c}{h} - \frac{2cd}{hk} & -\frac{2c}{hk} \\ \frac{a}{h} - \frac{2bc}{hk} & \frac{1}{h} & -\frac{c}{h} + \frac{2cd}{hk} & \frac{2c}{hk} \\ \frac{b}{k} & 0 & 1 - \frac{d}{k} & -\frac{1}{k} \\ -\frac{b}{k} & 0 & \frac{d}{k} & \frac{1}{k} \end{pmatrix} \tag{40}$$

if i = n, where in all cases

$$a = \frac{\Delta\tau}{4}\bar{b}_{1\,i}^{\,j+1}, \quad b = \frac{\Delta\tau\alpha_1^2}{4\alpha_2}, \quad c = \frac{\Delta\tau s\bar{A}\alpha_2}{4\bar{I}},$$

$$d = \frac{\Delta\tau}{4}\bar{b}_{2\,i}^{\,j+1}, \quad h = 1 + 2a, \text{ and}$$

$$k = (1 + 2d) + 4bc\delta_{oi}\delta_{ni}.$$

The quantities of physical interest are obtained from the solution of equation (36) with the help of the formulas

$$\zeta_i^{j+1} = \zeta_i^o + \frac{\alpha_1 L^2 \Delta\tau}{2\sqrt{s}} \sum_{k=0}^{j} \left[(v_1 - v_2)_i^{k+1} + (v_1 - v_2)_i^k \right] \tag{41}$$

$$\phi_i^{j+1} = \phi_i^o + 6\alpha_2 L^4 \Delta\tau \sum_{k=0}^{j} \left[(v_3 - v_4)_i^{k+1} + (v_3 - v_4)_i^k \right] \tag{42}$$

$$\bar{V}_i^{j+1} = (v_1 + v_2)_i^{j+1} \tag{43}$$

and

$$\bar{M}_i^{j+1} = (v_3 + v_4)_i^{j+1} \tag{44}$$

RESULTS

The algorithm described above has been incorporated into a computer code for solving the damped, Timoshenko beam equations with free-free boundary conditions and prescribed initial data. A number of special cases have been investigated and, where appropriate, comparisons have been made with earlier results. In order to facilitate these comparisons, the time scale t_o was taken to be the period of the first mode of an equivalent Euler beam (ref. 7):

$$t_o = \frac{2\pi L^2}{(4.730)^2}\left(\frac{\rho_o A}{E_o I}\right)^{\frac{1}{2}} \tag{45}$$

and results were obtained for different slenderness ratios, SLR = $L(A/I)^{\frac{1}{2}}$, and velocity ratios, $V_R = (G_o/E_o)^{\frac{1}{2}}$.

The graphs in appendixes A through F show the undamped displacement response to initial data of the form

$$\varepsilon(\xi,0) = \frac{1}{2}\left[1 + \cos\left\{\frac{2\pi}{\lambda}\left(\xi - \frac{1}{2}\right)\right\}\right] H\left[\lambda^2 - (2\xi - 1)^2\right] \tag{46}$$

$$\phi(\xi,0) = -\frac{\pi}{\lambda}\sin\left\{\frac{2\pi}{\lambda}\left(\xi - \frac{1}{2}\right)\right\} H\left[\lambda^2 - (2\xi - 1)^2\right] \tag{47}$$

$$V(\xi,0) = 0 \tag{48}$$

and

$$M(\xi,0) = 0 \tag{49}$$

where $H(x) = \begin{cases} 1, & x > 0 \\ 0, & x < 0 \end{cases}$ is the heavyside function.

Appendixes A and B deal with the cases $V_R = 0.62$, SLR = 50.0, and $\lambda = 0.5$ and 0.1, respectively. The results given here agree with those obtained by the modal method (ref. 2) and also by the direct finite-difference method (ref. 3). A comparison of machine time used shows that the method of characteristics is about 20 times faster than the direct finite-difference method. It appears, however, that the characteristic method is not as efficient as the modal method especially when short wave lengths are involved. This is because the high spatial resolution required to see short waves demands that very small time steps be used, and the resulting buildup error quickly swamps out the desired solution. Appendixes C, D, E, and F show corresponding results for the cases $V_R = 0.3$, SLR = 50.0, $\lambda = 0.5$; $V_R = 0.3$, SLR = 50.0, $\lambda = 0.1$; $V_R = 0.1$, SLR = 50.0, $\lambda = 0.5$, and $V_R = 0.1$, SLR = 50.0, $\lambda = 0.1$, respectively.

Appendixes G through K show how the displacement, bending angle, shear and bending moment respond to initial data of the type represented by equations (46) to (49) in the presence of uniform velocity damping. Results are presented for the cases $\bar{b}_1 = 0.0$, $\bar{b}_2 = 0.0$; $\bar{b}_1 = 1.5$, $\bar{b}_2 = 0.0$; $\bar{b}_1 = 3.0$, $\bar{b}_2 = 0.0$; $\bar{b}_1 = 0.0$, $\bar{b}_2 = 3.0$, and $\bar{b}_1 = 0.0$, $\bar{b}_2 = 12.0$, respectively, with $V_R = 0.62$, SLR = 50.0, and $\lambda = 0.2$. A comparison of the solutions obtained shows that transverse damping is much more effective than rotational damping.

An attempt was made to analyze local damping and point-load-rate effects. While results due to Leonard (ref. 5) could be reproduced approximately, in general the method proved to be poor for this class of problems. Again it is found that the high spatial resolution requires results in very small time steps and buildup error which quickly swamps out the desired solution.

REFERENCES

1. Hyer, M. W.: Preliminary Investigations into the Active Control of Large Space Structures—Character of Motions in an Infinite Beam. Progress Report for NASA grant NSG 1279, April 1977.

2. Hyer, M. W.: Preliminary Investigations into the Active Control of Large Space Structures—Character of Motions in a Finite-Length Beam. Progress Report for NASA grant NSG 1279, June 1978.

3. Tweed, J.: Preliminary Investigations into the Active Control of Large Space Structures—A Finite Difference Program for the Solution of the Timoshenko Beam Equations. Progress Report for NASA grant NSG 1279, June 1978.

4. Leonard, R. W.; and Budiansky, B.: On Travelling Waves in Beams. NACA Report 1173, 1954.

5. Leonard, R. W.: On Solutions for the Transient Response of Beams. NACA Report R-21, 1958.

6. Kruszewski, E. T.: Effect of Transverse Shear and Rotary Inertia on the Natural Frequency of a Uniform Beam. NACA-TN-1909, May 1949.

7. Skudrzyk, Eugen: Simple and Complex Vibratory Systems. The Penn. State Univ. Press, 1968.

APPENDIX A

Displacement response to a (1 + cos) initial disturbance;
$V_R = 0.62$, SLR = 50, $\lambda = 0.5$.

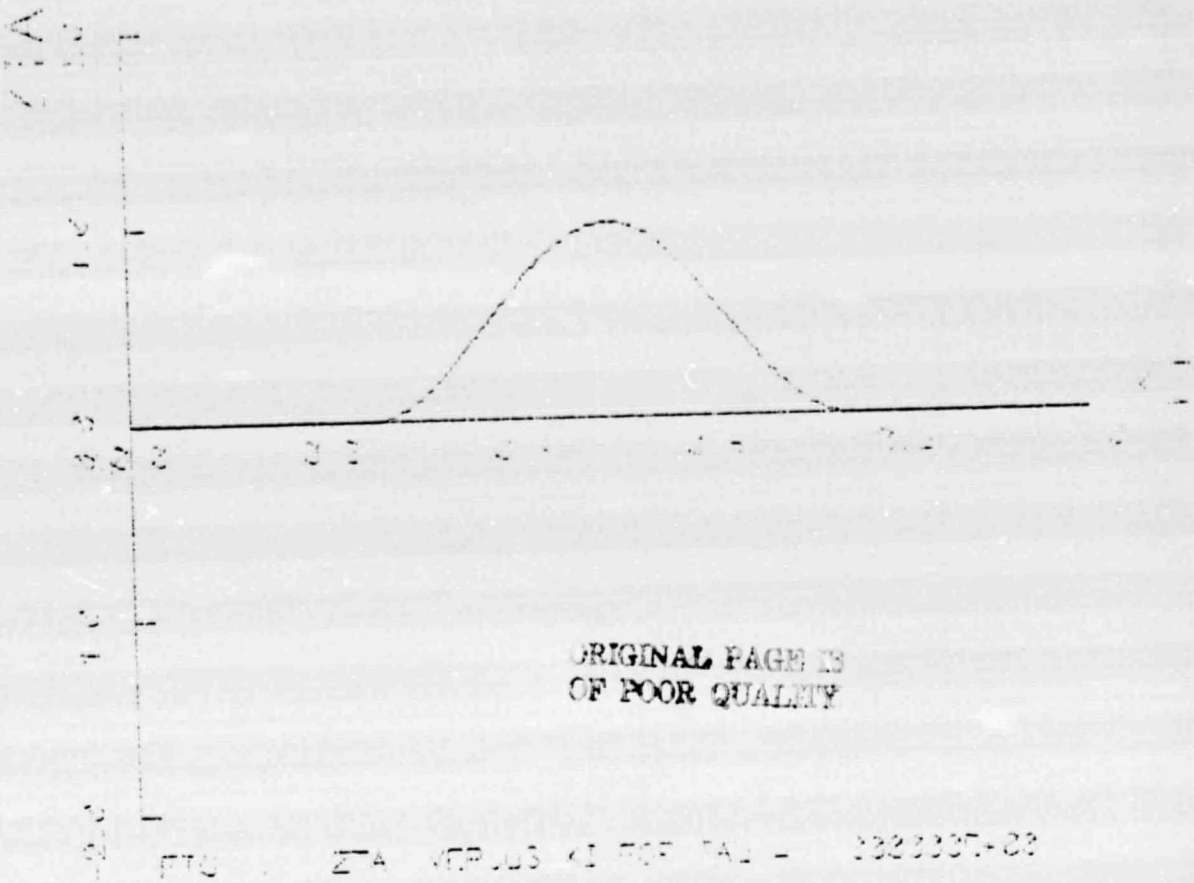

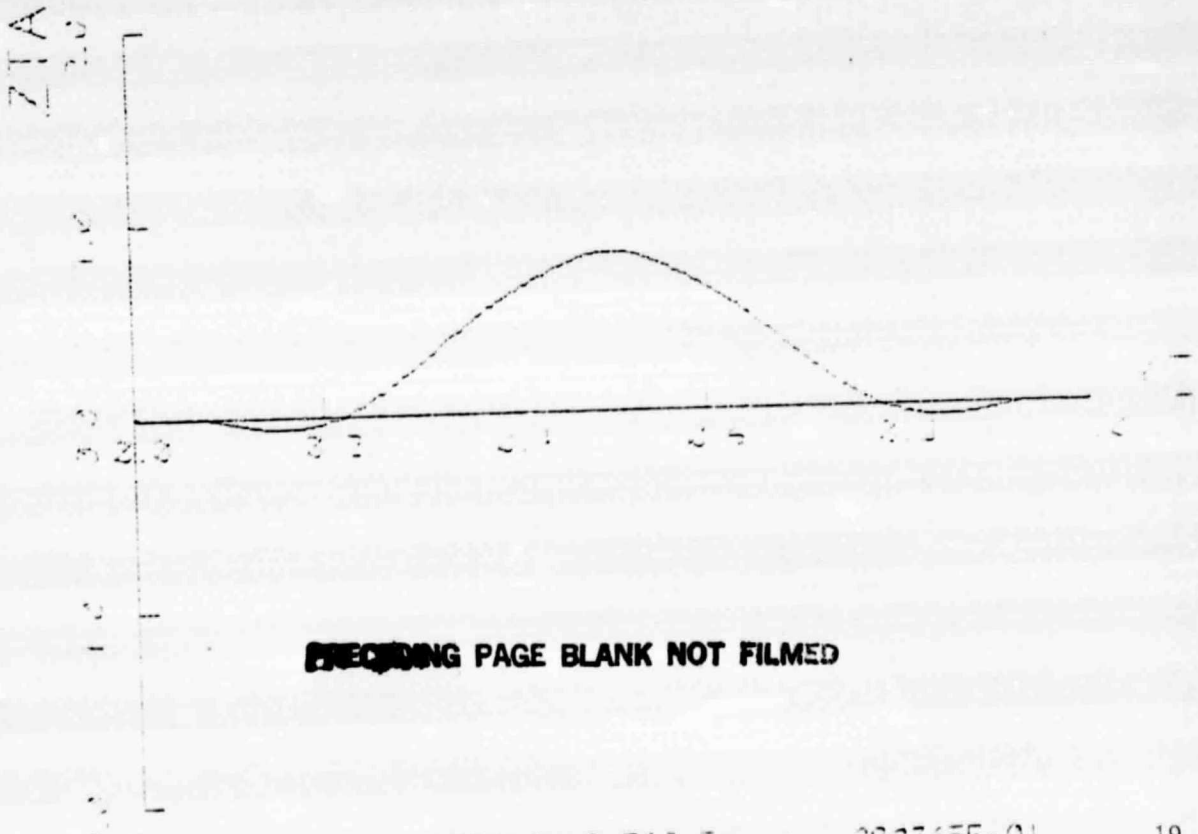

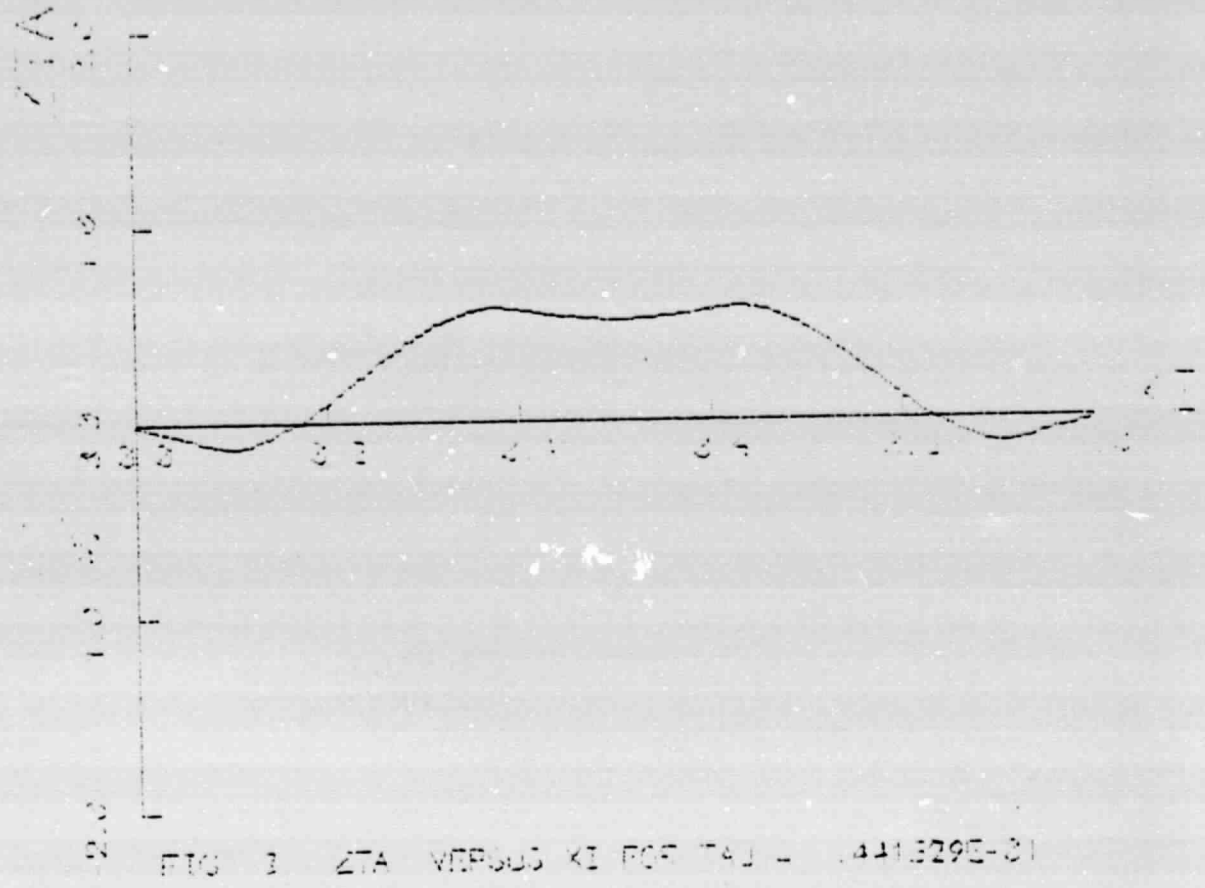

FIG 3 ZTA VERSUS KI FOR TAU = .411329E-01

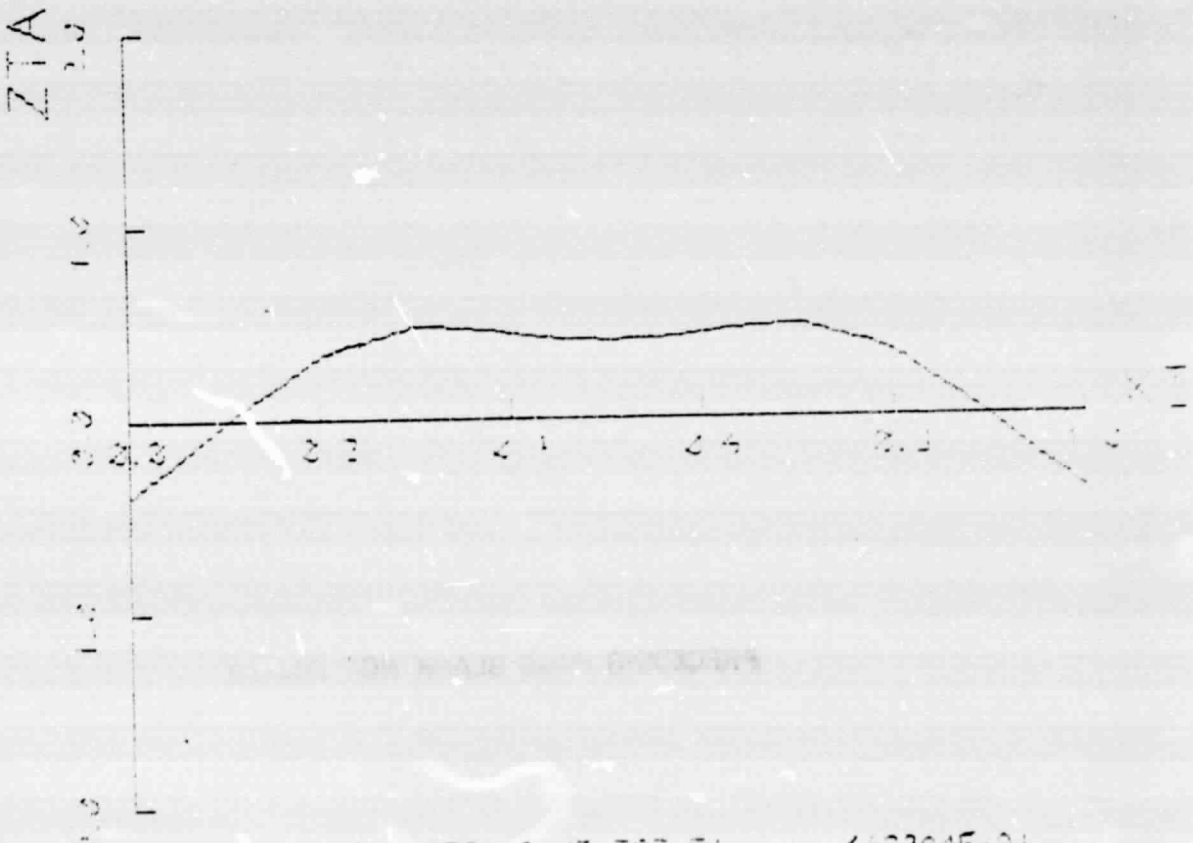

FIG 4 ZTA VERSUS KI FOR TAU = .462294E-01

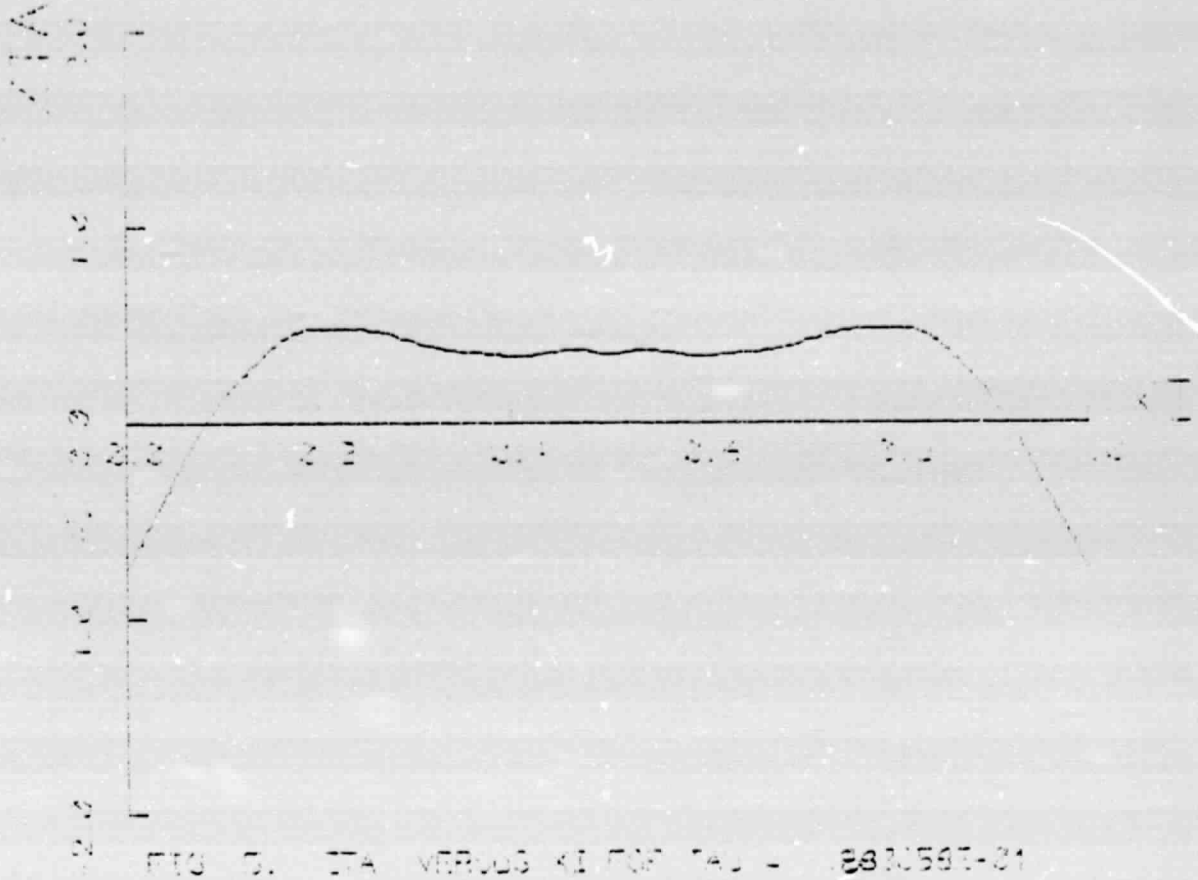

FIG 5. ZTA VERSUS XI FOR TAU = 8810561-01

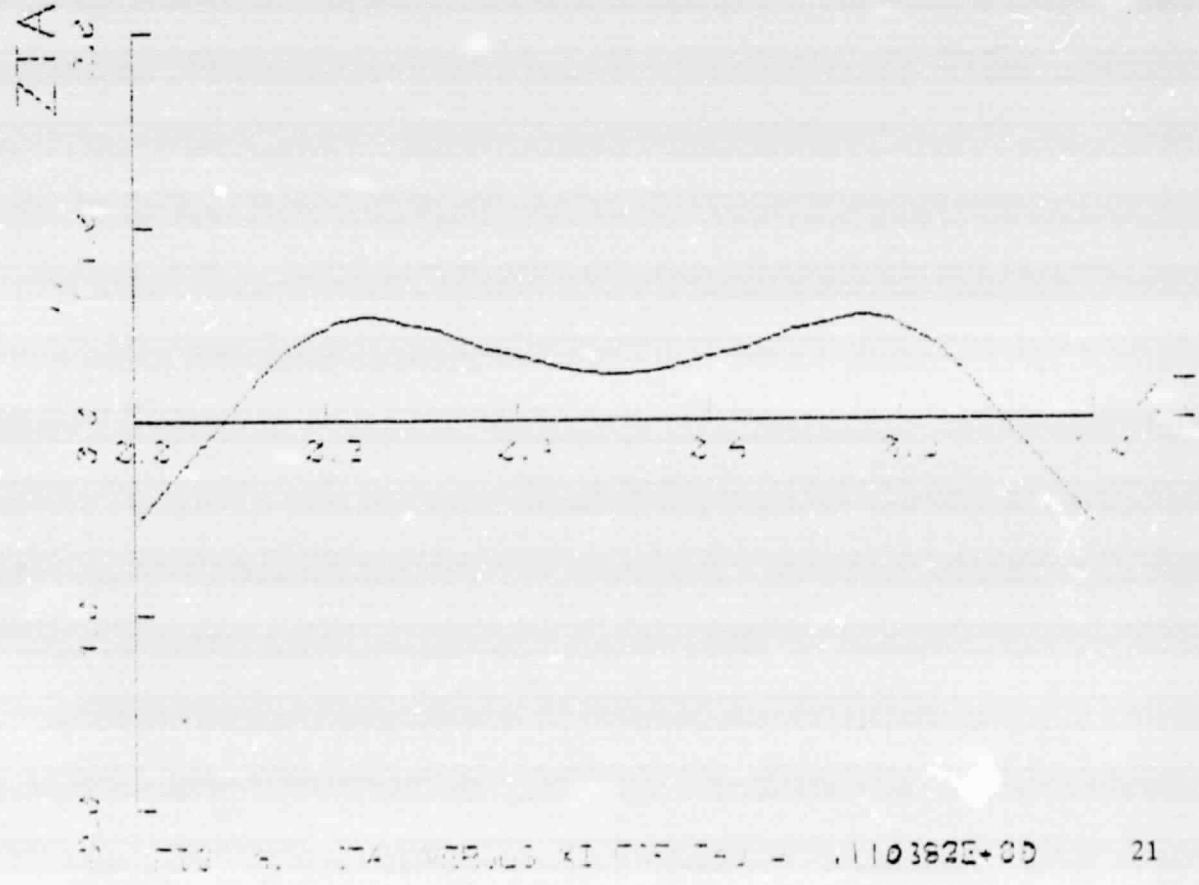

FIG 6. ZTA VERSUS XI FOR TAU = .1103625+00

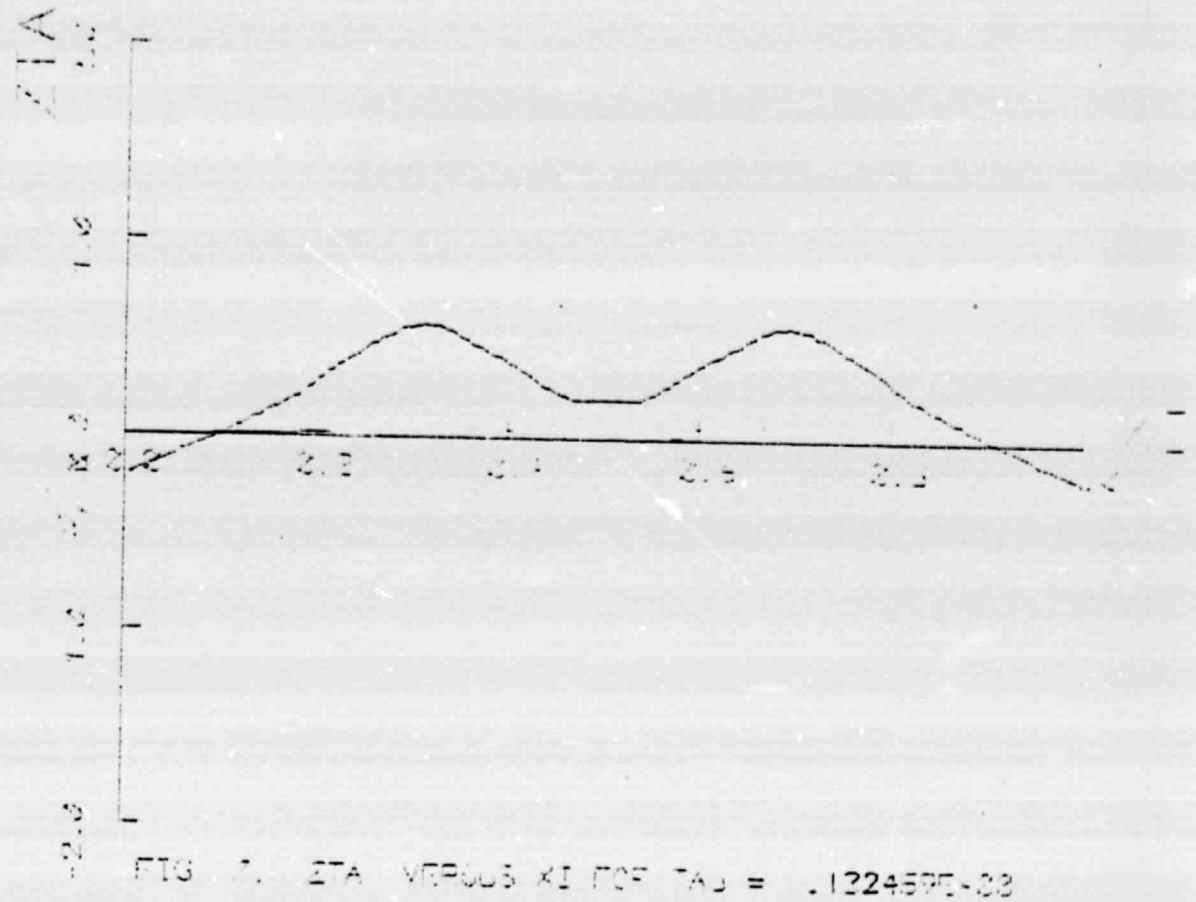

FIG 2. ZTA VERSUS KI FOR TAU = .1224577E-03

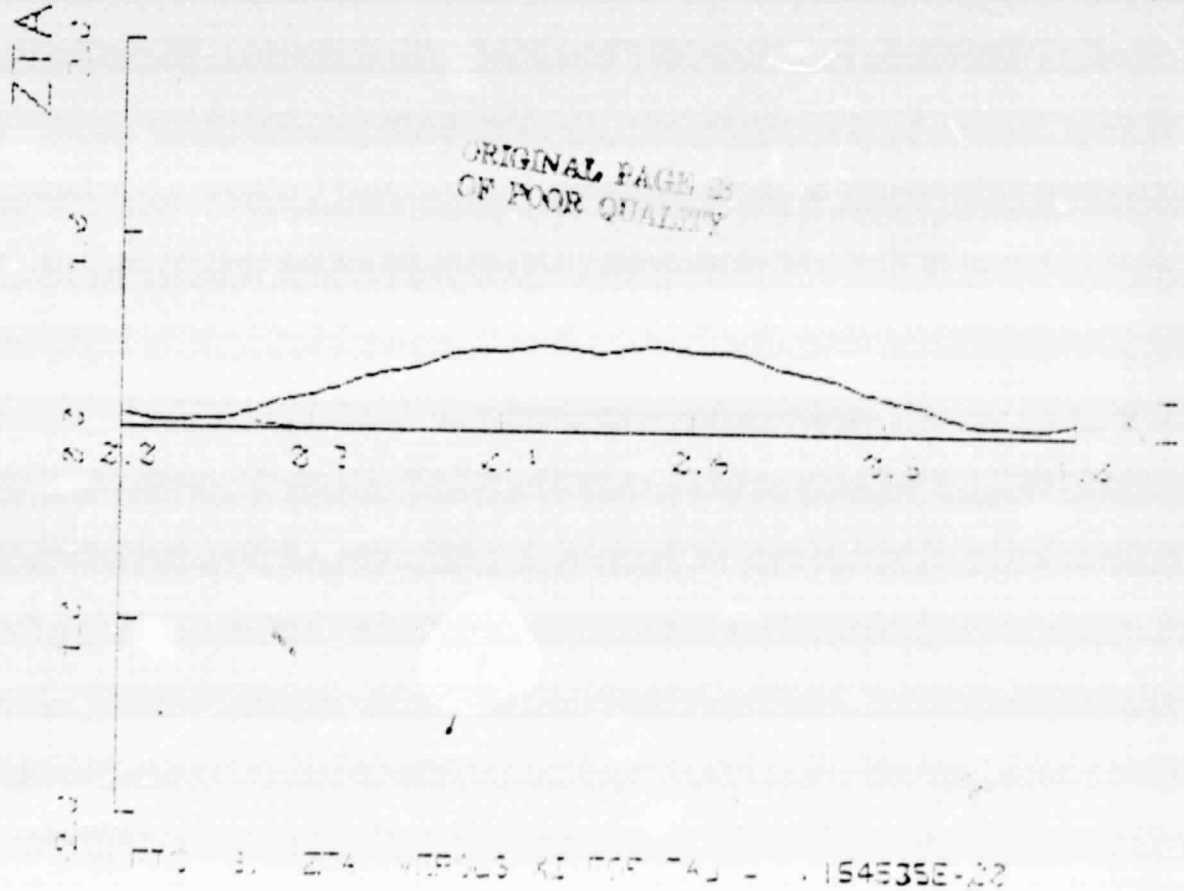

FIG 3. ZTA VERSUS KI FOR TAU = .1545358-03

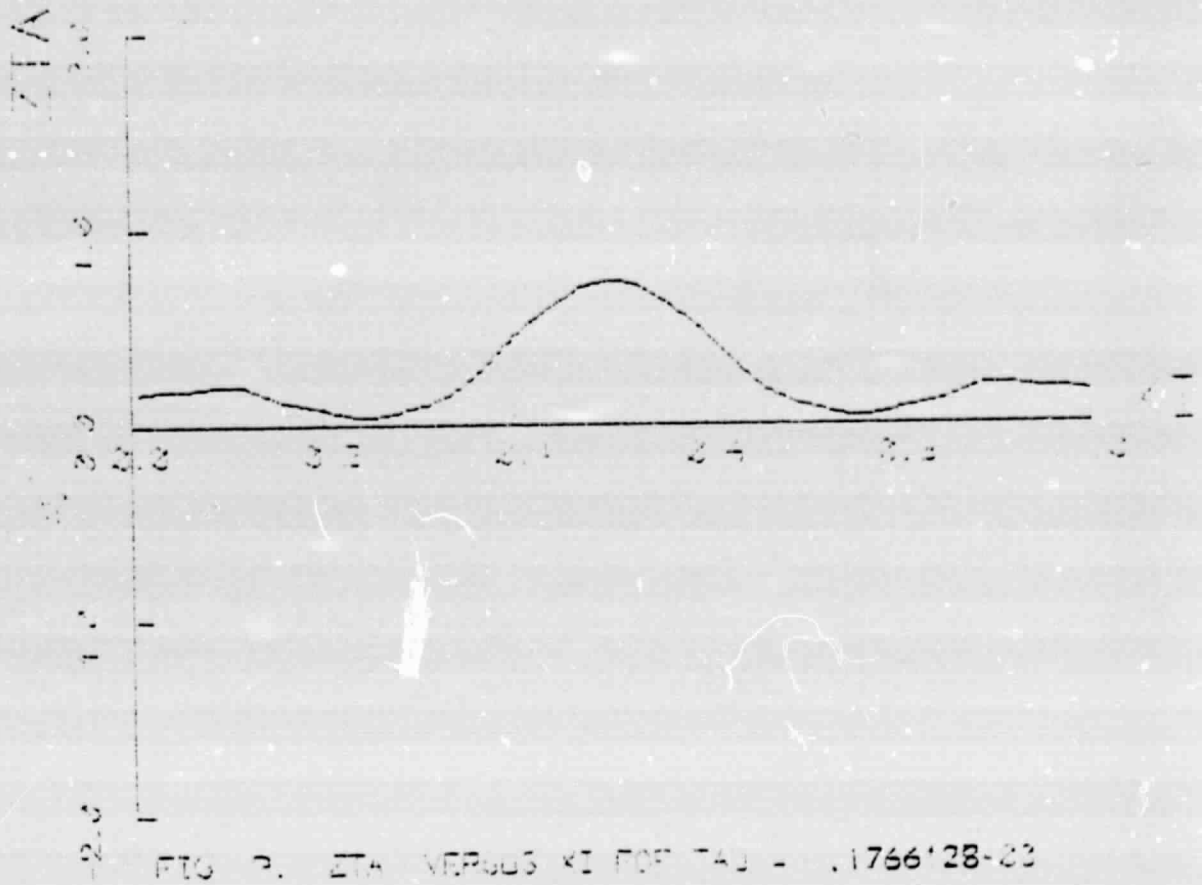

FIG 3. ZTA VERSUS XI FOR TAU = .1766'28-03

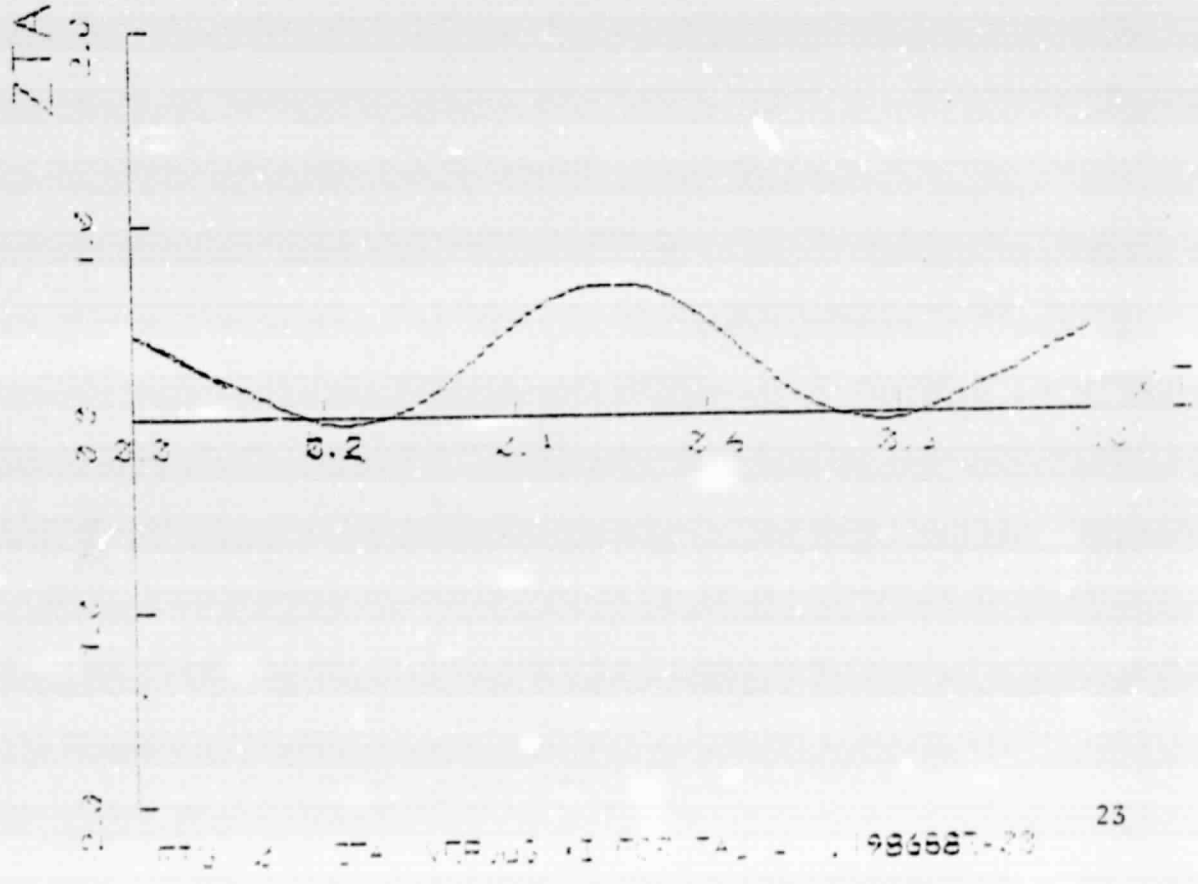

FIG 4. ZTA VERSUS XI FOR TAU = .98668T-03

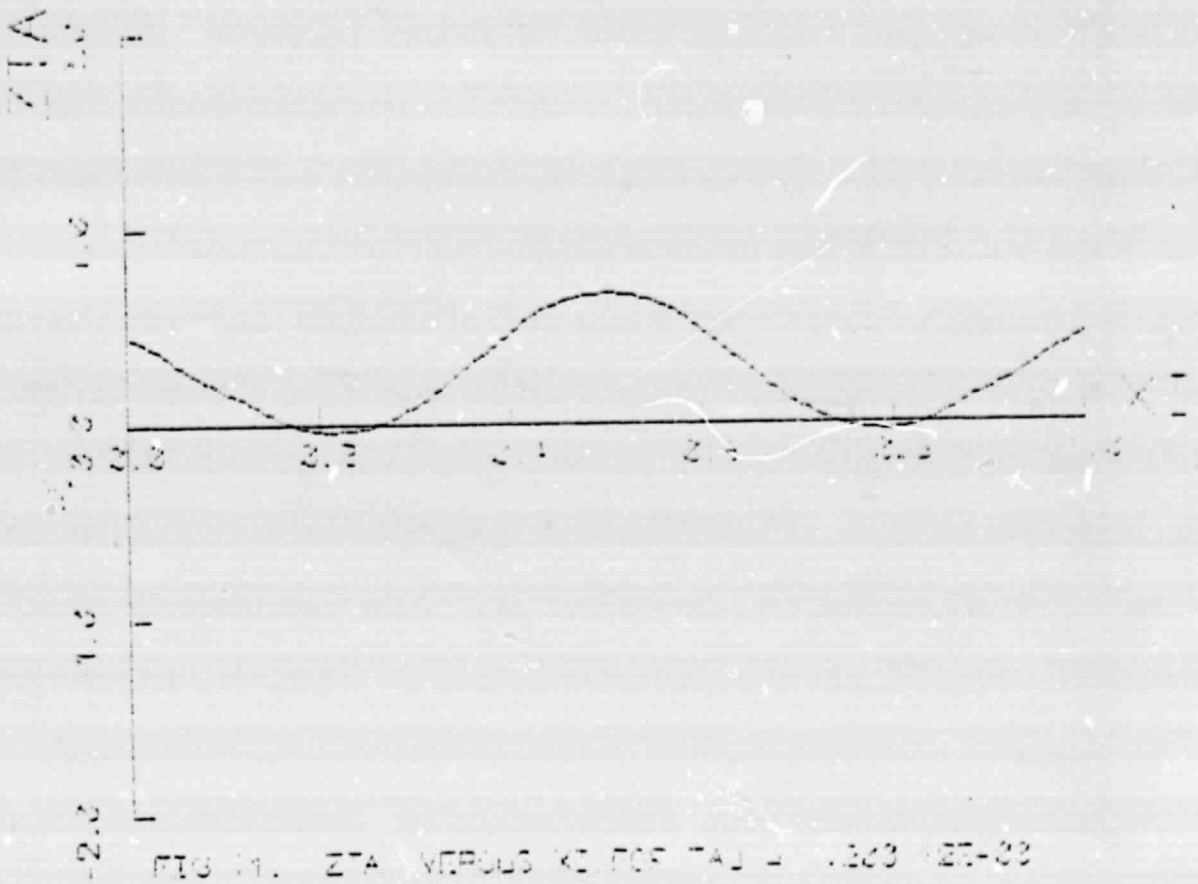

FIG 11. ZETA VERSUS K FOR TAU = .363 (ET-33

ORIGINAL PAGE IS
OF POOR QUALITY

APPENDIX B

Displacement response to a (1 + cos) initial disturbance;
$V_R = 0.62$, SLR = 50, $\lambda = 0.1$.

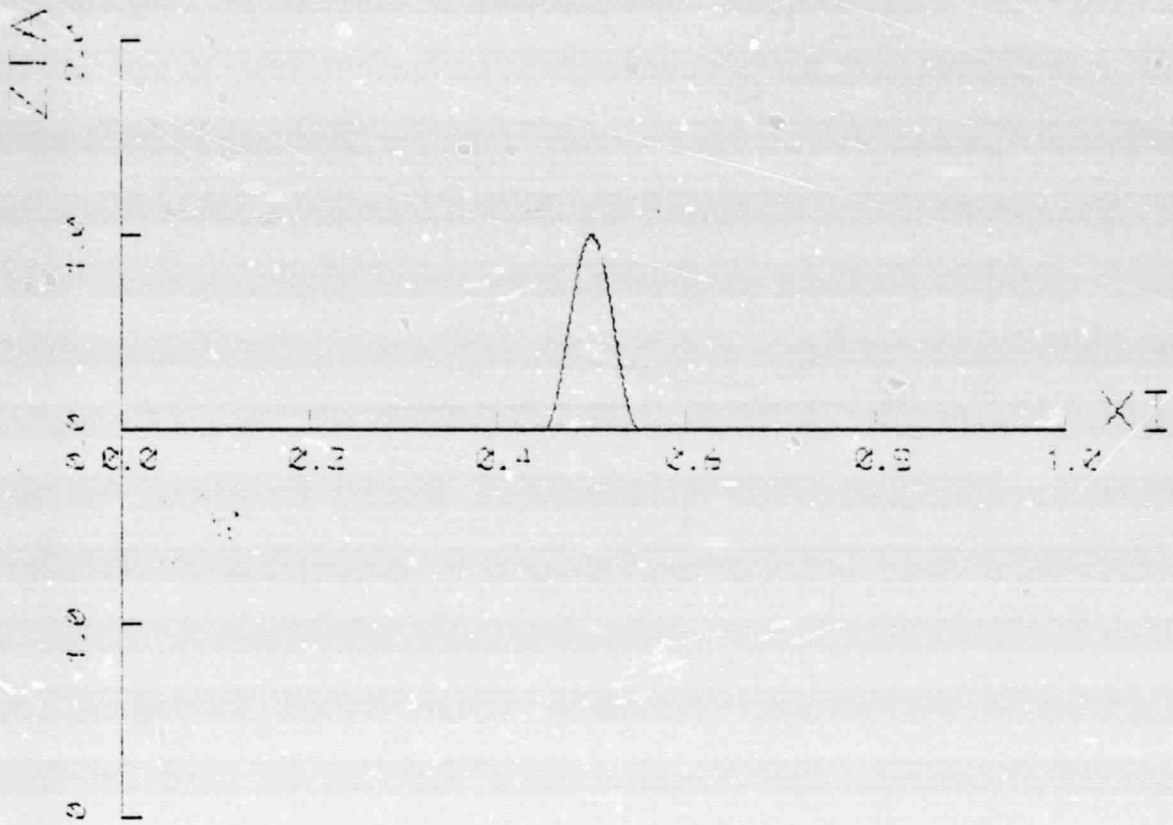

FIG 1. ZTA VERSUS XI FOR TAU = .000000E-00

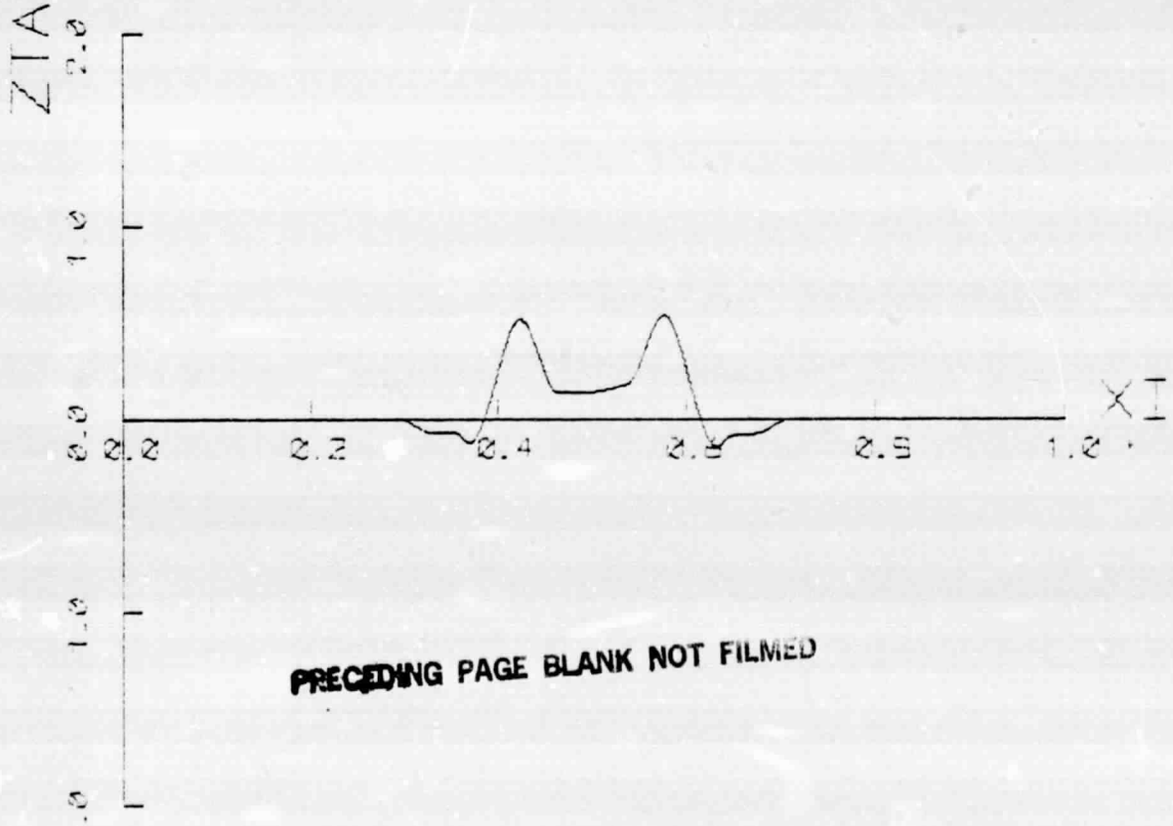

PRECEDING PAGE BLANK NOT FILMED

FIG 2. ZTA VERSUS XI FOR TAU = .111094E-01

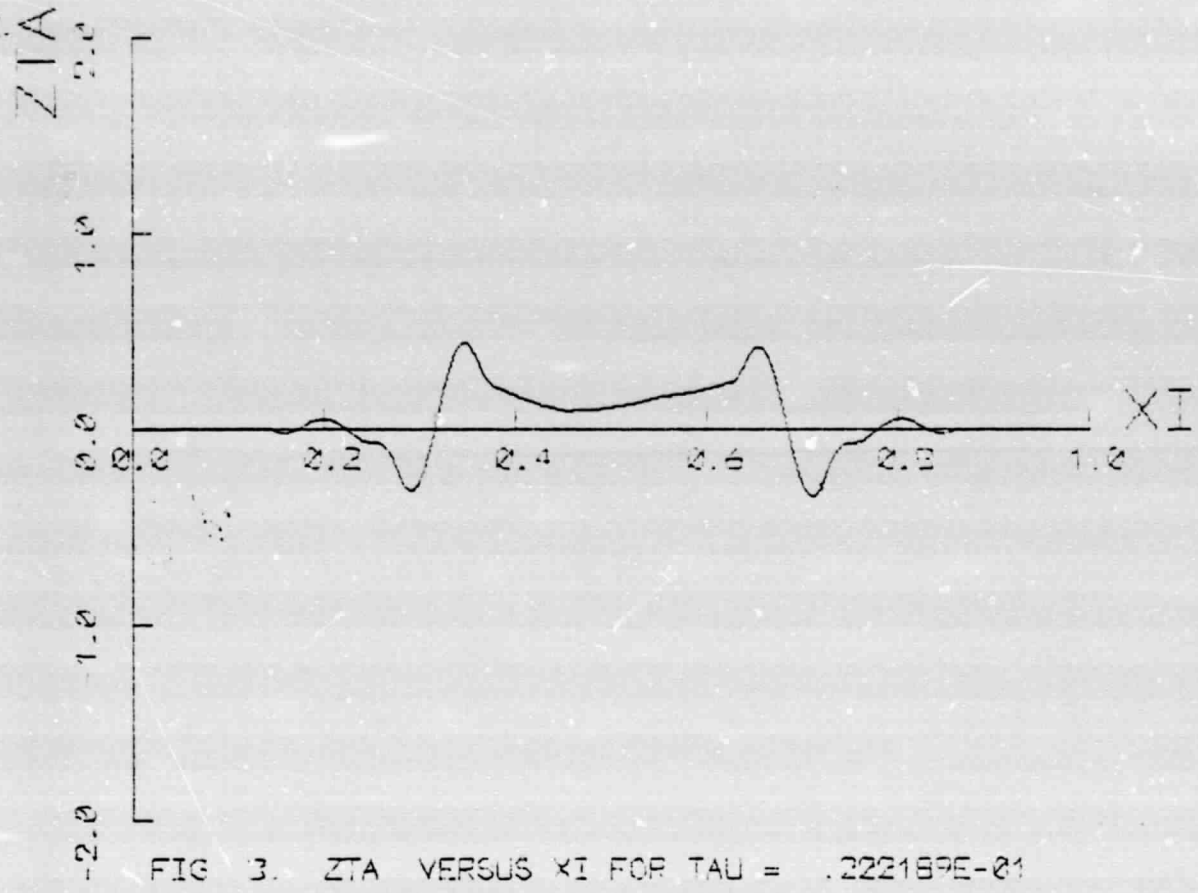

FIG 3. ZTA VERSUS XI FOR TAU = .222189E-01

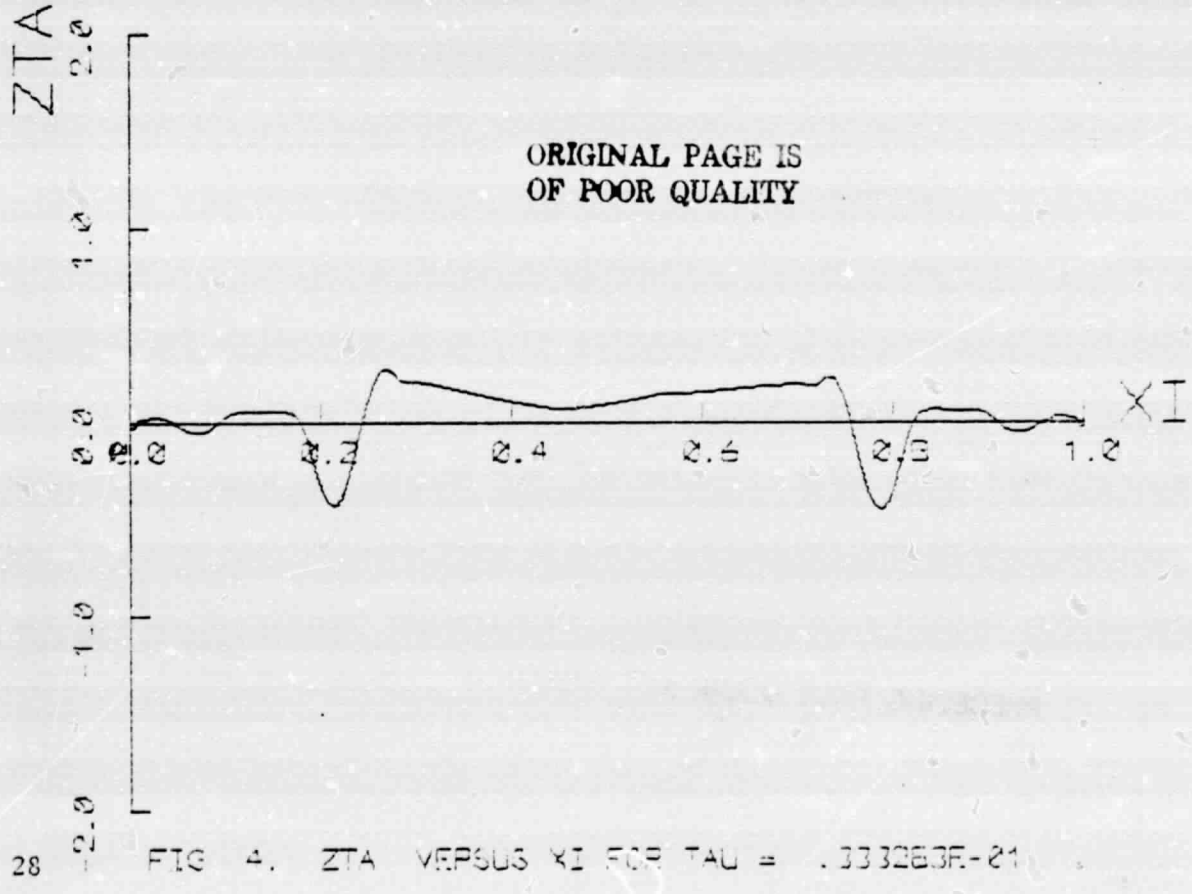

FIG 4. ZTA VERSUS XI FOR TAU = .333283E-01

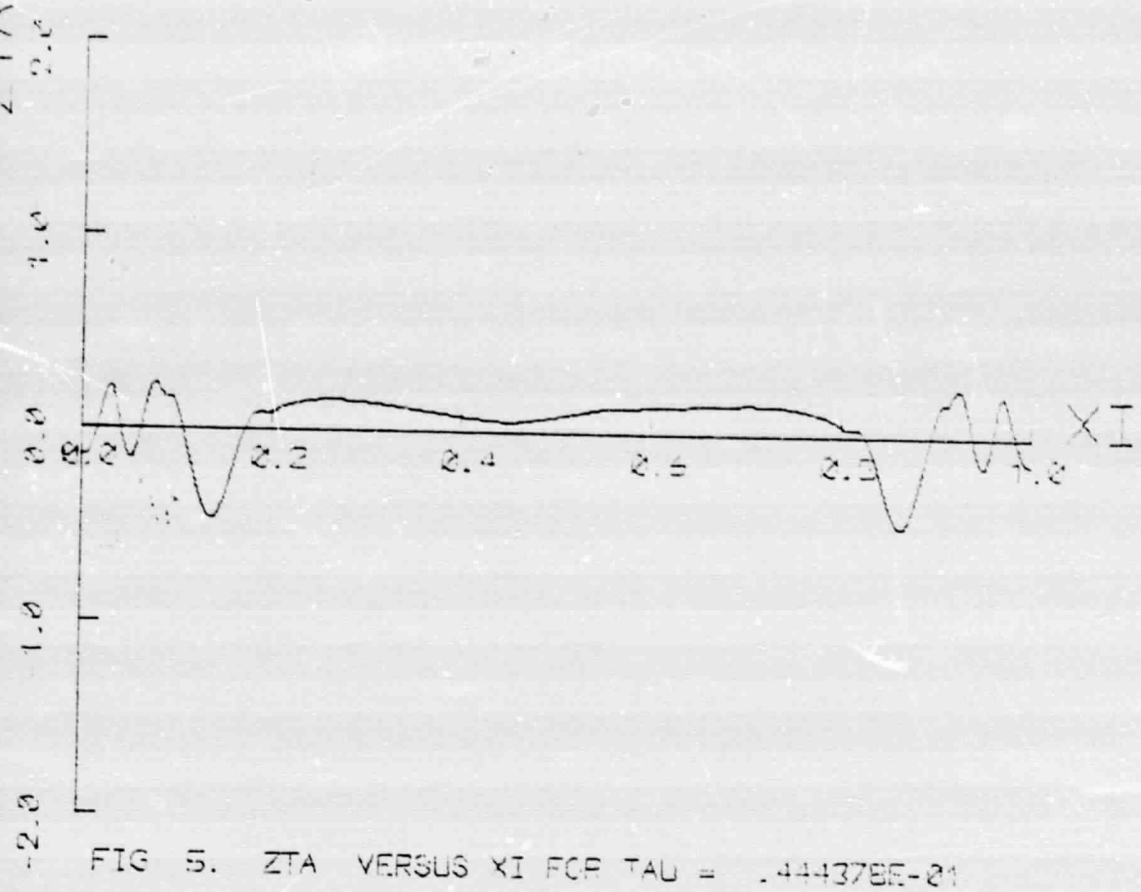

FIG 5. ZTA VERSUS XI FOR TAU = .444378E-01

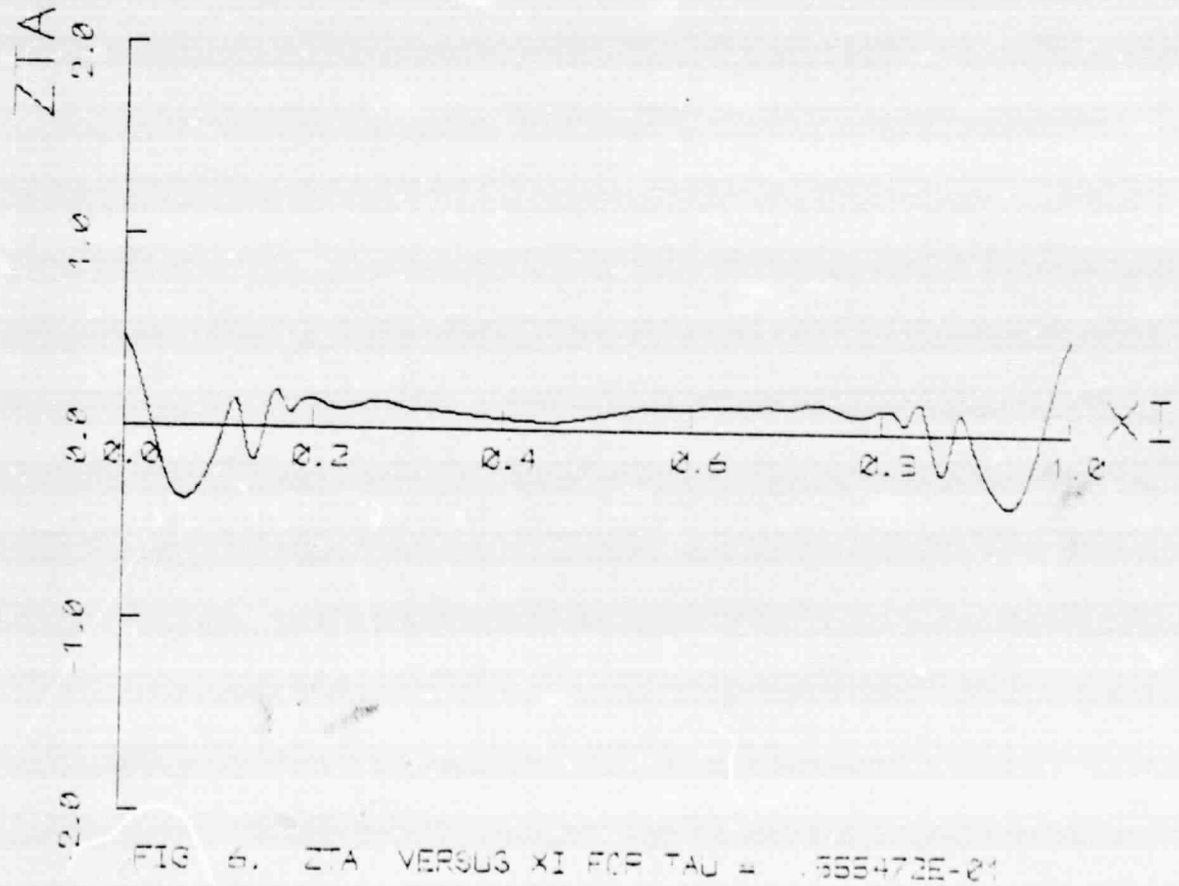

FIG 6. ZTA VERSUS XI FOR TAU = .555472E-01

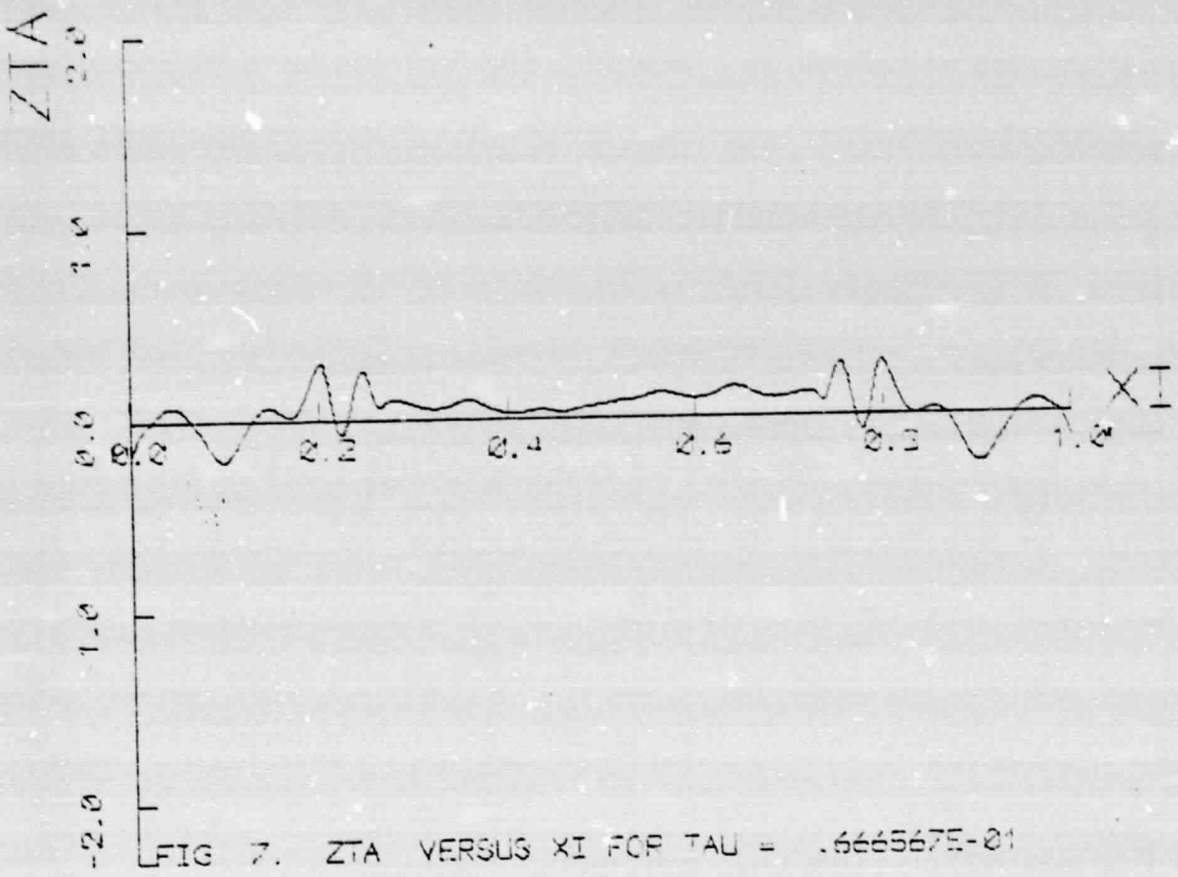

FIG 7. ZTA VERSUS XI FOR TAU = .6665675E-01

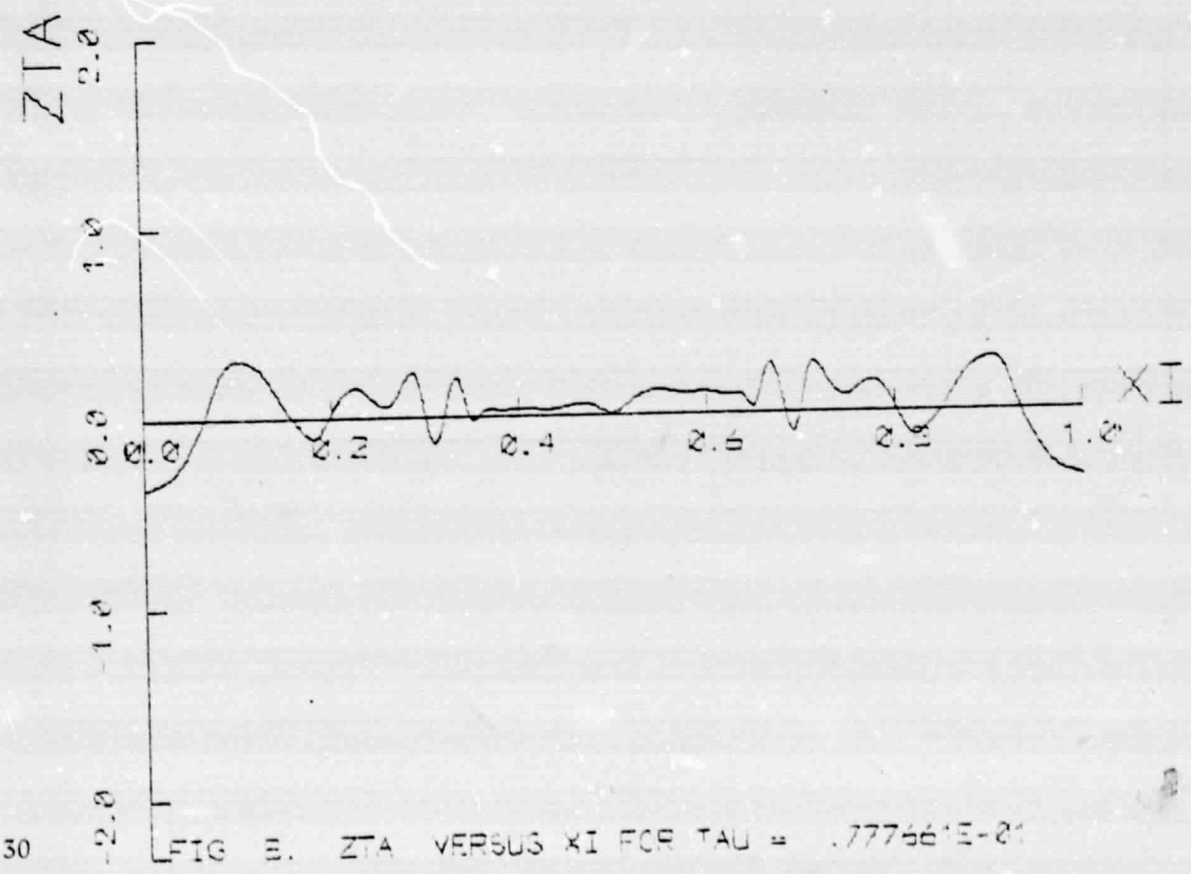

FIG 8. ZTA VERSUS XI FOR TAU = .7776613E-01

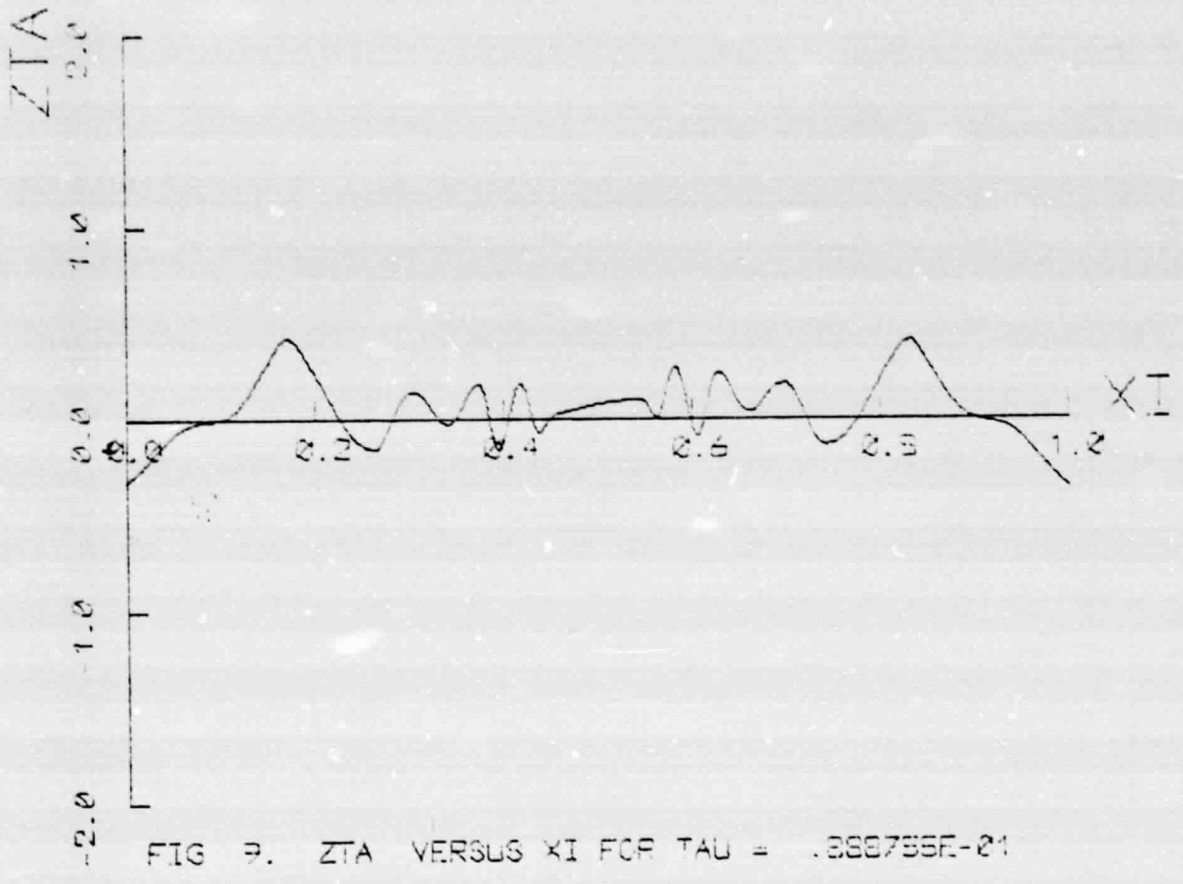

FIG 9. ZTA VERSUS XI FOR TAU = .888755E-01

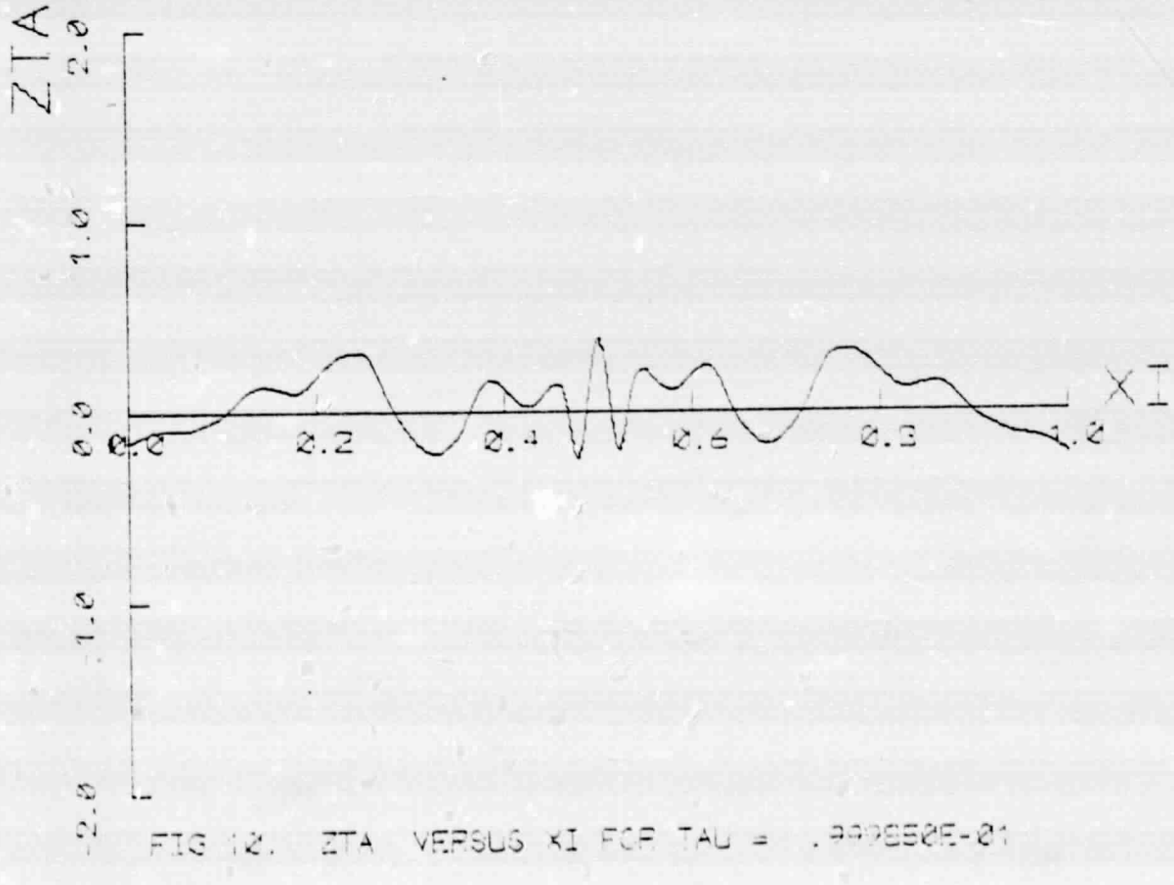

FIG 10. ZTA VERSUS XI FOR TAU = .999560E-01

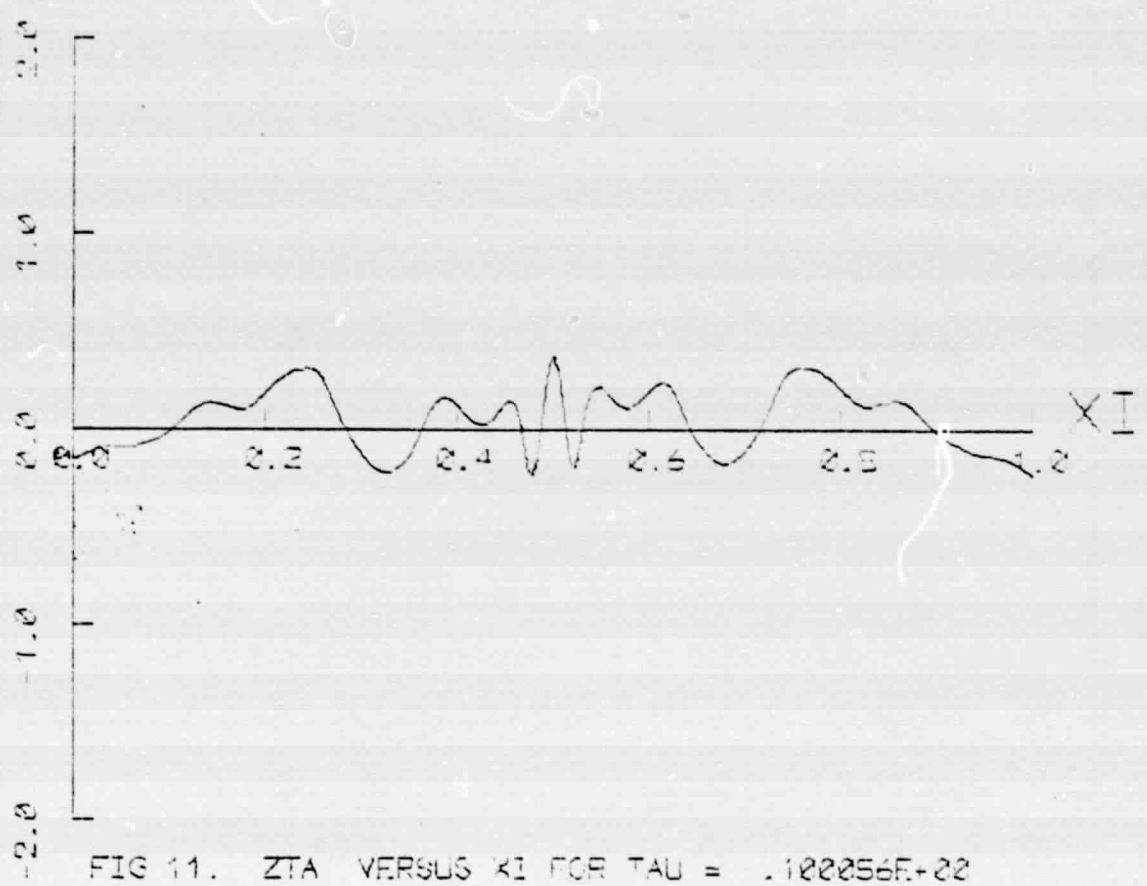

FIG 11. ZTA VERSUS XI FOR TAU = .100056E+02

APPENDIX C

Displacement response to a (1 + cos) initial disturbance;

$V_R = 0.3$, SLR = 50, $\lambda = 0.5$

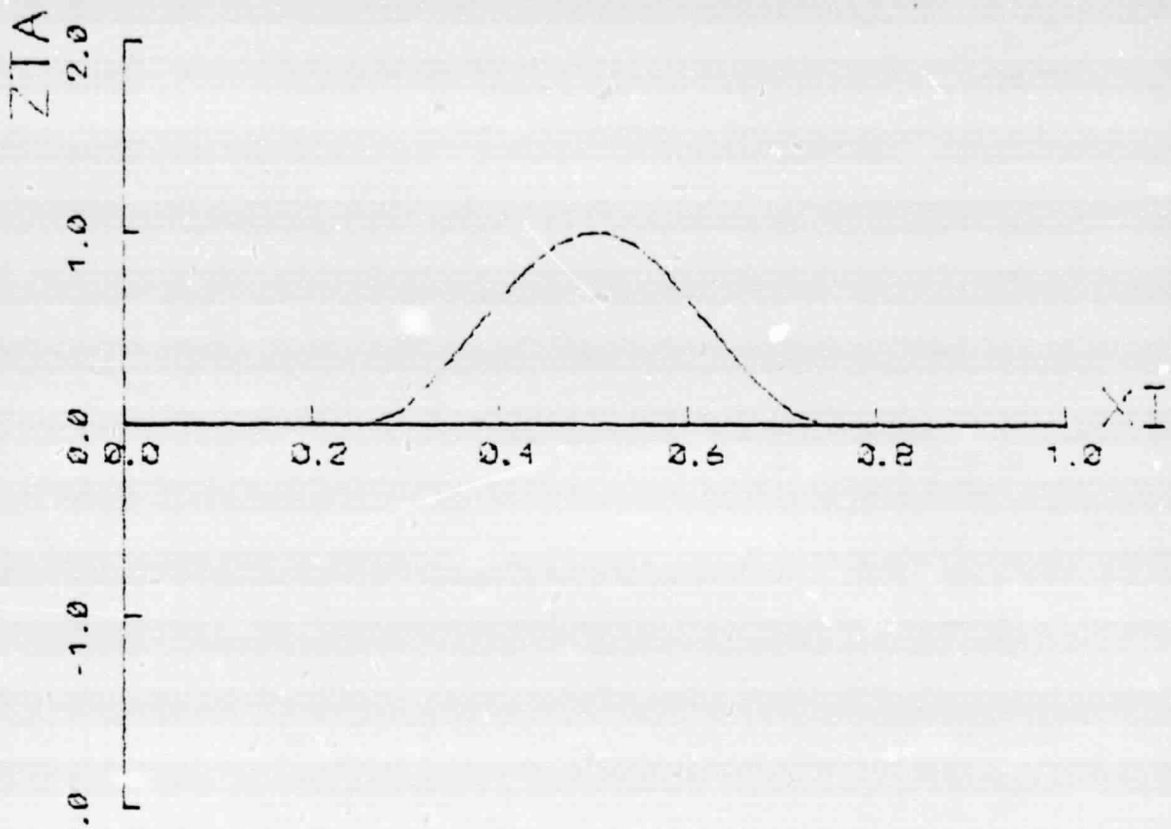

FIG 1. ZTA VERSUS XI FOR TAU = .200000E+00

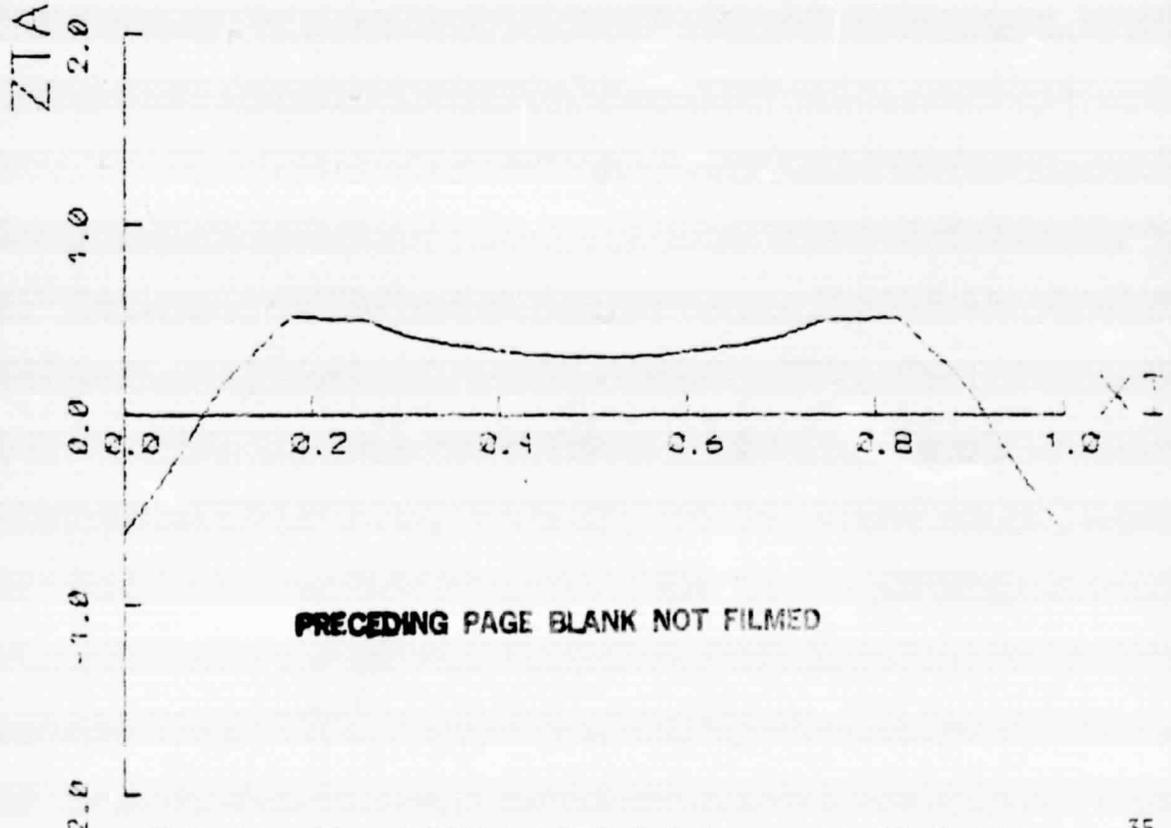

PRECEDING PAGE BLANK NOT FILMED

FIG 2. ZTA VERSUS XI FOR TAU = .111094E+00

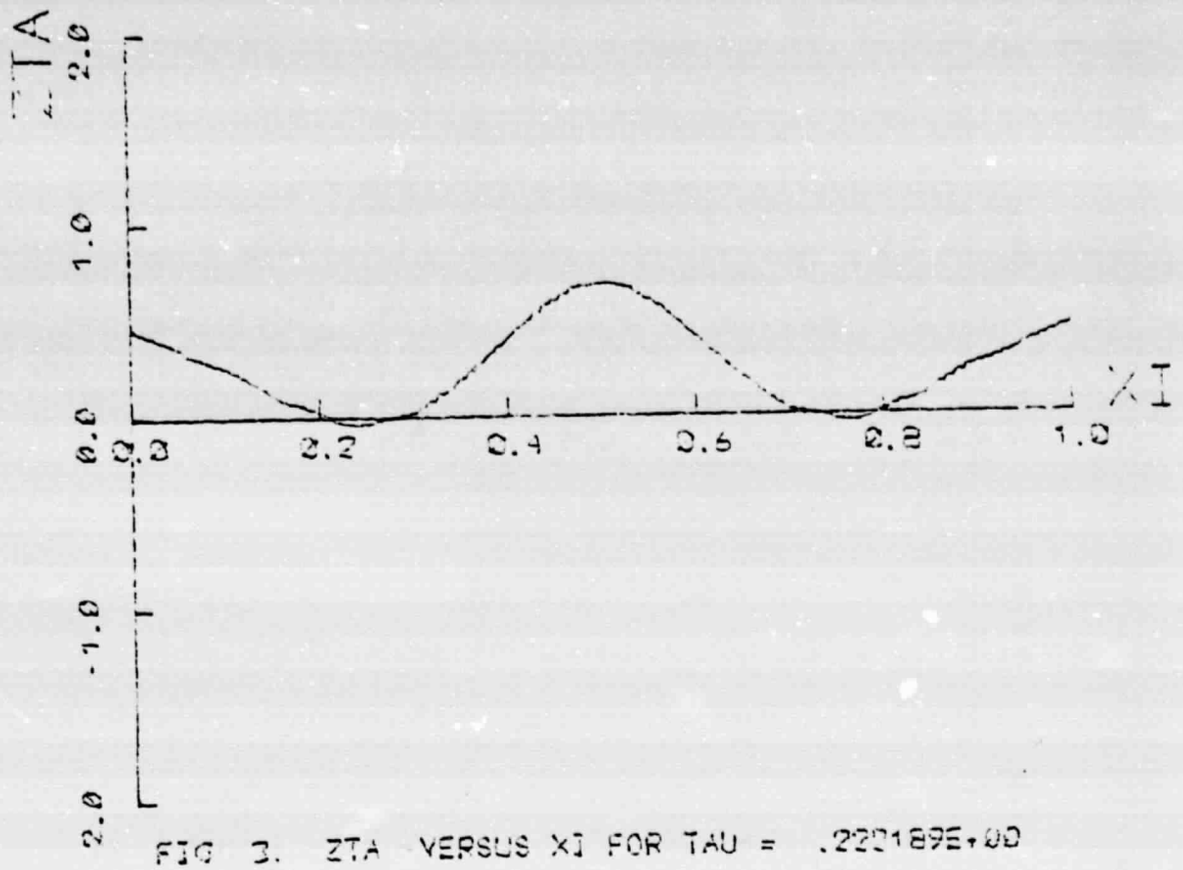

FIG 3. ZTA VERSUS XI FOR TAU = .220189E+00

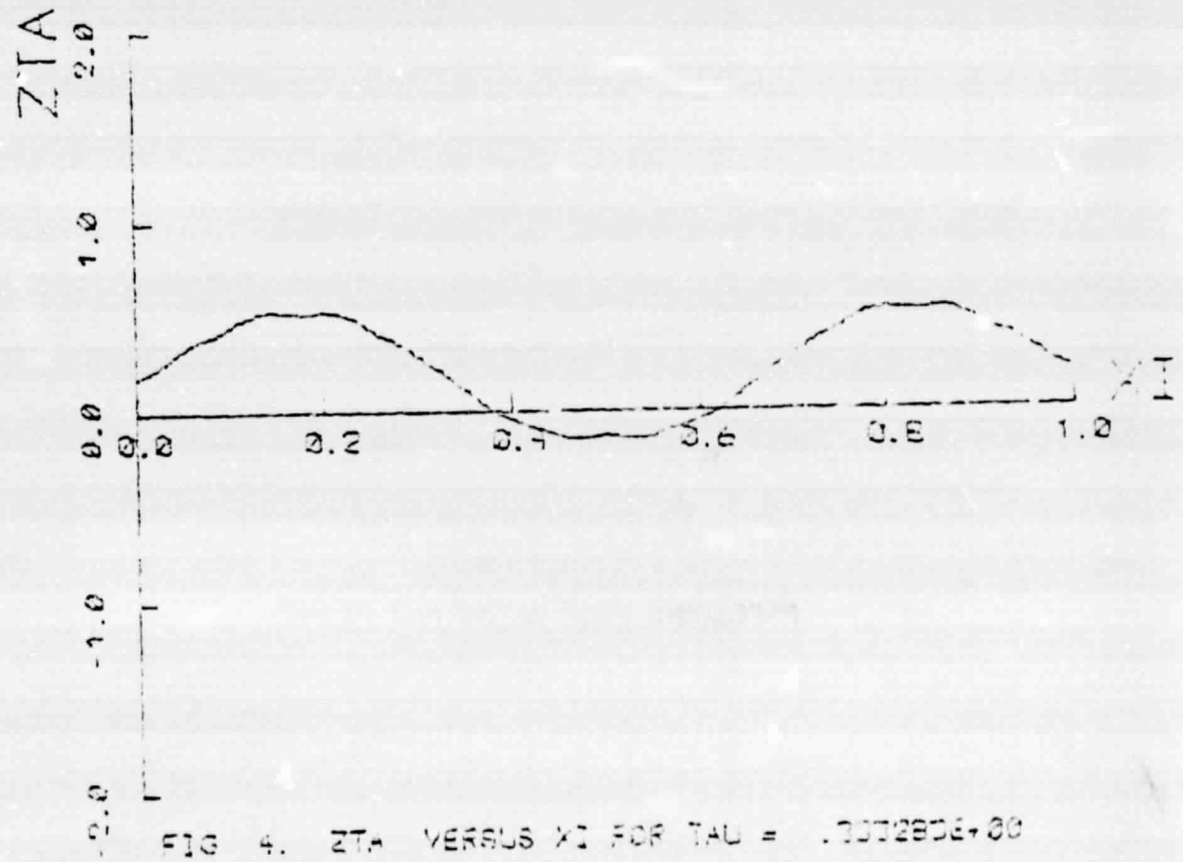

FIG 4. ZTA VERSUS XI FOR TAU = .[illegible]

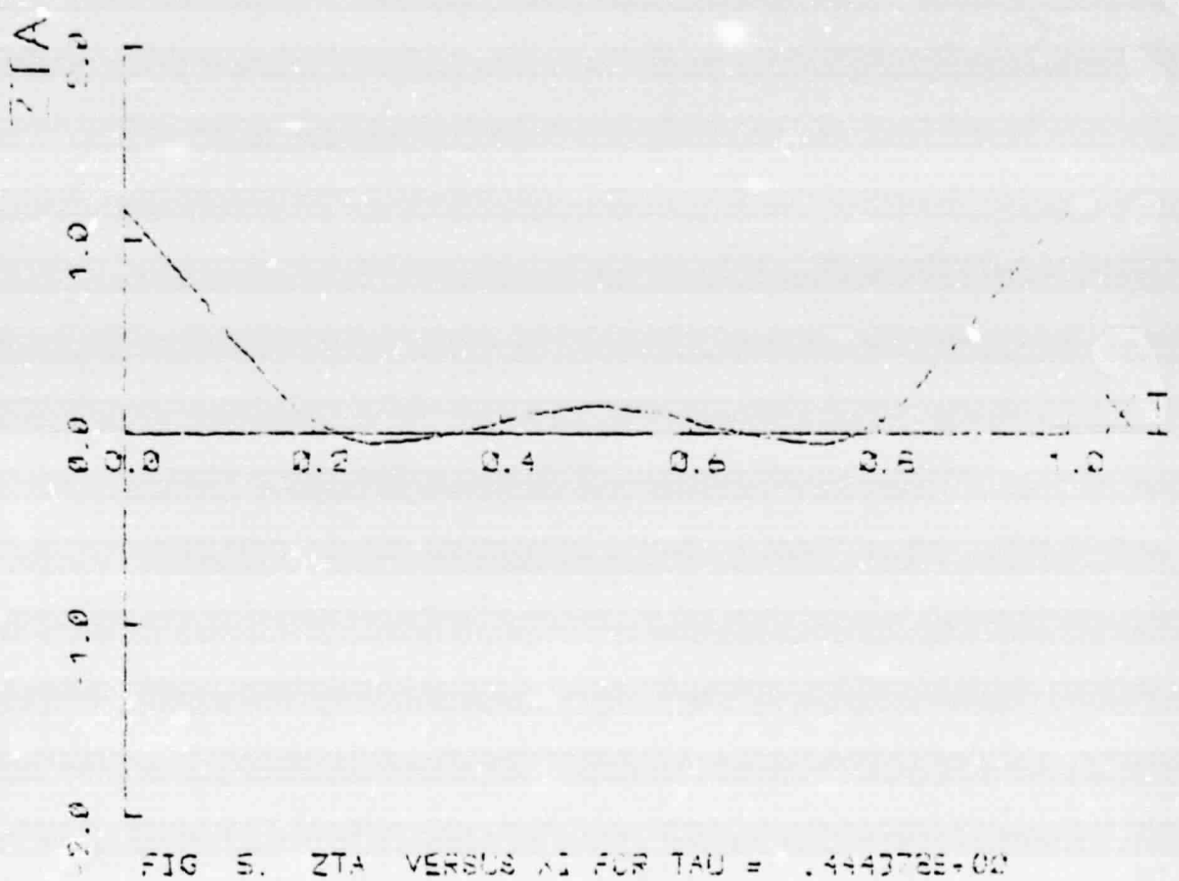

FIG 5. ZTA VERSUS XI FOR TAU = .4443788+00

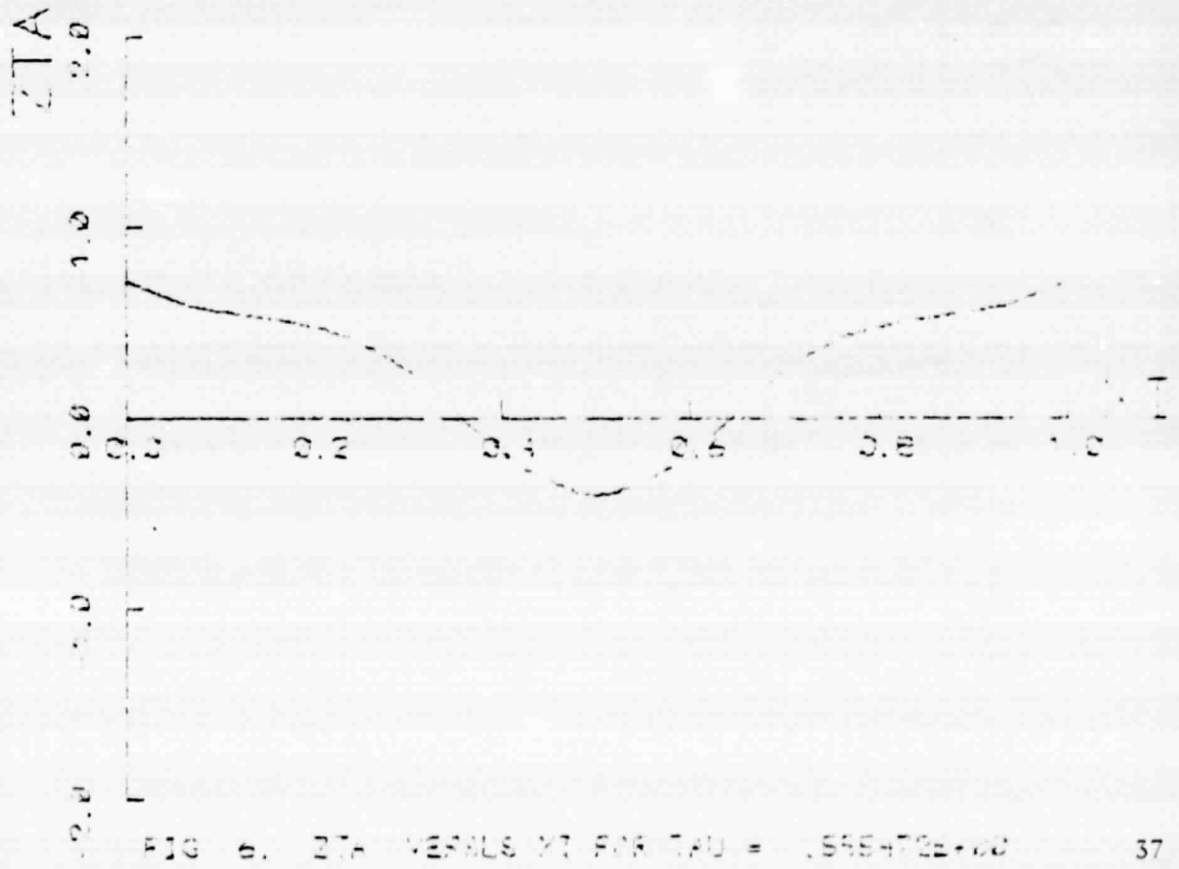

FIG 6. ZTA VERSUS XI FOR TAU = .5454782+00

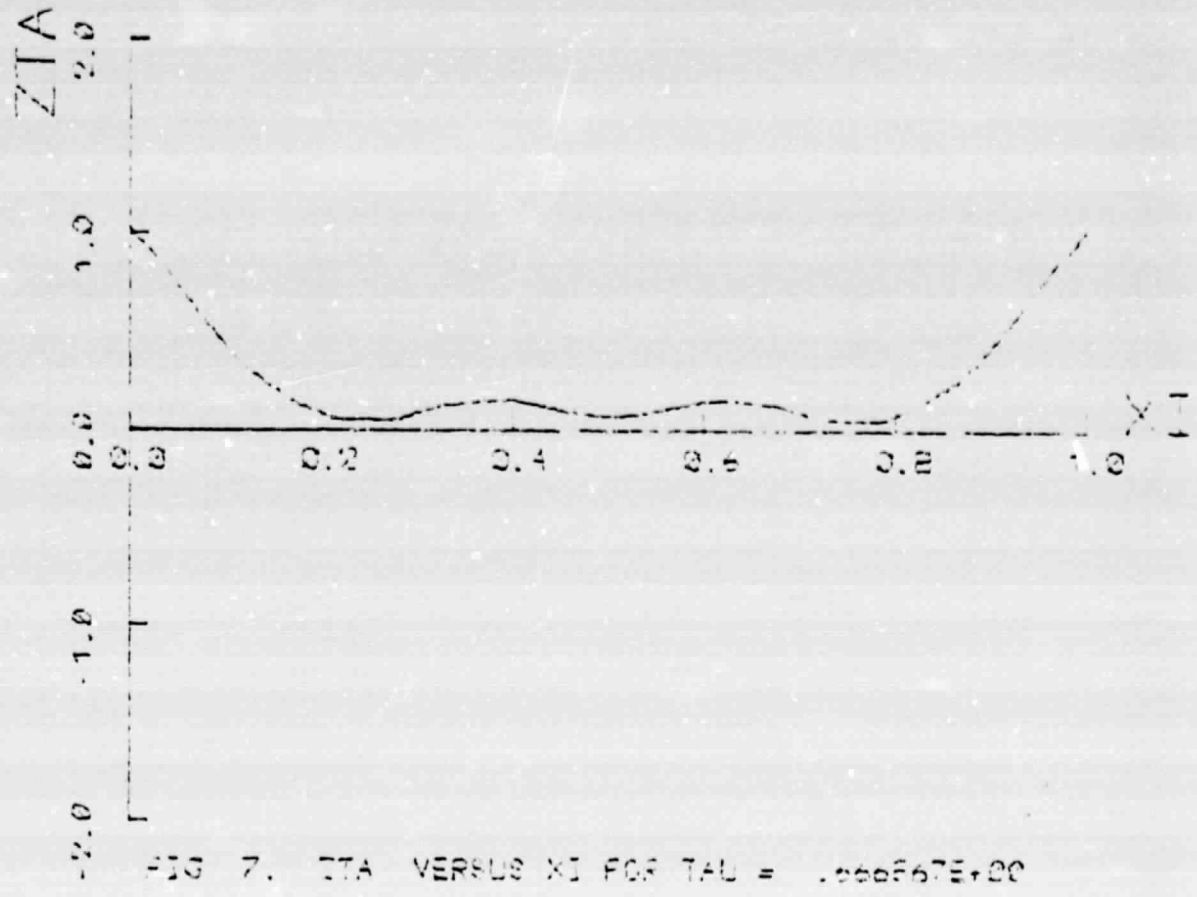

FIG 7. ZTA VERSUS XI FOR TAU = .966F67E+00

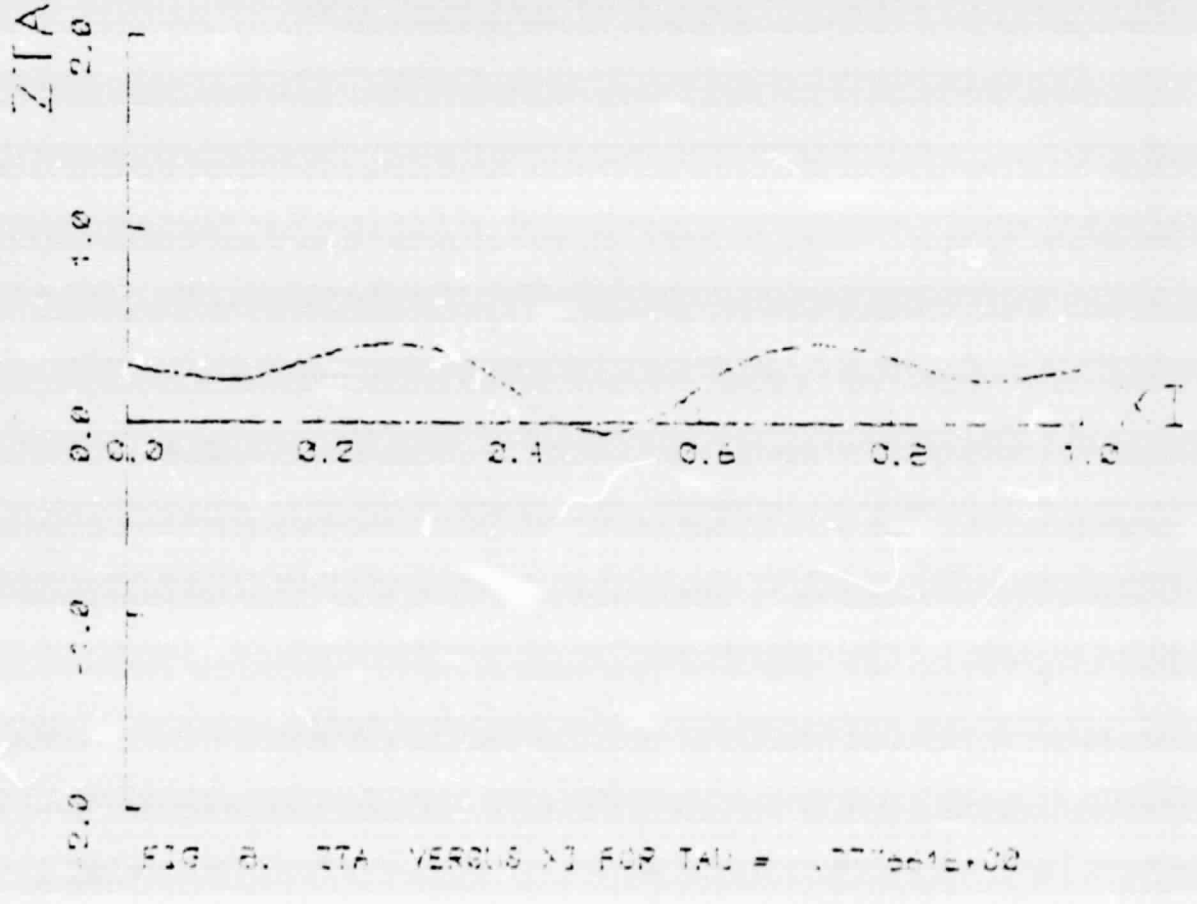

FIG 8. ZTA VERSUS XI FOR TAU = .[illegible]E+02

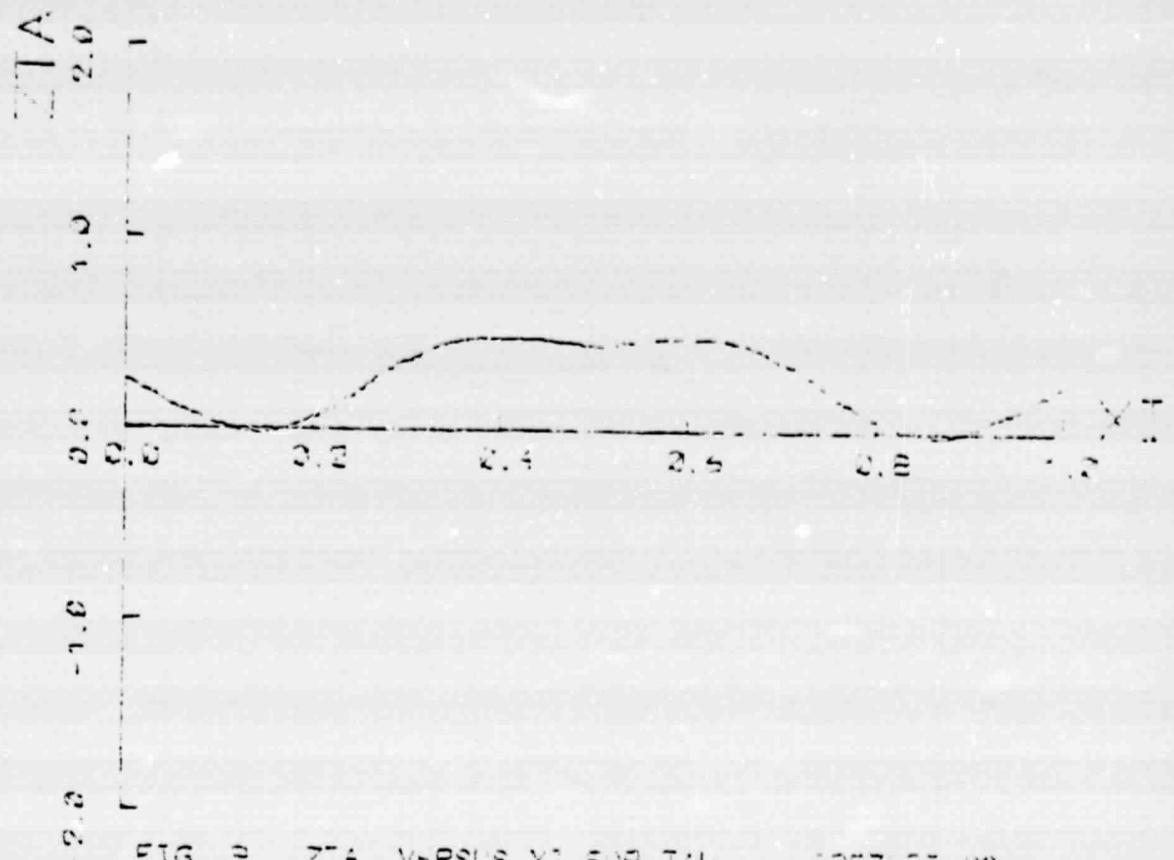

FIG 9. ZTA VERSUS XI FOR TAU = .ABETaSE-10

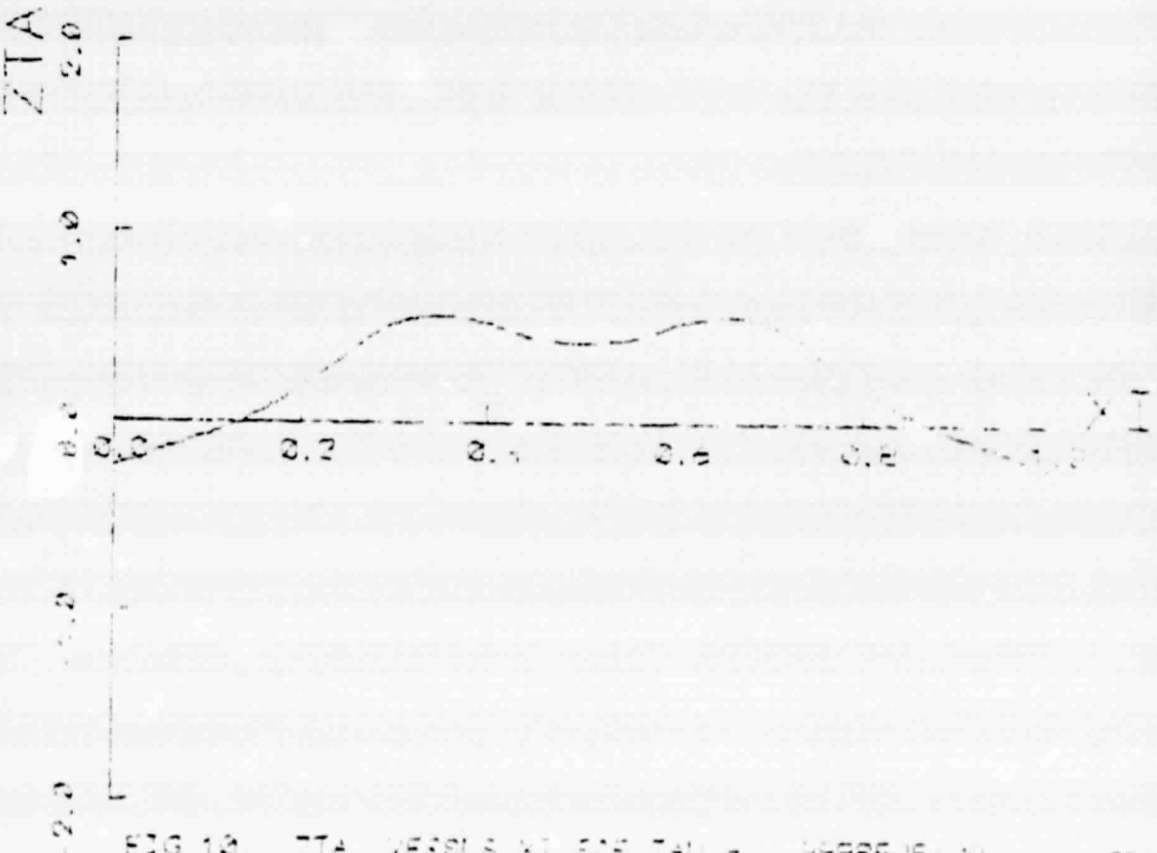

FIG 10. ZTA VERSUS XI FOR TAU = .AFFBE-10

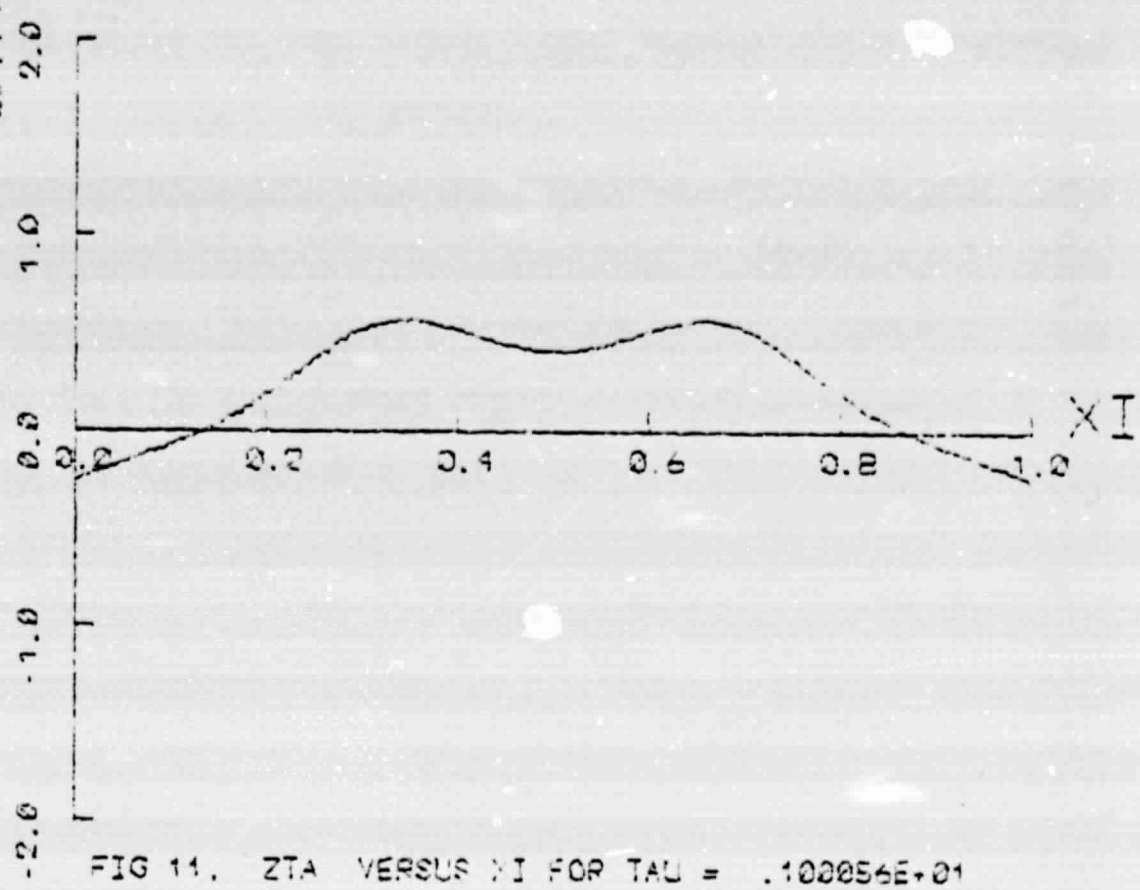

FIG 11. ZTA VERSUS XI FOR TAU = .100056E+01

APPENDIX D

Displacement response to a (1 + cos) initial disturbance;
$V_R = 0.3$, SLR = 50, $\lambda = 0.1$.

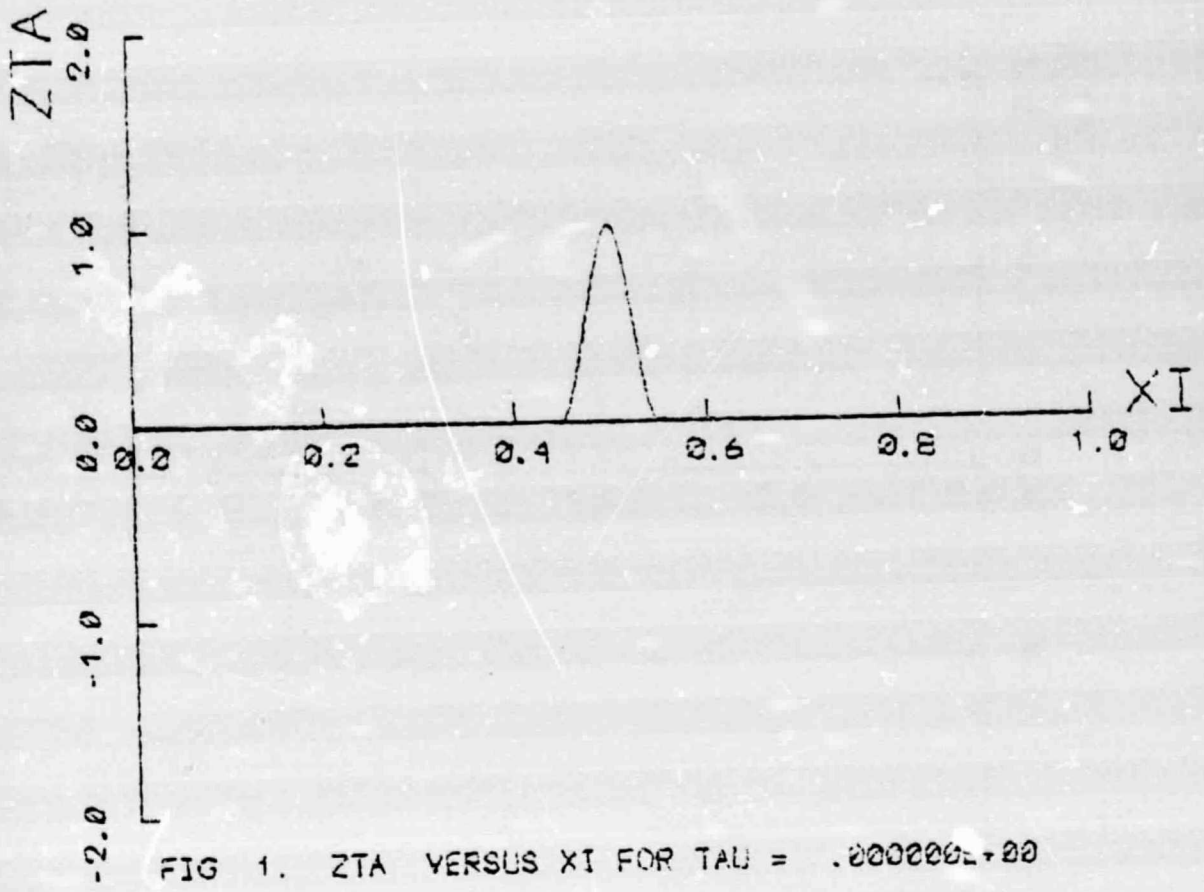

FIG 1. ZTA VERSUS XI FOR TAU = .000000E+00

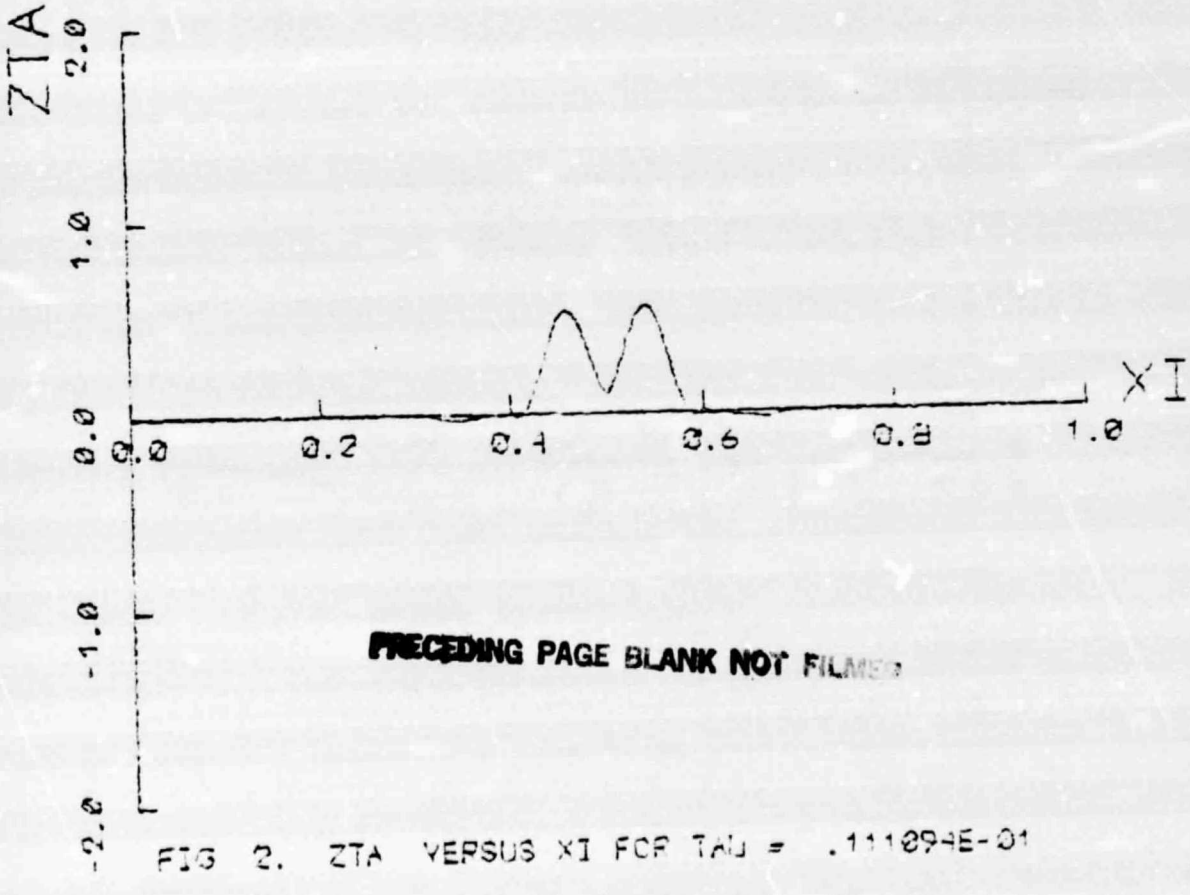

FIG 2. ZTA VERSUS XI FOR TAU = .111094E-01

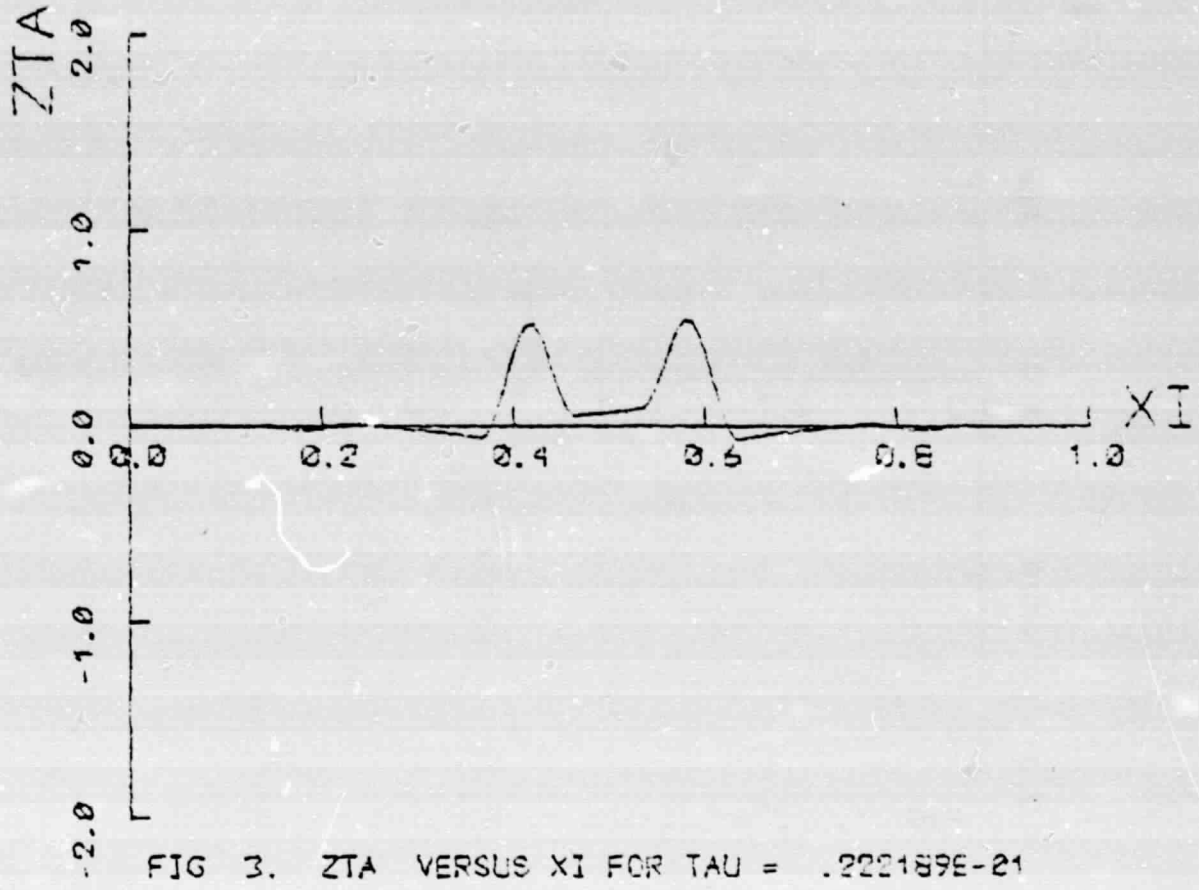

FIG 3. ZTA VERSUS XI FOR TAU = .2221899E-01

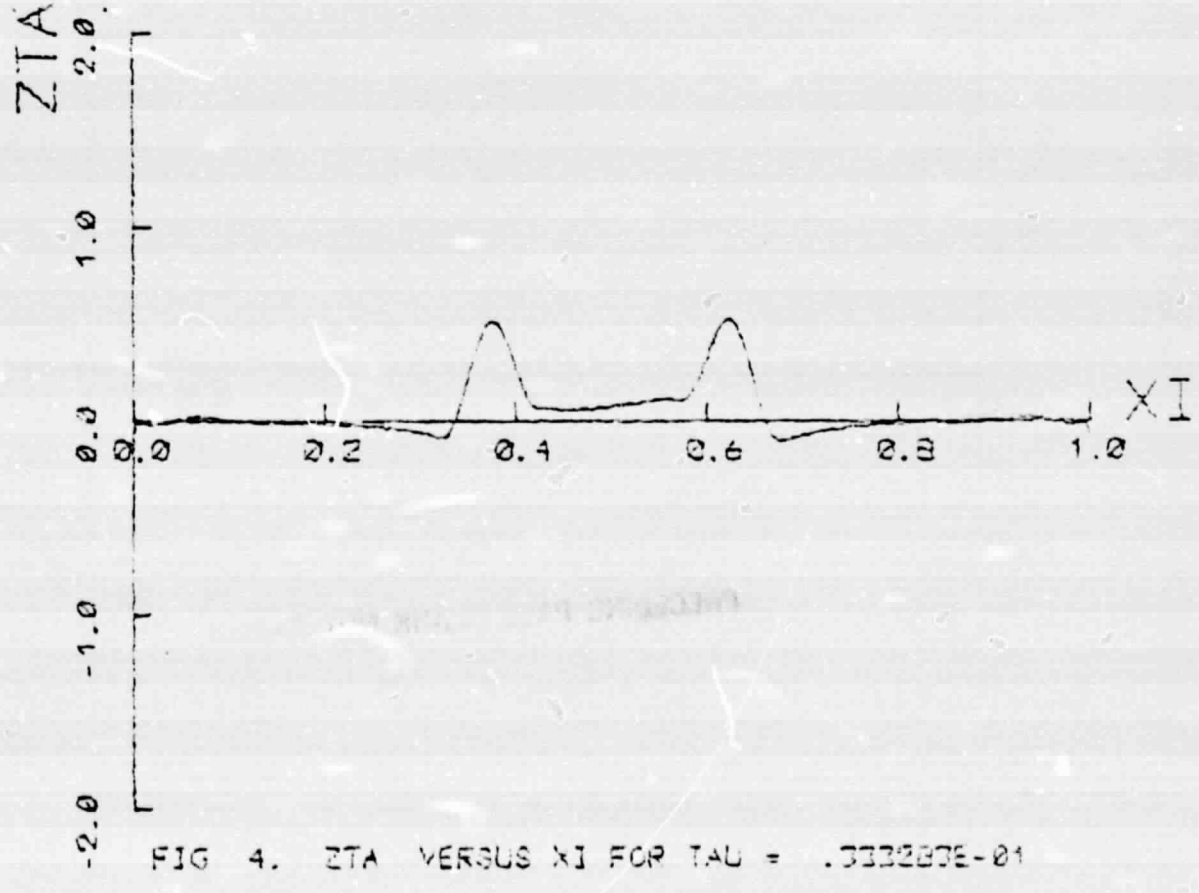

FIG 4. ZTA VERSUS XI FOR TAU = .3332837E-01

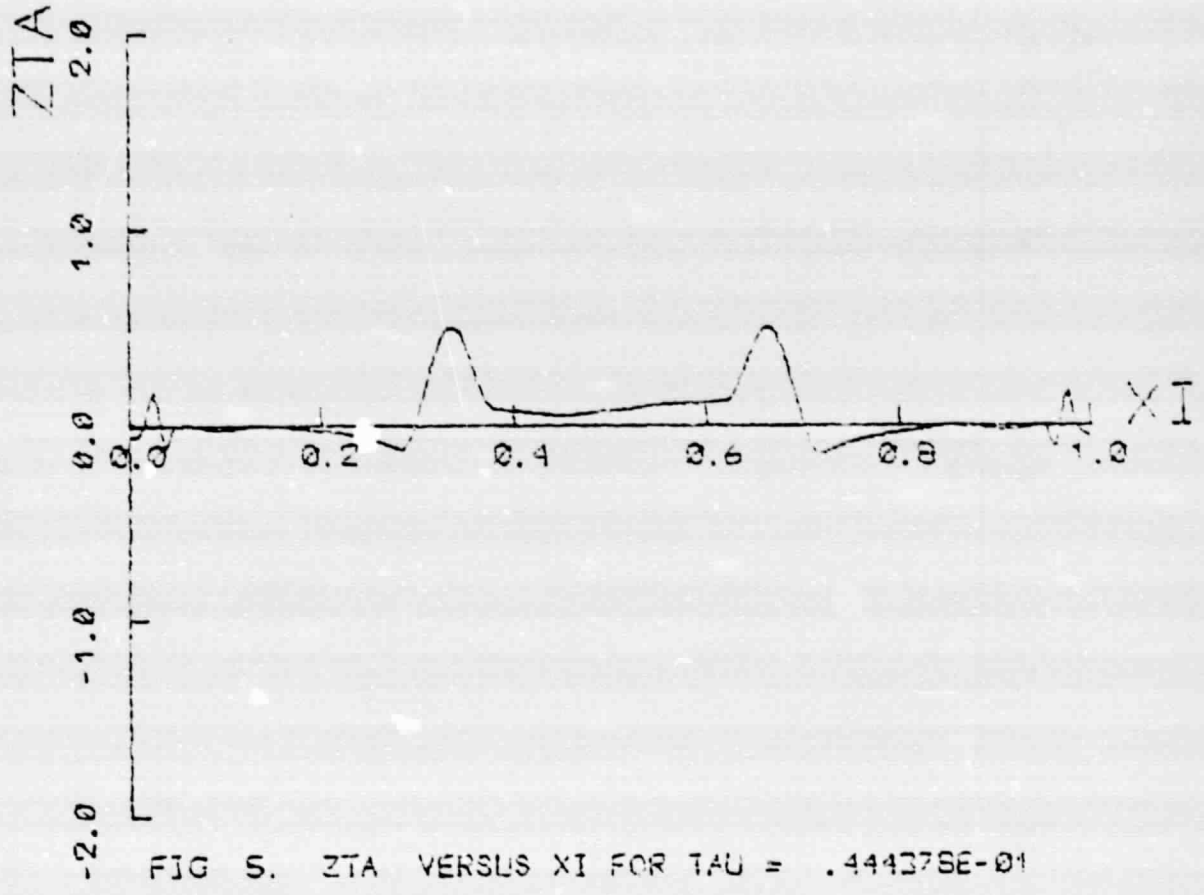

FIG 5. ZTA VERSUS XI FOR TAU = .444378E-01

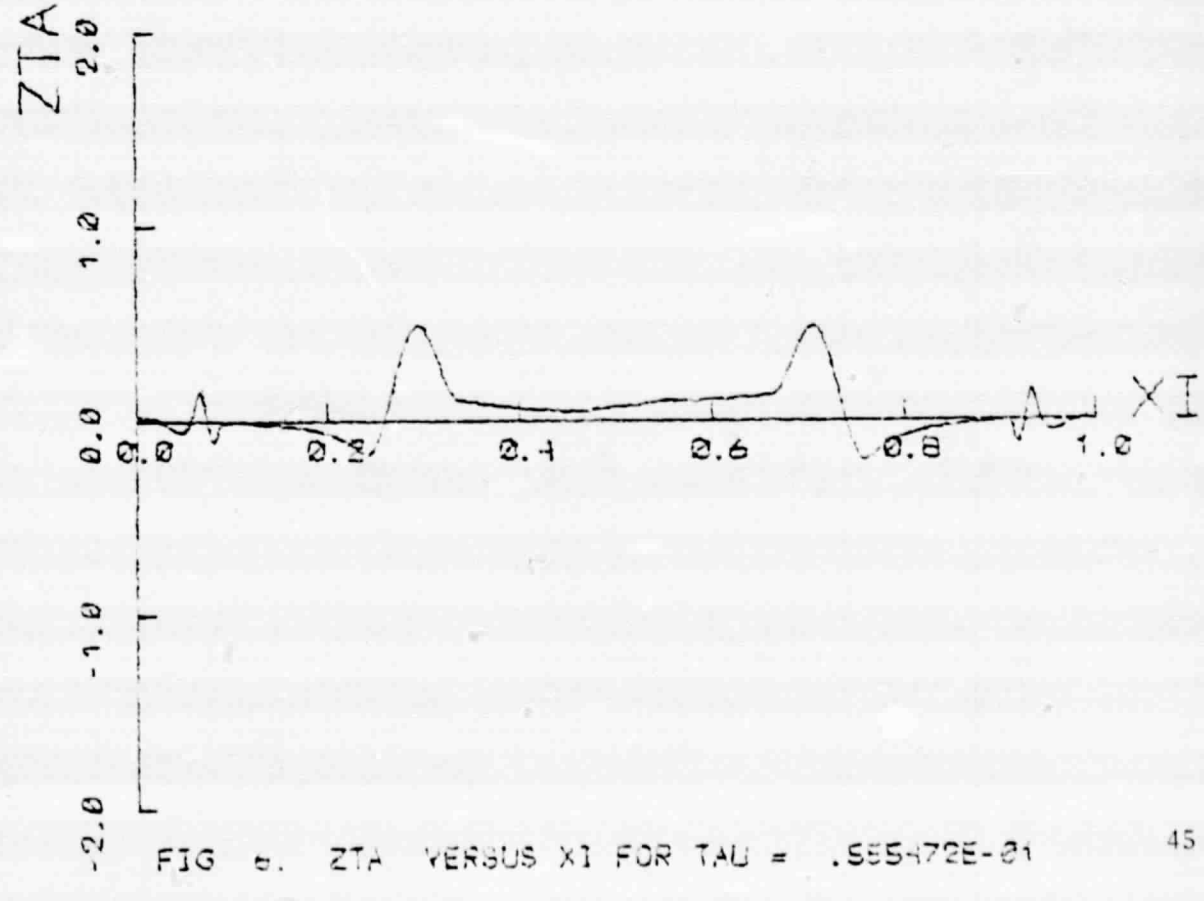

FIG 6. ZTA VERSUS XI FOR TAU = .555472E-01

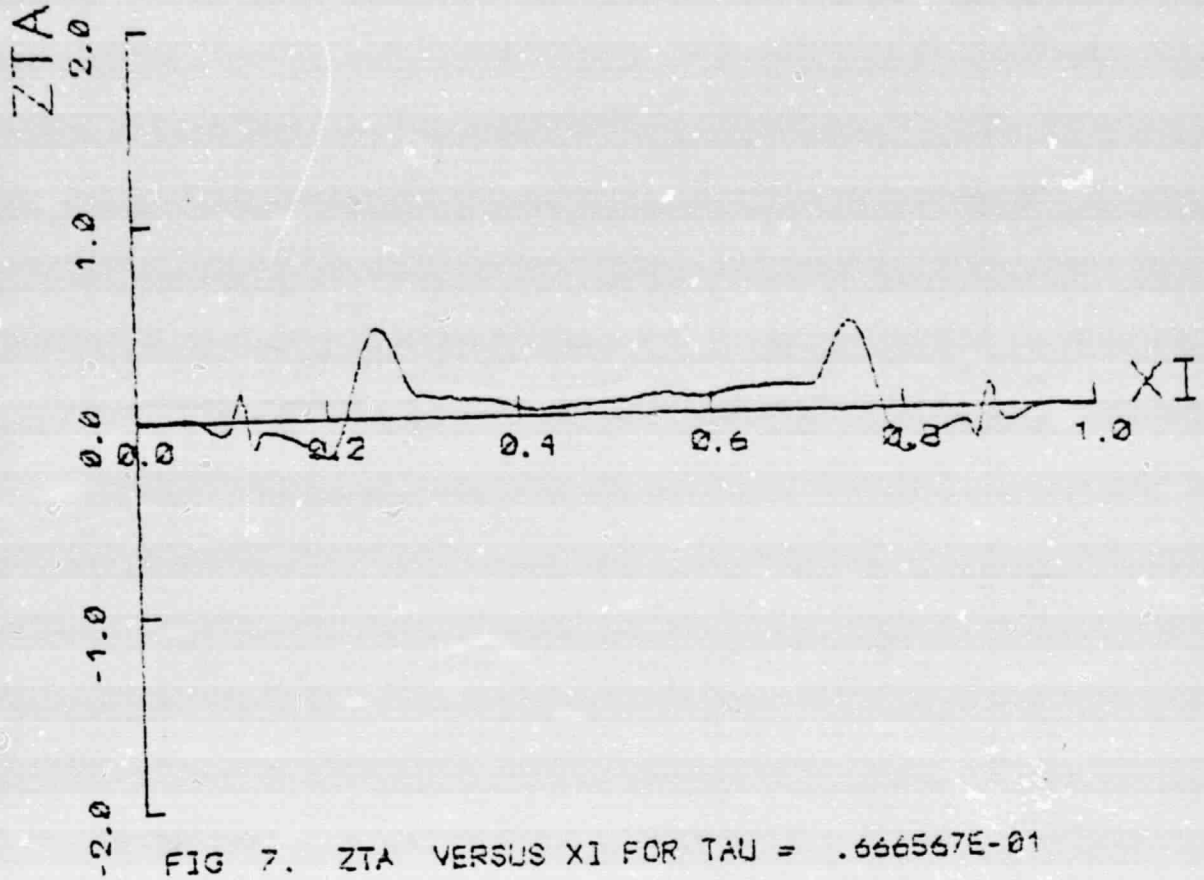

FIG 7. ZTA VERSUS XI FOR TAU = .666567E-01

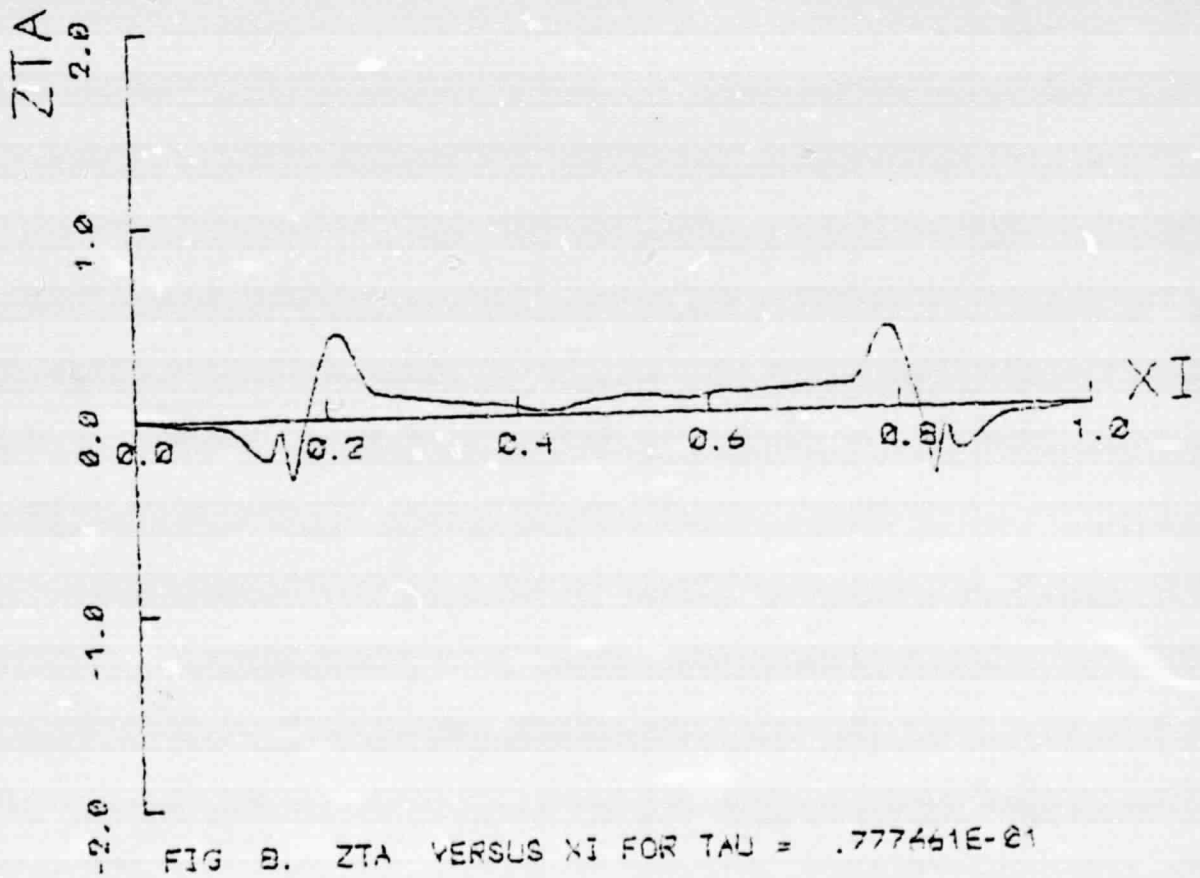

FIG 8. ZTA VERSUS XI FOR TAU = .777461E-01

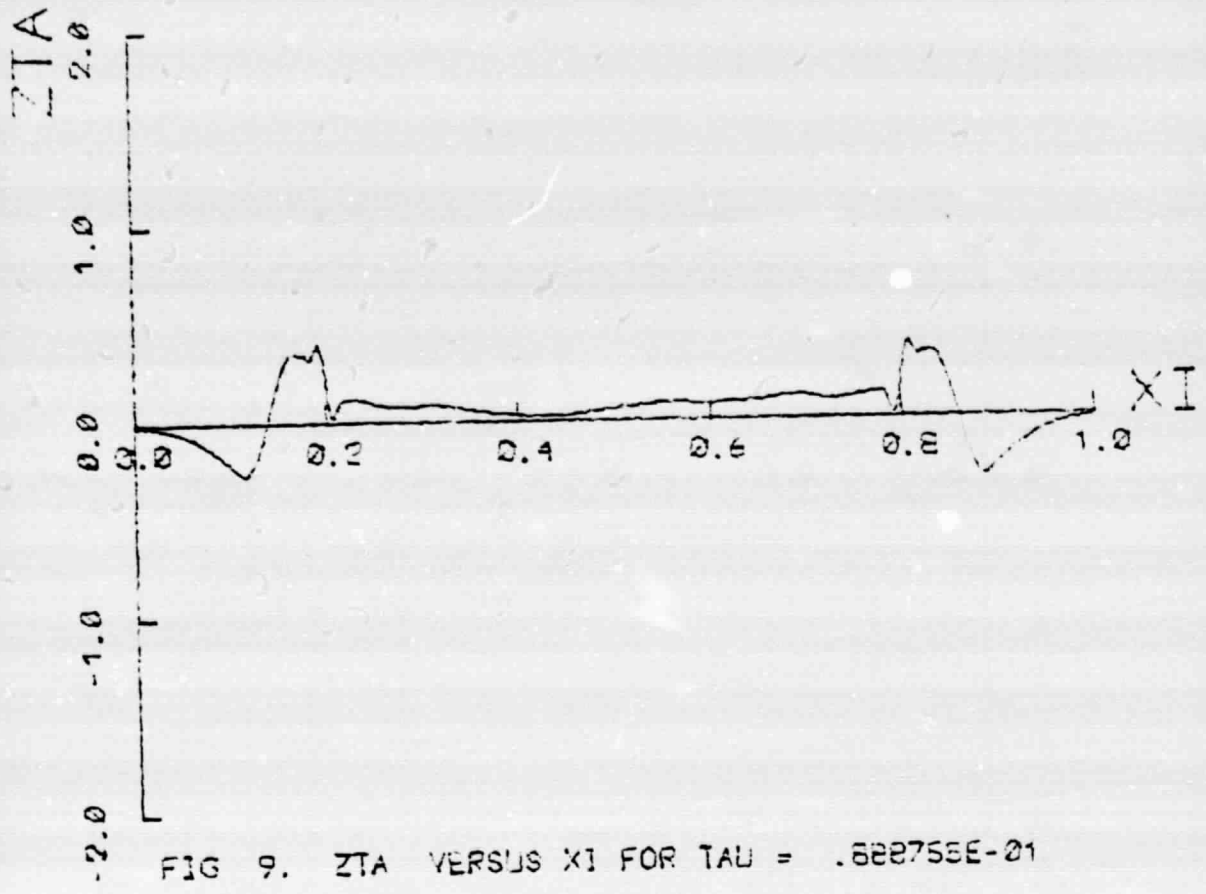

FIG 9. ZTA VERSUS XI FOR TAU = .8887588E-01

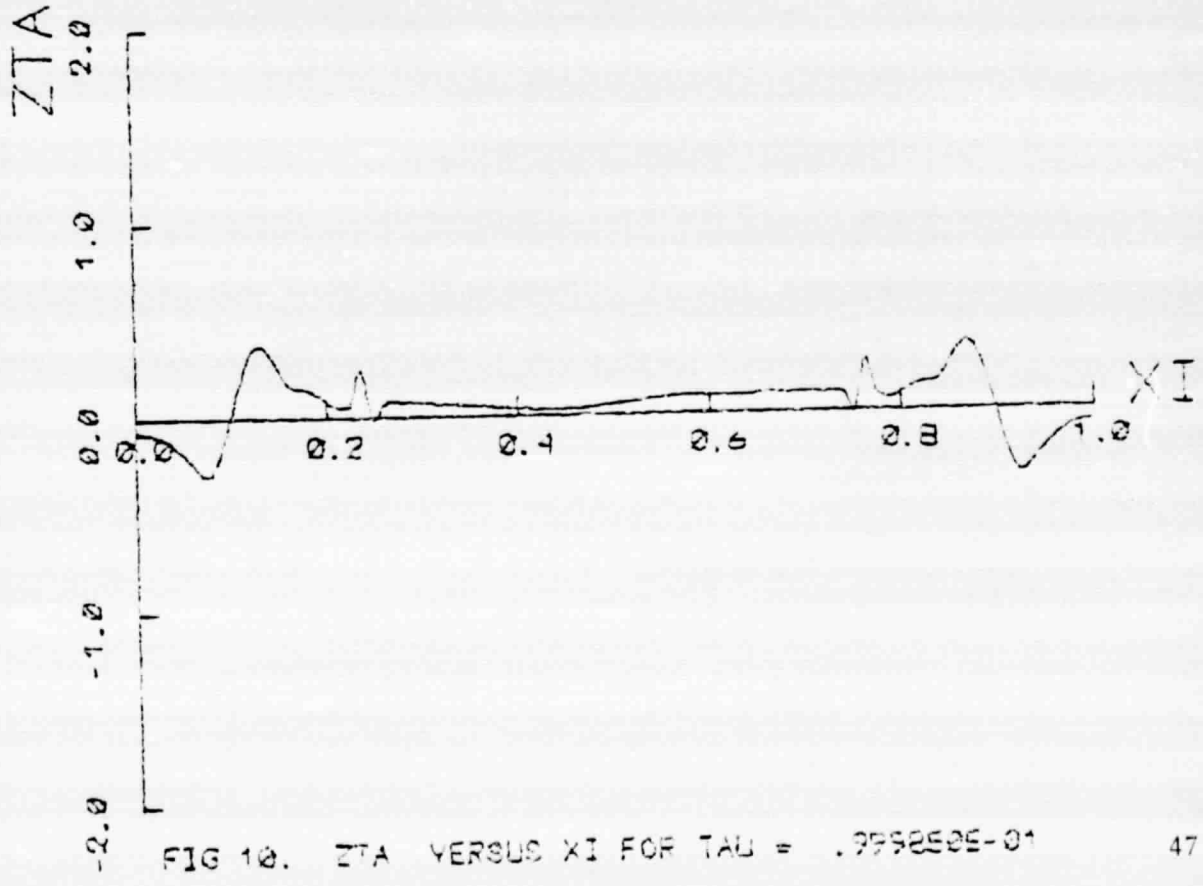

FIG 10. ZTA VERSUS XI FOR TAU = .9958588E-01

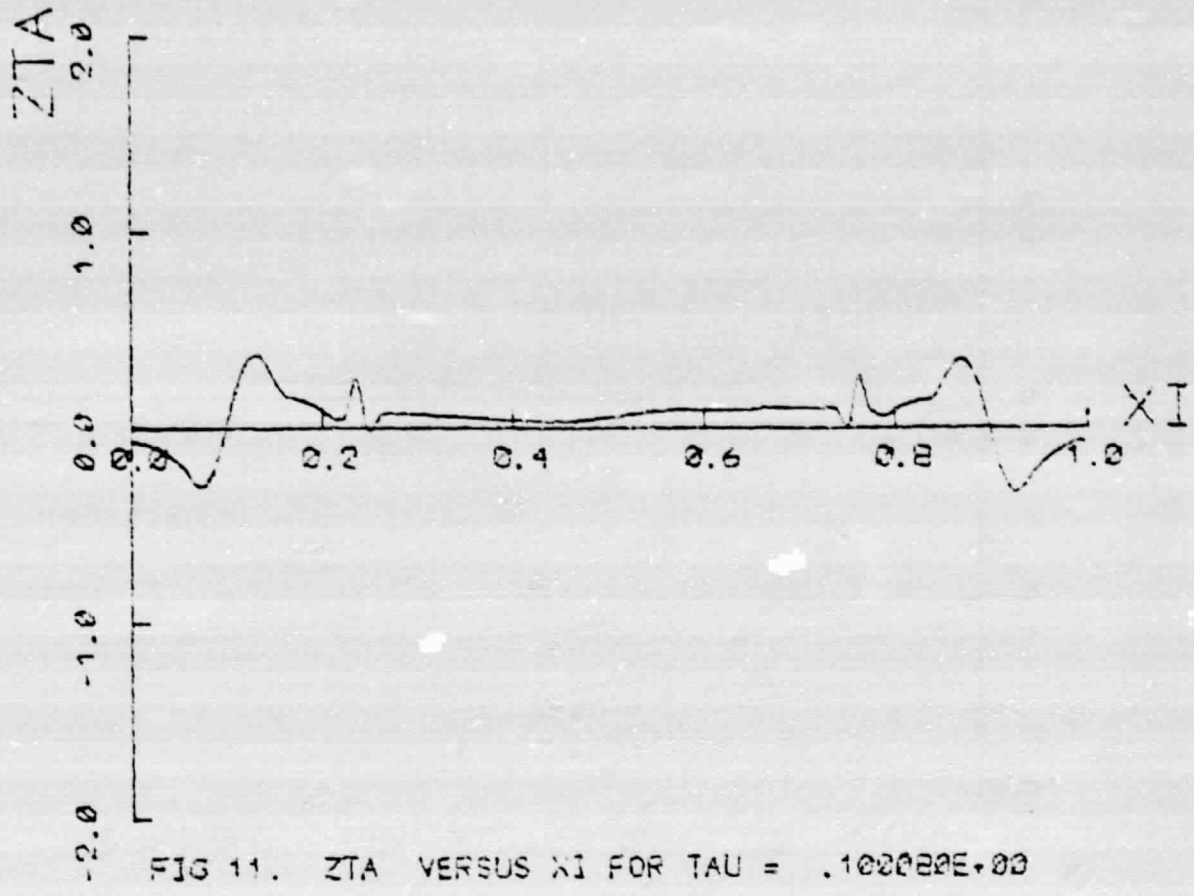

FIG 11. ZTA VERSUS XI FOR TAU = .100000E+00

APPENDIX E

Displacement response to a (1 + cos) initial disturbance;

$V_R = 0.1$, SLR = 50, $\lambda = 0.5$.

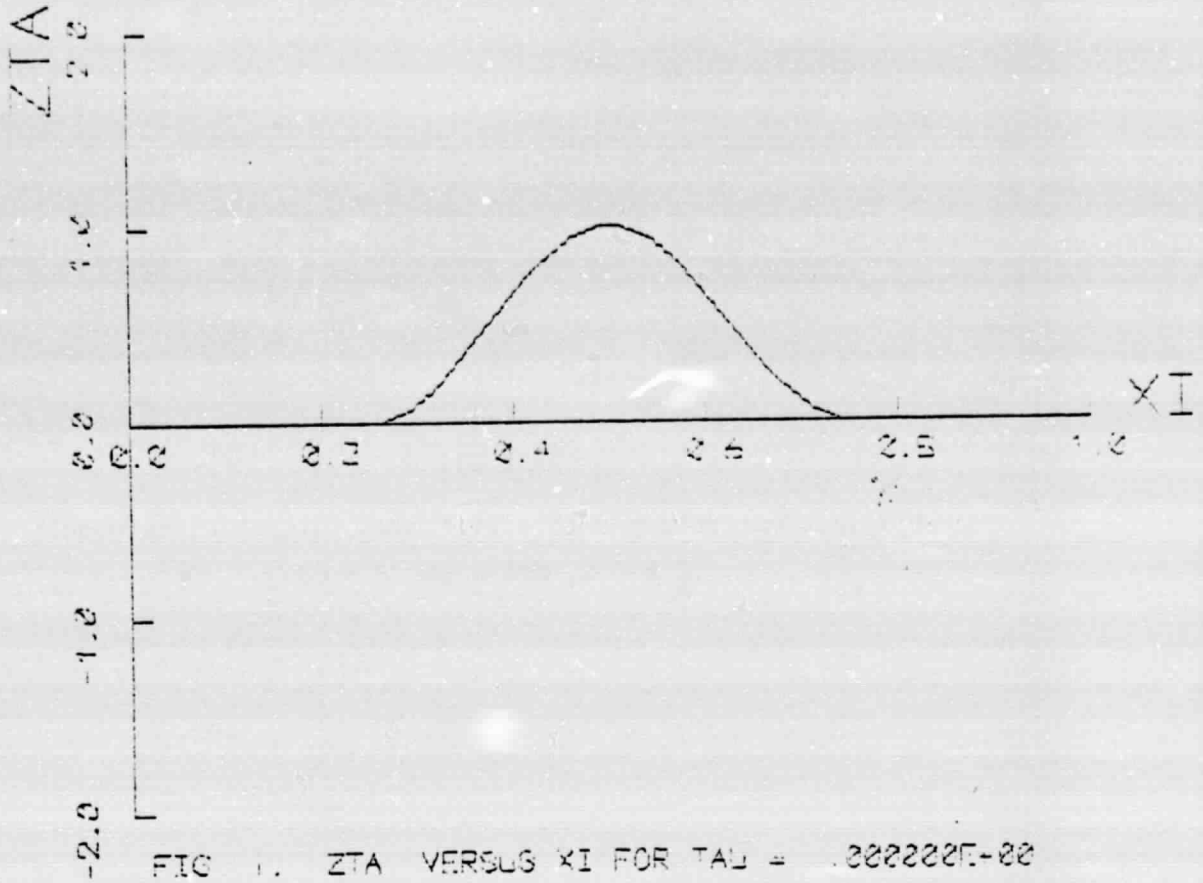

FIG 1. ZTA VERSUS XI FOR TAU = .000000E-00

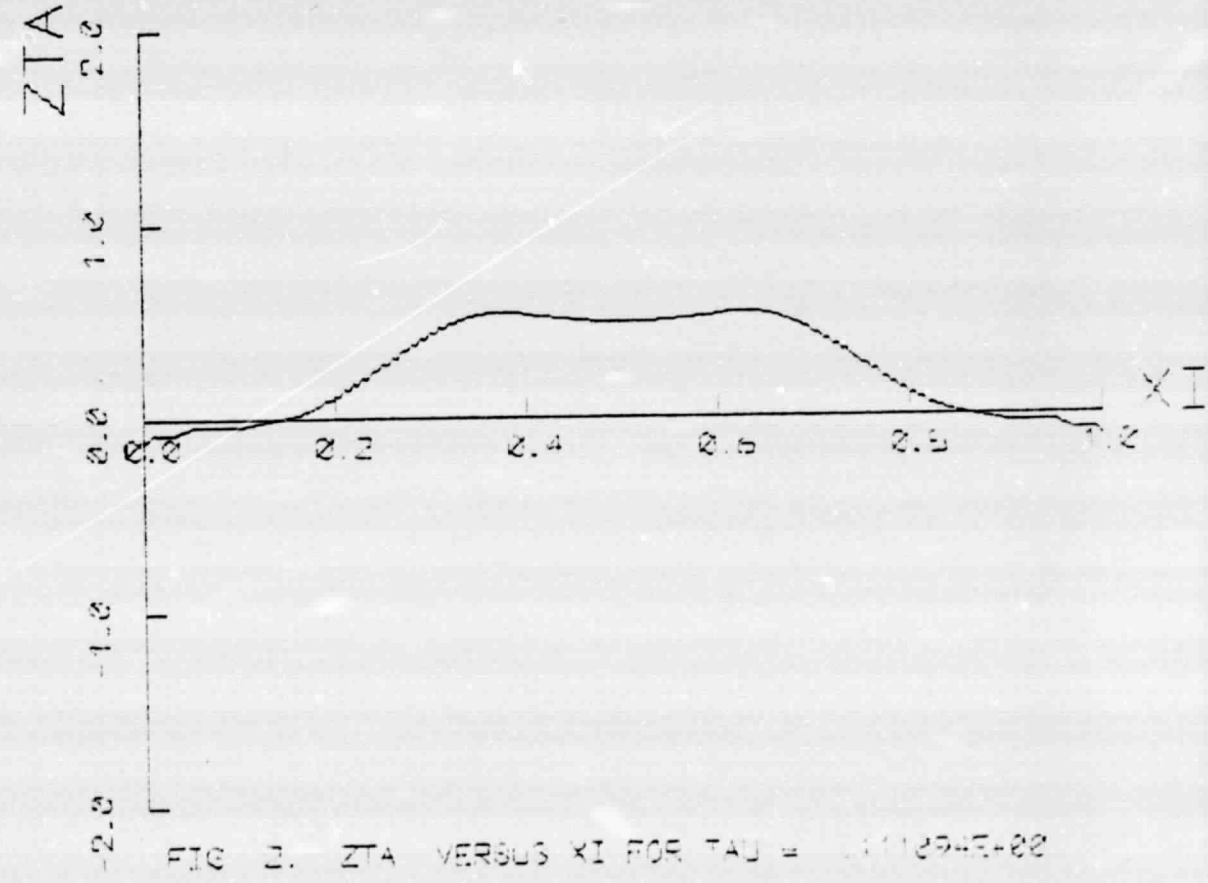

FIG 2. ZTA VERSUS XI FOR TAU = .111654E-02

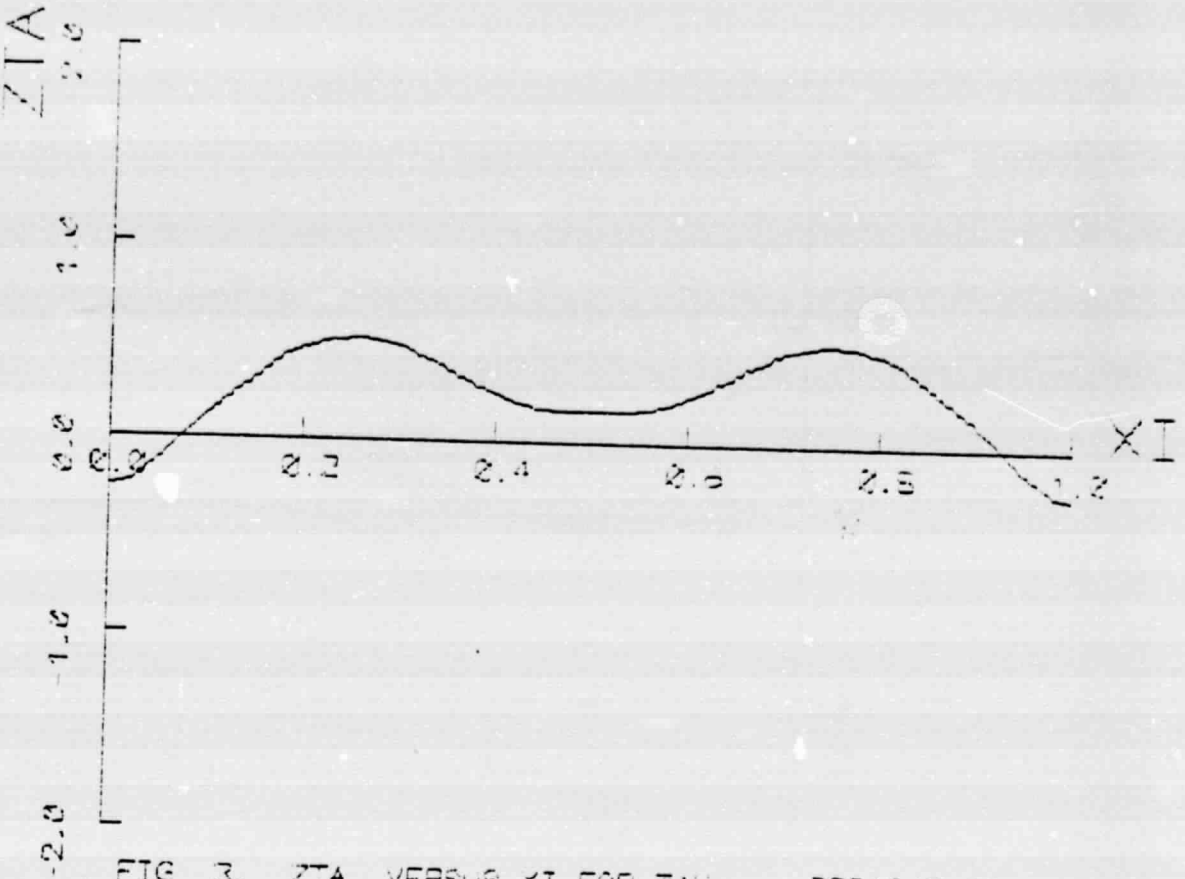

FIG 3. ZTA VERSUS XI FOR TAU = .3221B4E+00

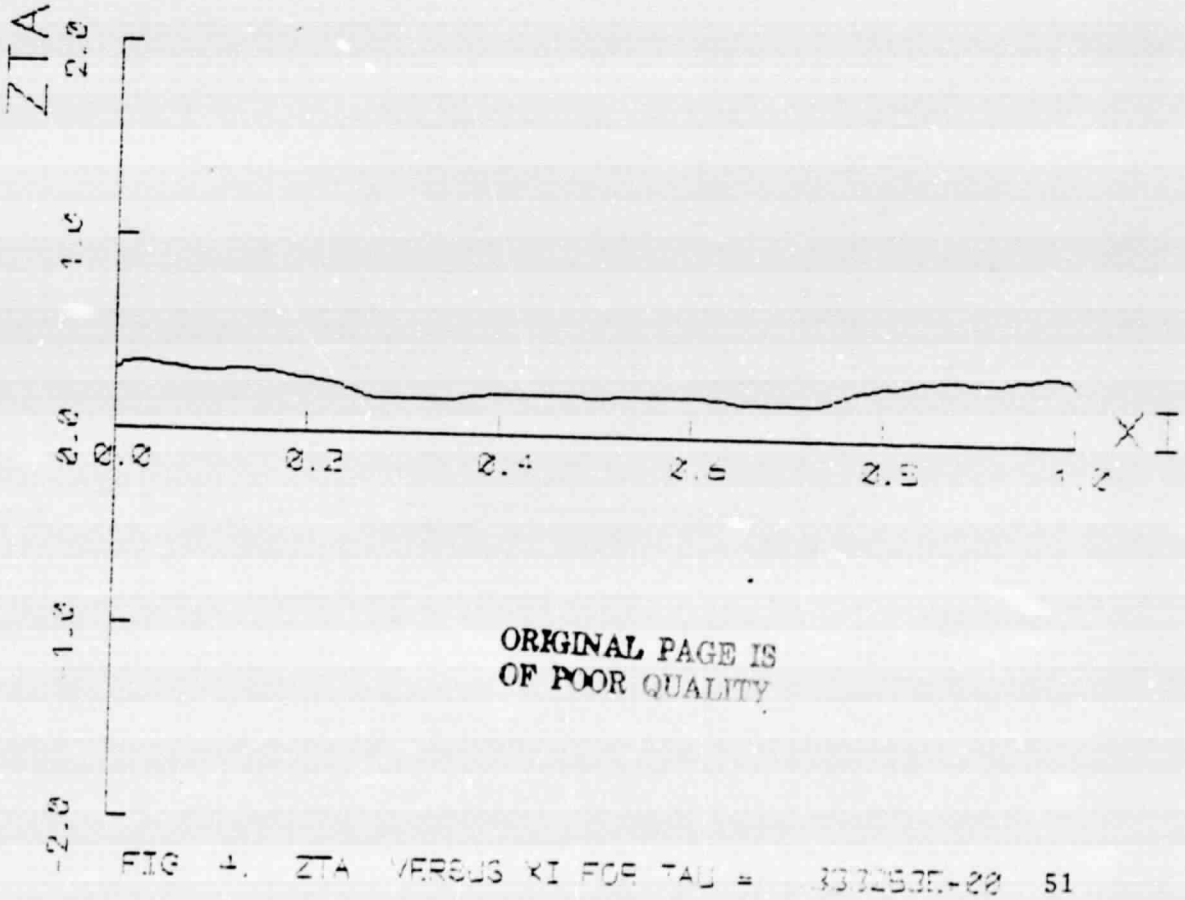

ORIGINAL PAGE IS
OF POOR QUALITY

FIG 4. ZTA VERSUS XI FOR TAU = .3312B3E-00

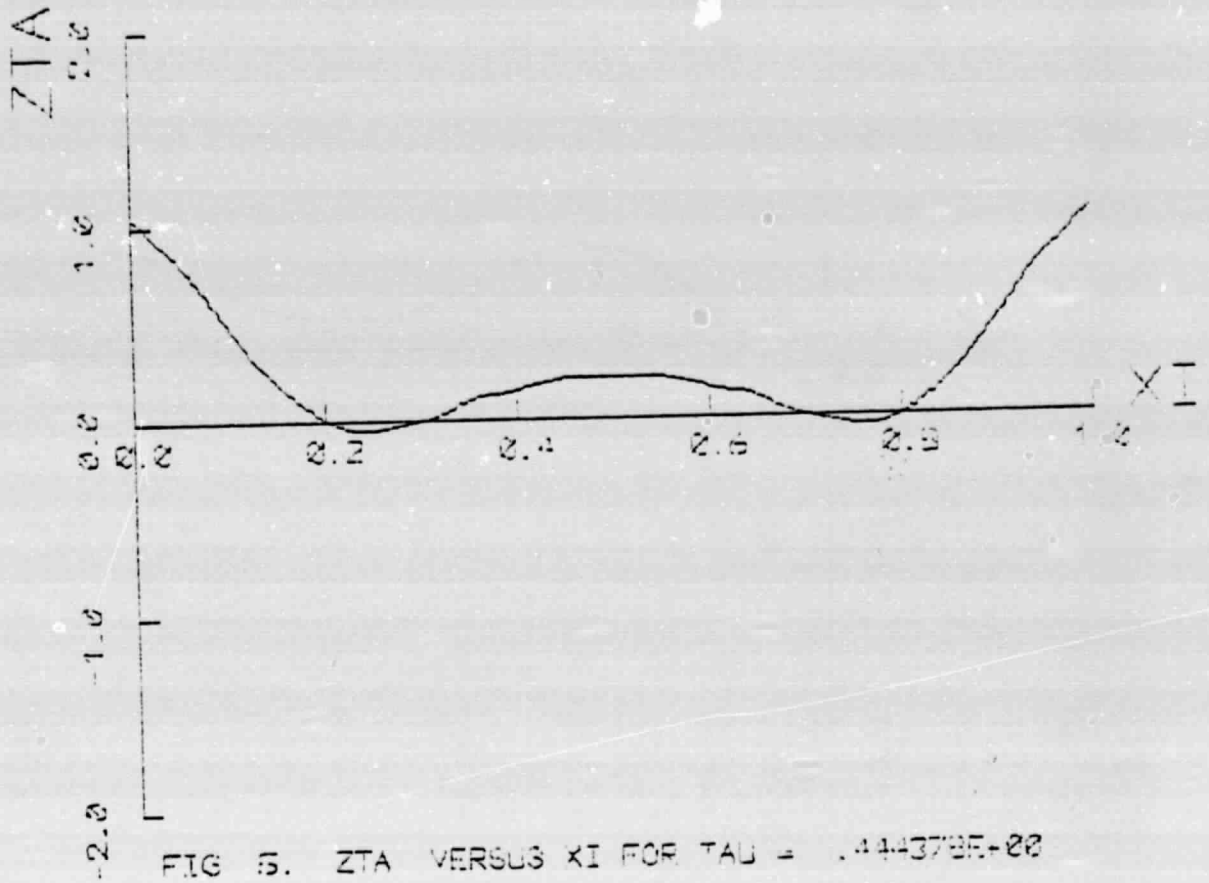

FIG 5. ZTA VERSUS XI FOR TAU = .444378E+00

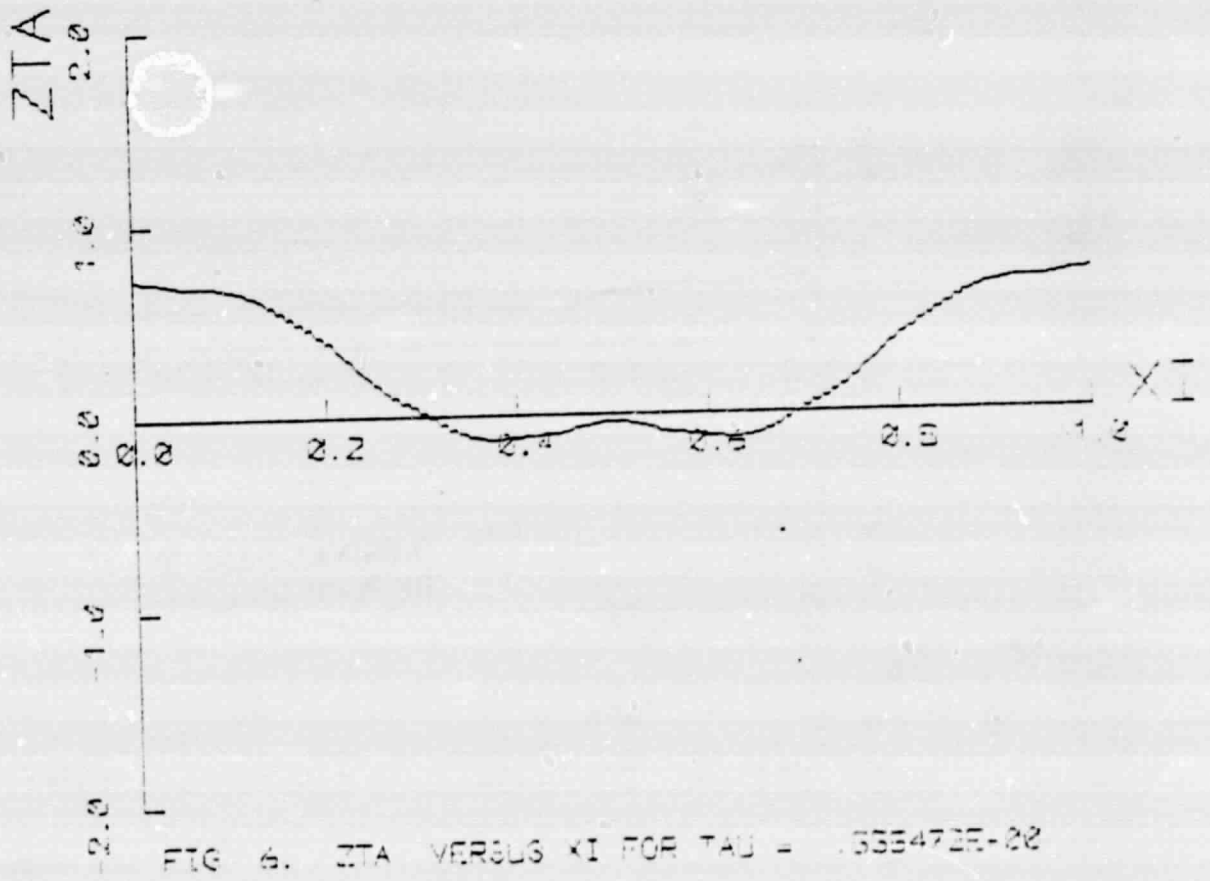

FIG 6. ZTA VERSUS XI FOR TAU = .333472E-02

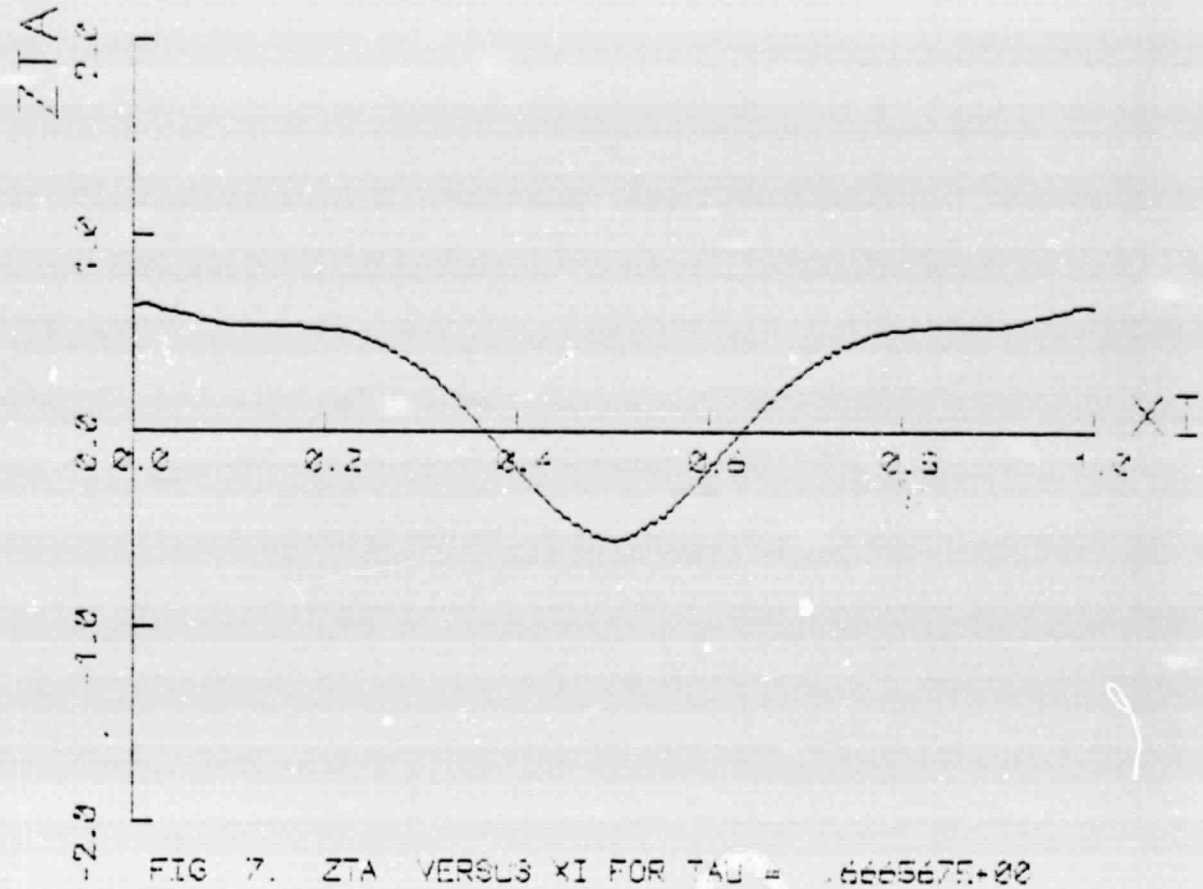

FIG 7. ZTA VERSUS XI FOR TAU = .6665675+00

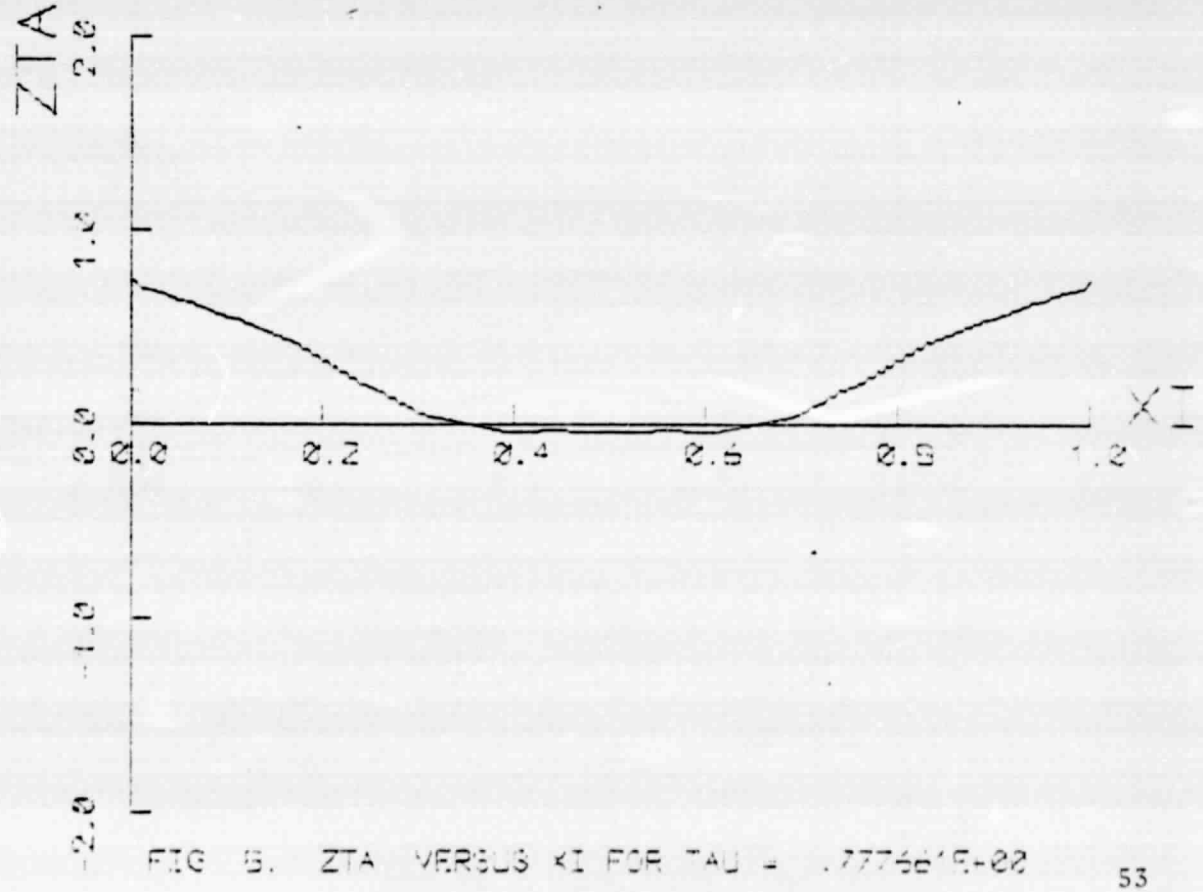

FIG 8. ZTA VERSUS XI FOR TAU = .7776615+00

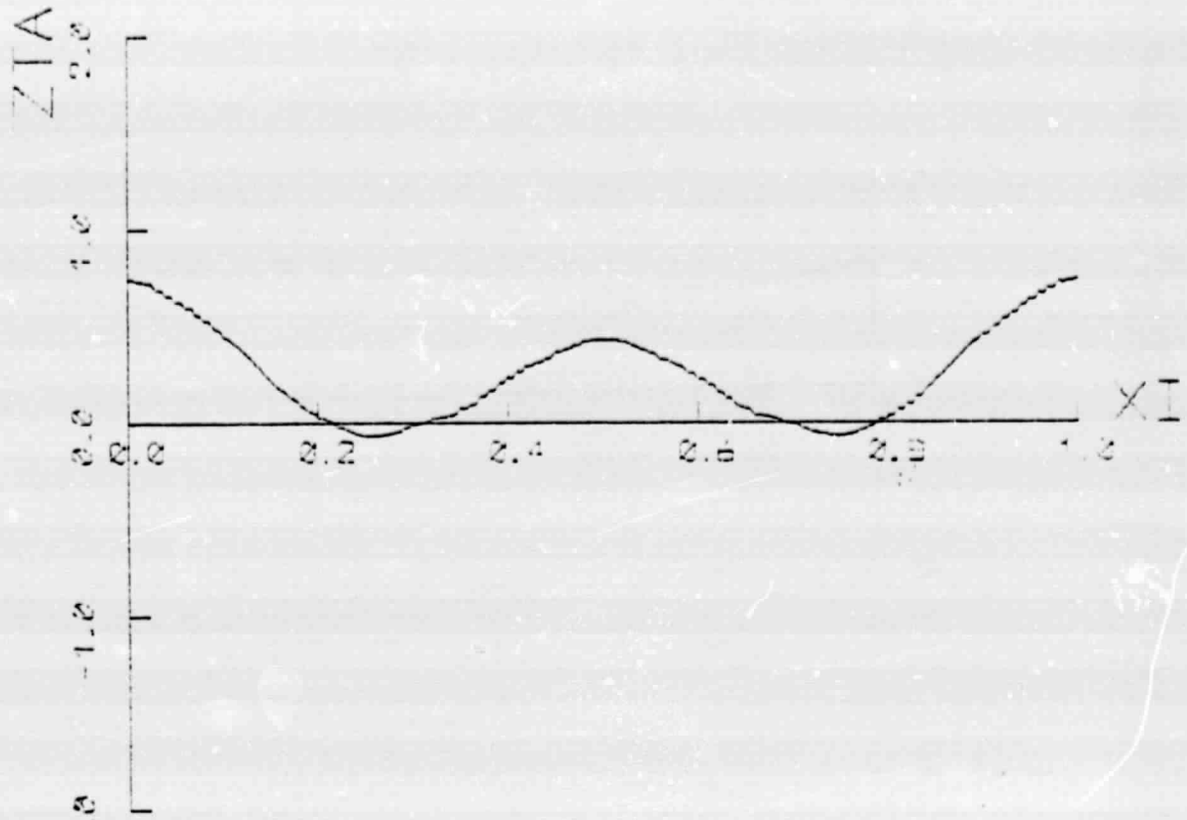

FIG 3. ZTA VERSUS XI FOR TAU = .3557655E-00

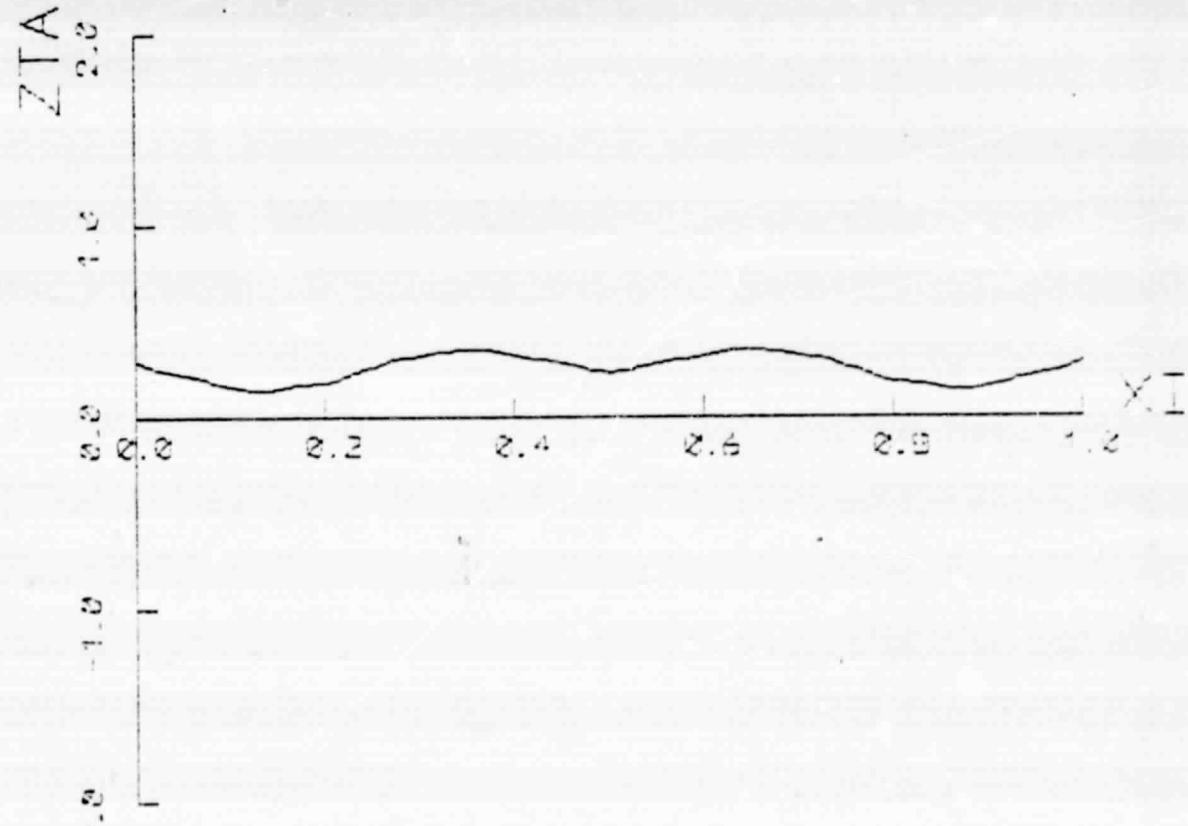

FIG 4. ZTA VERSUS XI FOR TAU = .9999502E-00

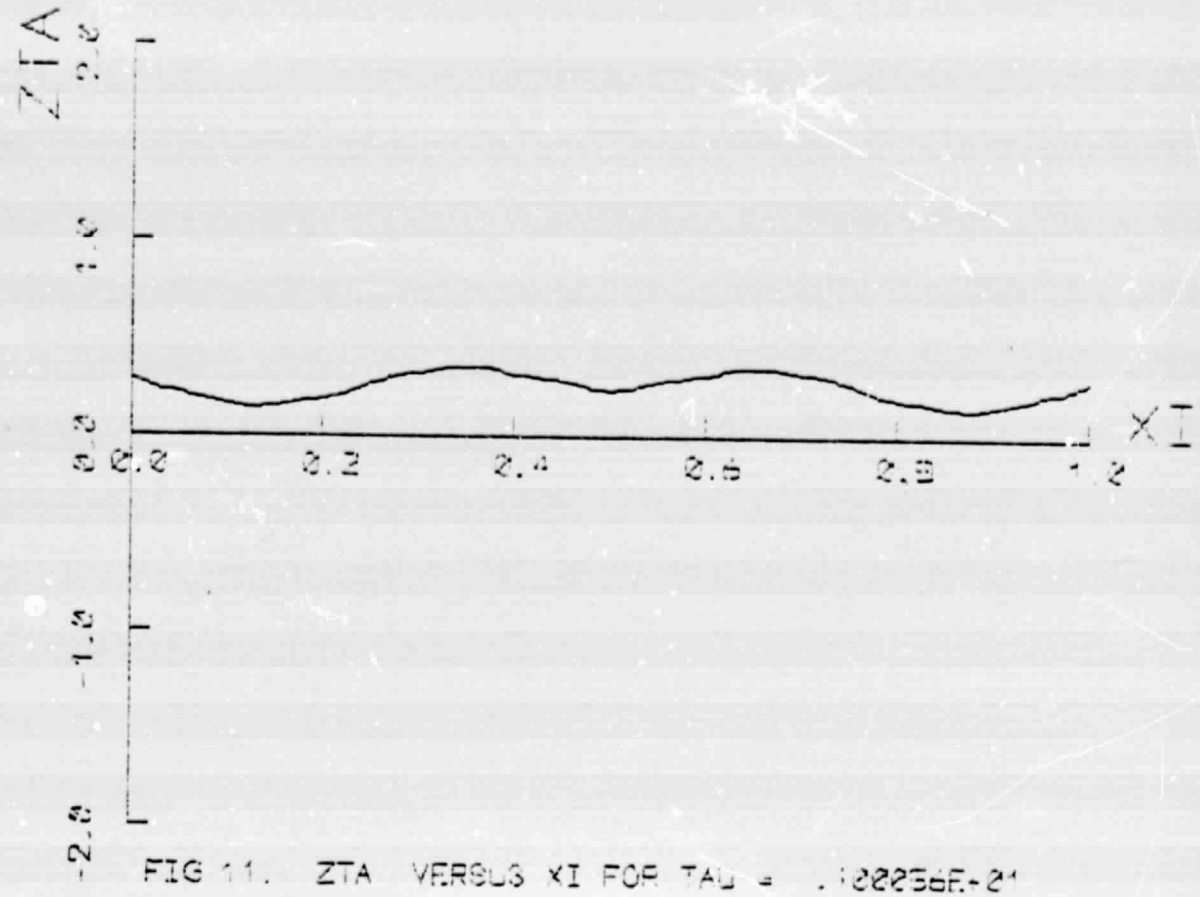

FIG 11. ZTA VERSUS XI FOR TAU = .1222E6E-21

APPENDIX F

Displacement response to a (1 + cos) initial disturbance;

$V_R = 0.1$, SLR = 50, $\lambda = 0.1$.

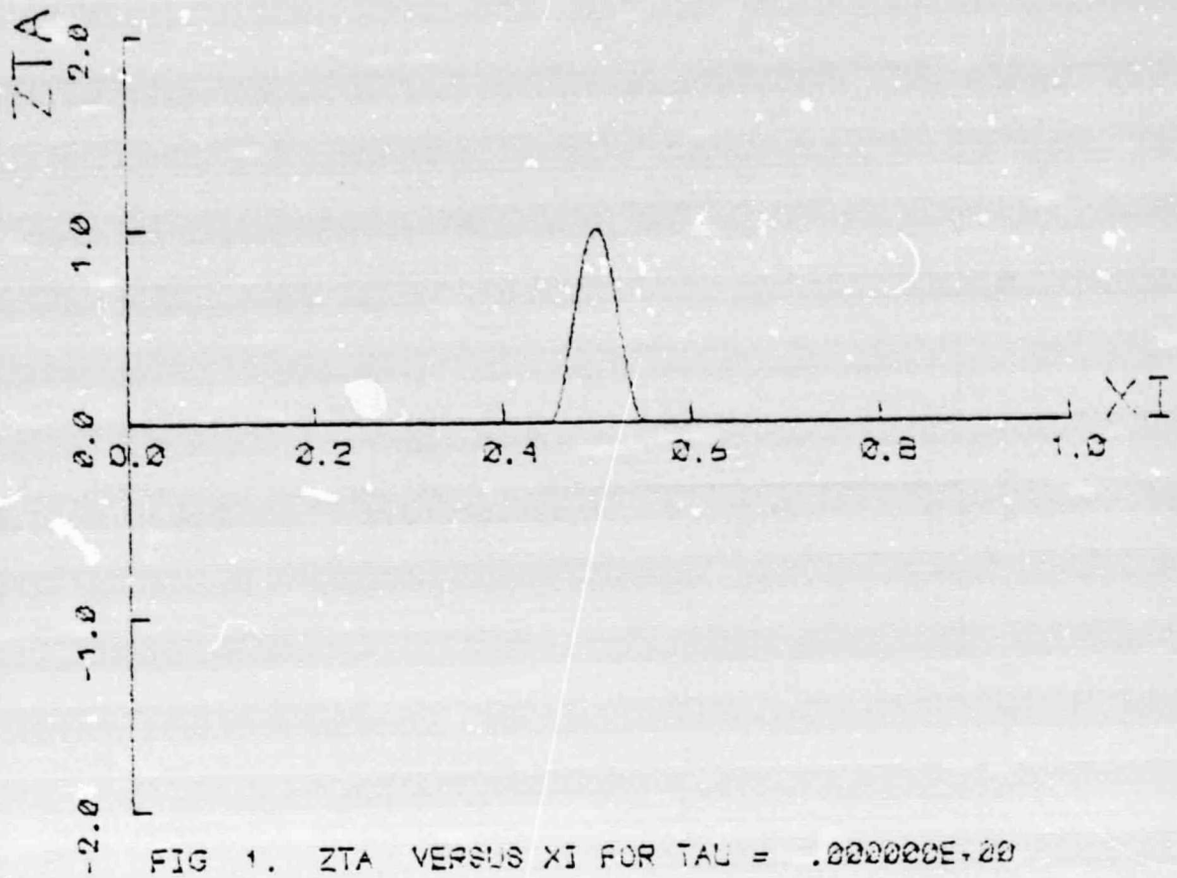

FIG 1. ZTA VERSUS XI FOR TAU = .000000E+00

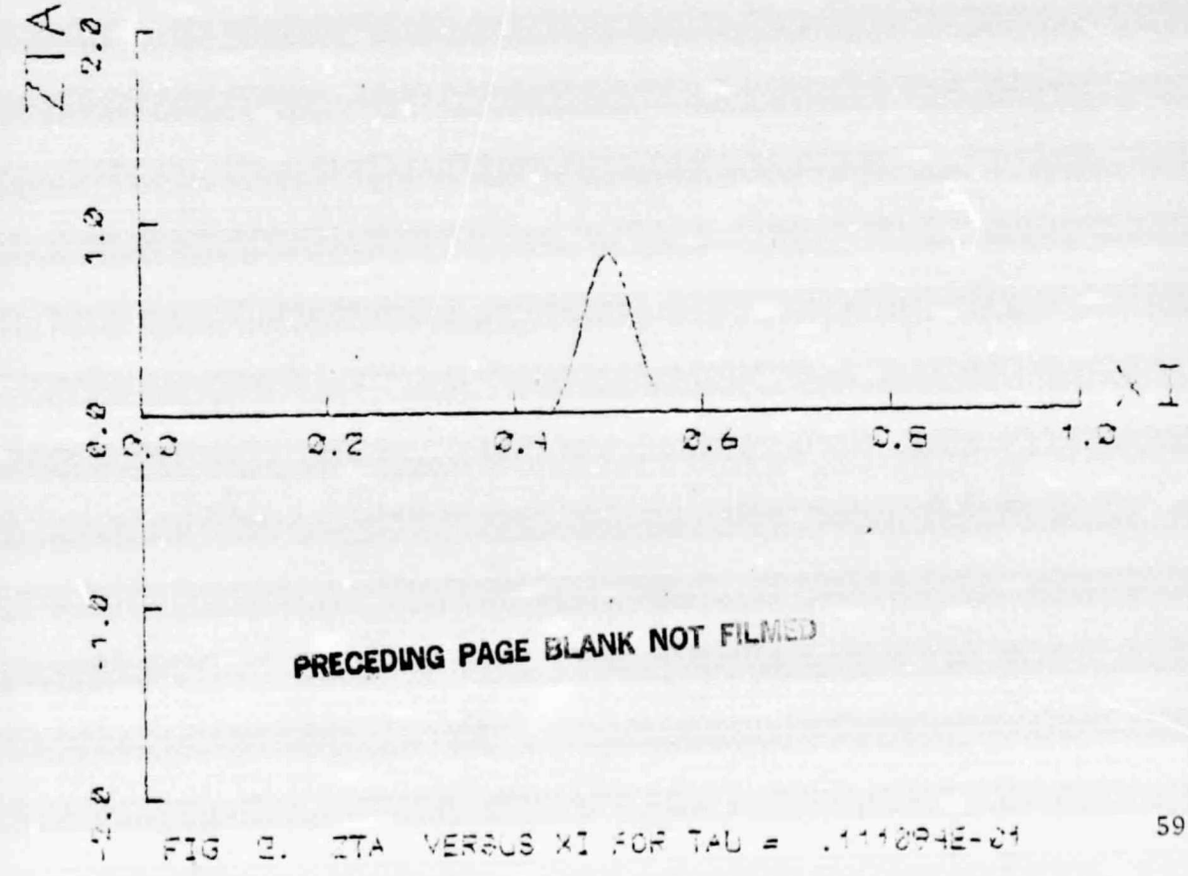

PRECEDING PAGE BLANK NOT FILMED

FIG 2. ZTA VERSUS XI FOR TAU = .111894E-01

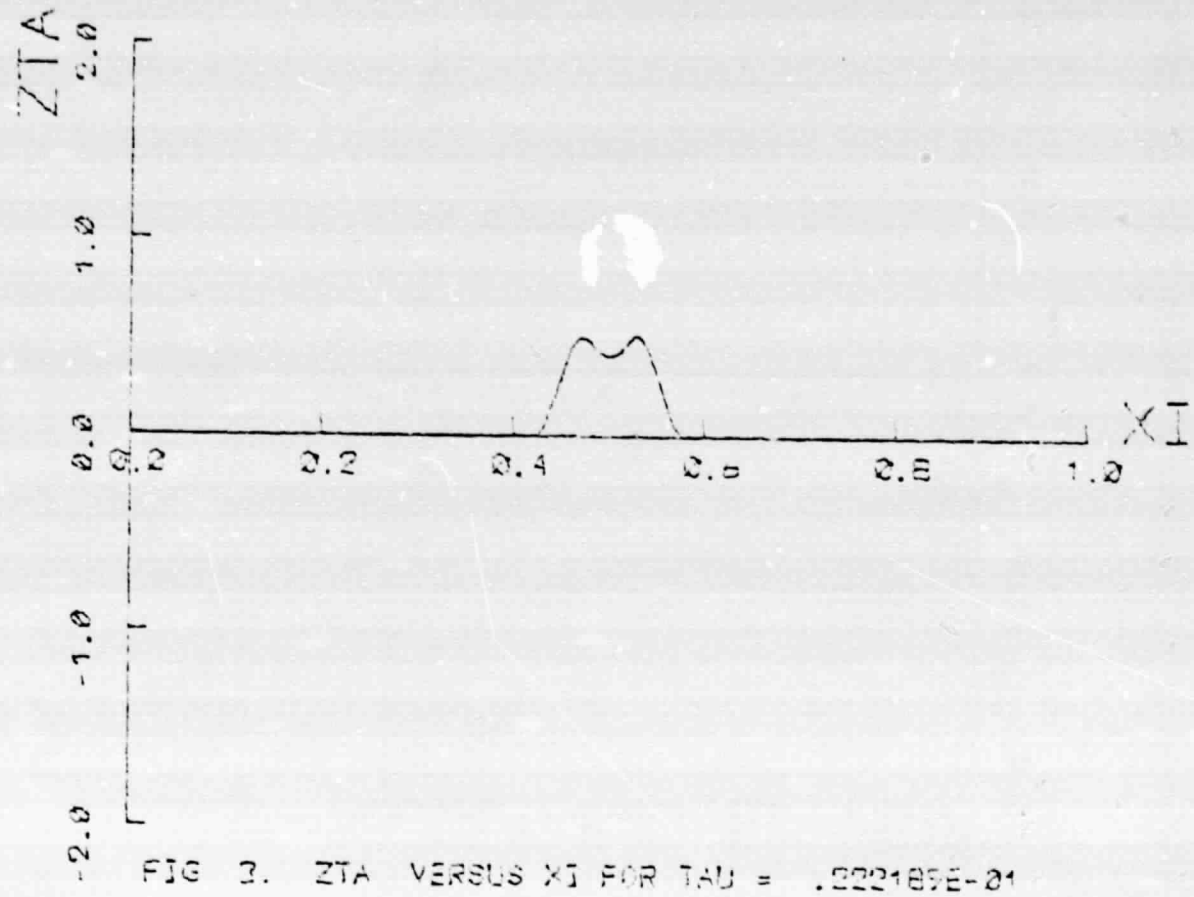

FIG 3. ZTA VERSUS XI FOR TAU = .0221859E-01

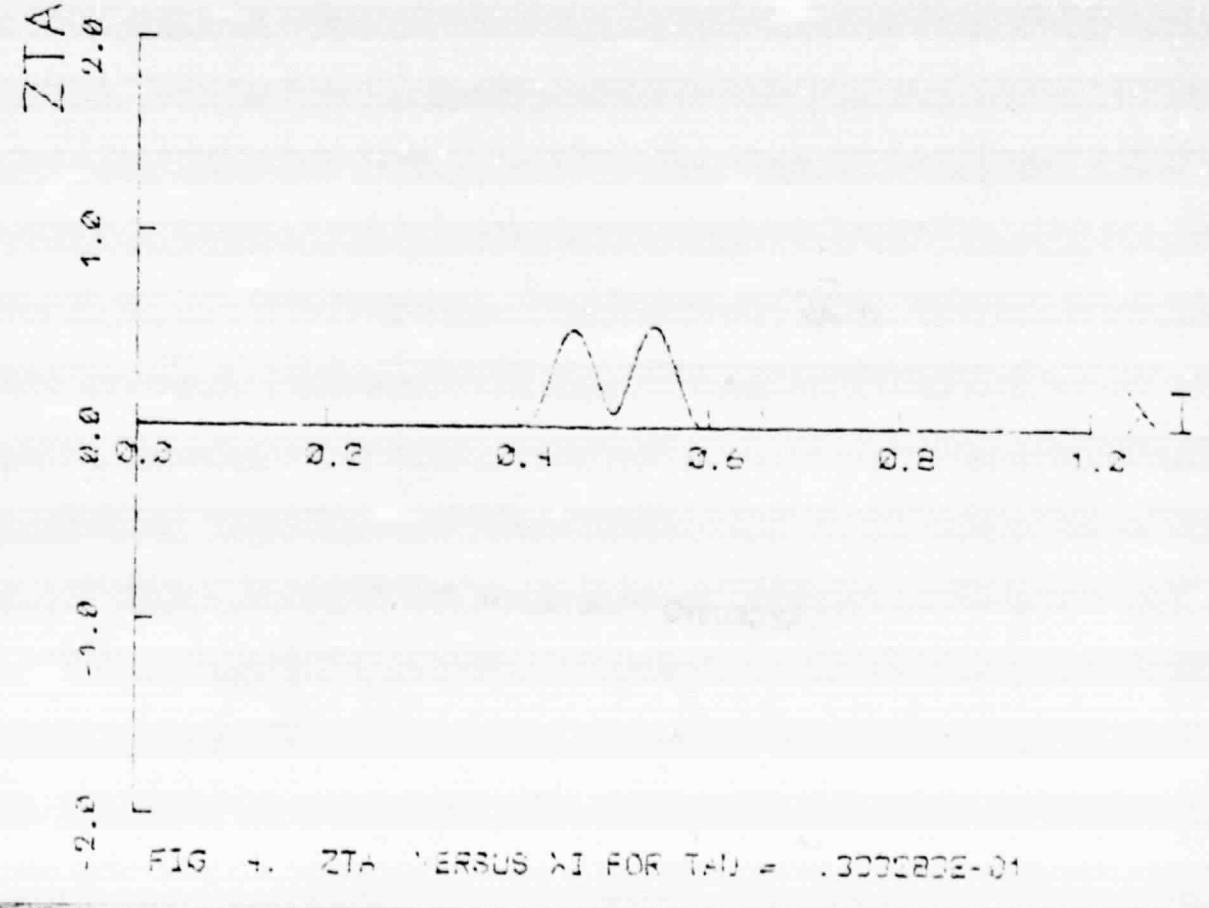

FIG 4. ZTA VERSUS XI FOR TAU = .3333333E-01

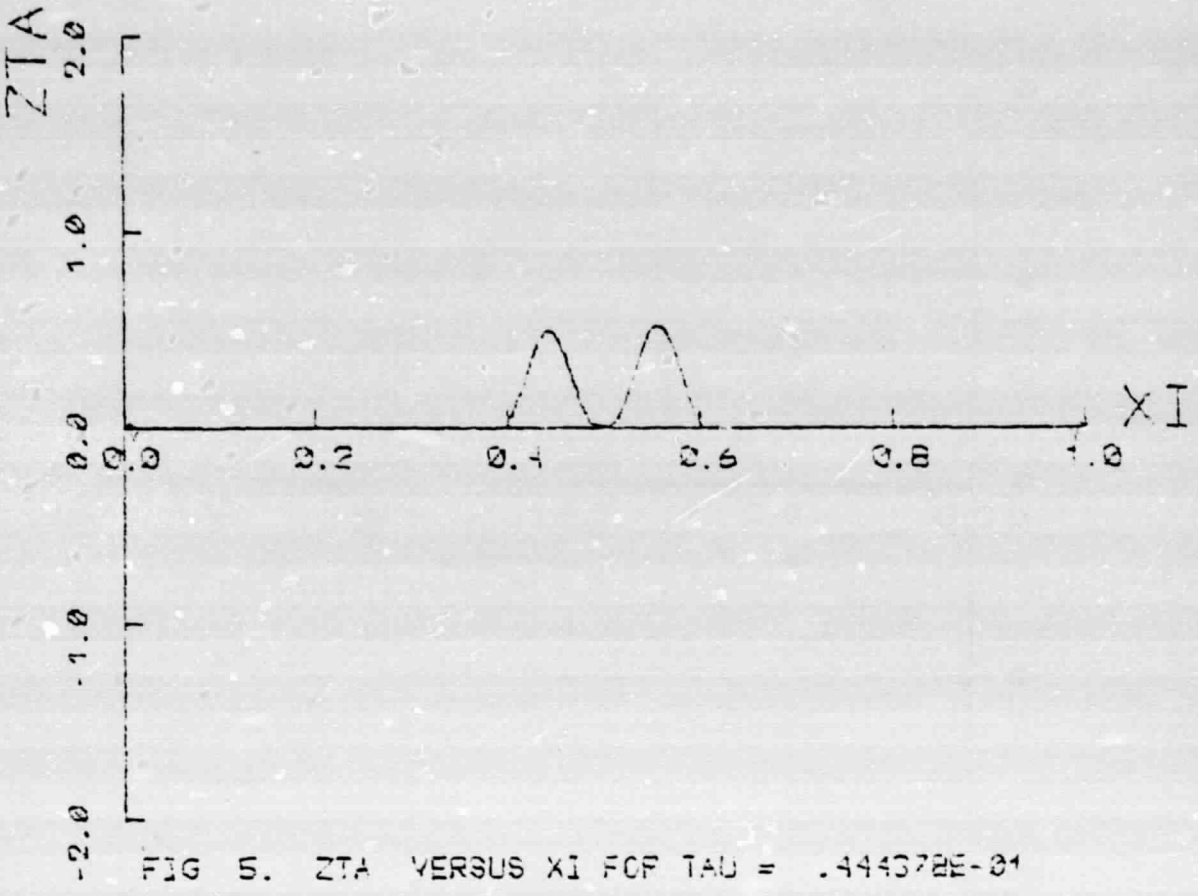

FIG 5. ZTA VERSUS XI FOR TAU = .444372E-01

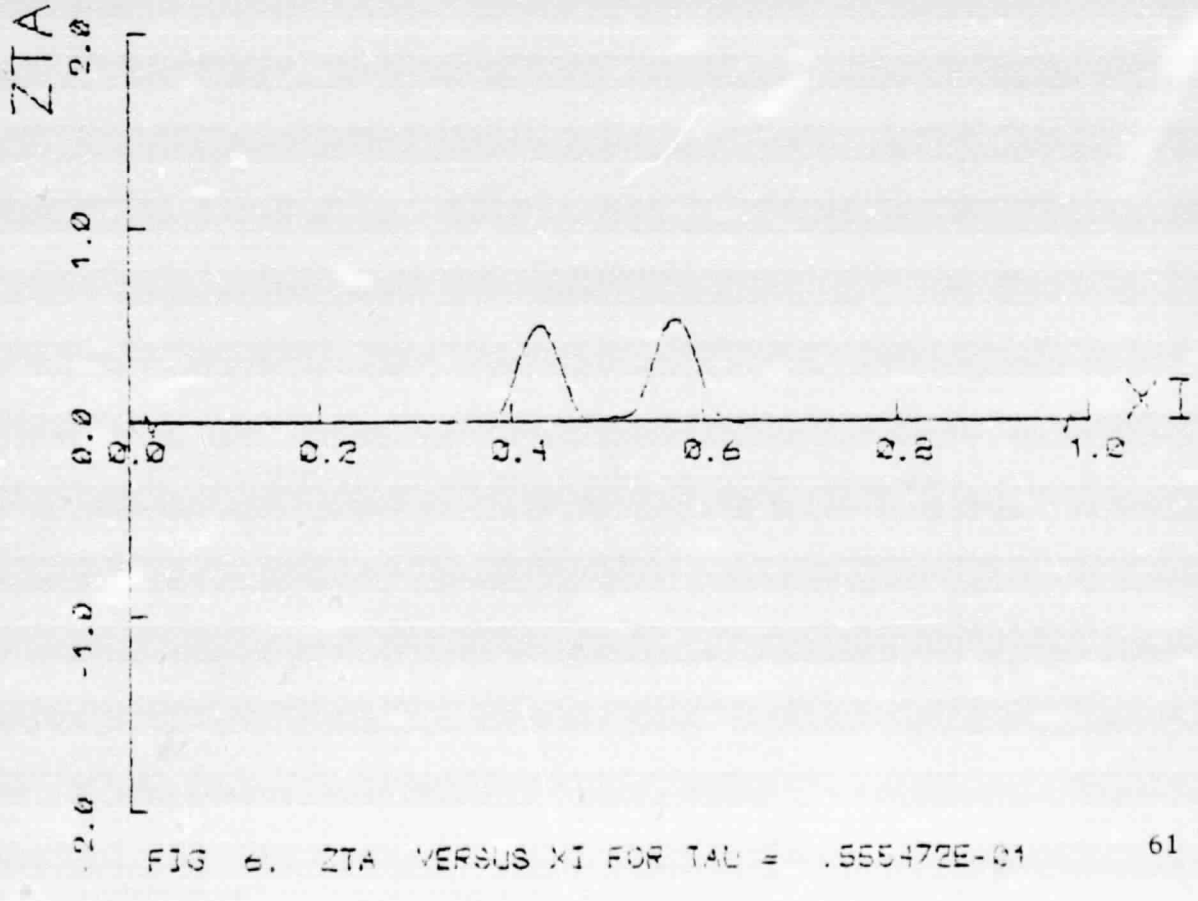

FIG 6. ZTA VERSUS XI FOR TAU = .555472E-01

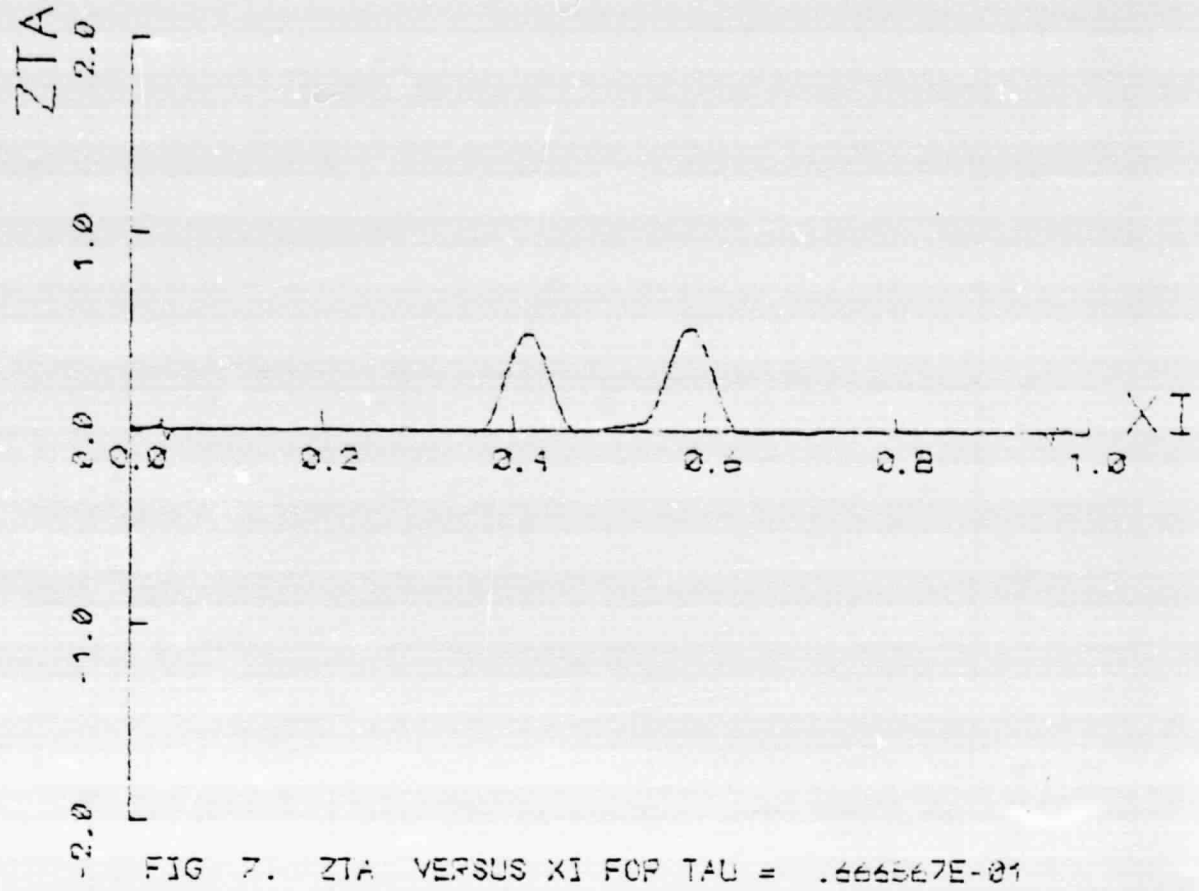

FIG 7. ZTA VERSUS XI FOR TAU = .6665E7E-01

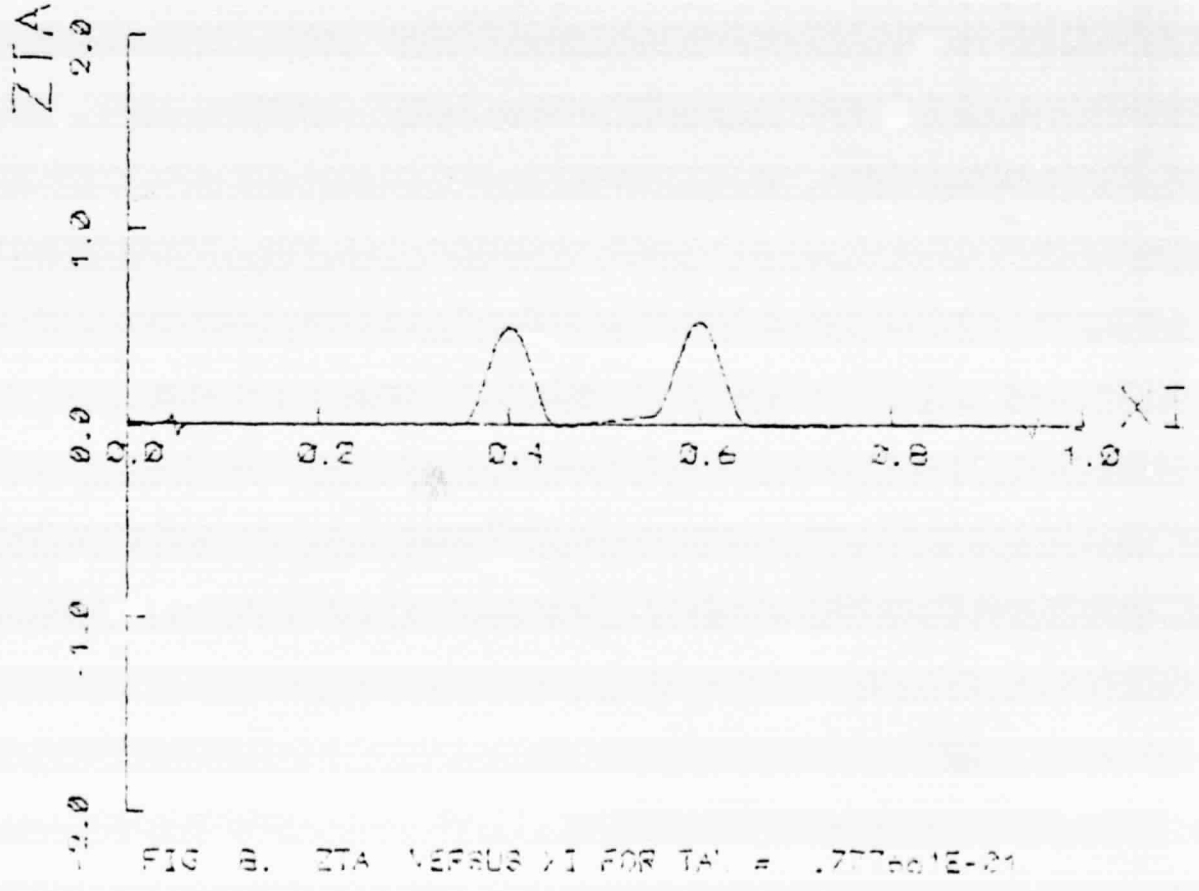

FIG 8. ZTA VERSUS XI FOR TAU = .7776E-01

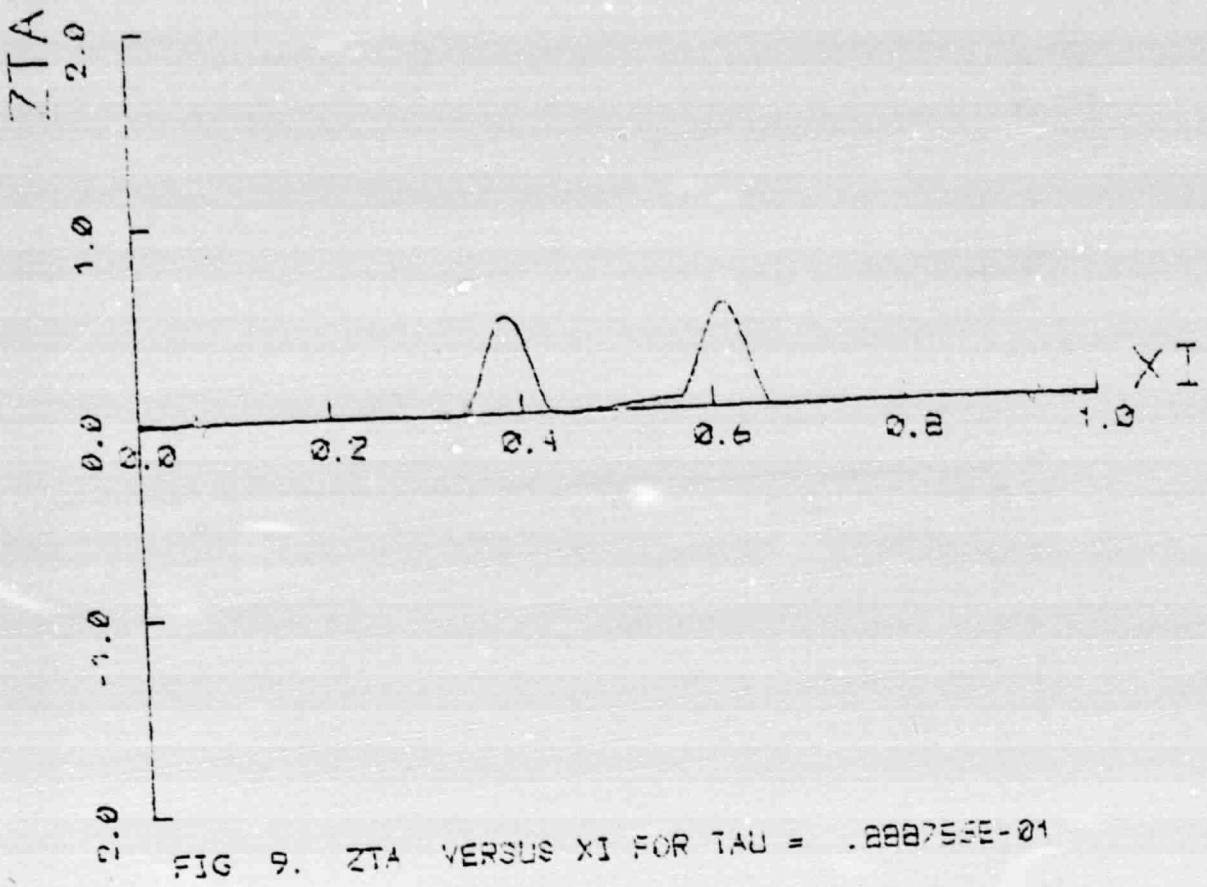

FIG 9. ZTA VERSUS XI FOR TAU = .8887555E-01

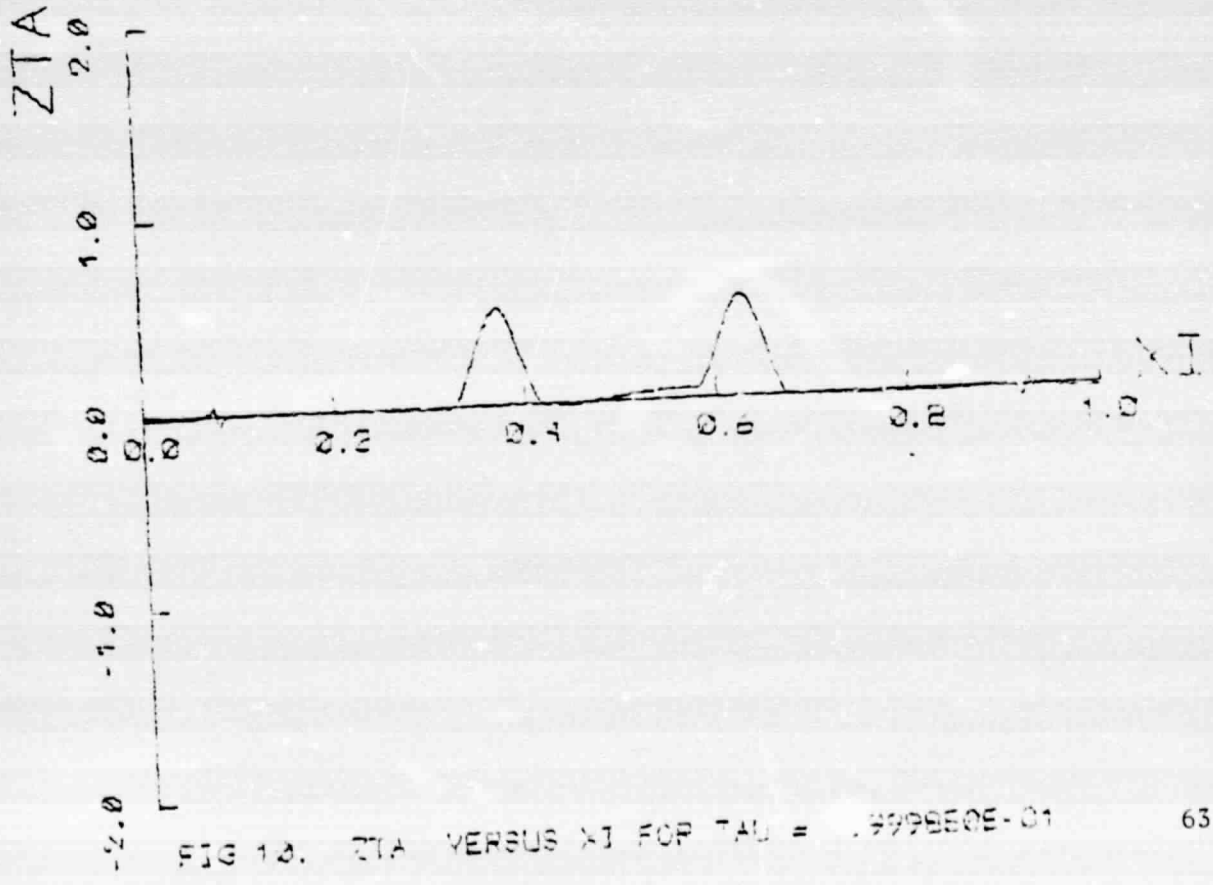

FIG 10. ZTA VERSUS XI FOR TAU = .9995605E-01

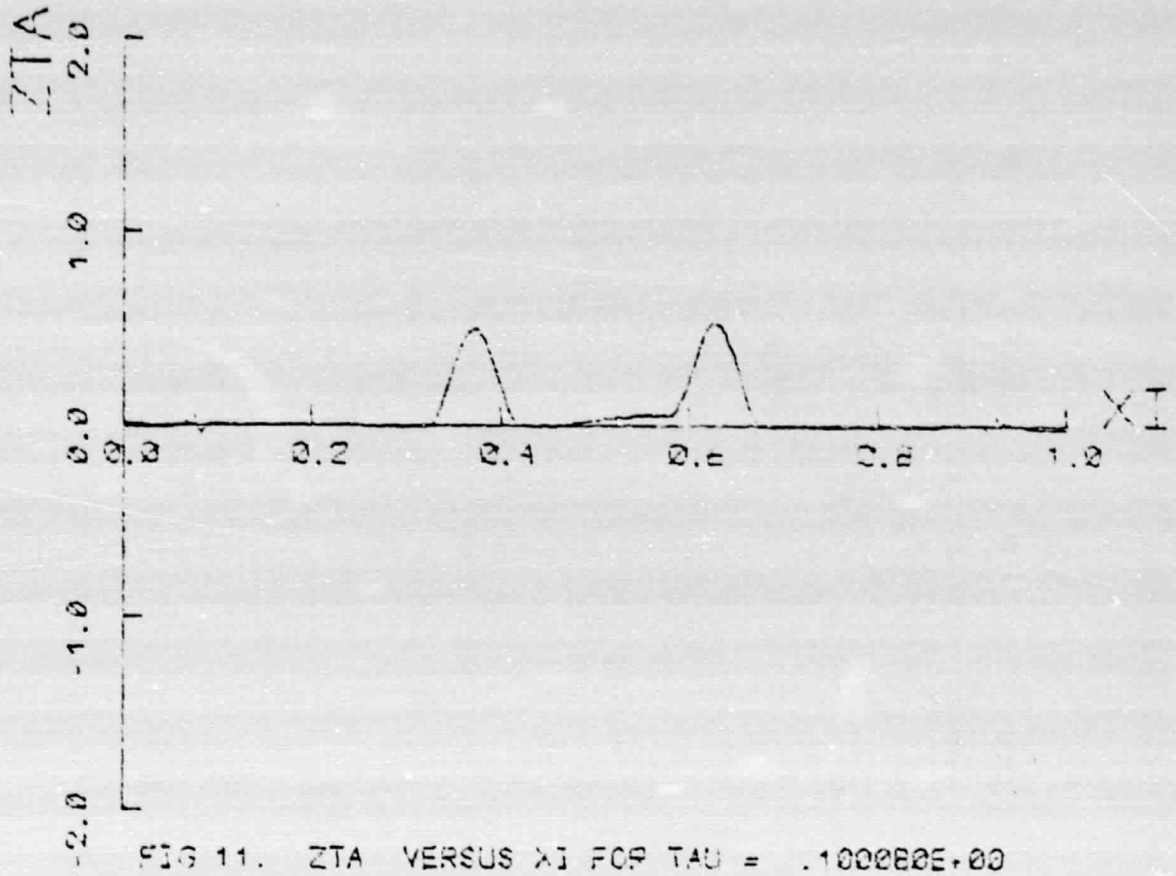

FIG 11. ZTA VERSUS XI FOR TAU = .100000E+00

APPENDIX G

Response to a (1 + cos) initial displacement;
$V_R = 0.62$, SLR = 50, $\lambda = 0.2$, $\overline{b}_1 = 0.0$, $\overline{b}_2 = 0.0$.

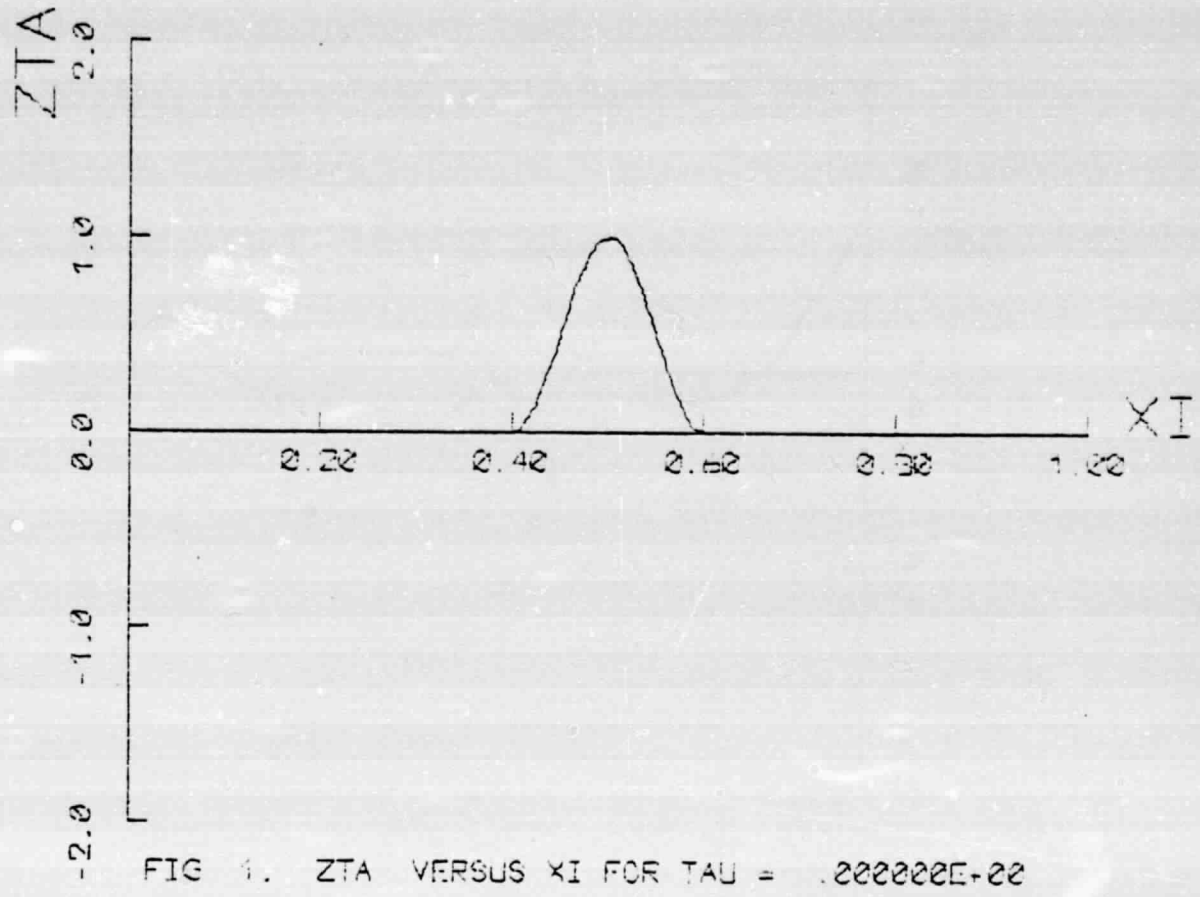

FIG 1. ZTA VERSUS XI FOR TAU = .000000E+00

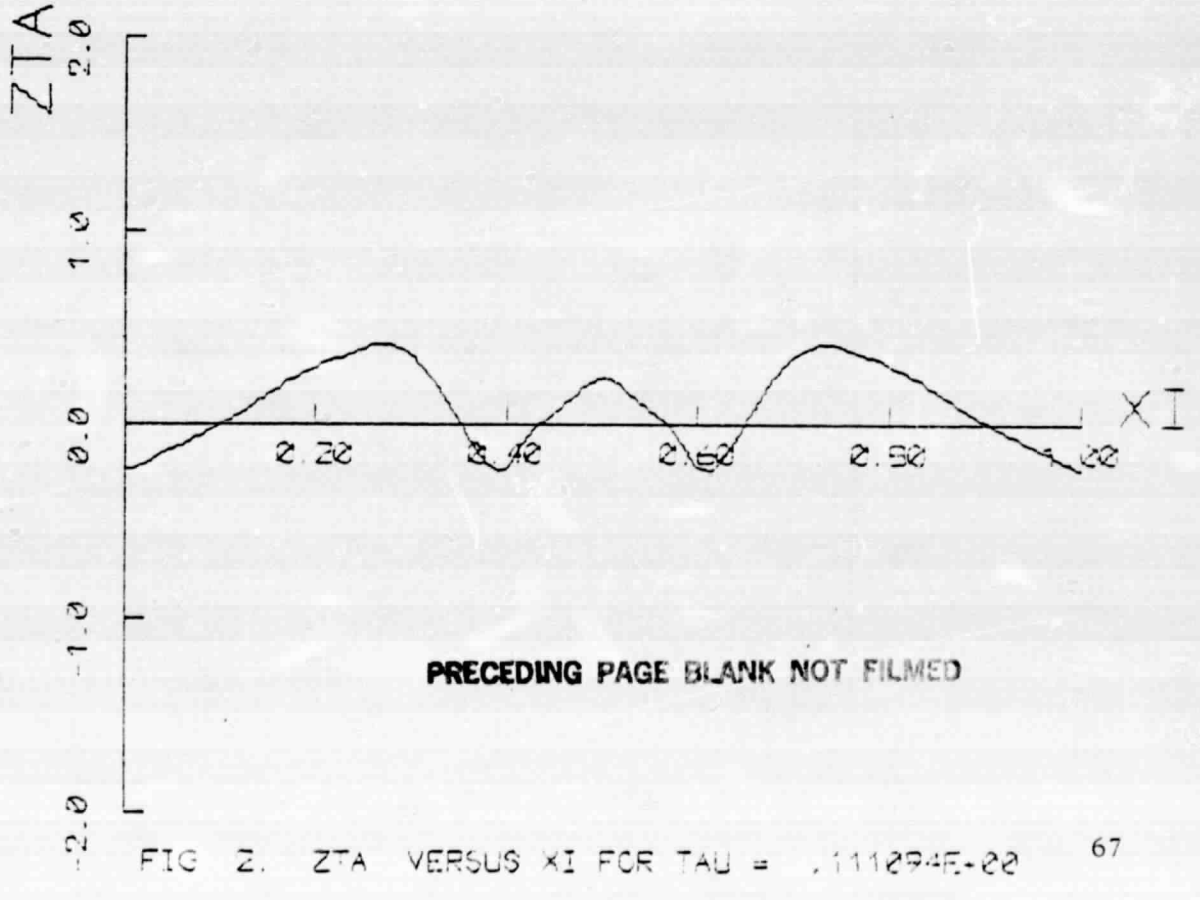

FIG 2. ZTA VERSUS XI FOR TAU = .111284E-02

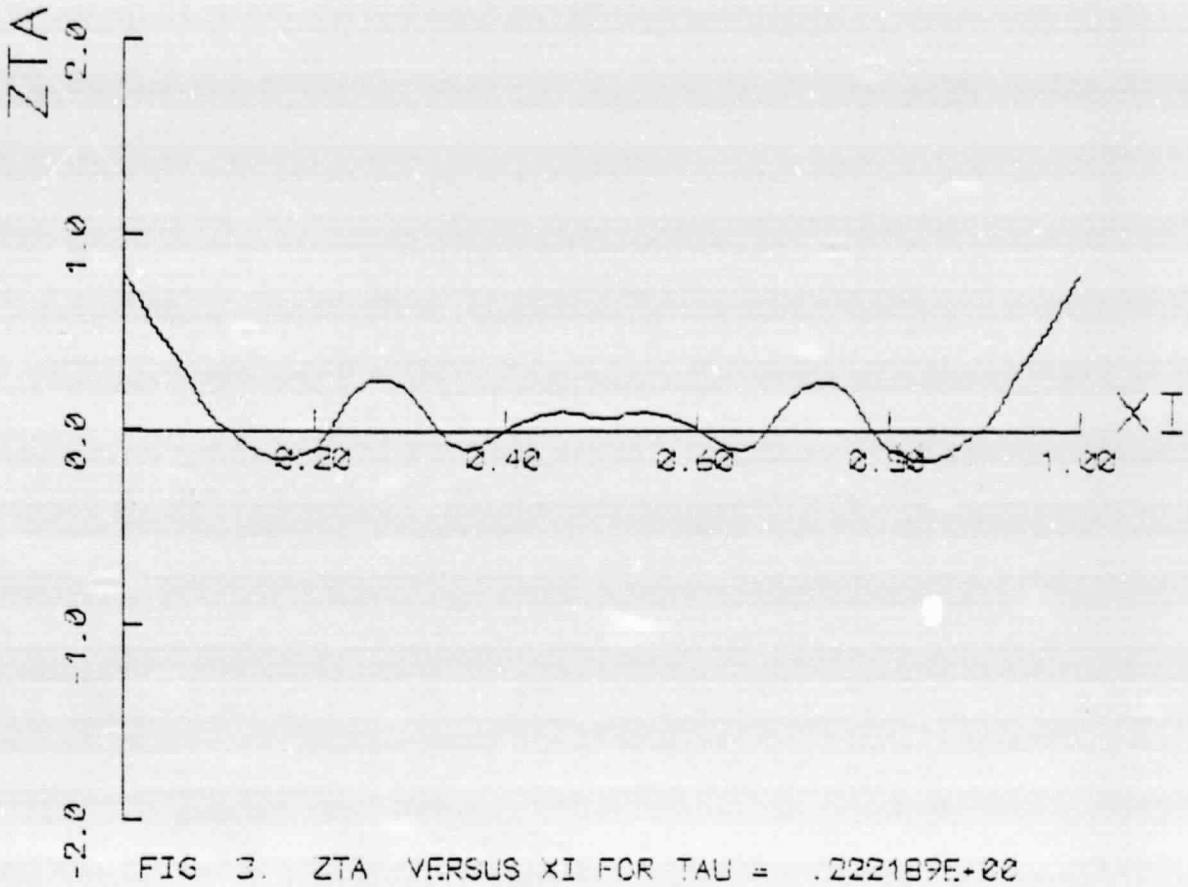

FIG 3. ZTA VERSUS XI FOR TAU = .2221875E+00

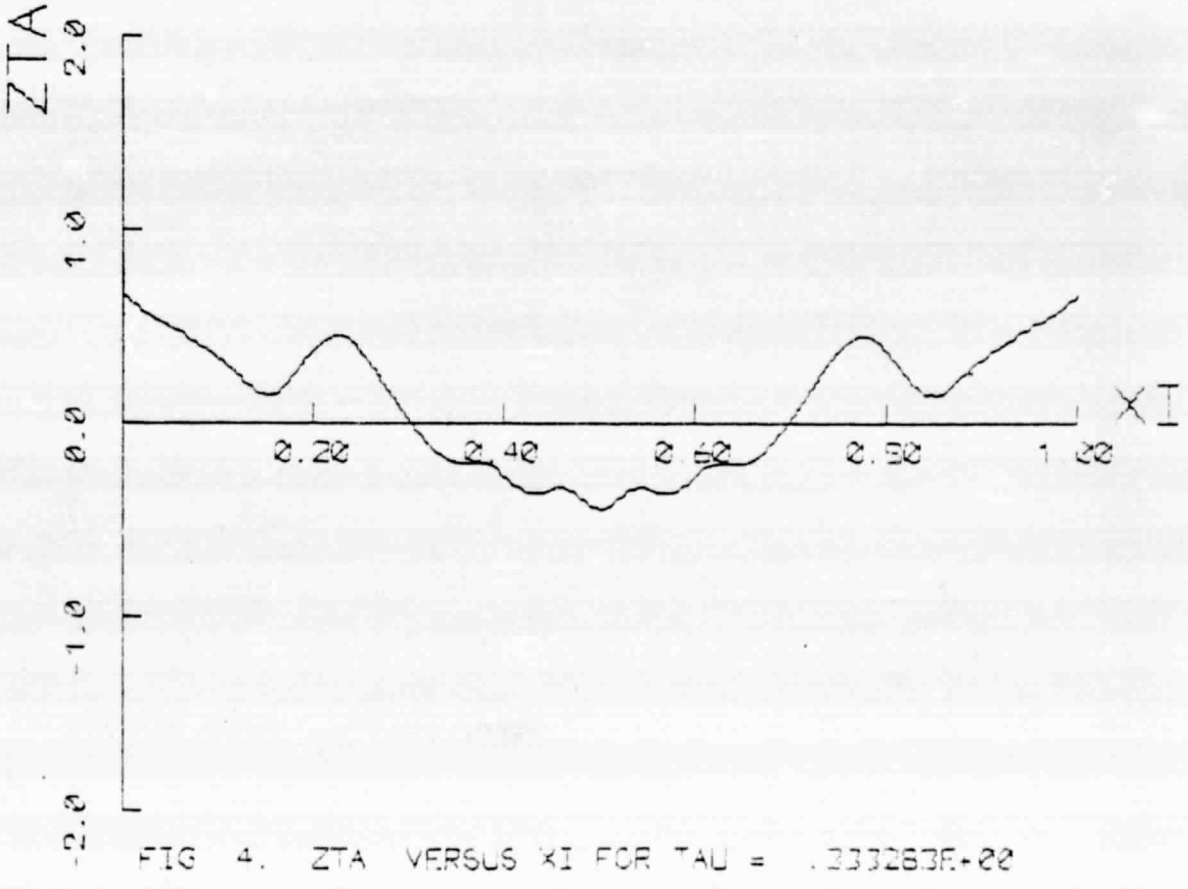

FIG 4. ZTA VERSUS XI FOR TAU = .3332813E+00

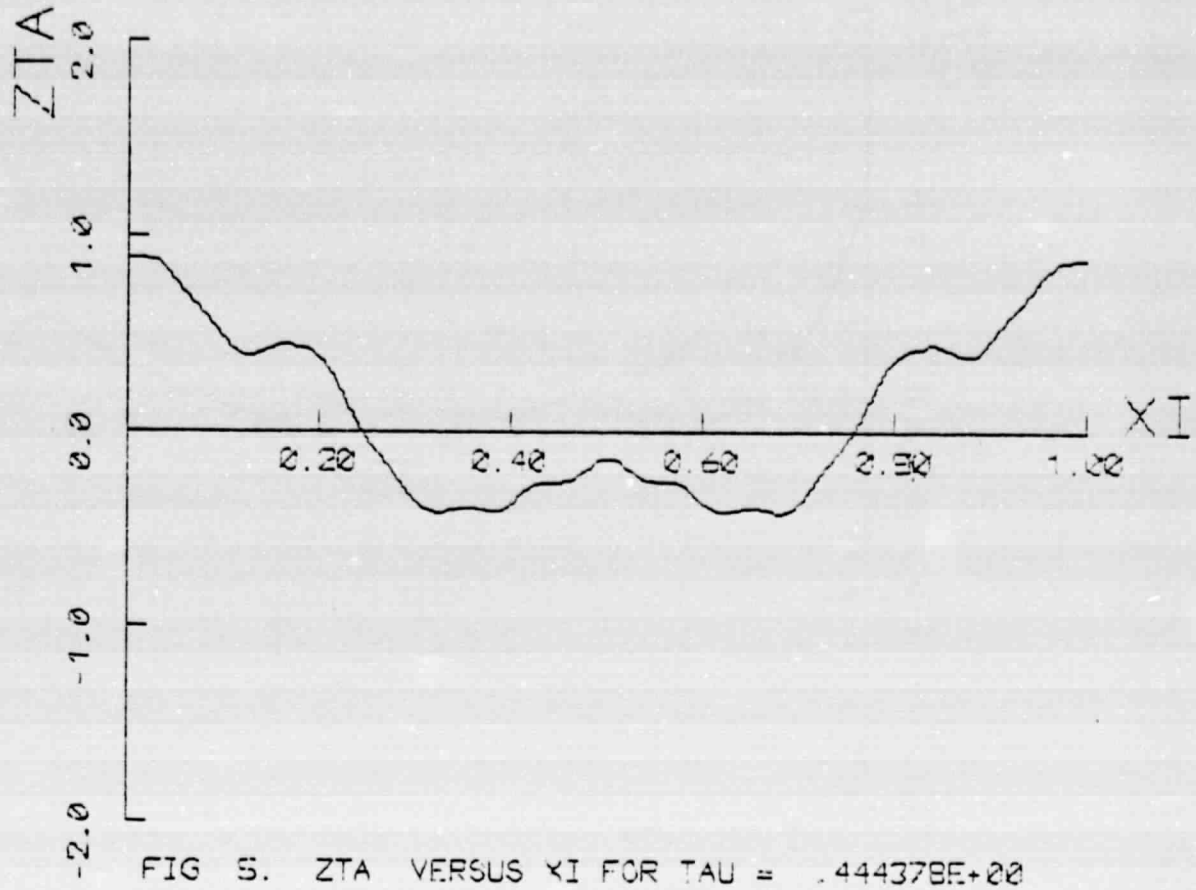

FIG 5. ZTA VERSUS XI FOR TAU = .444378E+00

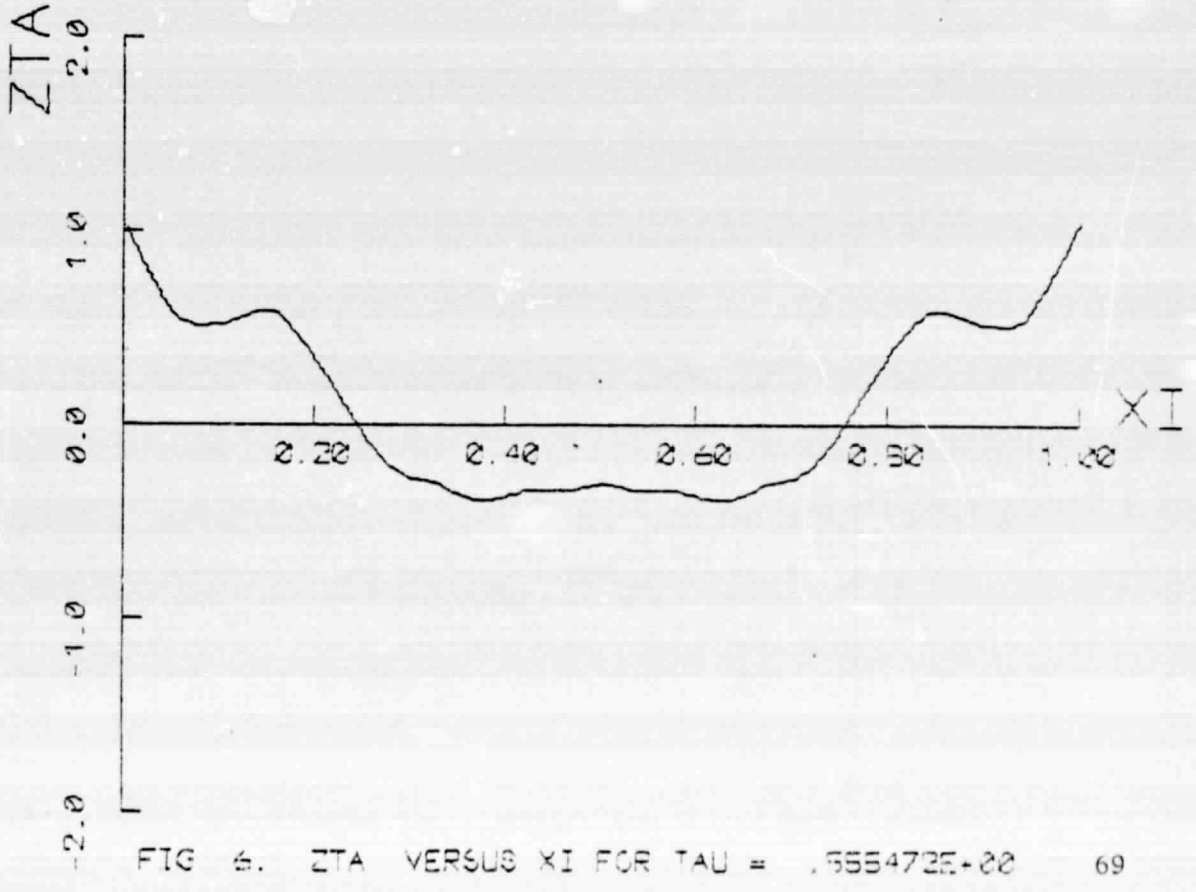

FIG 6. ZTA VERSUS XI FOR TAU = .555472E+00

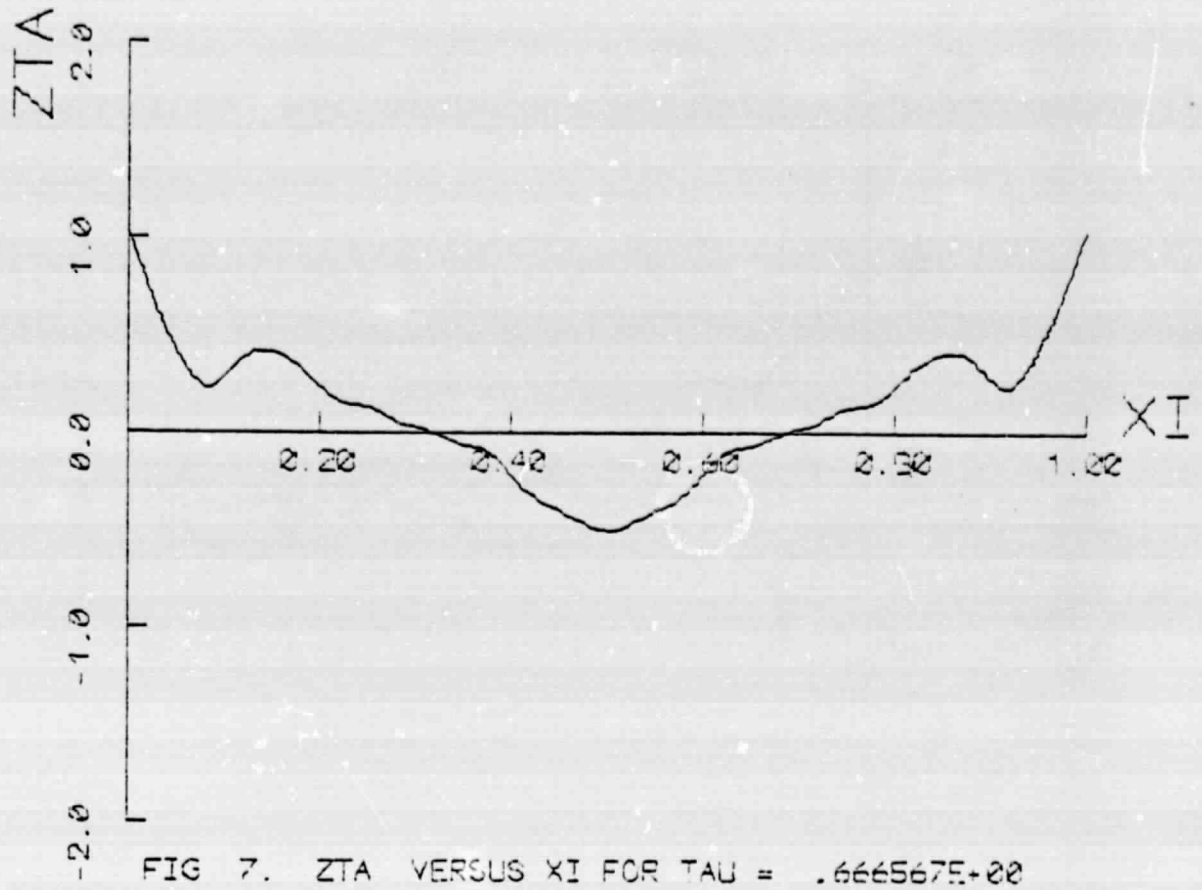

FIG 7. ZTA VERSUS XI FOR TAU = .6665675+00

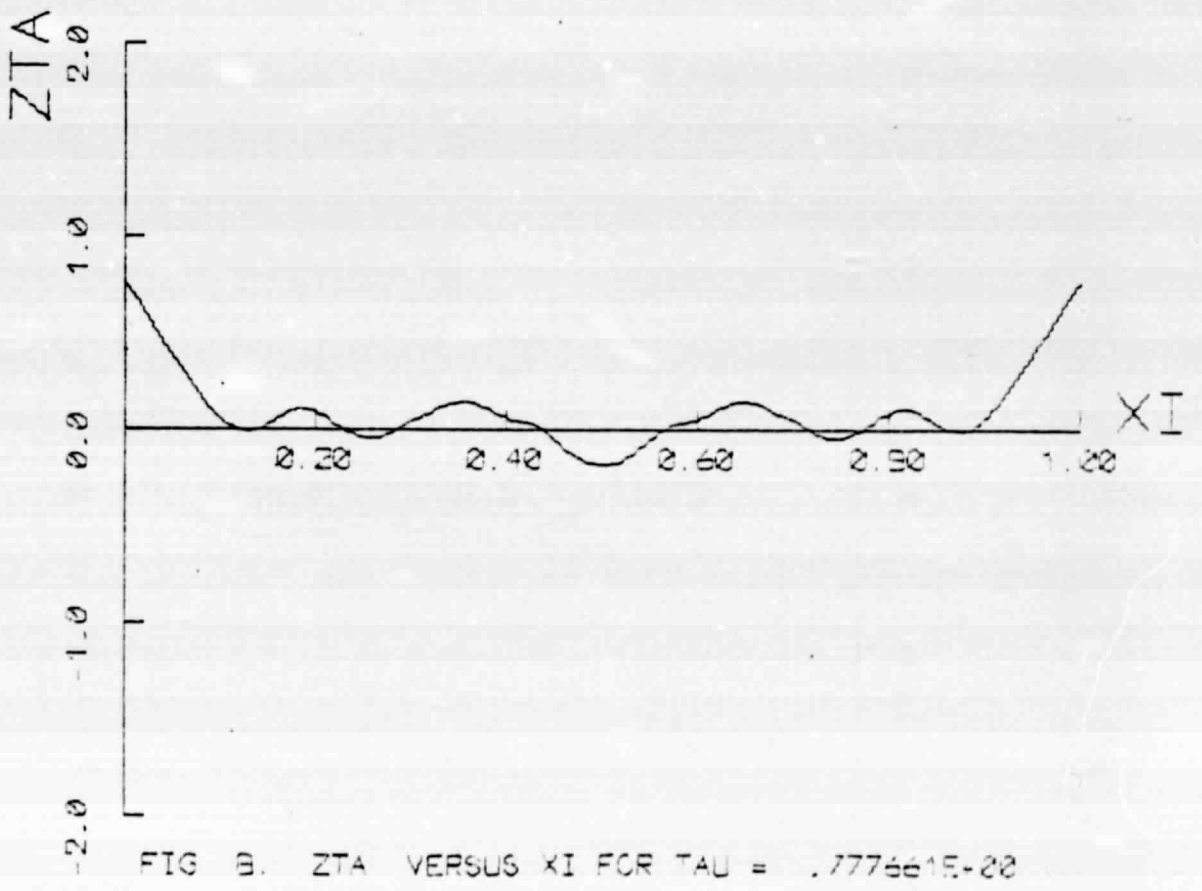

FIG 8. ZTA VERSUS XI FOR TAU = .7776615-00

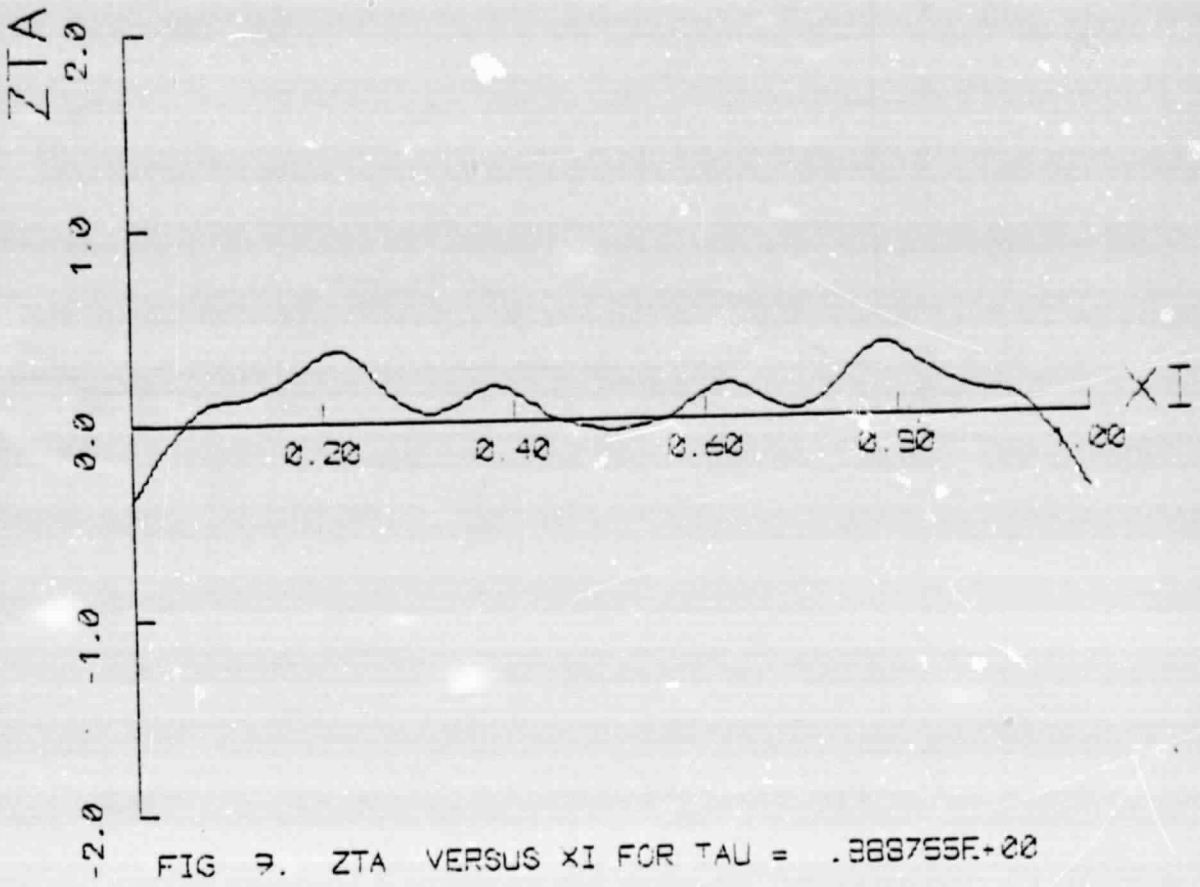

FIG 9. ZTA VERSUS XI FOR TAU = .888755E+00

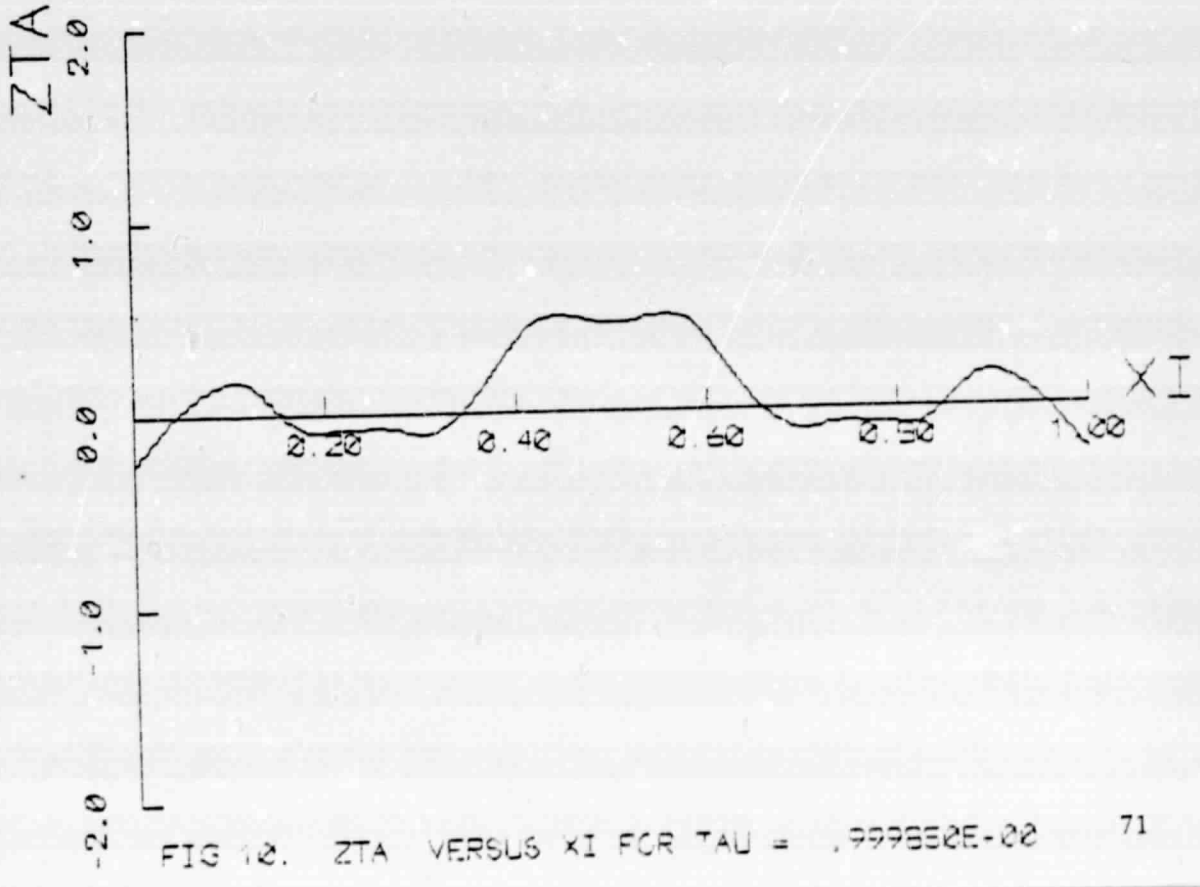

FIG 10. ZTA VERSUS XI FOR TAU = .999882E-00

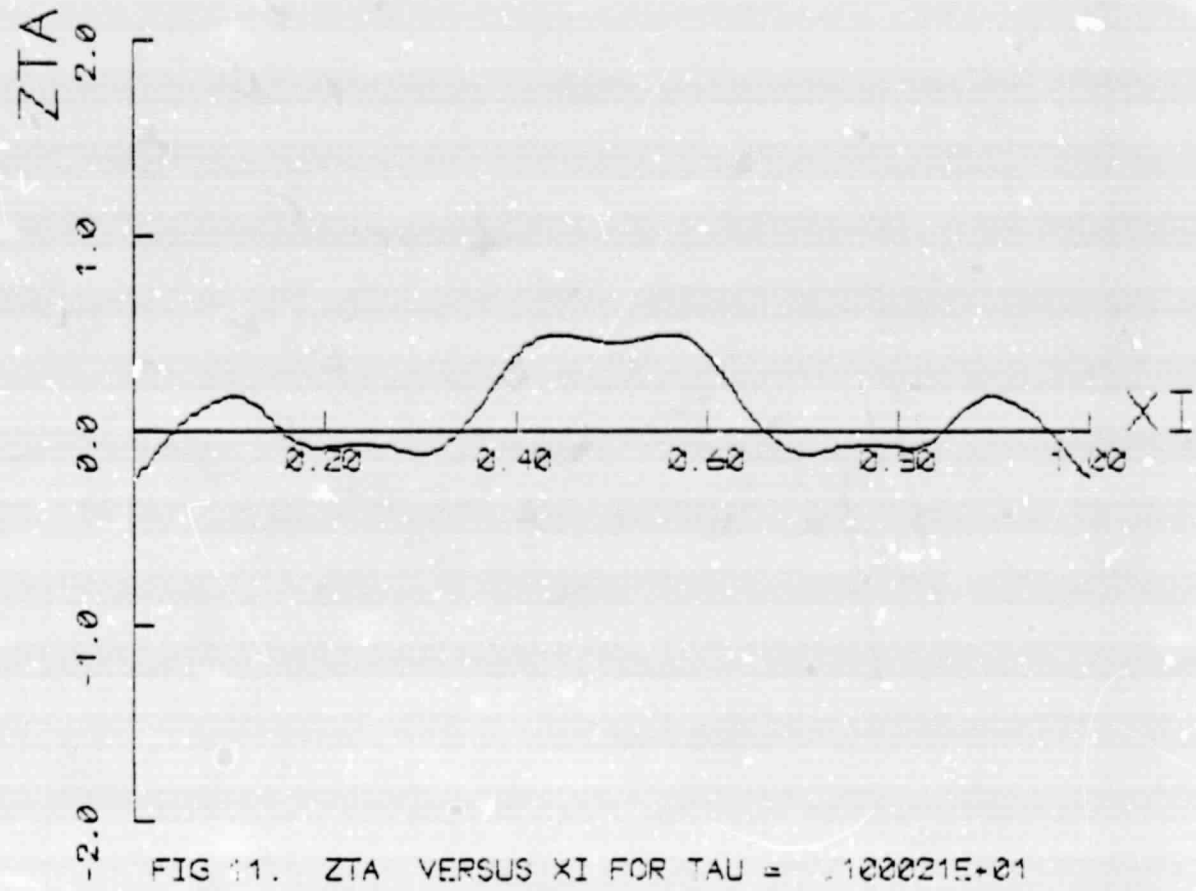

FIG 11. ZTA VERSUS XI FOR TAU = .100021E+01

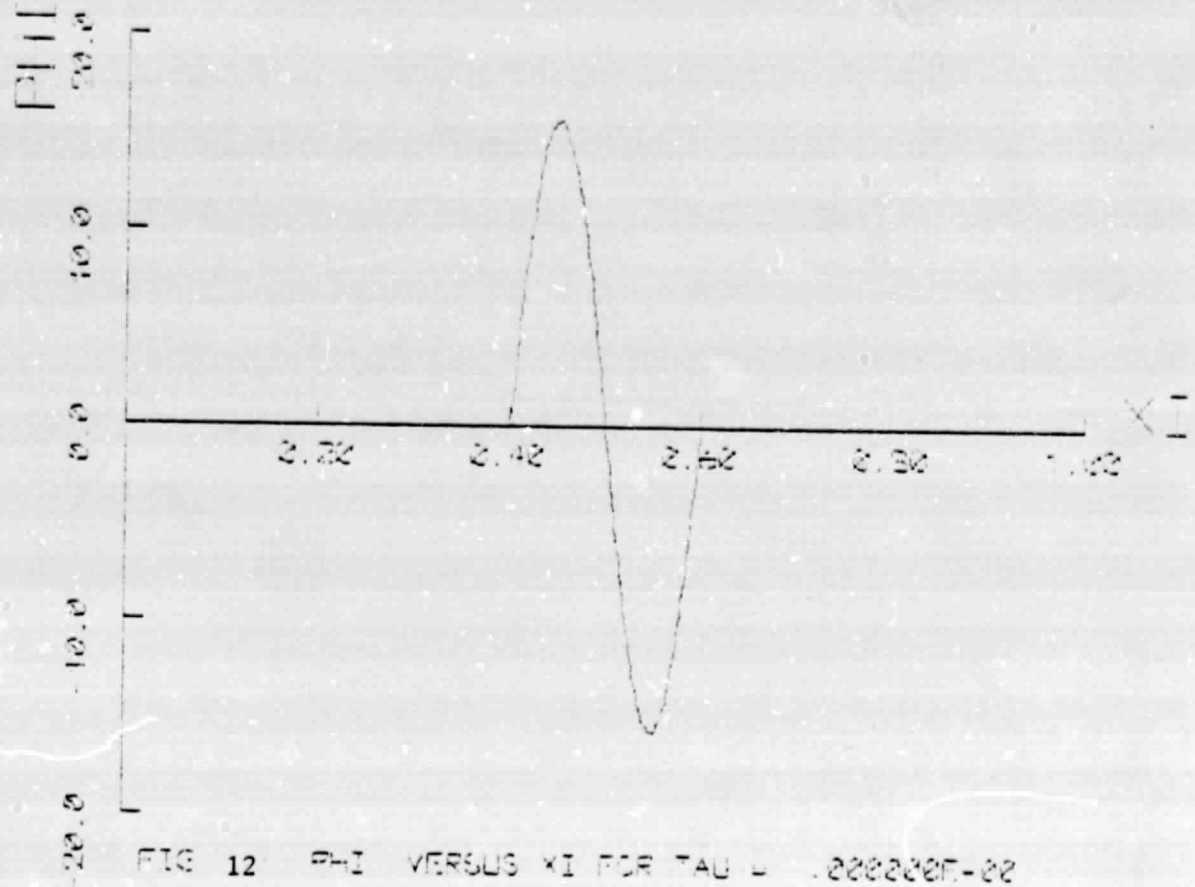

FIG 12 PHI VERSUS XI FOR TAU = .2000000E-02

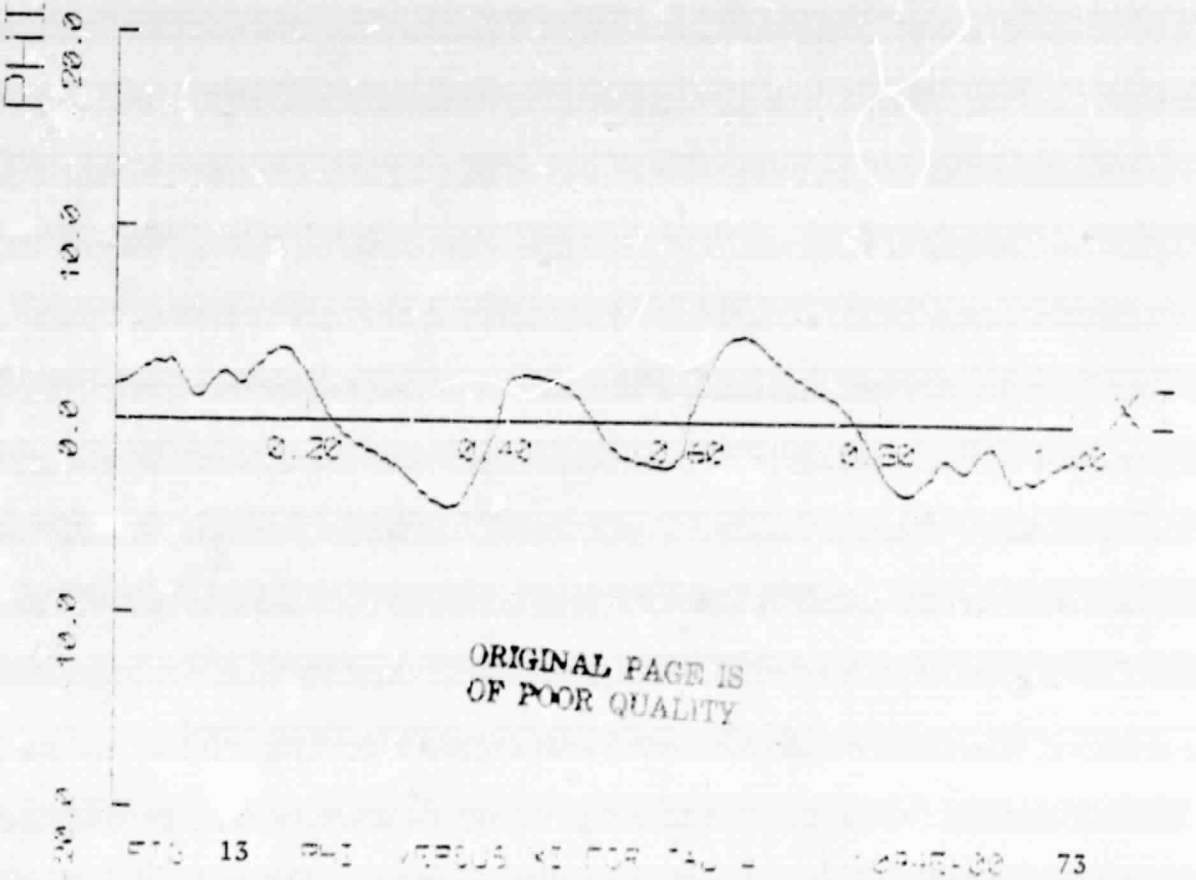

FIG 13 PHI VERSUS XI FOR TAU = .4000000E-02

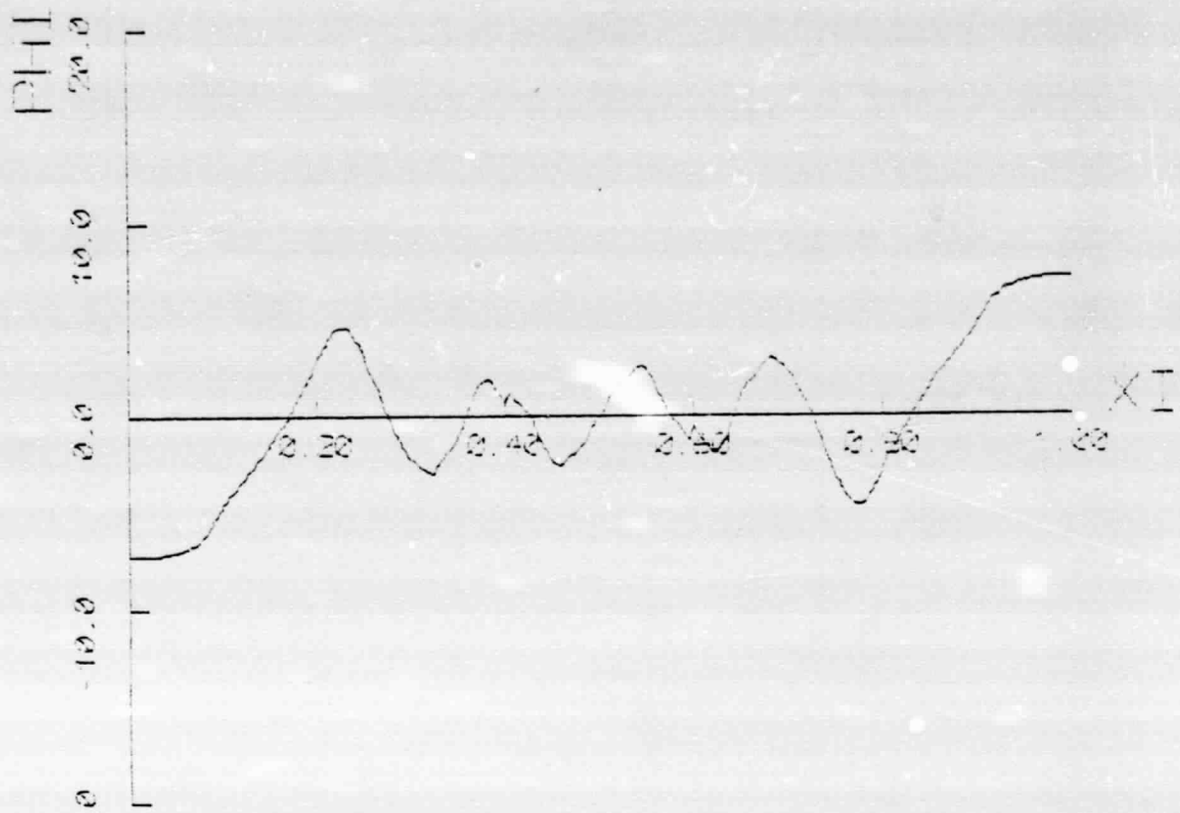

FIG 14 PHI VERSUS XI FOR TAU = .222187E-00

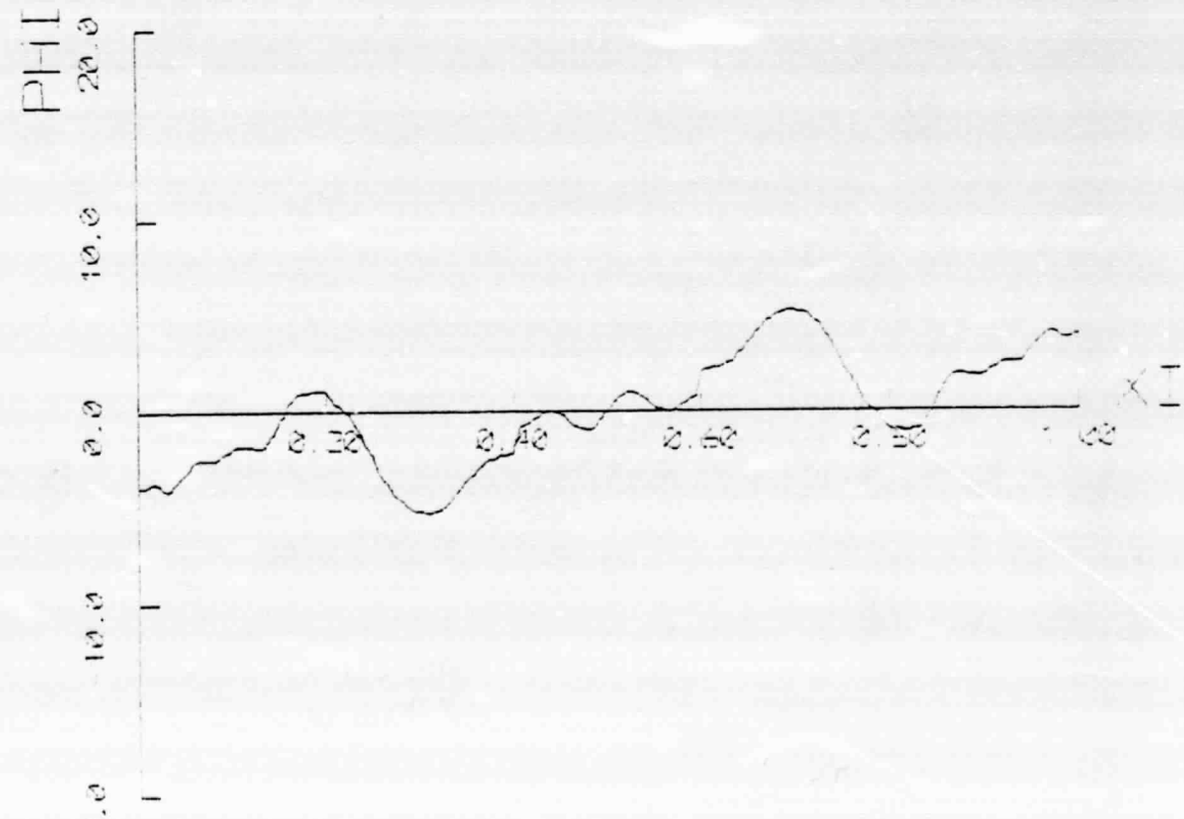

FIG 15 PHI VERSUS XI FOR TAU = .333333E-00

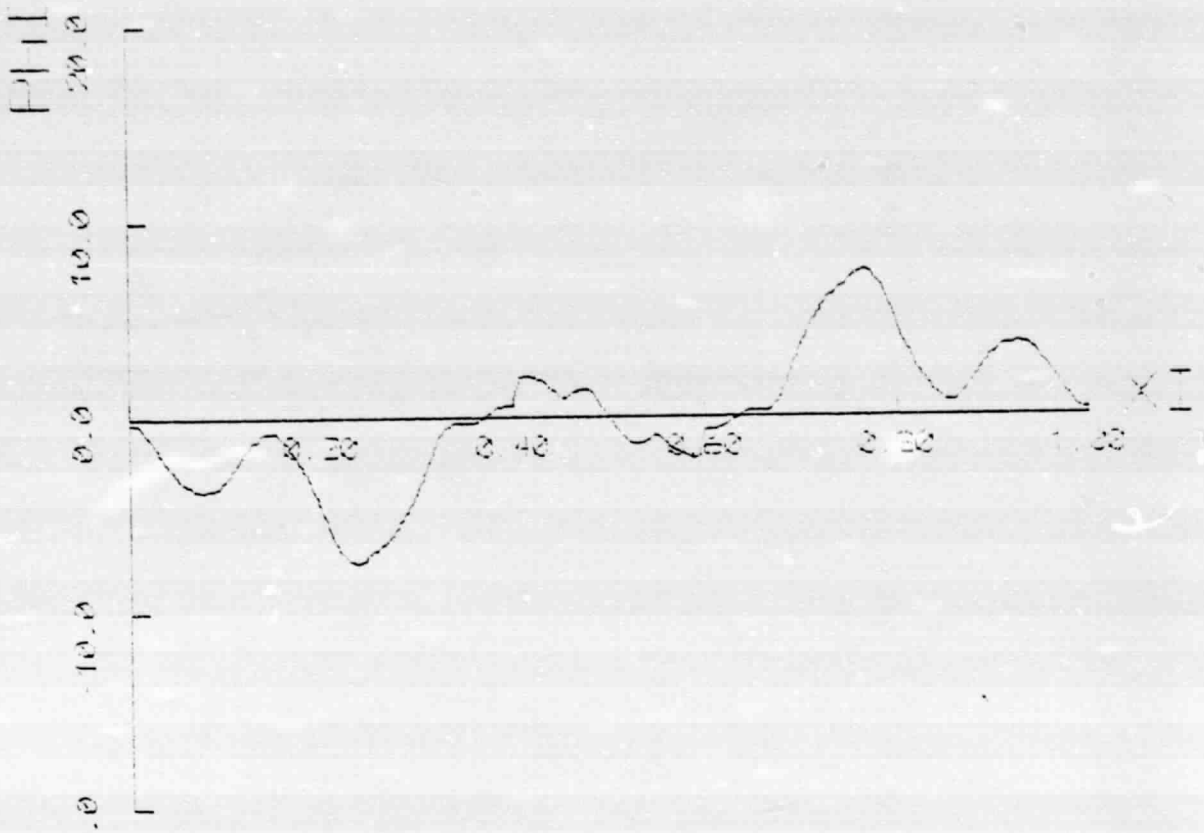

FIG 16 PHI VERSUS XI FOR TAU = .4443750E-00

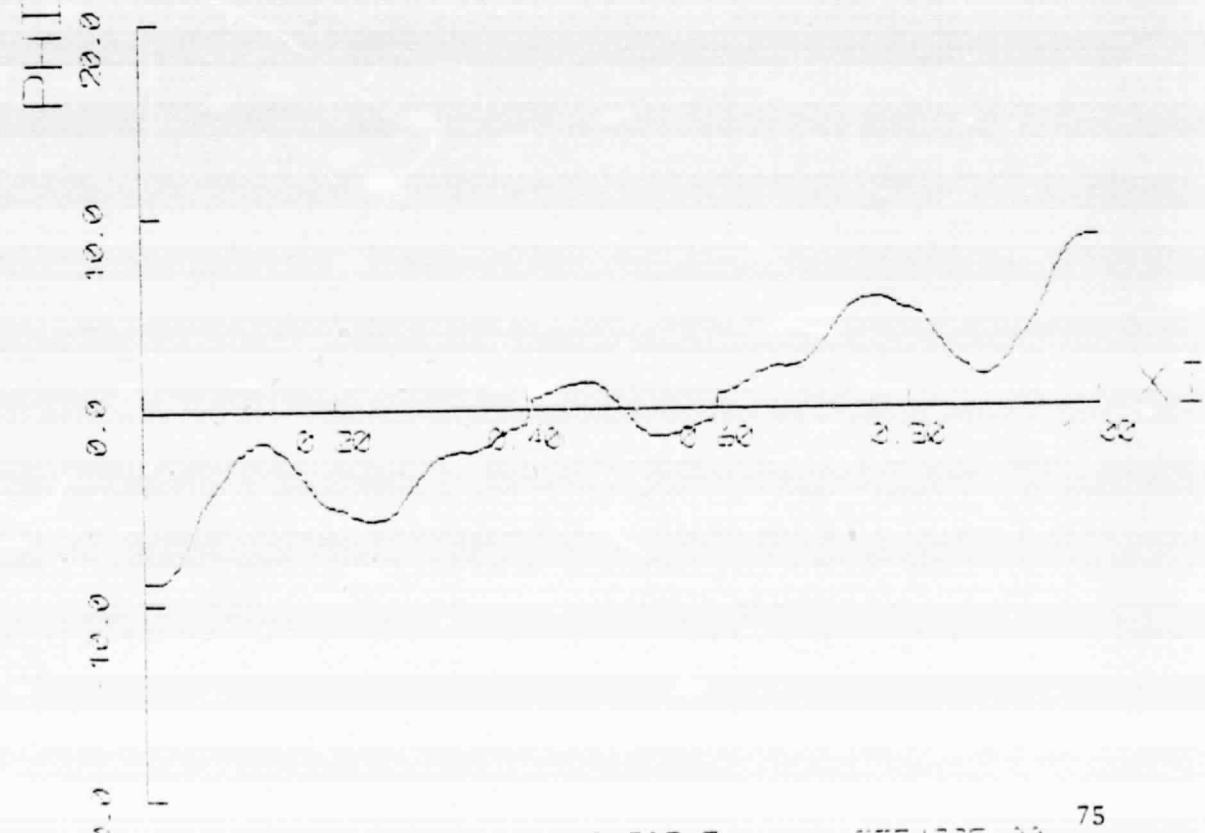

FIG 17 PHI VERSUS XI FOR TAU = .8884720E-00

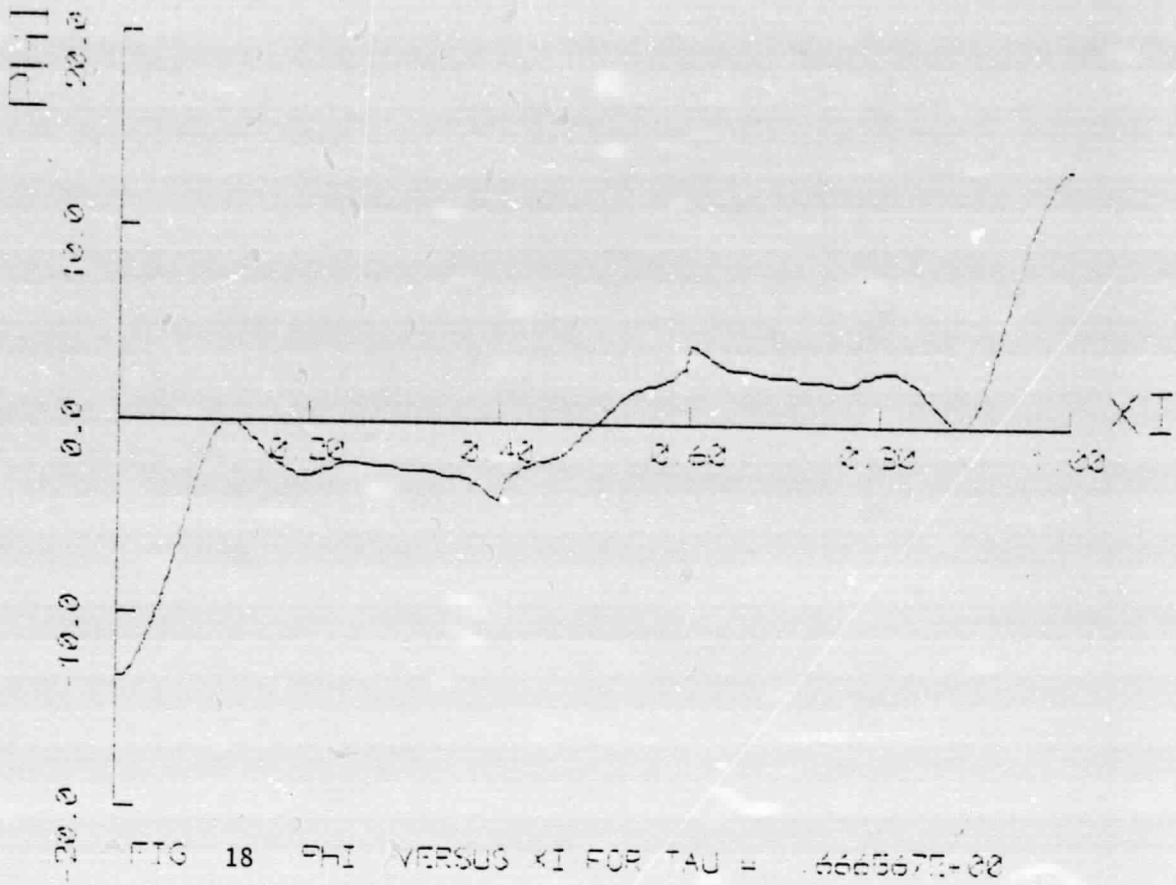

FIG 18 PHI VERSUS XI FOR TAU = .6663677E-02

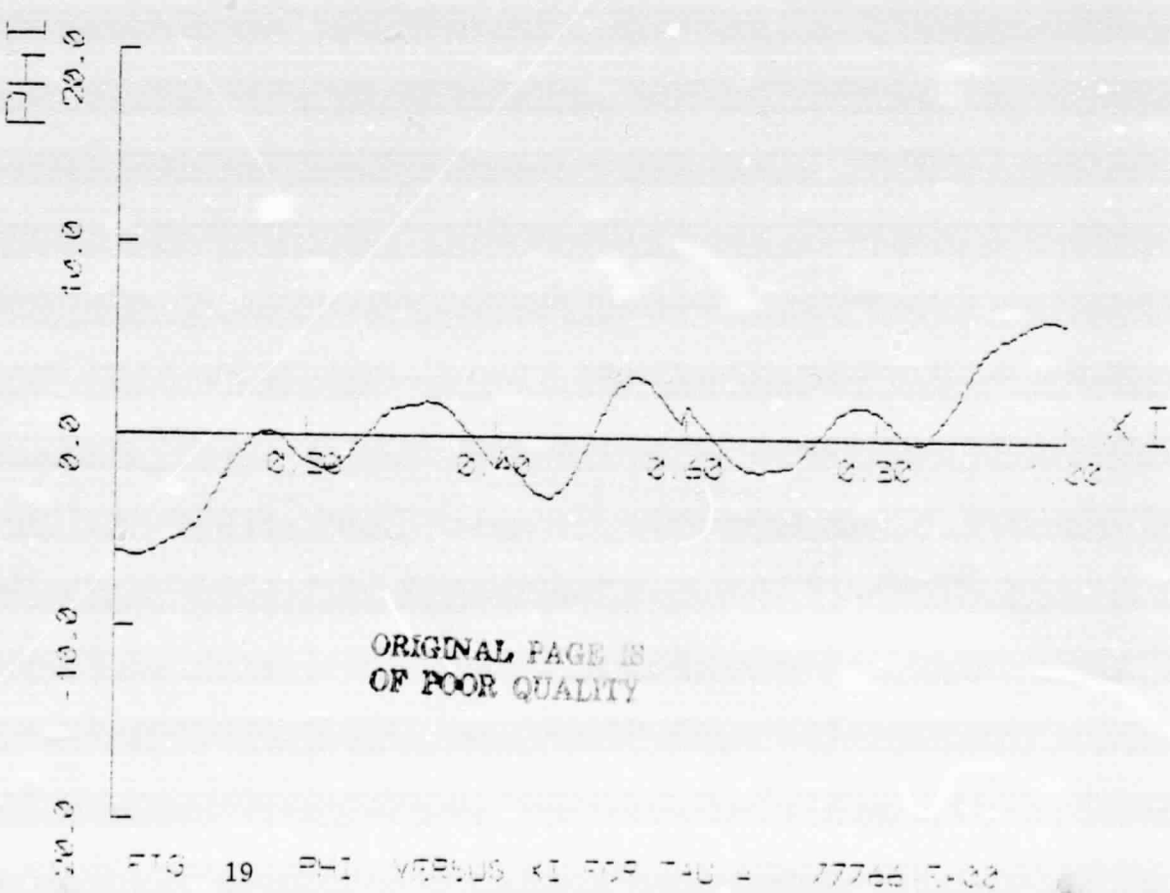

FIG 19 PHI VERSUS XI FOR TAU = .7766E-02

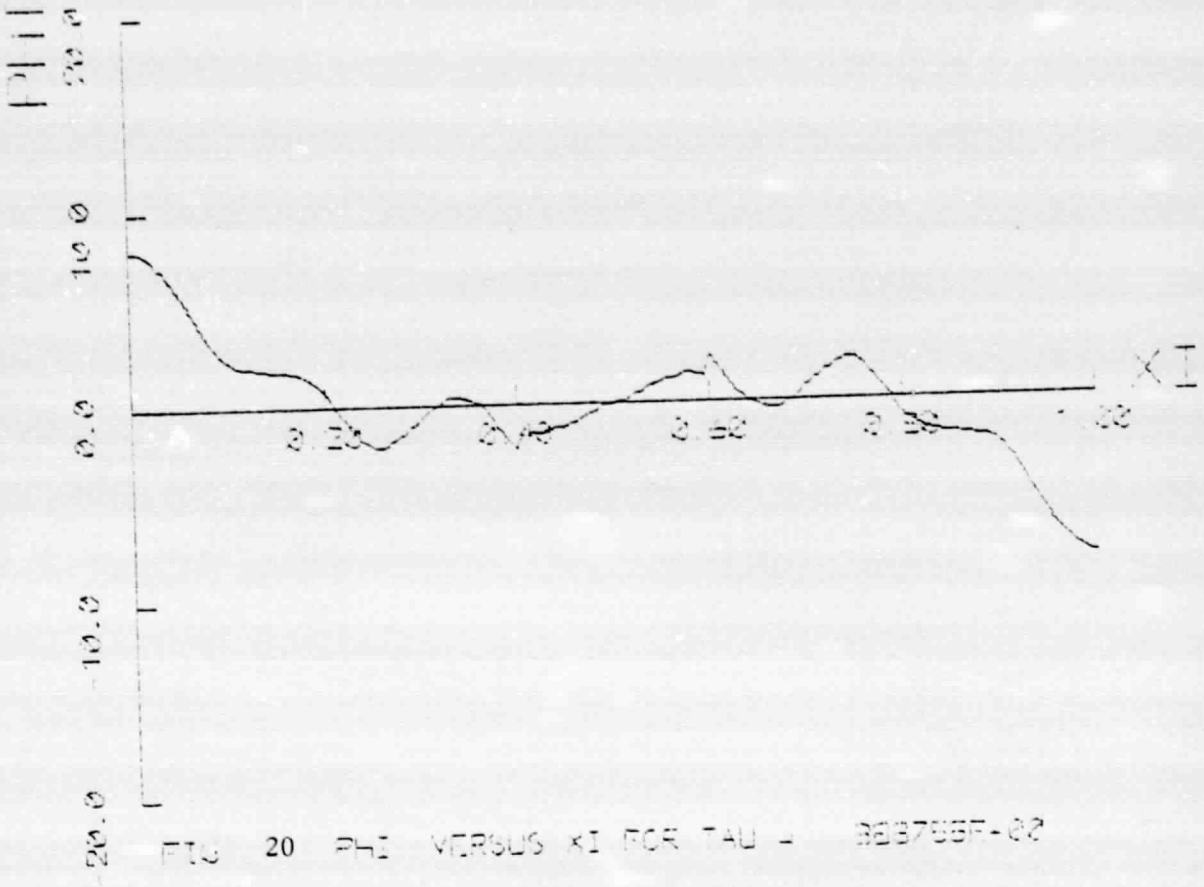

FIG 20 PHI VERSUS XI FOR TAU = 3.837E-02

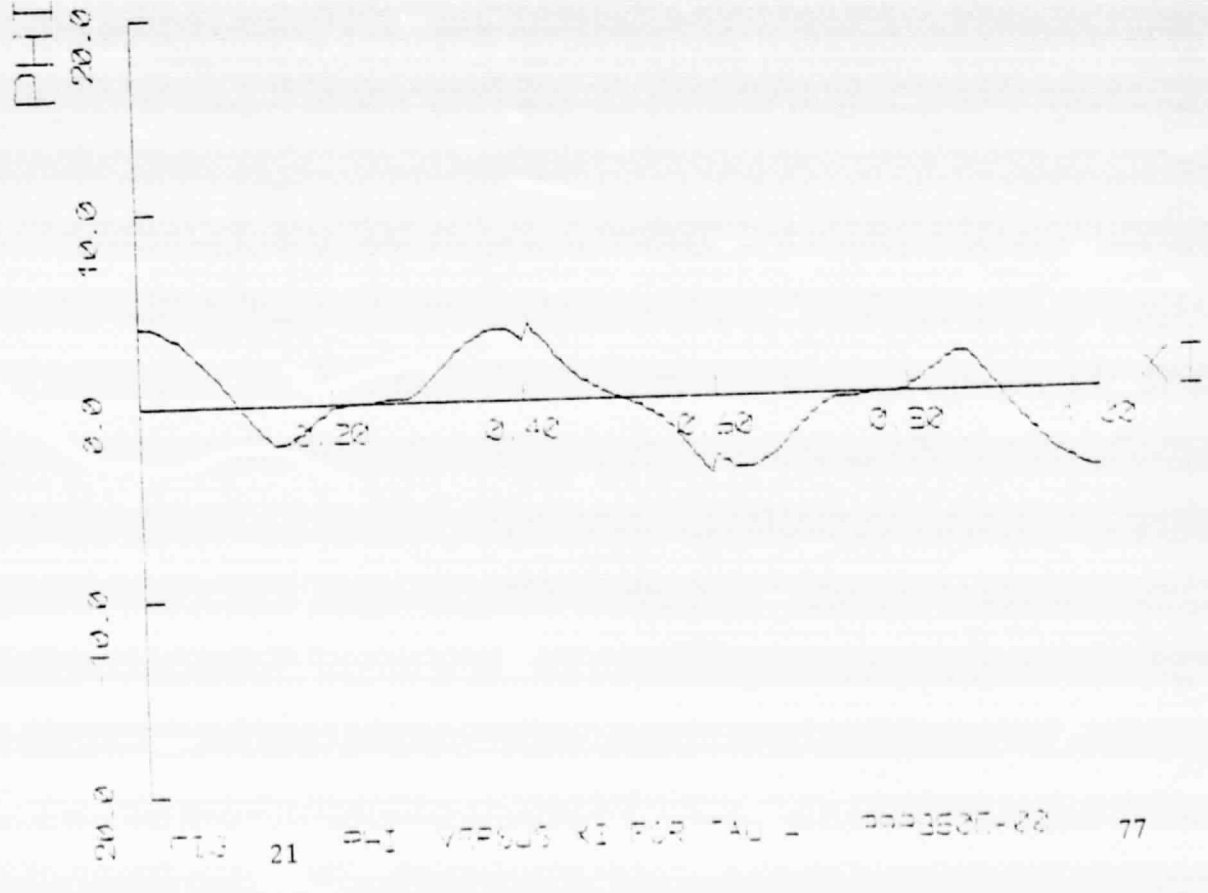

FIG 21 PHI VERSUS XI FOR TAU = 3.731E-02

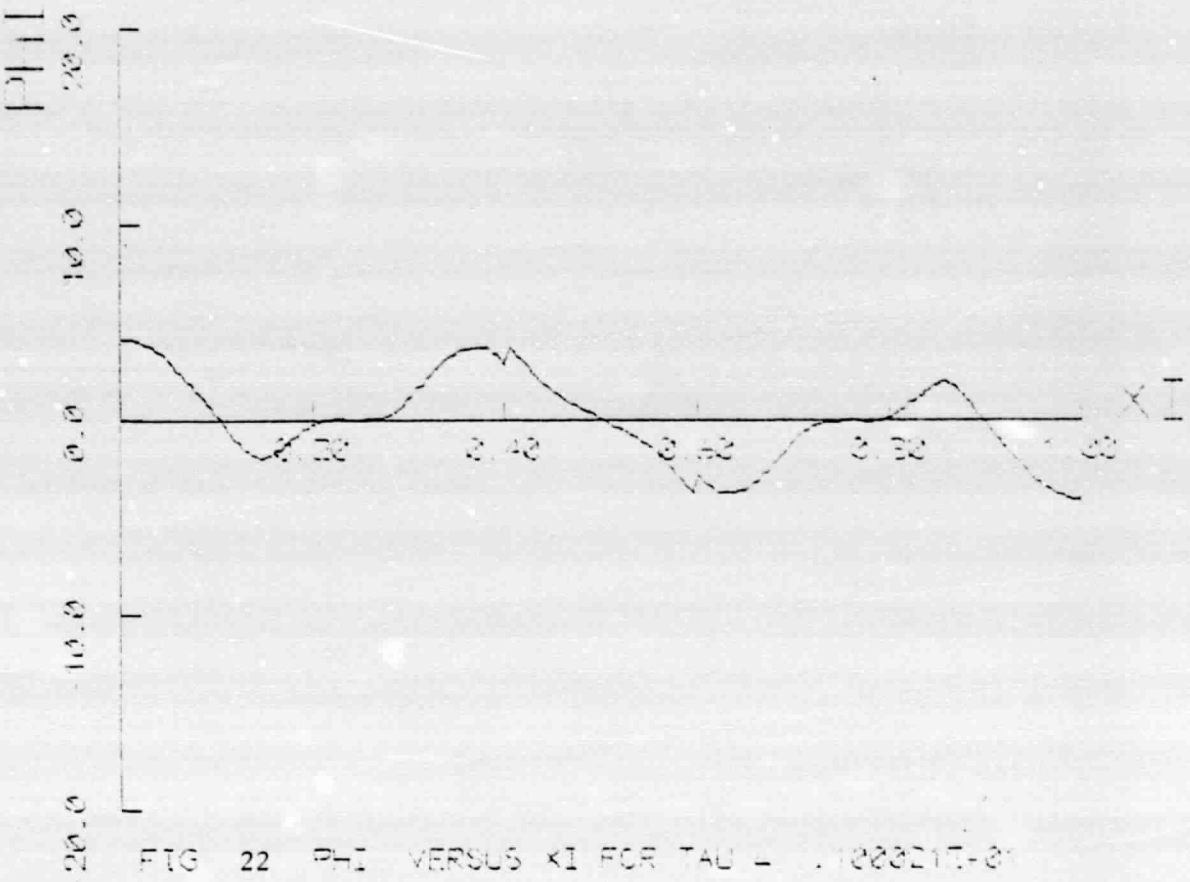

FIG 22 PHI VERSUS XI FOR TAU = .1000E-01

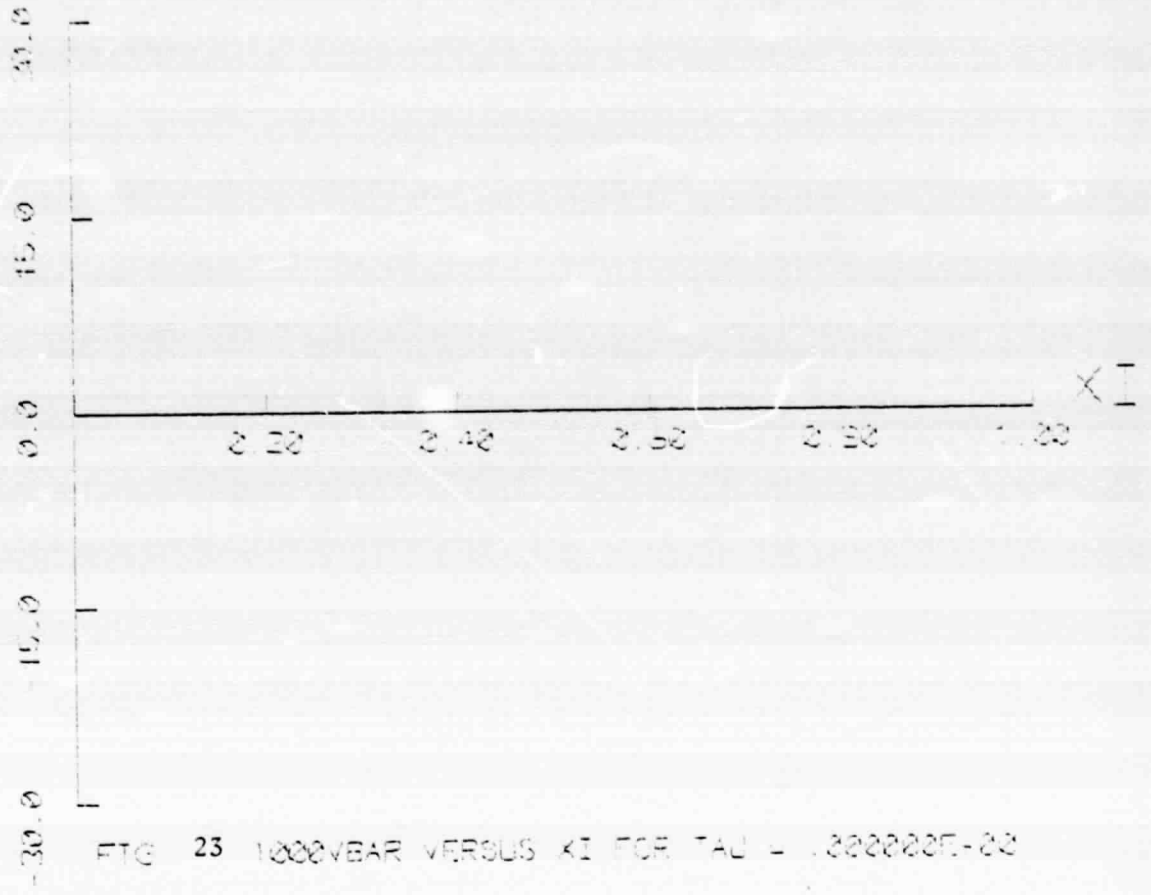

FIG 23 1000VBAR VERSUS XI FOR TAU = .3000000E-02

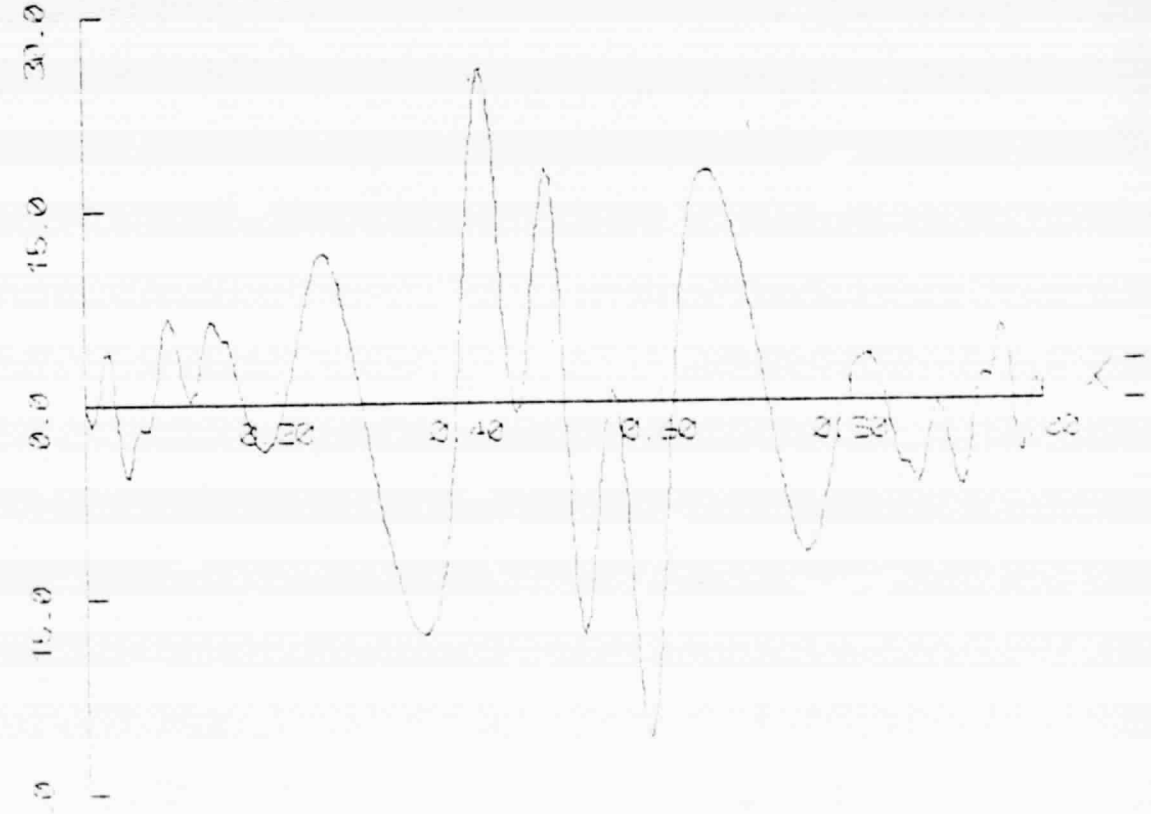

FIG 24 1000.BAR VERSUS XI FOR TAU = .3000000E-02

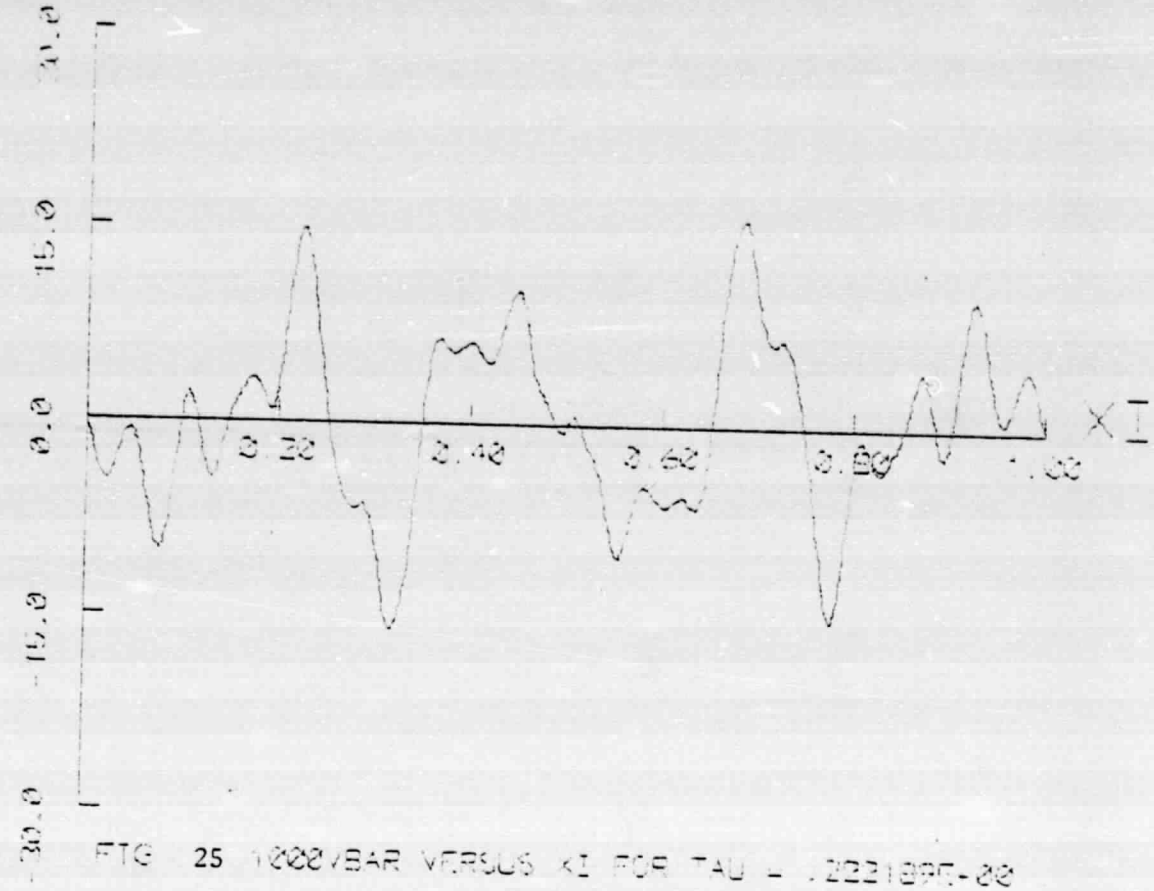

FIG 25 1000/BAR VERSUS XI FOR TAU = .2221E0E-00

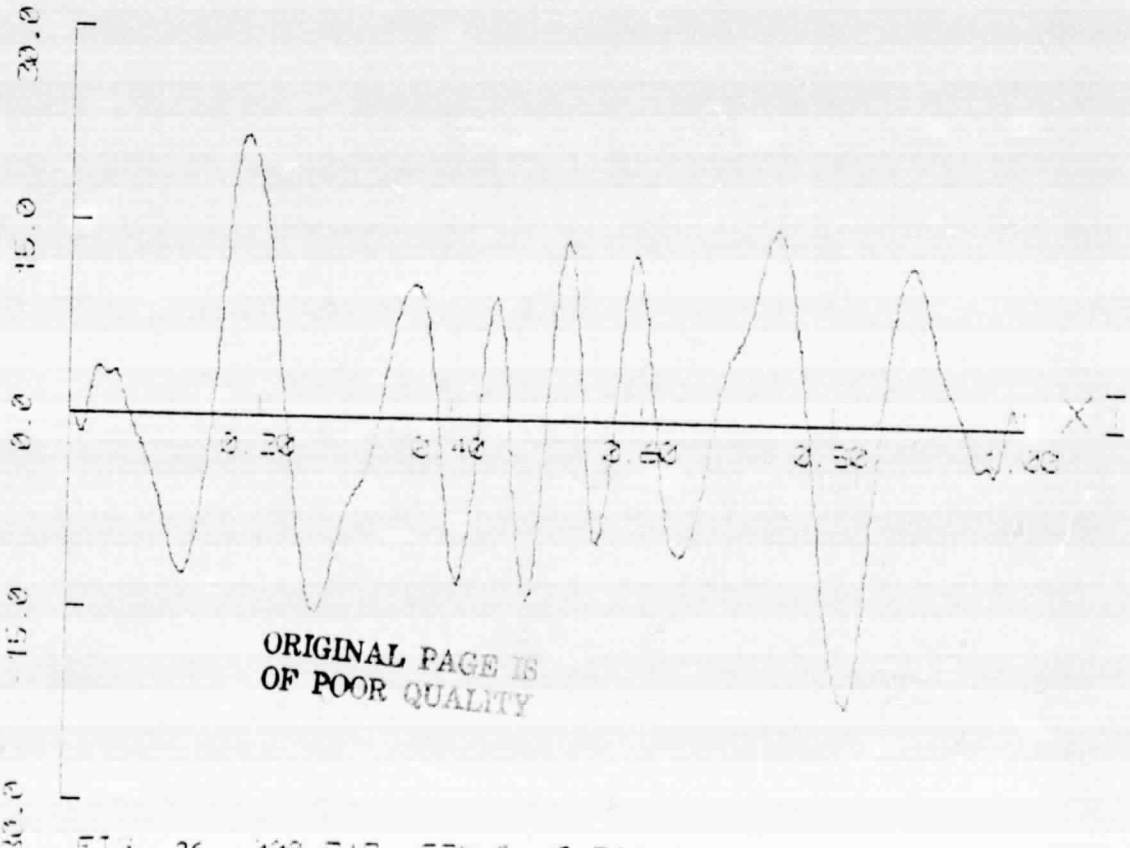

FIG 26 1000/BAR VERSUS XI FOR TAU = .3332E0E-00

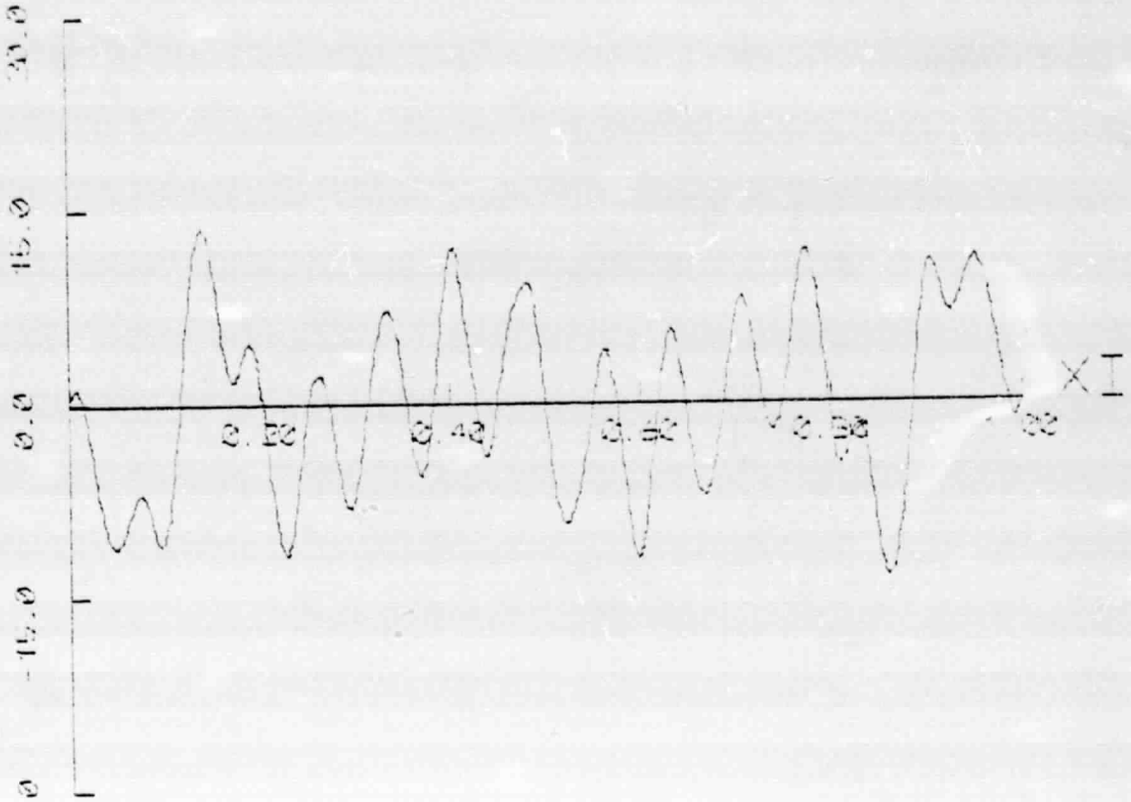

FIG 27 1000VBAR VERSUS XI FOR TAU = .4443785-00

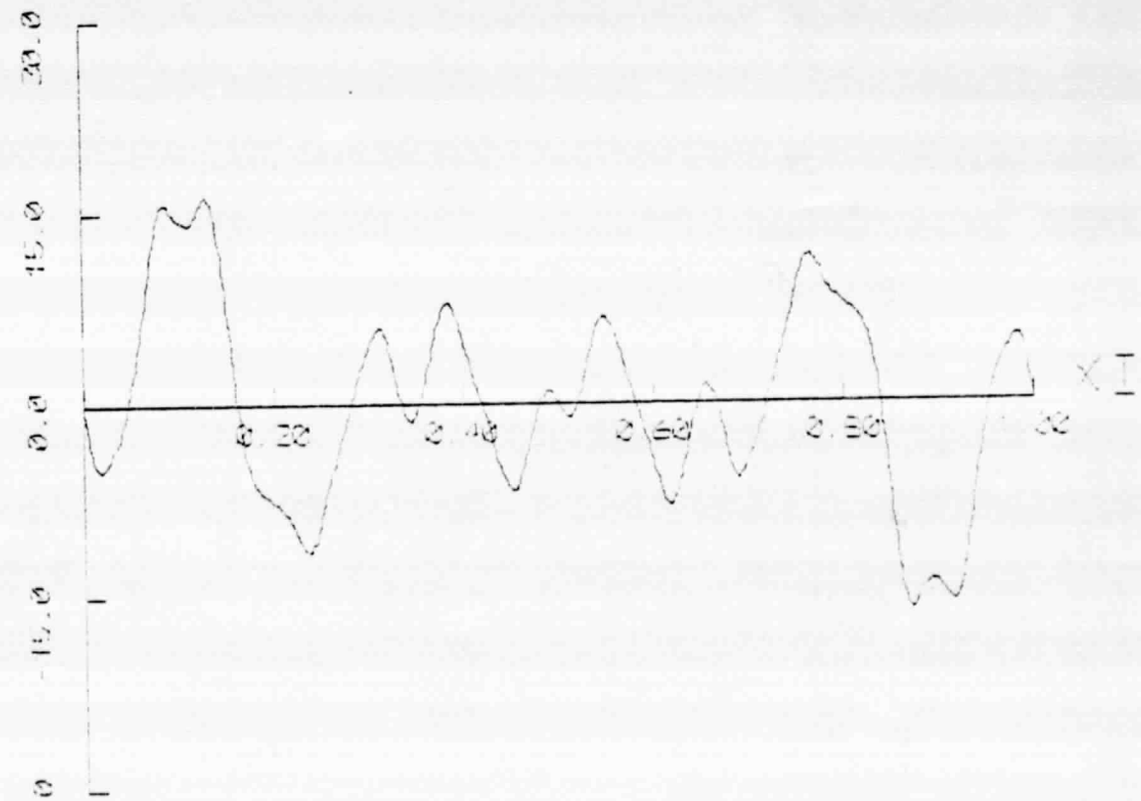

FIG 28 1000VBAR VERSUS XI FOR TAU = .9884725-00

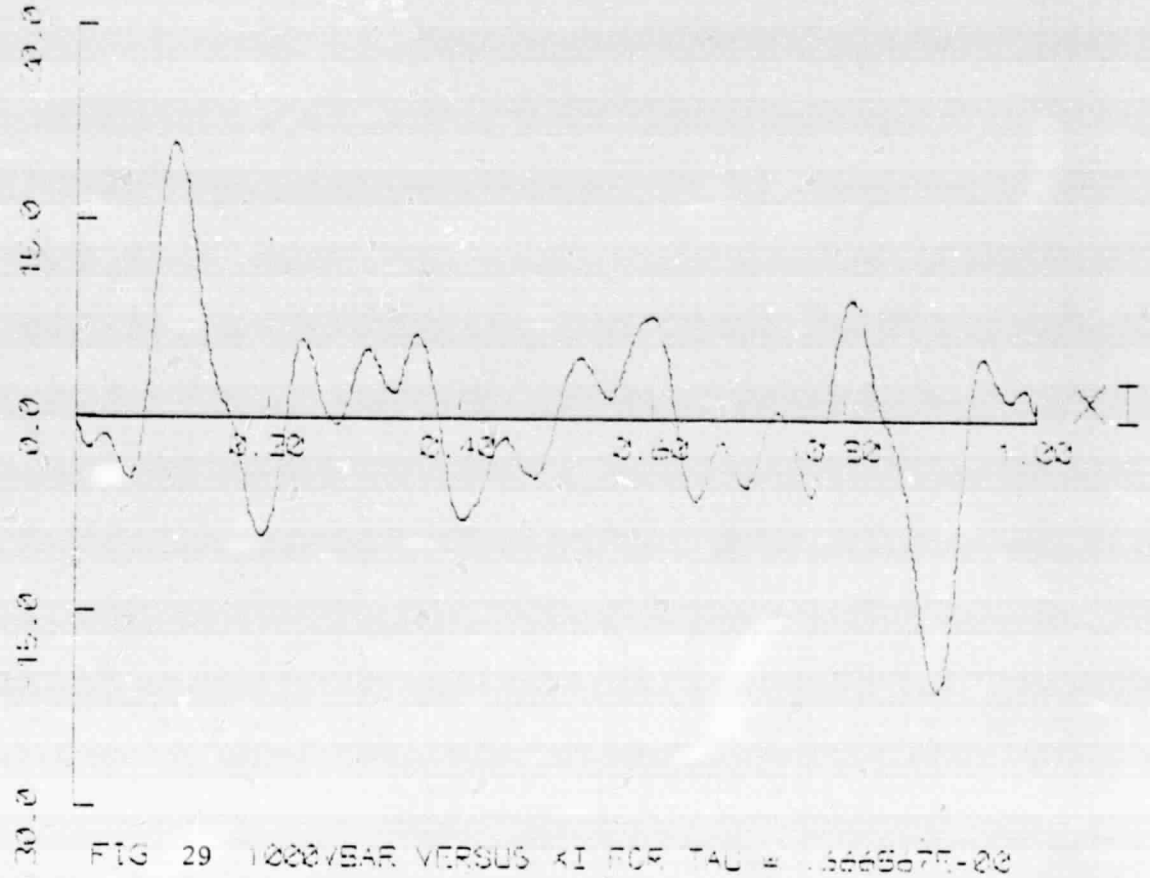

FIG 29 1000*BAR VERSUS XI FOR TAU = .6666E77-00

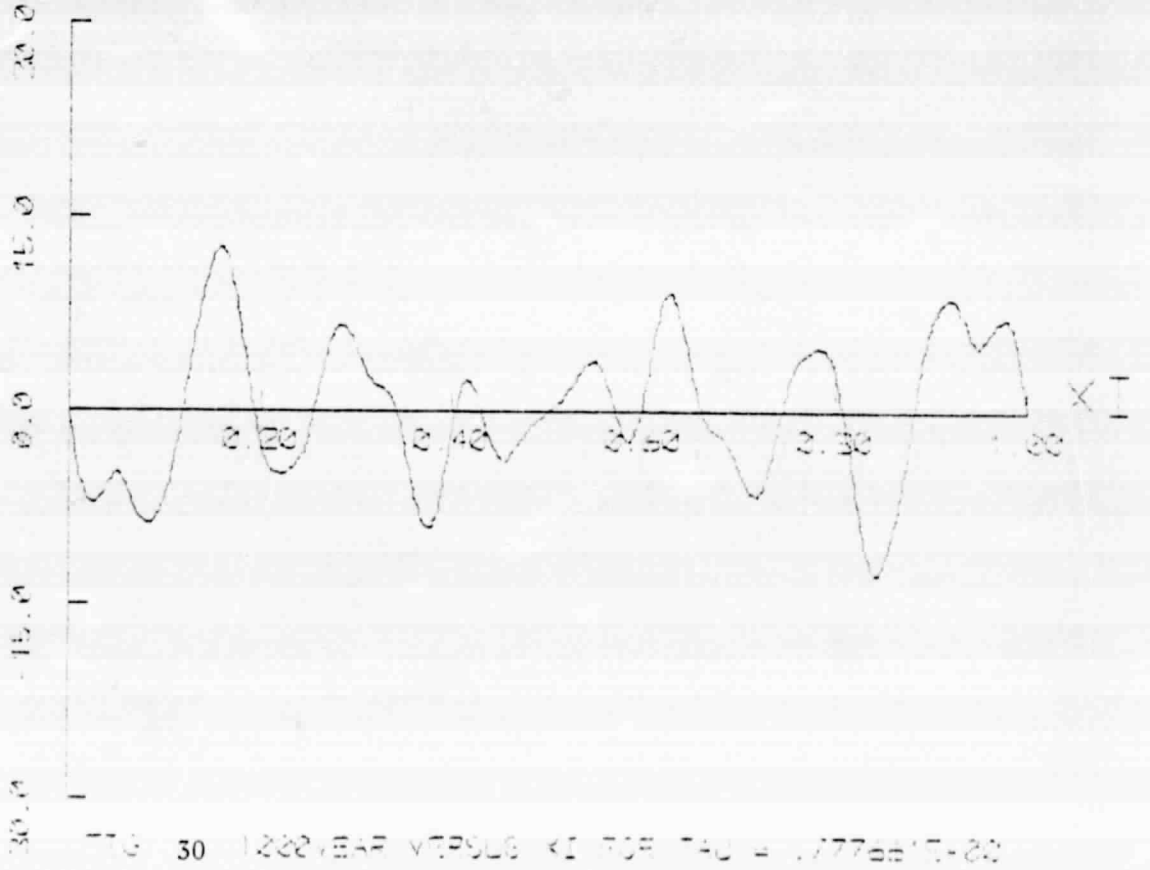

FIG 30 1000*BAR VERSUS XI FOR TAU = .7778E77-00

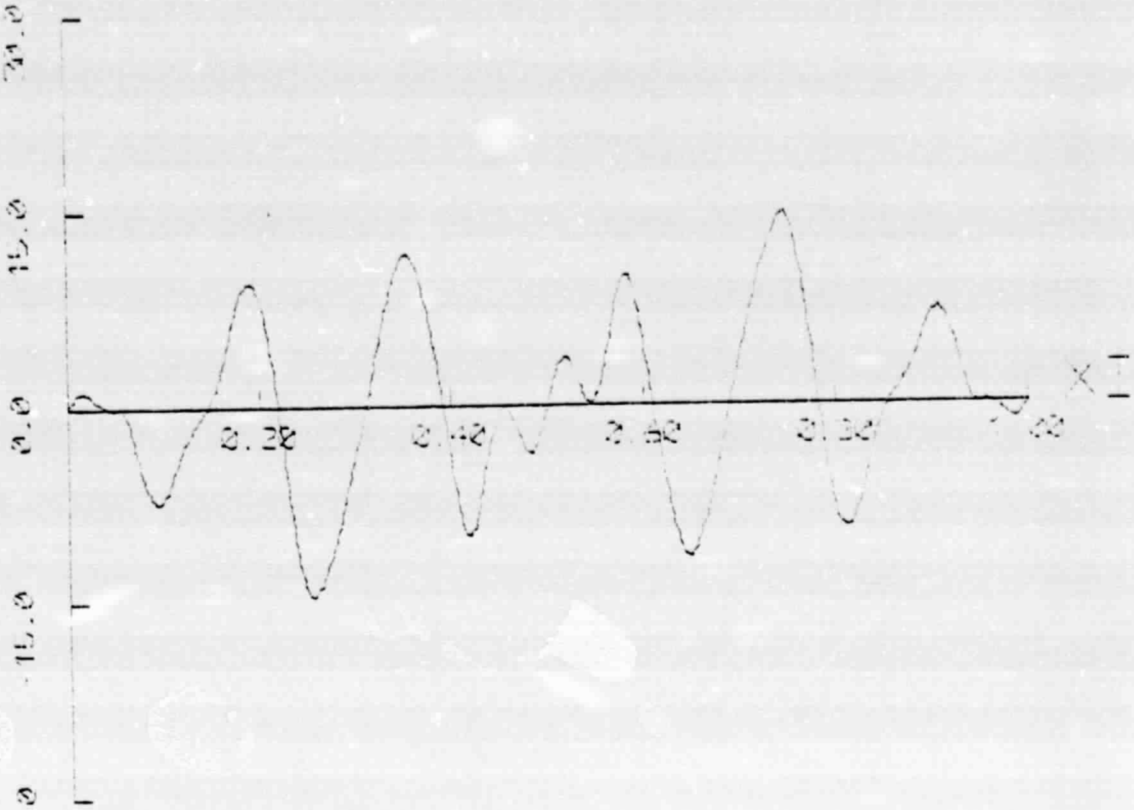

FIG 31 1000VBAR VERSUS XI FOR TAU = .988750E-00

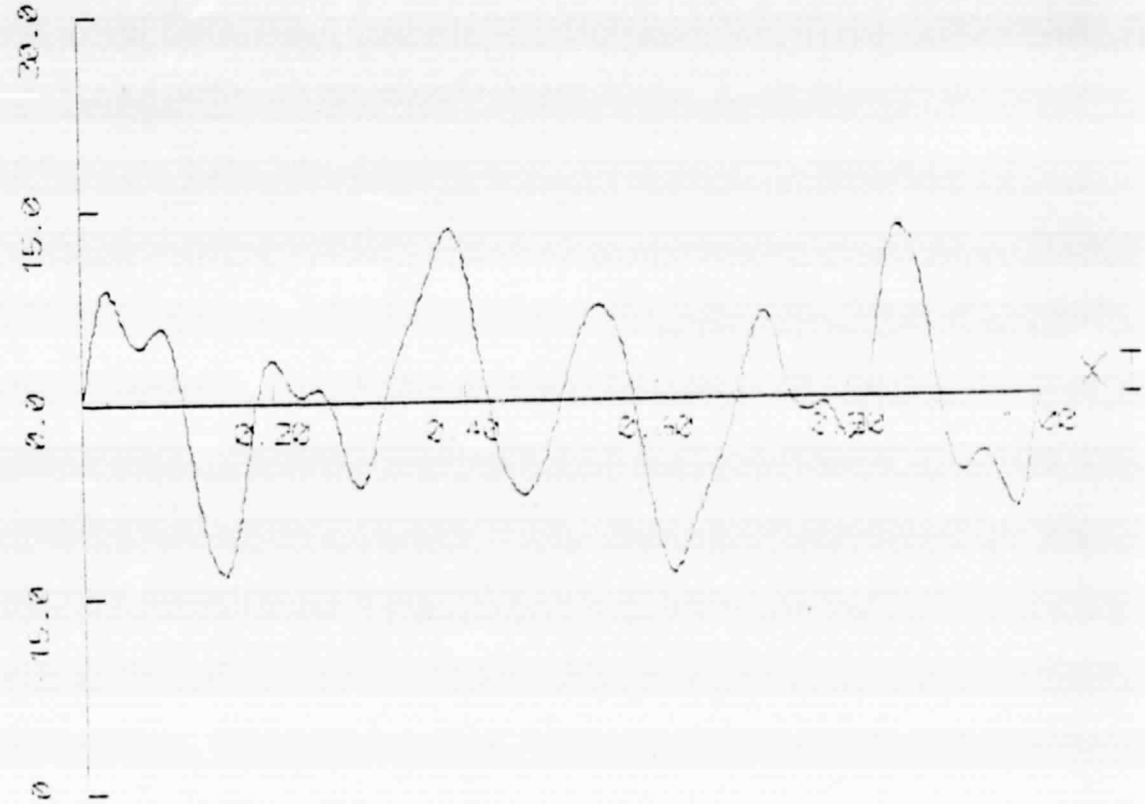

FIG 32 1000VBAR VERSUS XI FOR TAU = [illegible]

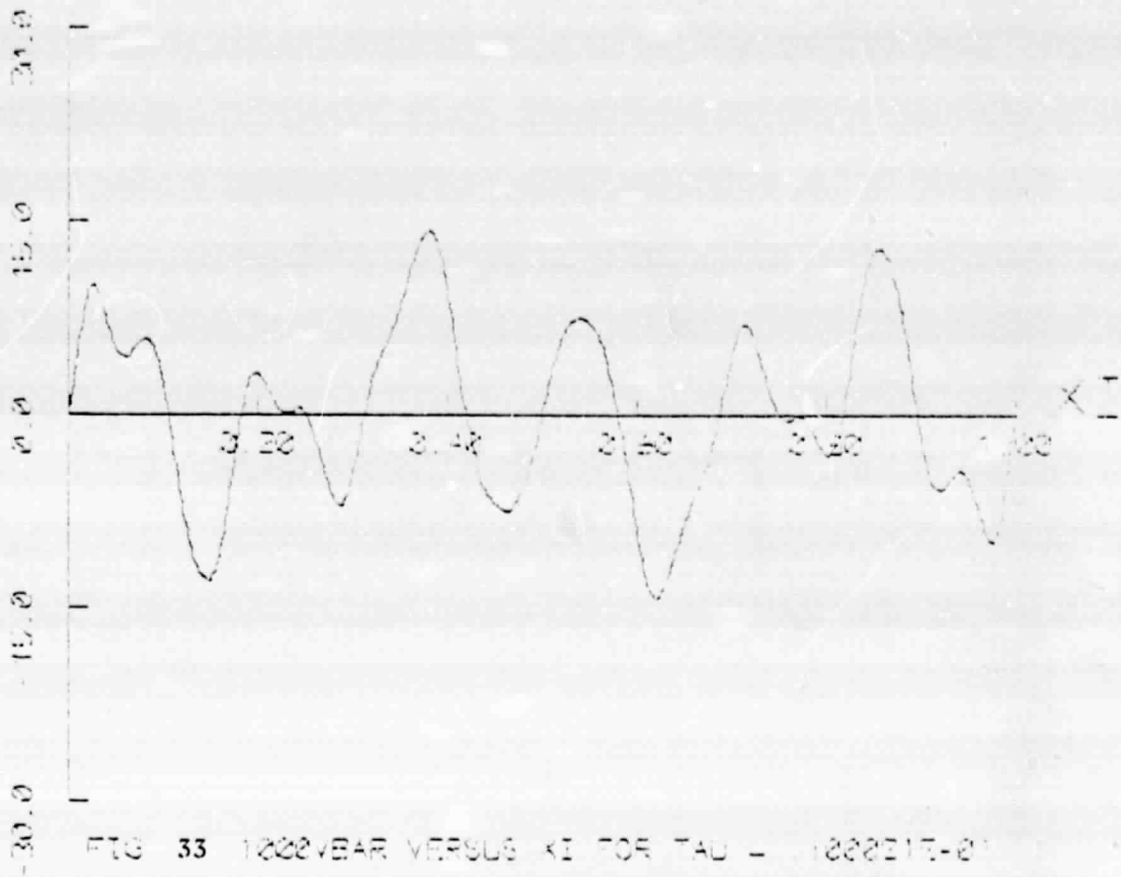

FIG 33 1000*BAR VERSUS XI FOR TAU = 1.0222E17-01

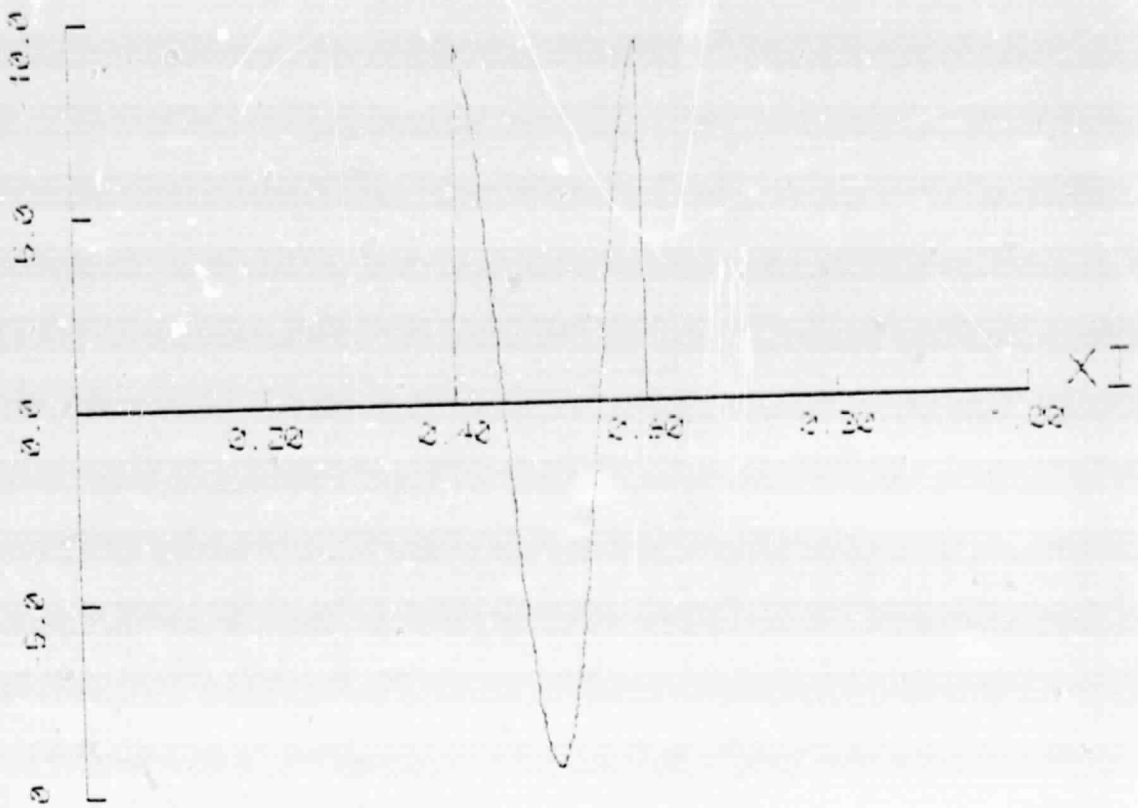

FIG 34 100000*BAR VERSUS XI FOR TAU = .2000000E-00

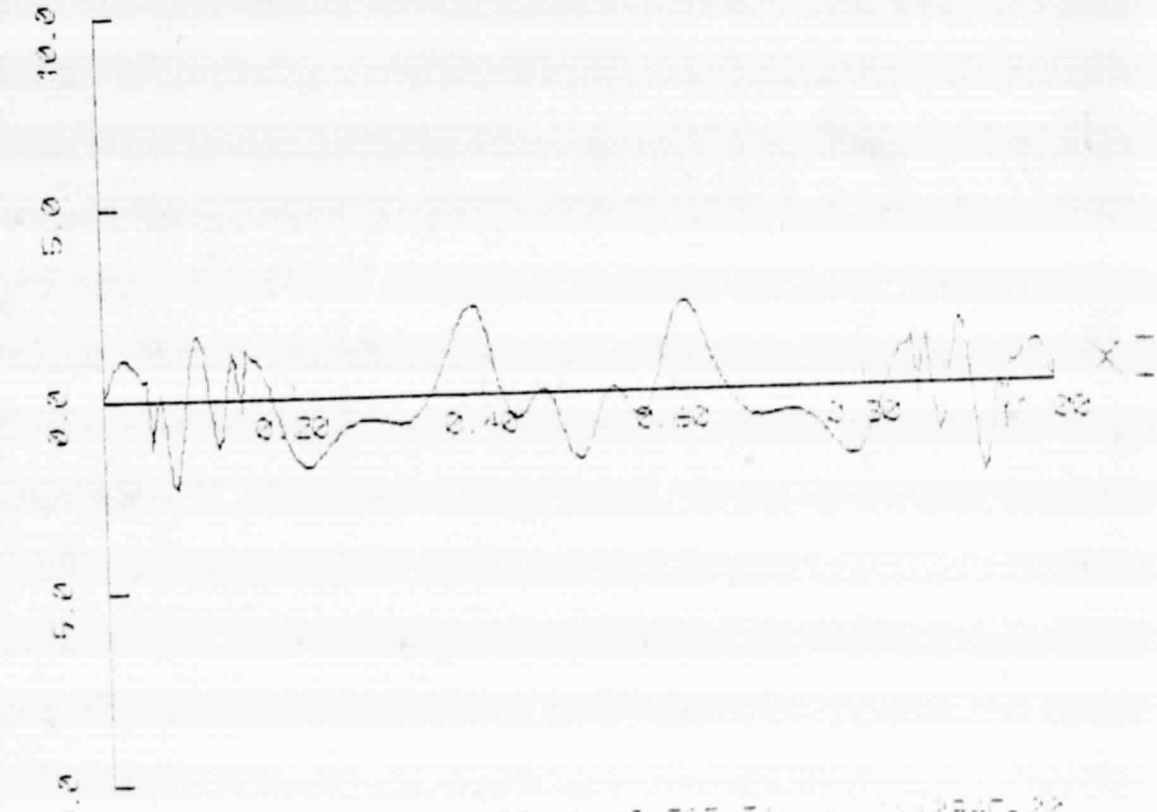

FIG 35 .2000000E-F VERSUS XI FOR TAU = .[illegible]E-02

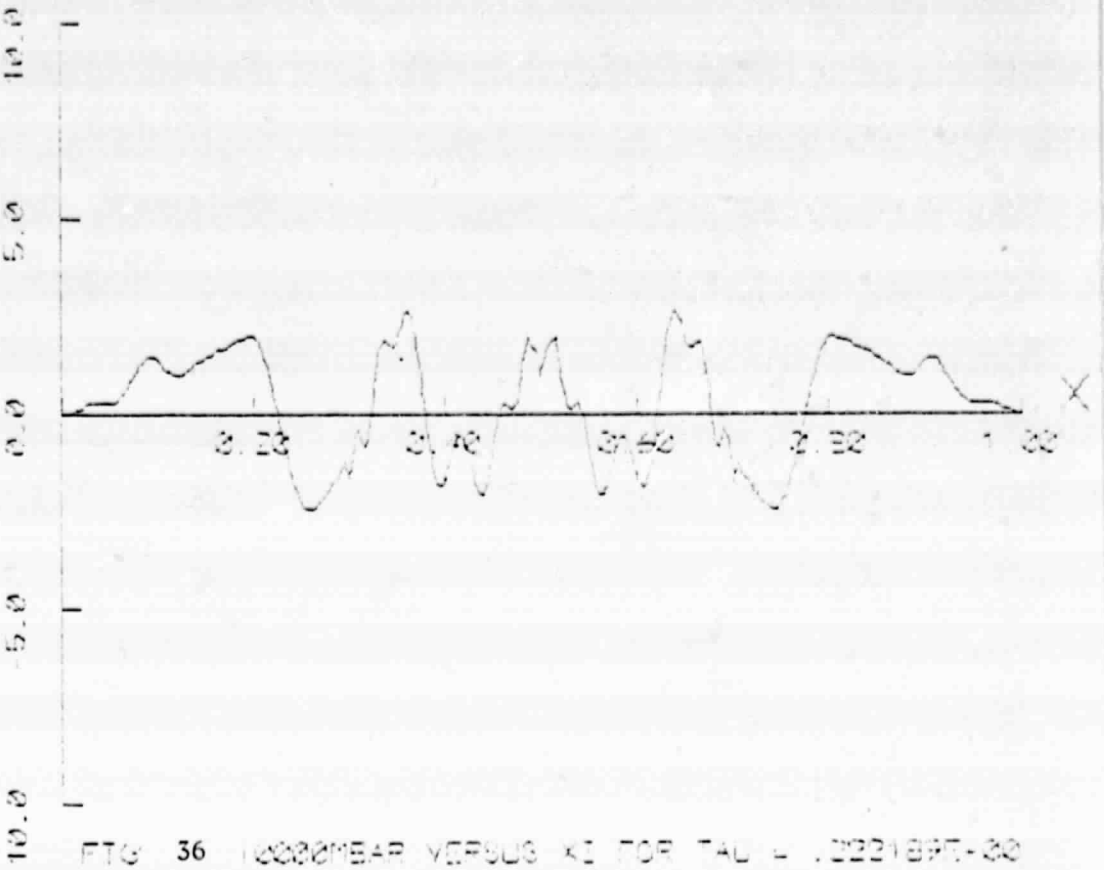

FIG 36 400000MBAR VERSUS KI FOR TAU = .0221897-00

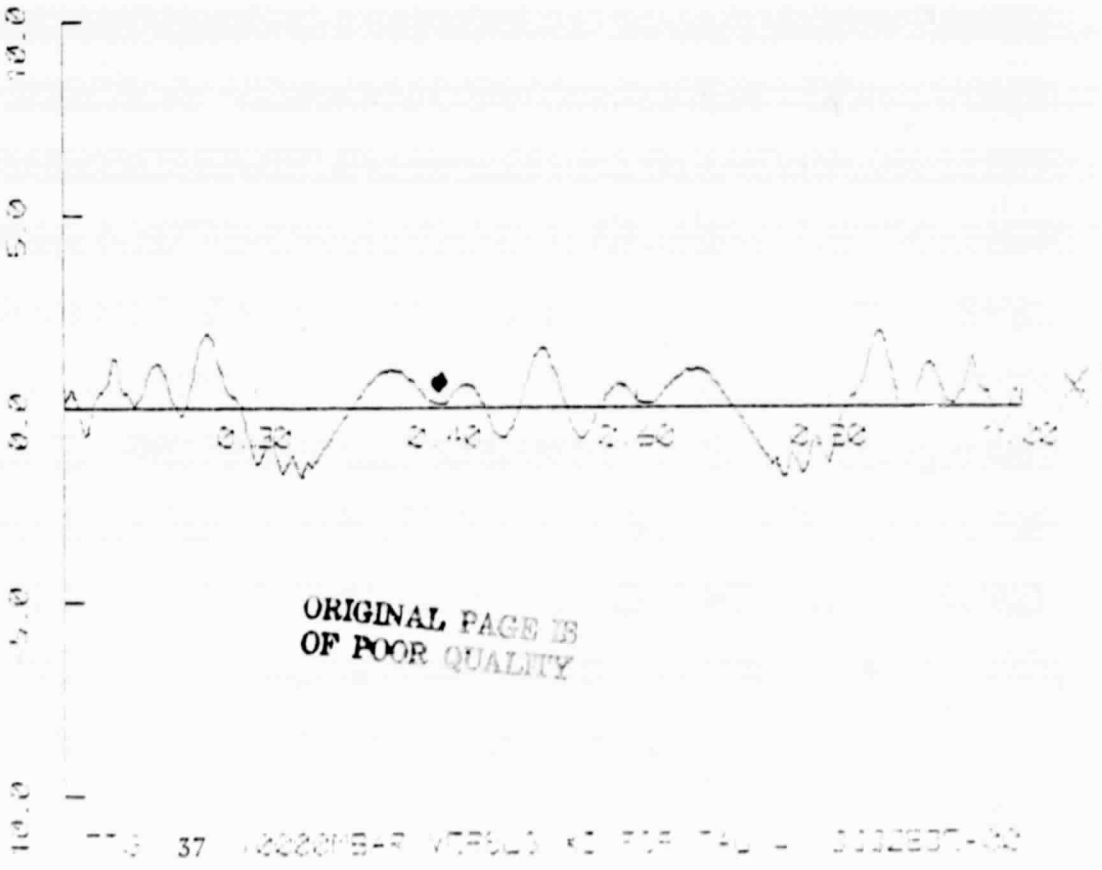

ORIGINAL PAGE IS
OF POOR QUALITY

FIG 37 400000MBAR VERSUS KI FOR TAU = .0112837-00

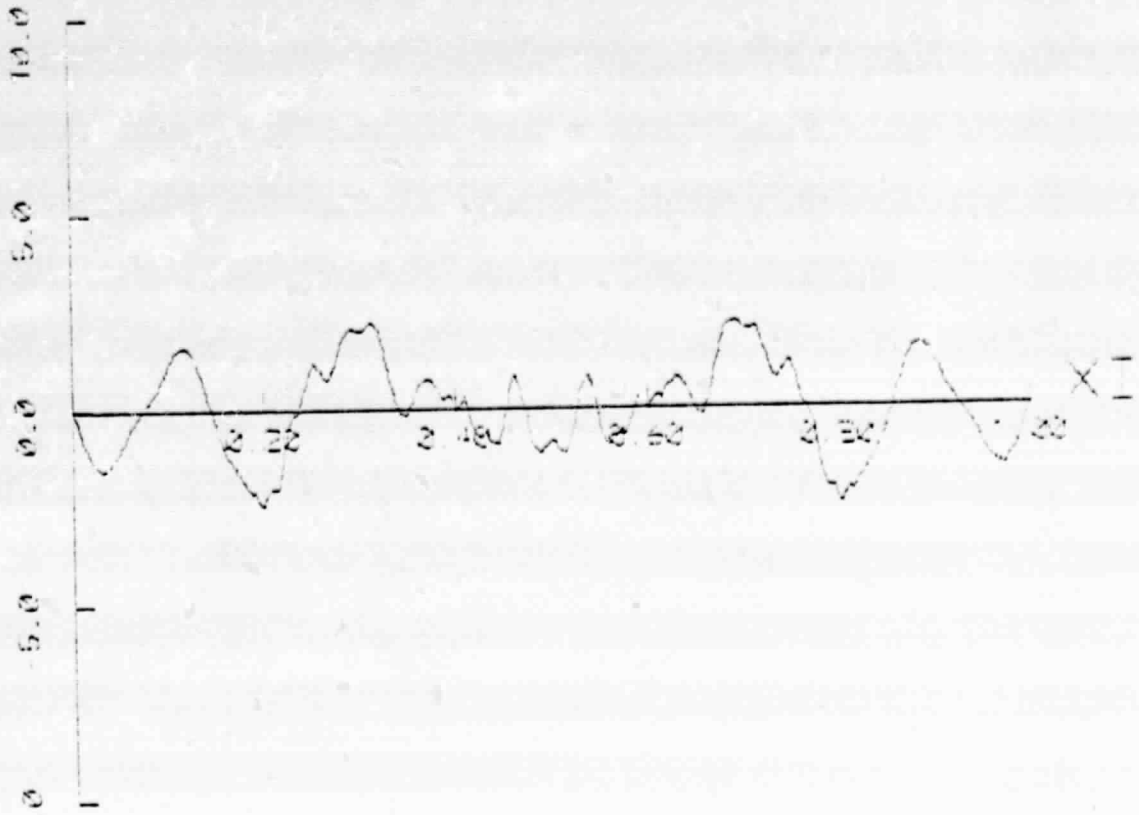

FIG 38 12000MBAR VERSUS XI FOR TAU = .4443750E-02

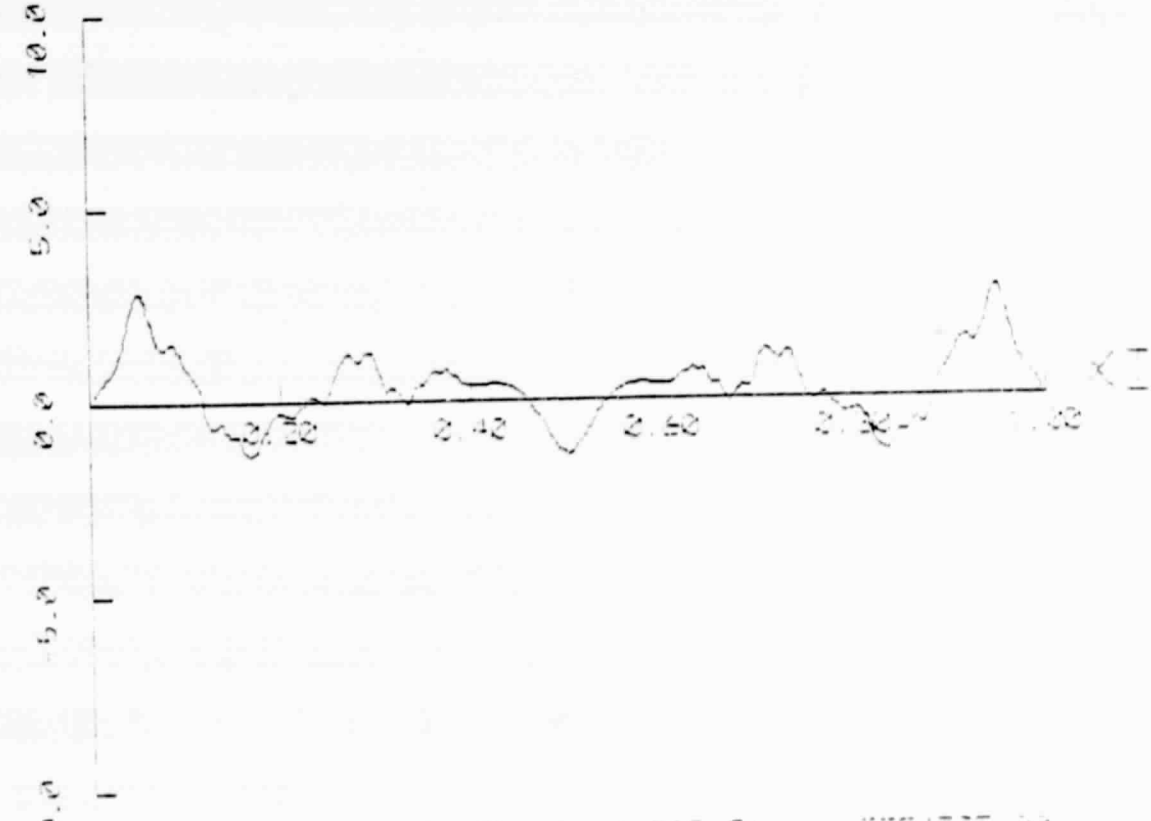

FIG 39 12000MBAR VERSUS XI FOR TAU = 0.0000000E+00

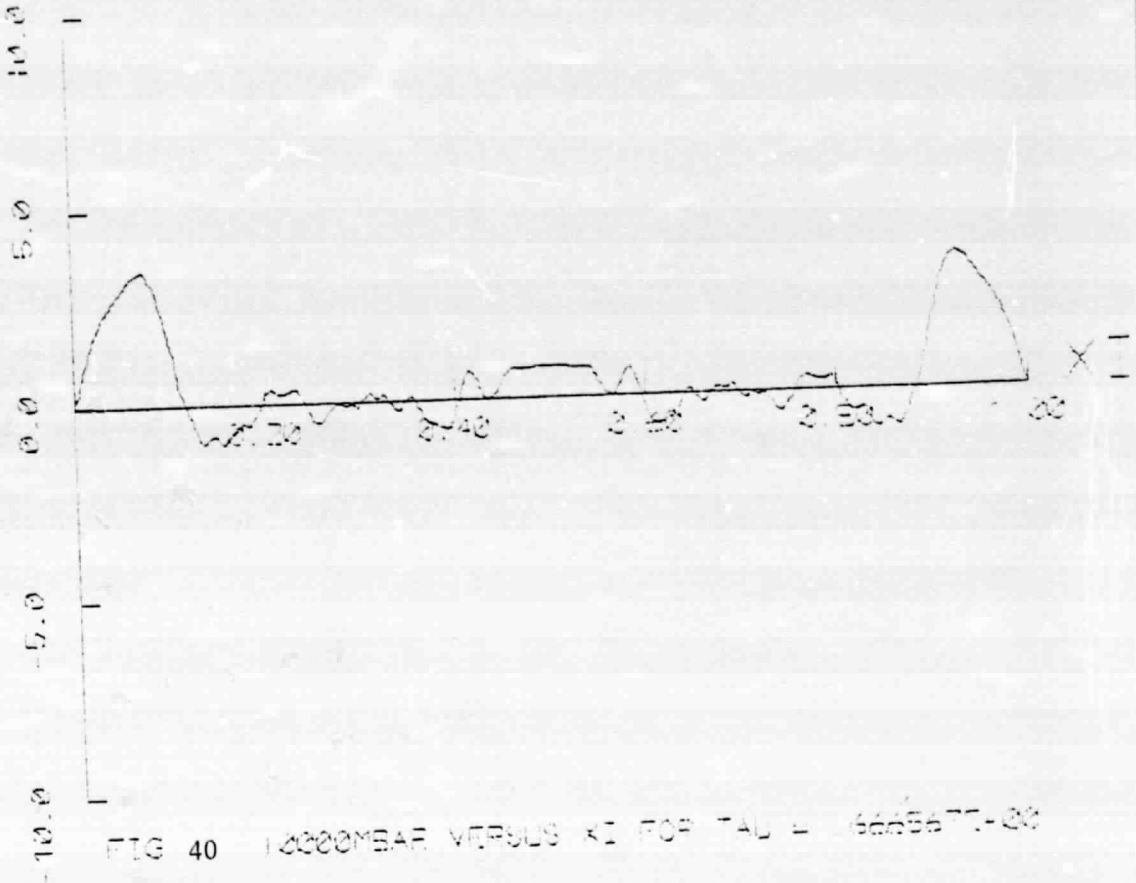

FIG 40 16000MBAR VERSUS KI FOR TAU = 66656T-00

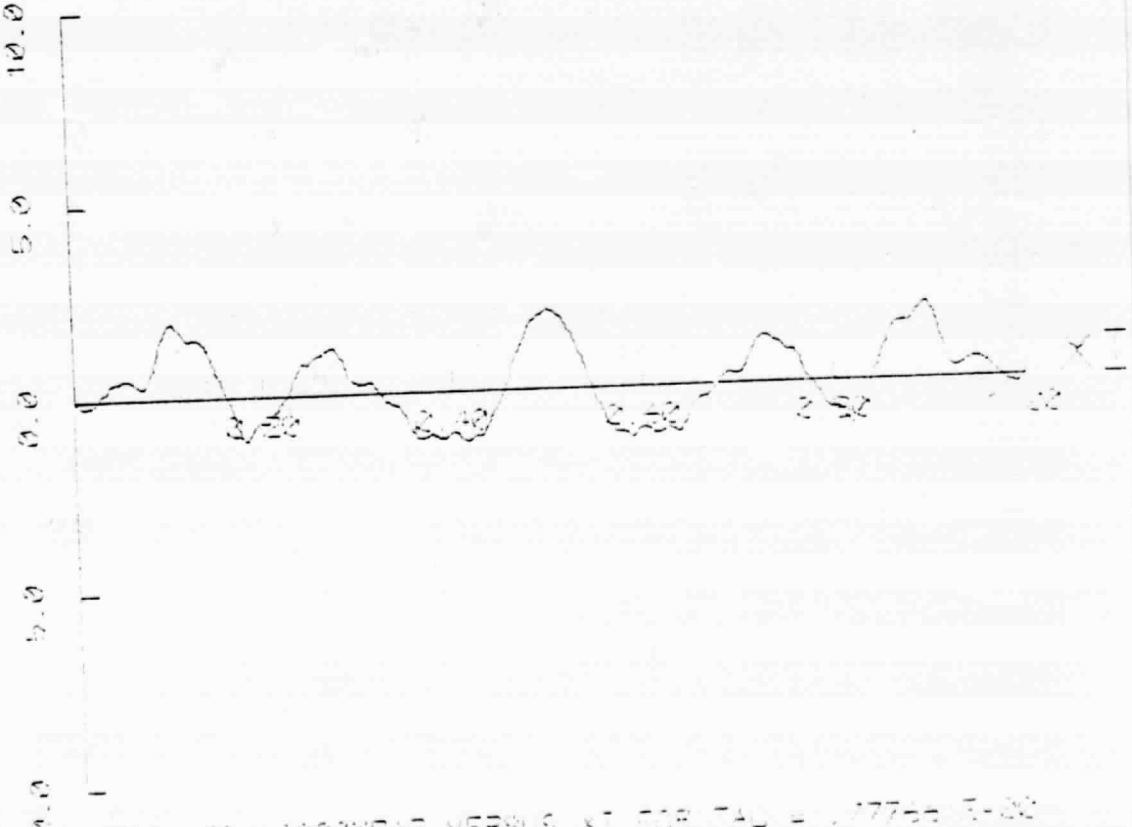

FIG 41 16000MBAR VERSUS KI FOR TAU = .177E-02

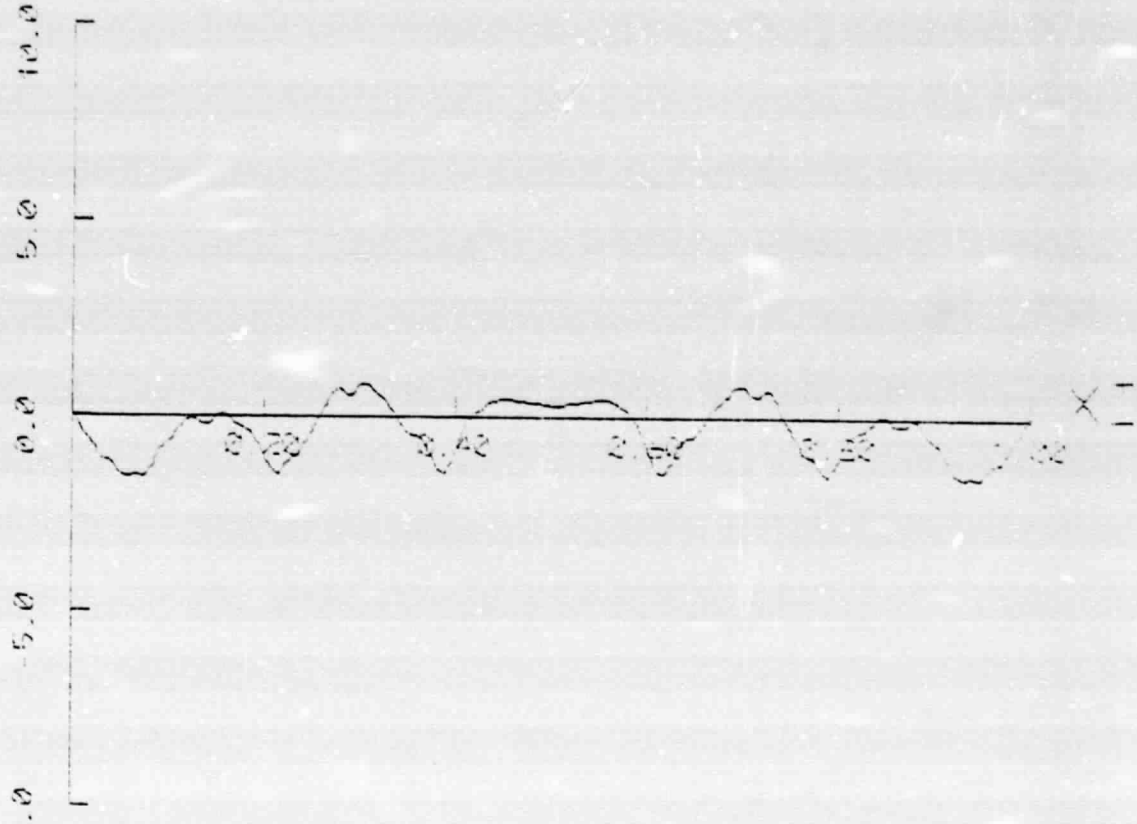

FIG 42 10000MBAR VERSUS XI FOR TAU = .8887557-04

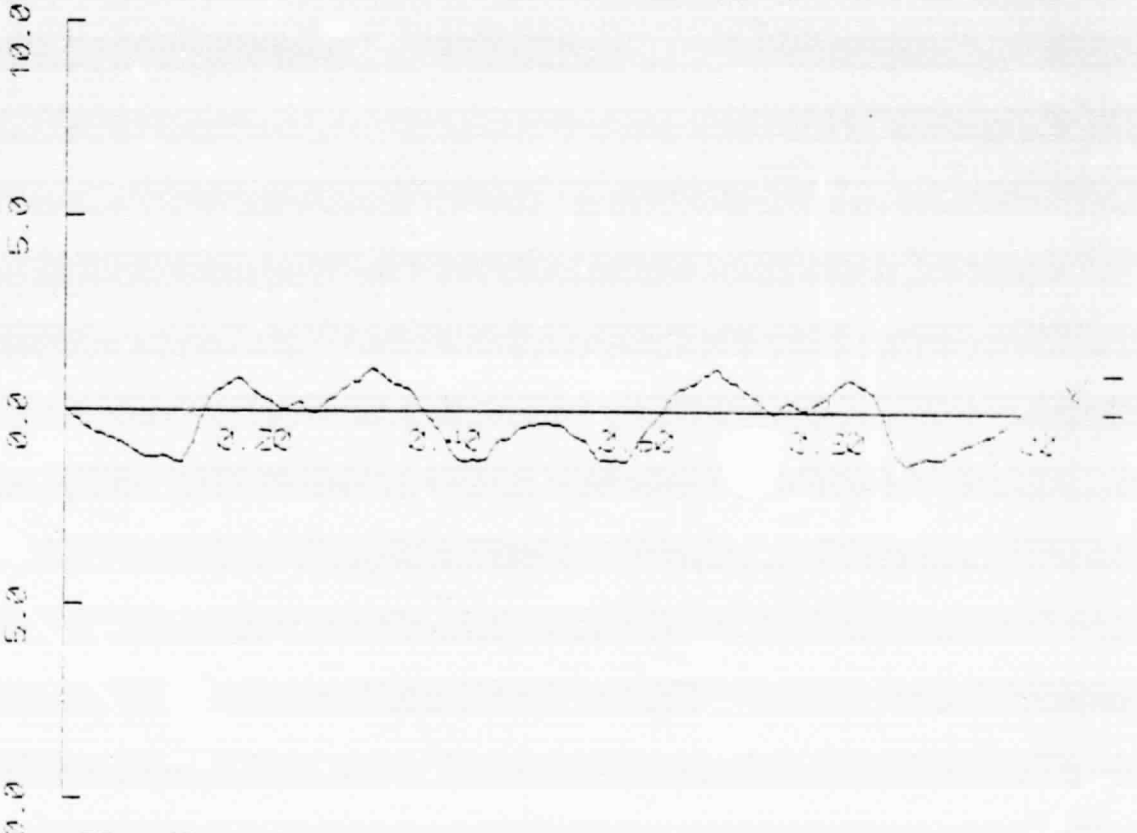

FIG 43 10000MBAR VERSUS XI FOR TAU = .8887557-04

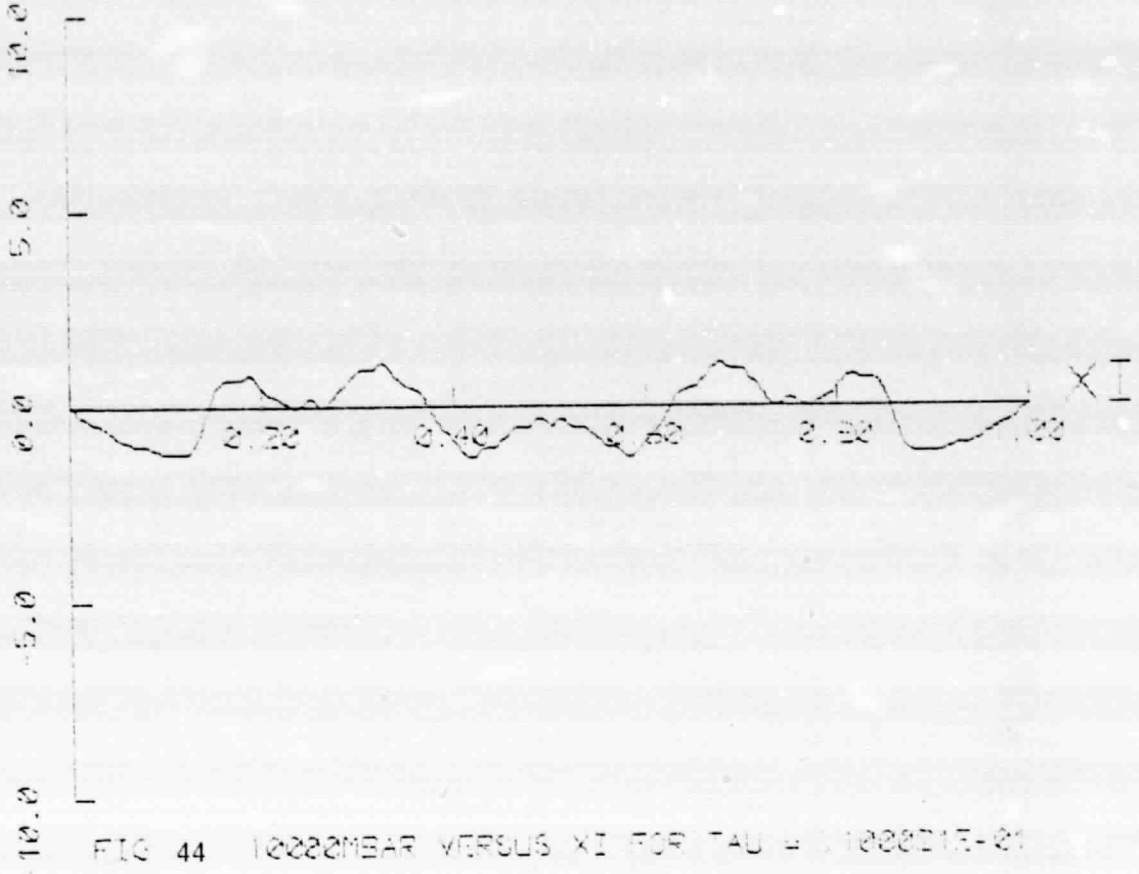

FIG 44 10000MBAR VERSUS XI FOR TAU = .1000E1E-01

APPENDIX H

Response to a (1 + cos) initial displacement;
$V_R = 0.62$, SLR = 50, $\lambda = 0.2$, $\overline{b}_1 = 1.5$, $\overline{b}_2 = 0$.

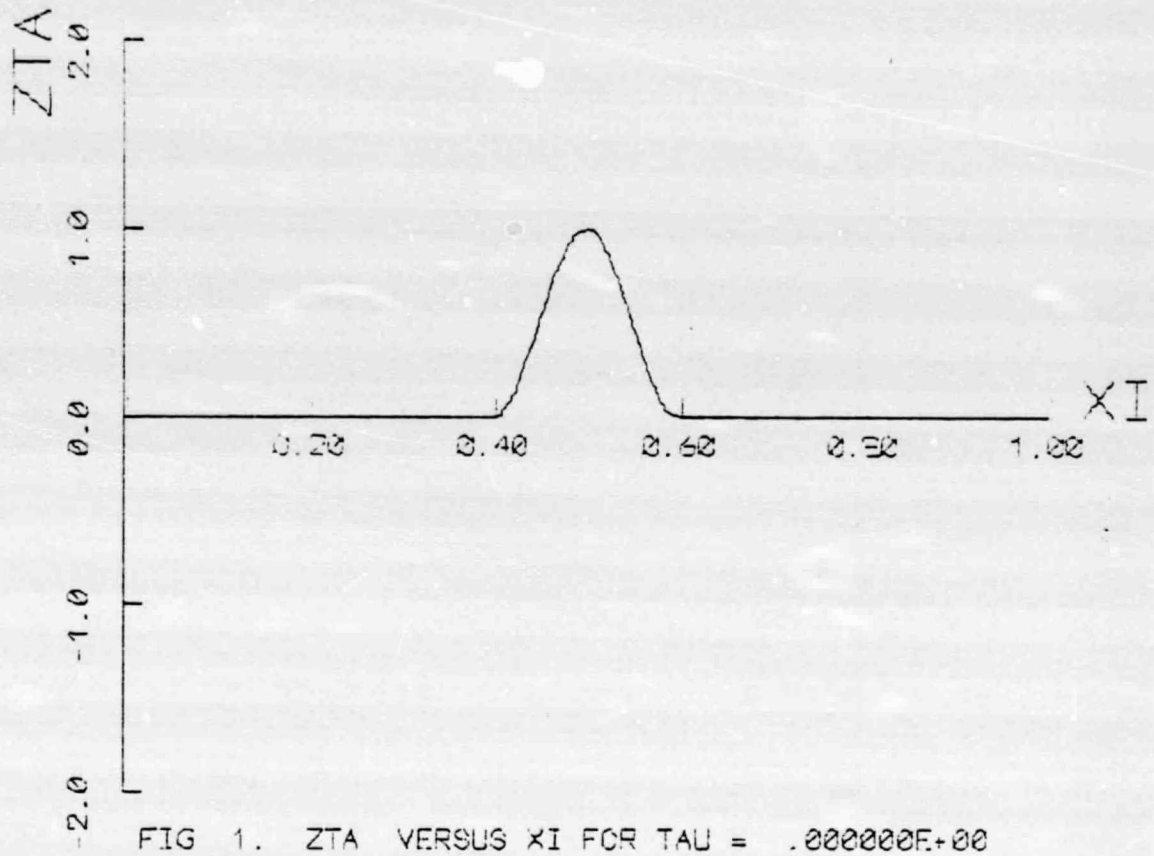

FIG 1. ZTA VERSUS XI FOR TAU = .000000E+00

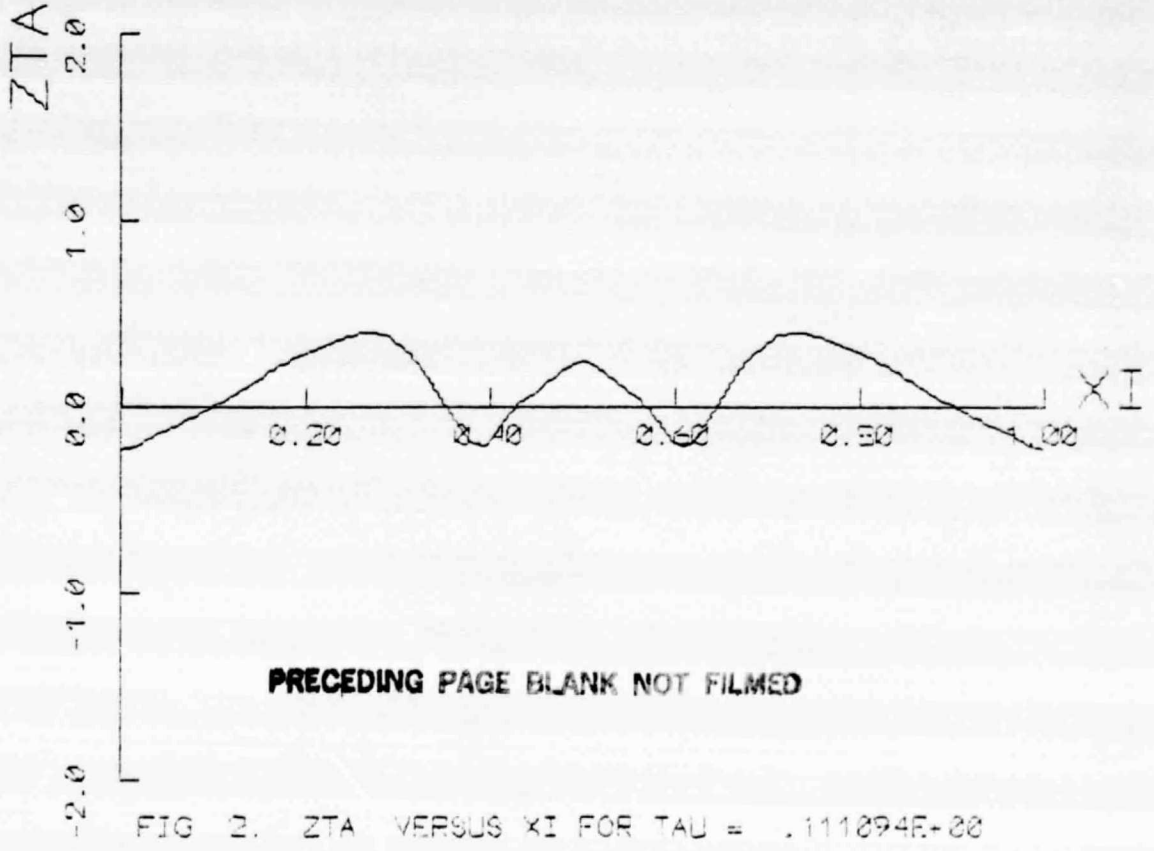

PRECEDING PAGE BLANK NOT FILMED

FIG 2. ZTA VERSUS XI FOR TAU = .111894E+00

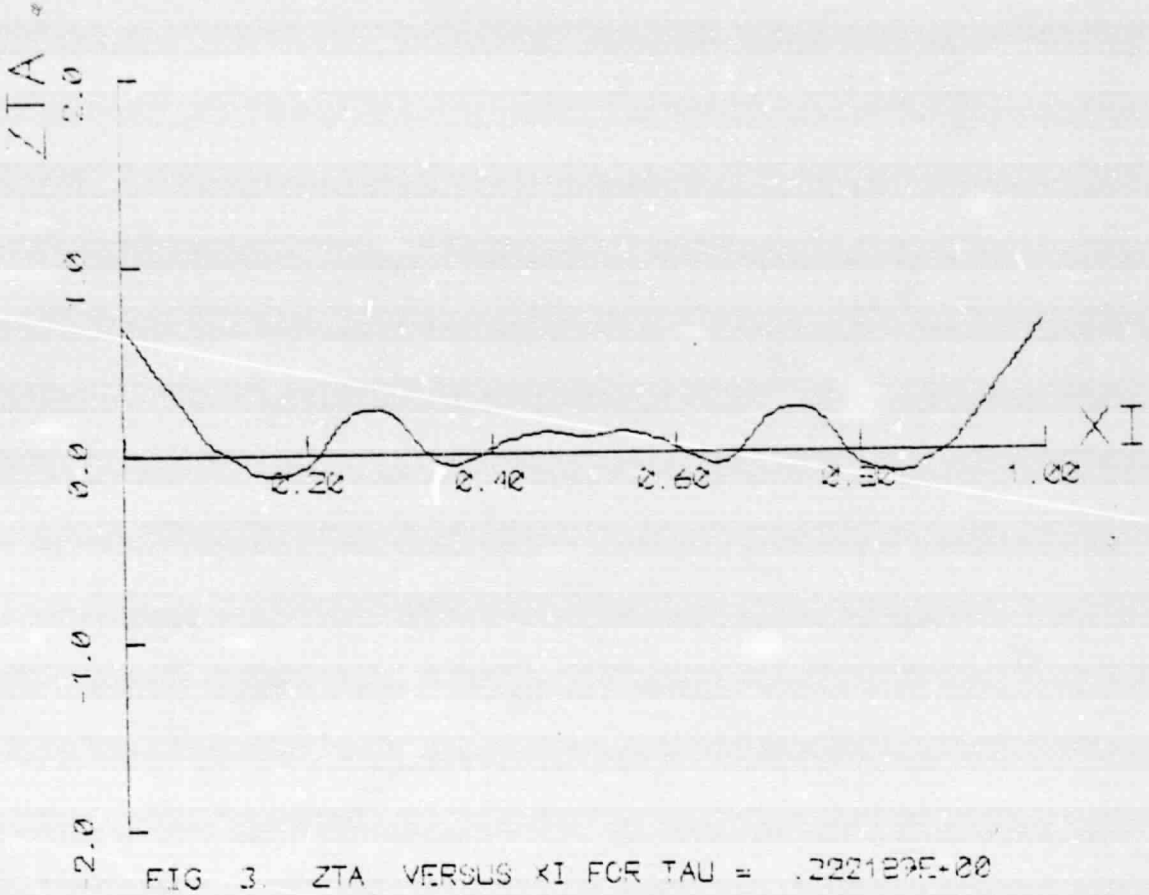

FIG 3. ZTA VERSUS XI FOR TAU = .2221E-00

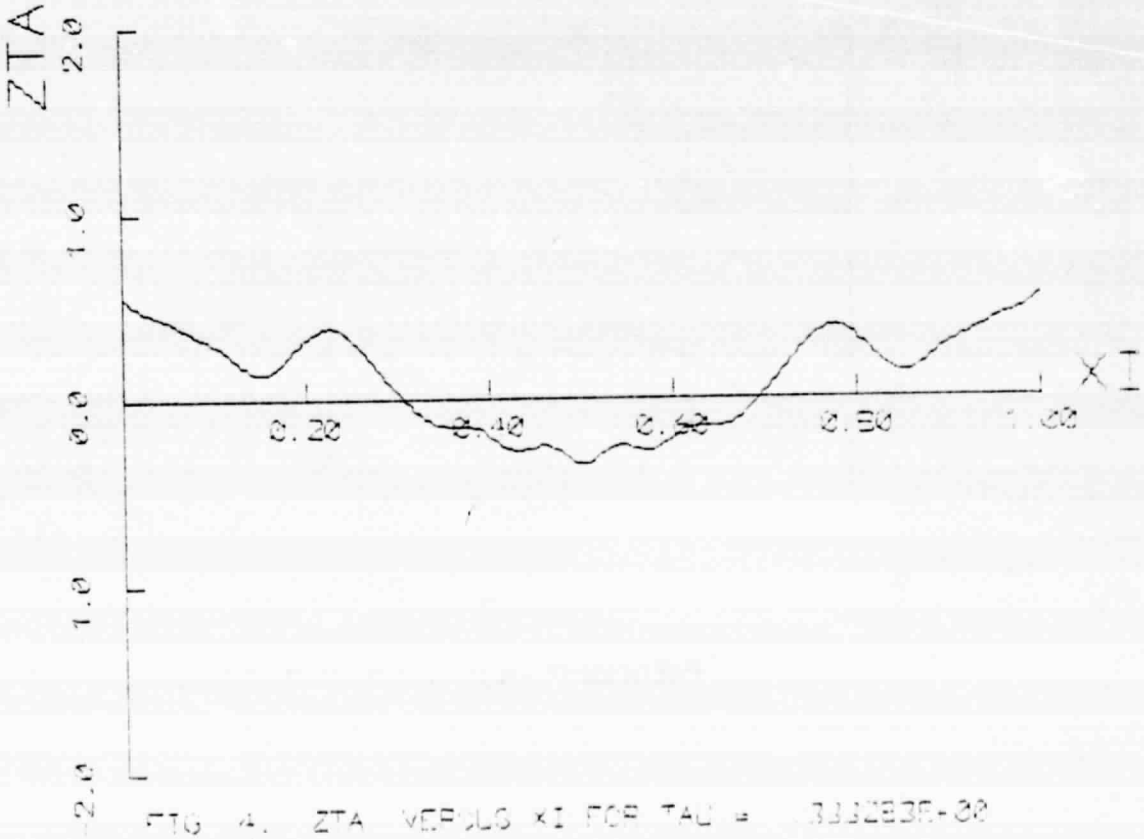

FIG 4. ZTA VERSUS XI FOR TAU = [illegible]

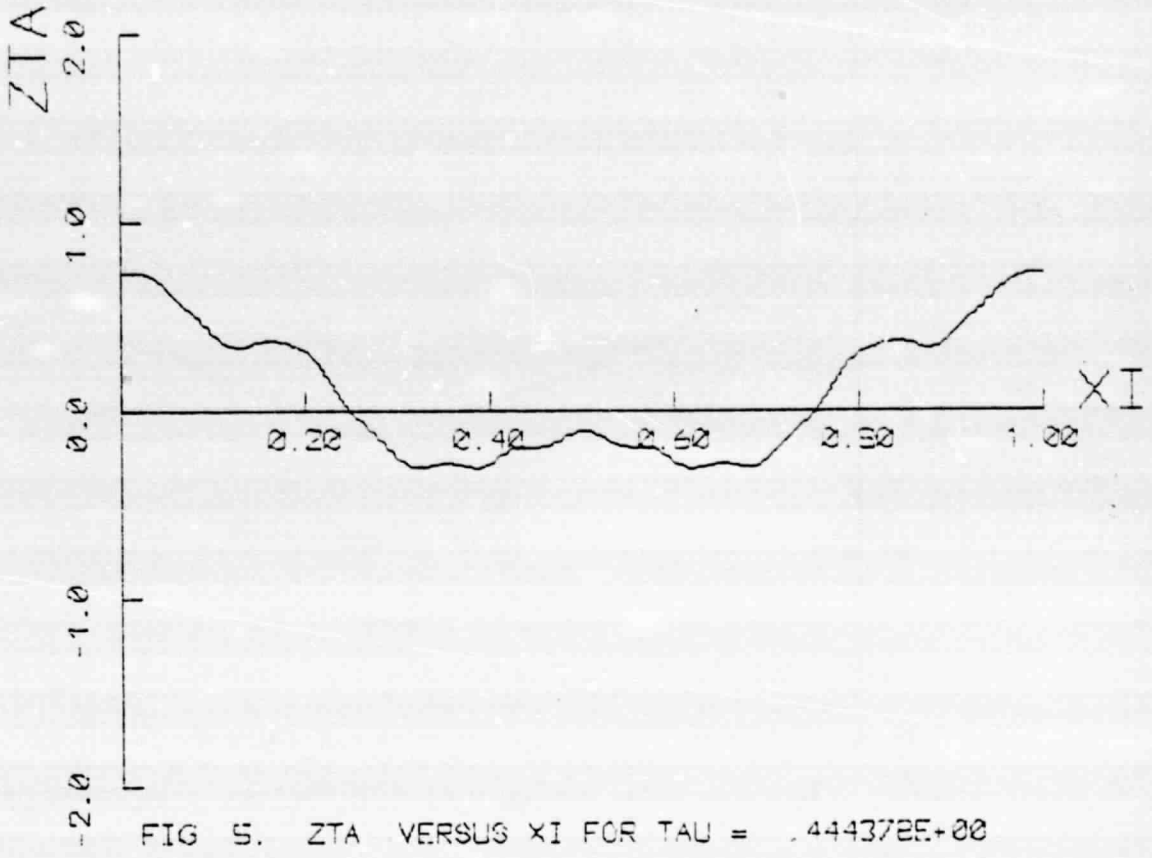

FIG 5. ZTA VERSUS XI FOR TAU = .444372E+00

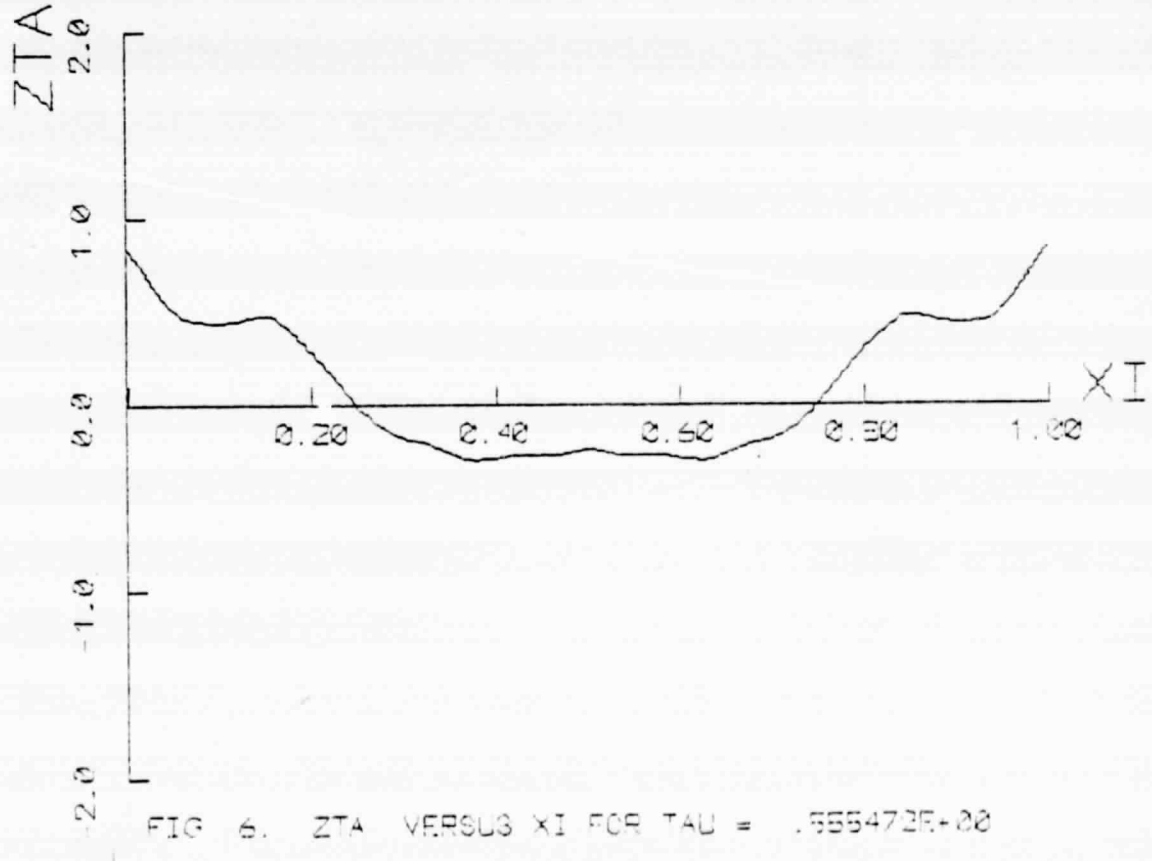

FIG 6. ZTA VERSUS XI FOR TAU = .555472E+00

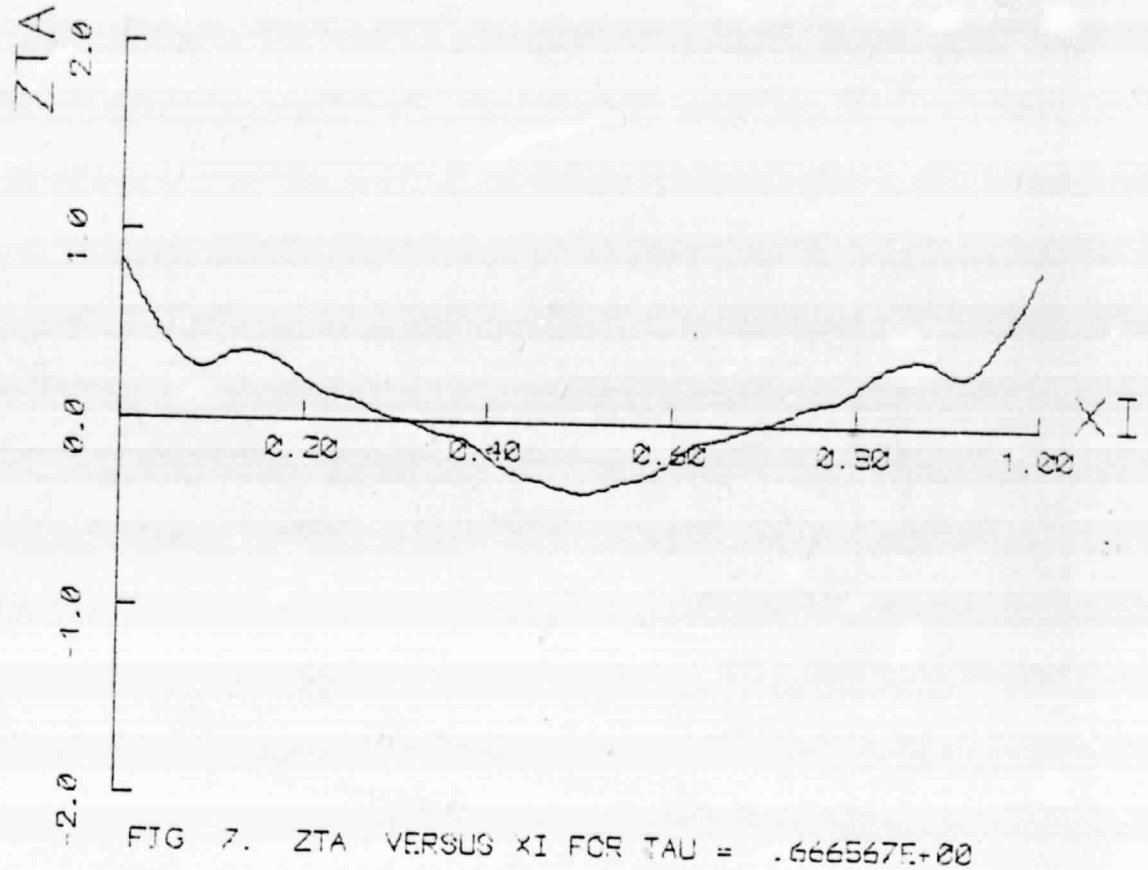

FIG 7. ZTA VERSUS XI FOR TAU = .666567E+00

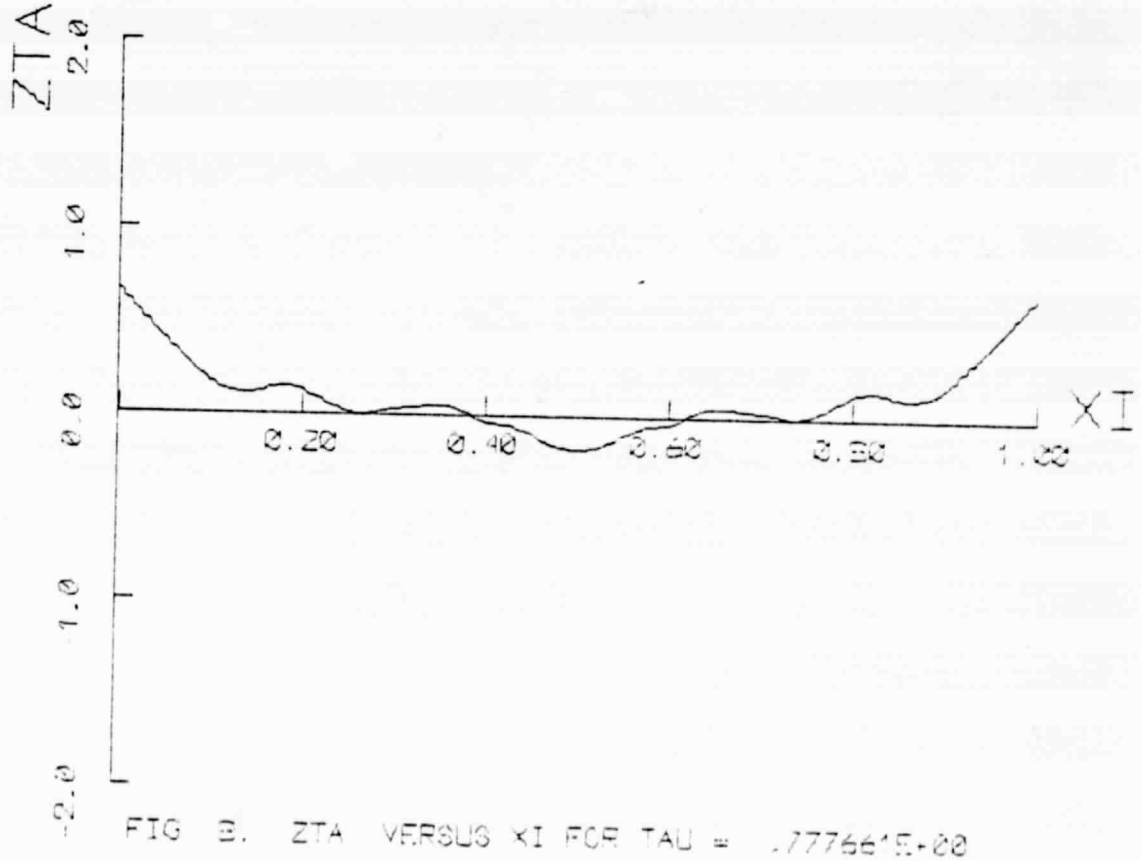

FIG 8. ZTA VERSUS XI FOR TAU = .777661E+00

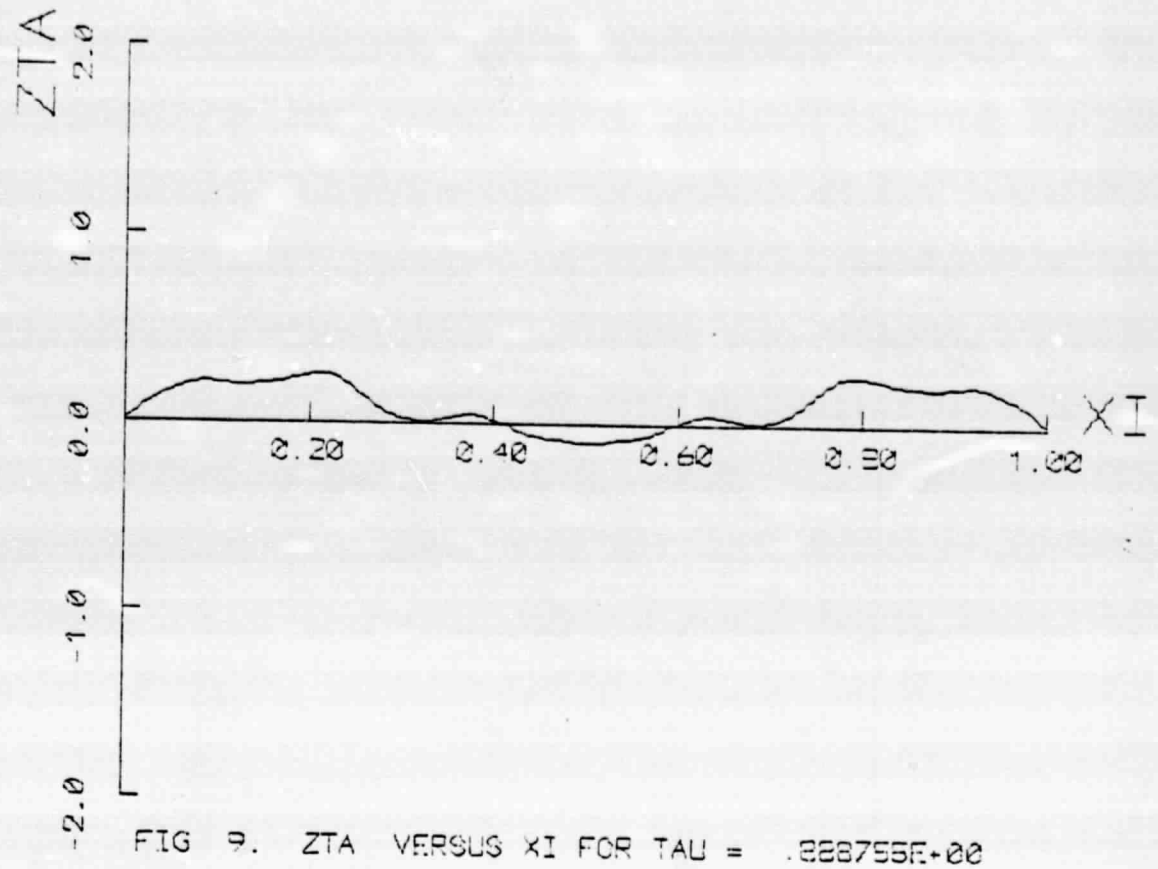

FIG 9. ZTA VERSUS XI FOR TAU = .888755E+00

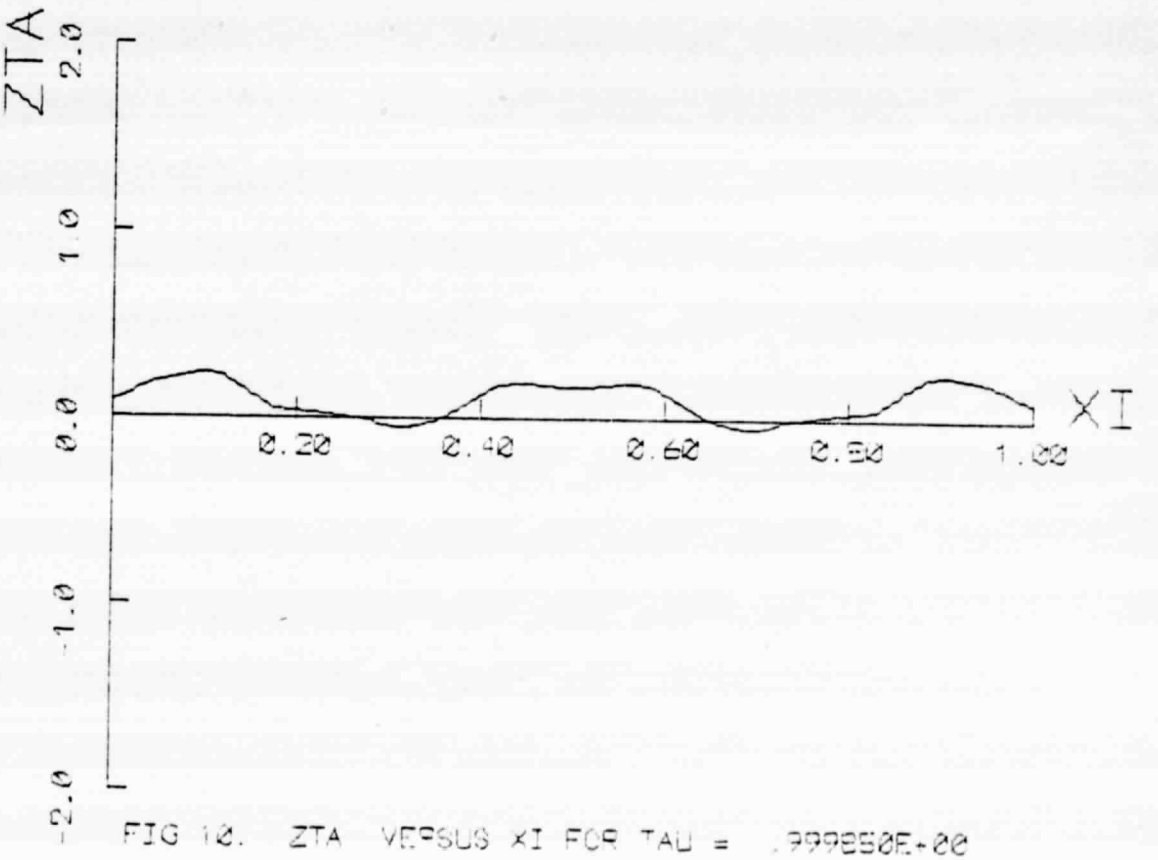

FIG 10. ZTA VERSUS XI FOR TAU = .999850E+00

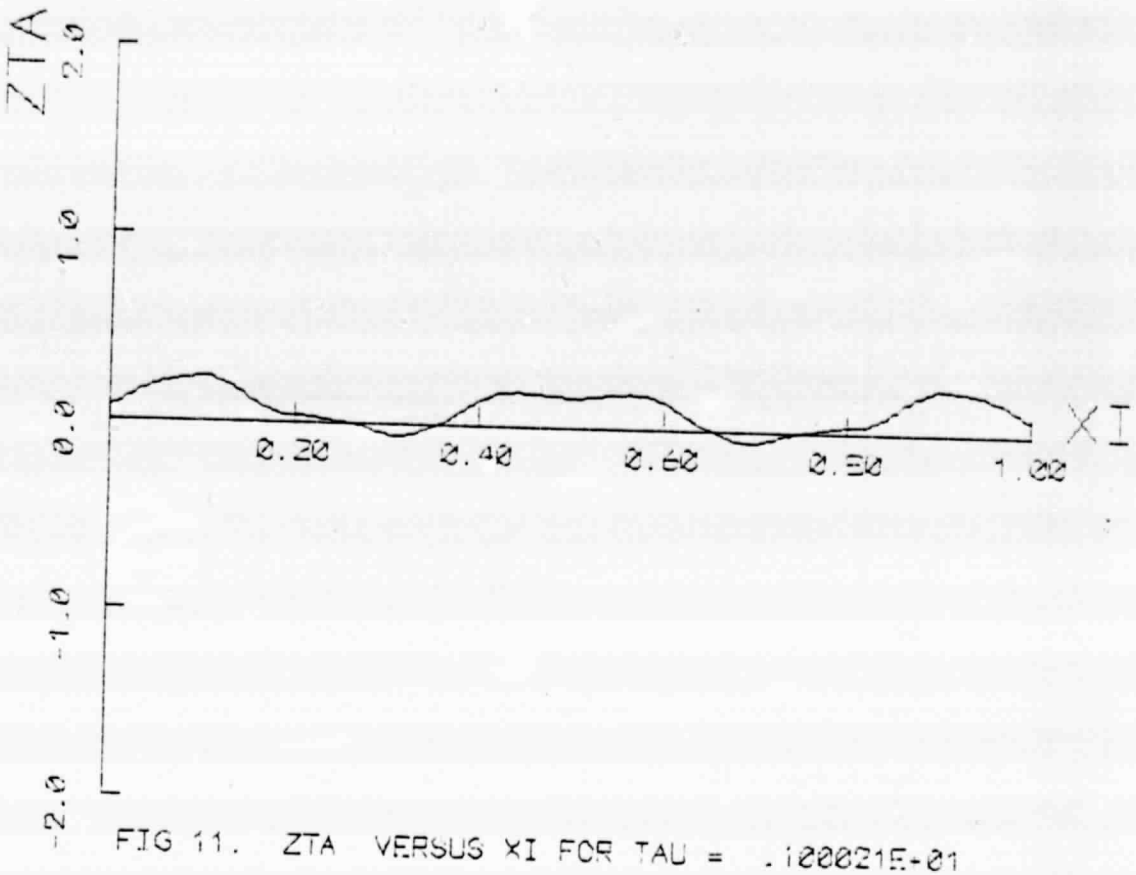

FIG 11. ZTA VERSUS XI FOR TAU = .100021E-01

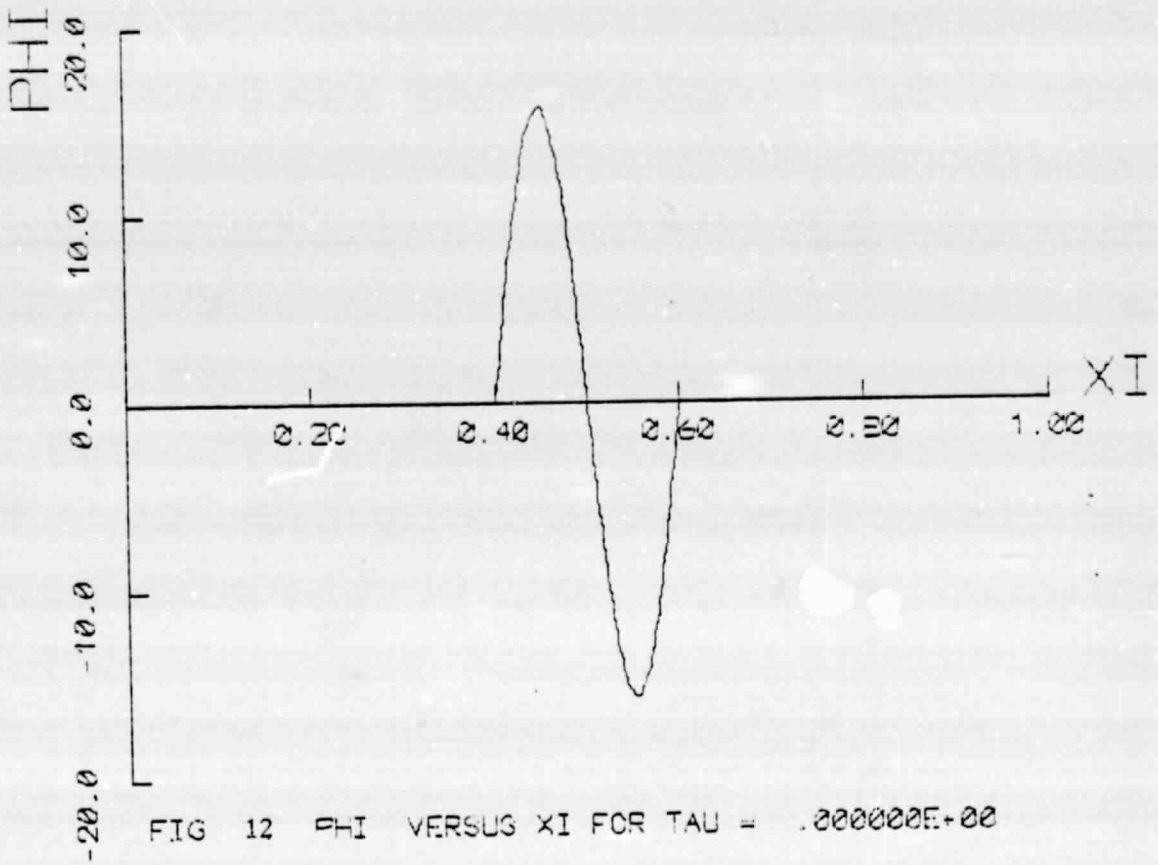

FIG 12 PHI VERSUS XI FOR TAU = .000000E+00

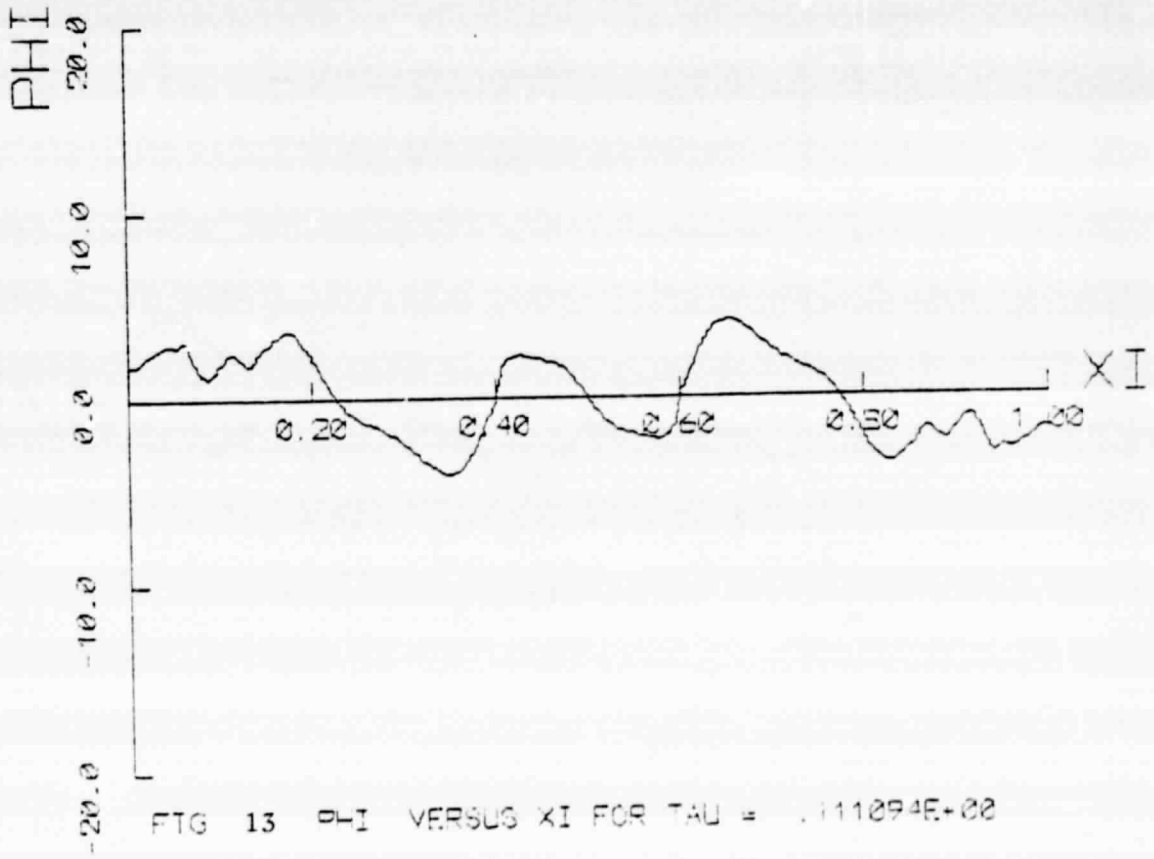

FIG 13 PHI VERSUS XI FOR TAU = .111094E+00

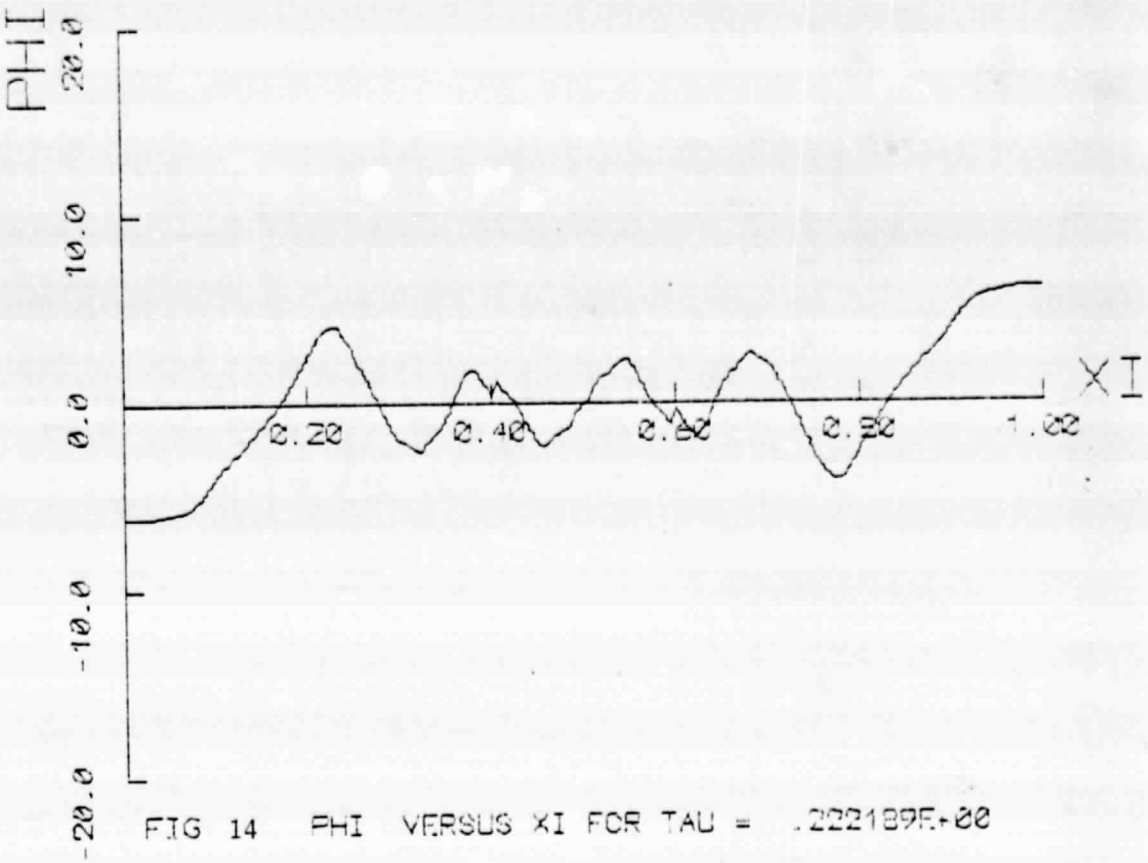

FIG 14 PHI VERSUS XI FOR TAU = .222189E+00

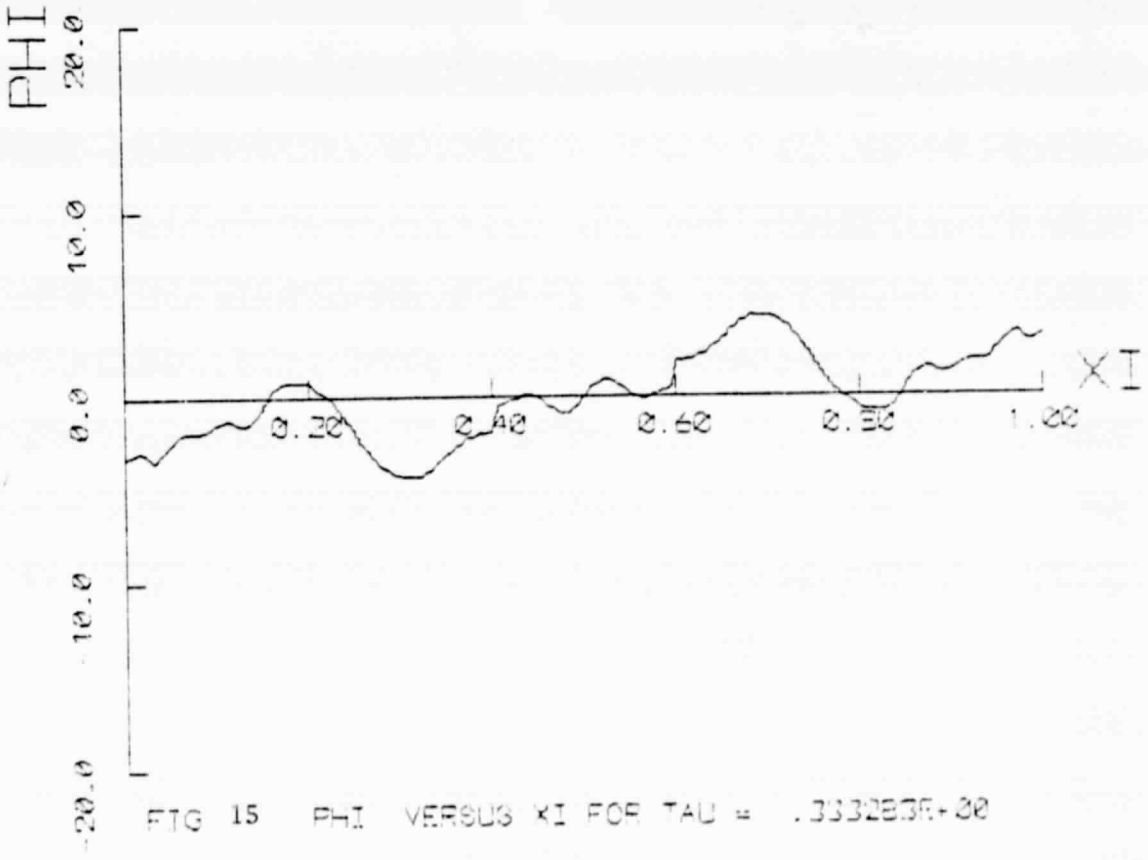

FIG 15 PHI VERSUS XI FOR TAU = .333283E+00

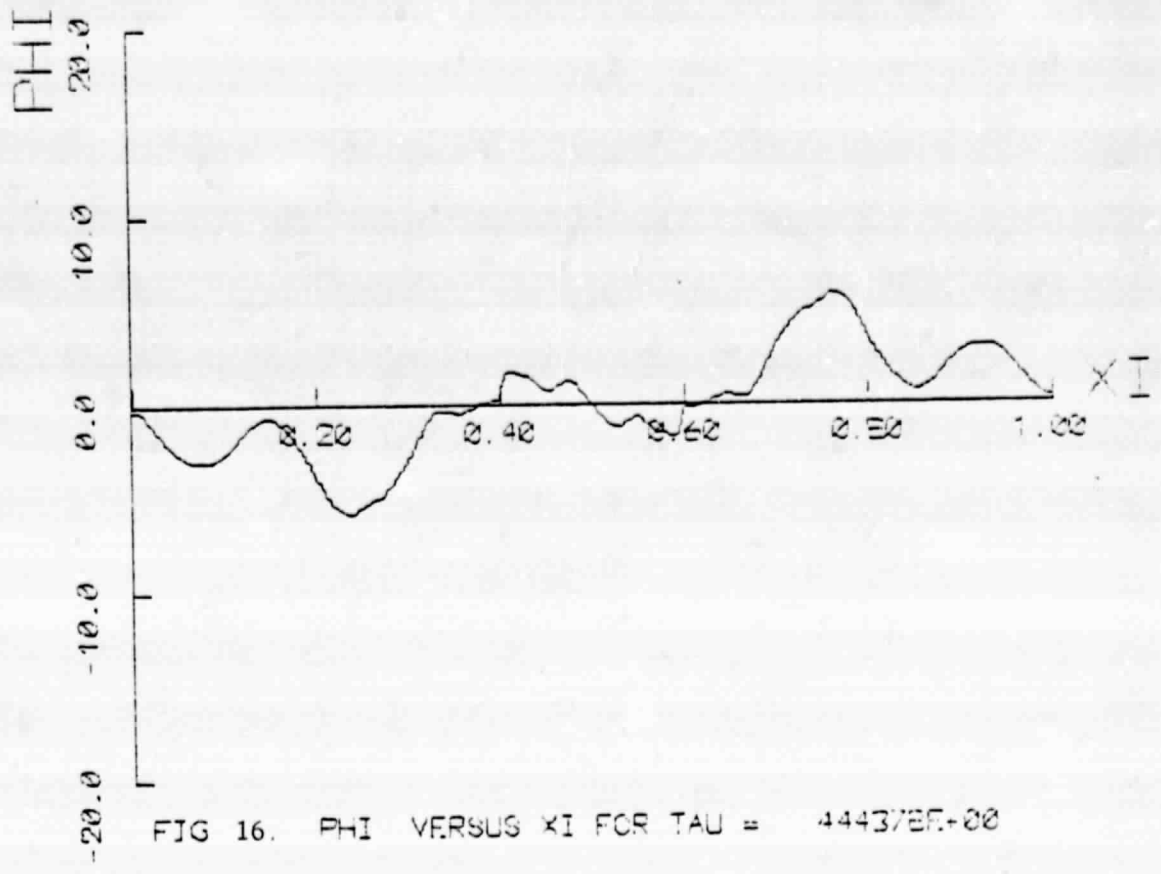

FIG 16. PHI VERSUS XI FOR TAU = 4443?E-00

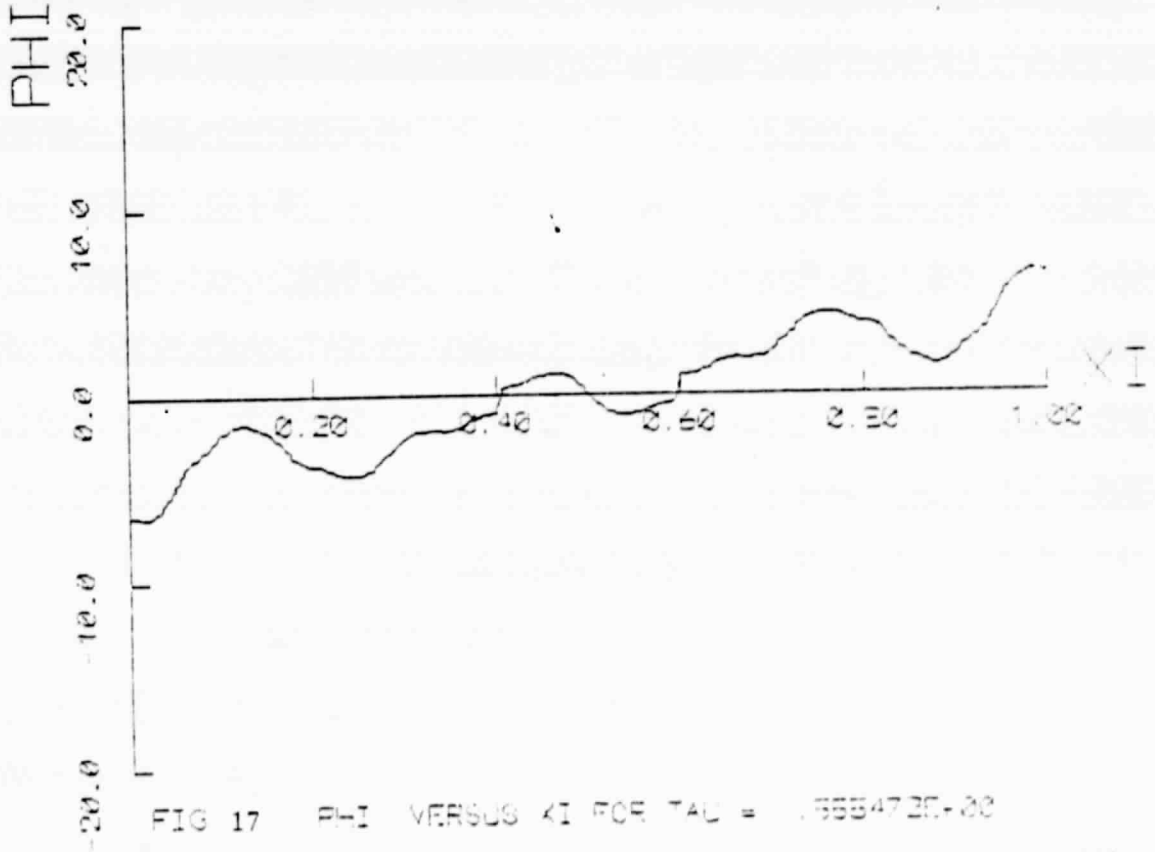

FIG 17 PHI VERSUS XI FOR TAU = .55547?E-00

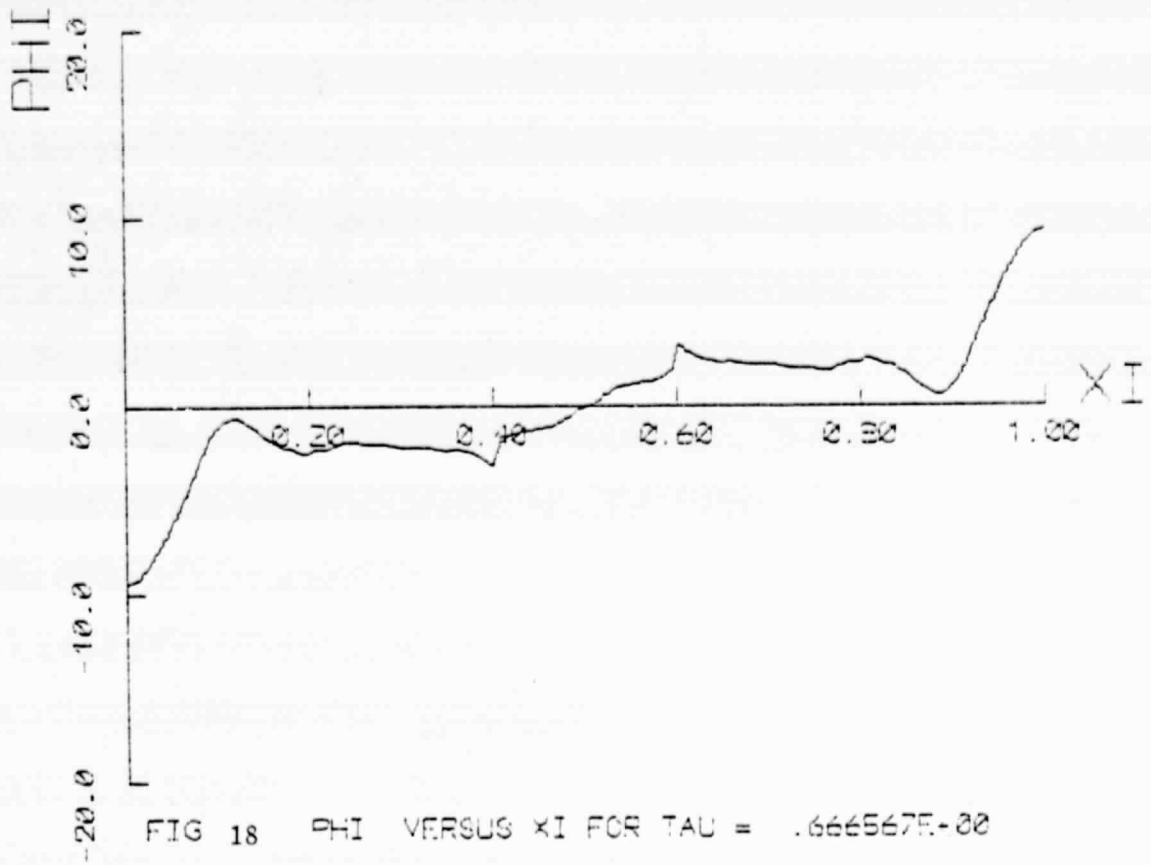

FIG 18 PHI VERSUS XI FOR TAU = .6666667E-00

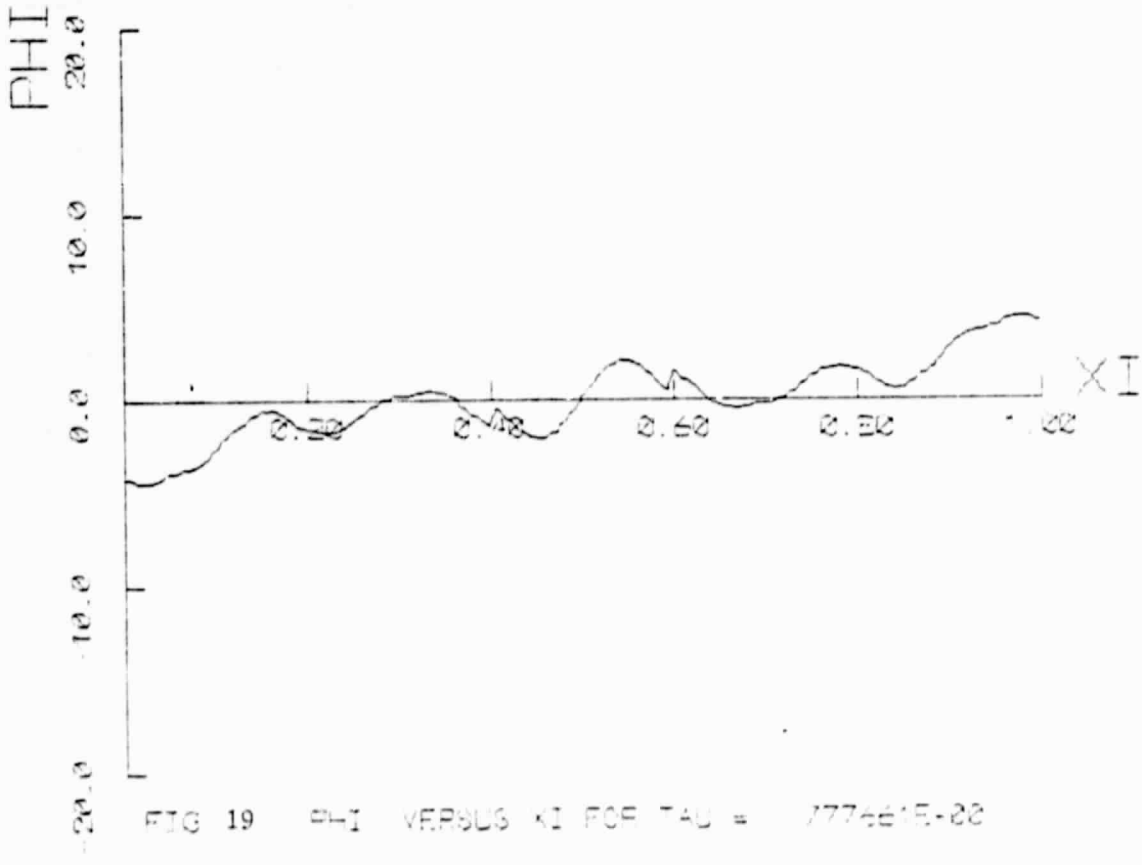

FIG 19 PHI VERSUS XI FOR TAU = .7776615-00

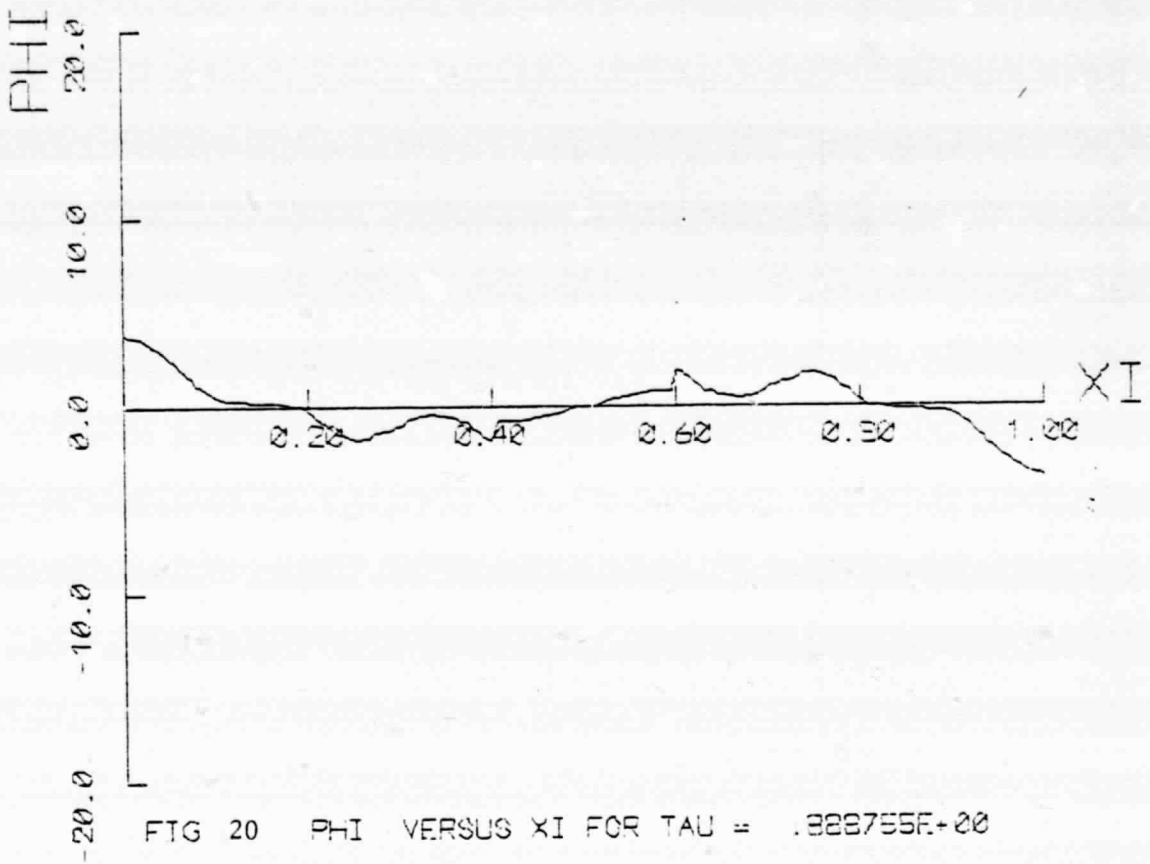

FIG 20 PHI VERSUS XI FOR TAU = .888755E+00

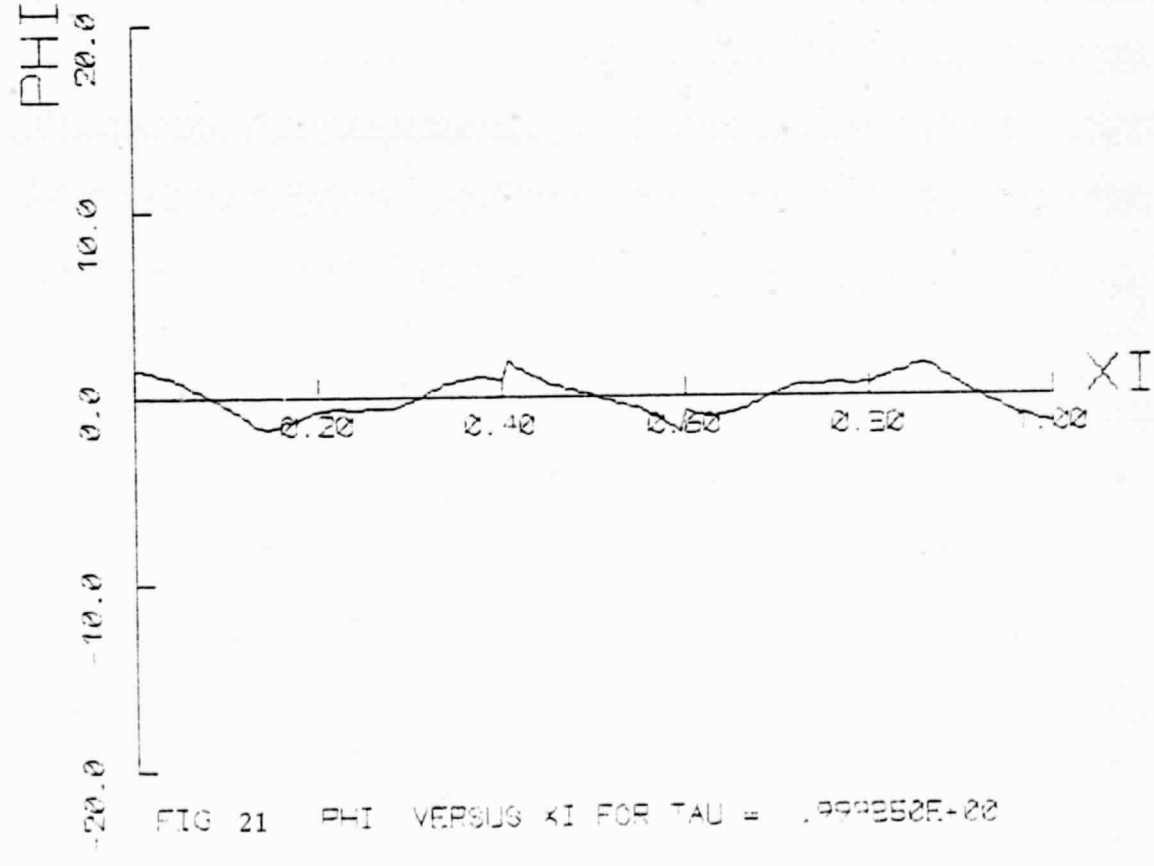

FIG 21 PHI VERSUS XI FOR TAU = .999350E+00

C-2

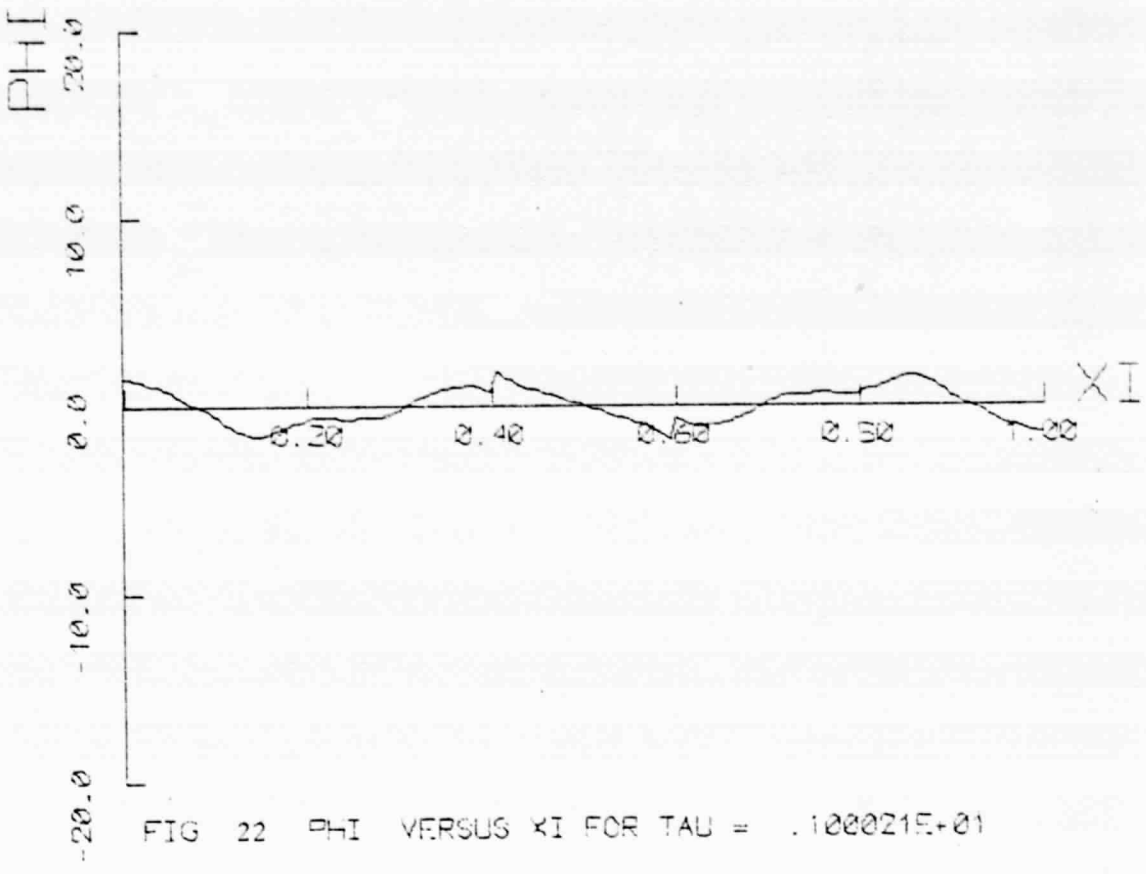

FIG 22 PHI VERSUS XI FOR TAU = .100021E+01

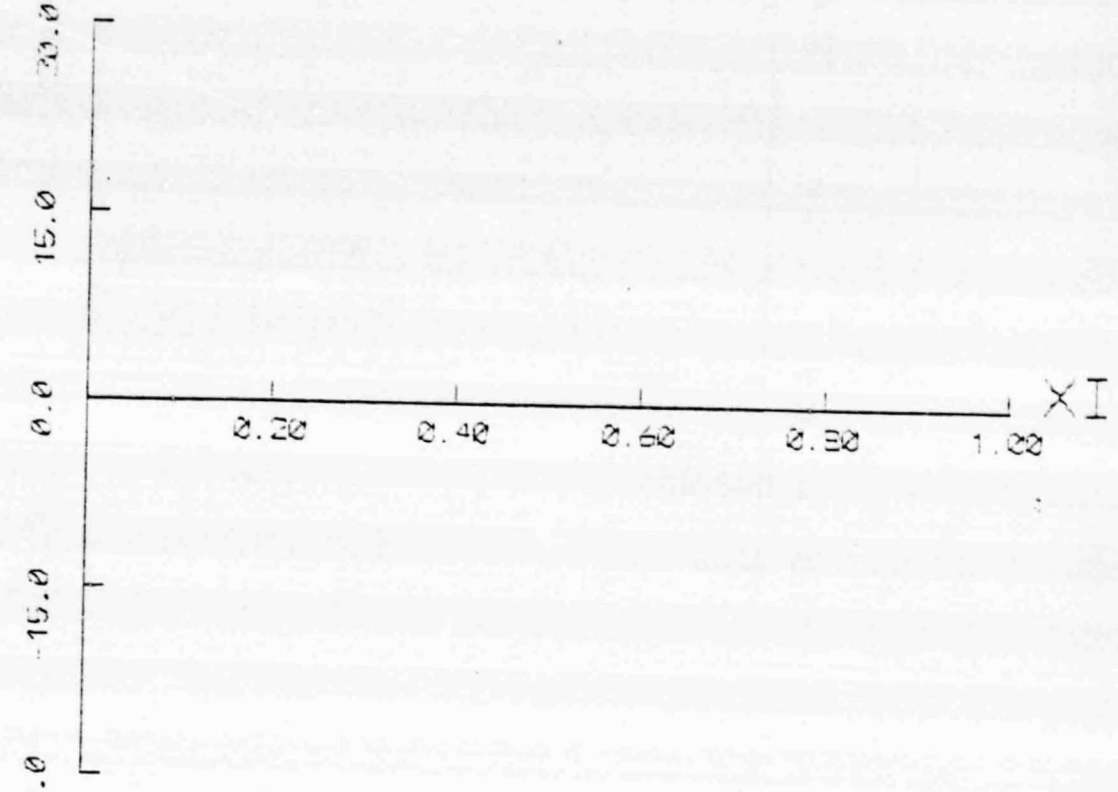

FIG 23 1000VBAR VERSUS XI FOR TAU = .000000E+00

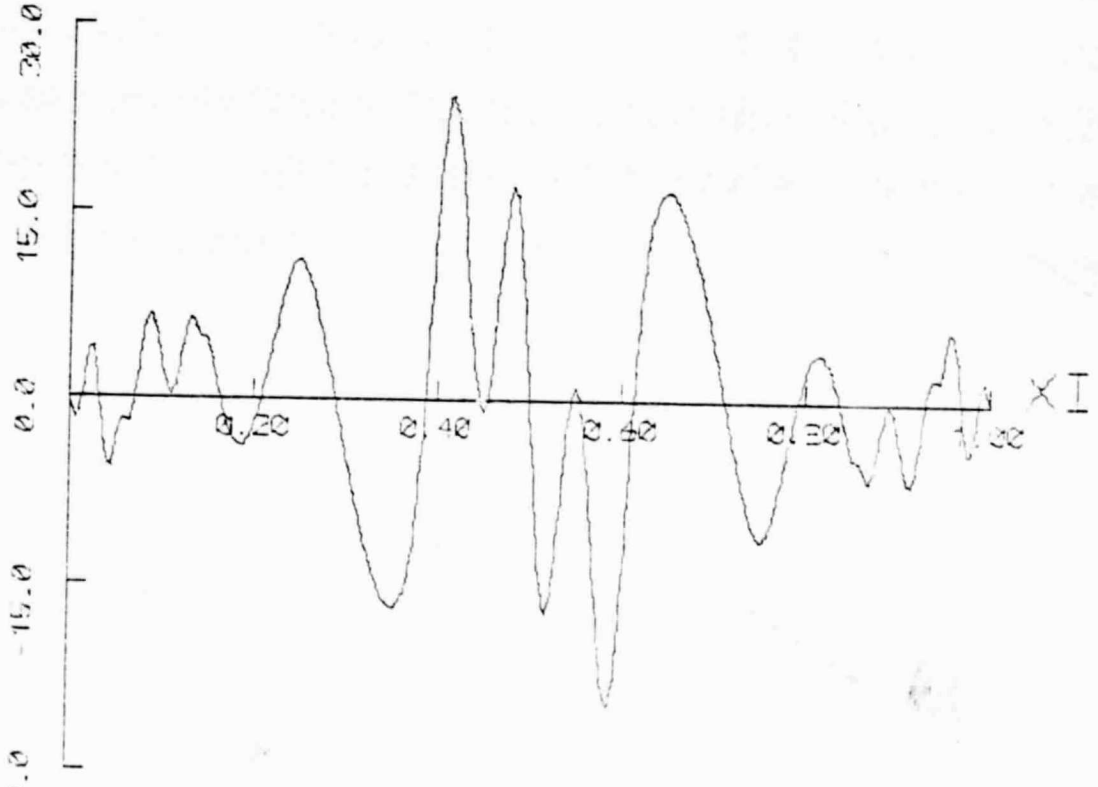

FIG 24 1000VBAR VERSUS XI FOR TAU = .111094E-00

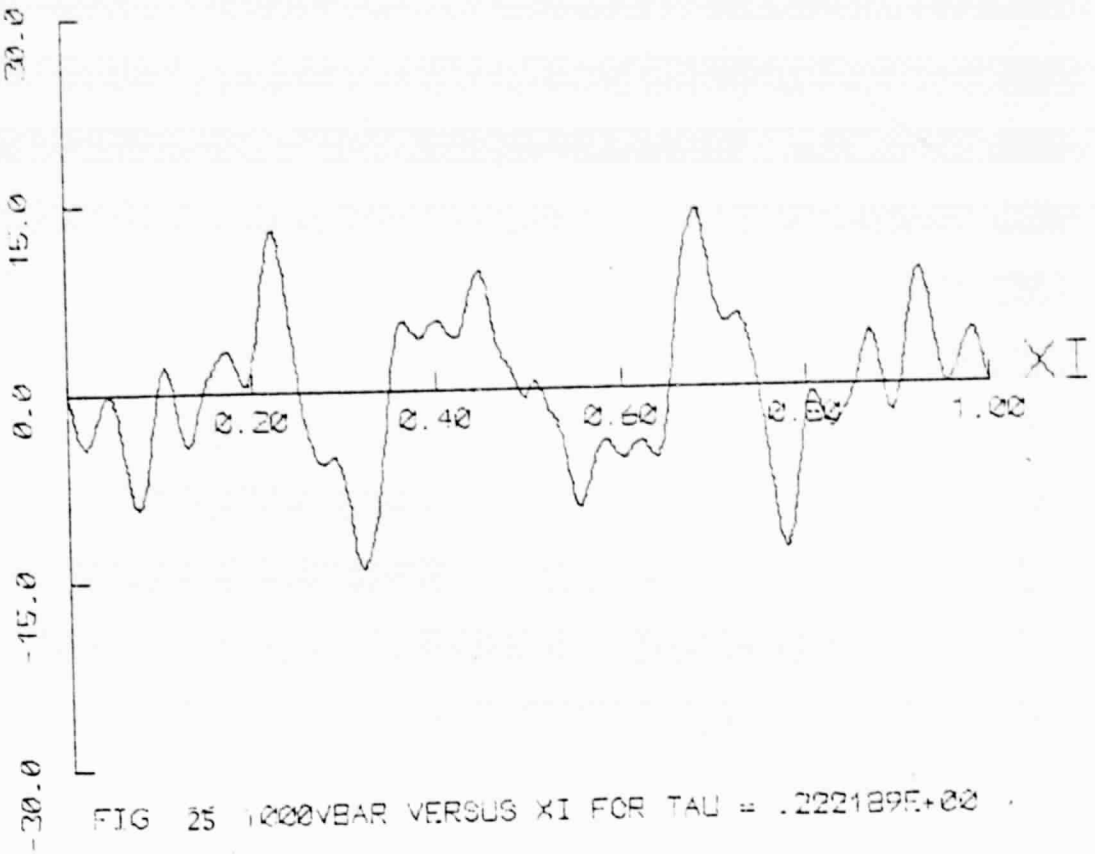

FIG 25 1000VBAR VERSUS XI FOR TAU = .222189E+00

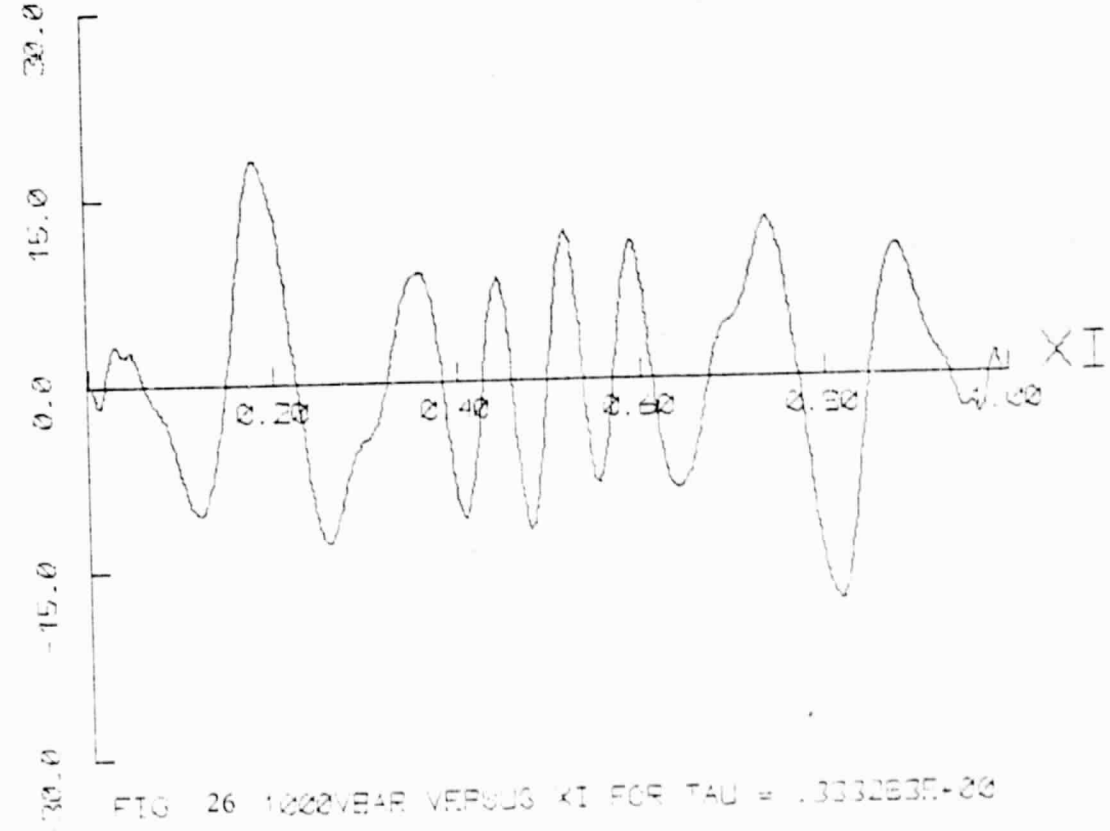

FIG 26 1000VBAR VERSUS XI FOR TAU = .333283E+00

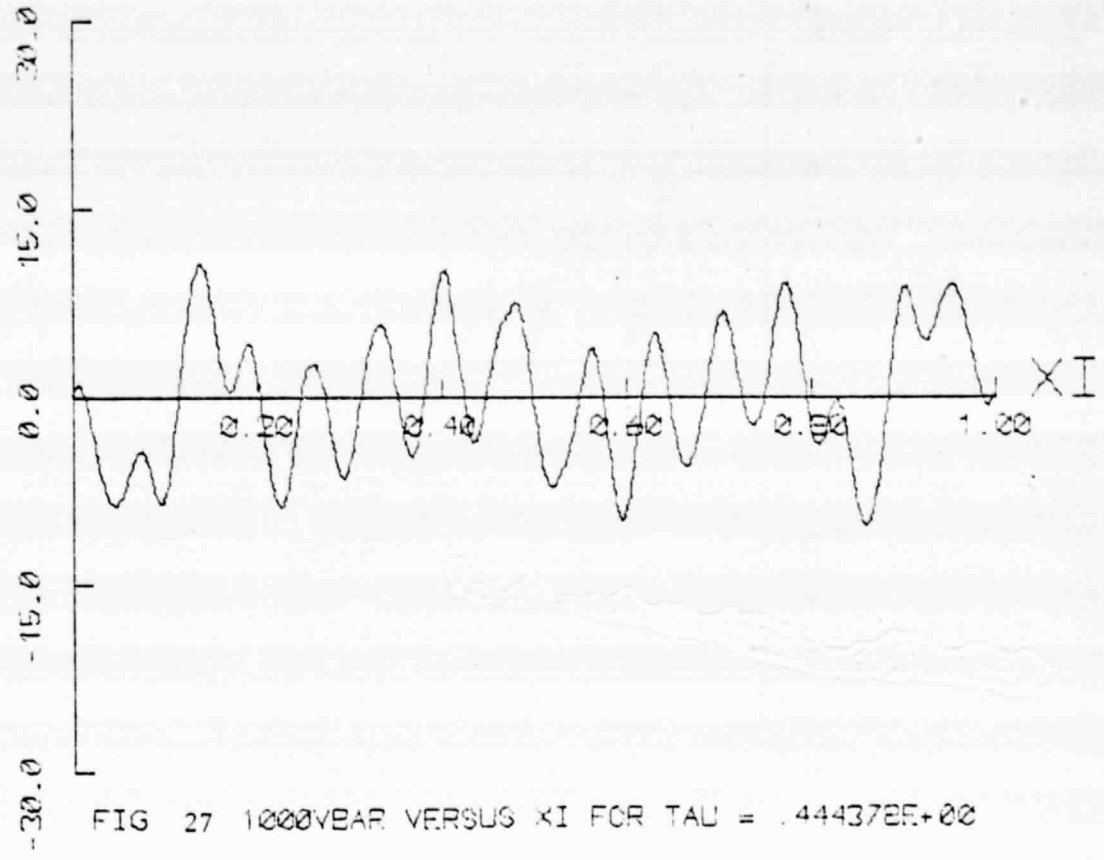

FIG 27 1000VBAR VERSUS XI FOR TAU = .444372E+00

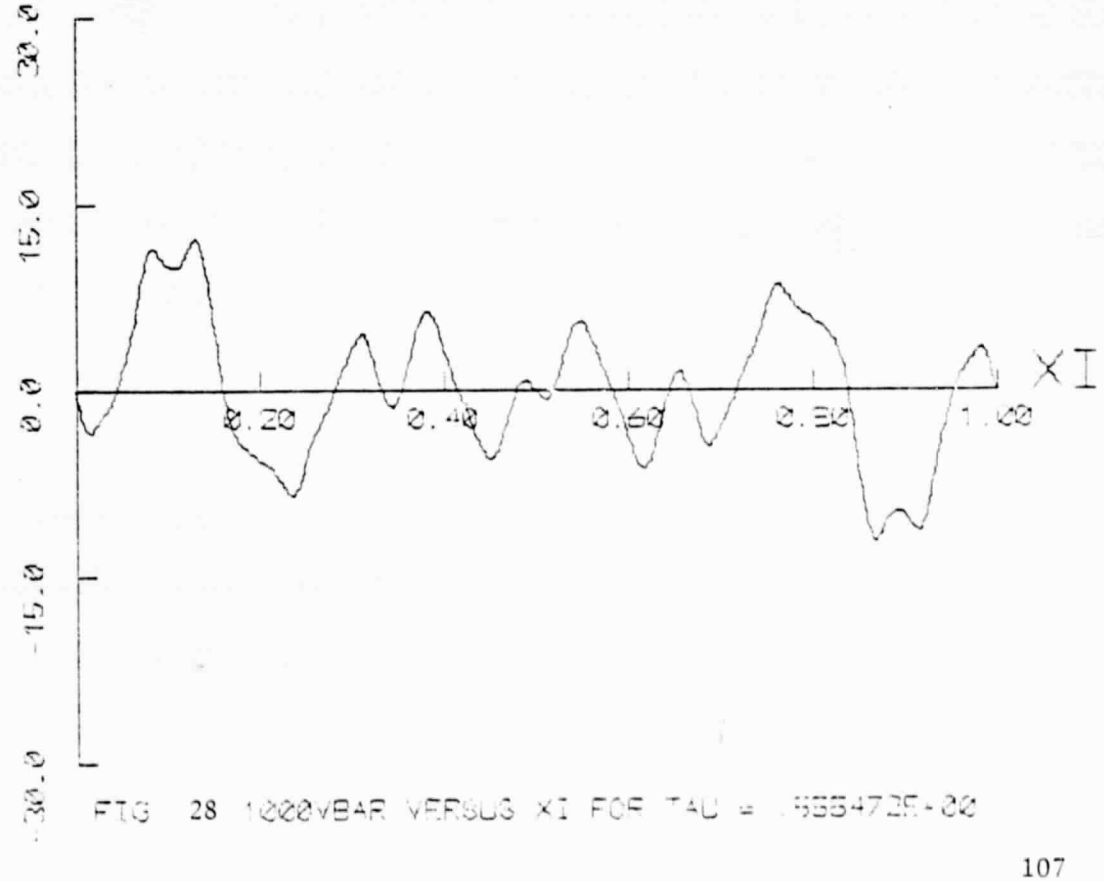

FIG 28 1000VBAR VERSUS XI FOR TAU = .553472E+00

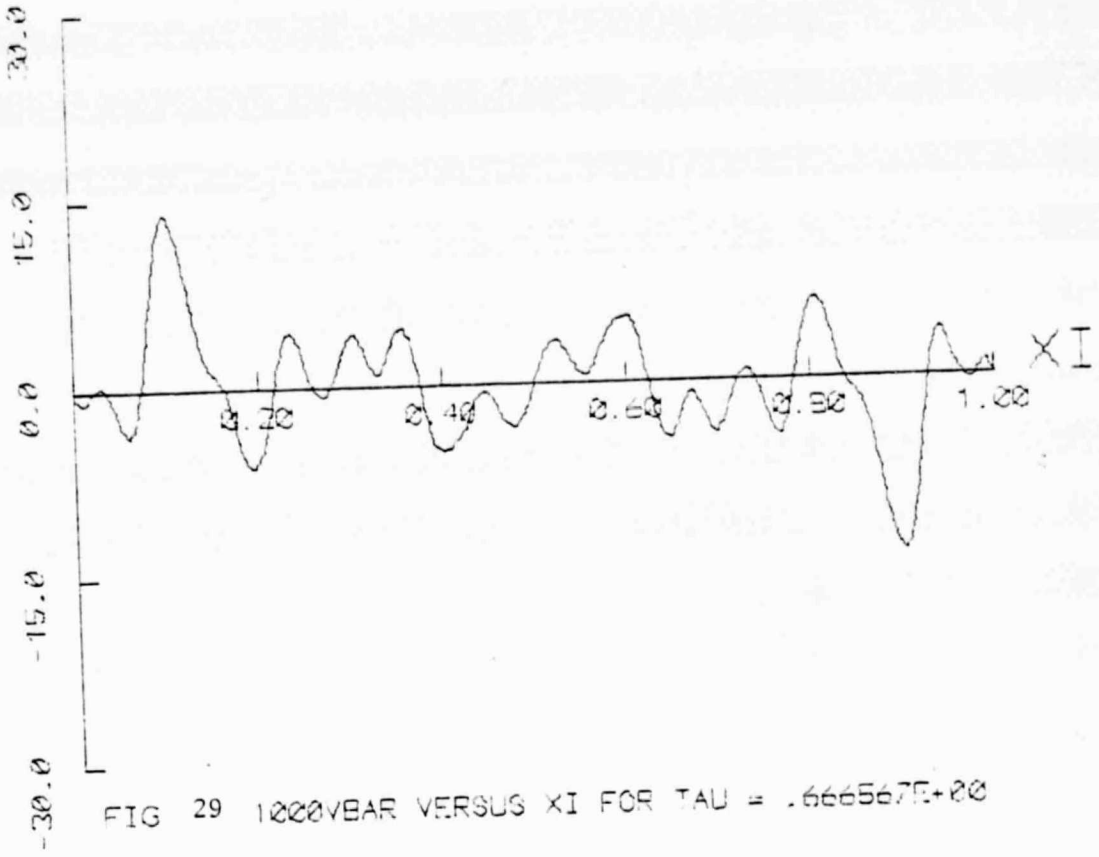

FIG 29 1000VBAR VERSUS XI FOR TAU = .6665677E+00

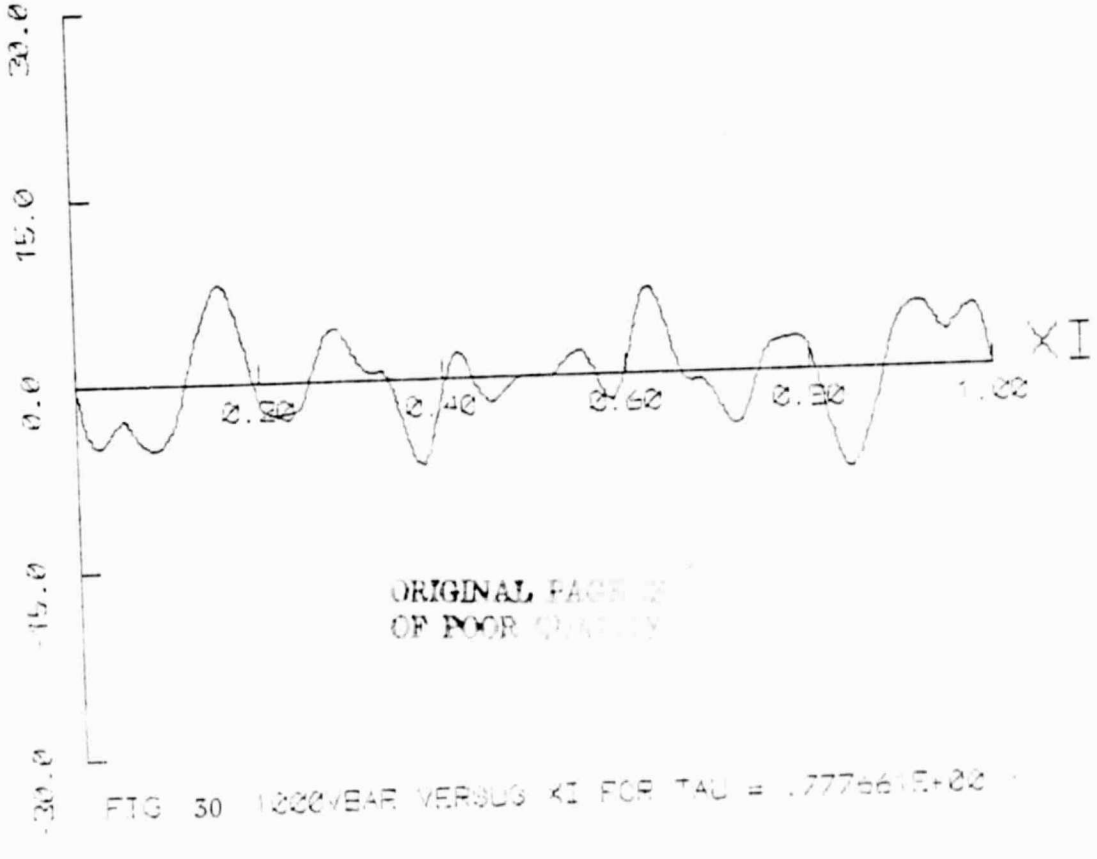

FIG 30 1000VBAR VERSUS XI FOR TAU = .7776661E+00

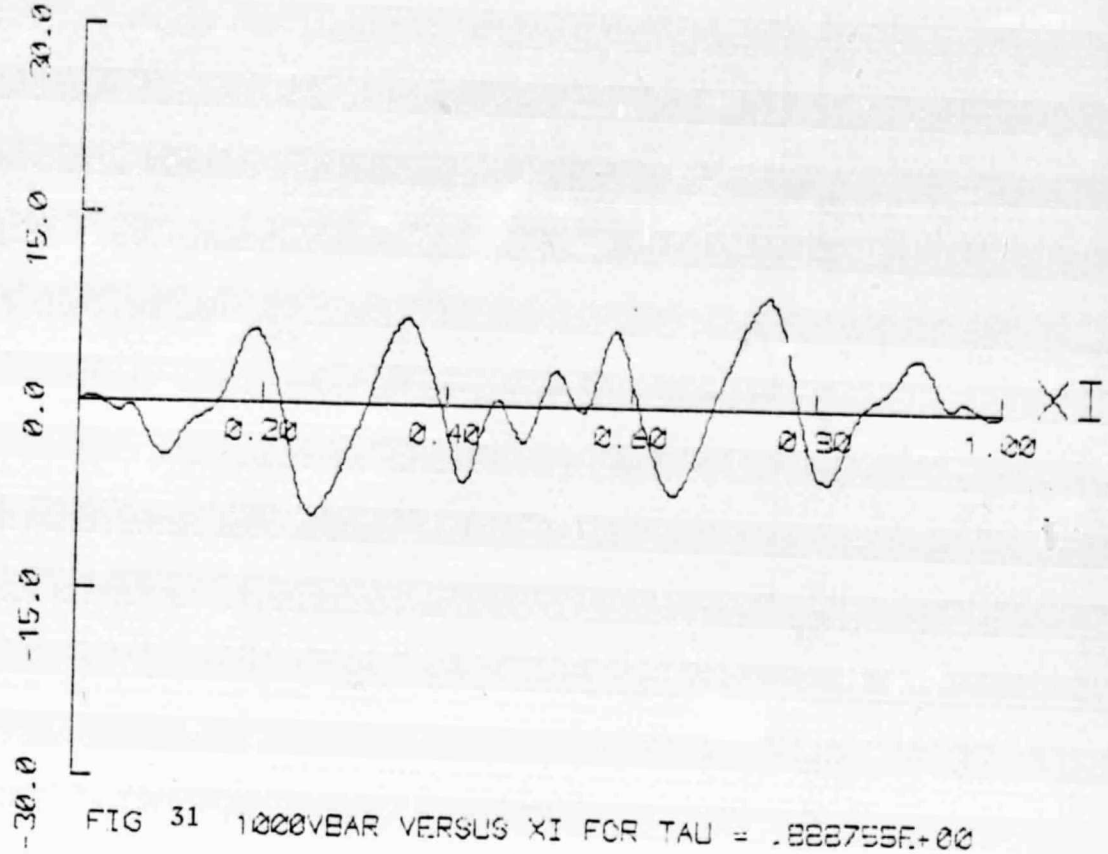

FIG 31 1000VBAR VERSUS XI FOR TAU = .888755E+00

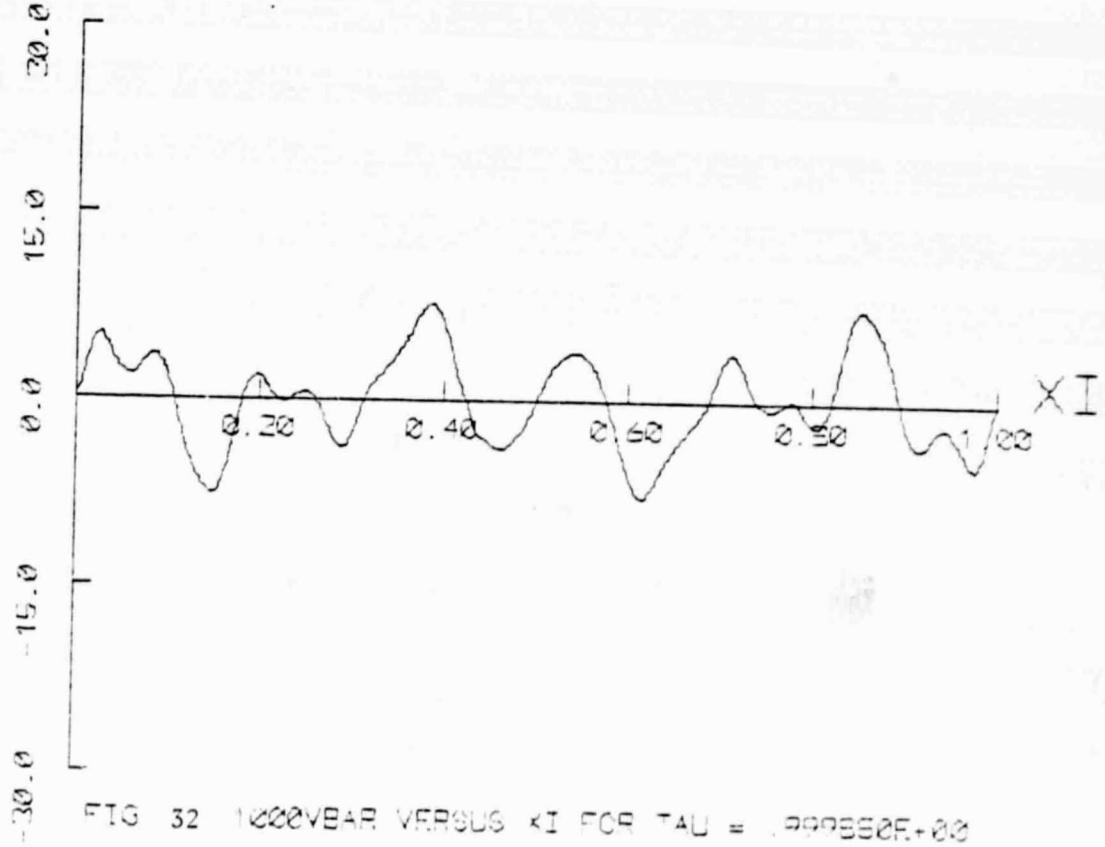

FIG 32 1000VBAR VERSUS XI FOR TAU = .999550E+00

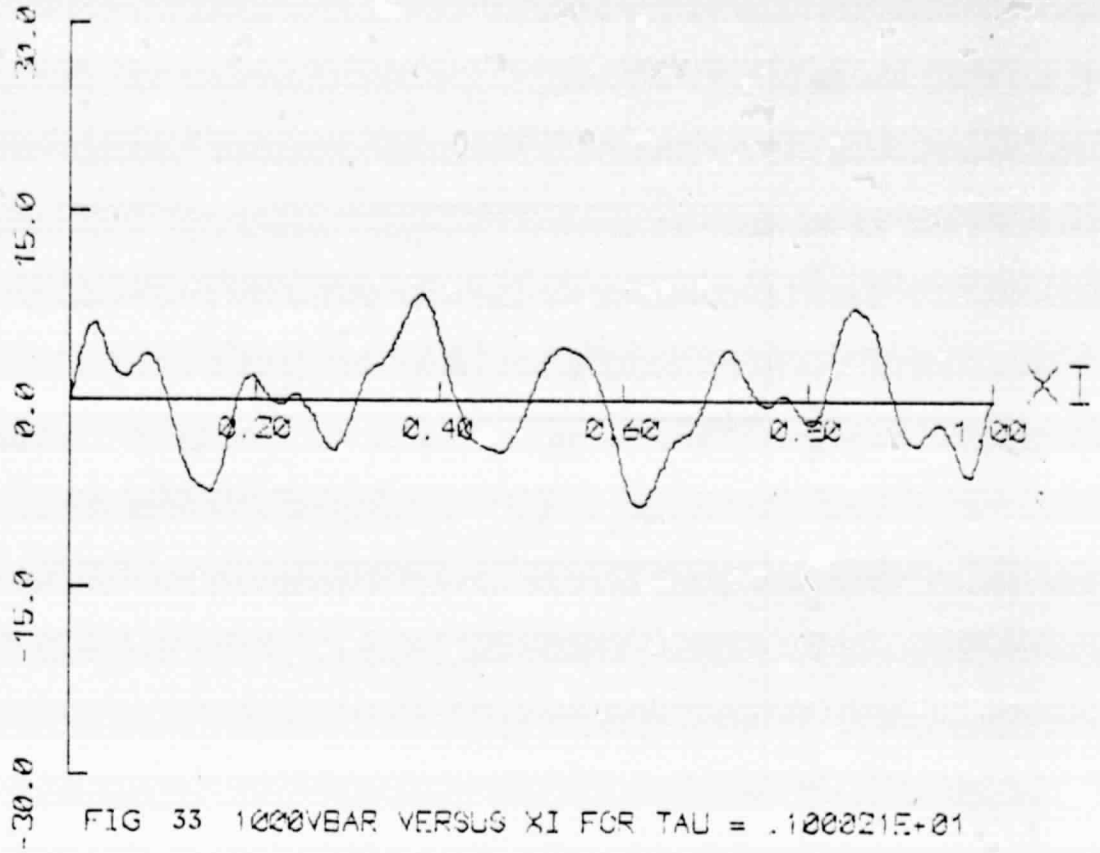

FIG 33 1000VBAR VERSUS XI FOR TAU = .100021E+01

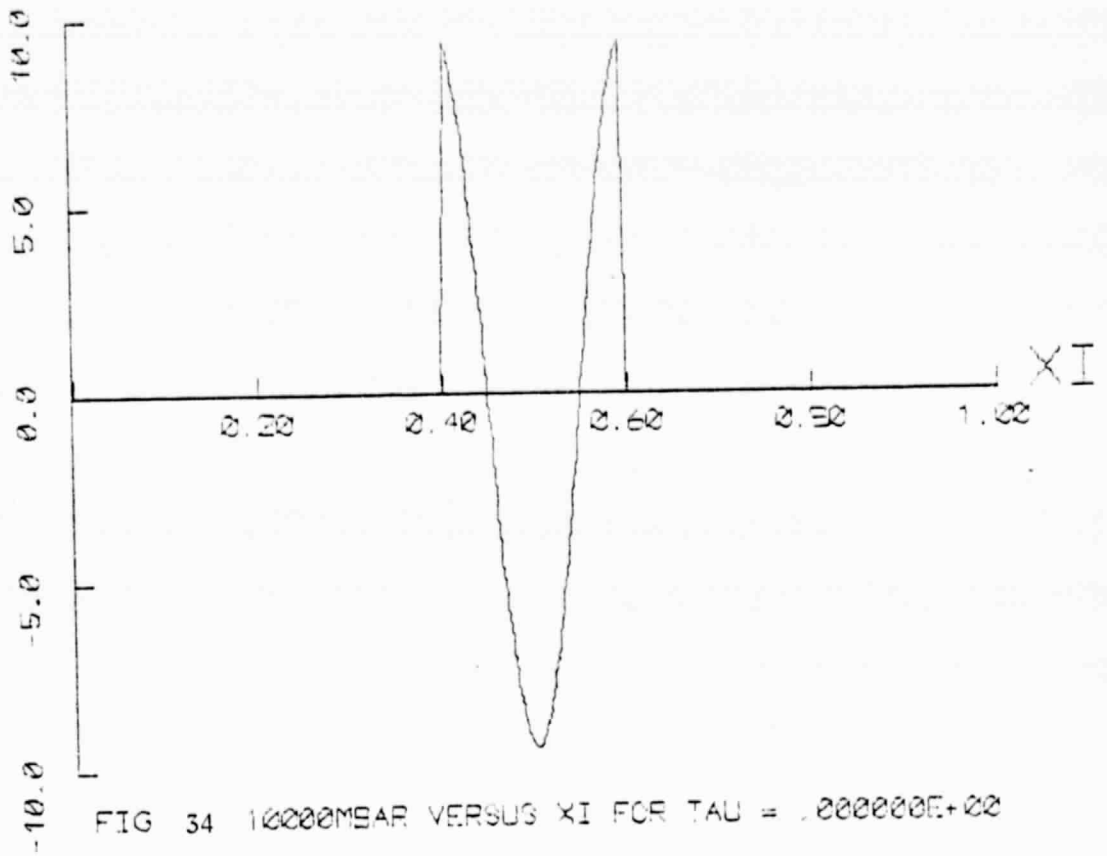

FIG 34 10000MSAR VERSUS XI FOR TAU = .000000E+00

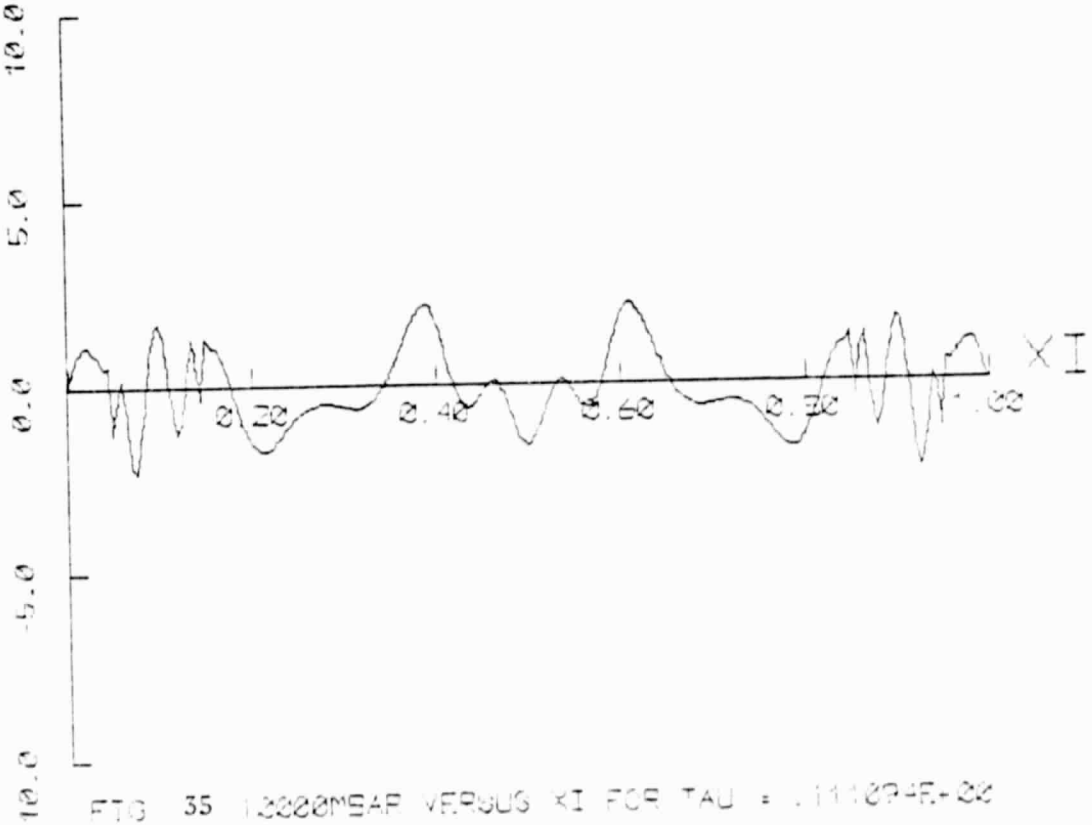

FIG 35 10000MSAR VERSUS XI FOR TAU = .111074E+00

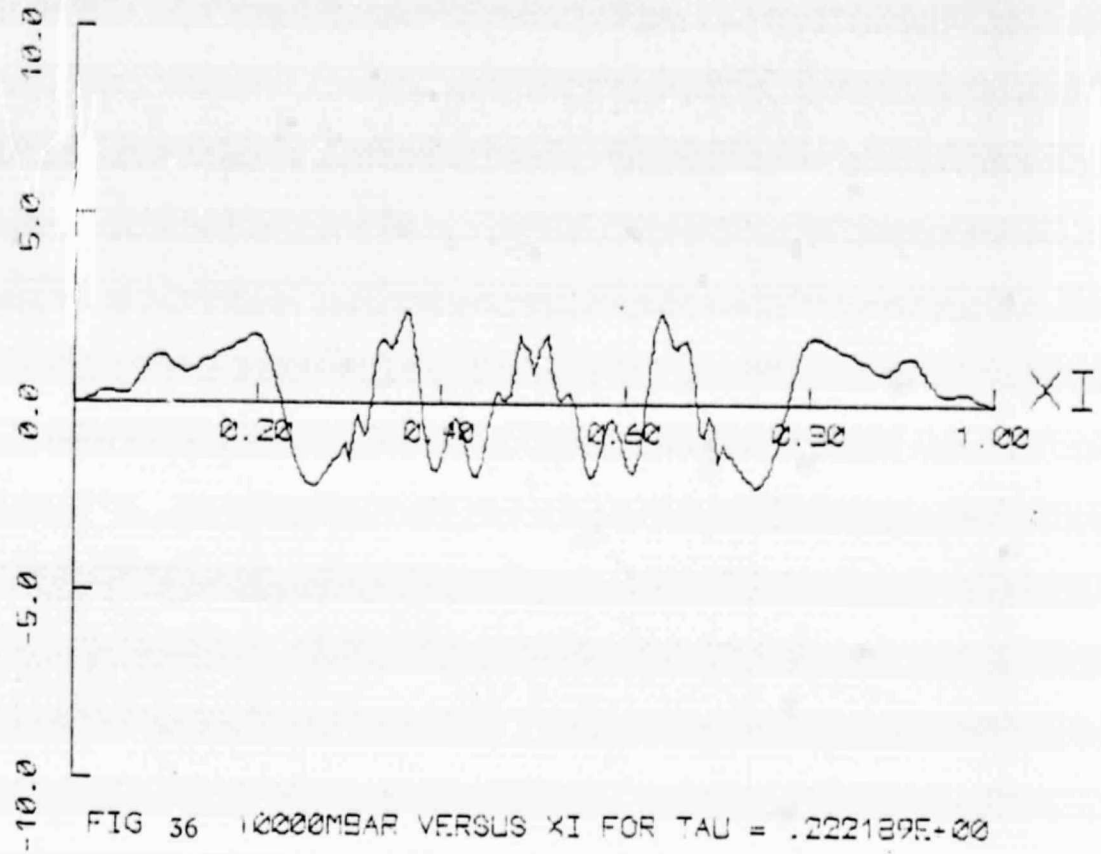

FIG 36 10000MBAR VERSUS XI FOR TAU = .2221895-00

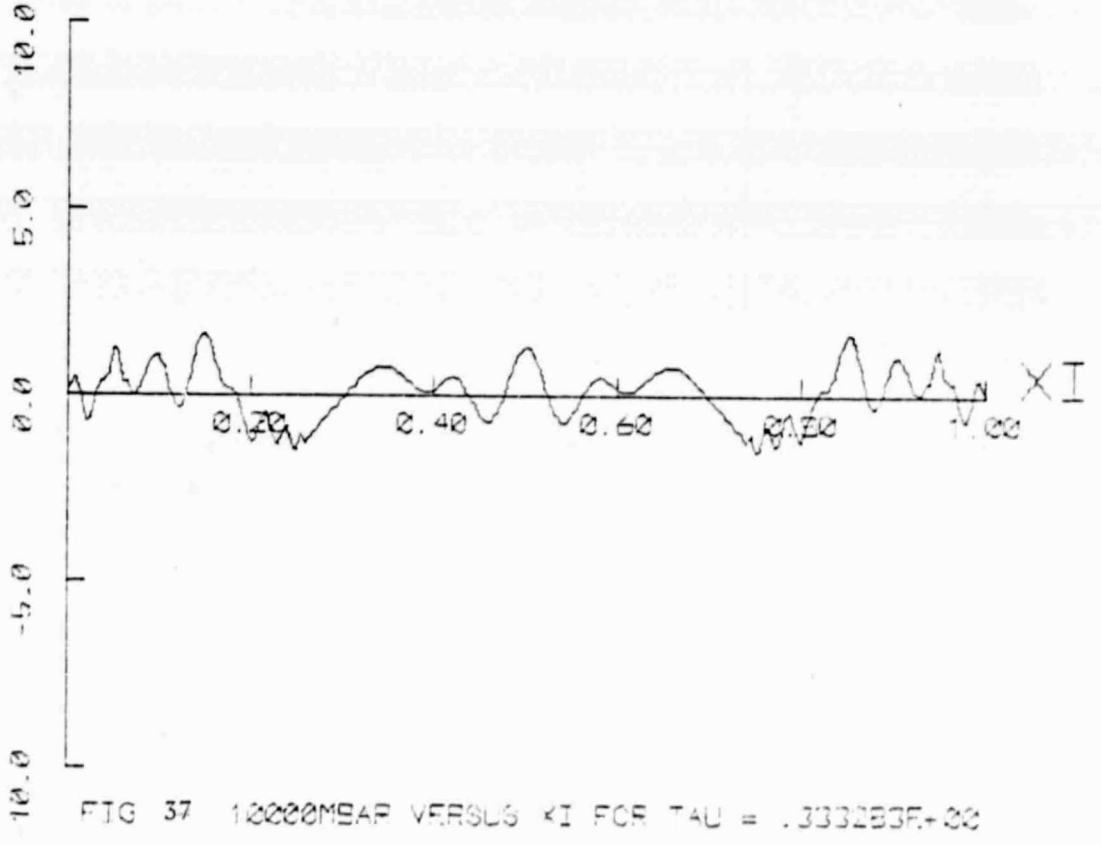

FIG 37 10000MBAR VERSUS XI FOR TAU = .3332835-00

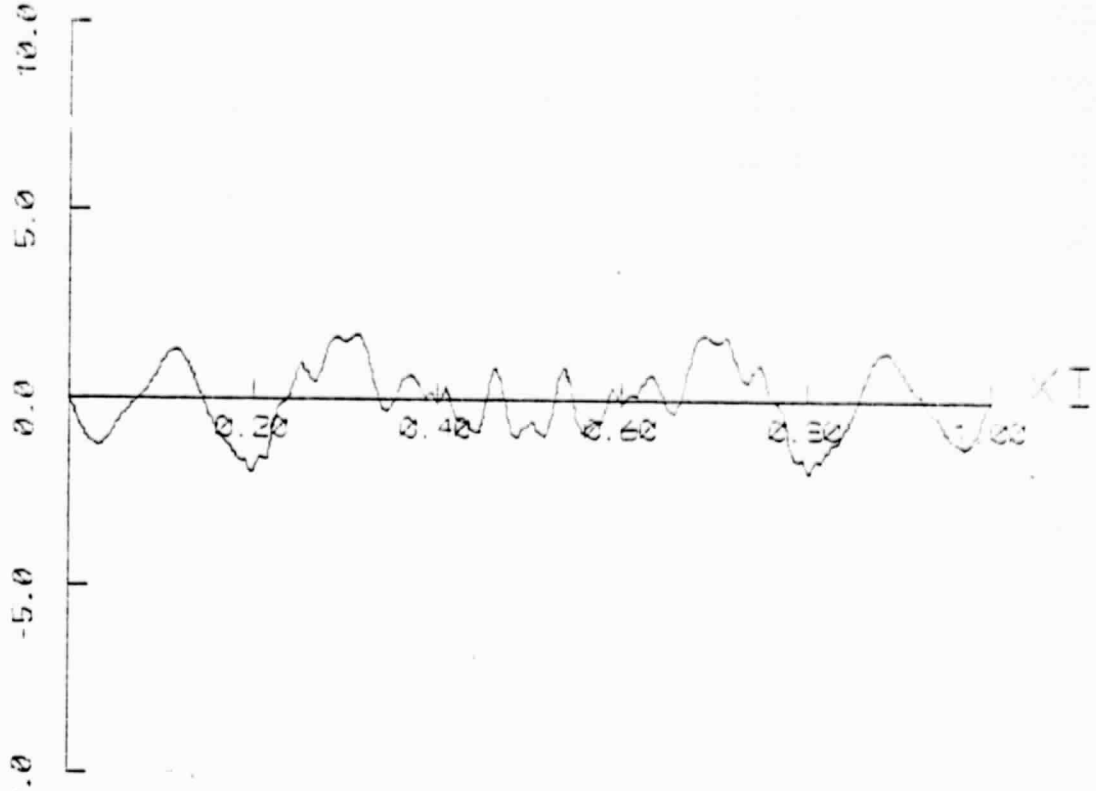

FIG 38 10000MEAR VERSUS XI FOR TAU = .4443/E0-00

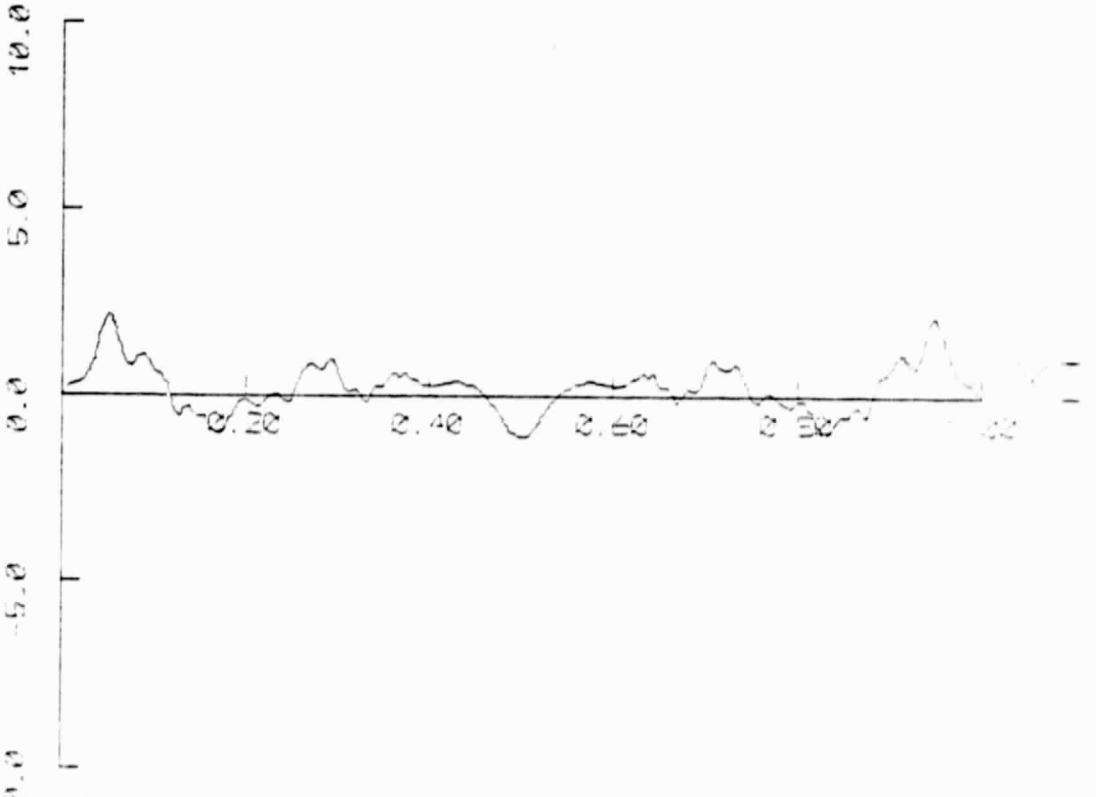

FIG 39 10000MEAR VERSUS XI FOR TAU = .4334715E-00

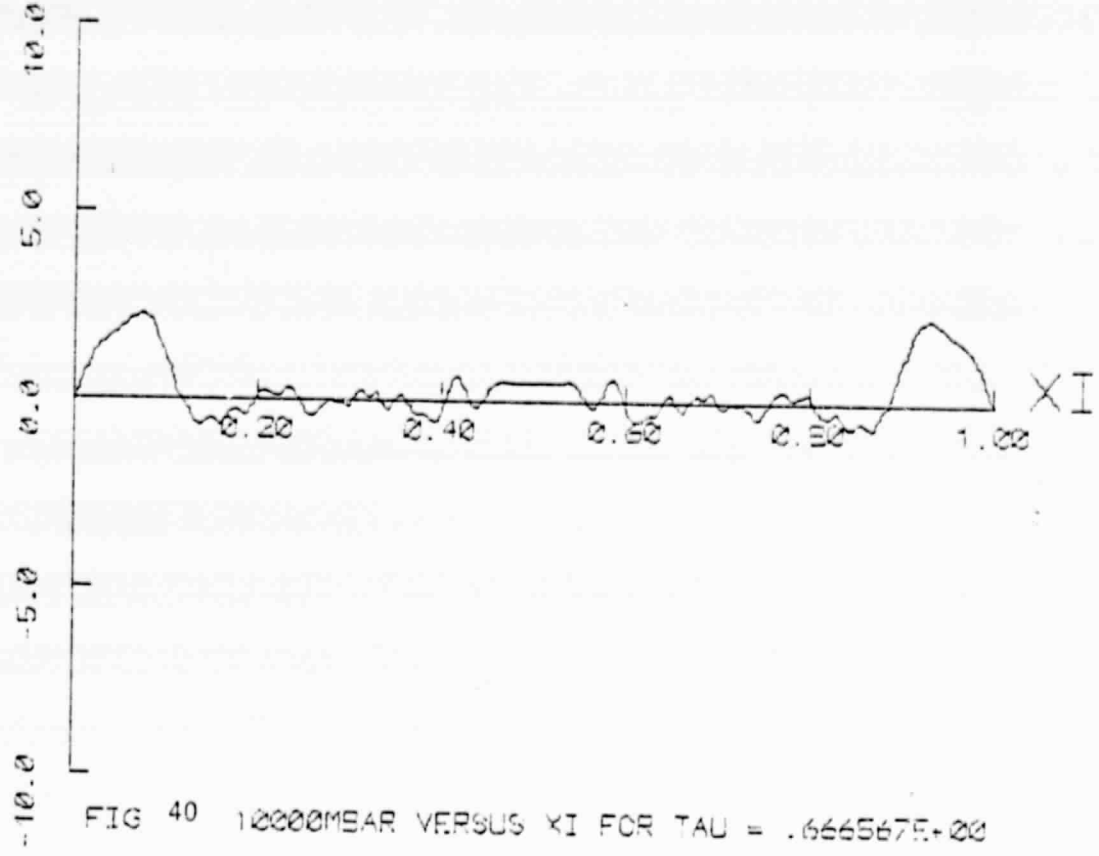

FIG 40 10000MBAR VERSUS XI FOR TAU = .666567E+00

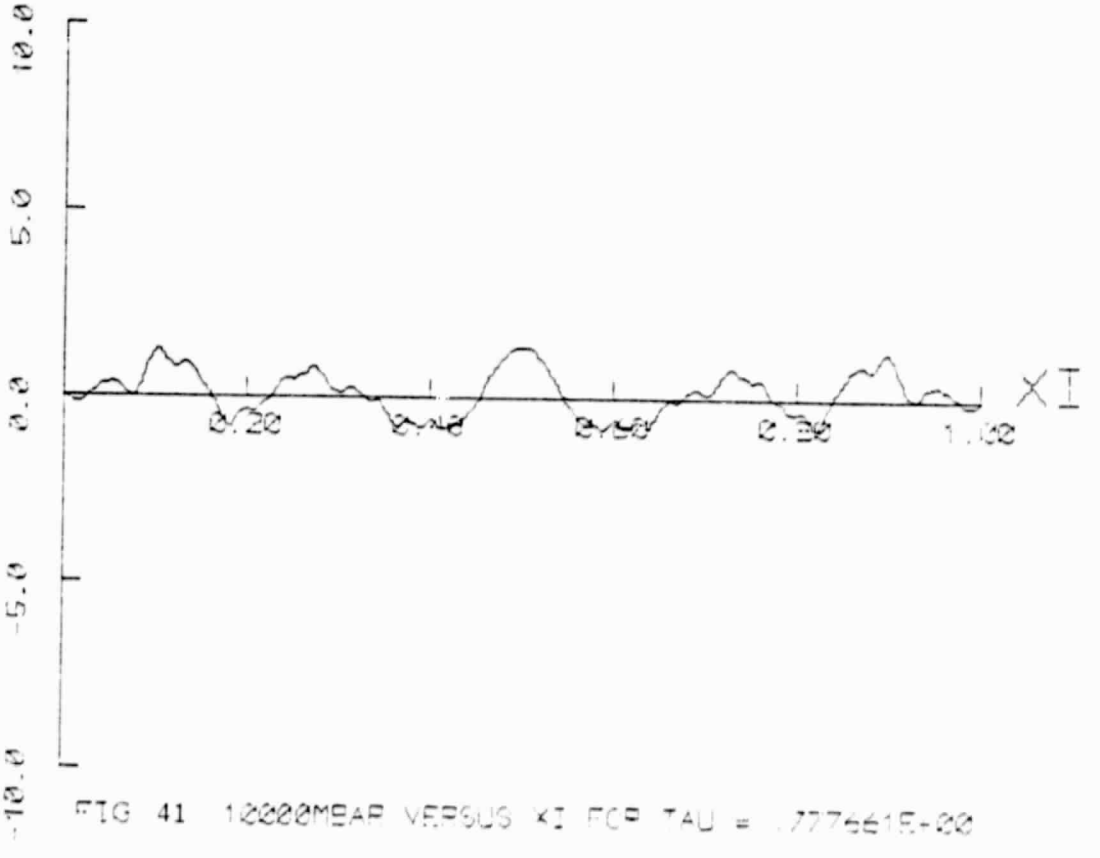

FIG 41 10000MBAR VERSUS XI FOR TAU = .777661E+00

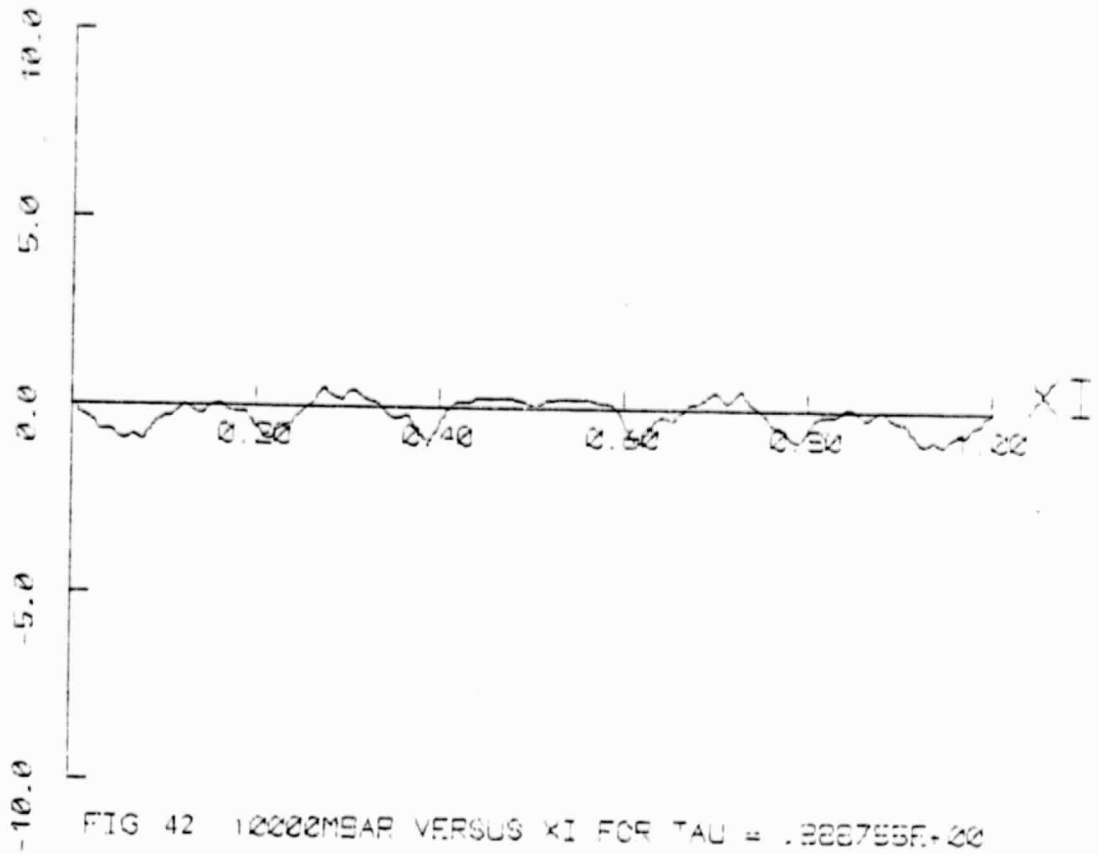

FIG 42 10000MBAR VERSUS XI FOR TAU = .3887553E+00

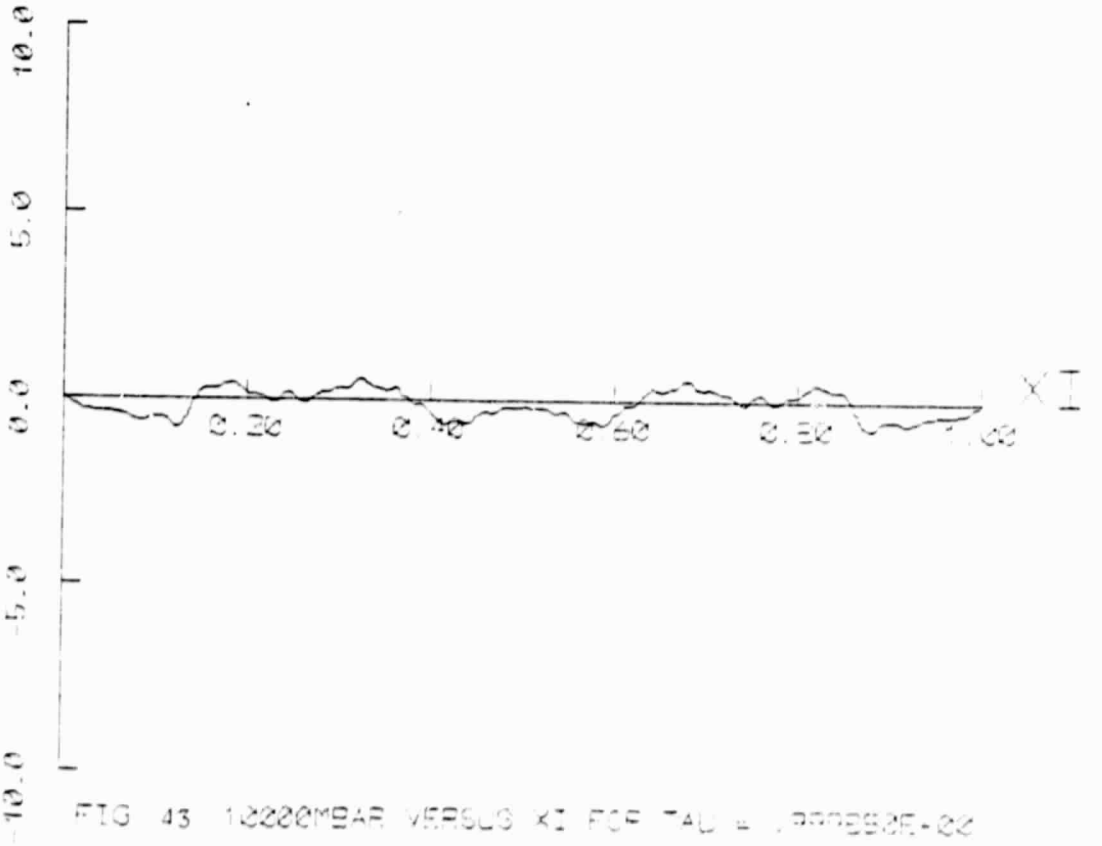

FIG 43 10000MBAR VERSUS XI FOR TAU = .8773530E+00

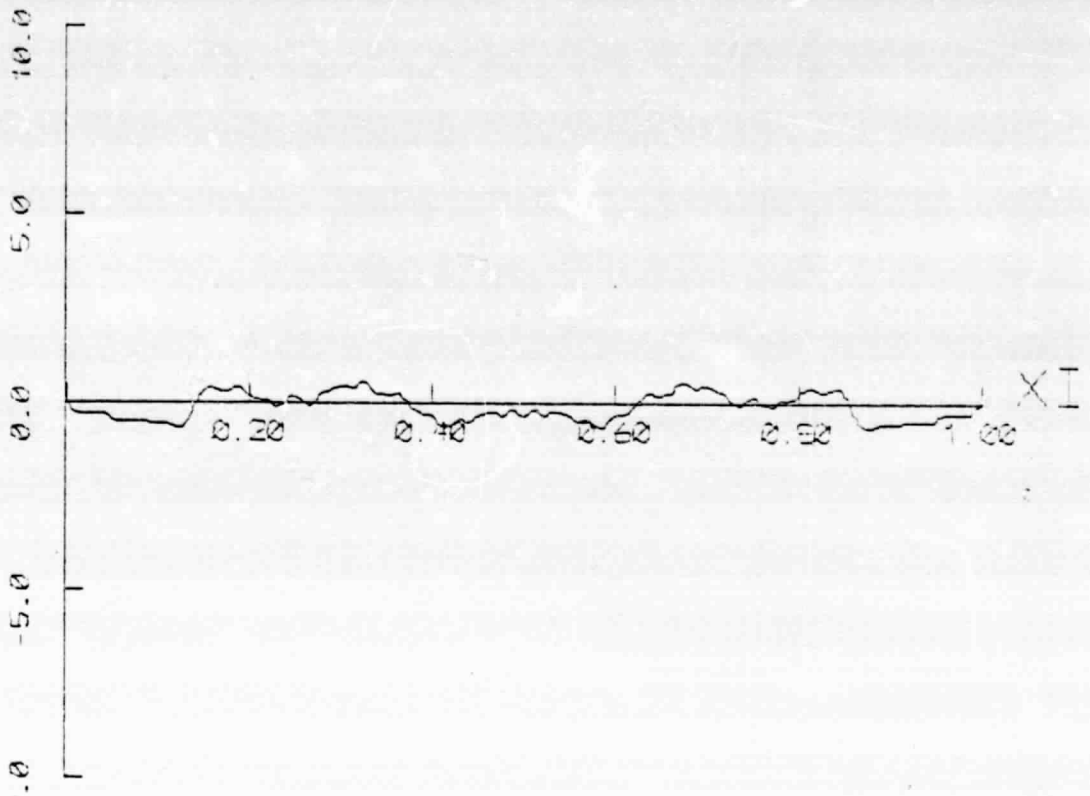

FIG 44 10000MSAR VERSUS XI FOR TAU = .1000215+01

APPENDIX I

Response to a (1 + cos) initial displacement;
V_R = 0.62. SLR = 50, λ = 0.2, b_1 = 3.0, b_2 = 0.0.

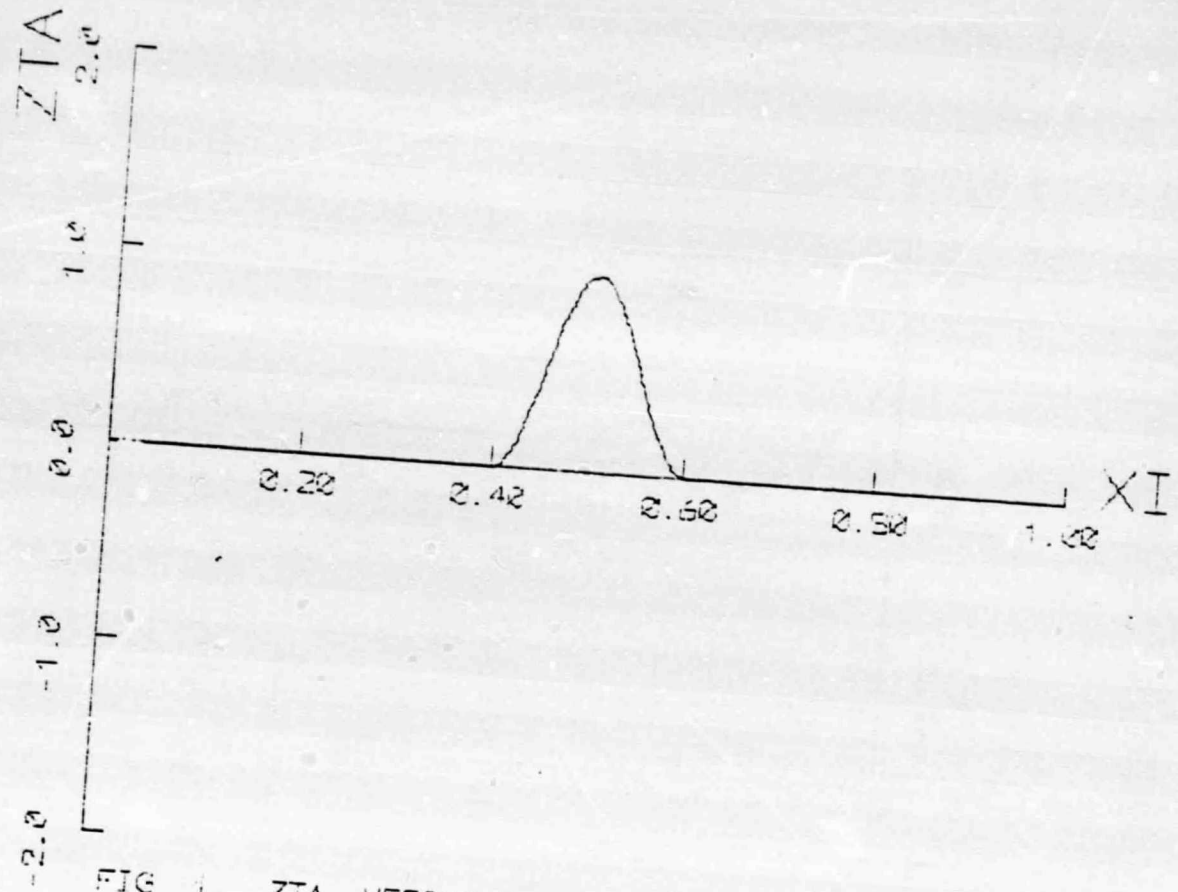

FIG 1. ZTA VERSUS XI FOR TAU = .200000E-00

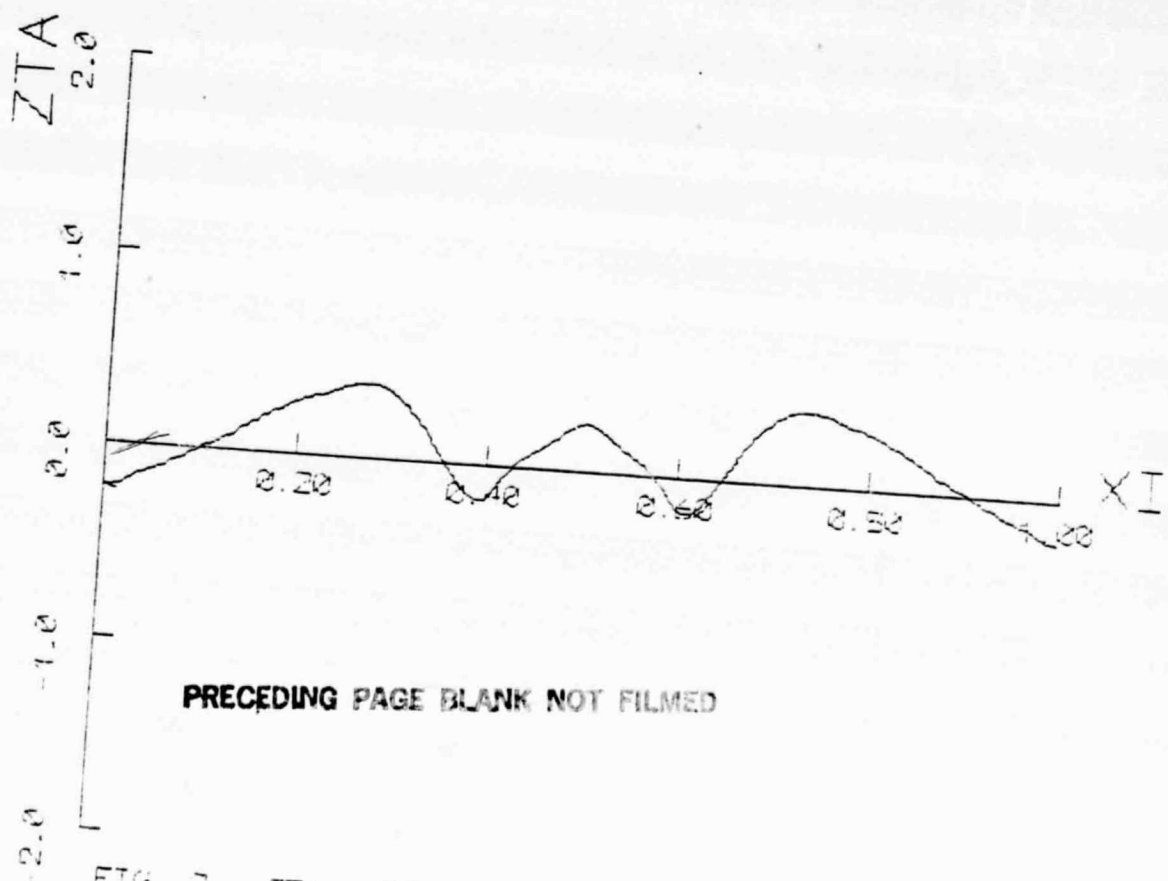

FIG 2. ZTA VERSUS XI FOR TAU = .110P-01-00

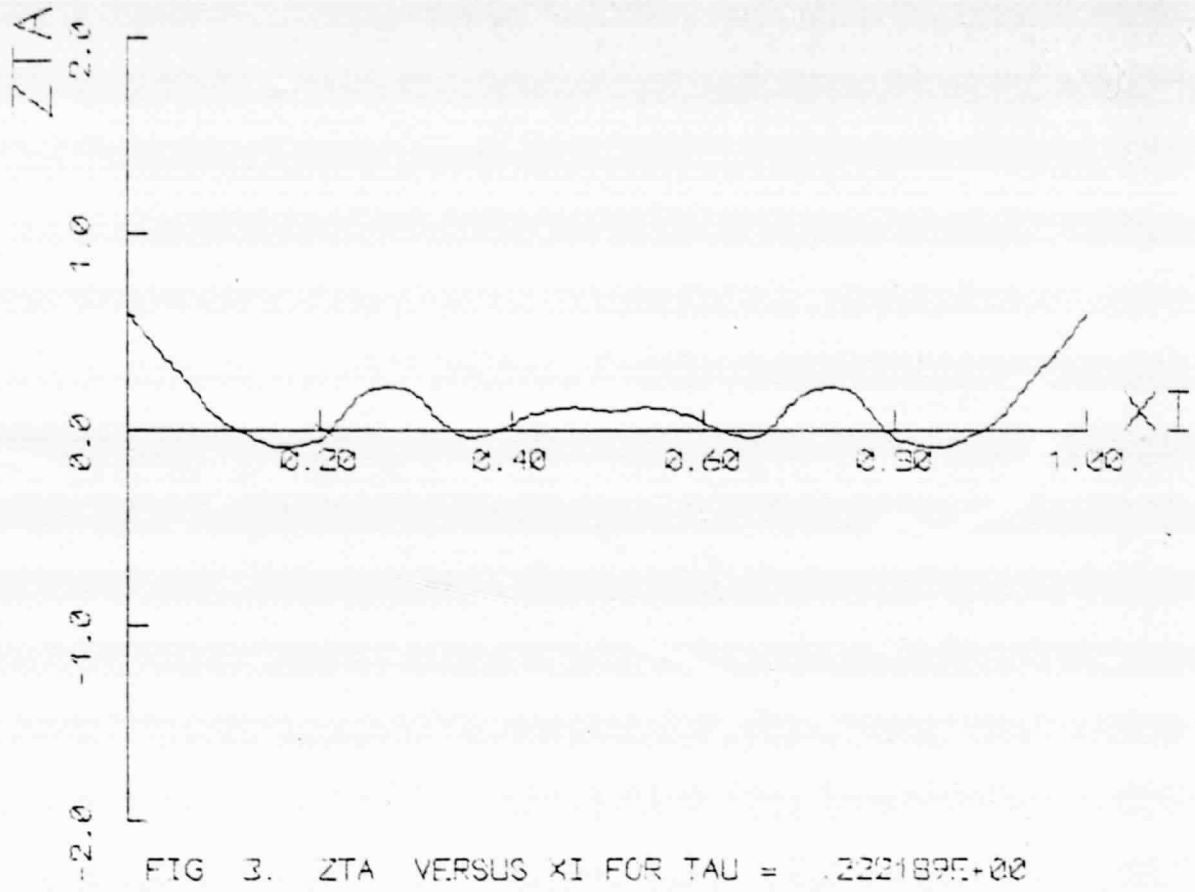

FIG 3. ZTA VERSUS XI FOR TAU = .2221895E+00

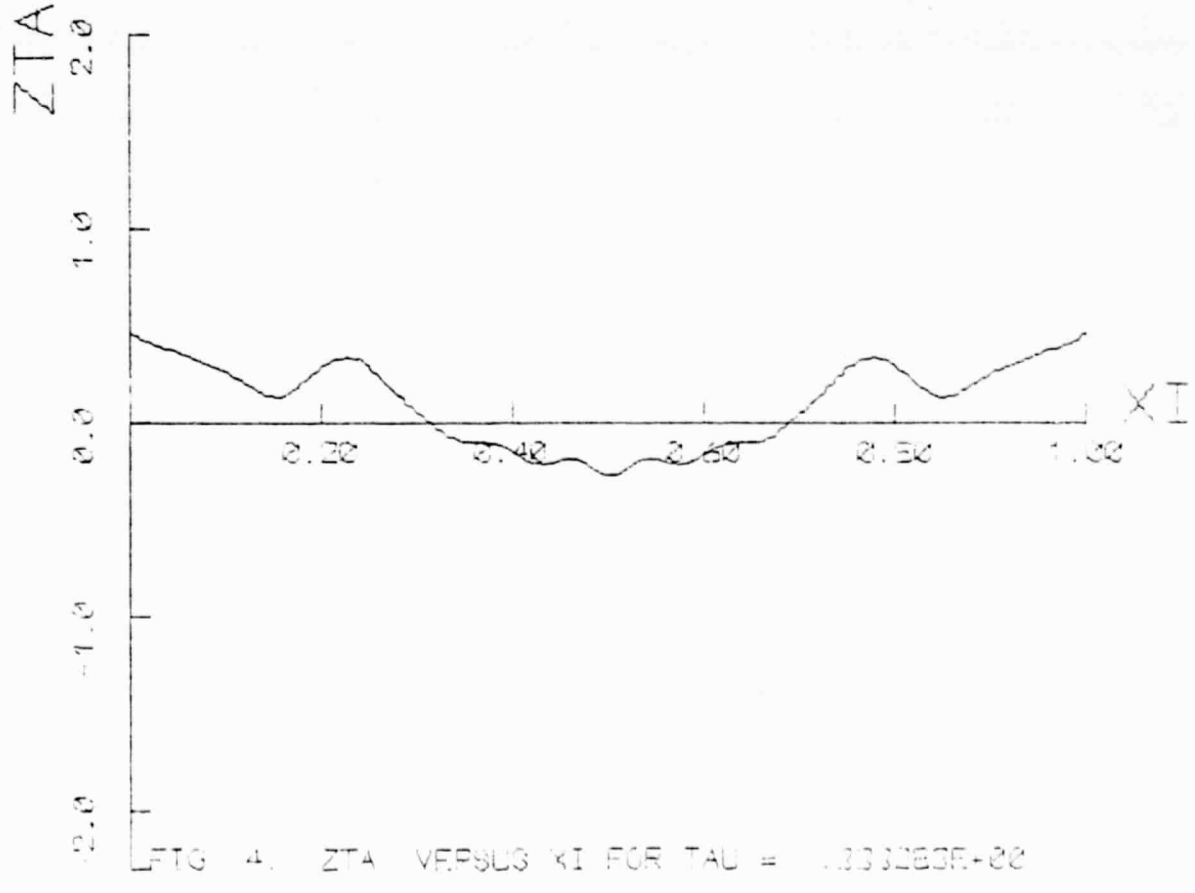

FIG 4. ZTA VERSUS XI FOR TAU = .3332838E+00

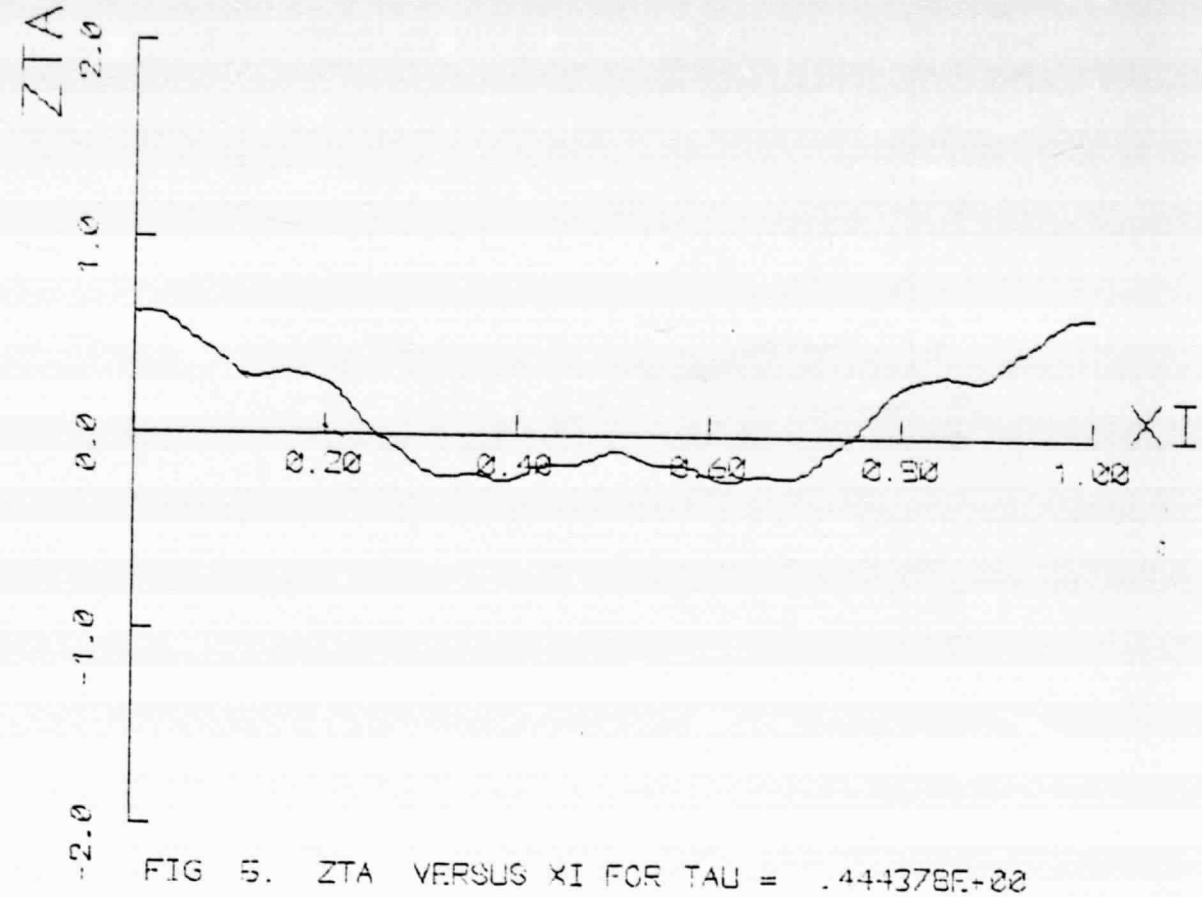

FIG 5. ZTA VERSUS XI FOR TAU = .444378E+00

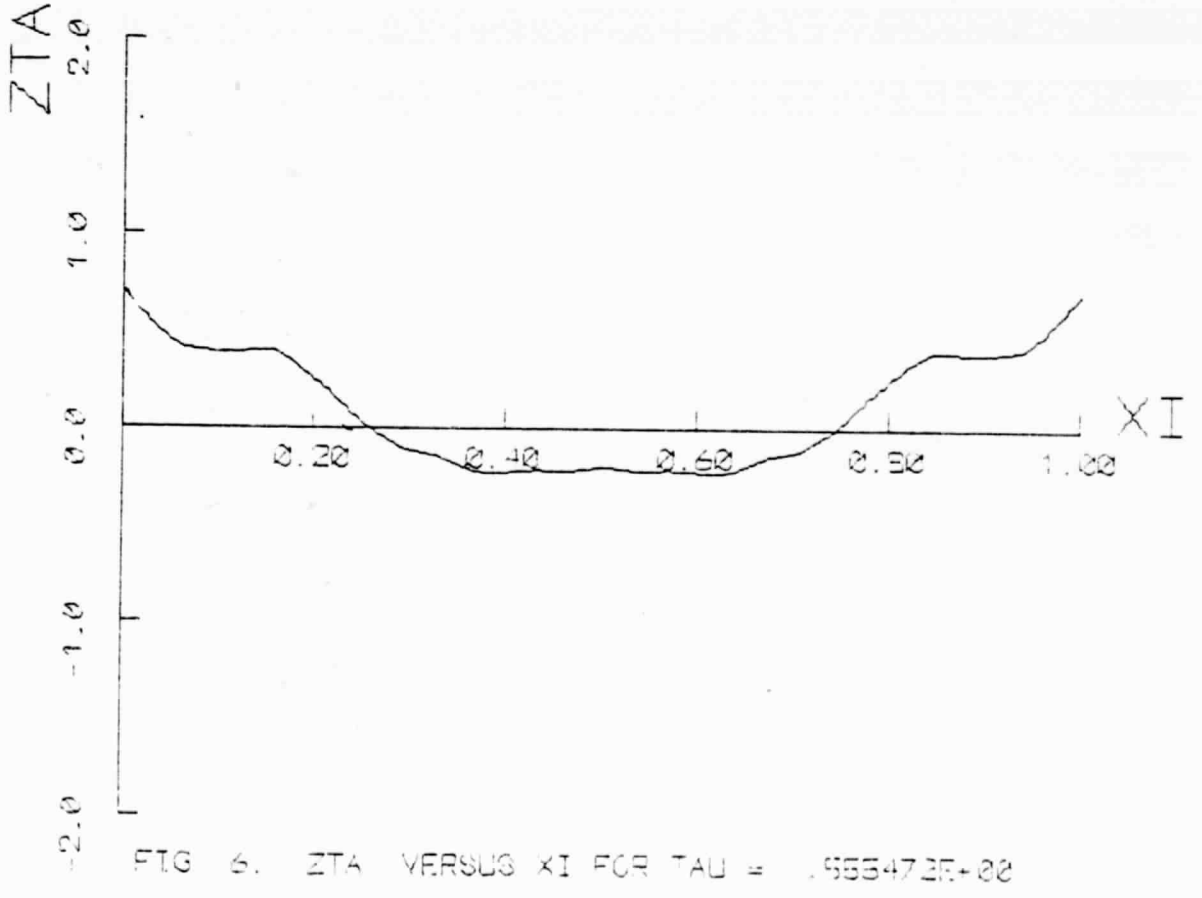

FIG 6. ZTA VERSUS XI FOR TAU = .555472E+00

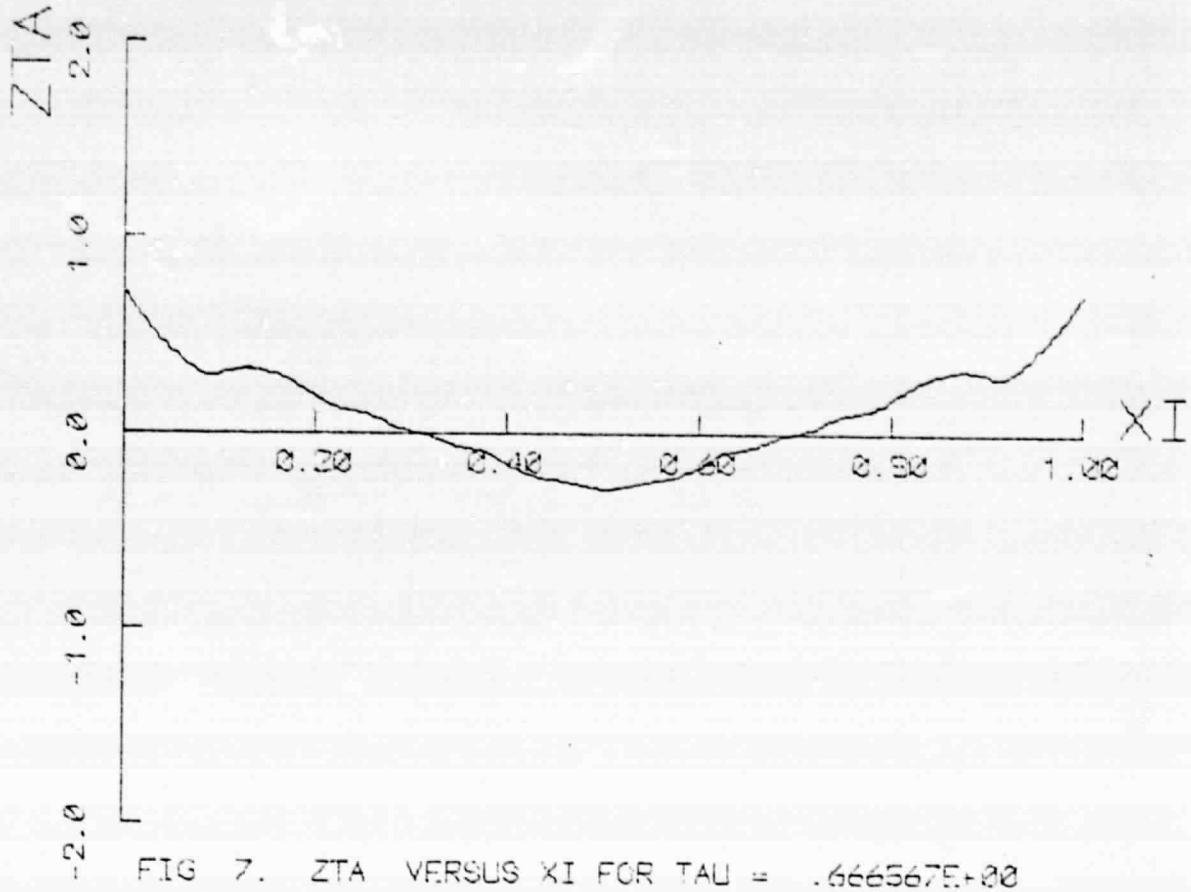

FIG 7. ZTA VERSUS XI FOR TAU = .6665675E+00

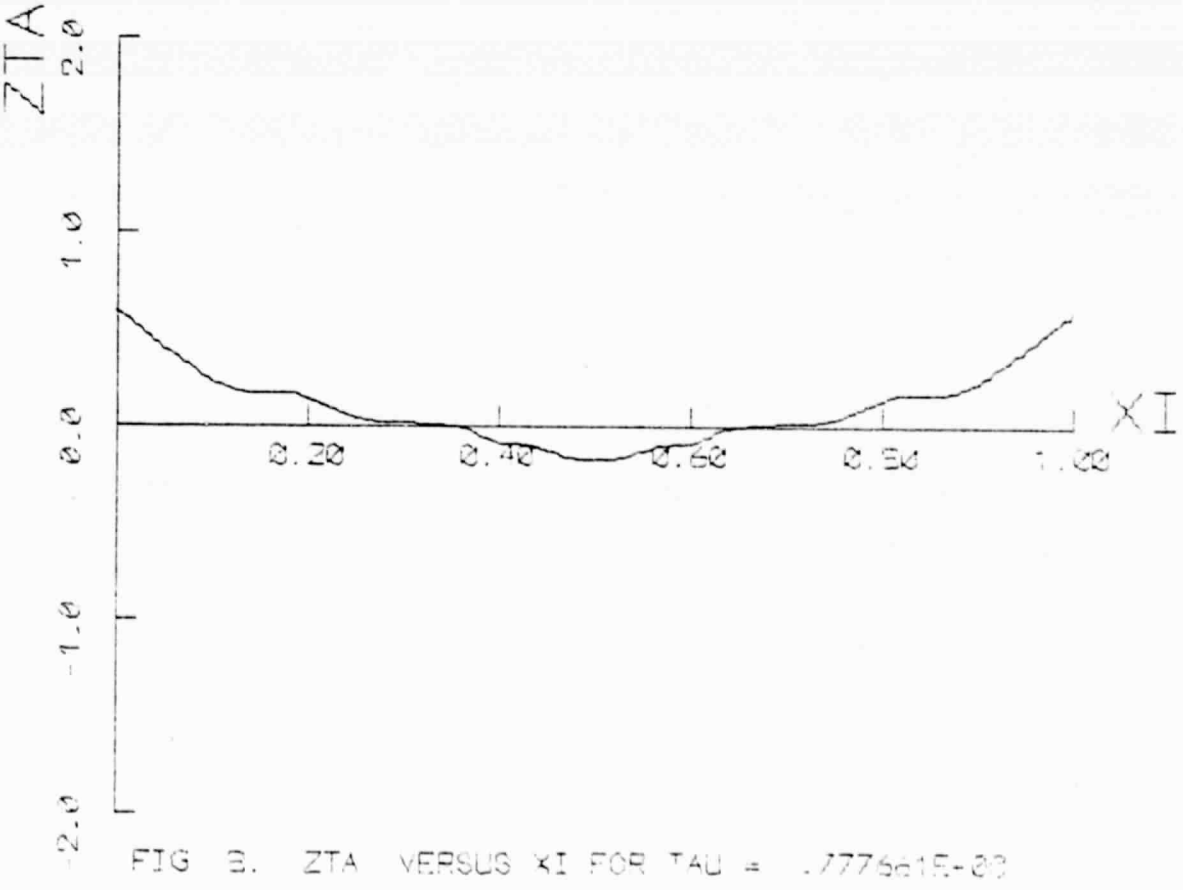

FIG 8. ZTA VERSUS XI FOR TAU = .7776615E-03

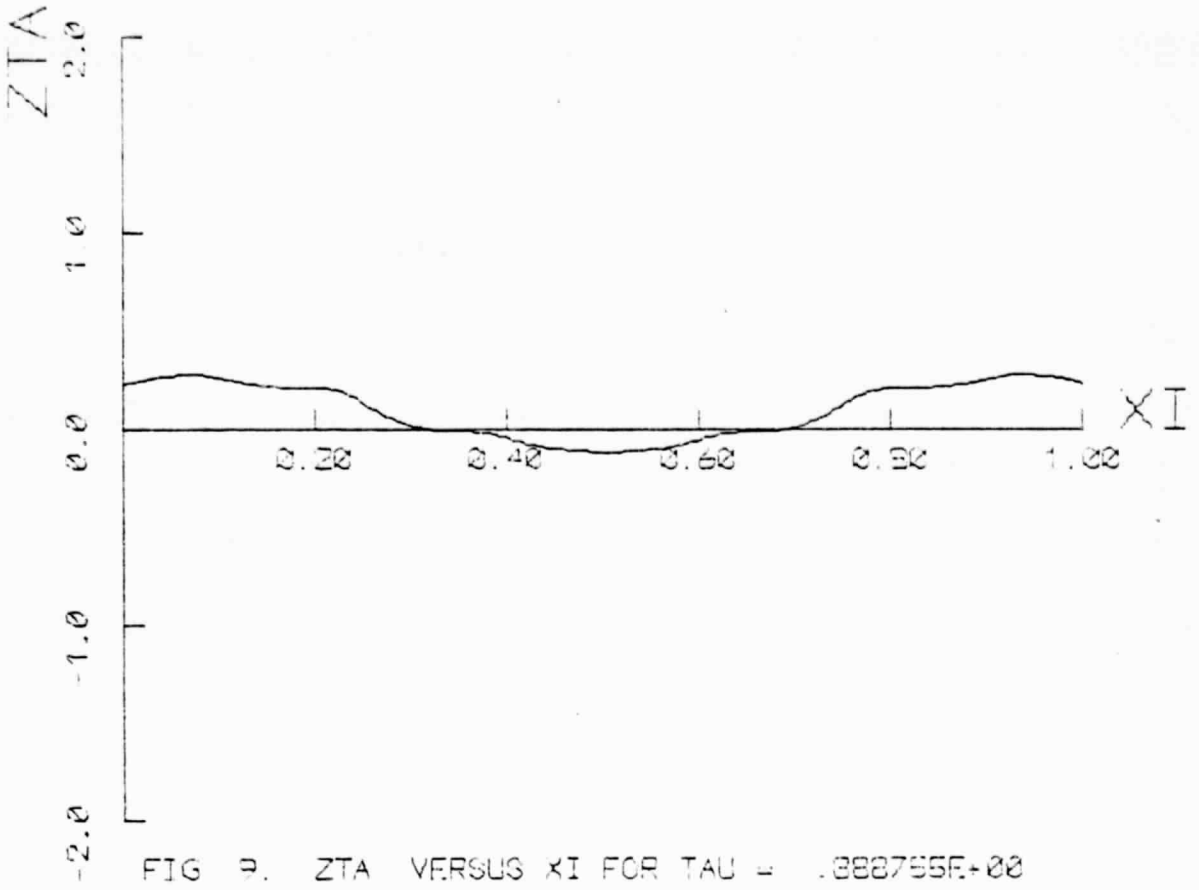

FIG 9. ZTA VERSUS XI FOR TAU = .888755E+00

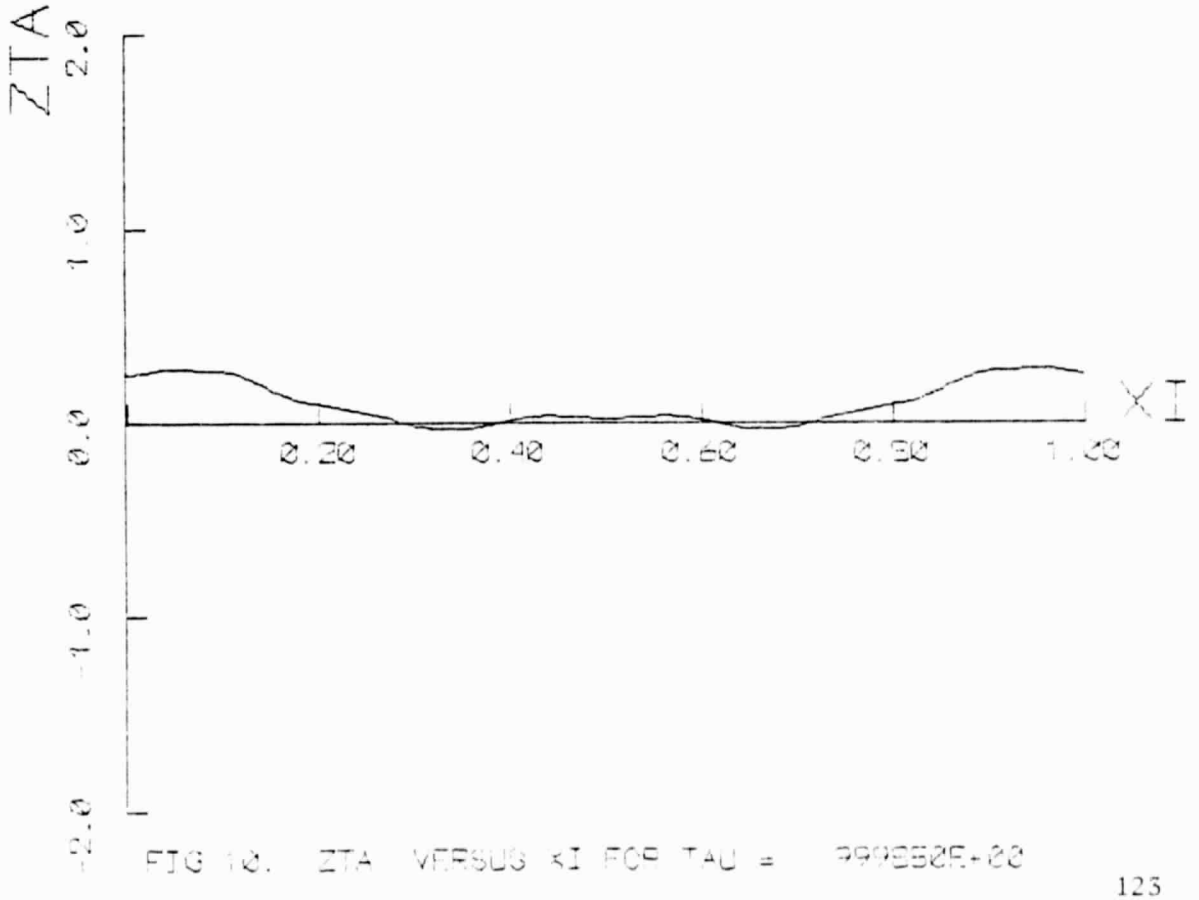

FIG 10. ZTA VERSUS XI FOR TAU = .999850E+00

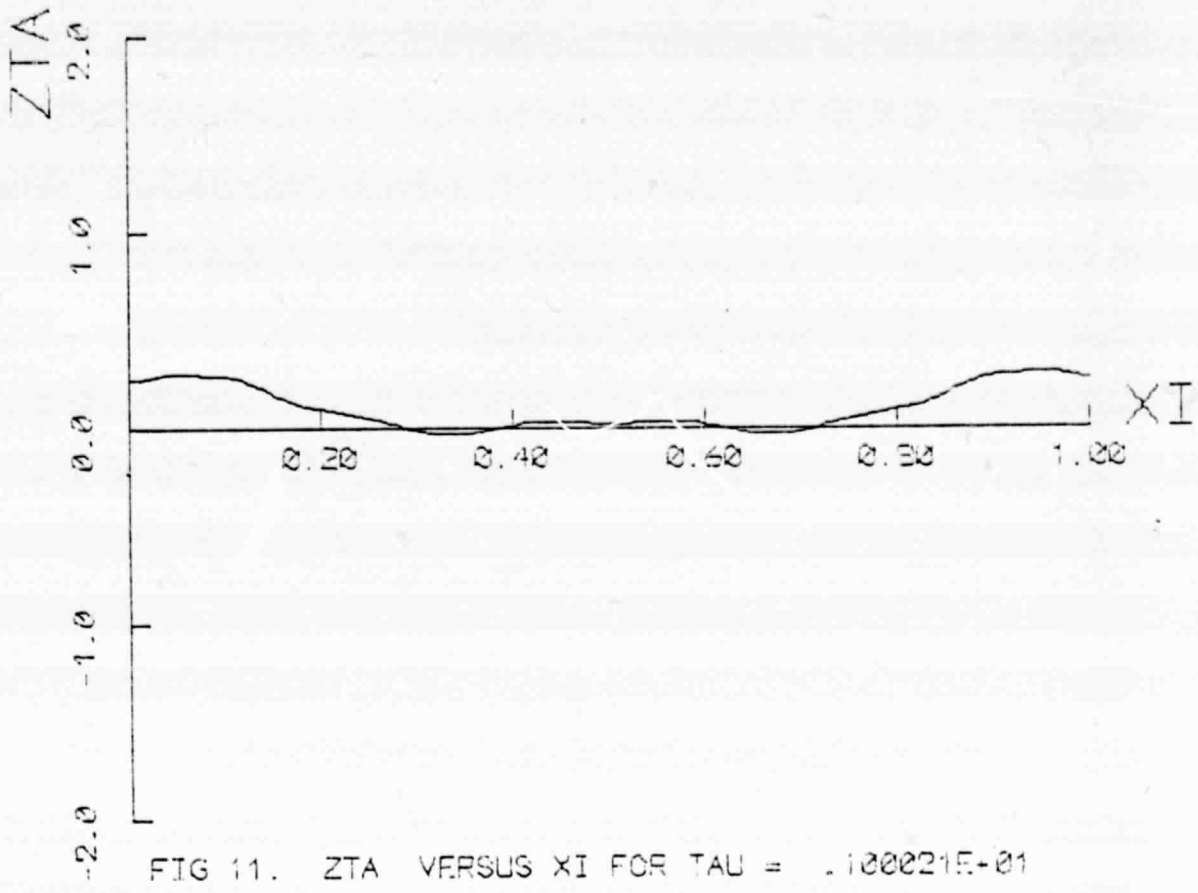

FIG 11. ZTA VERSUS XI FOR TAU = .100021E-01

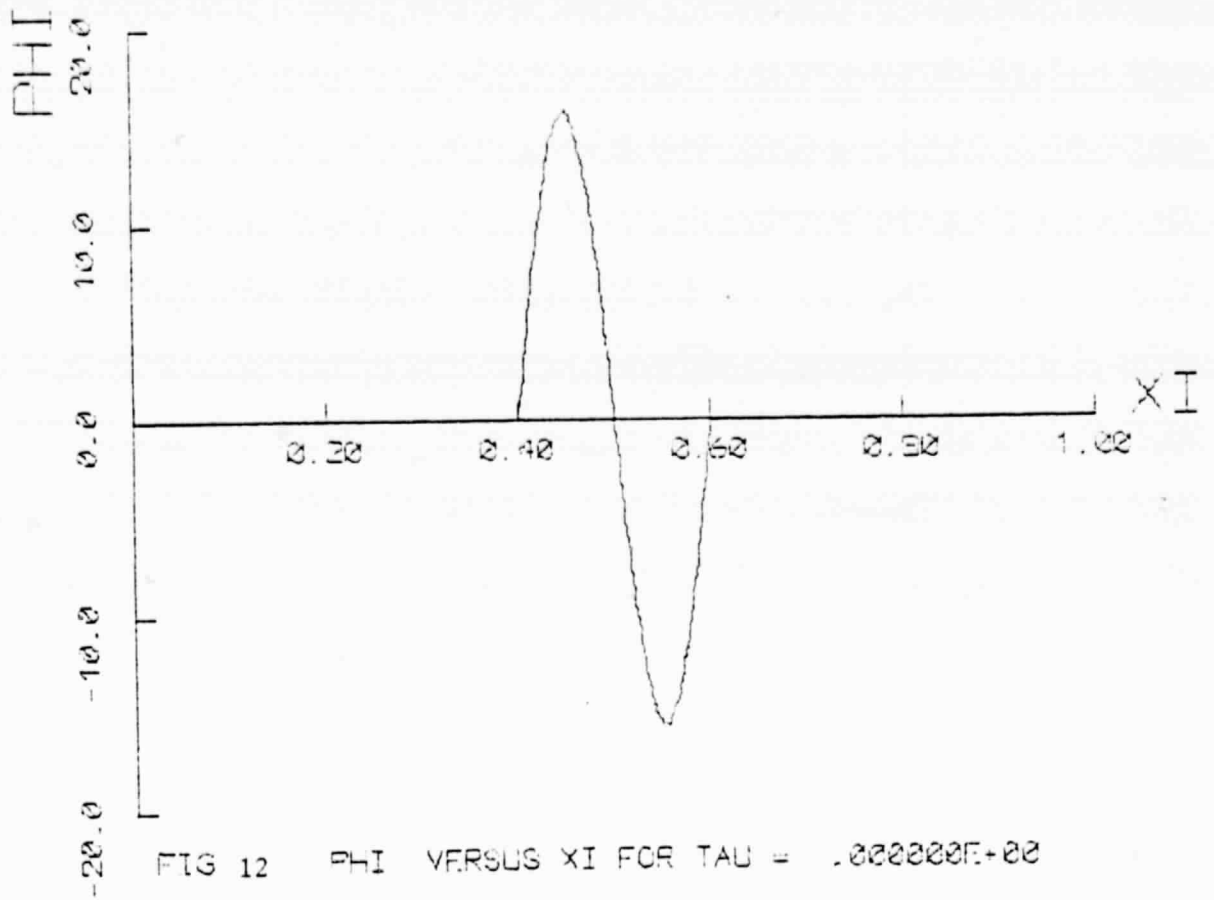

FIG 12 PHI VERSUS XI FOR TAU = .0000000E+00

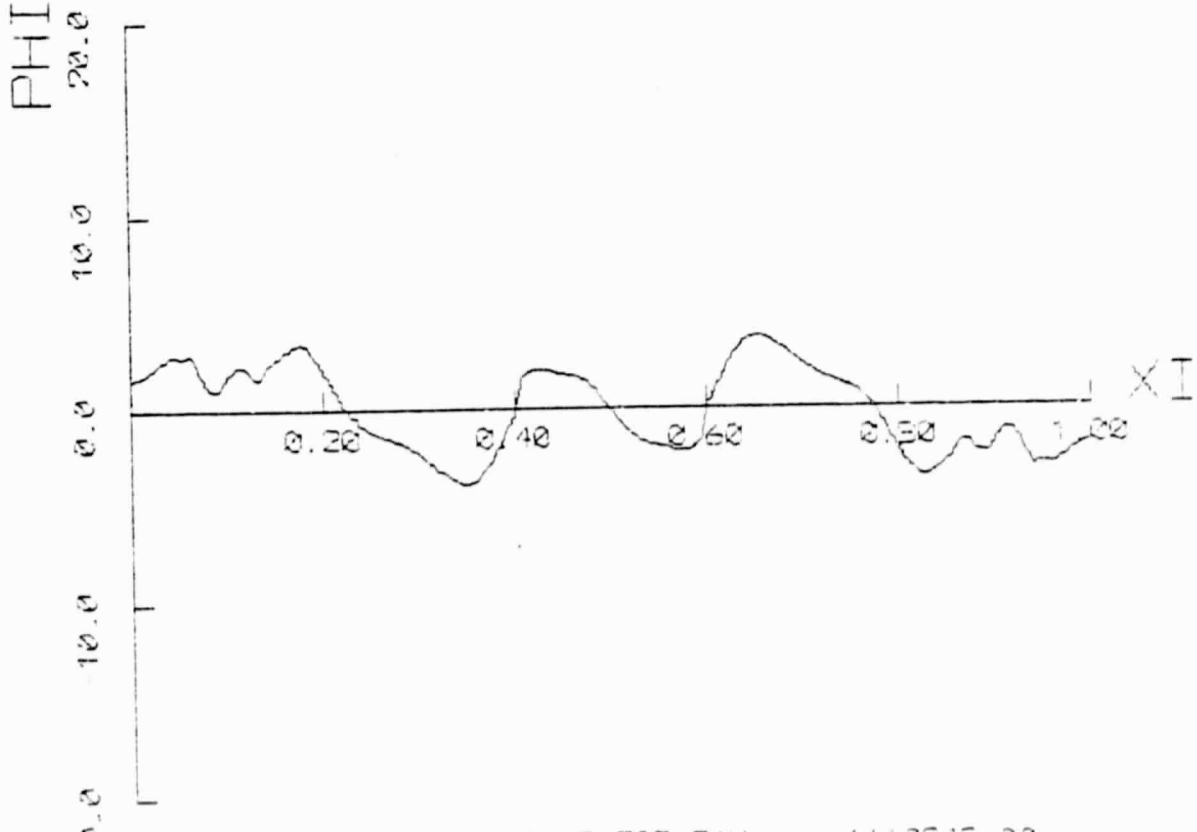

FIG 13 PHI VERSUS XI FOR TAU = .1112945E+00

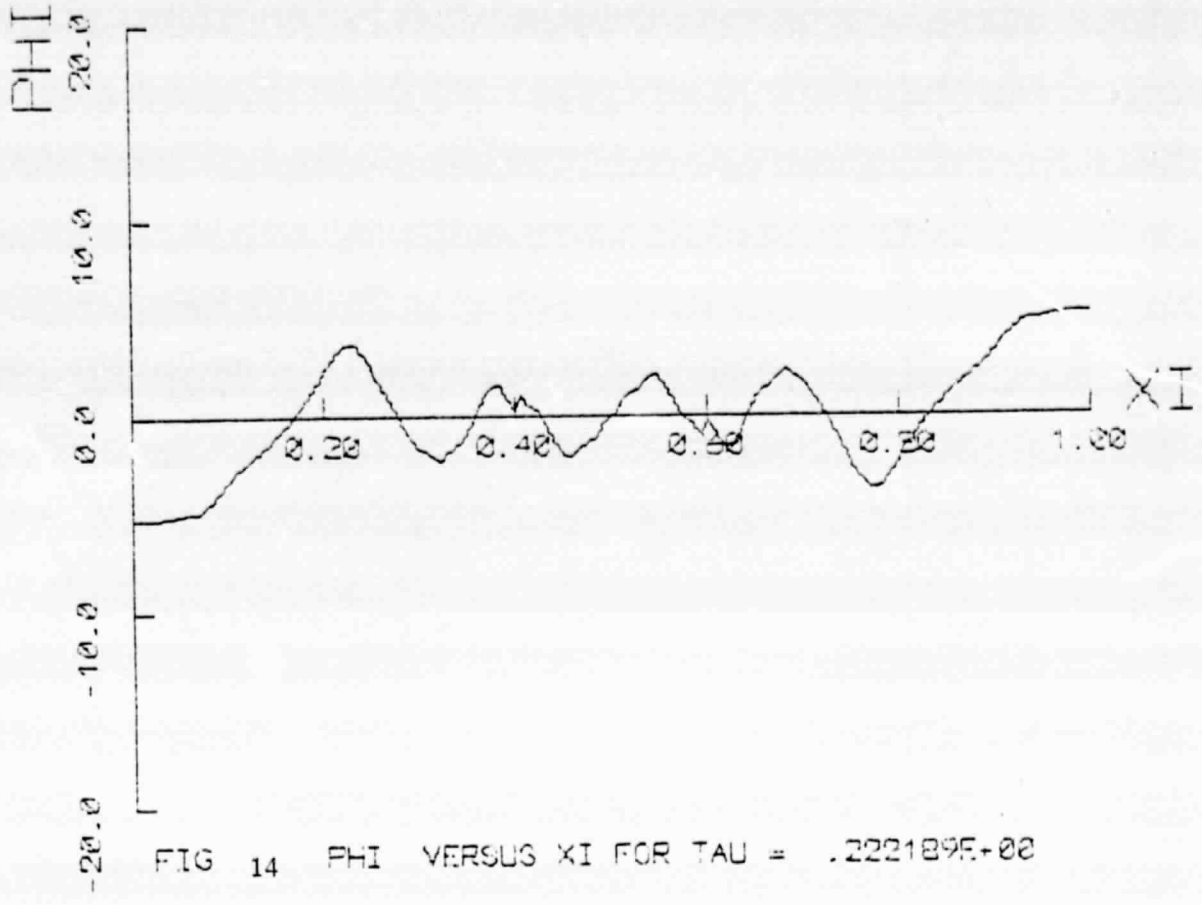

FIG 14 PHI VERSUS XI FOR TAU = .222189E+00

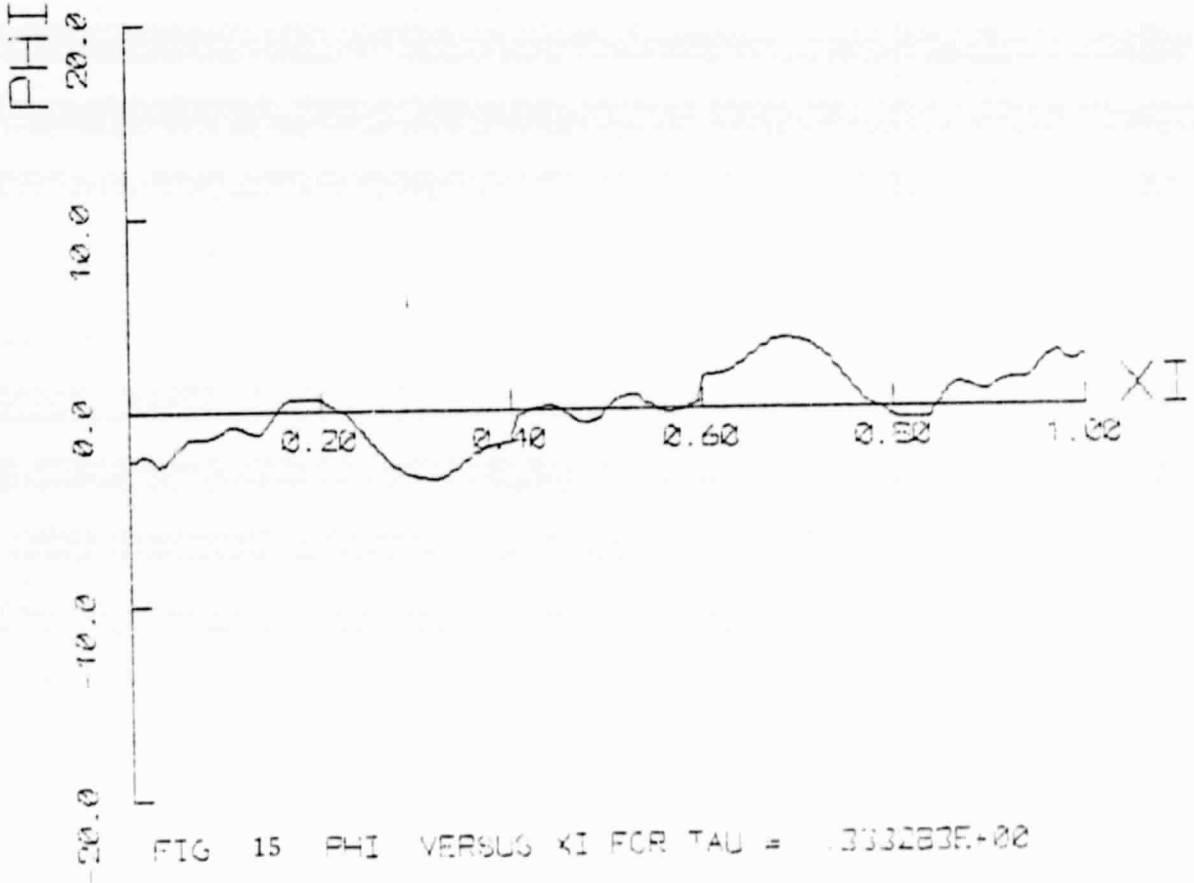

FIG 15 PHI VERSUS XI FOR TAU = .333283E+00

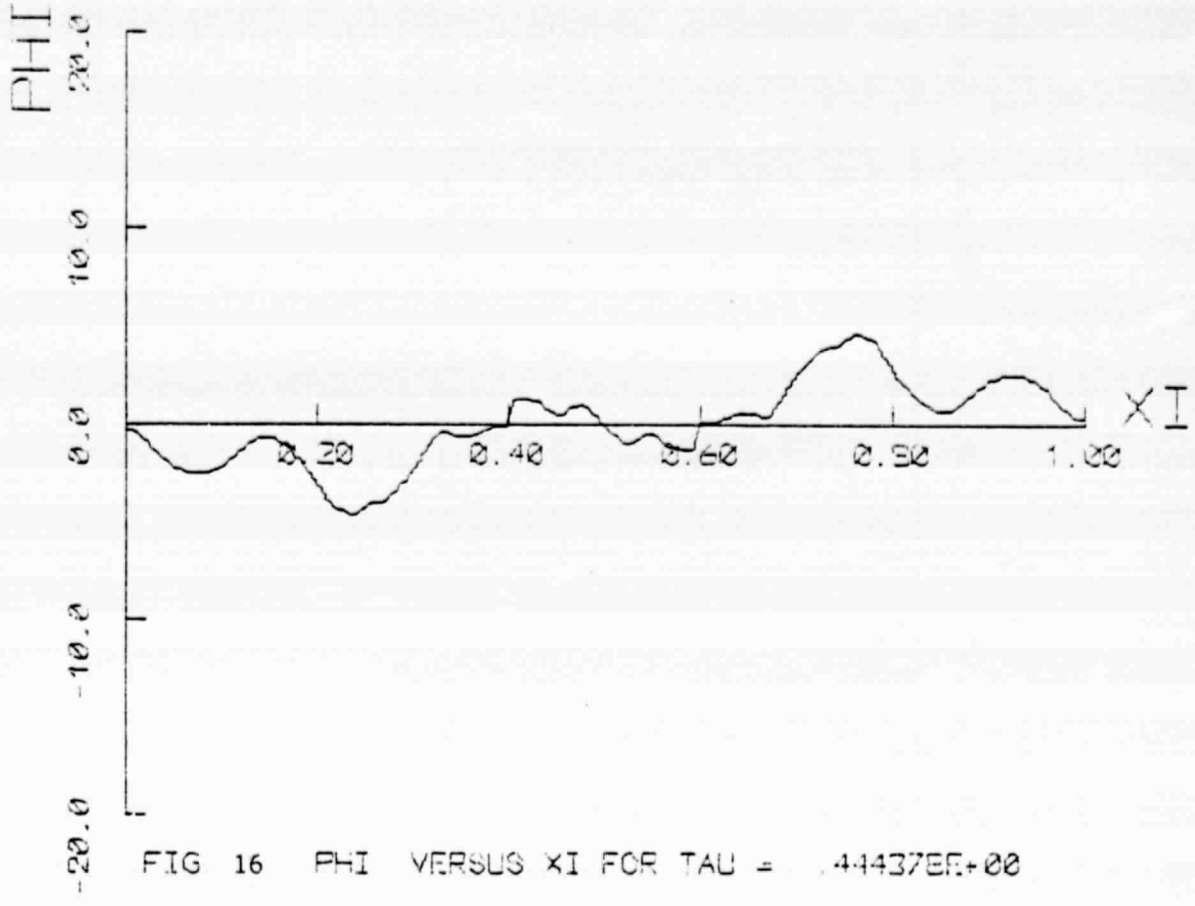

FIG 16 PHI VERSUS XI FOR TAU = .444376E+00

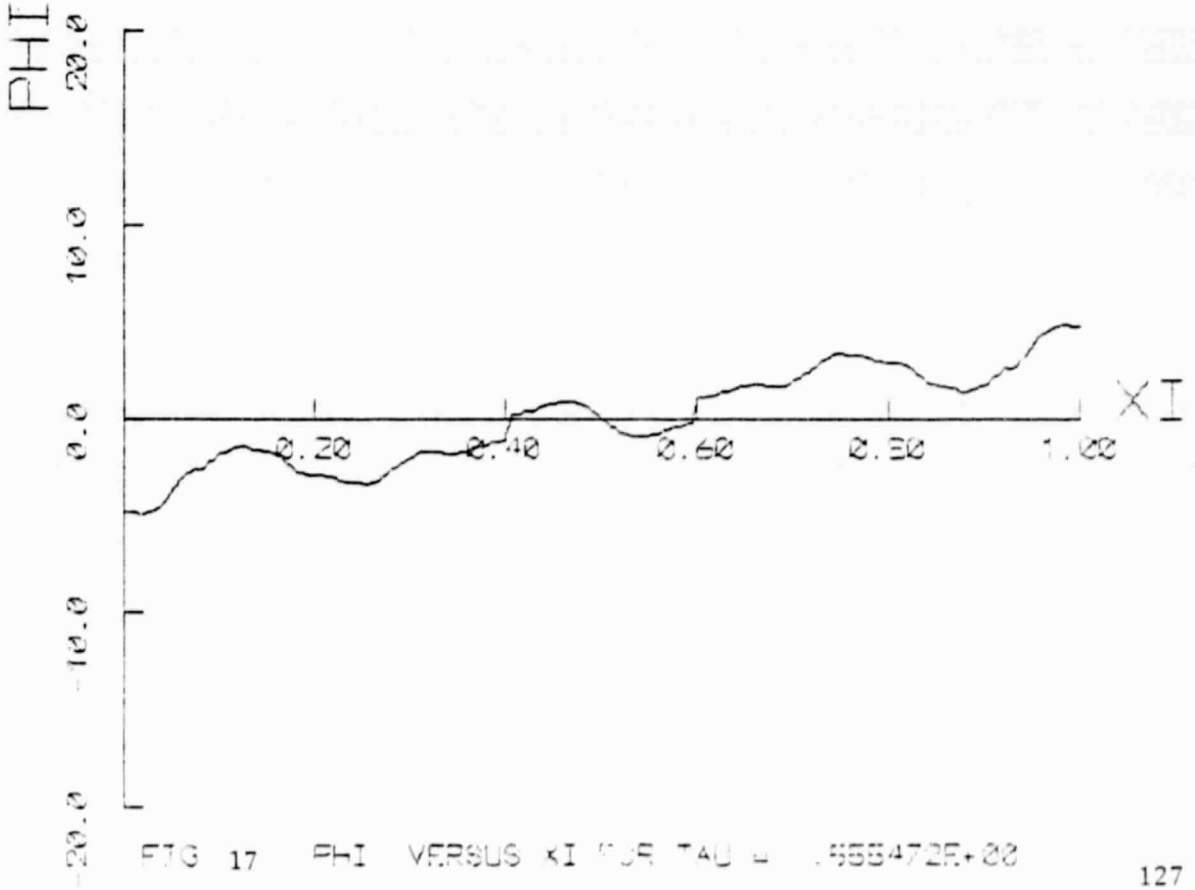

FIG 17 PHI VERSUS XI FOR TAU = .555472E+00

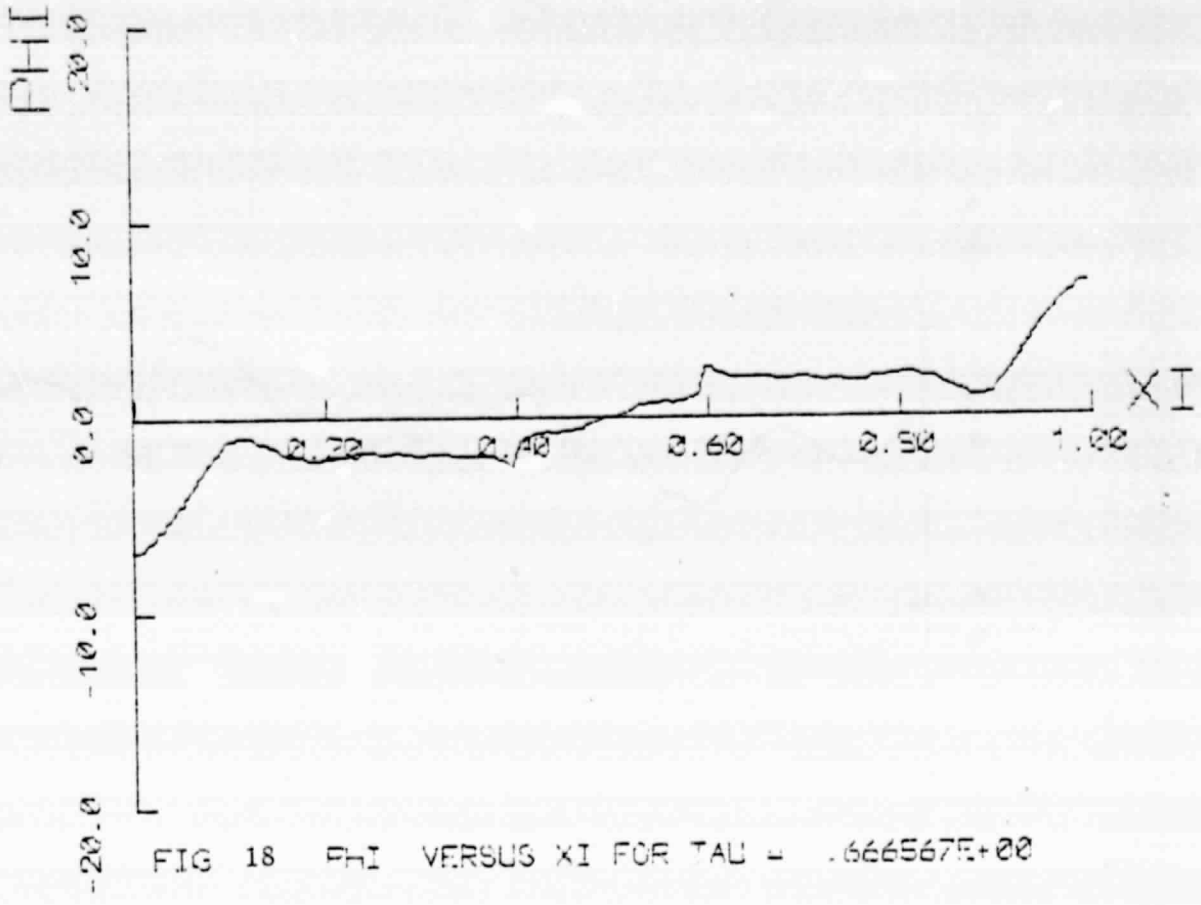

FIG 18 PHI VERSUS XI FOR TAU = .666567E+00

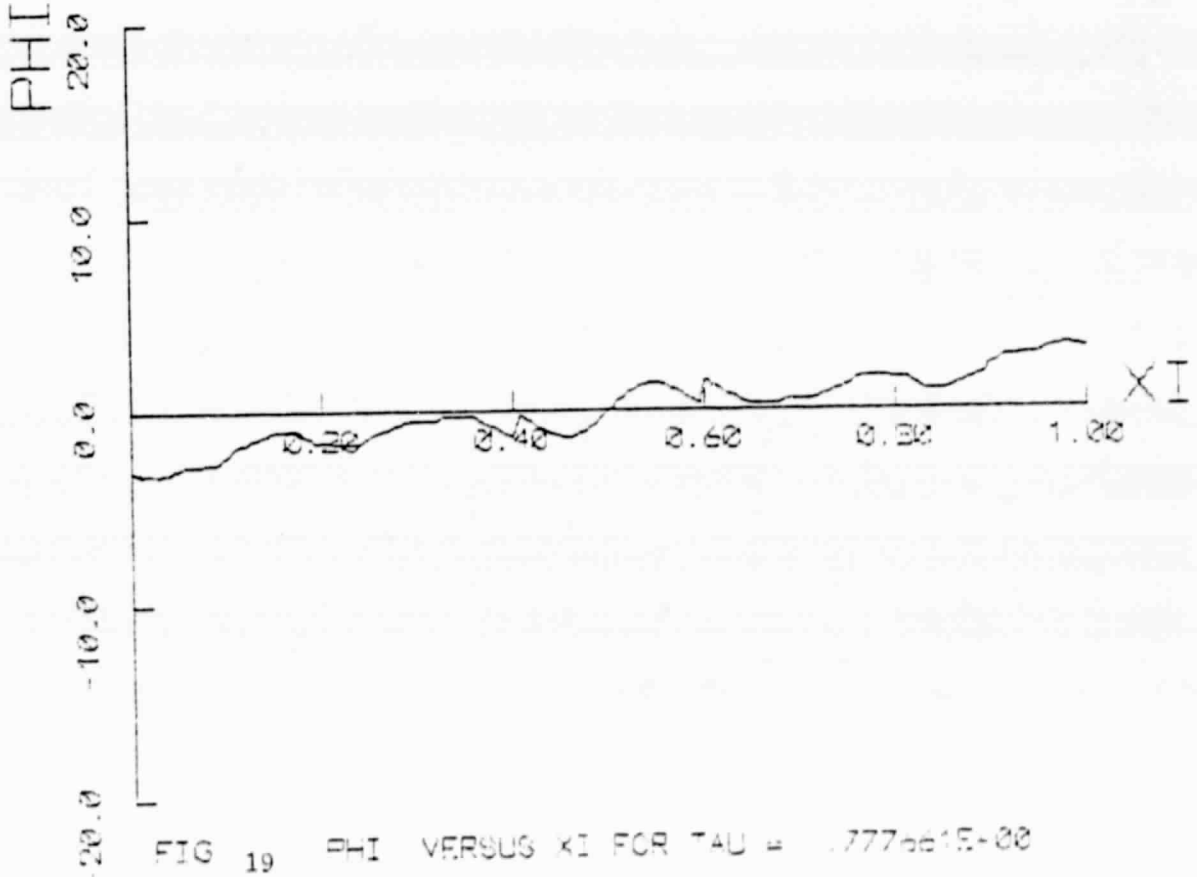

FIG 19 PHI VERSUS XI FOR TAU = .777e61E+00

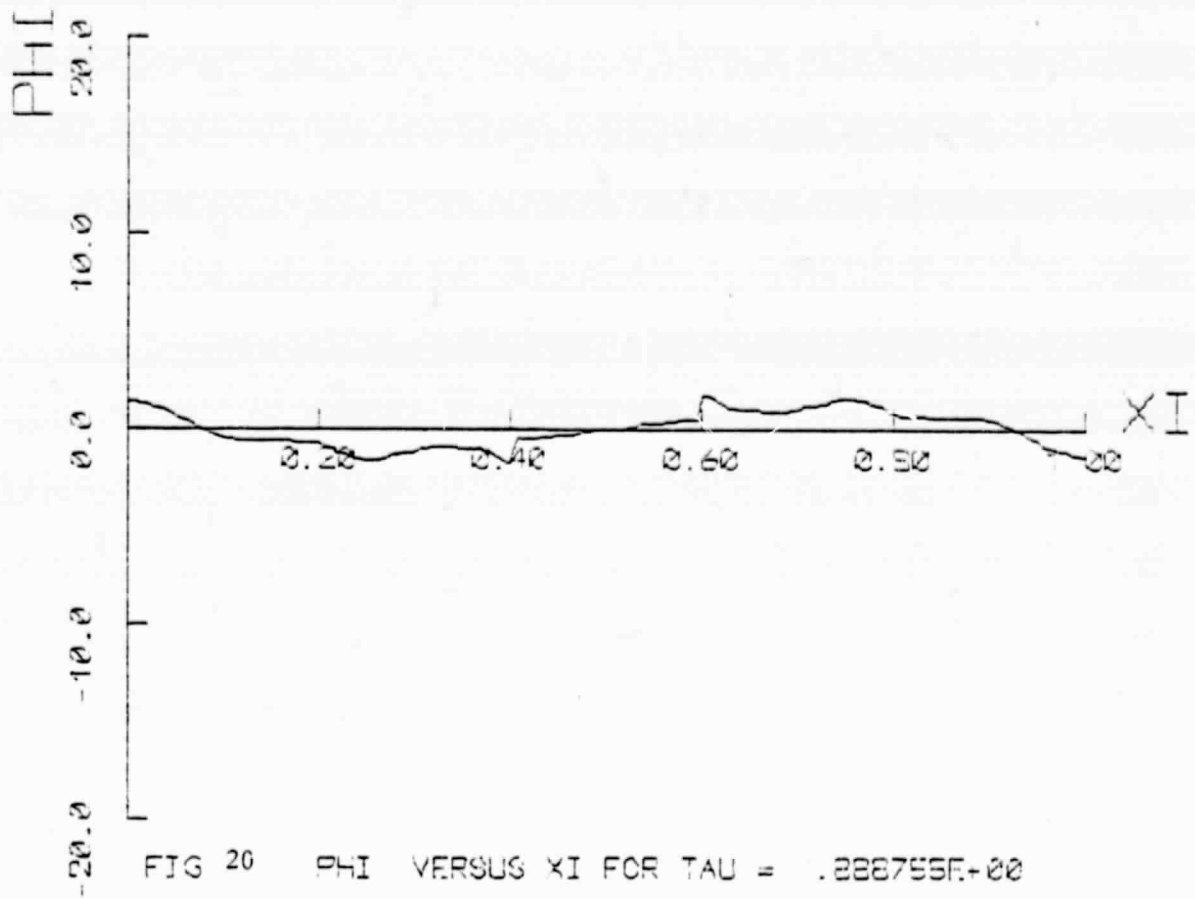

FIG 20 PHI VERSUS XI FOR TAU = .288755E+00

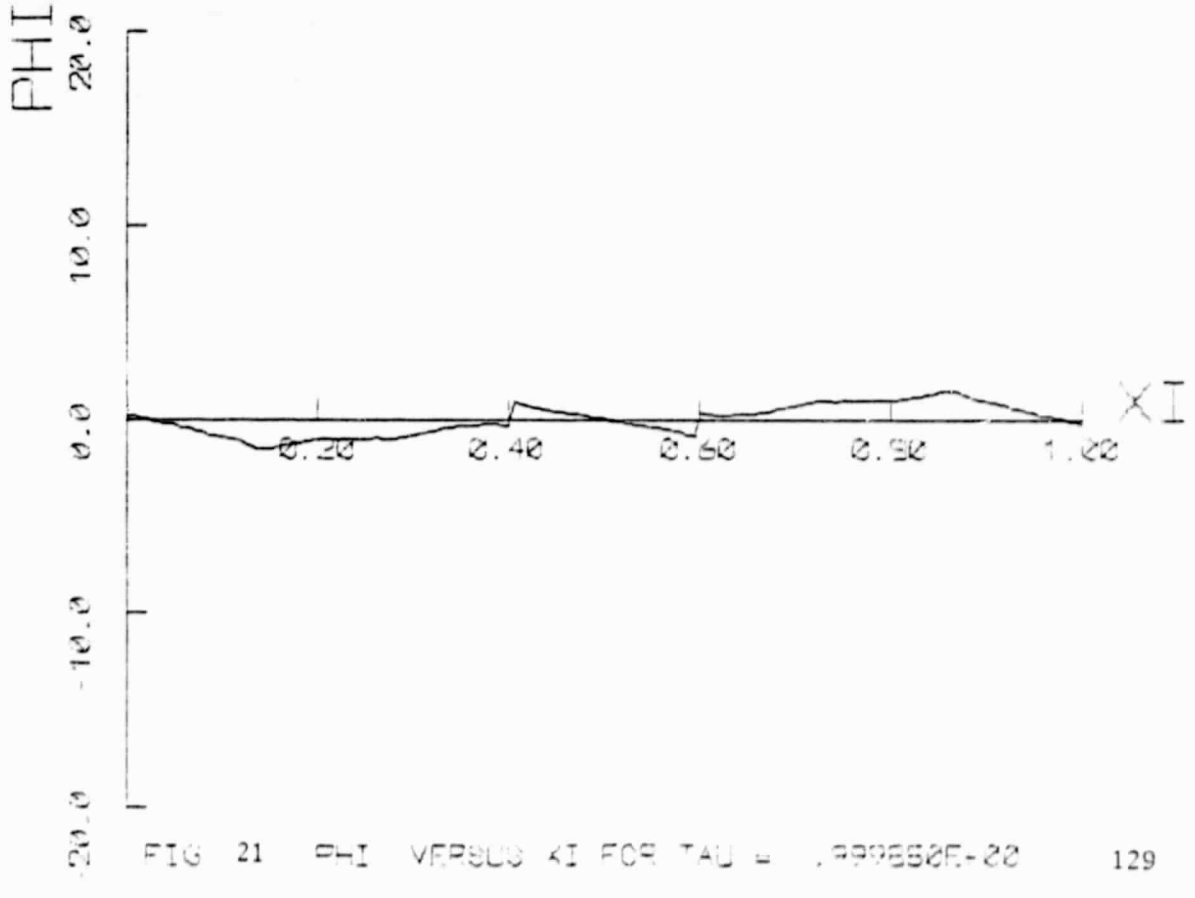

FIG 21 PHI VERSUS XI FOR TAU = .299650E+00

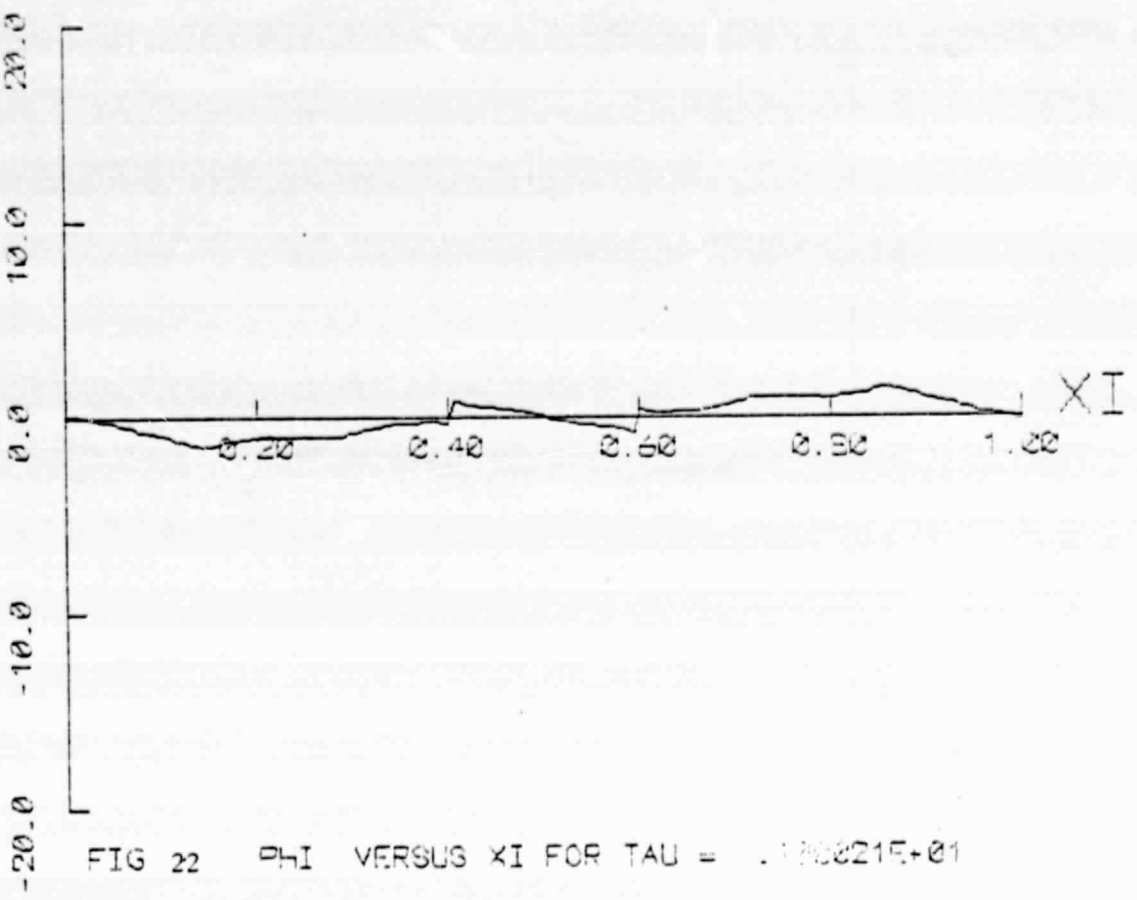

FIG 22 PHI VERSUS XI FOR TAU = .1[illegible]21E+01

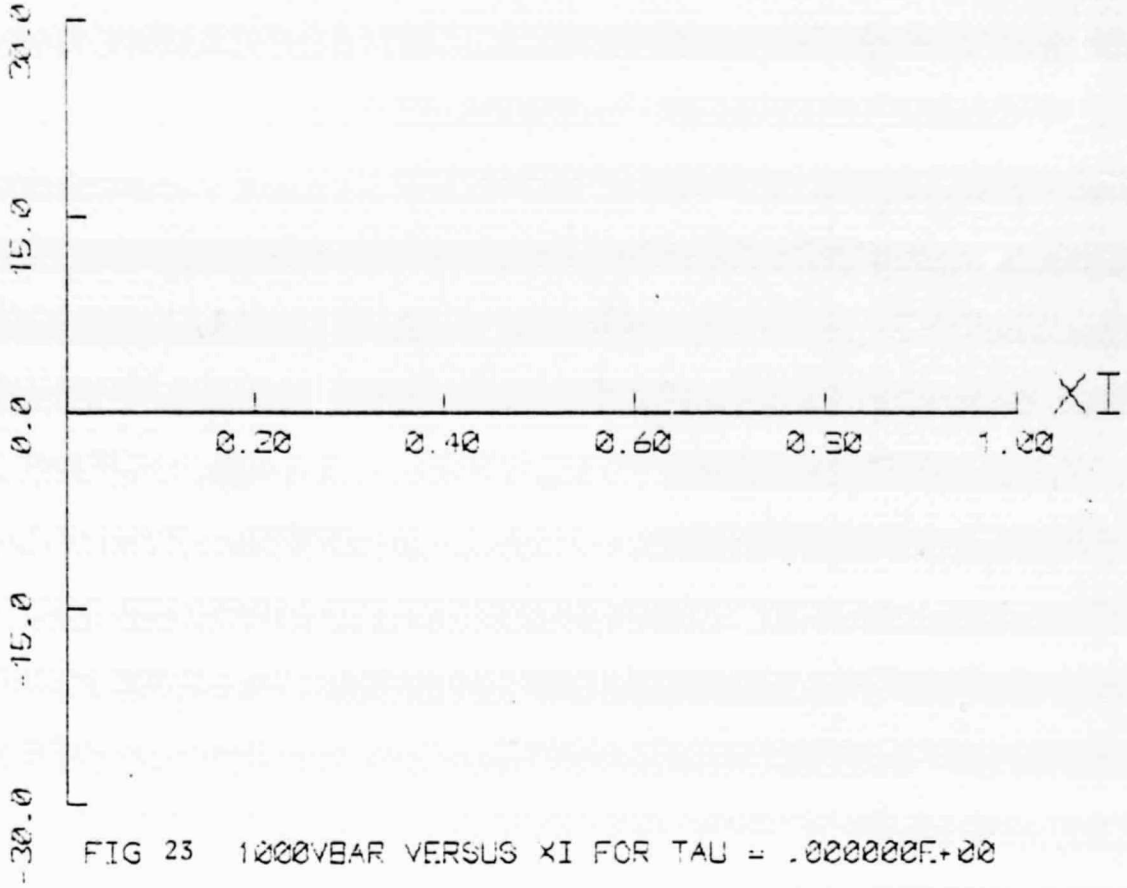

FIG 23 1000VBAR VERSUS XI FOR TAU = .000000E+00

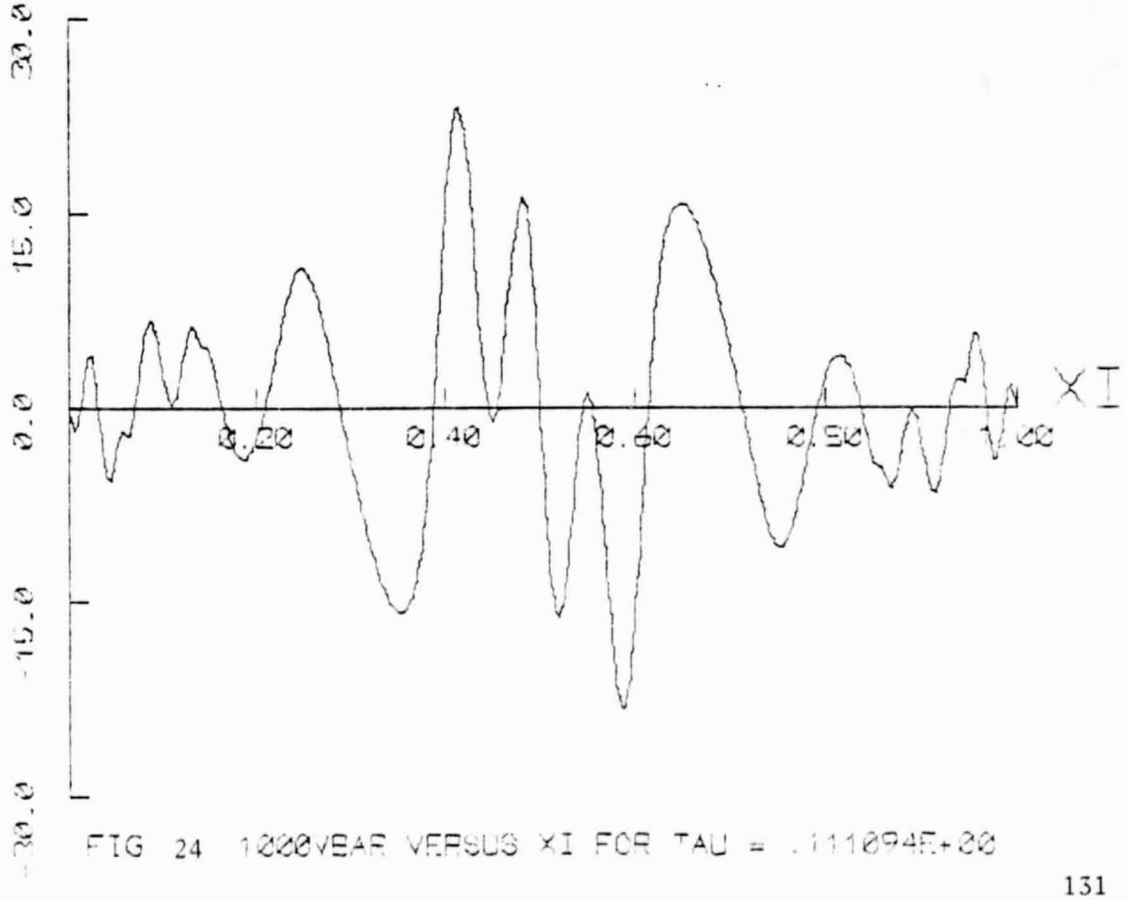

FIG 24 1000VBAR VERSUS XI FOR TAU = .111094E+00

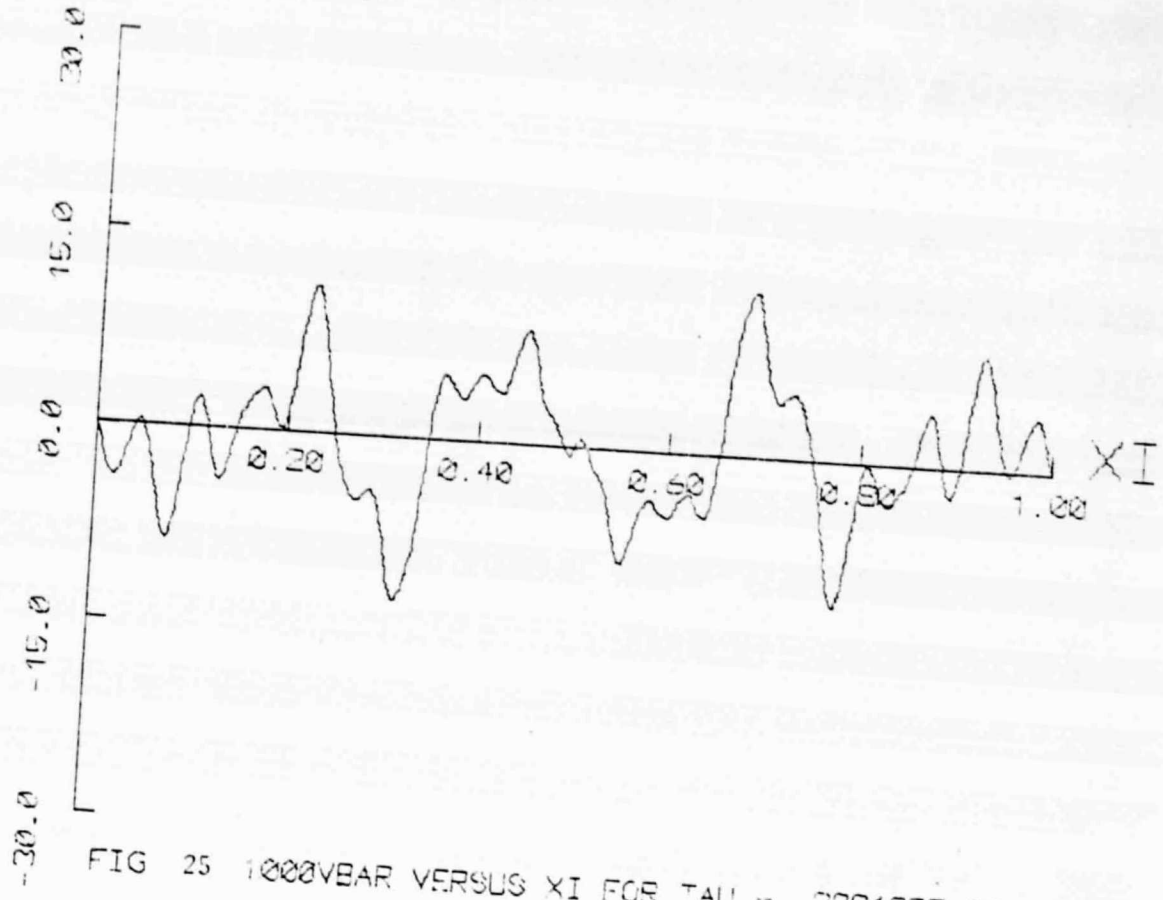

FIG 25 1000VBAR VERSUS XI FOR TAU = .2221895+00

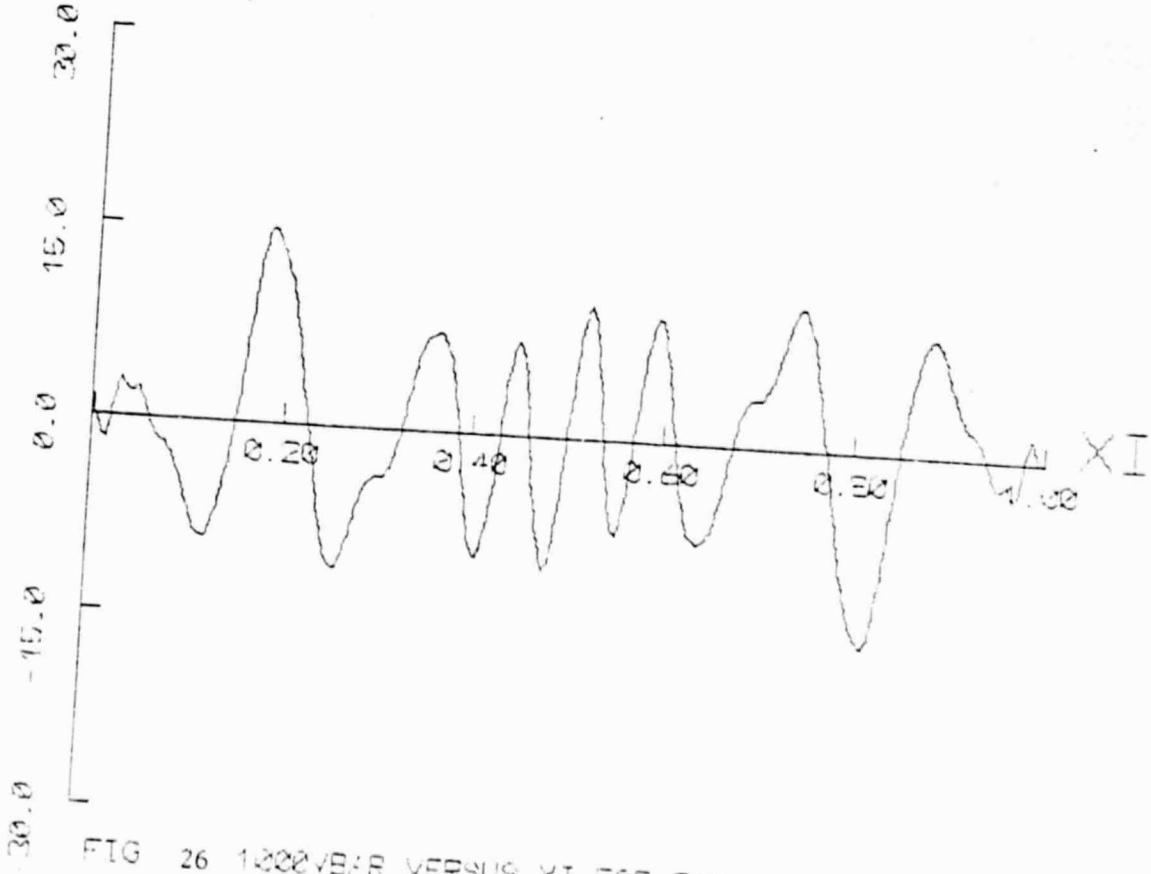

FIG 26 1000VBAR VERSUS XI FOR TAU = .3332835-00

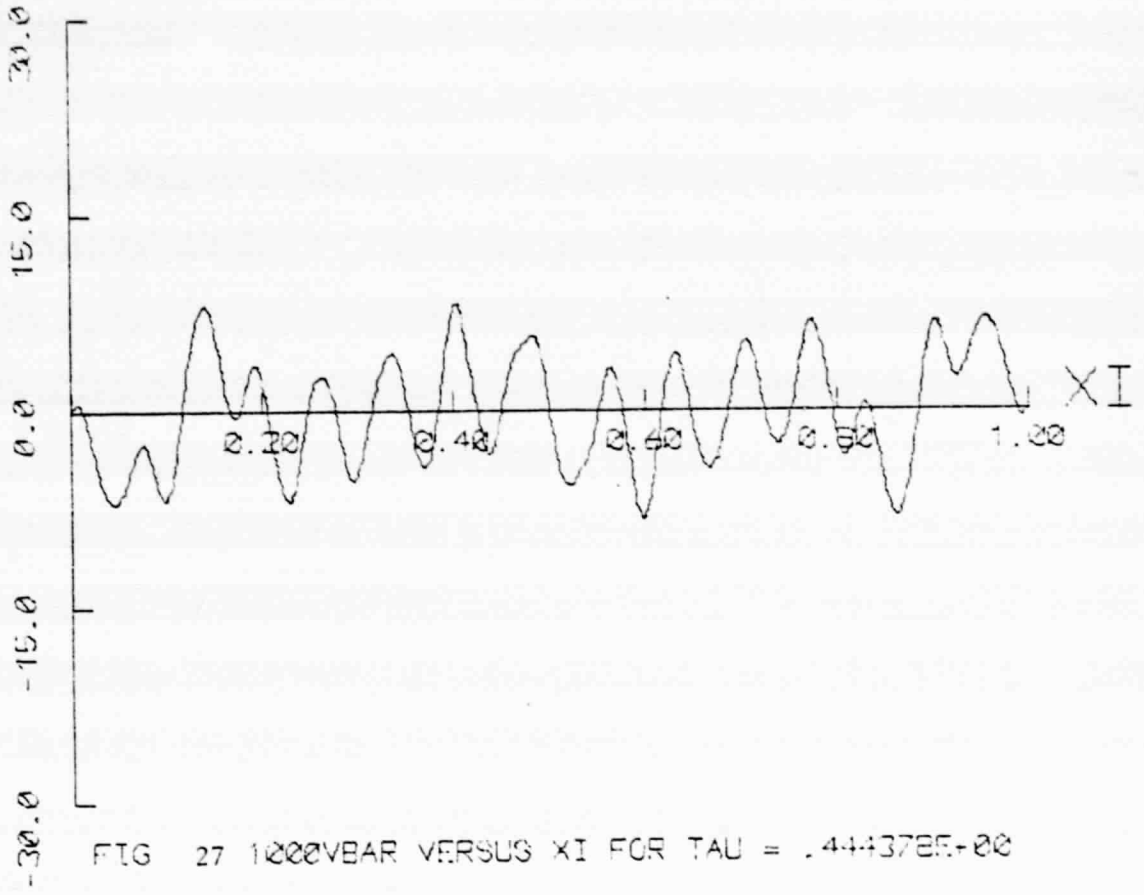

FIG 27 1000VBAR VERSUS XI FOR TAU = .444378E+00

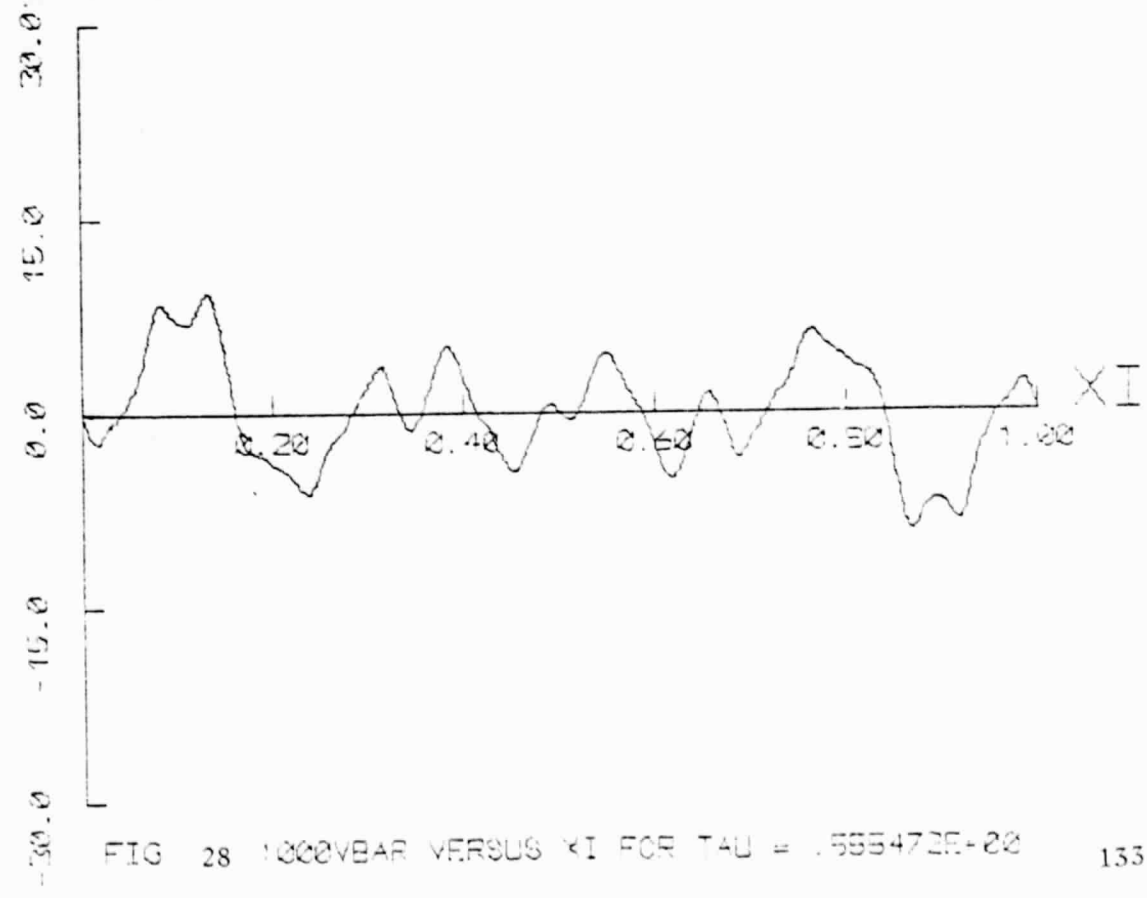

FIG 28 1000VBAR VERSUS XI FOR TAU = .555472E+00

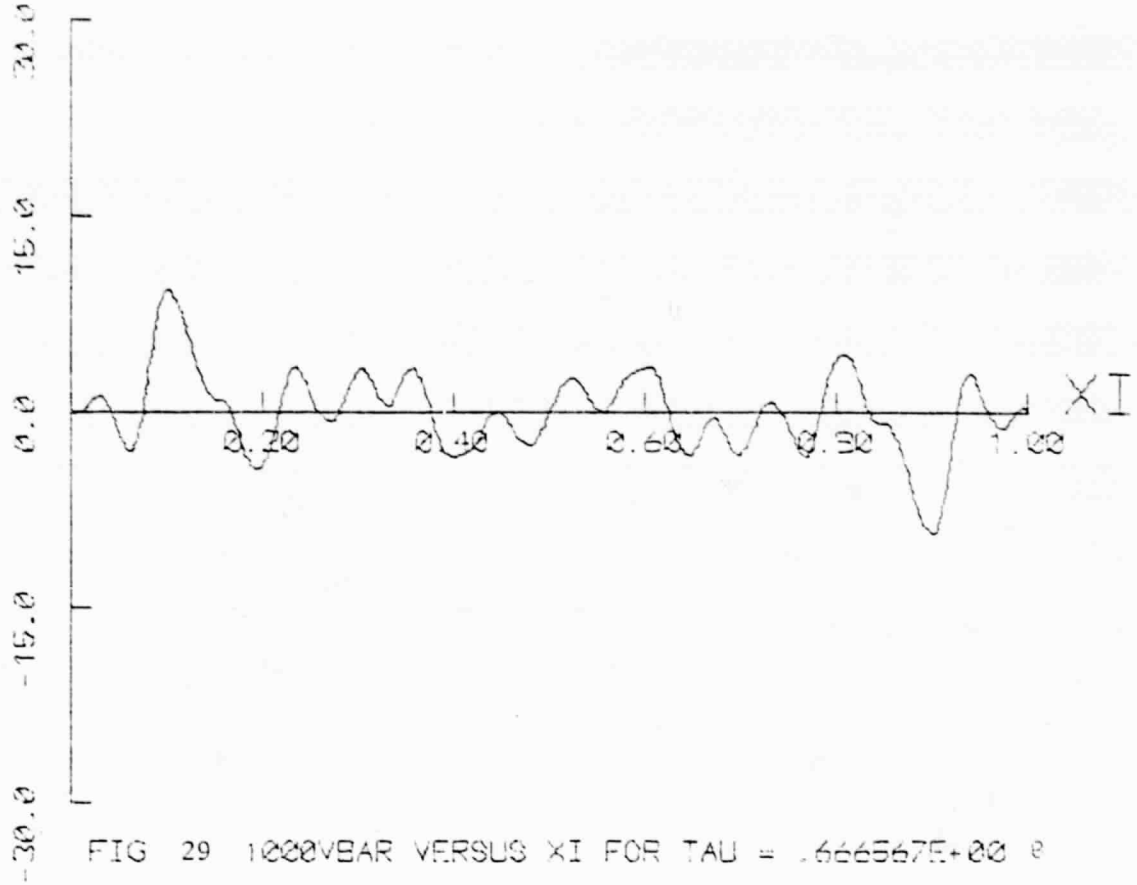

FIG 29 1000VBAR VERSUS XI FOR TAU = .6665675E+00

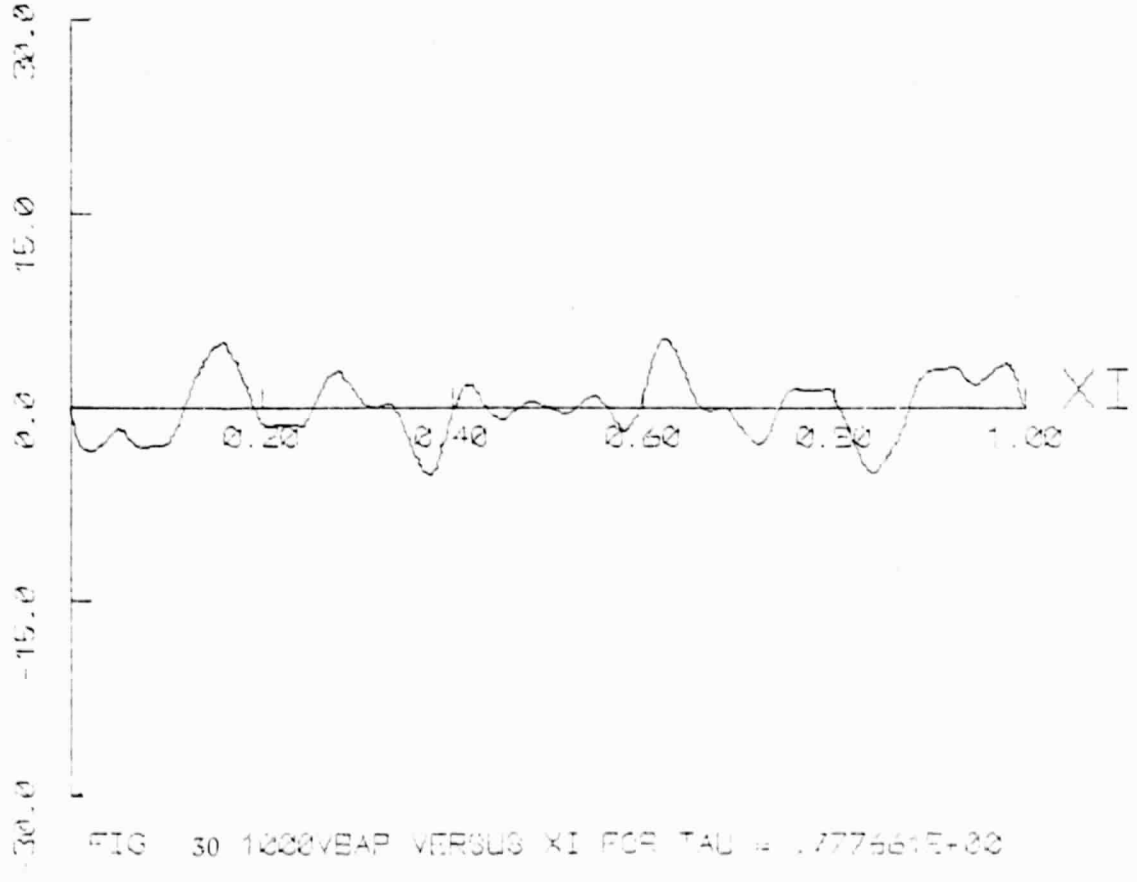

FIG 30 1000VBAR VERSUS XI FOR TAU = .7776615E+00

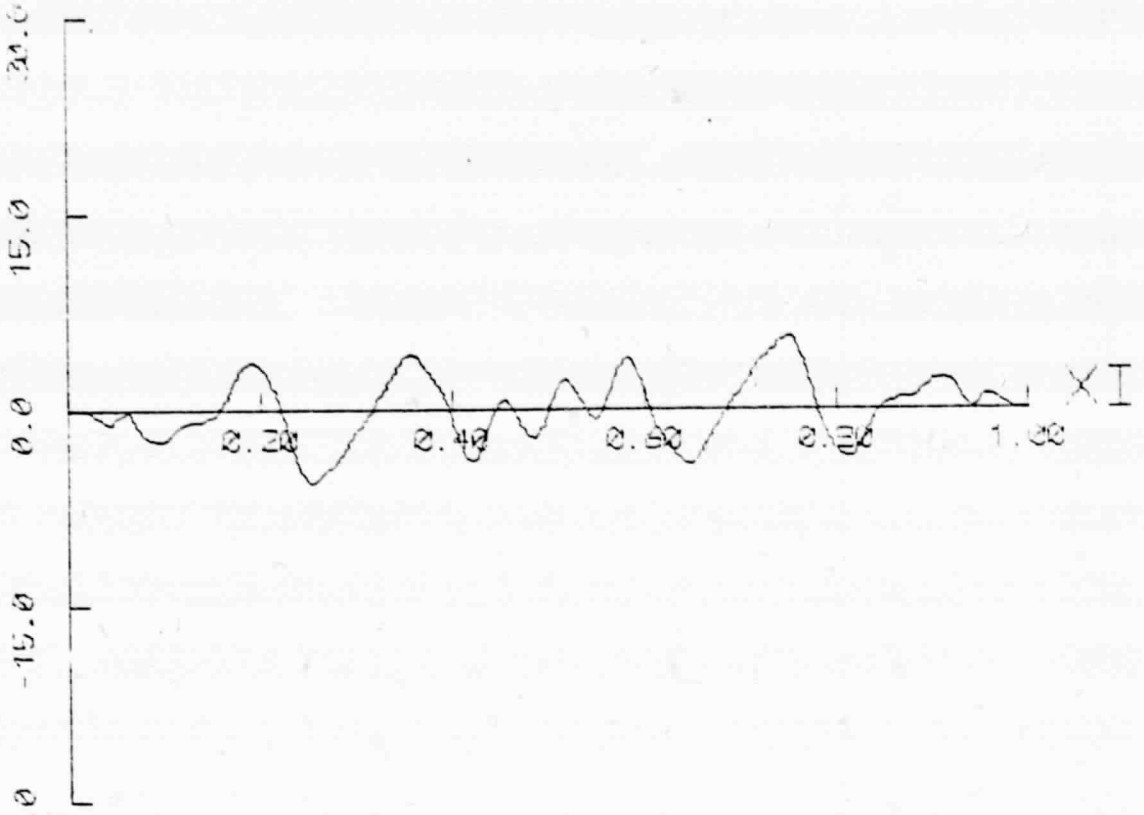

FIG 31 1000VBAR VERSUS XI FOR TAU = .888755E-00

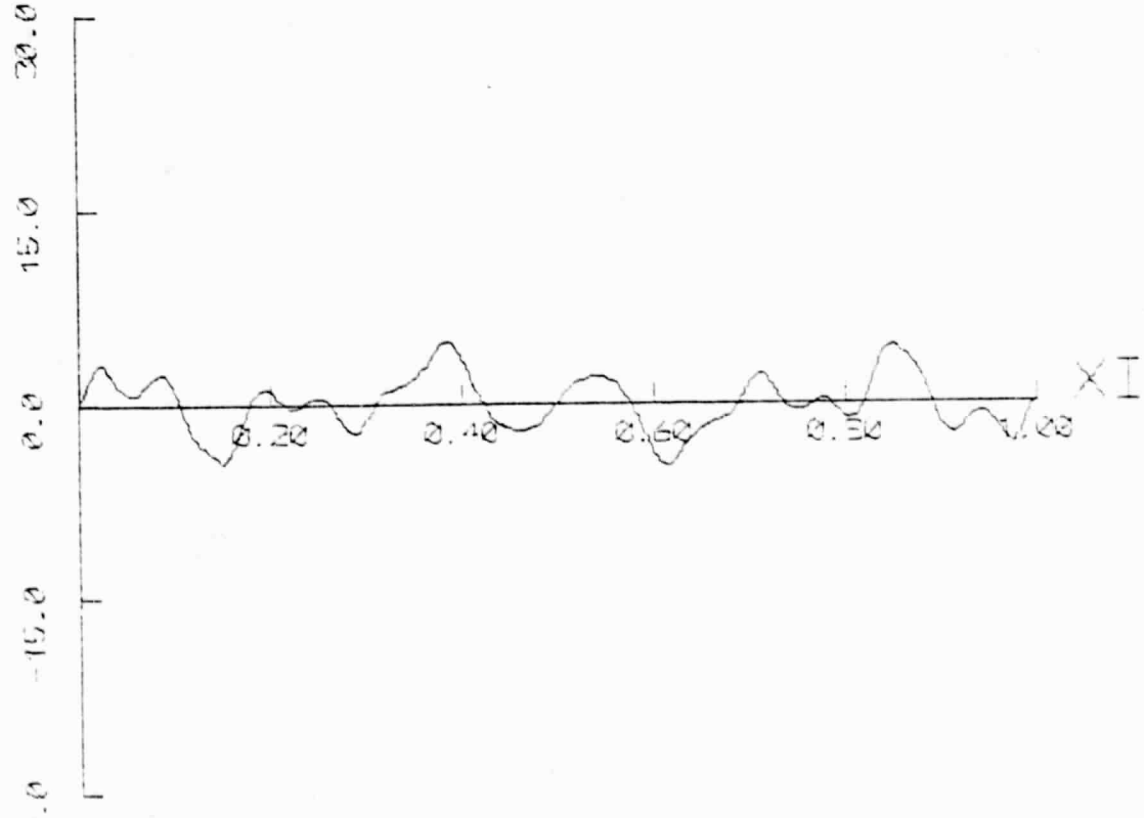

FIG 32 1000VBAR VERSUS XI FOR TAU = .999852E-00

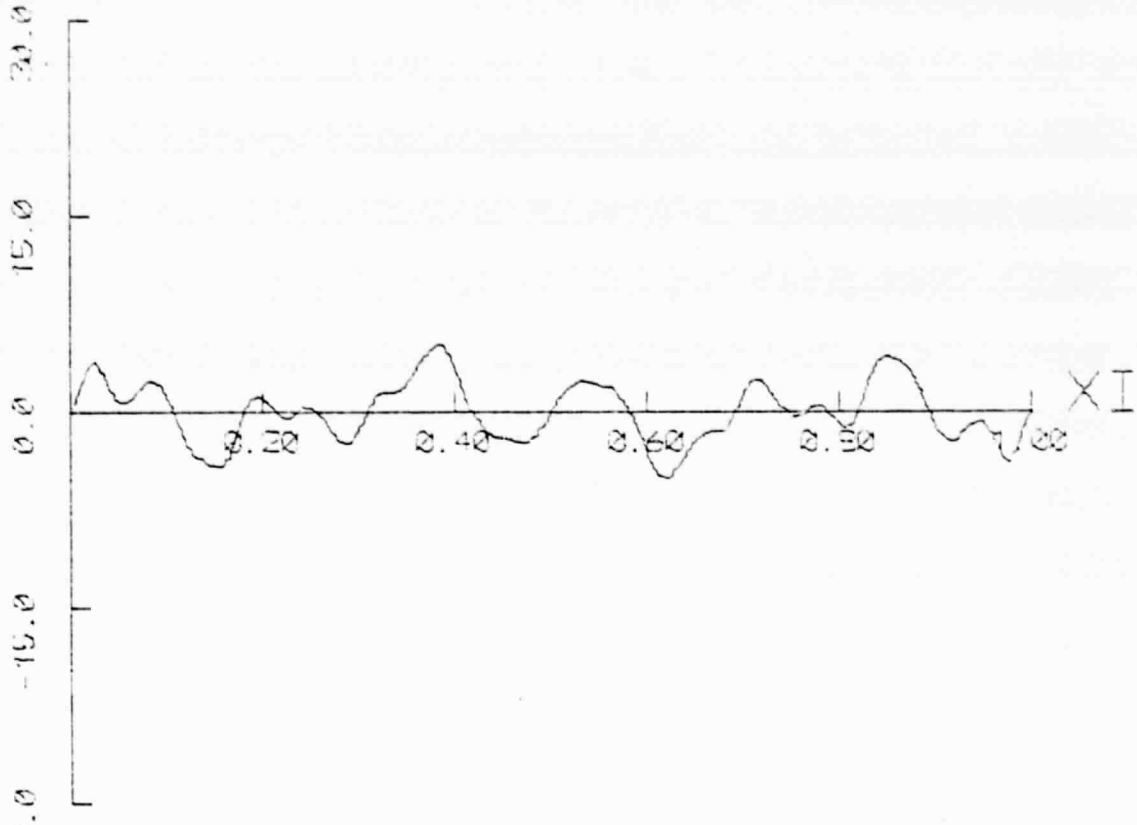

FIG 33 1000VBAR VERSUS XI FOR TAU = .1000215+01

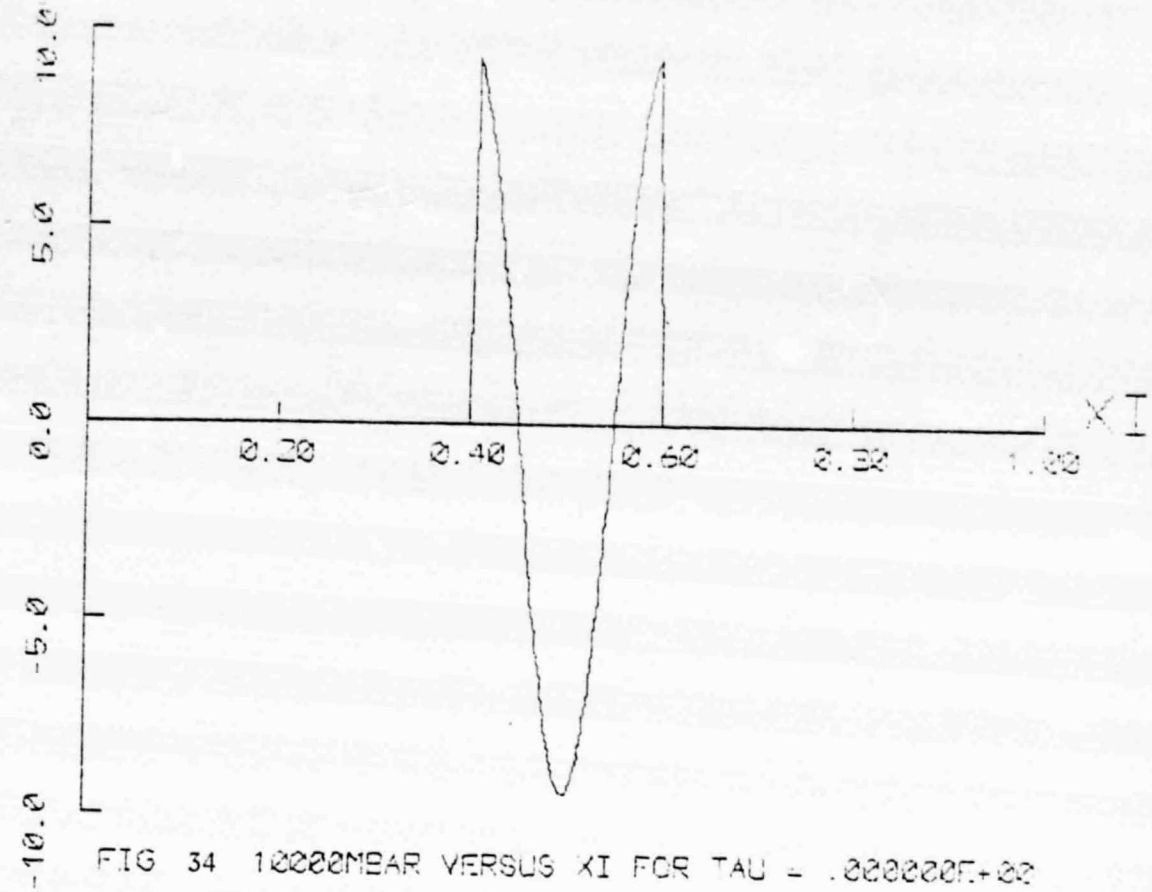

FIG 34 10000MBAR VERSUS XI FOR TAU = .000000E+00

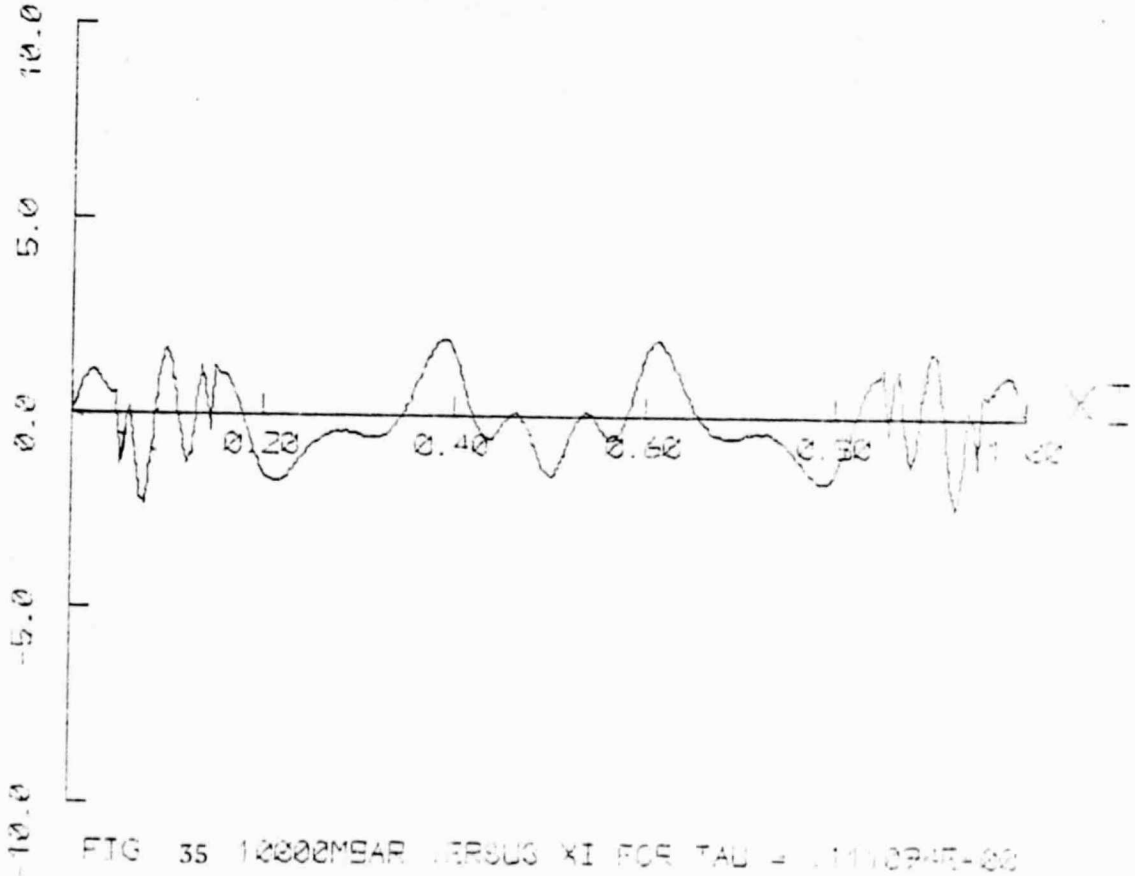

FIG 35 10000MBAR VERSUS XI FOR TAU = .111028E-00

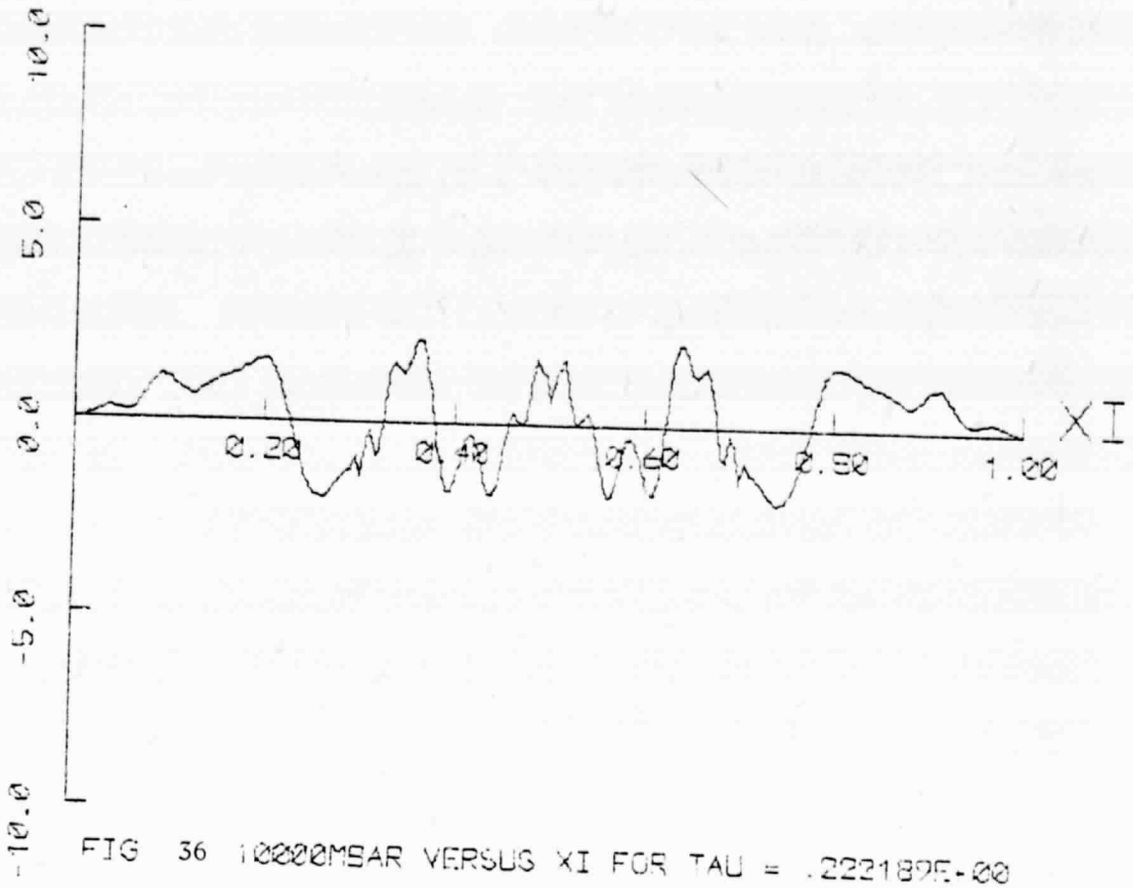

FIG 36 10000MBAR VERSUS XI FOR TAU = .2221805-00

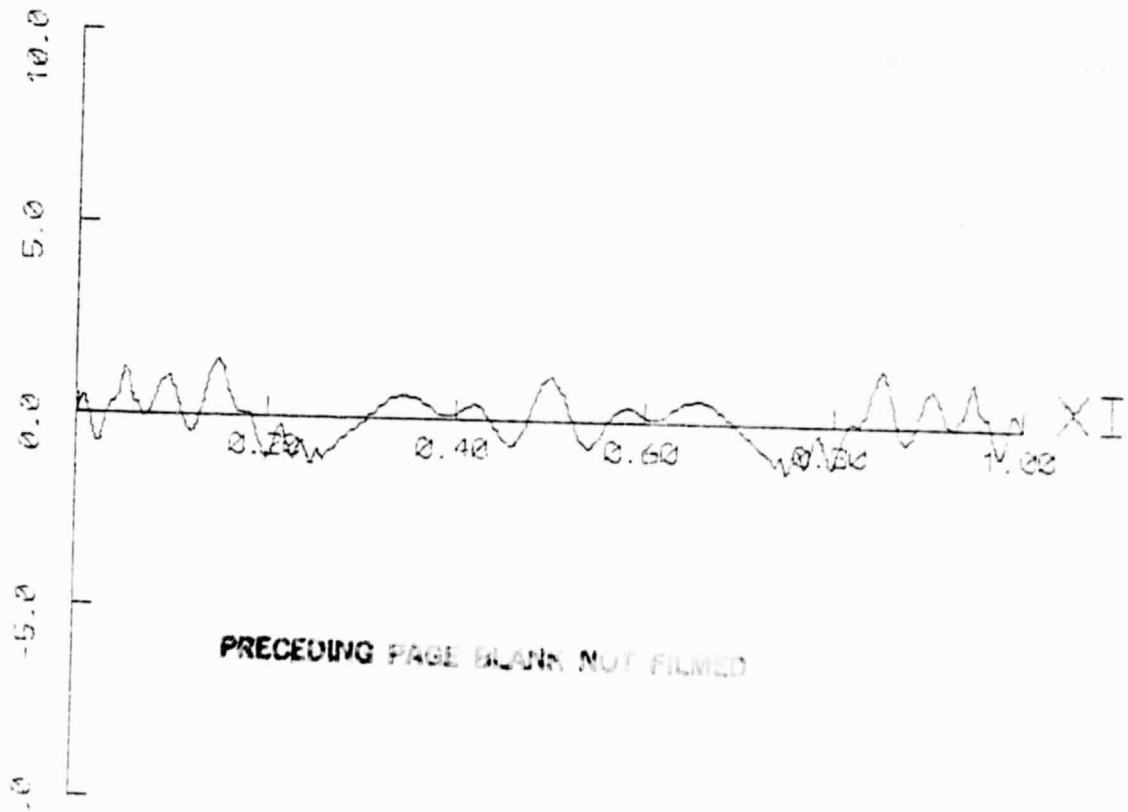

FIG 37 12000MBAR VERSUS XI FOR TAU = .3331830-00

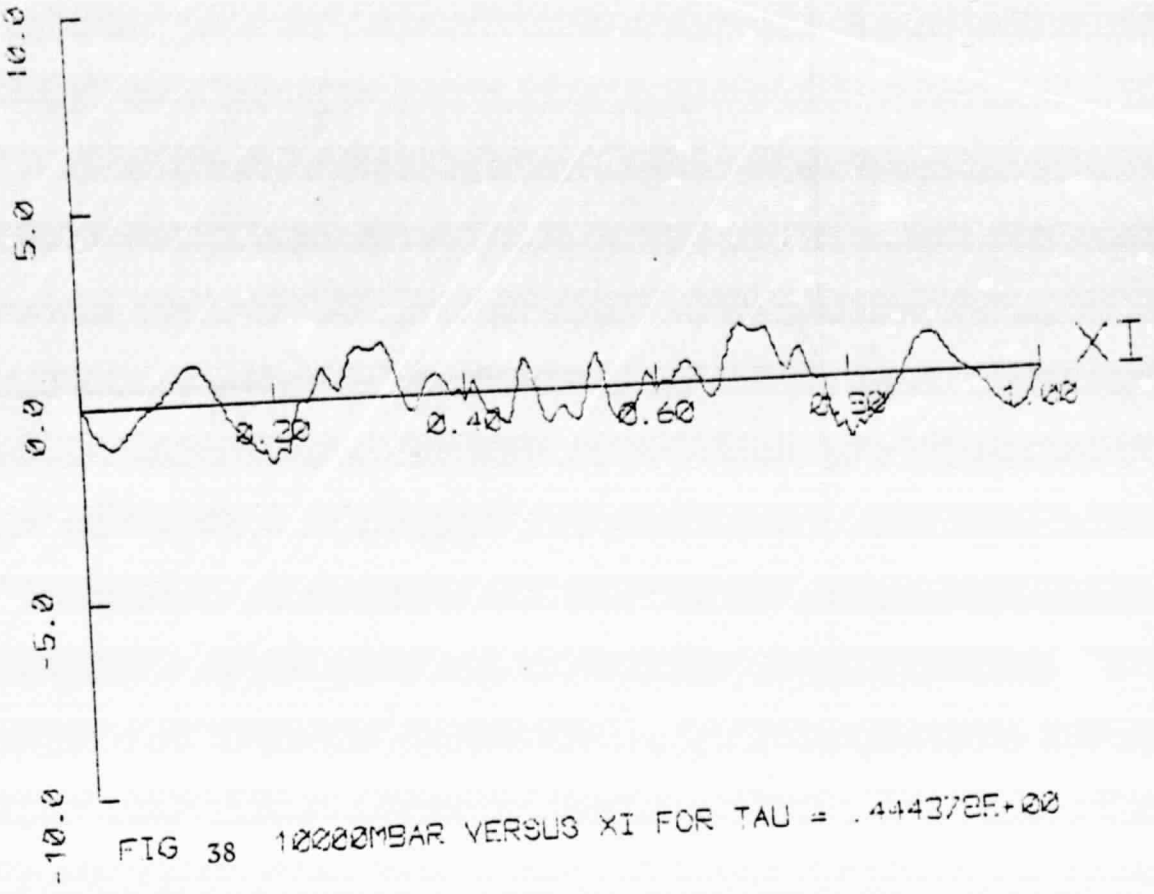

FIG 38 10000MBAR VERSUS XI FOR TAU = .444378E+00

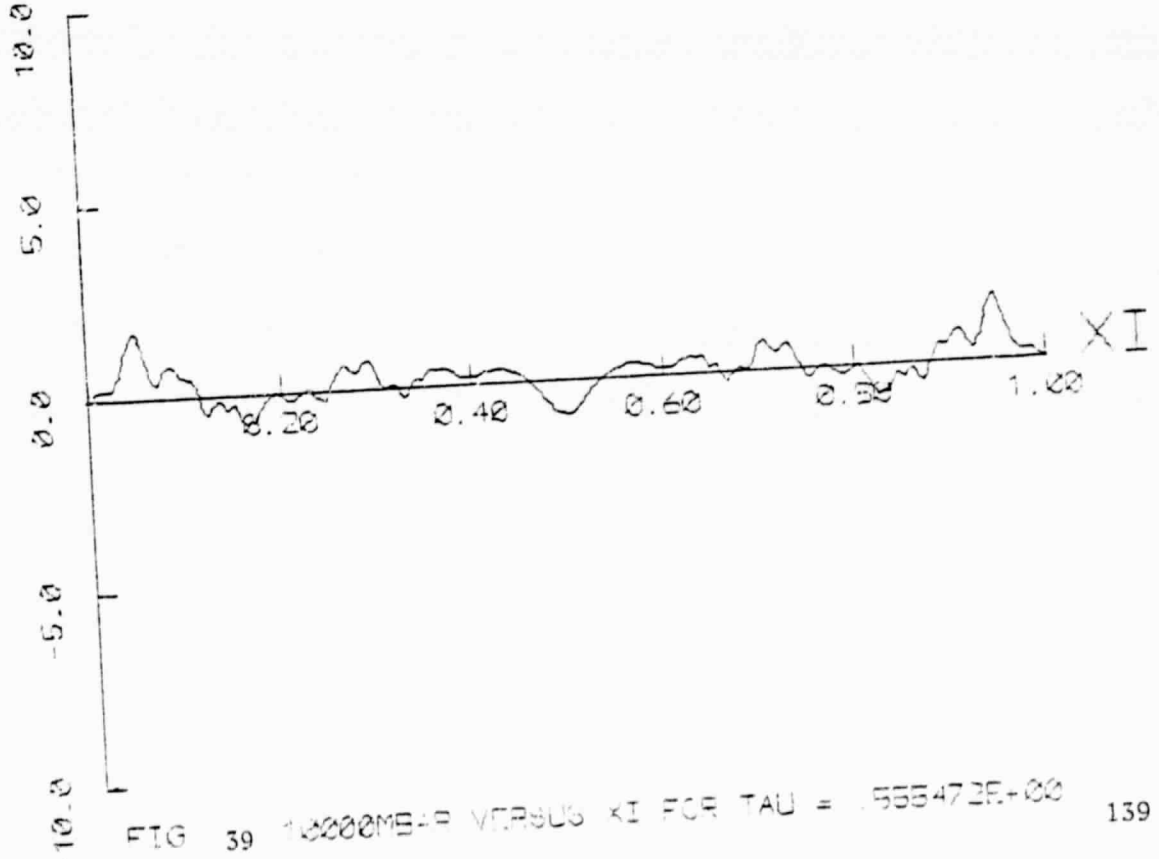

FIG 39 10000MBAR VERSUS XI FOR TAU = .555473E+00

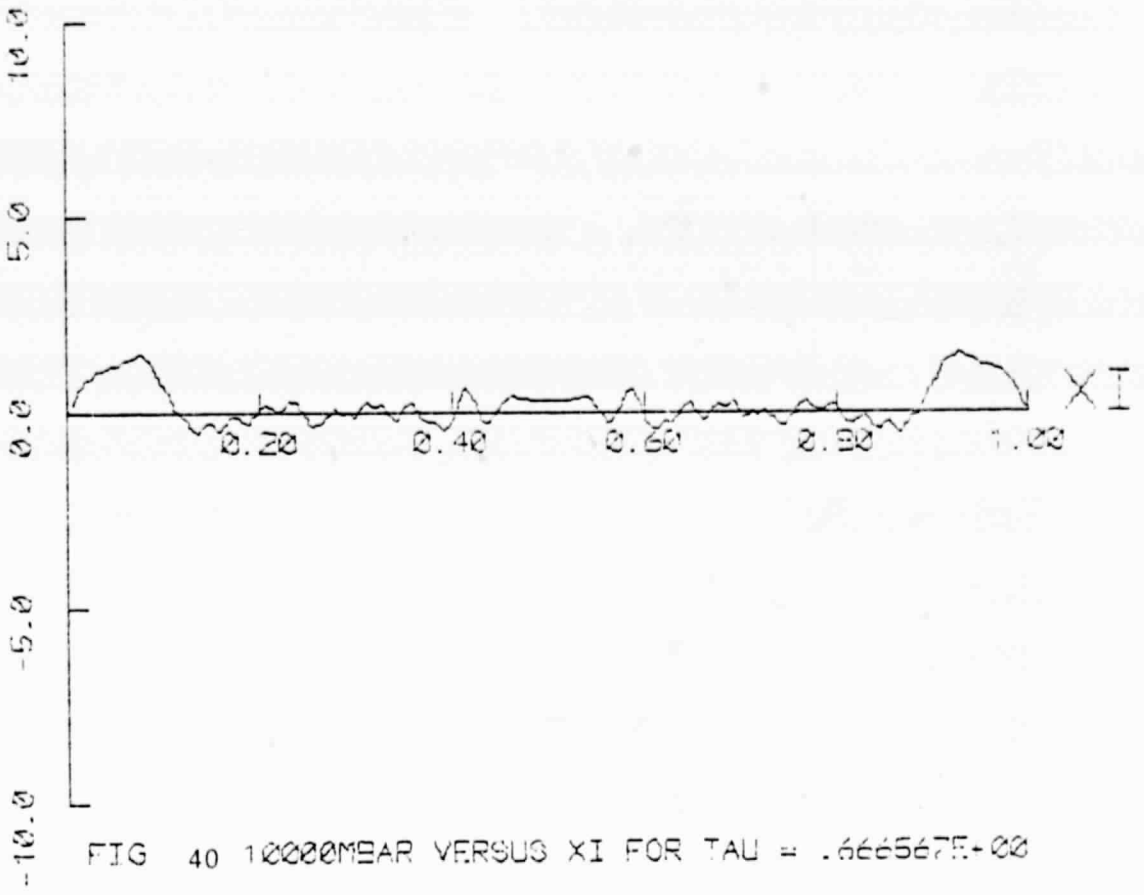

FIG 40 10000MBAR VERSUS XI FOR TAU = .6666675-00

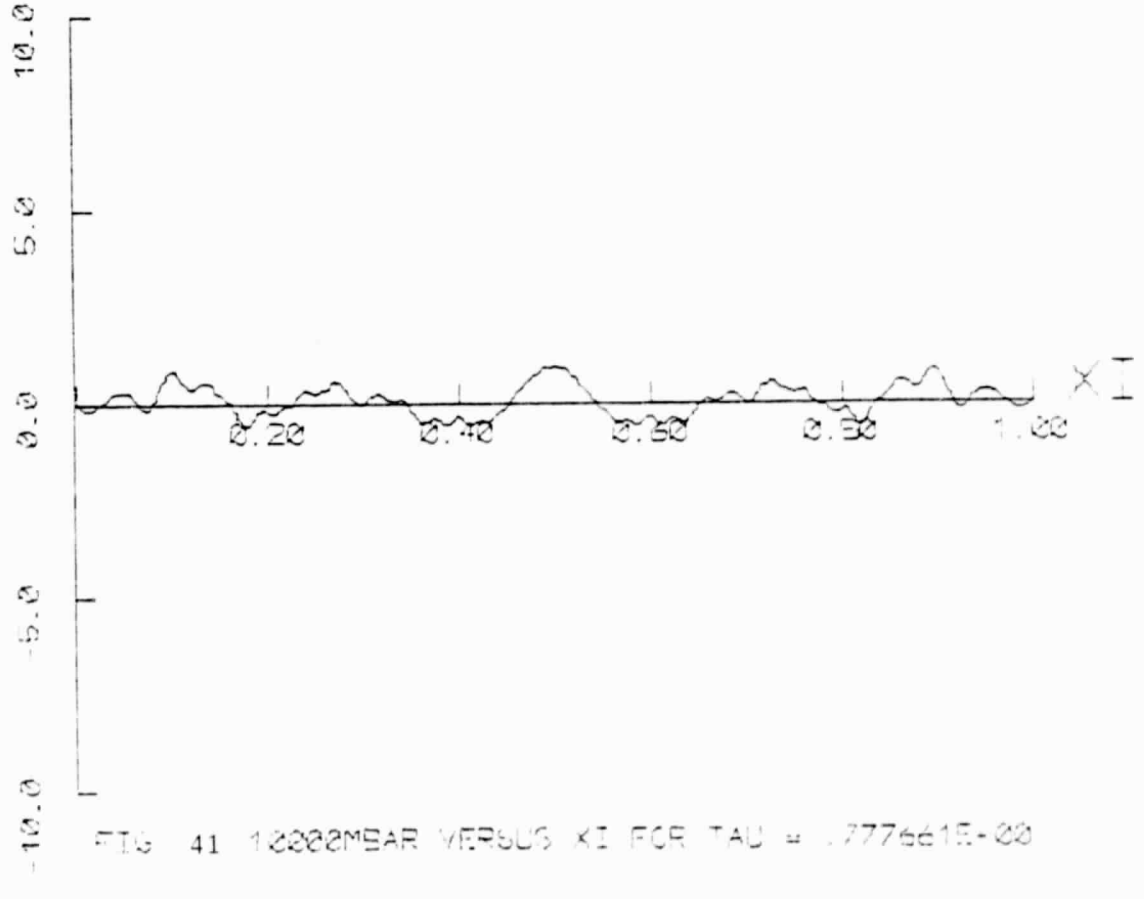

FIG 41 10000MBAR VERSUS XI FOR TAU = .7776615-00

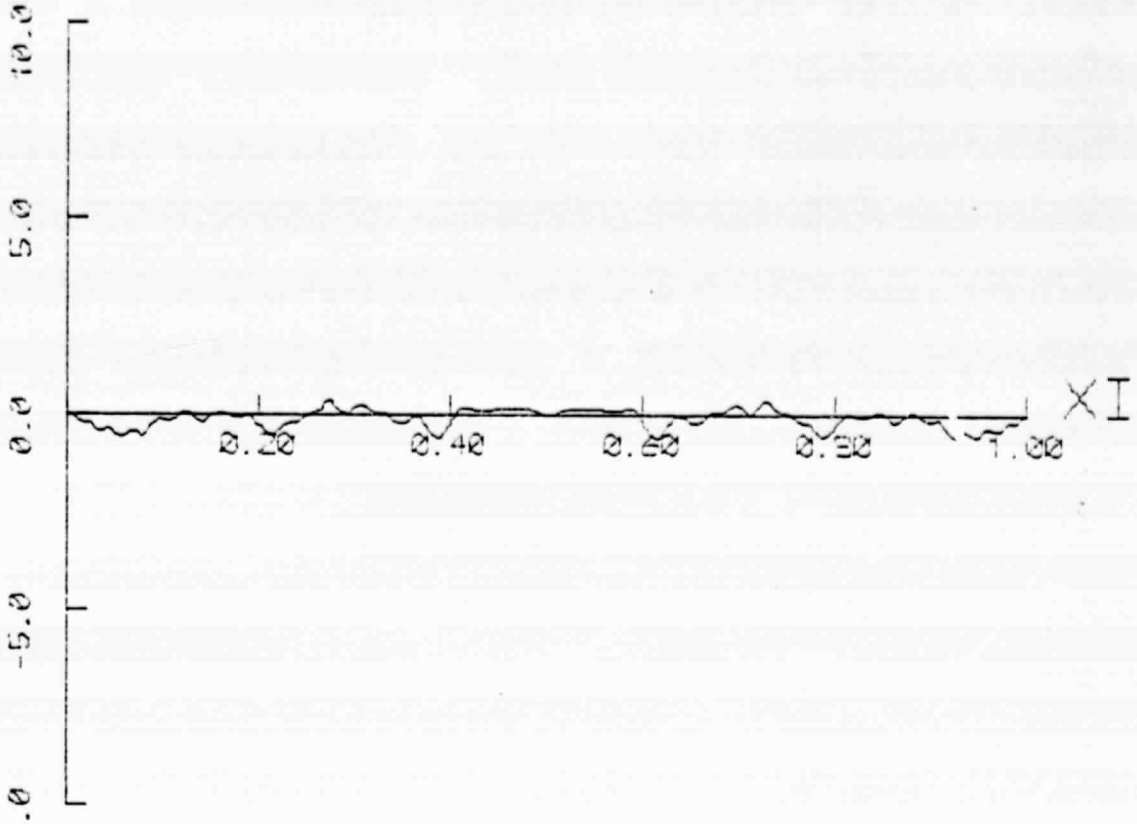

FIG 42 10000MBAR VERSUS XI FOR TAU = .888755E+00

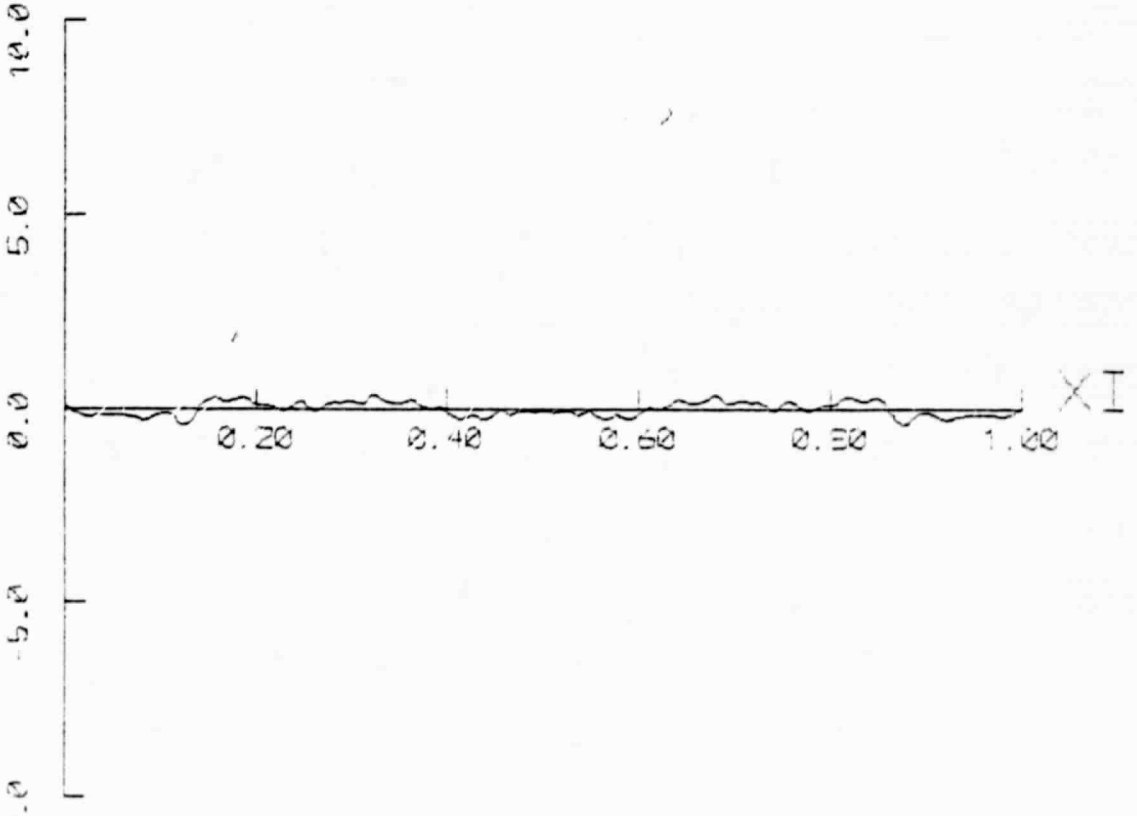

FIG 43 10000MBAR VERSUS XI FOR TAU = .999852E+00

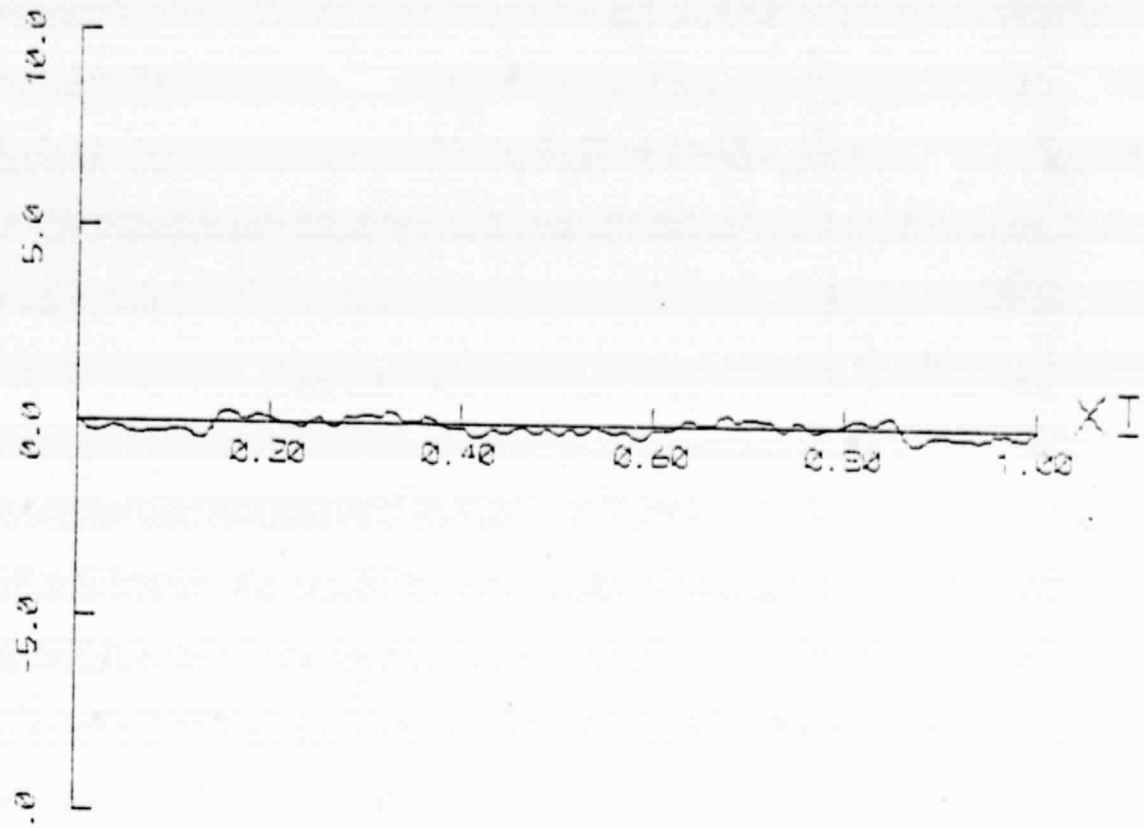

FIG 44 10000MBAR VERSUS XI FOR TAU = .100021E+01 -

APPENDIX J

Response to a (1 + cos) initial displacement;
$V_R = 0.62$, SLR = 50, $\lambda = 0.2$, $\overline{b}_1 = 0.0$, $\overline{b}_2 = 3.0$.

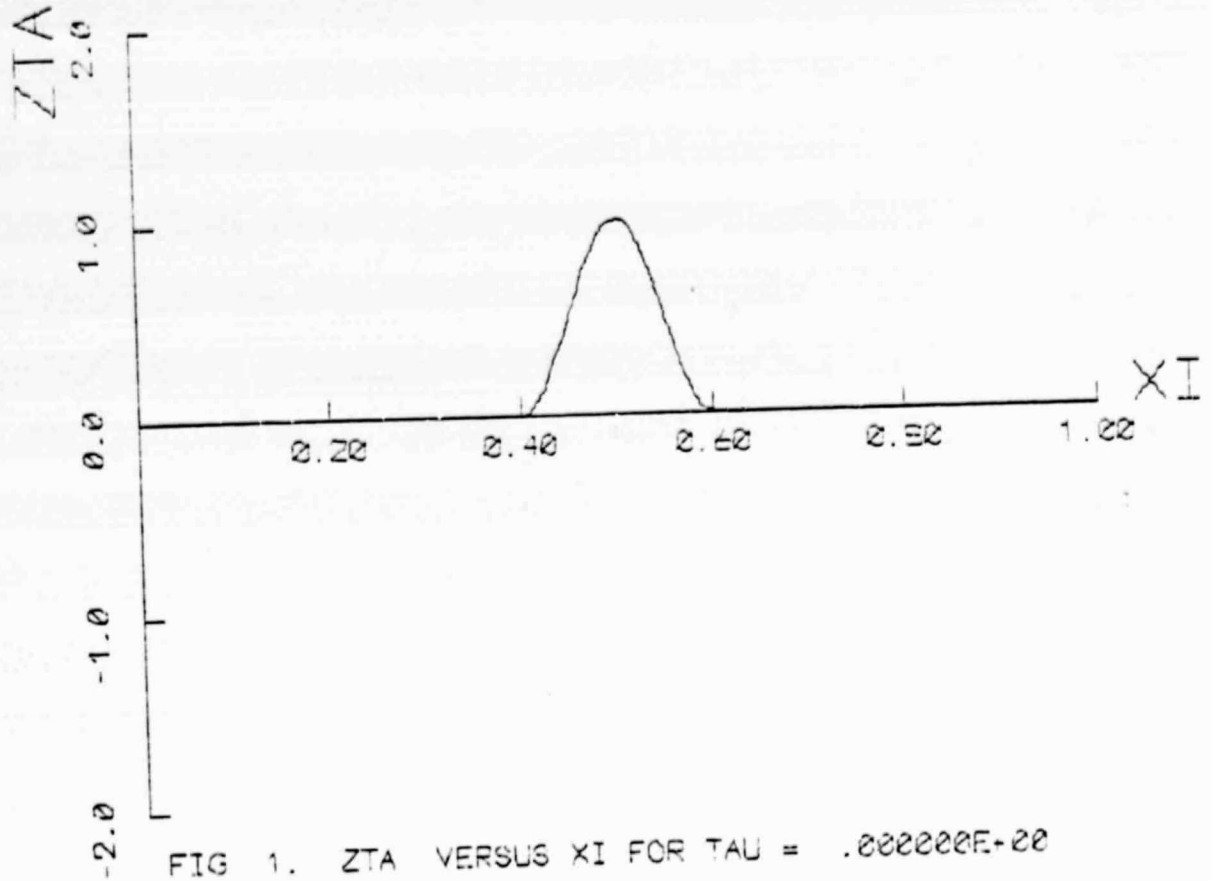

FIG 1. ZTA VERSUS XI FOR TAU = .000000E-00

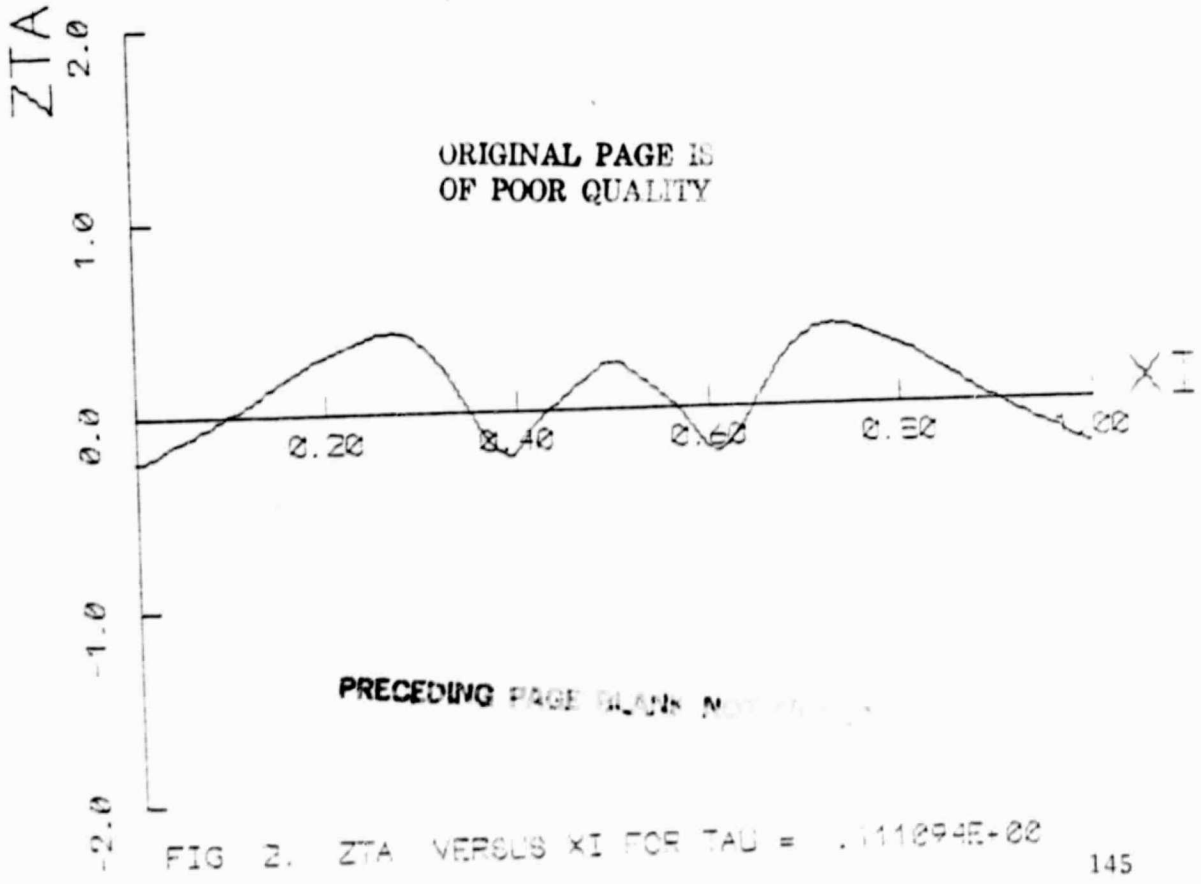

ORIGINAL PAGE IS
OF POOR QUALITY

PRECEDING PAGE BLANK NOT FILMED

FIG 2. ZTA VERSUS XI FOR TAU = .111094E-00

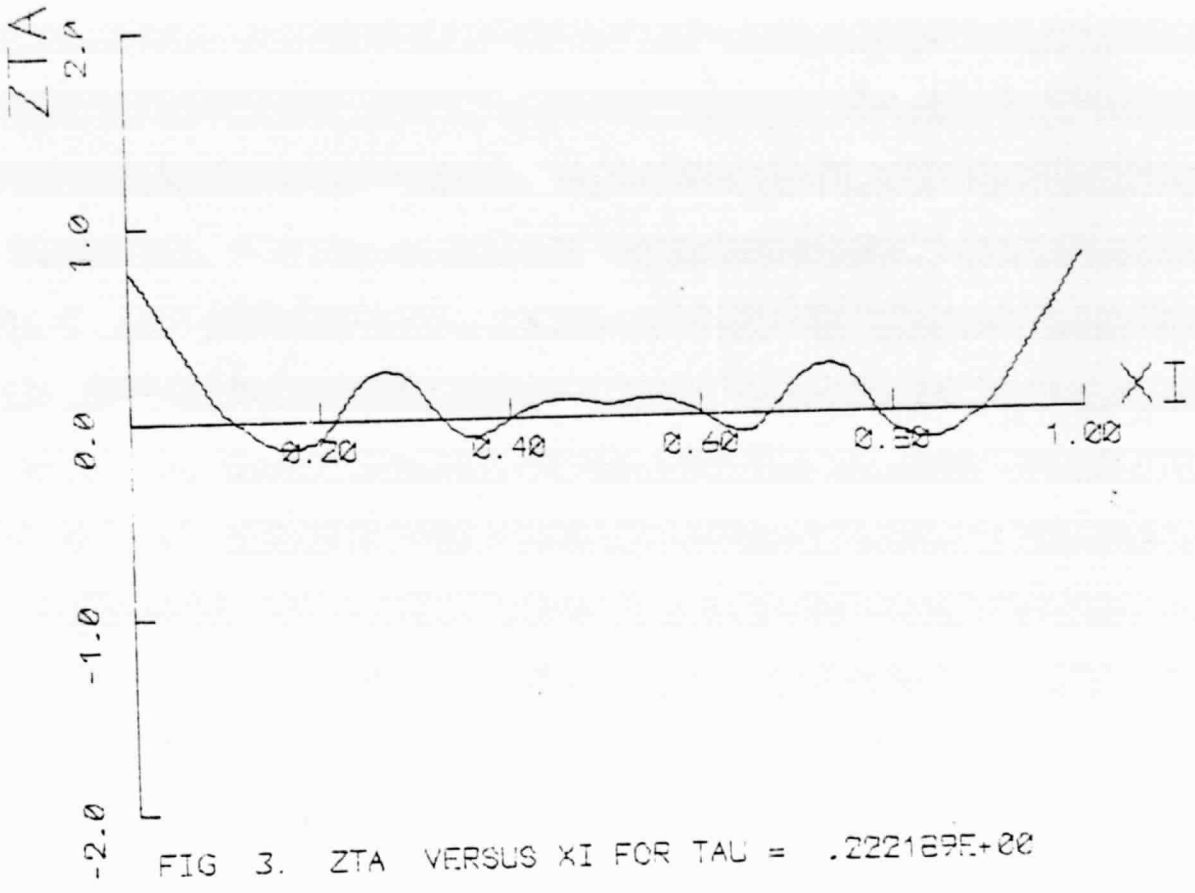

FIG 3. ZTA VERSUS XI FOR TAU = .222189E+00

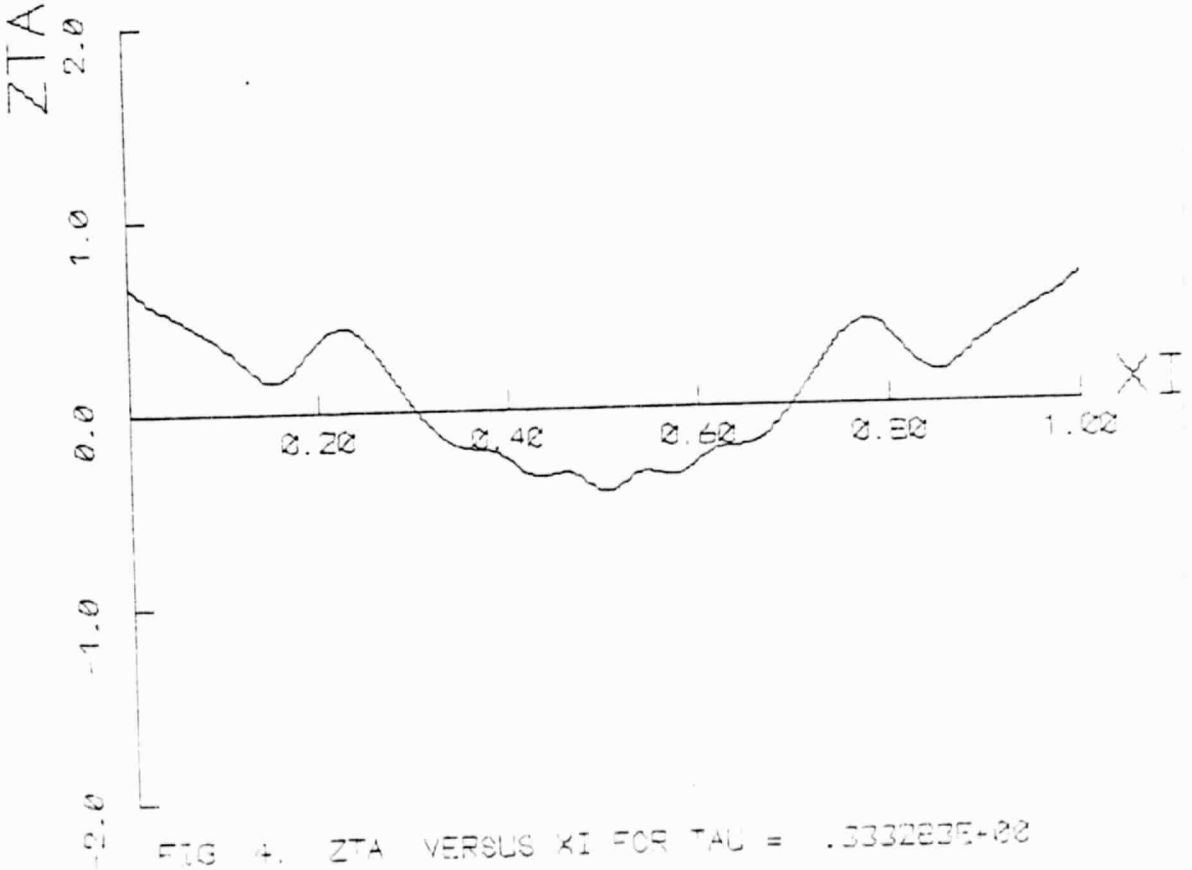

FIG 4. ZTA VERSUS XI FOR TAU = .333283E+00

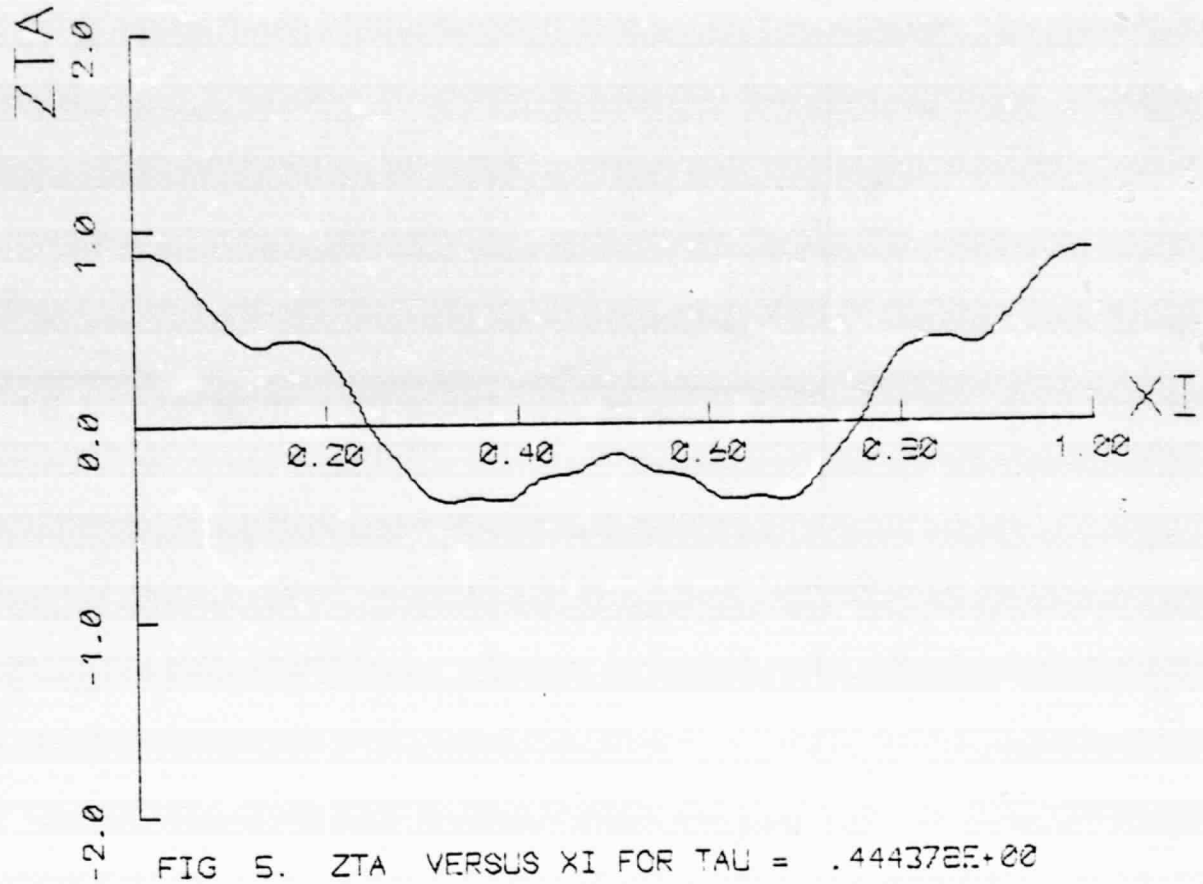

FIG 5. ZTA VERSUS XI FOR TAU = .444378E+00

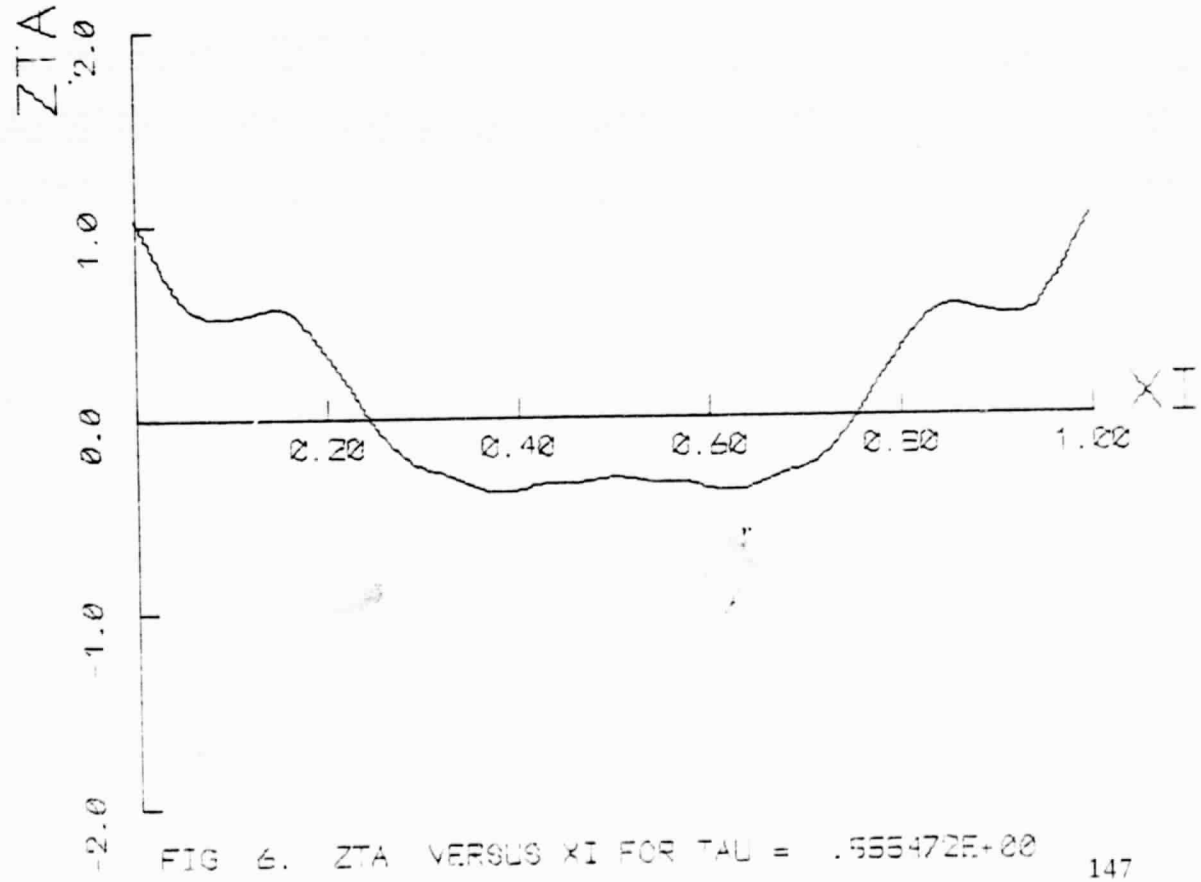

FIG 6. ZTA VERSUS XI FOR TAU = .555472E+00

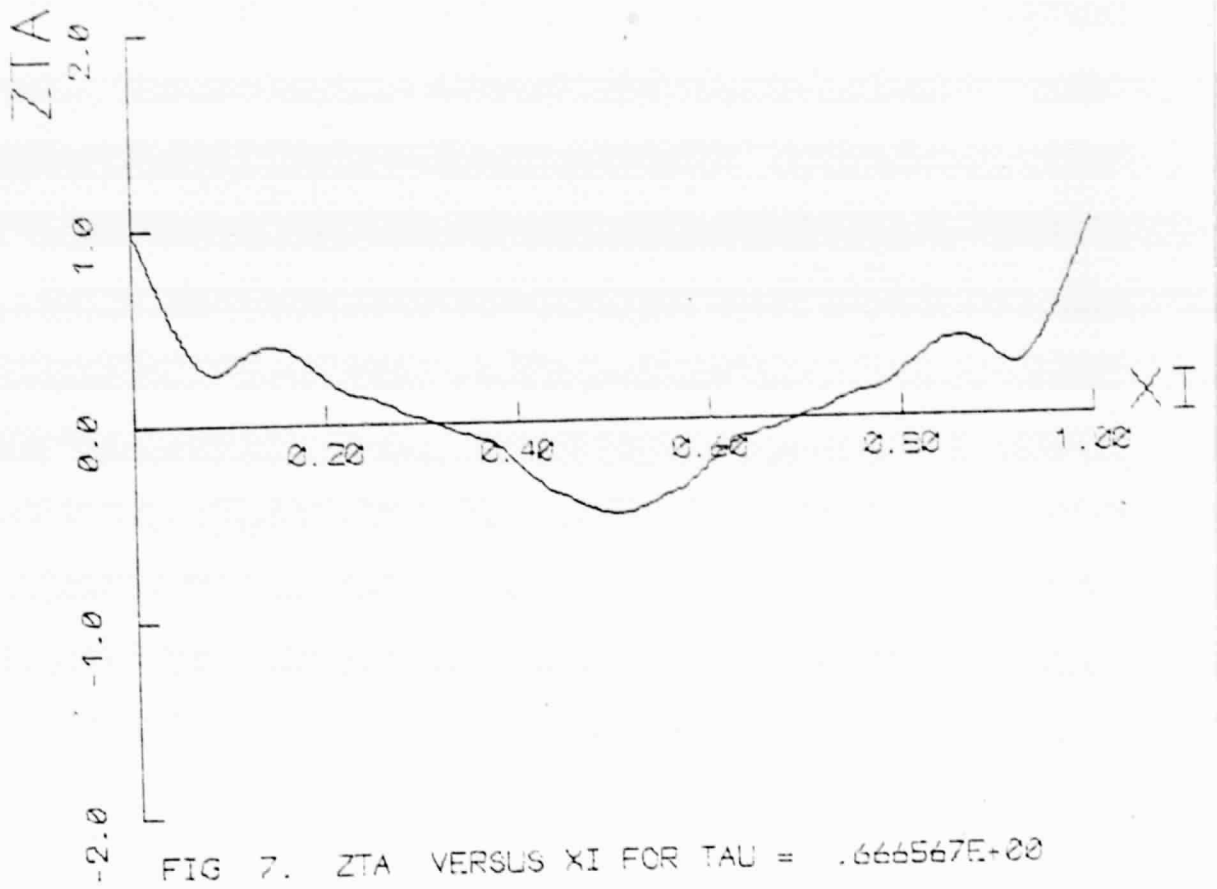

FIG 7. ZTA VERSUS XI FOR TAU = .666567E+00

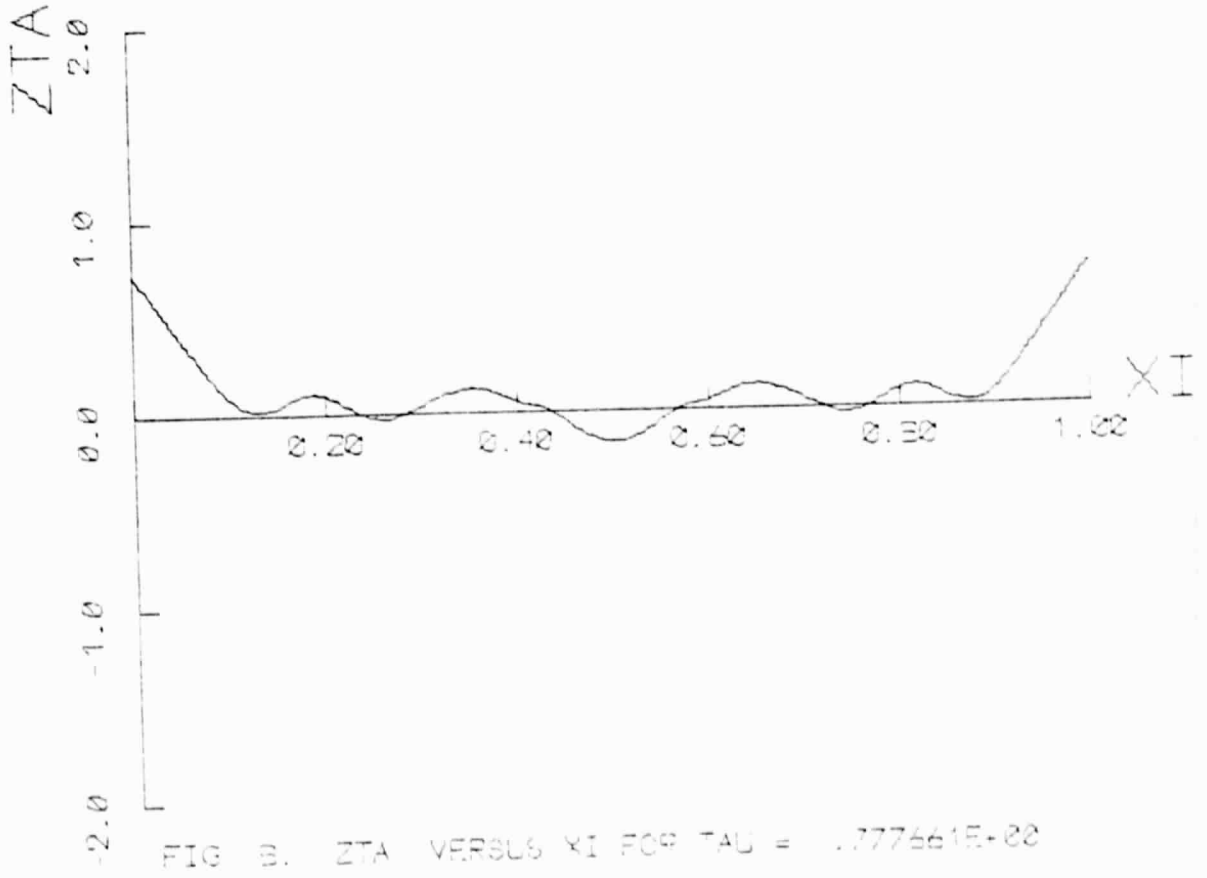

FIG 8. ZTA VERSUS XI FOR TAU = .777661E+00

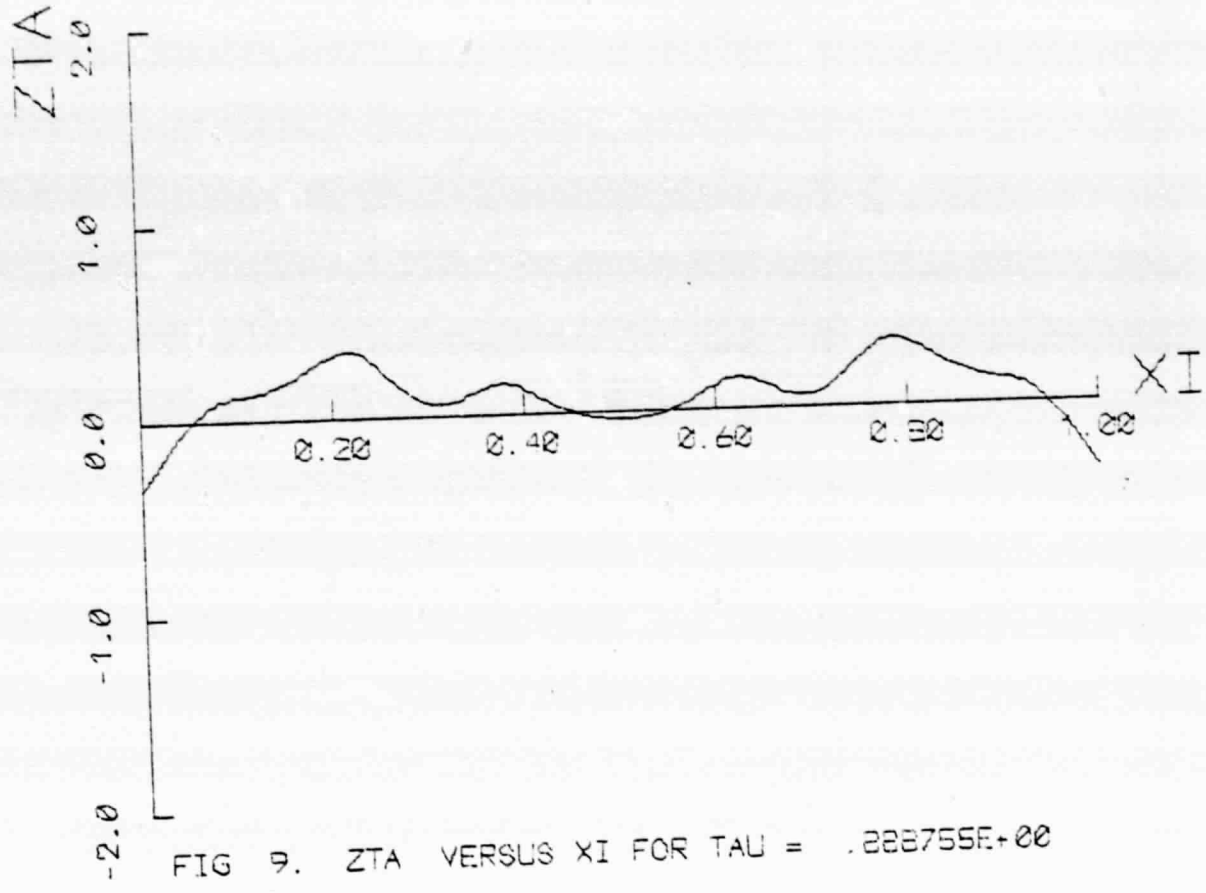

FIG 9. ZTA VERSUS XI FOR TAU = .888755E+00

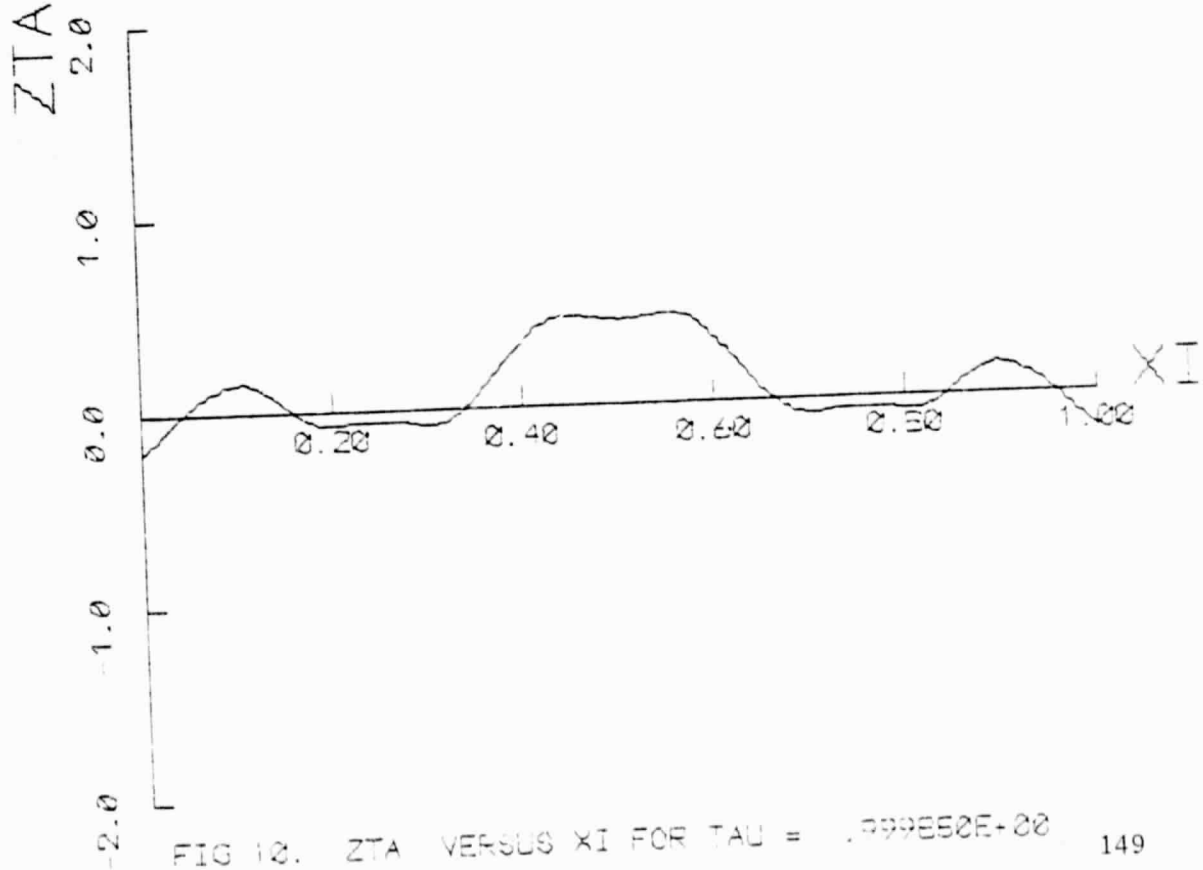

FIG 10. ZTA VERSUS XI FOR TAU = .999850E+00

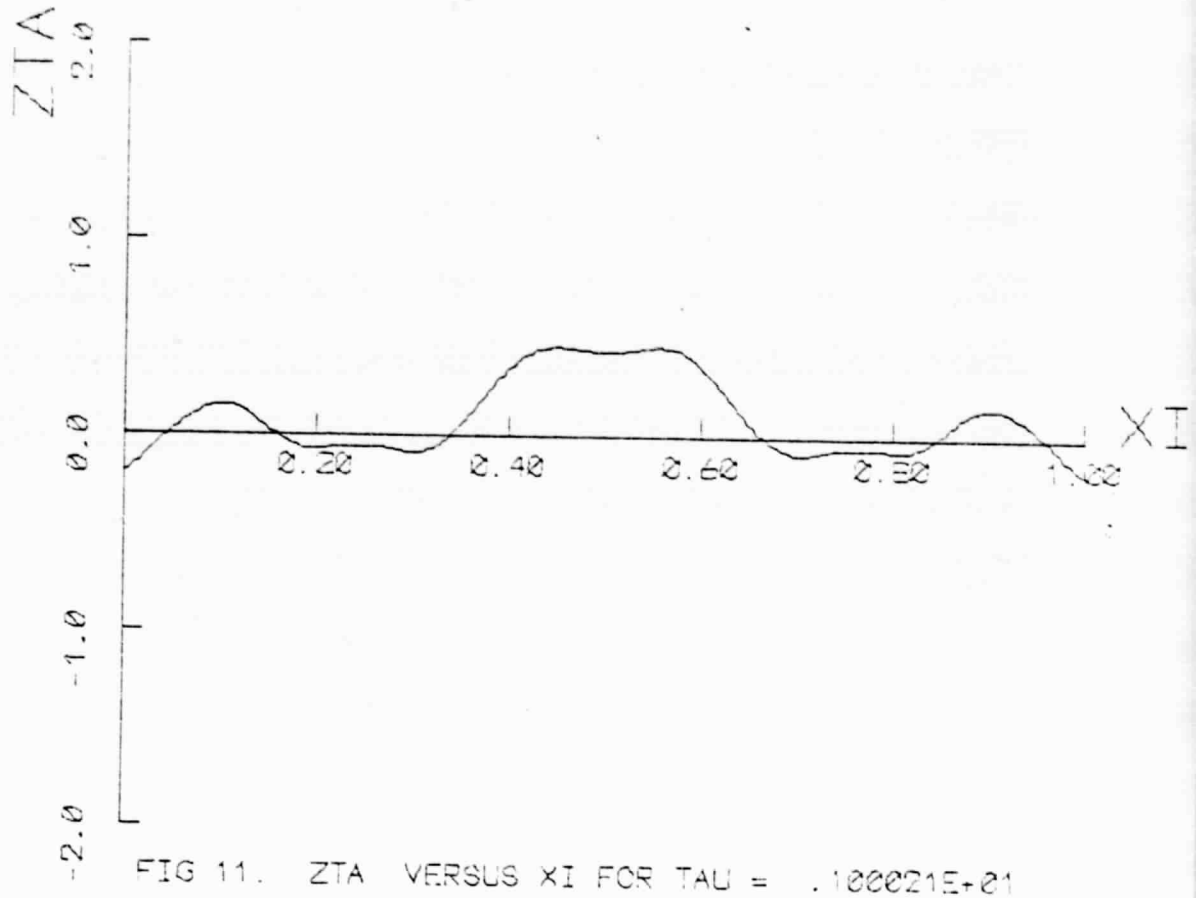

FIG 11. ZTA VERSUS XI FOR TAU = .100021E+01

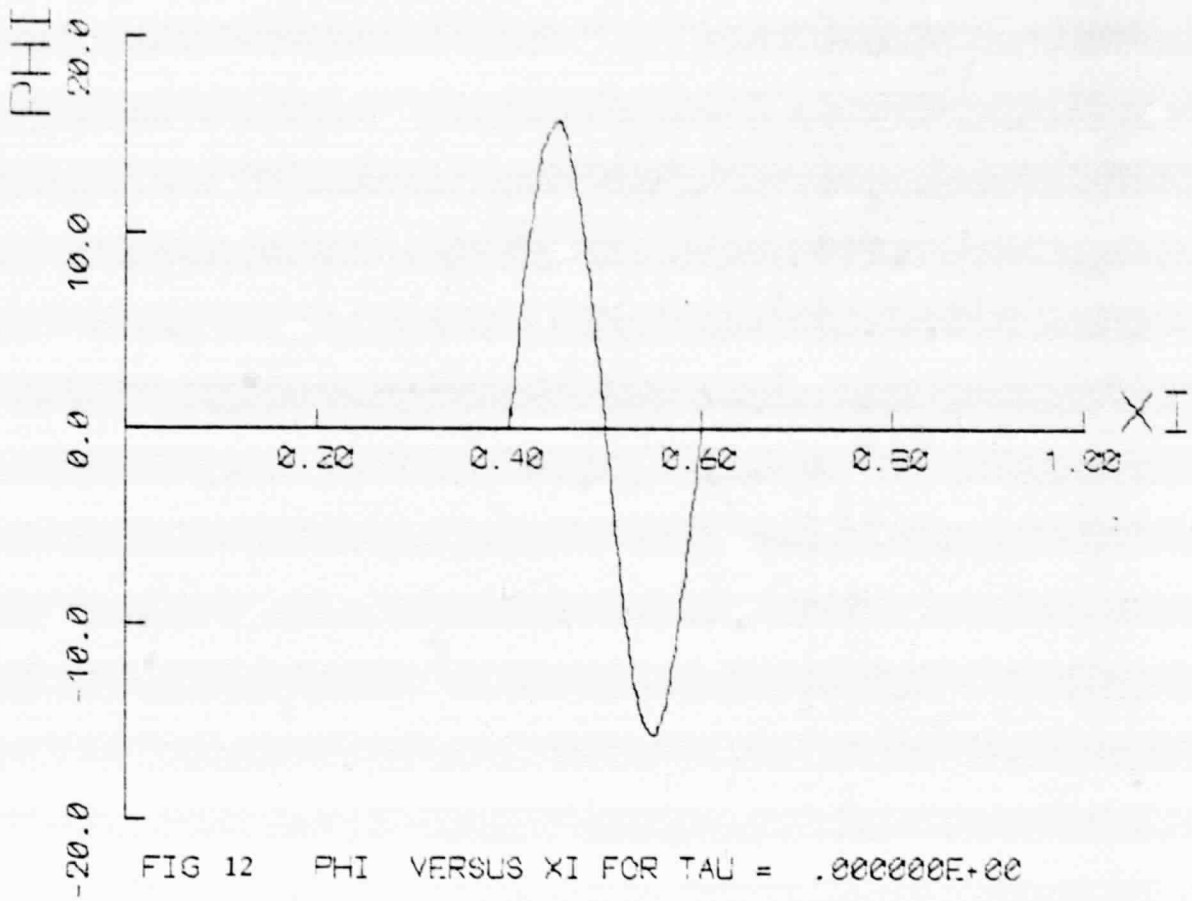

FIG 12 PHI VERSUS XI FOR TAU = .000000E+00

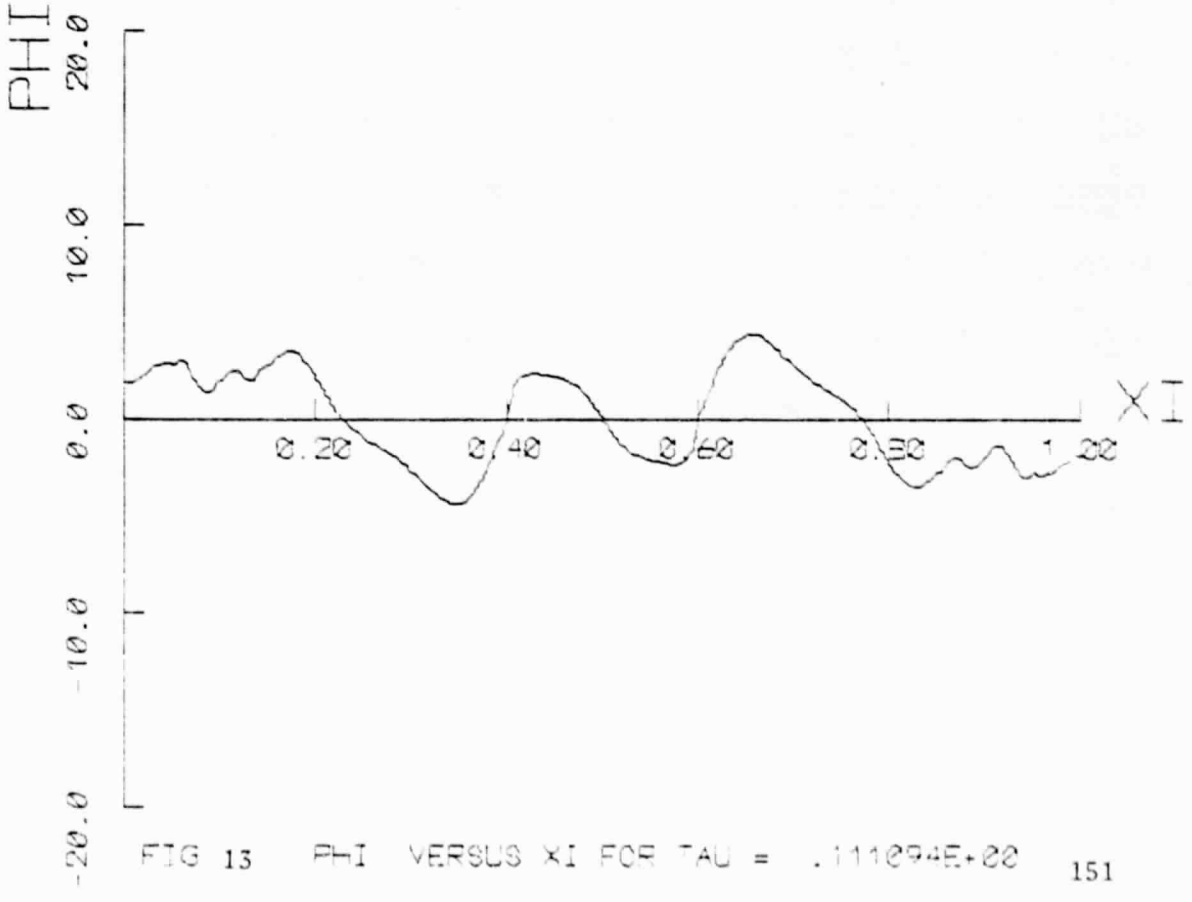

FIG 13 PHI VERSUS XI FOR TAU = .111094E+00

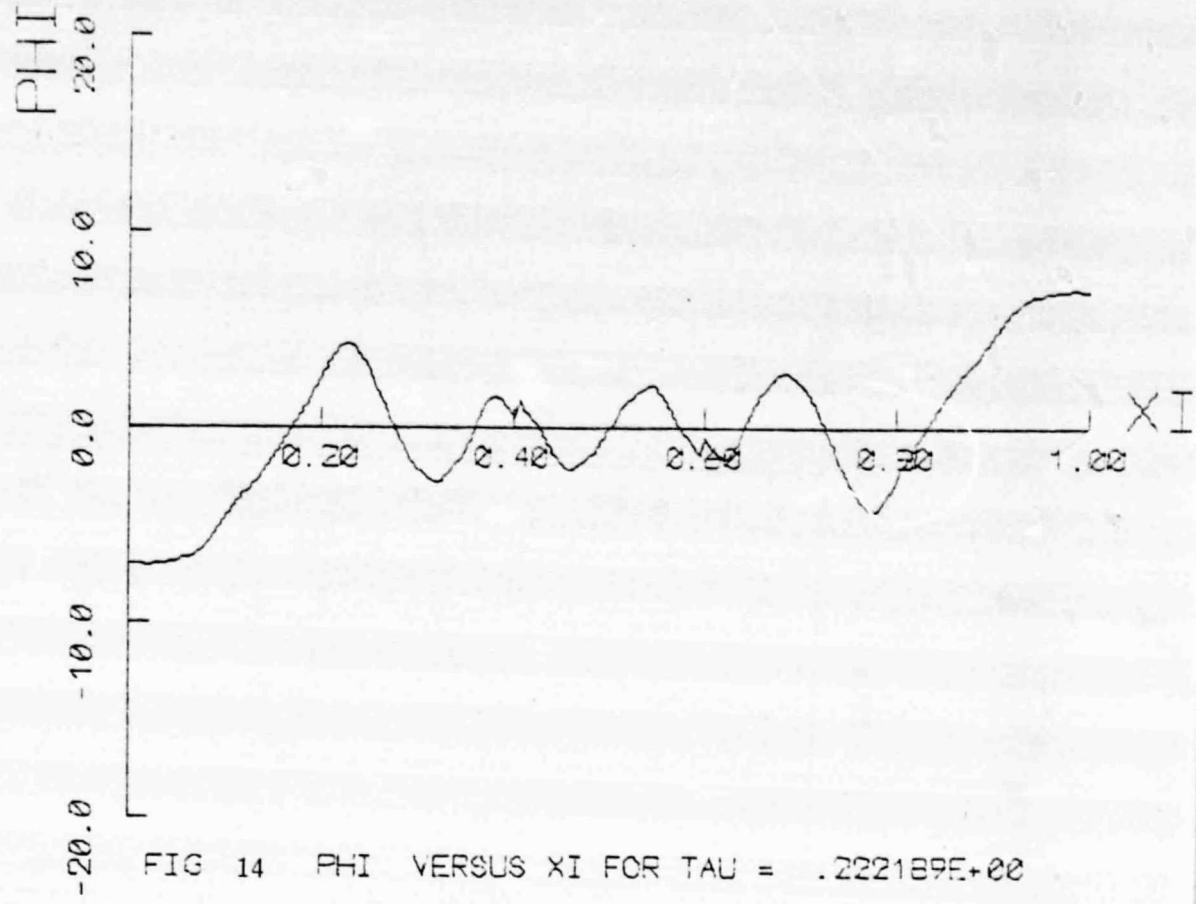

FIG 14 PHI VERSUS XI FOR TAU = .222189E+00

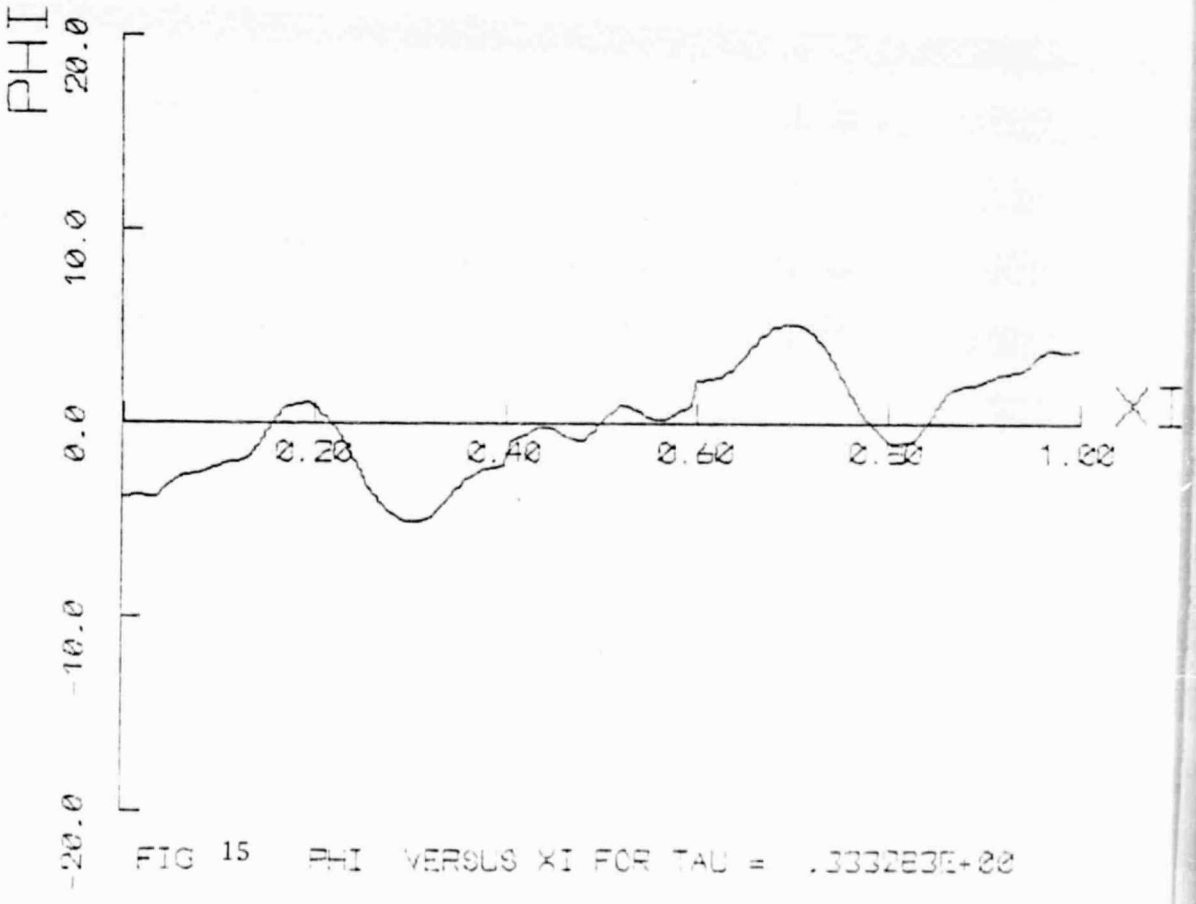

FIG 15 PHI VERSUS XI FOR TAU = .333283E+00

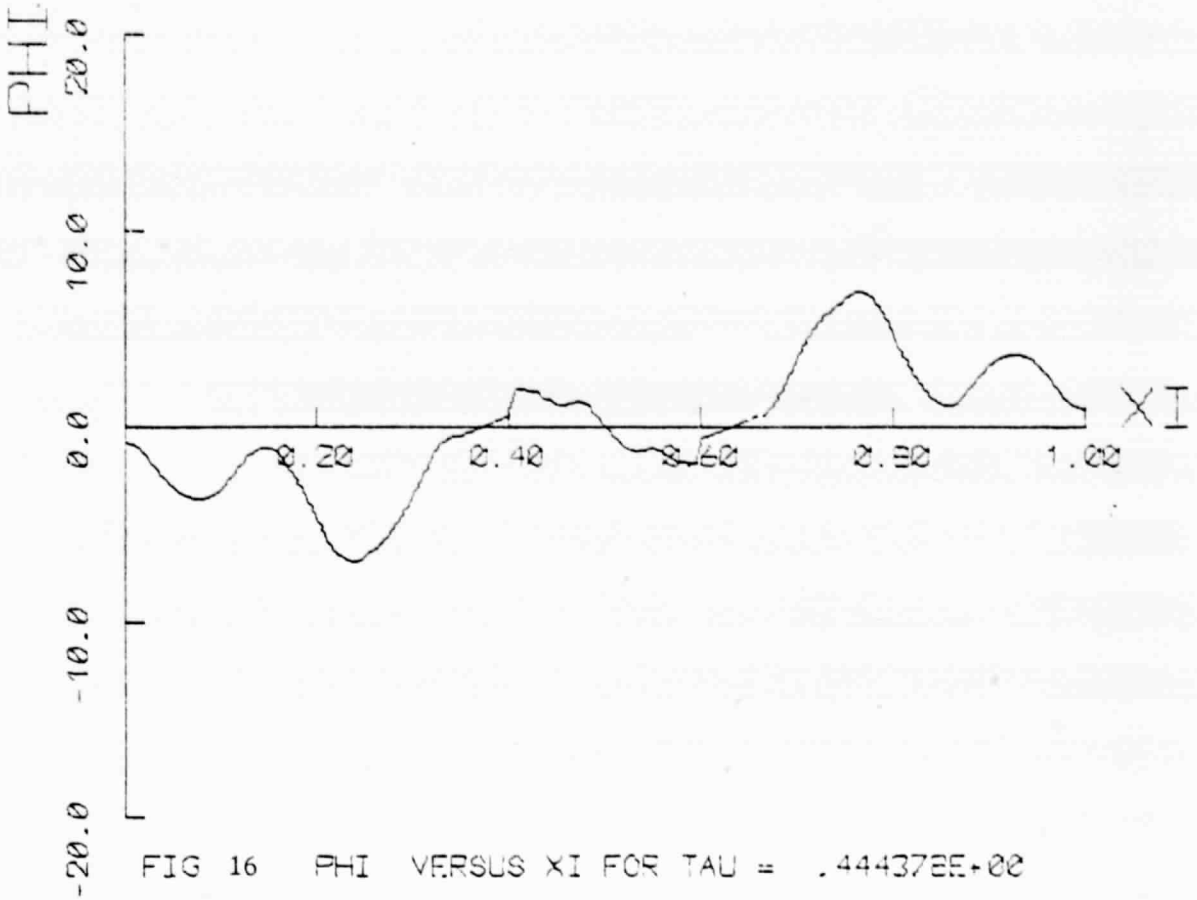

FIG 16 PHI VERSUS XI FOR TAU = .444373E+00

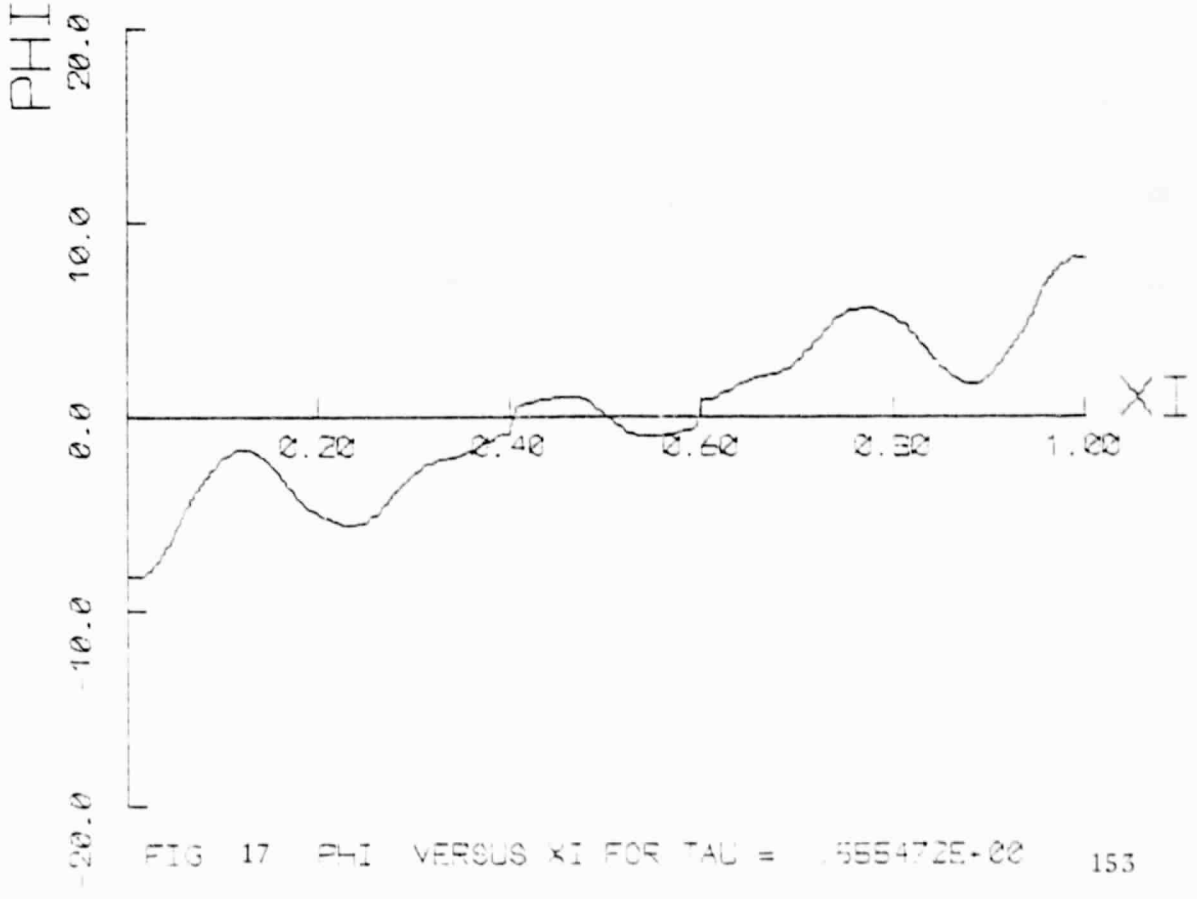

FIG 17 PHI VERSUS XI FOR TAU = .555472E+00

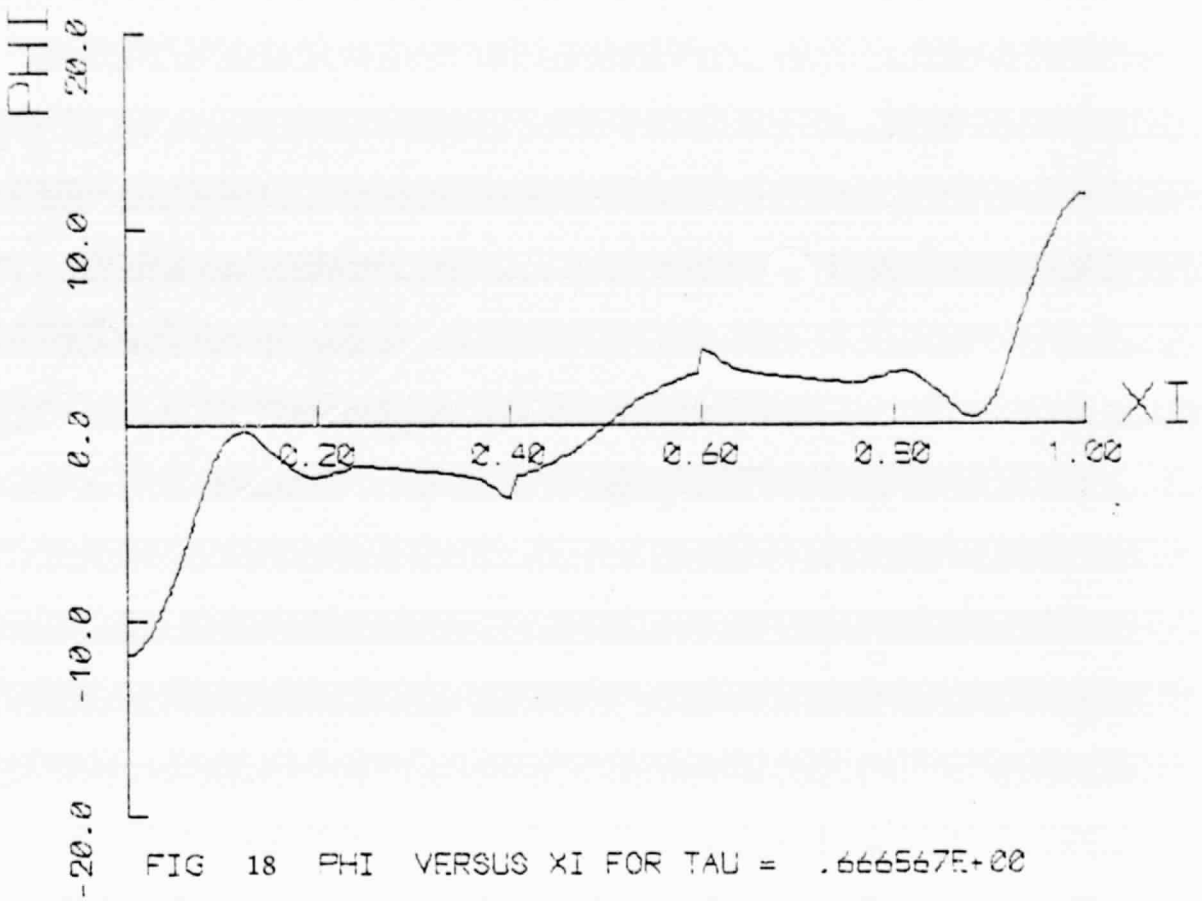

FIG 18 PHI VERSUS XI FOR TAU = .666567E+00

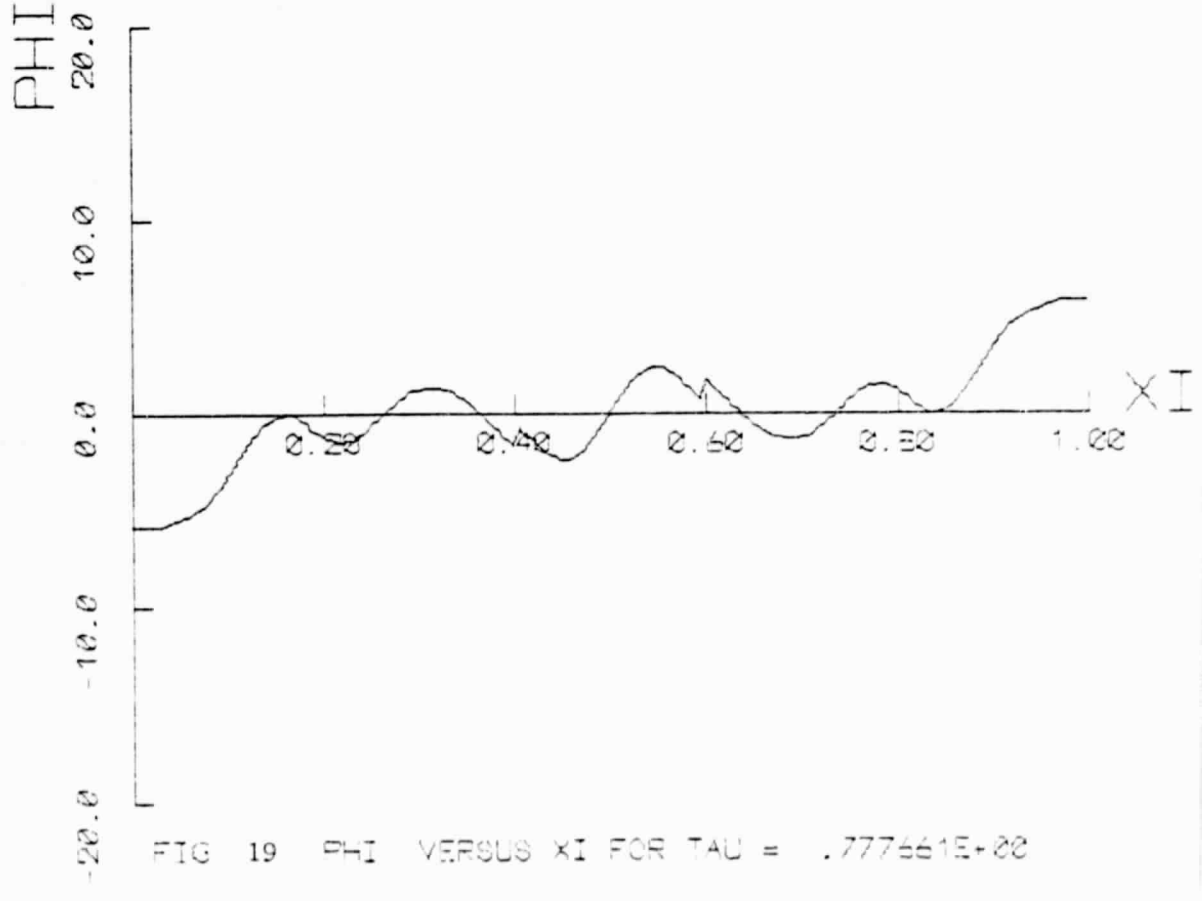

FIG 19 PHI VERSUS XI FOR TAU = .777661E+00

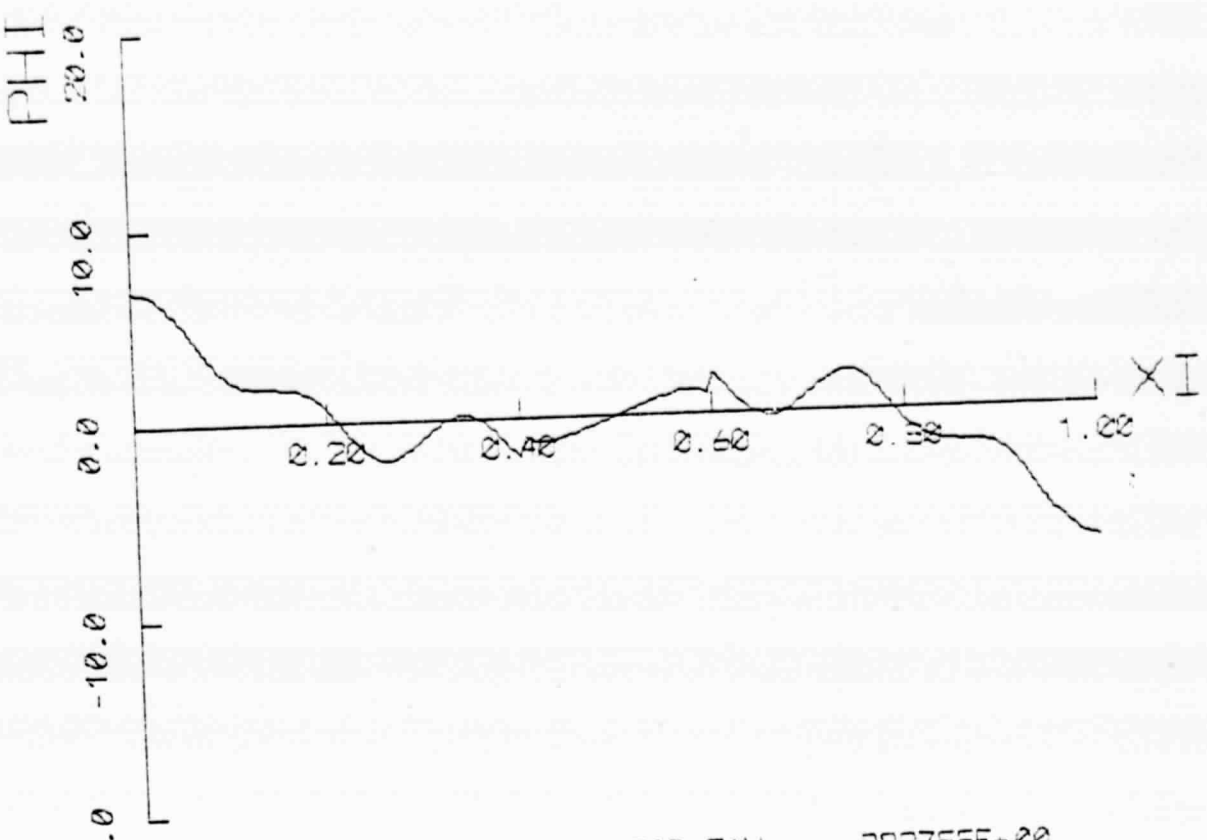

FIG 20 PHI VERSUS XI FOR TAU = .282755E+00

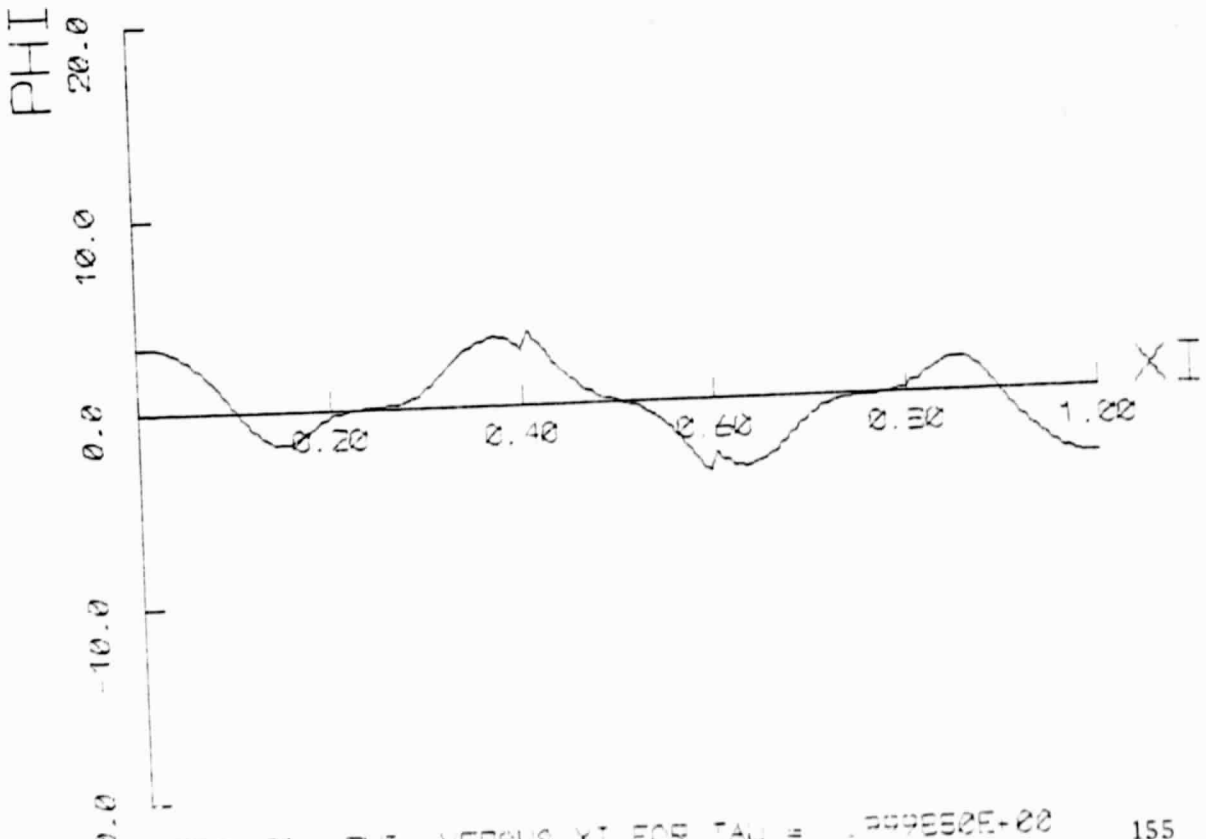

FIG 21 PHI VERSUS XI FOR TAU = .299582E+00

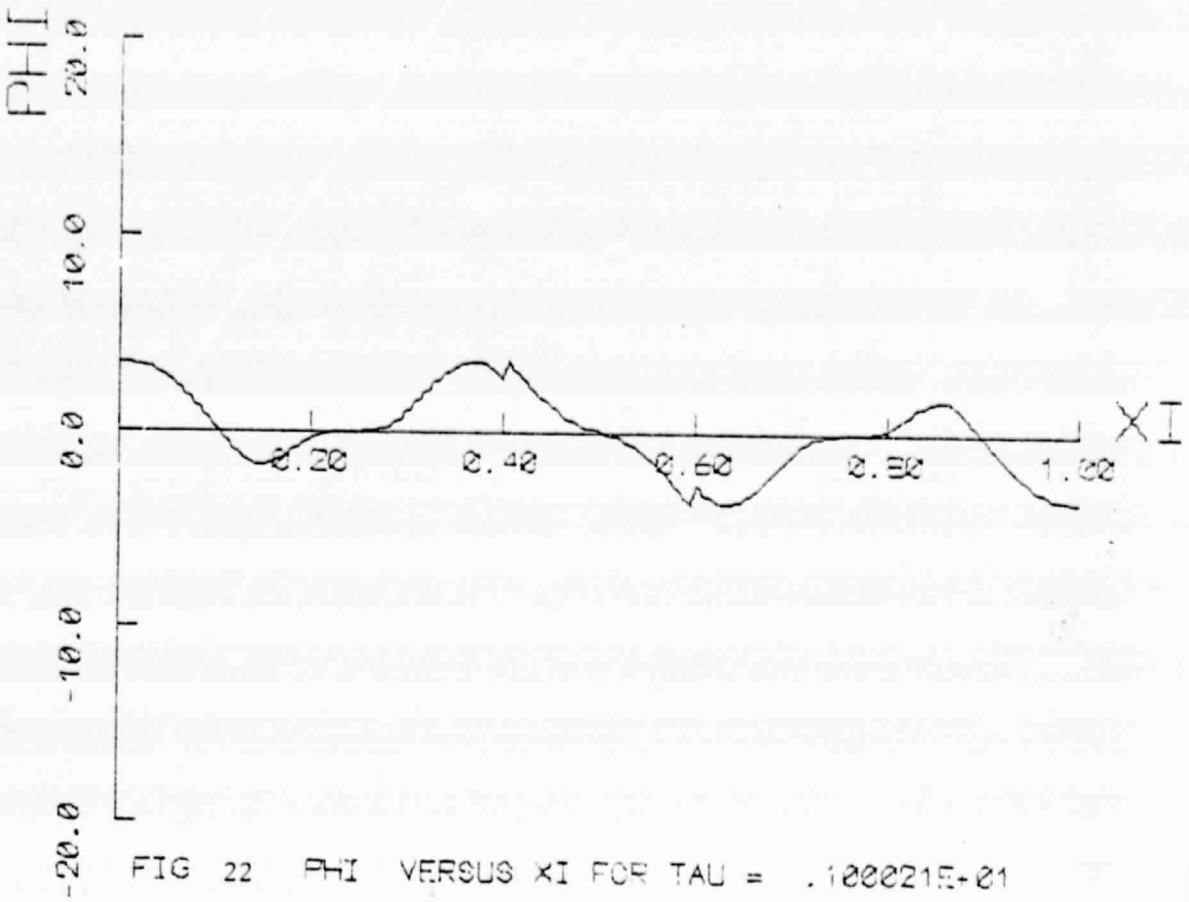

FIG 22 PHI VERSUS XI FOR TAU = .1000215-01

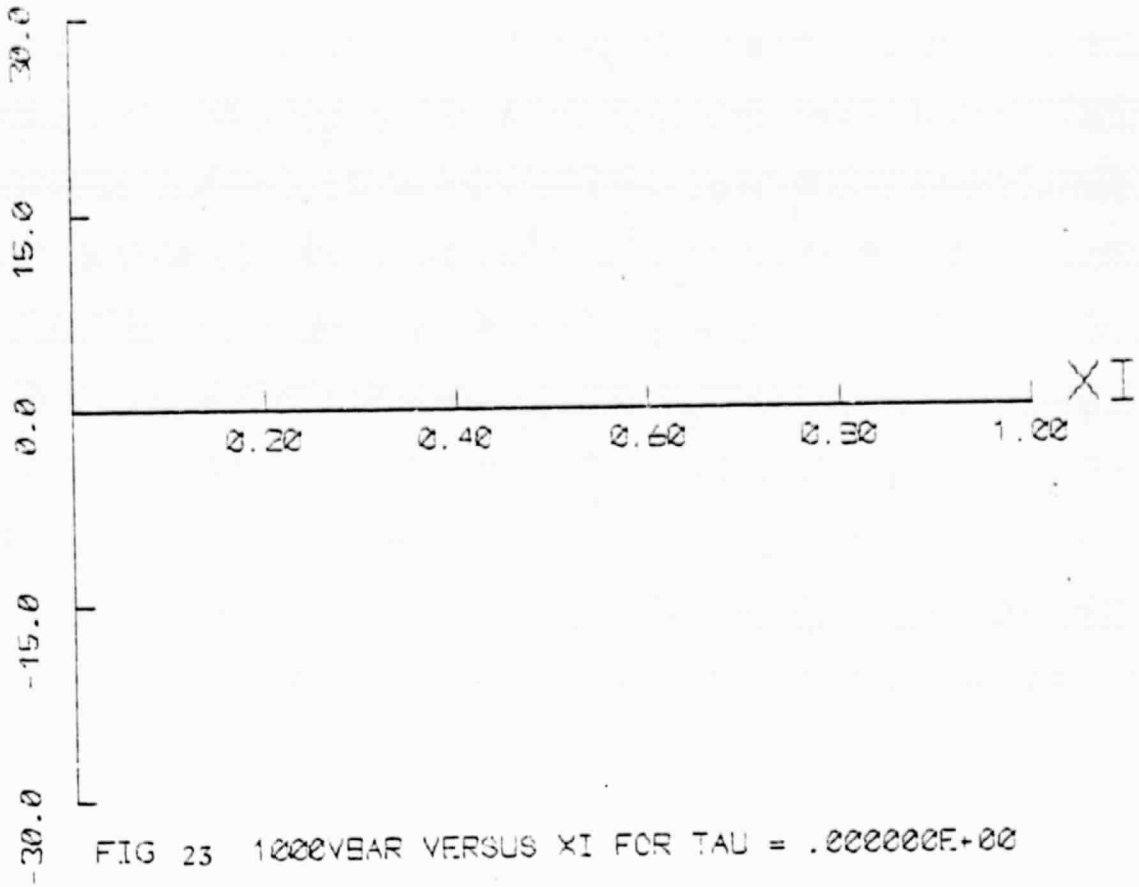

FIG 23 1000VBAR VERSUS XI FOR TAU = .000000E+00

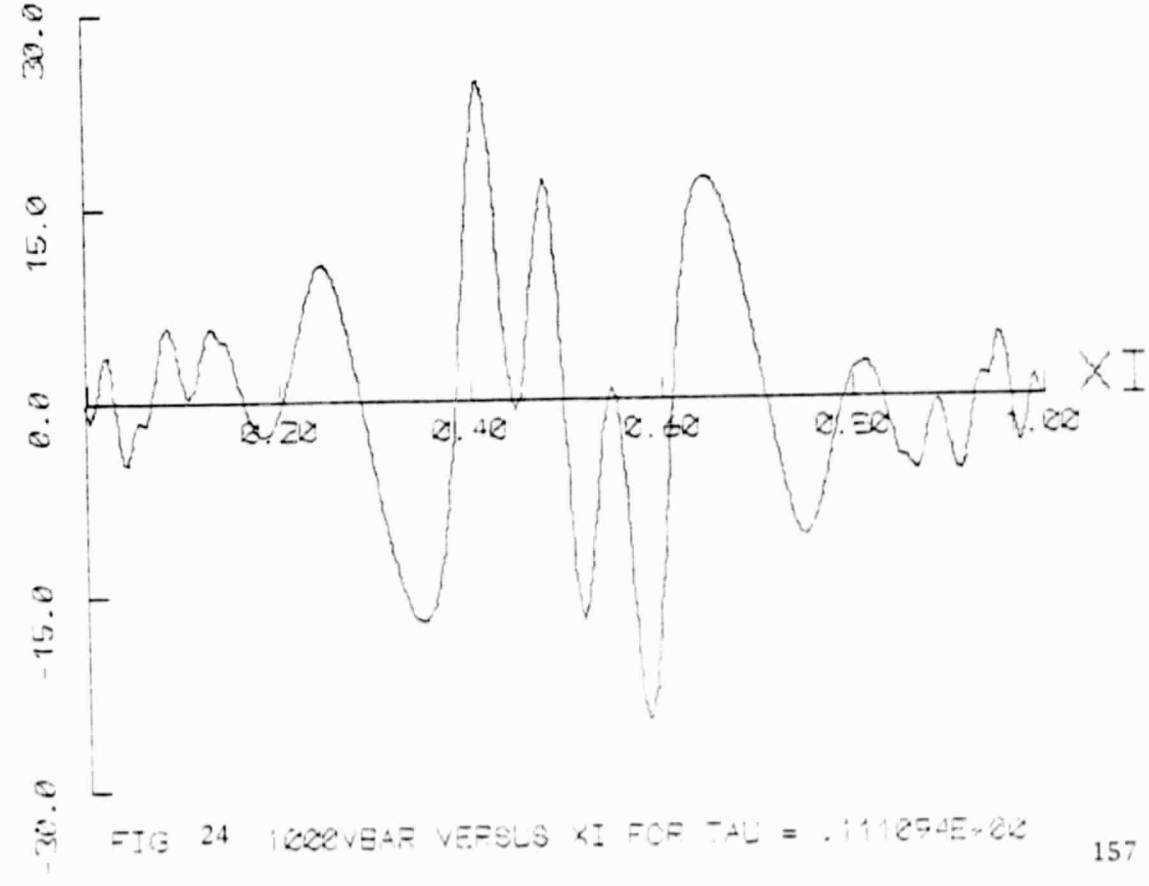

FIG 24 1000VBAR VERSUS XI FOR TAU = .111894E+00

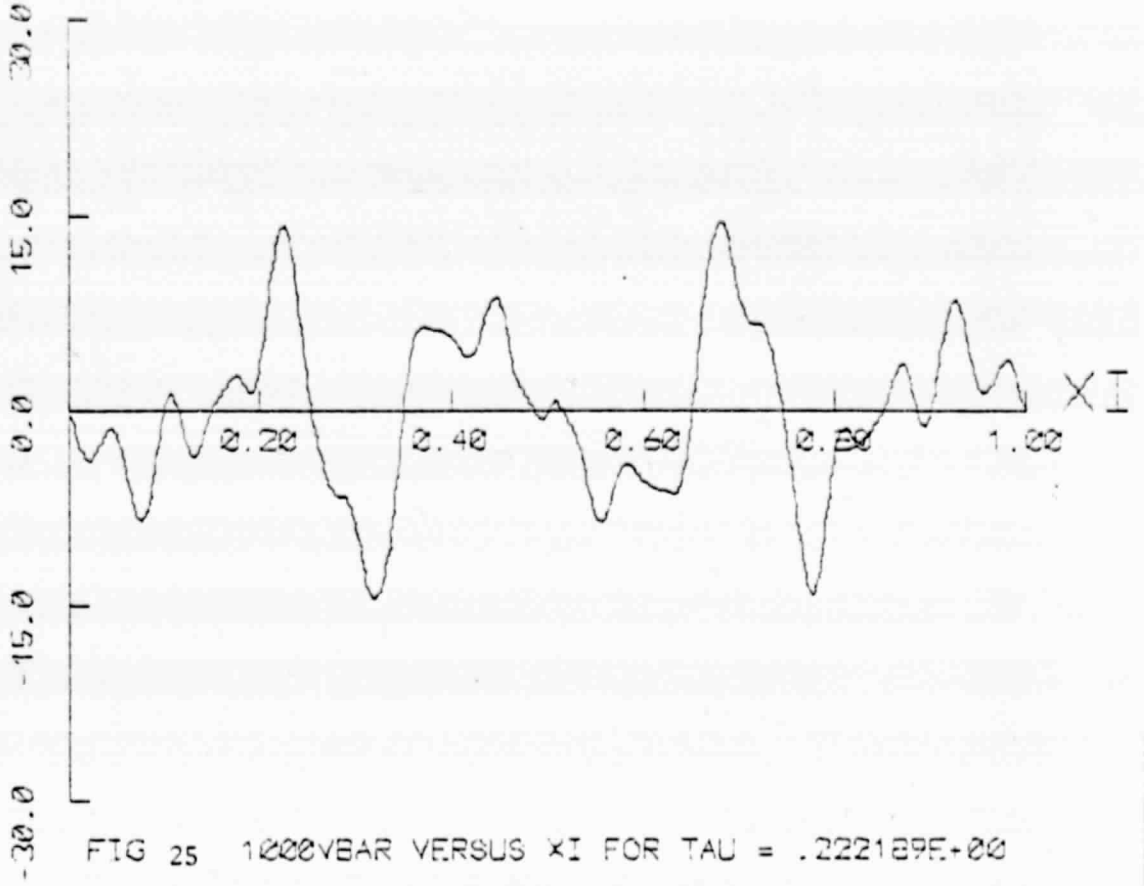

FIG 25 1000VBAR VERSUS XI FOR TAU = .222189E+00

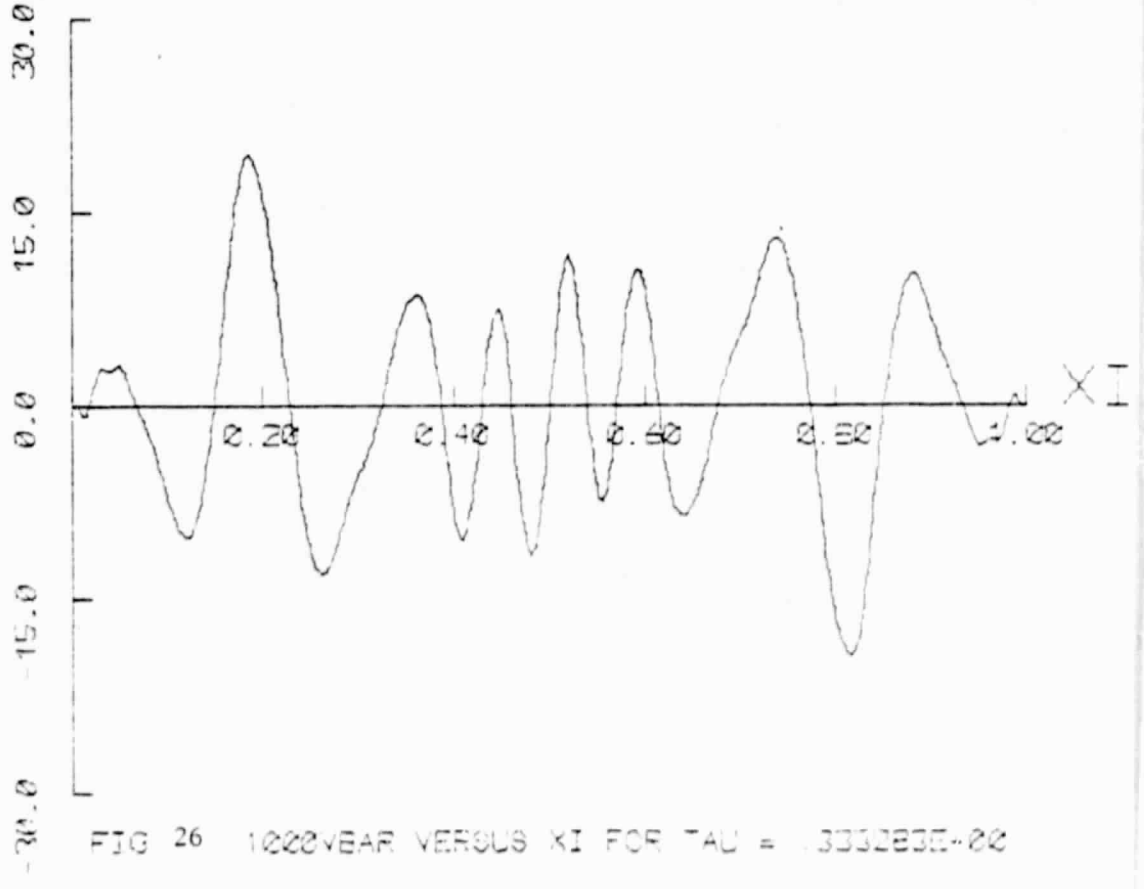

FIG 26 1000VBAR VERSUS XI FOR TAU = .333283E+00

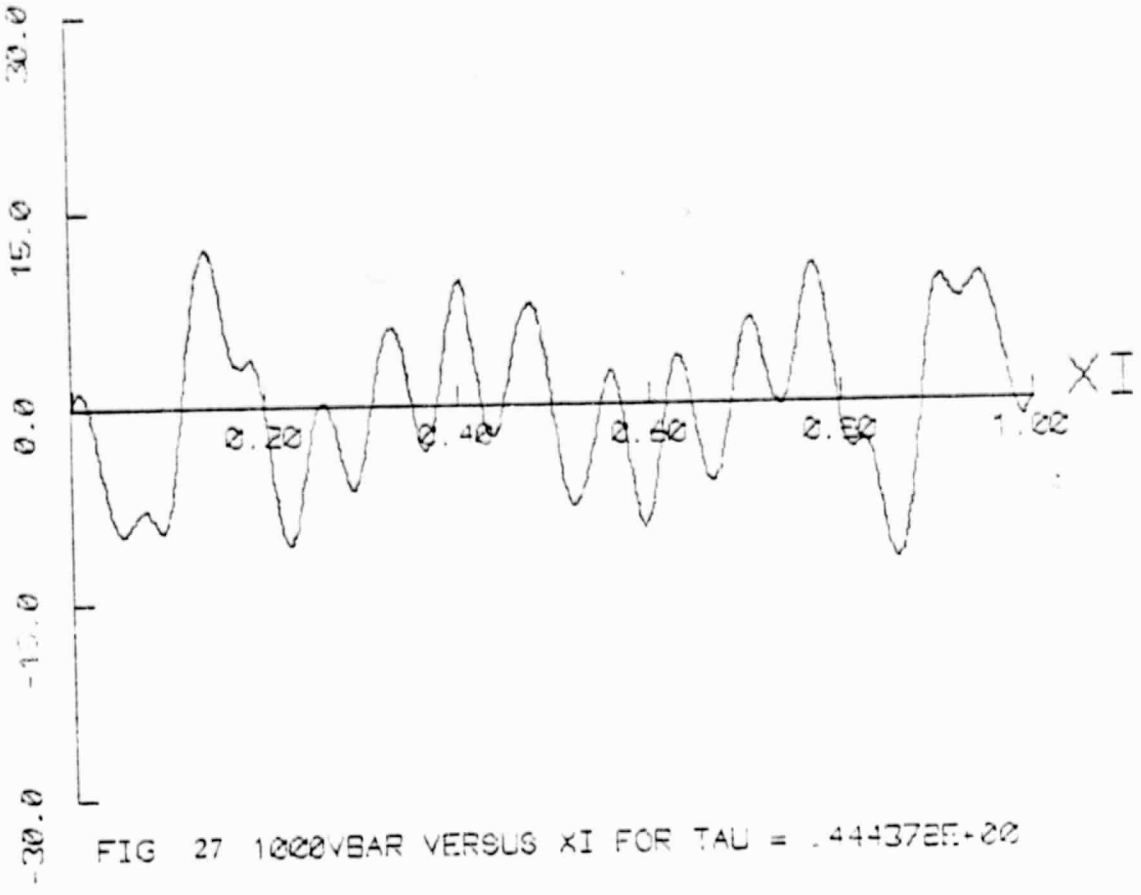

FIG 27 1000VBAR VERSUS XI FOR TAU = .444378E-00

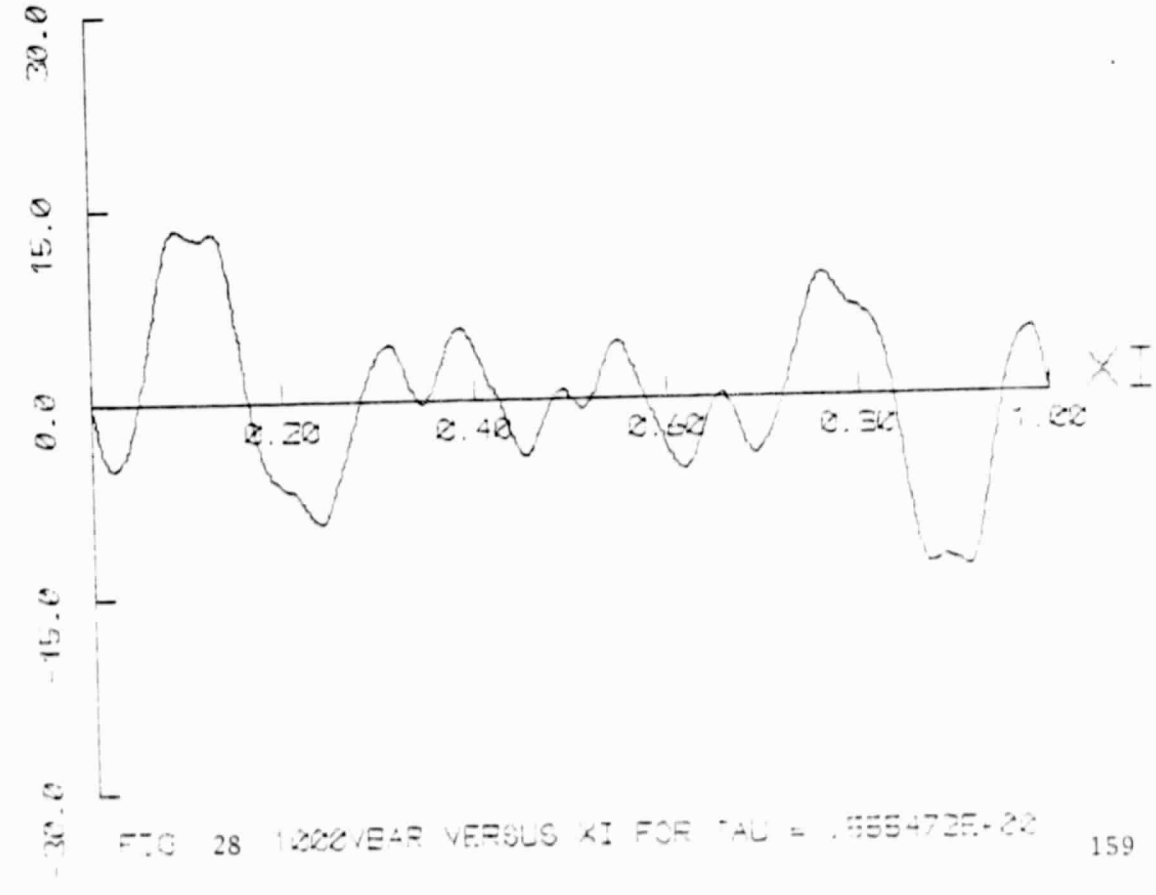

FIG 28 1000VBAR VERSUS XI FOR TAU = .855472E-00

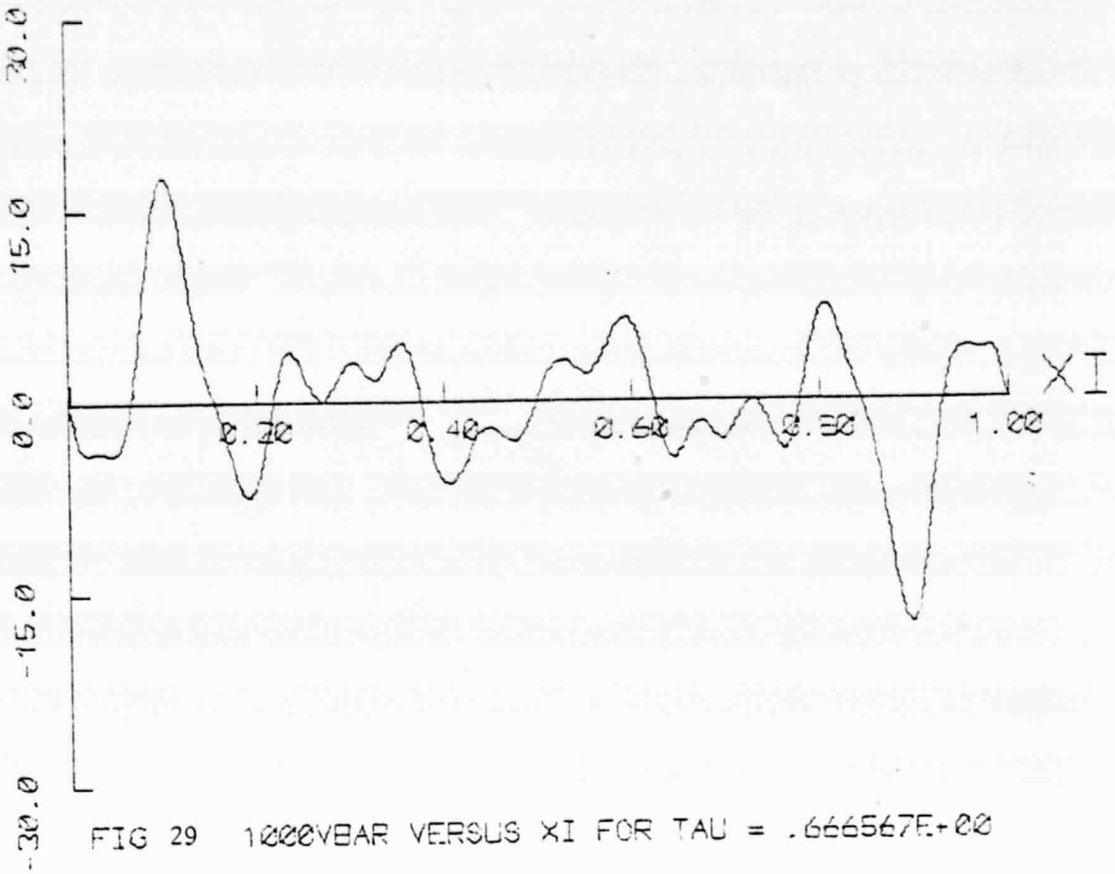

FIG 29 1000VBAR VERSUS XI FOR TAU = .666567E+00

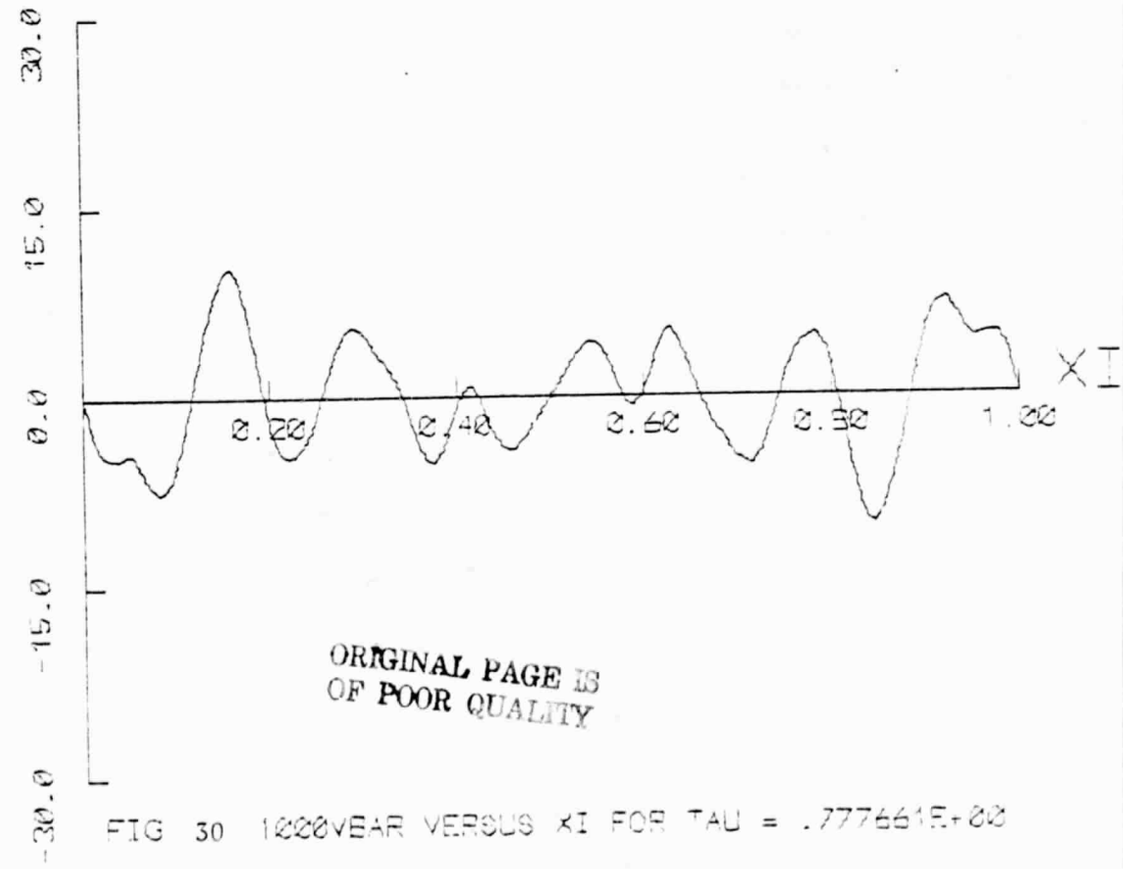

FIG 30 1000VBAR VERSUS XI FOR TAU = .777661E+00

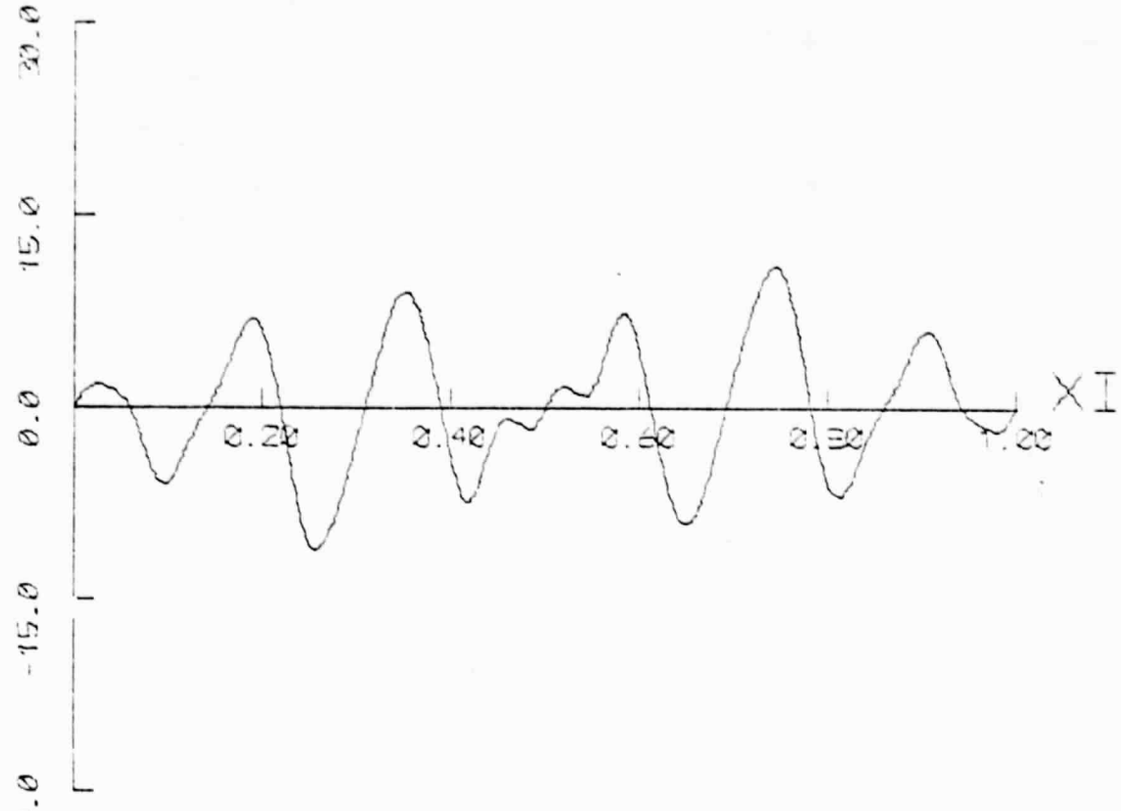

FIG 31 1000VBAR VERSUS XI FOR TAU = .288755E+00

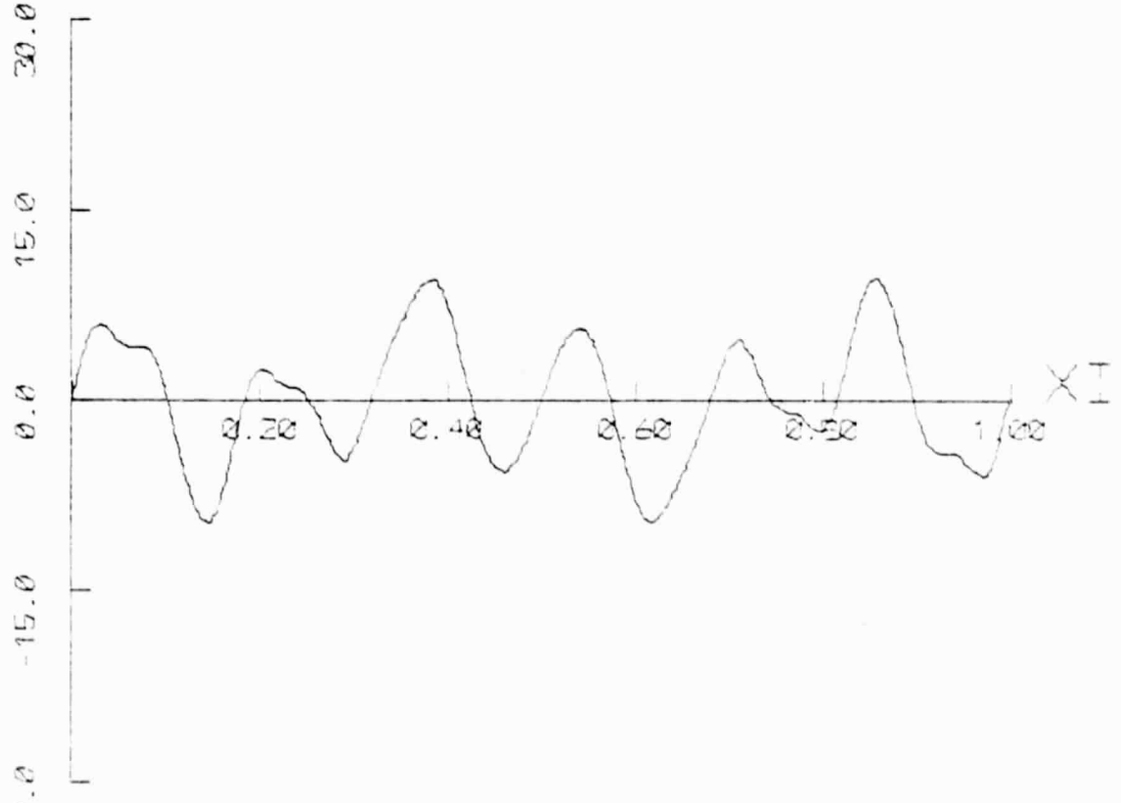

FIG 32 1000VBAR VERSUS XI FOR TAU = .499858E+00

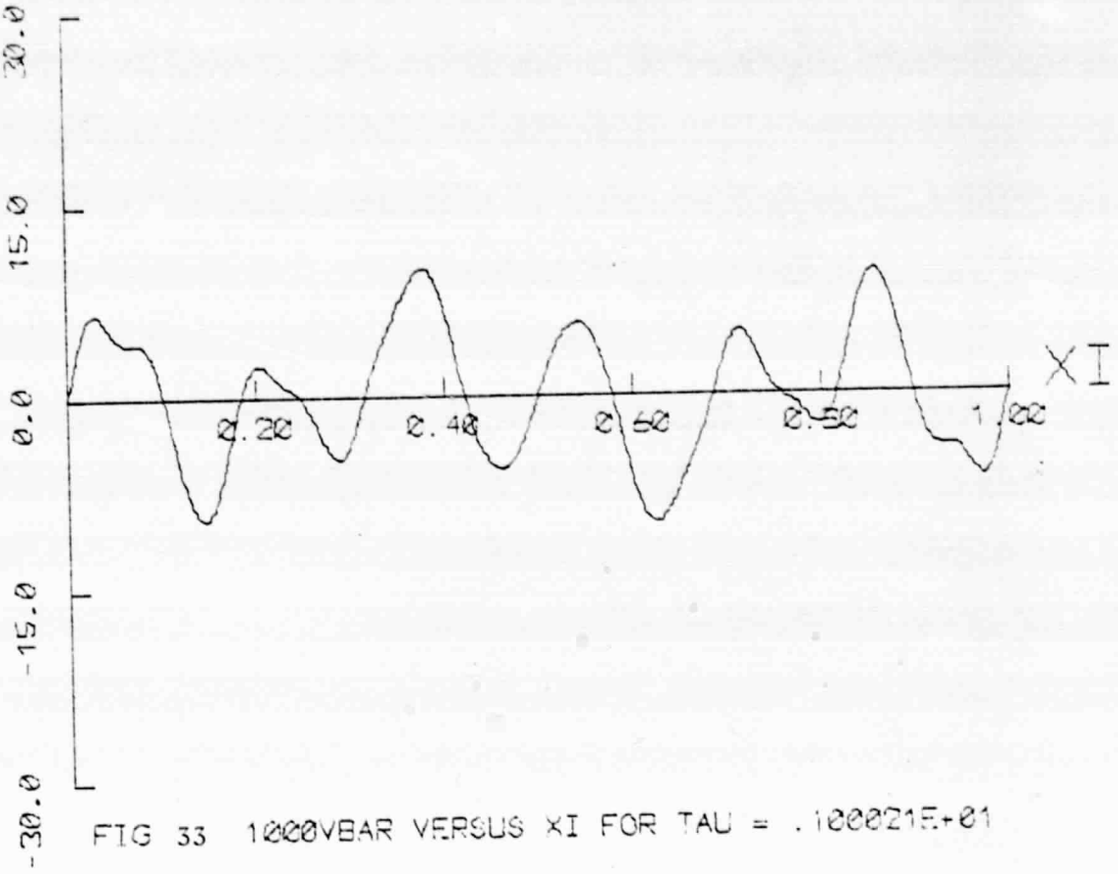

FIG 33 1000VBAR VERSUS XI FOR TAU = .100021E+01

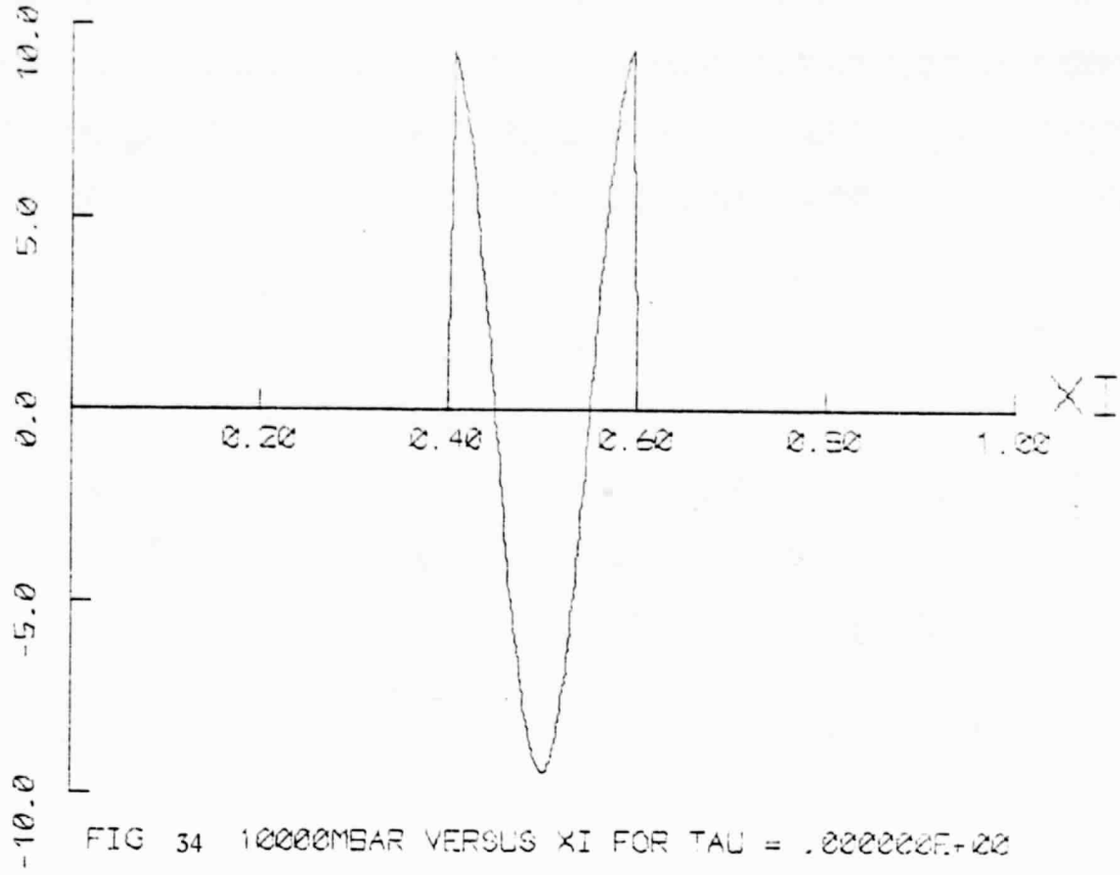

FIG 34 10000MBAR VERSUS XI FOR TAU = .000000E+00

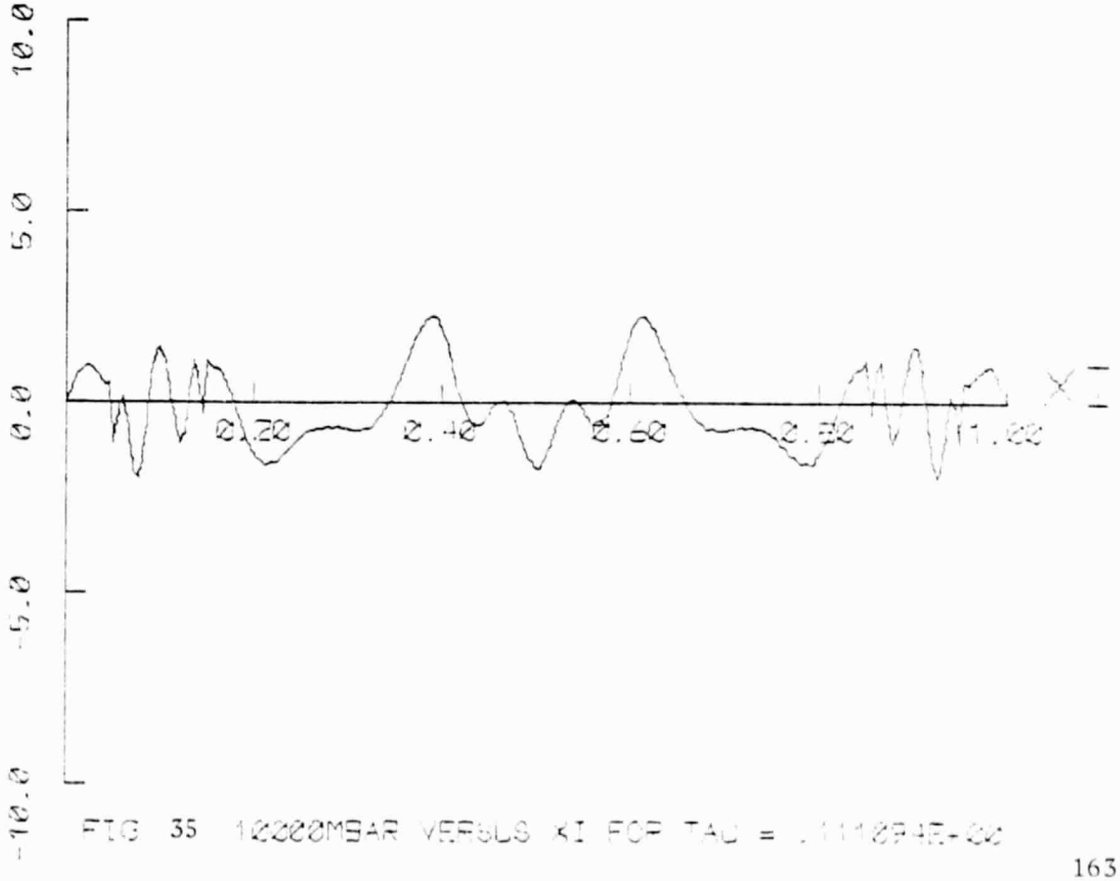

FIG 35 10000MBAR VERSUS XI FOR TAU = .111078E+00

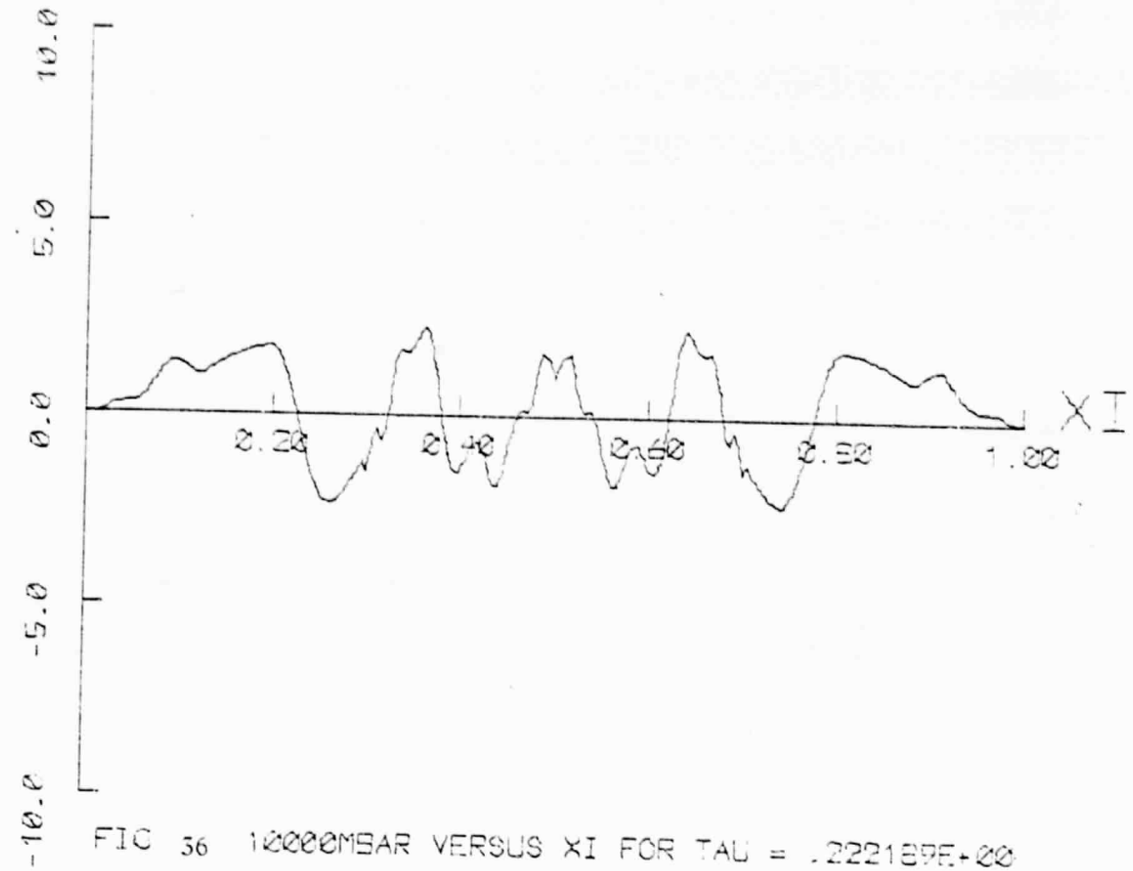

FIG 36 10000MBAR VERSUS XI FOR TAU = .222189E+00

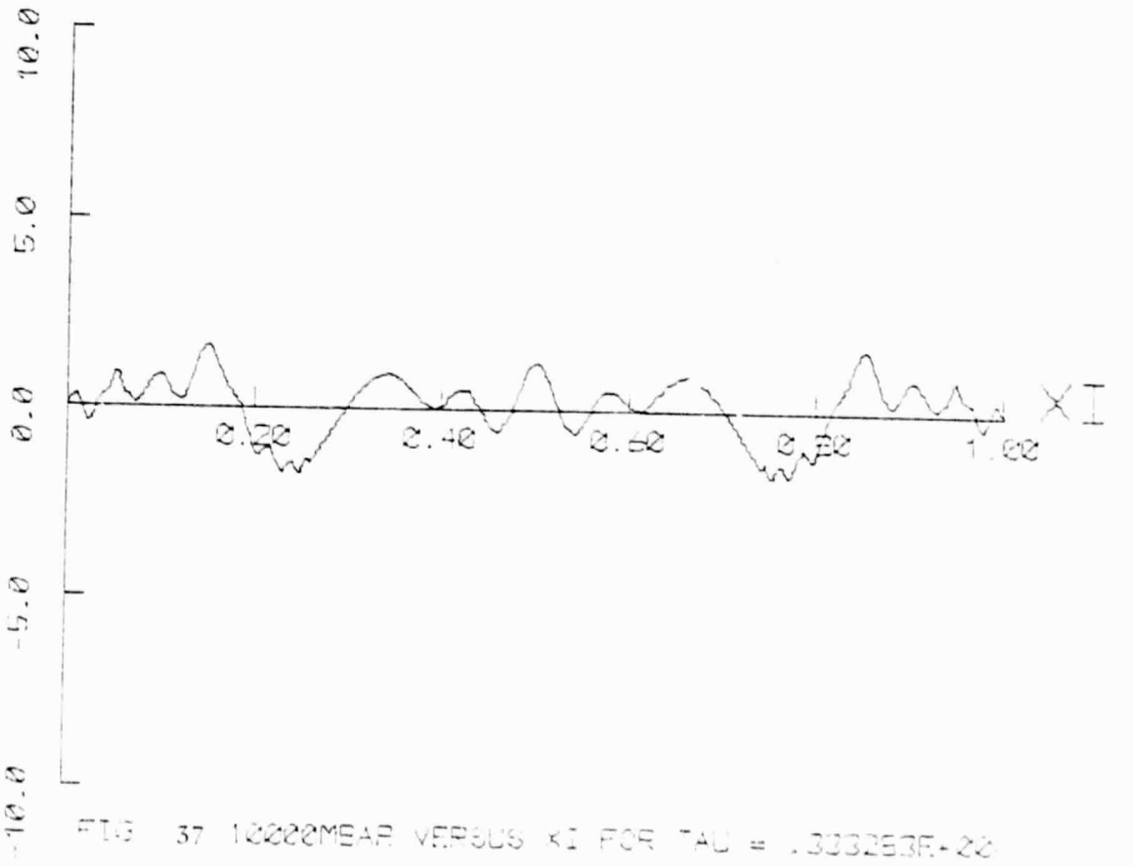

FIG 37 10000MBAR VERSUS XI FOR TAU = .333283E+00

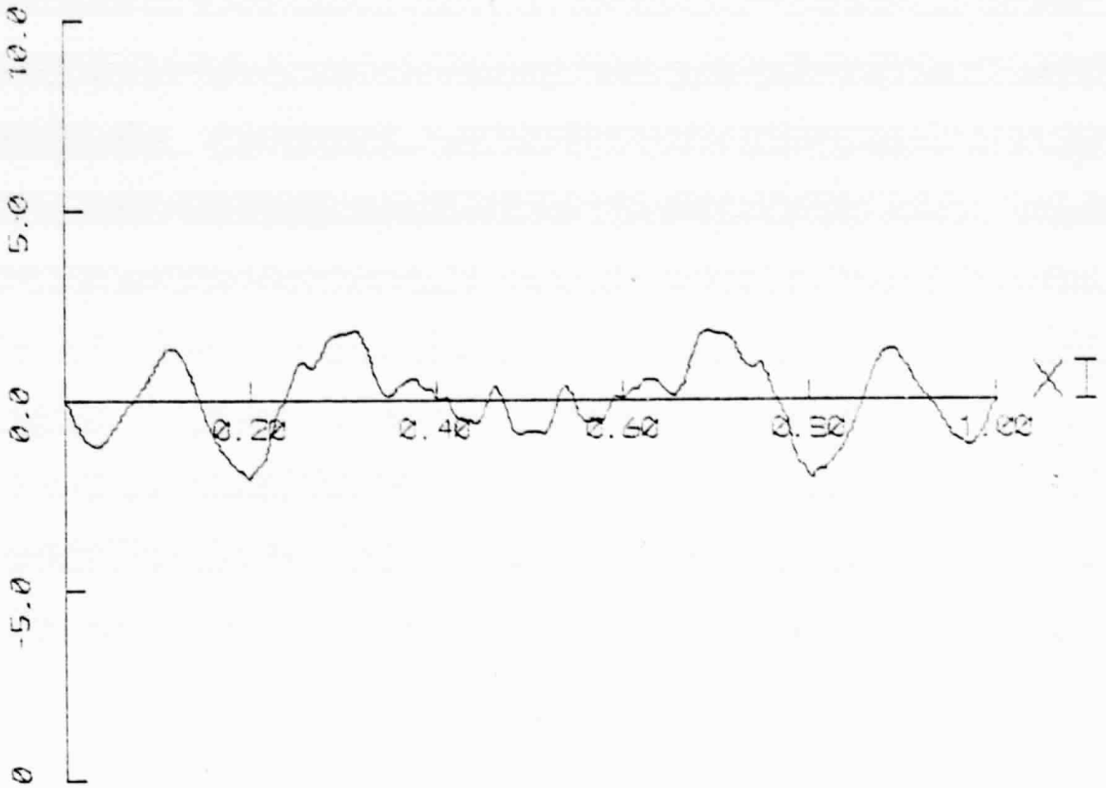

FIG 38 10000MBAR VERSUS XI FOR TAU = .444378E+00

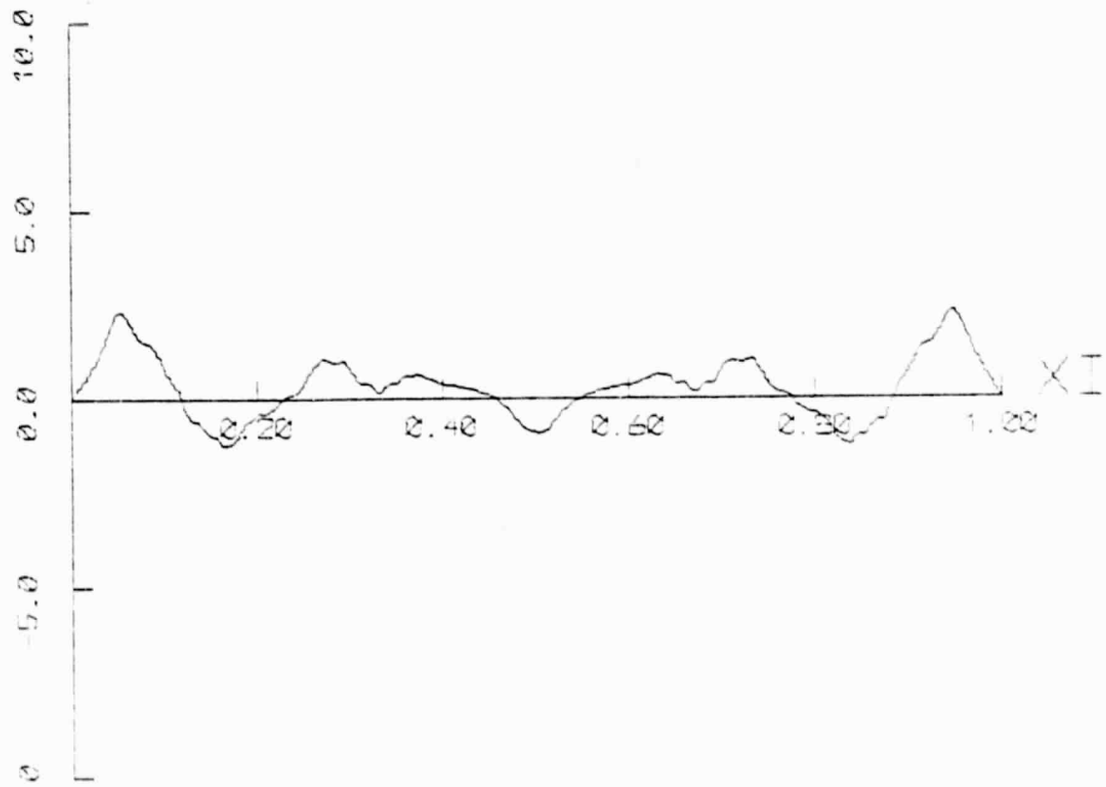

FIG 39 10000MBAR VERSUS XI FOR TAU = .955472E+00

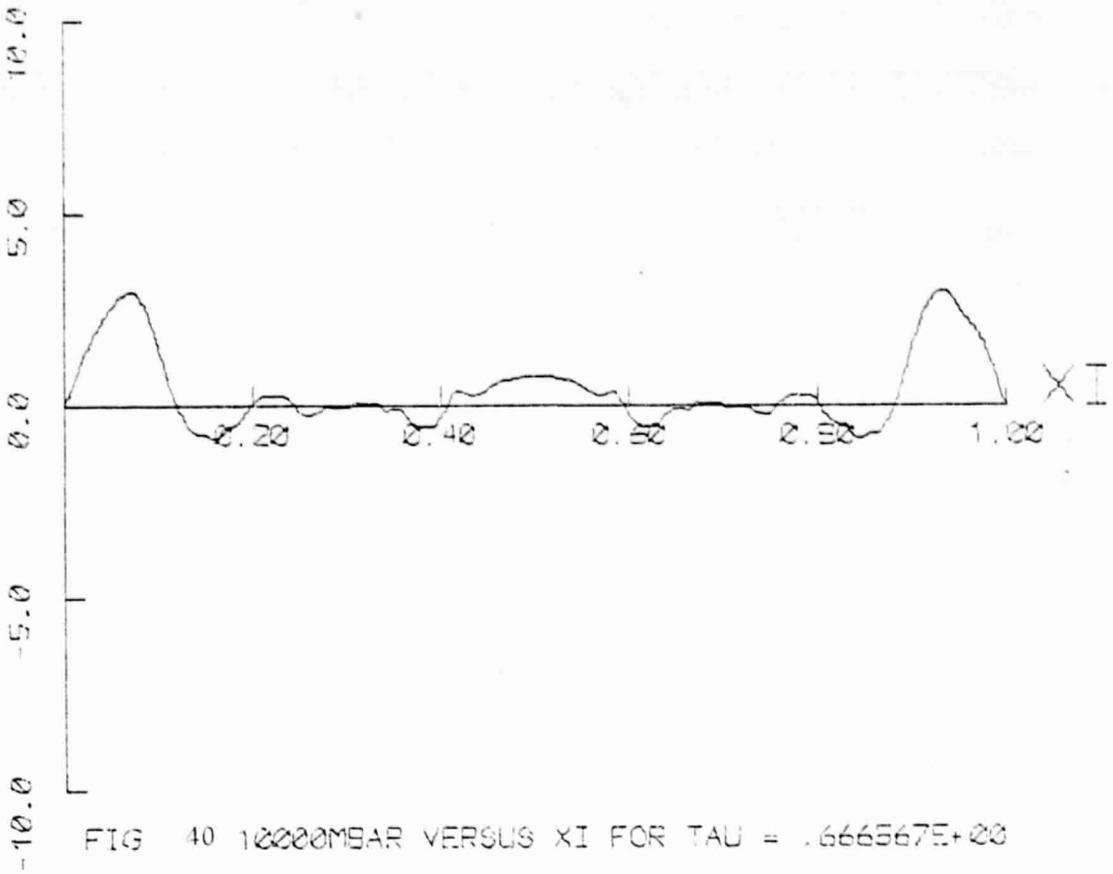

FIG 40 10000MBAR VERSUS XI FOR TAU = .6665675E+00

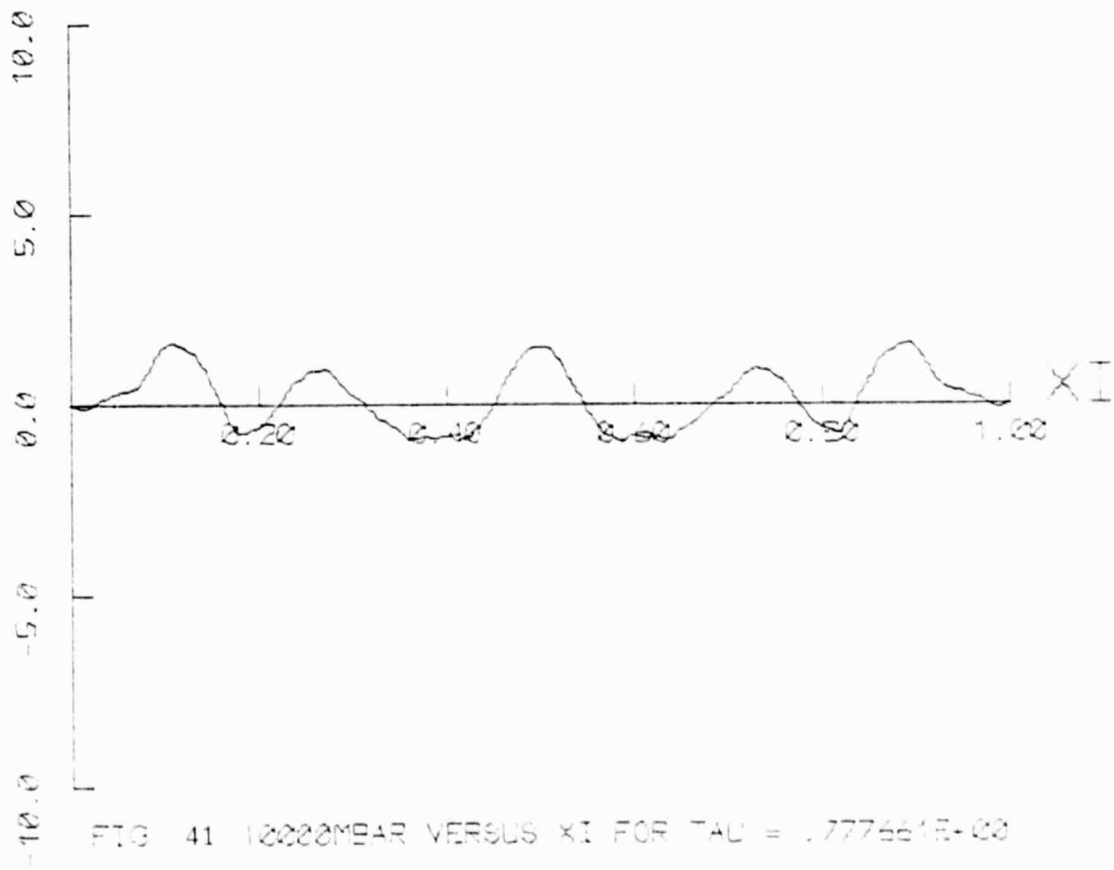

FIG 41 10000MBAR VERSUS XI FOR TAU = .7776615E+00

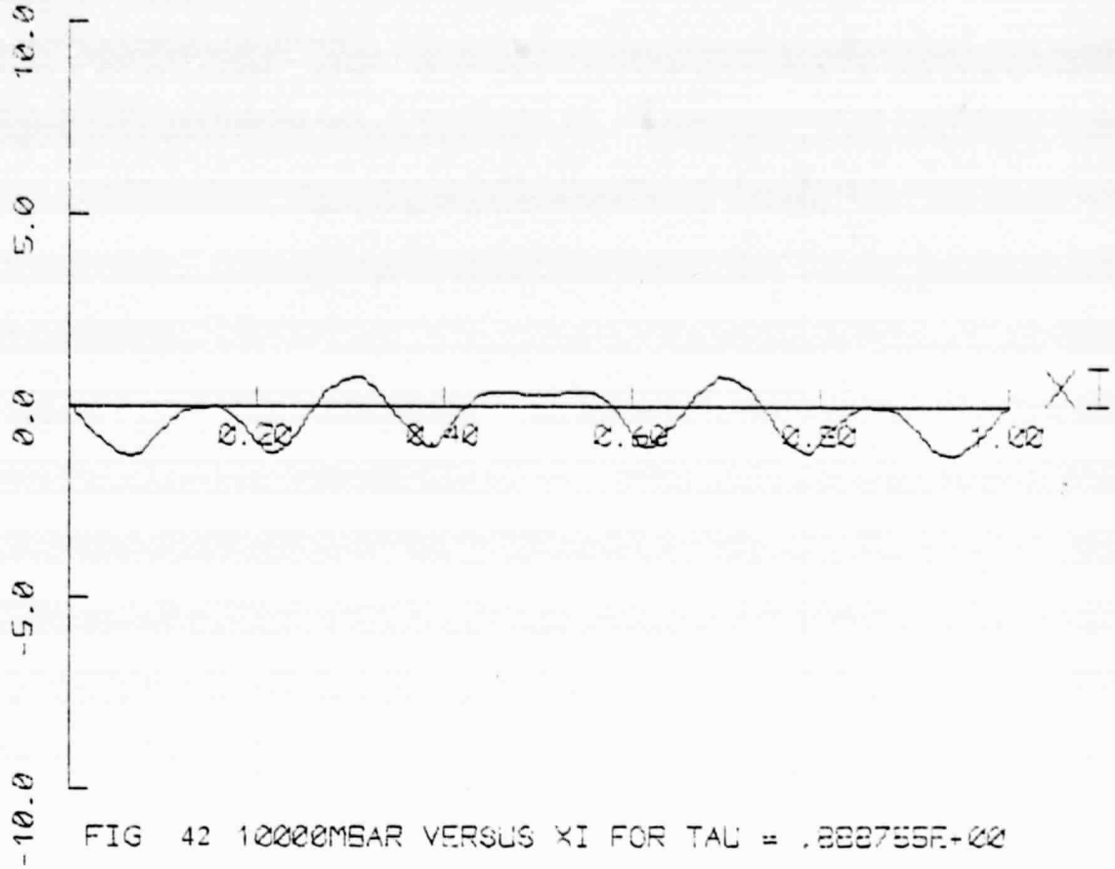

FIG 42 10000MBAR VERSUS XI FOR TAU = .888755E-00

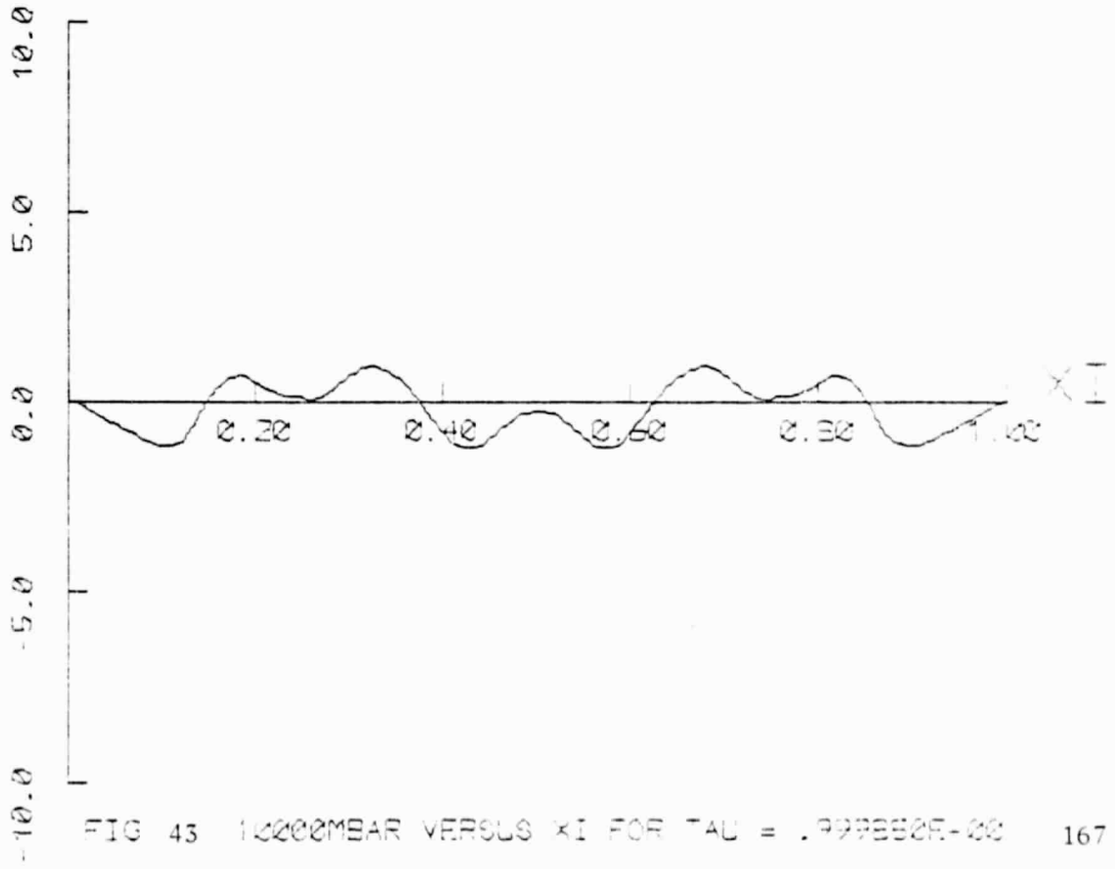

FIG 43 10000MBAR VERSUS XI FOR TAU = .999850E-00

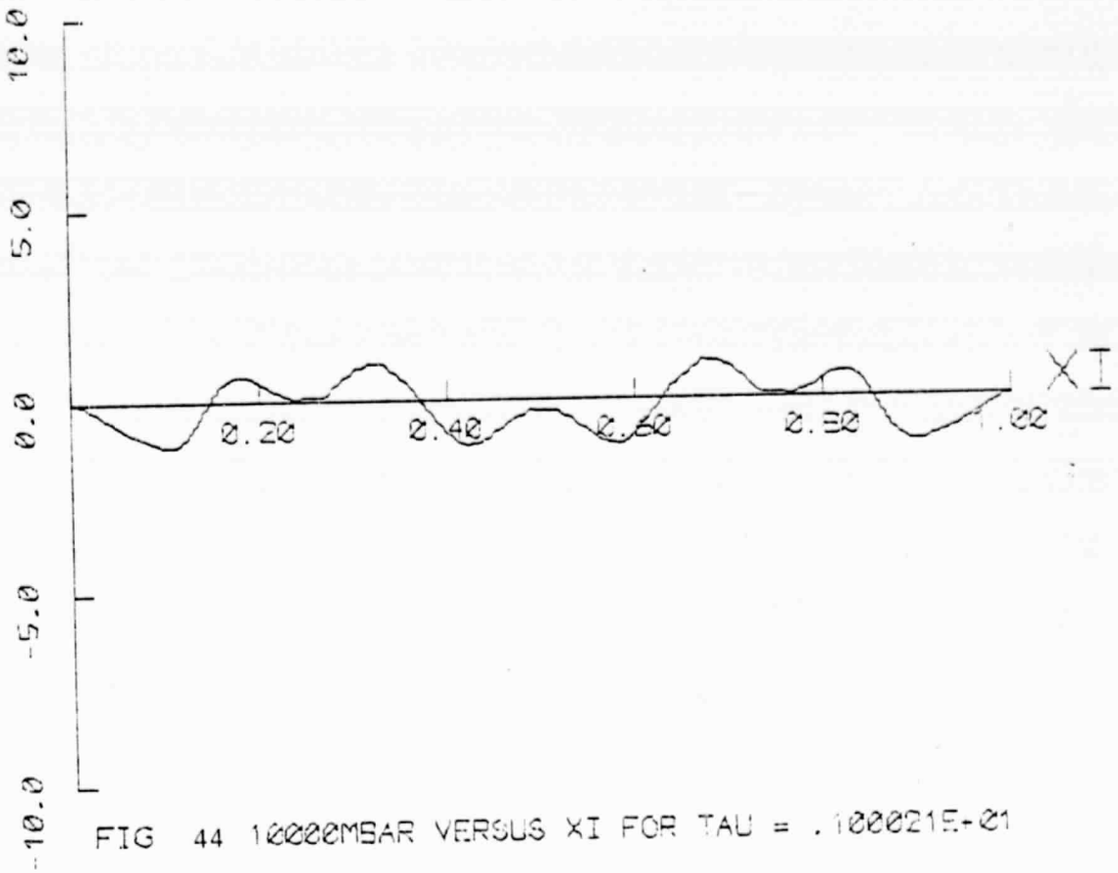

FIG 44 10000MBAR VERSUS XI FOR TAU = .100021E-01

APPENDIX K

Response to a (1 + cos) initial displacement;

$V_R = 0.62$, SLR = 50, $\lambda = 0.2$, $\bar{b}_1 = 0.0$, $\bar{b}_2 = 12.0$.

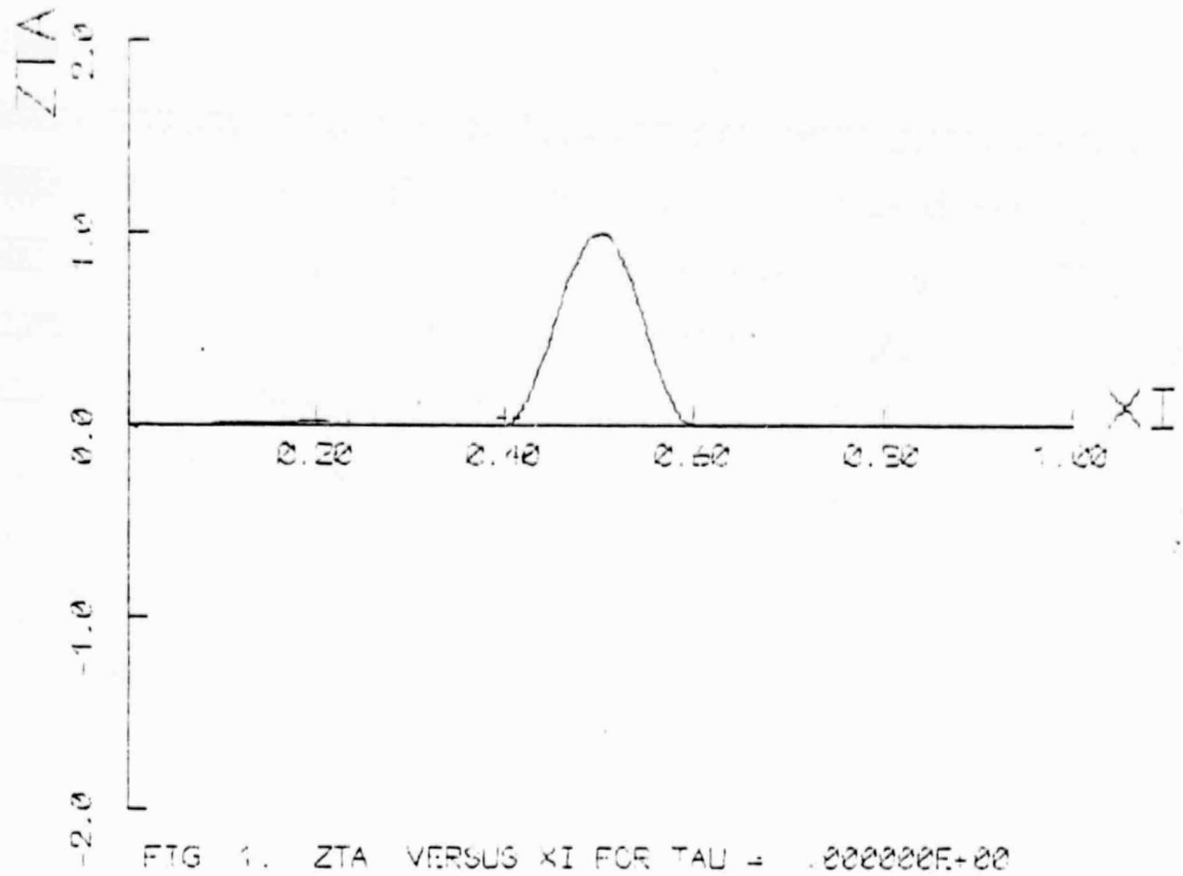

FIG 1. ZTA VERSUS XI FOR TAU = .000000E+00

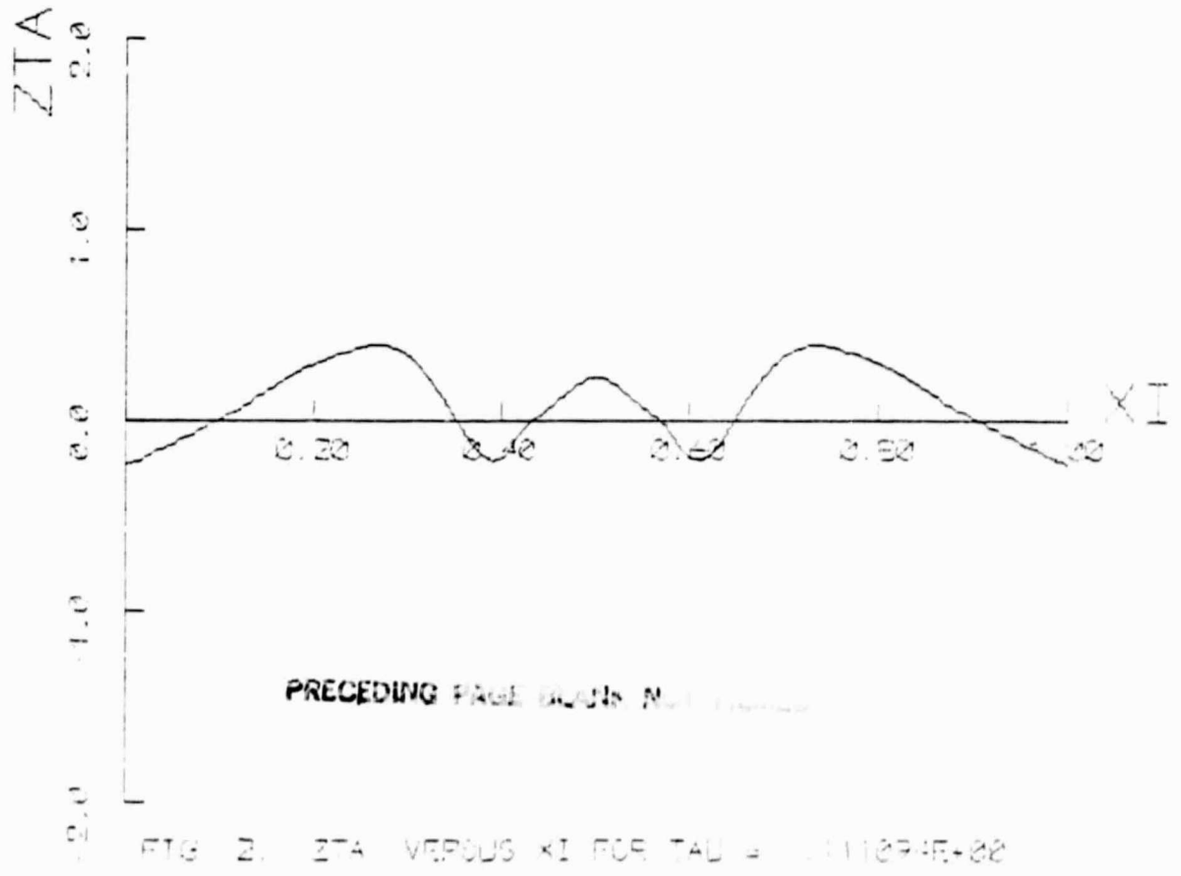

PRECEDING PAGE BLANK-NOT FILMED

FIG 2. ZTA VERSUS XI FOR TAU = .111674E+00

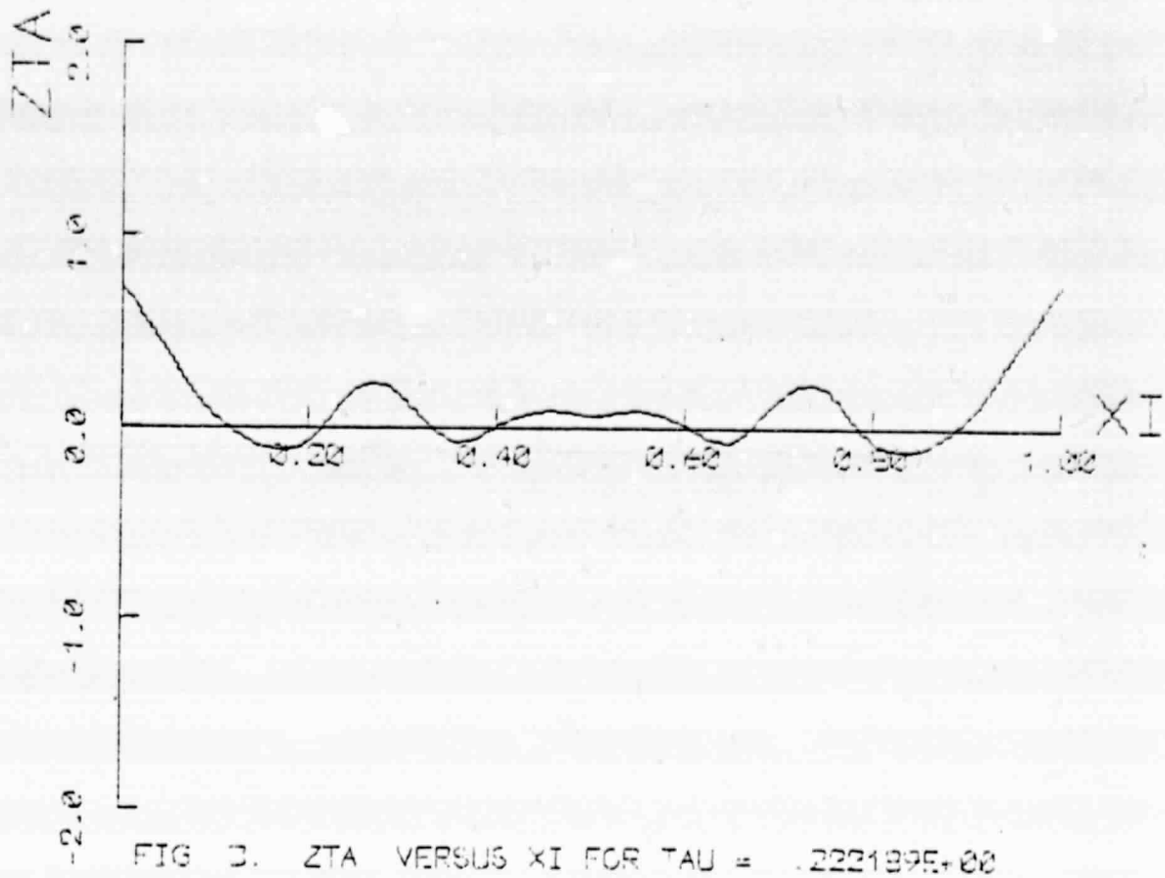

FIG 3. ZTA VERSUS XI FOR TAU = .2221895+00

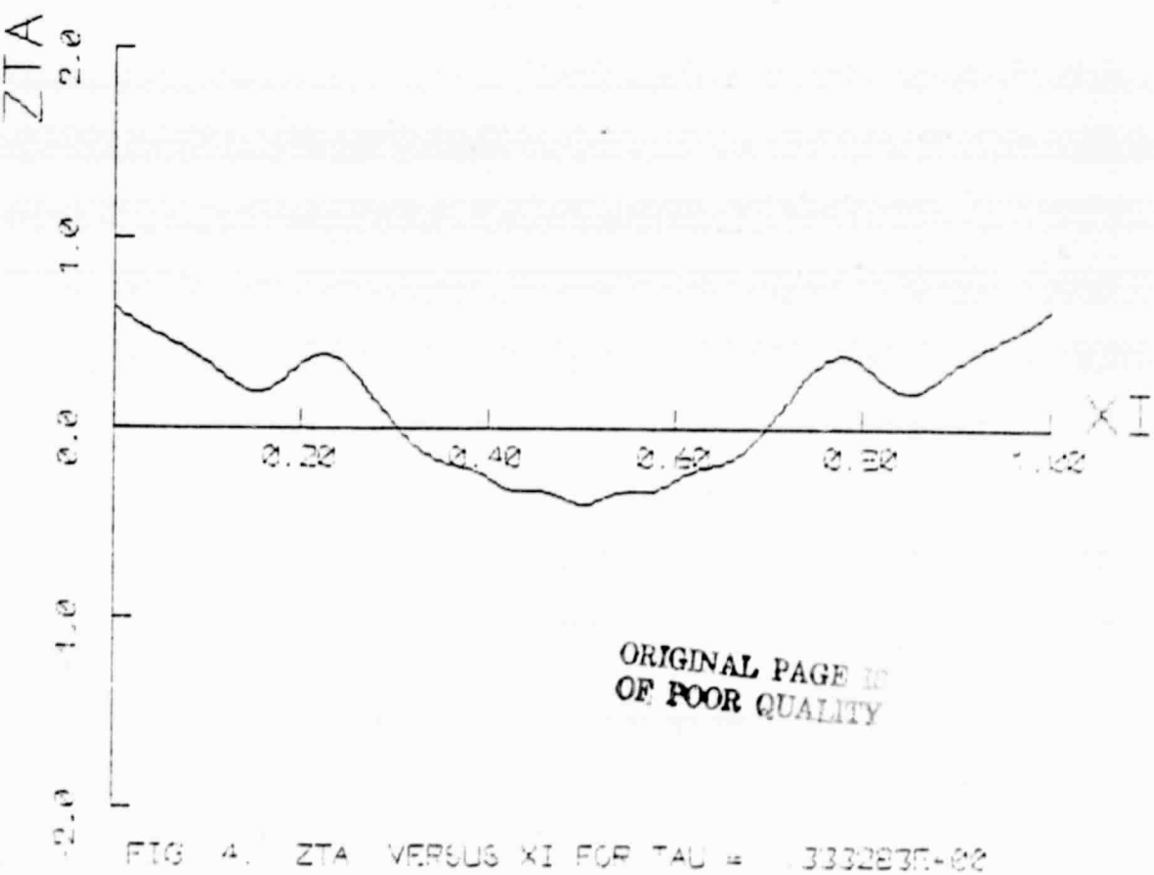

FIG 4. ZTA VERSUS XI FOR TAU = .3332837-00

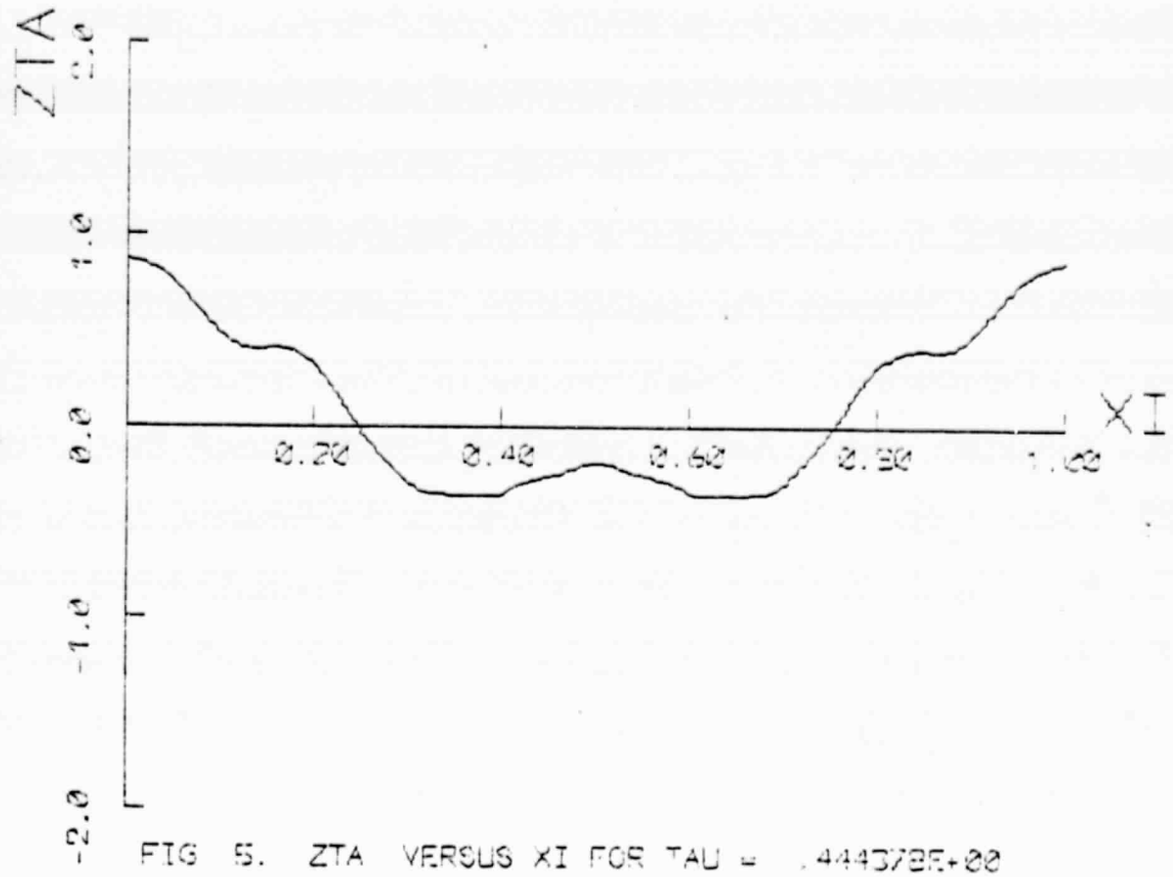

FIG 5. ZTA VERSUS XI FOR TAU = .444378E+00

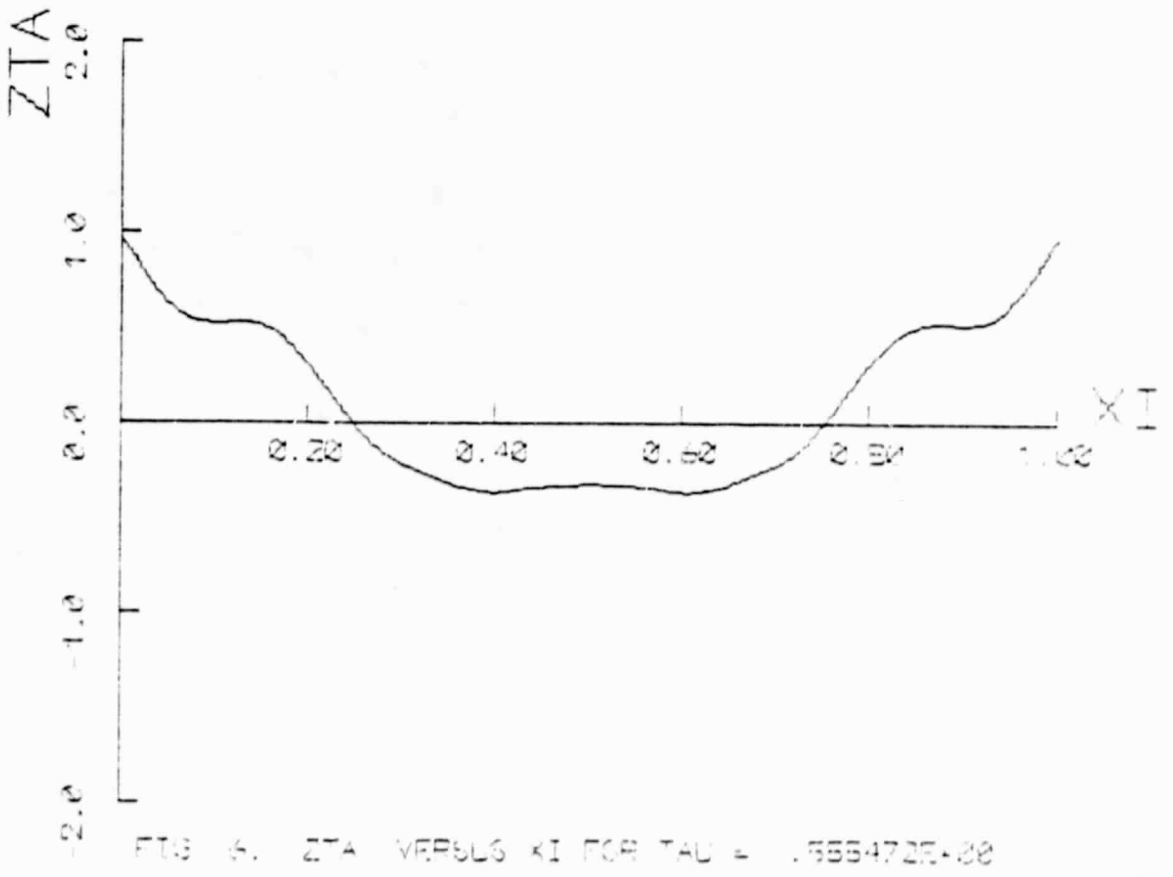

FIG 6. ZTA VERSUS XI FOR TAU = .555472E+00

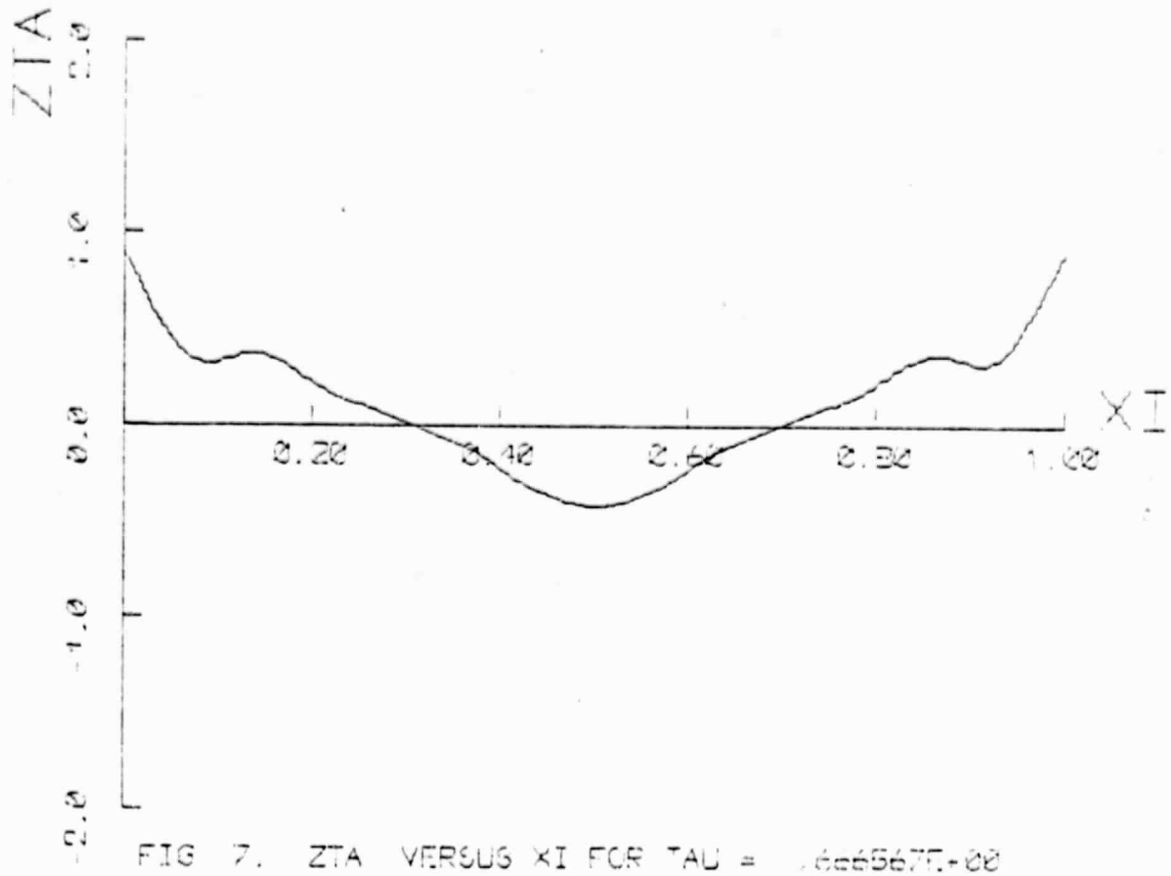

FIG 7. ZTA VERSUS XI FOR TAU = .6666567E-00

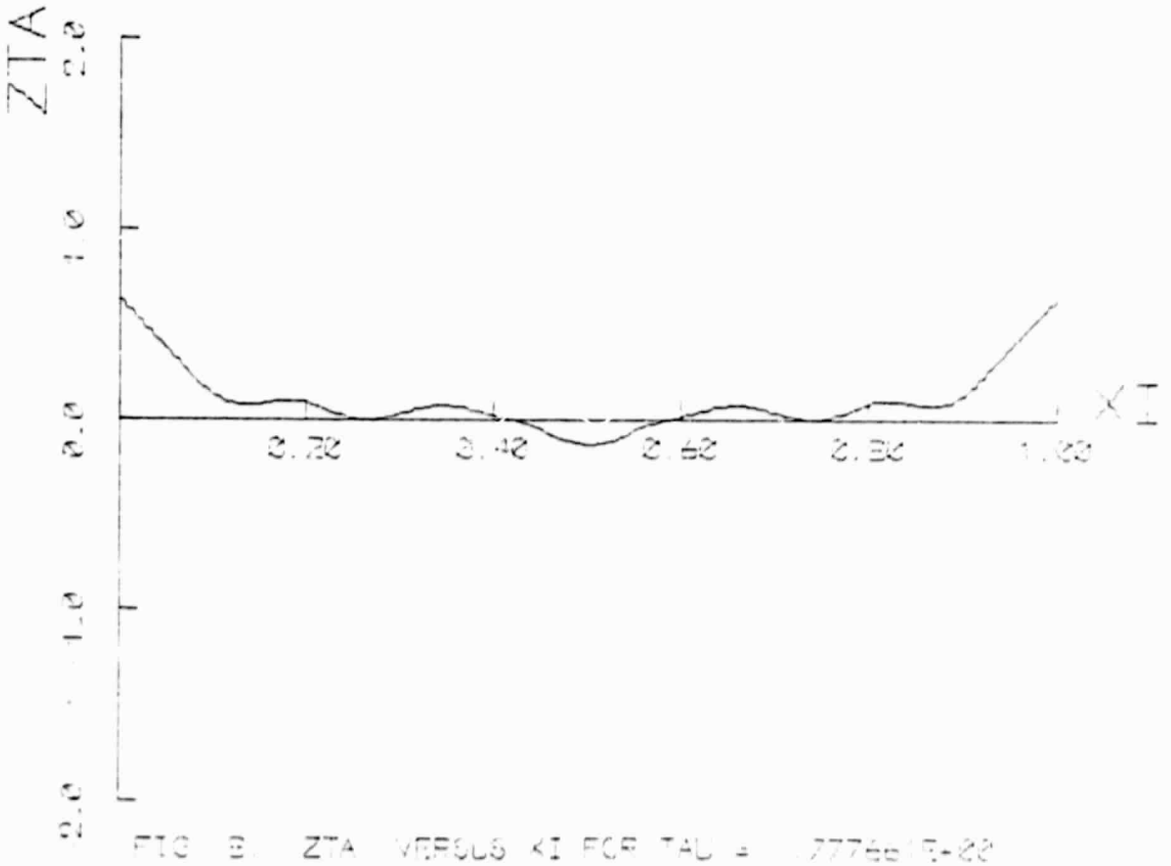

FIG 8. ZTA VERSUS XI FOR TAU = .7776667E-00

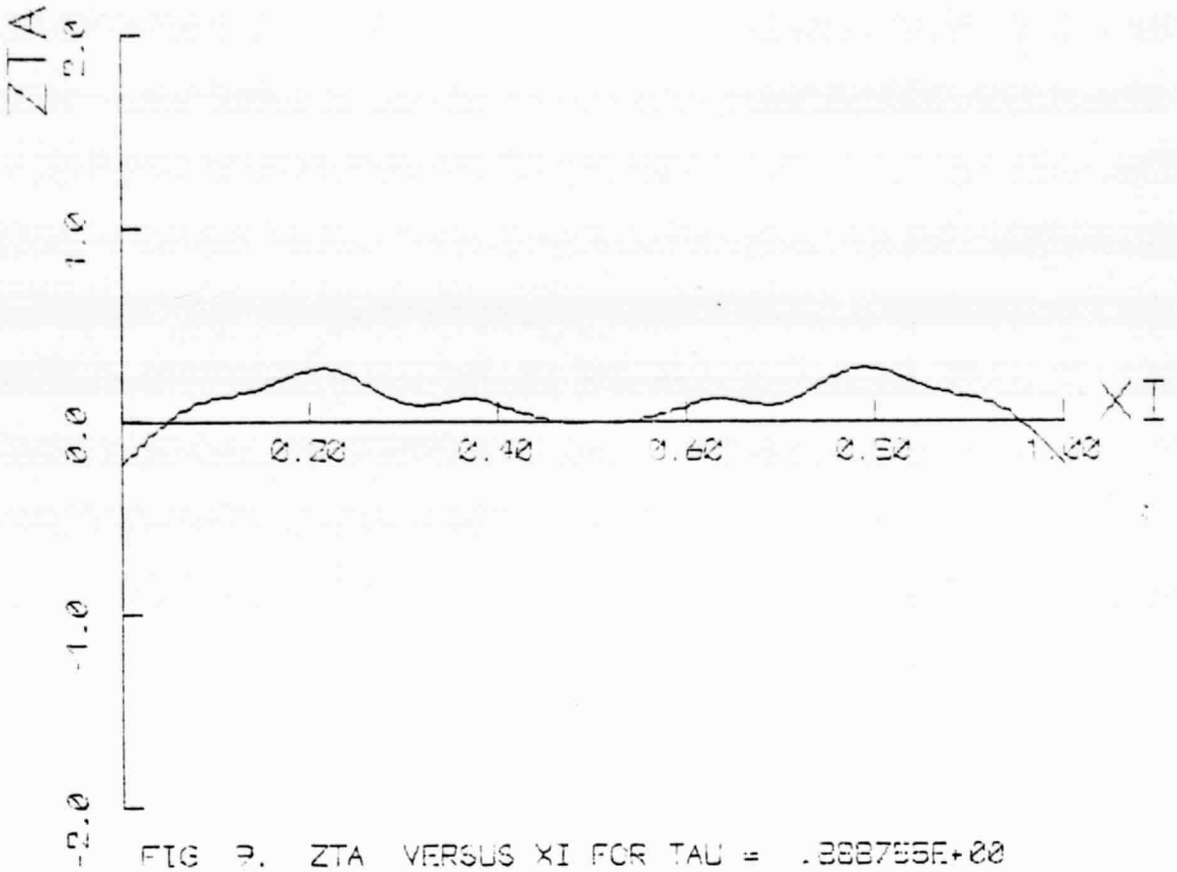

FIG 9. ZTA VERSUS XI FOR TAU = .888755E+00

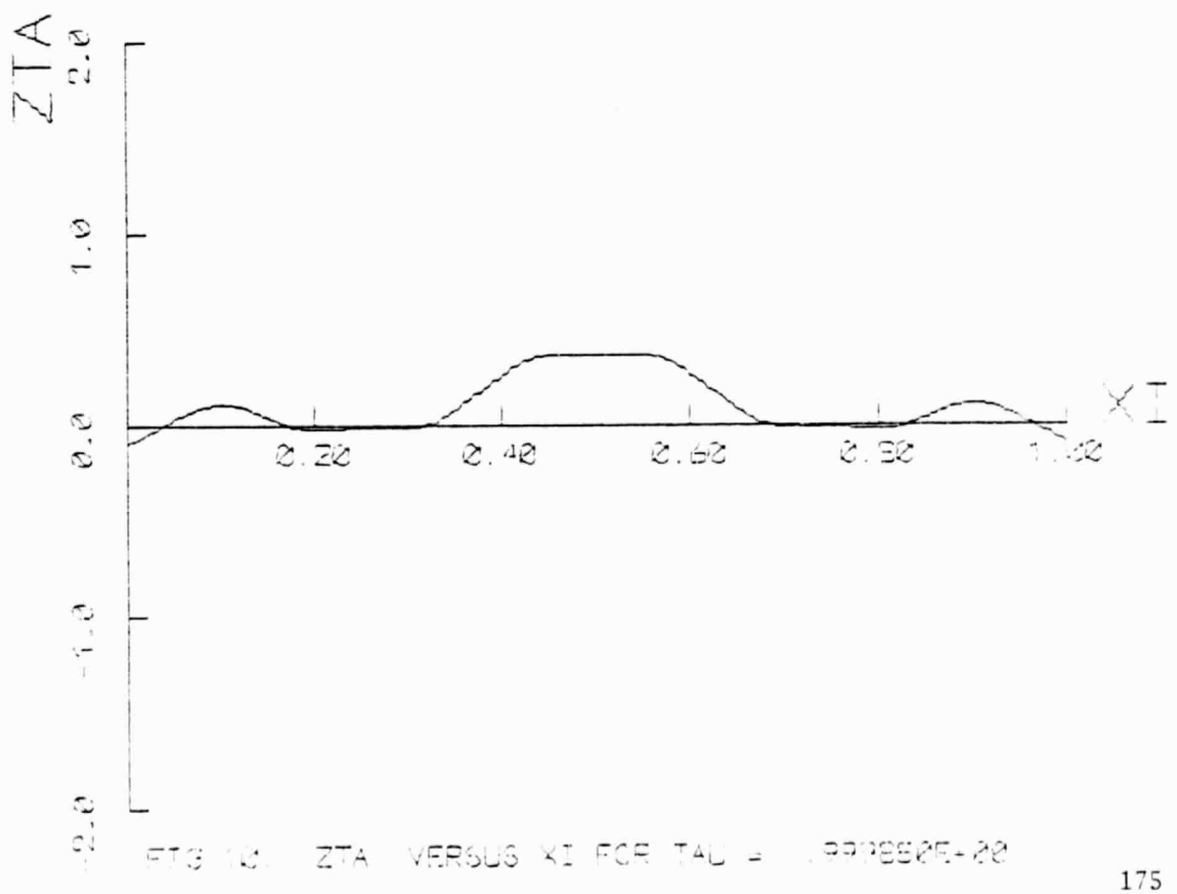

FIG 10. ZTA VERSUS XI FOR TAU = .999999E+00

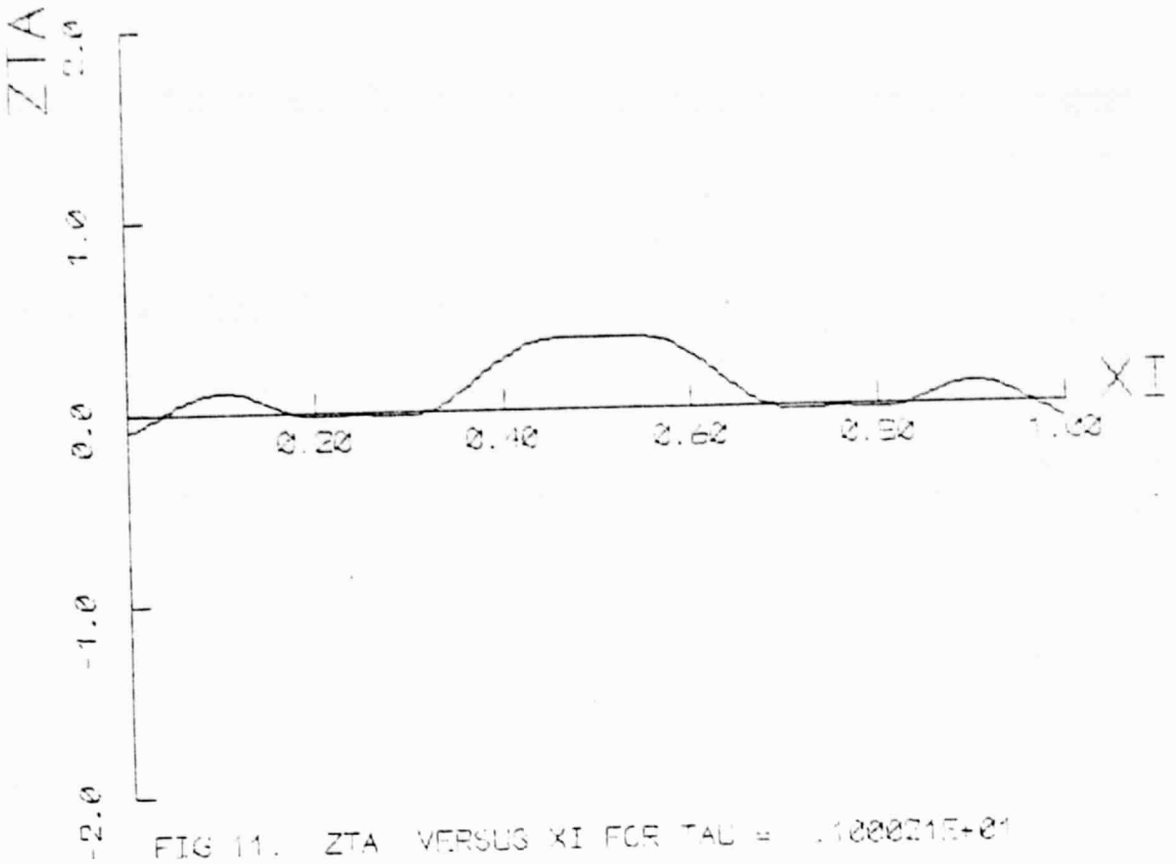

FIG 11. ZTA VERSUS XI FOR TAU = .1000E1E+01

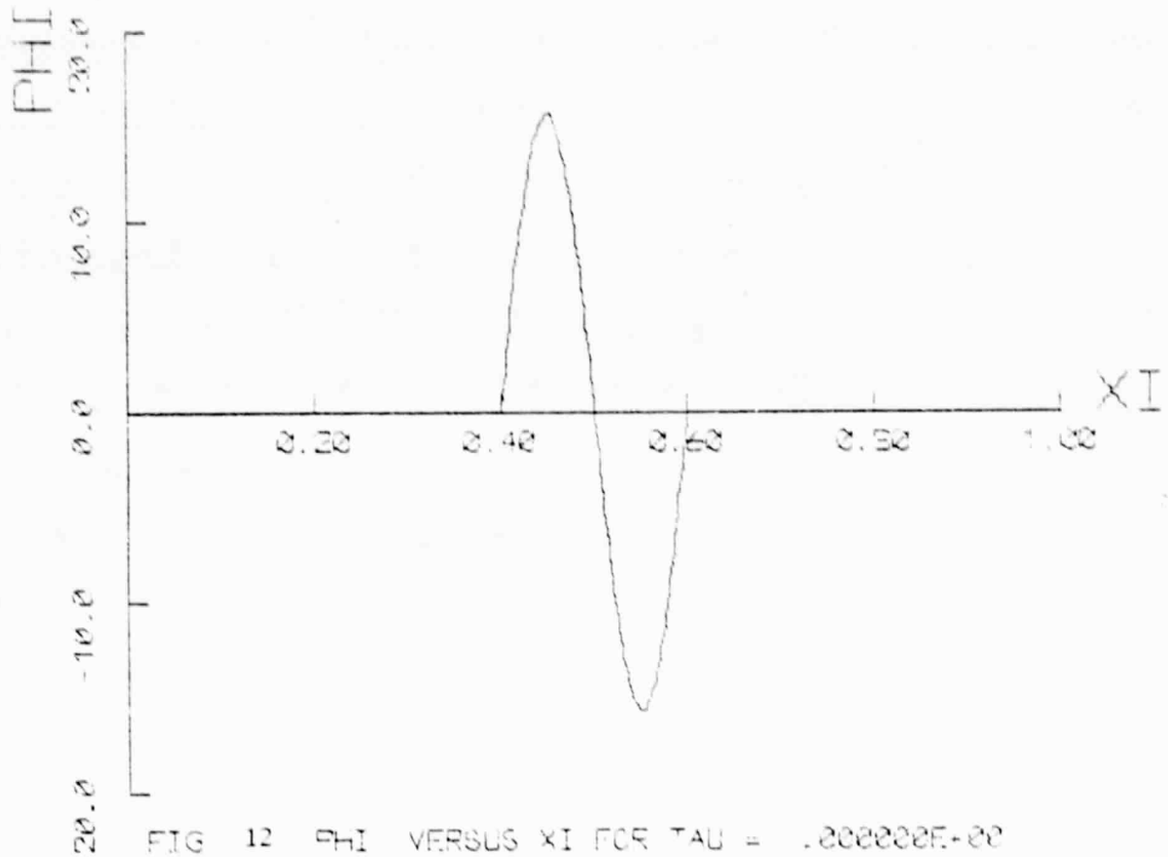

FIG 12 PHI VERSUS XI FOR TAU = .000000E-00

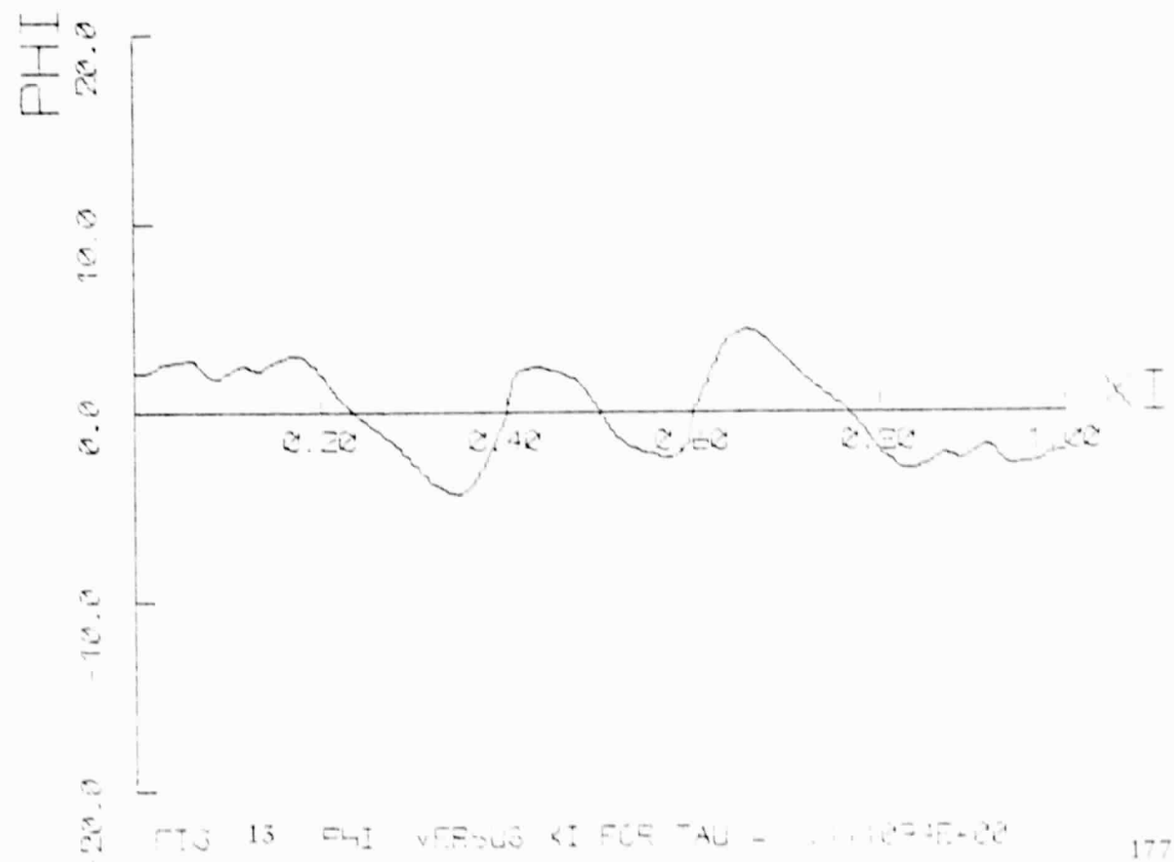

FIG 13 PHI VERSUS XI FOR TAU = [illegible]

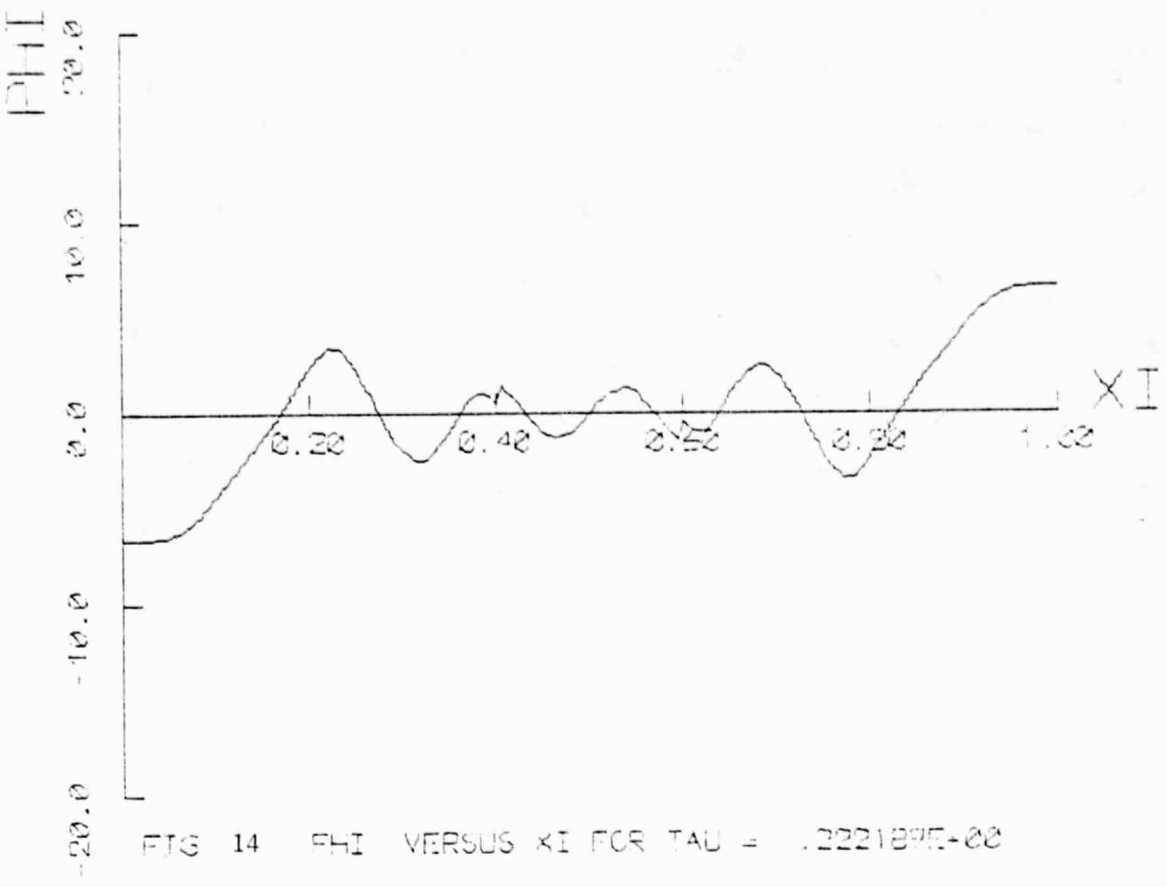

FIG 14 PHI VERSUS XI FOR TAU = .2221875E-00

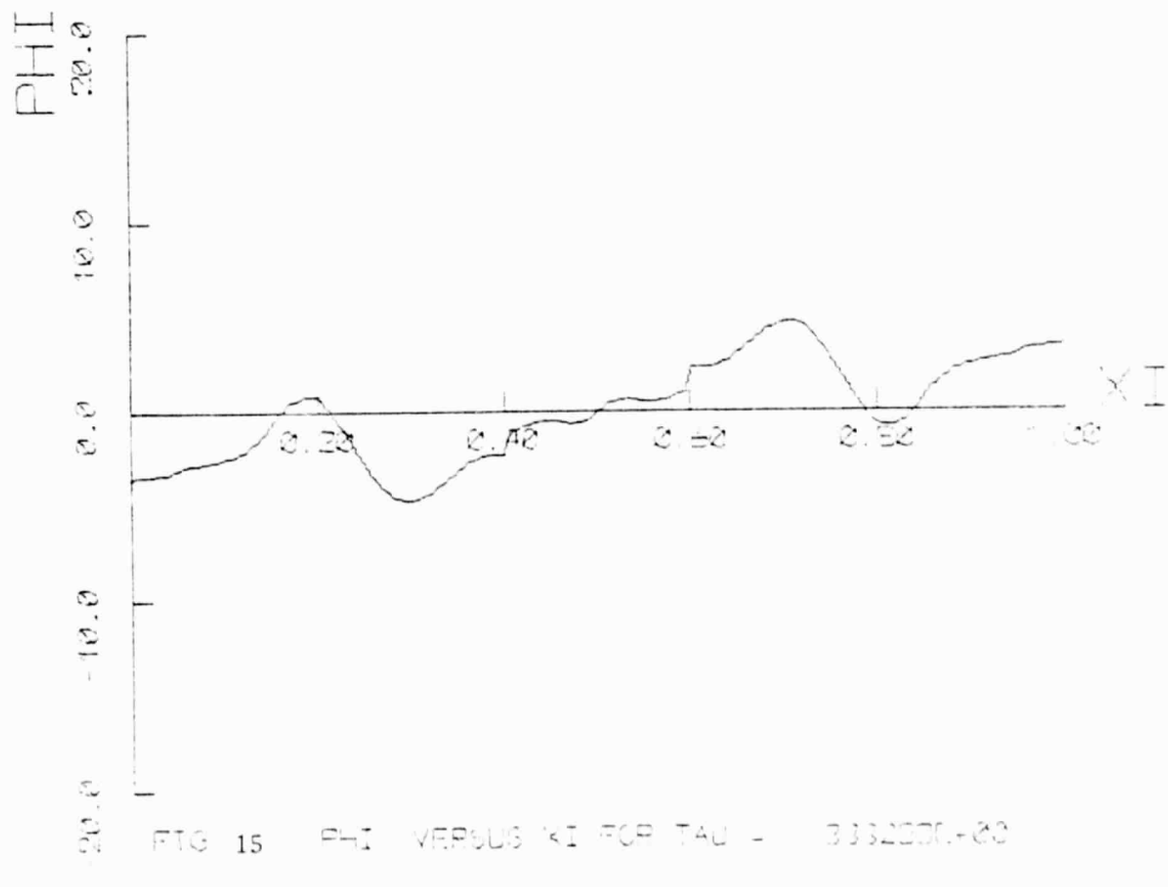

FIG 15 PHI VERSUS XI FOR TAU = 3.3312500E-00

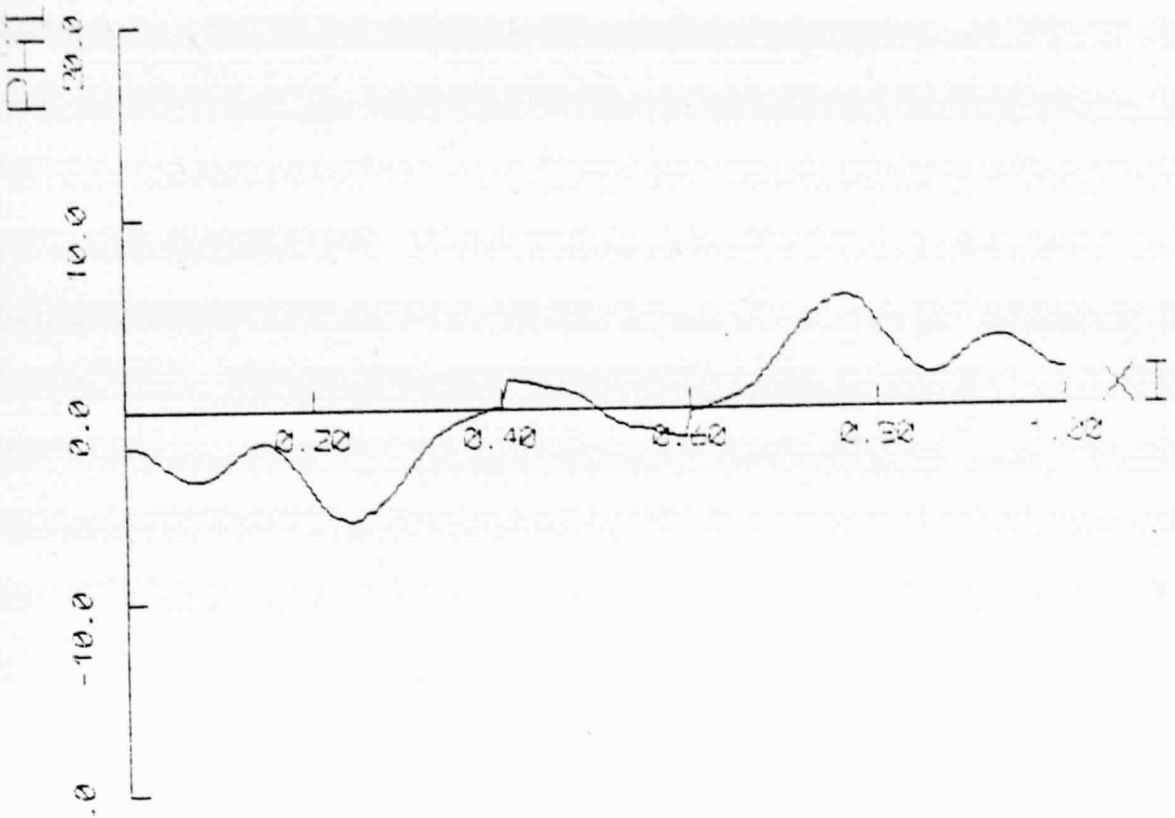

FIG 16 PHI VERSUS XI FOR TAU = .444378E+00

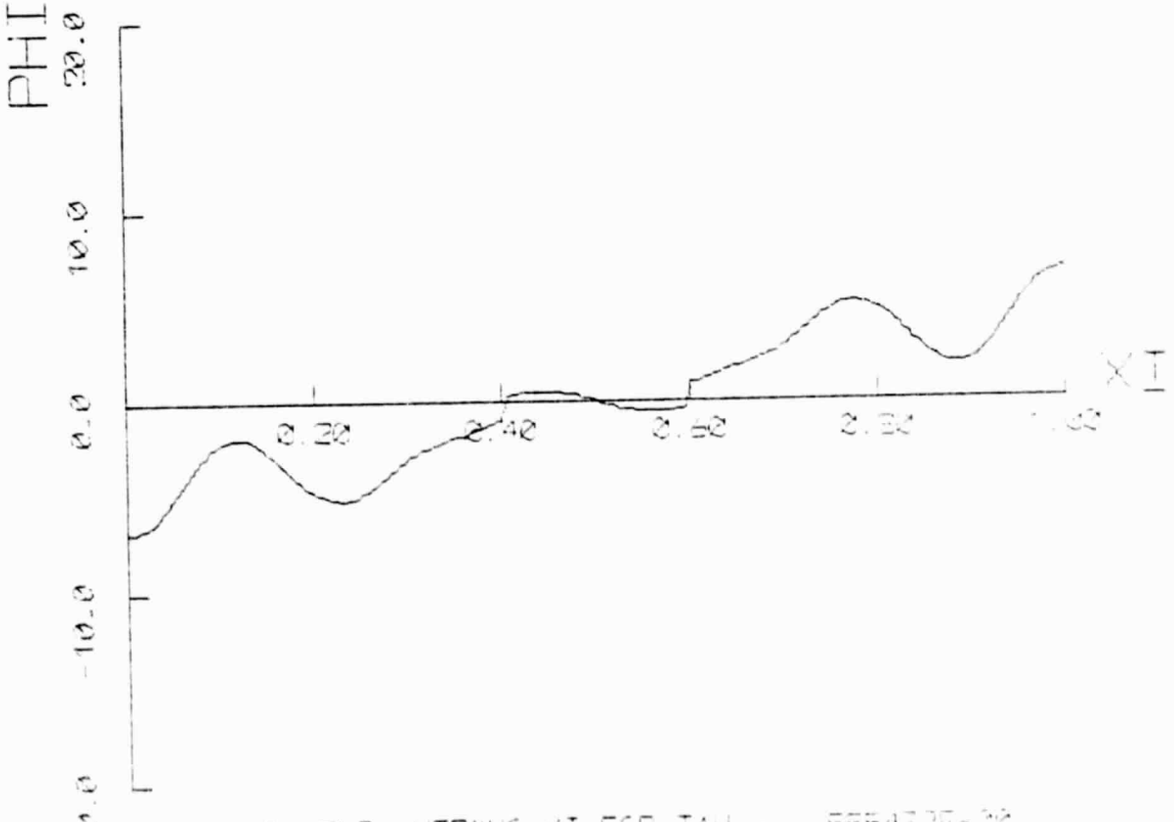

FIG 17 PHI VERSUS XI FOR TAU = .555472E+00

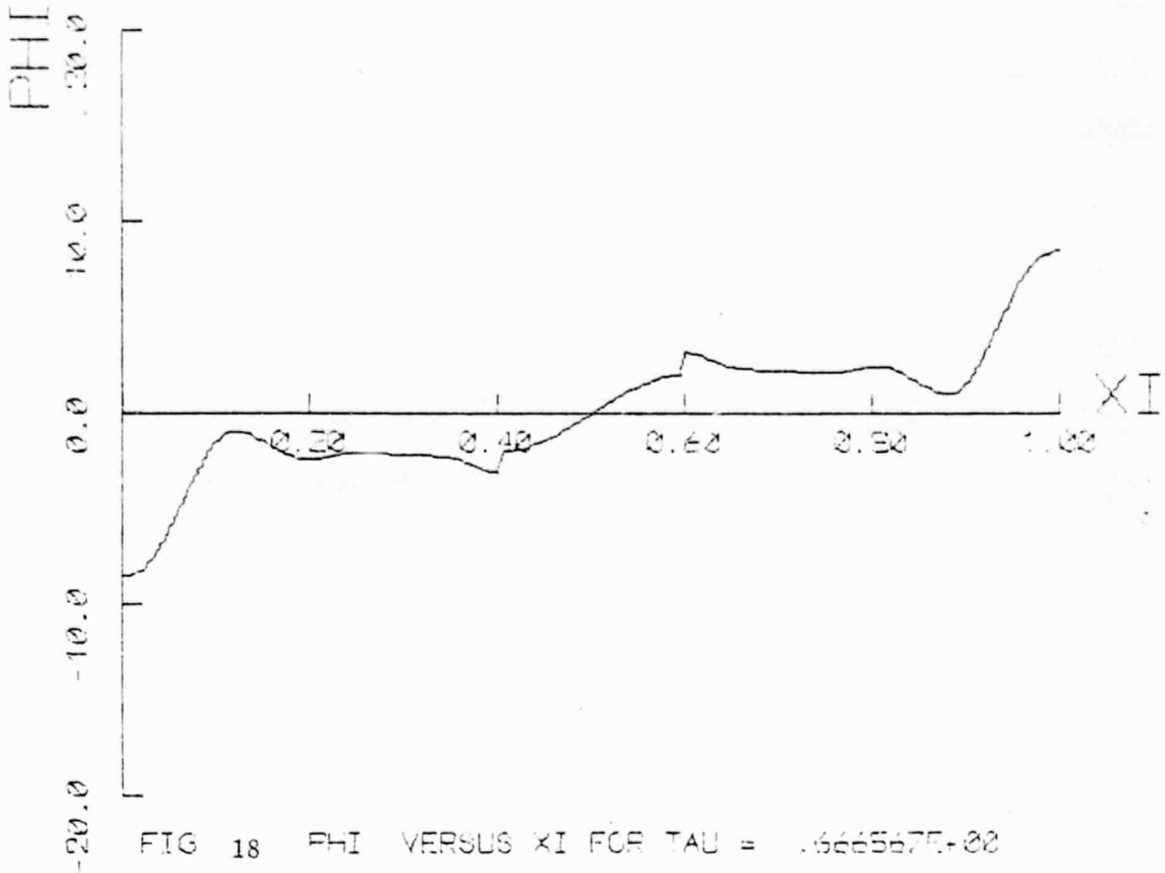

FIG 18 PHI VERSUS XI FOR TAU = .6665675+00

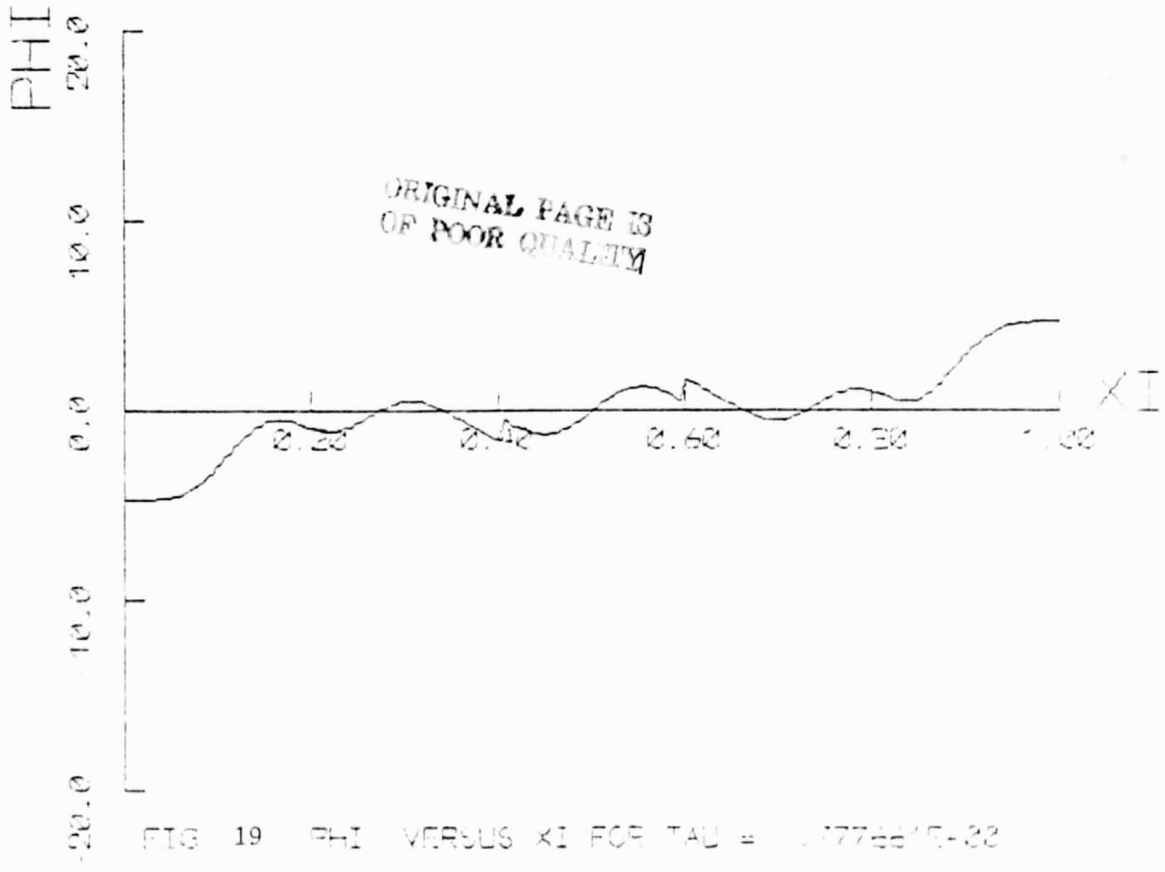

FIG 19 PHI VERSUS XI FOR TAU = .7776615+00

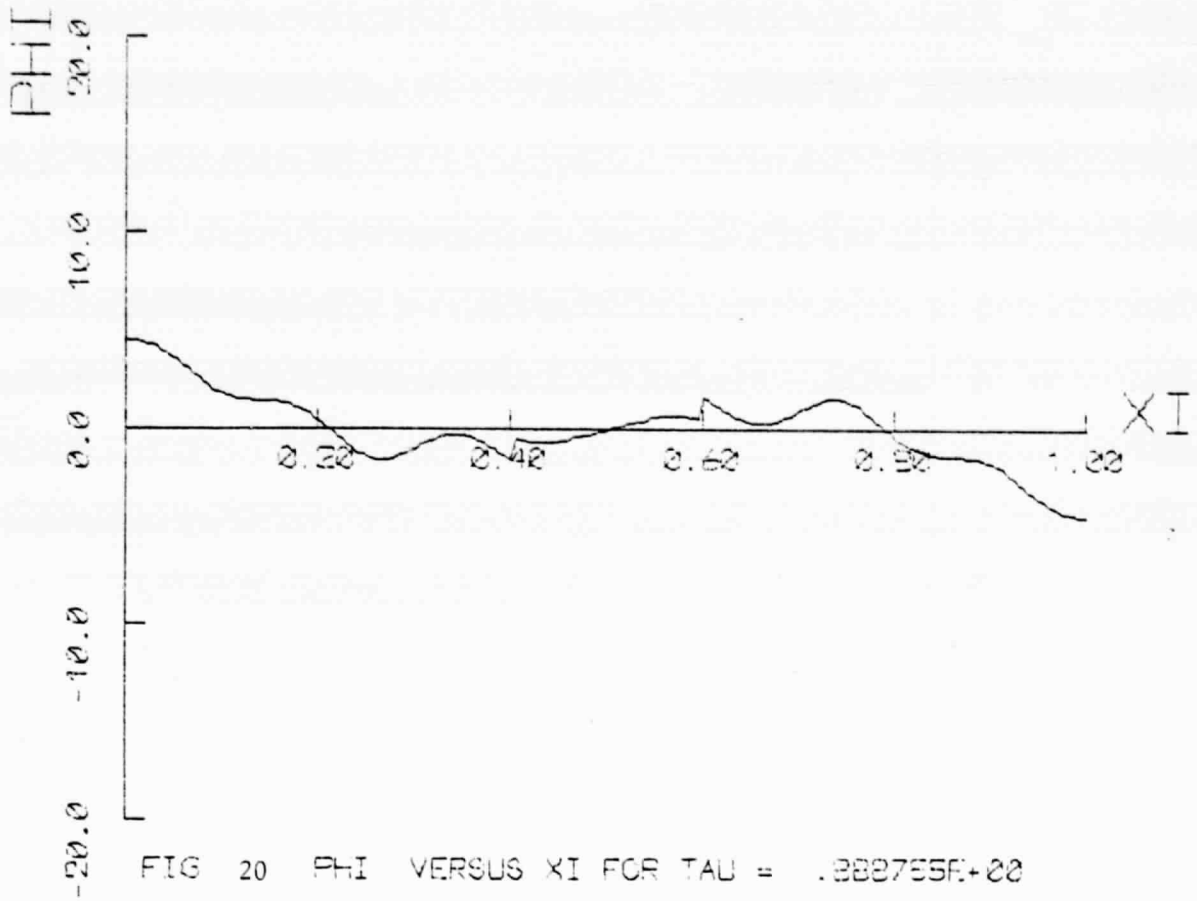

FIG 20 PHI VERSUS XI FOR TAU = .888755E+00

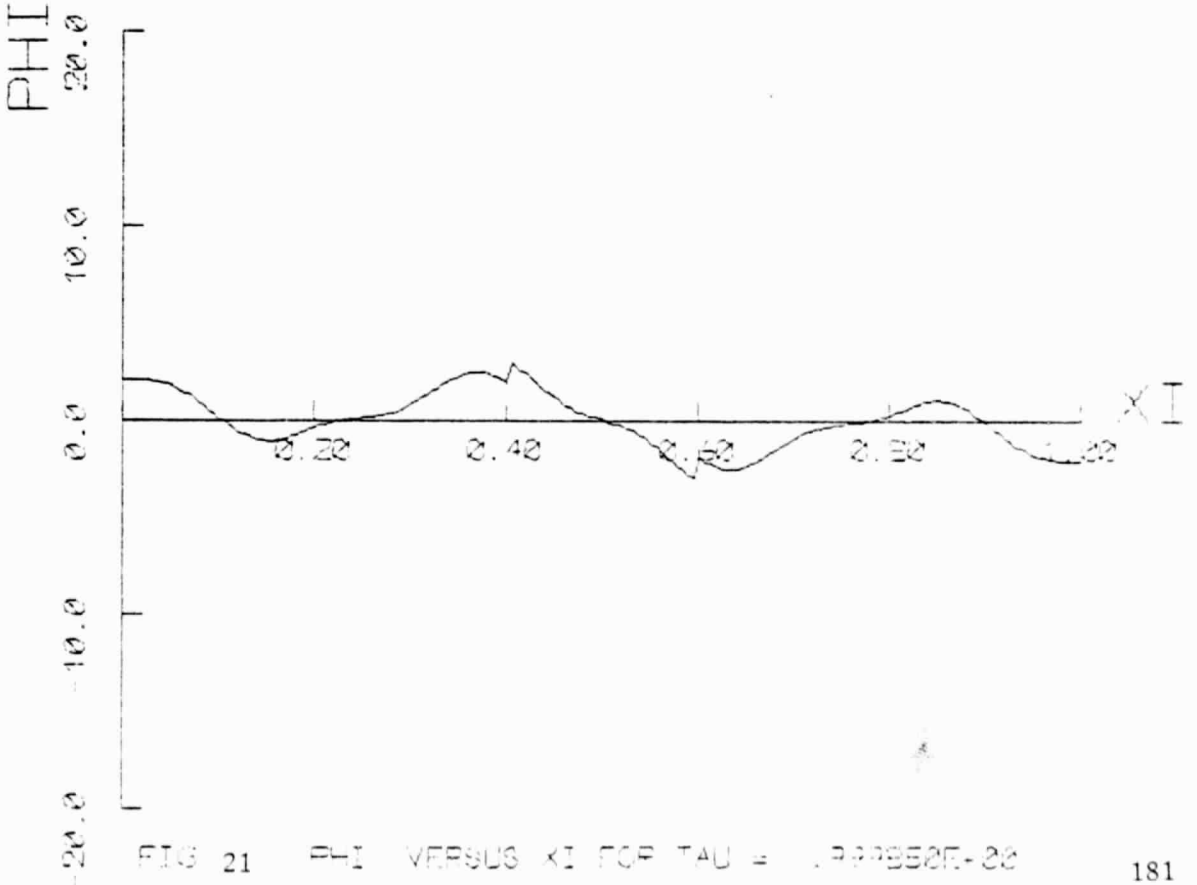

FIG 21 PHI VERSUS XI FOR TAU = .999950E+00

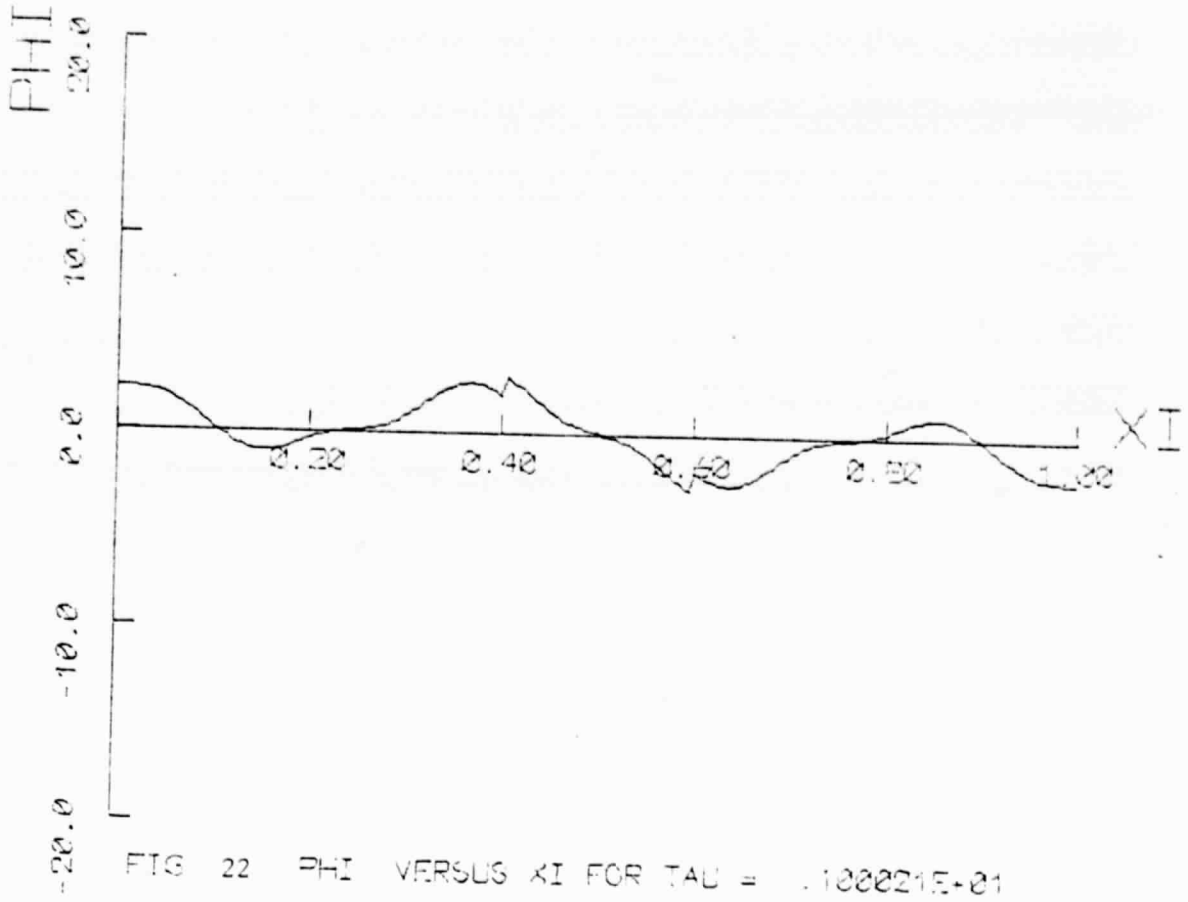

FIG 22 PHI VERSUS XI FOR TAU = .1000215+01

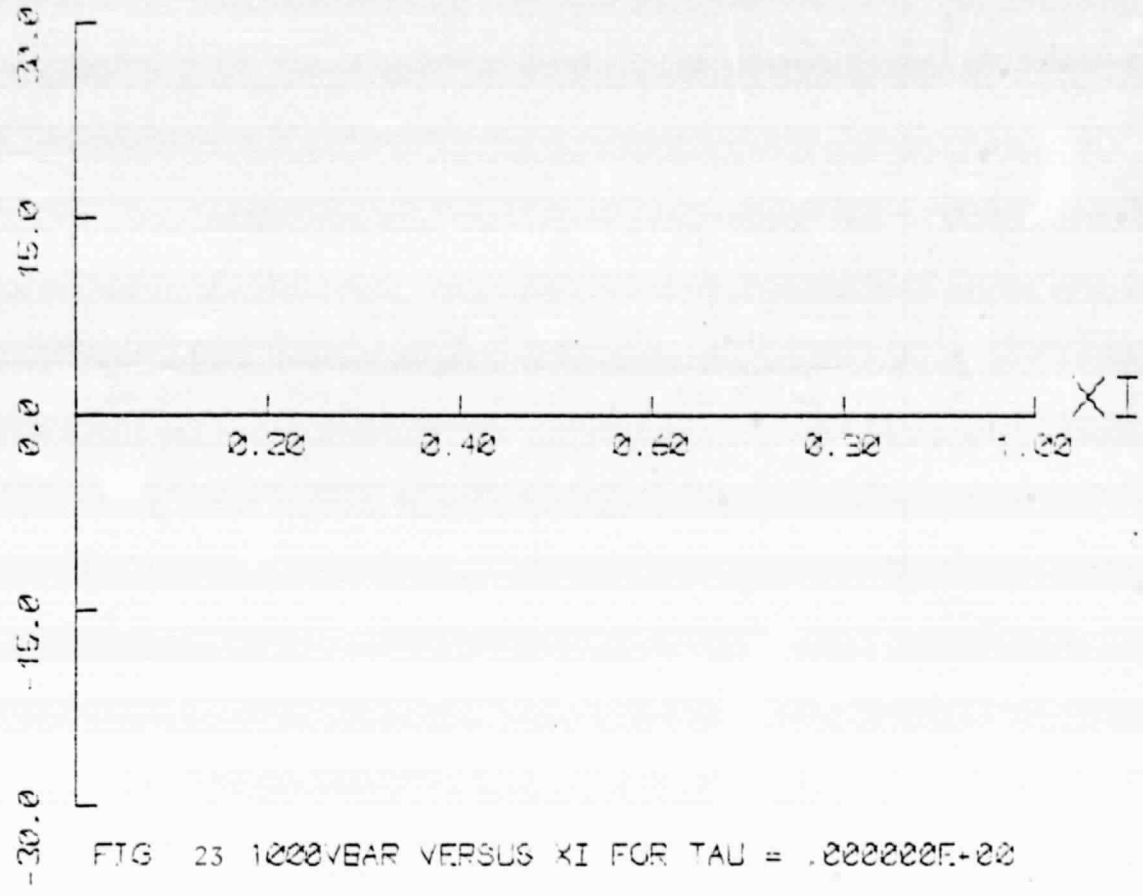

FIG 23 1000VBAR VERSUS XI FOR TAU = .000000E-00

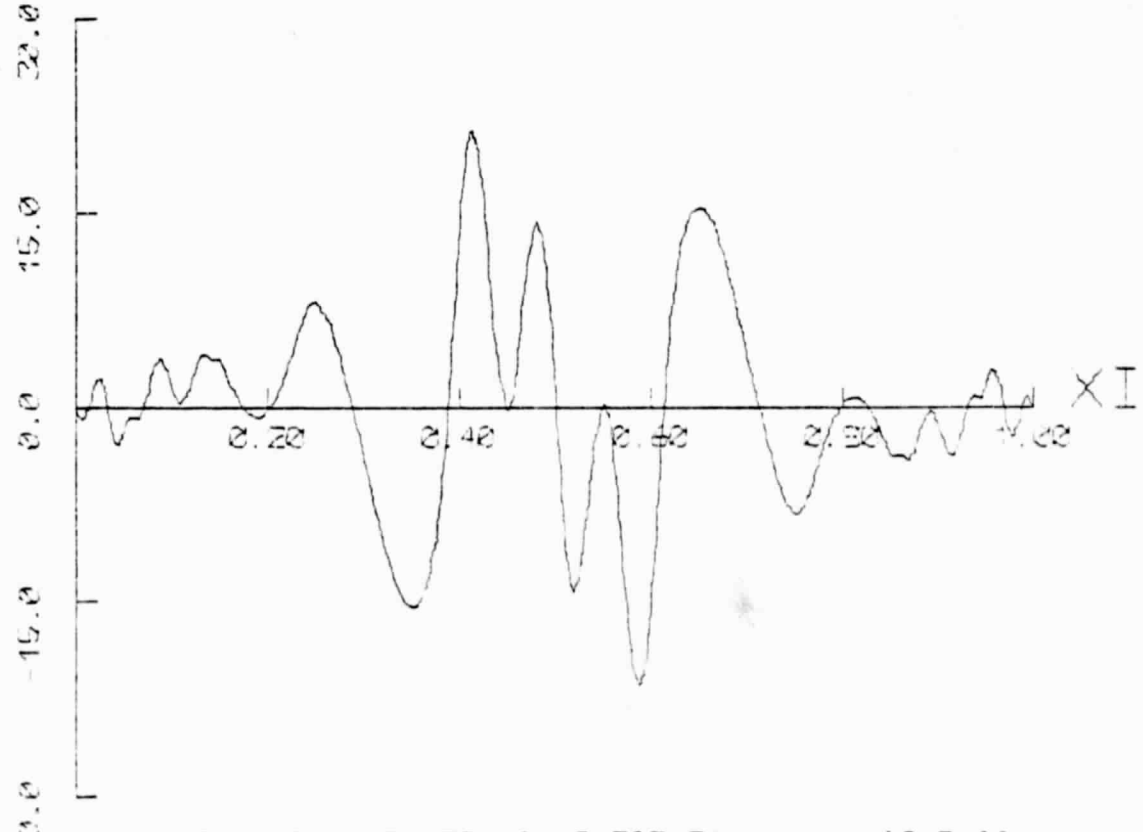

FIG 24 1000VBAR VERSUS XI FOR TAU = .111094E-00

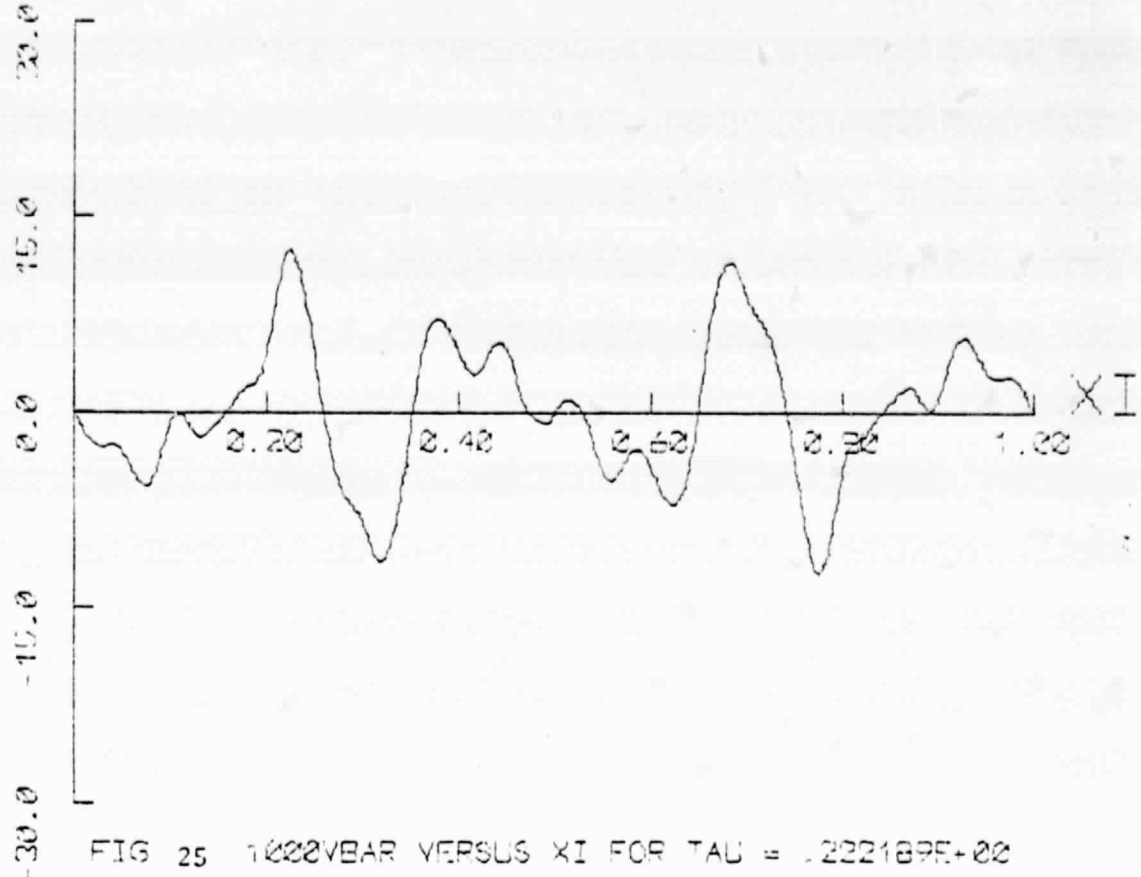

FIG 25 1000VBAR VERSUS XI FOR TAU = .22218PE+00

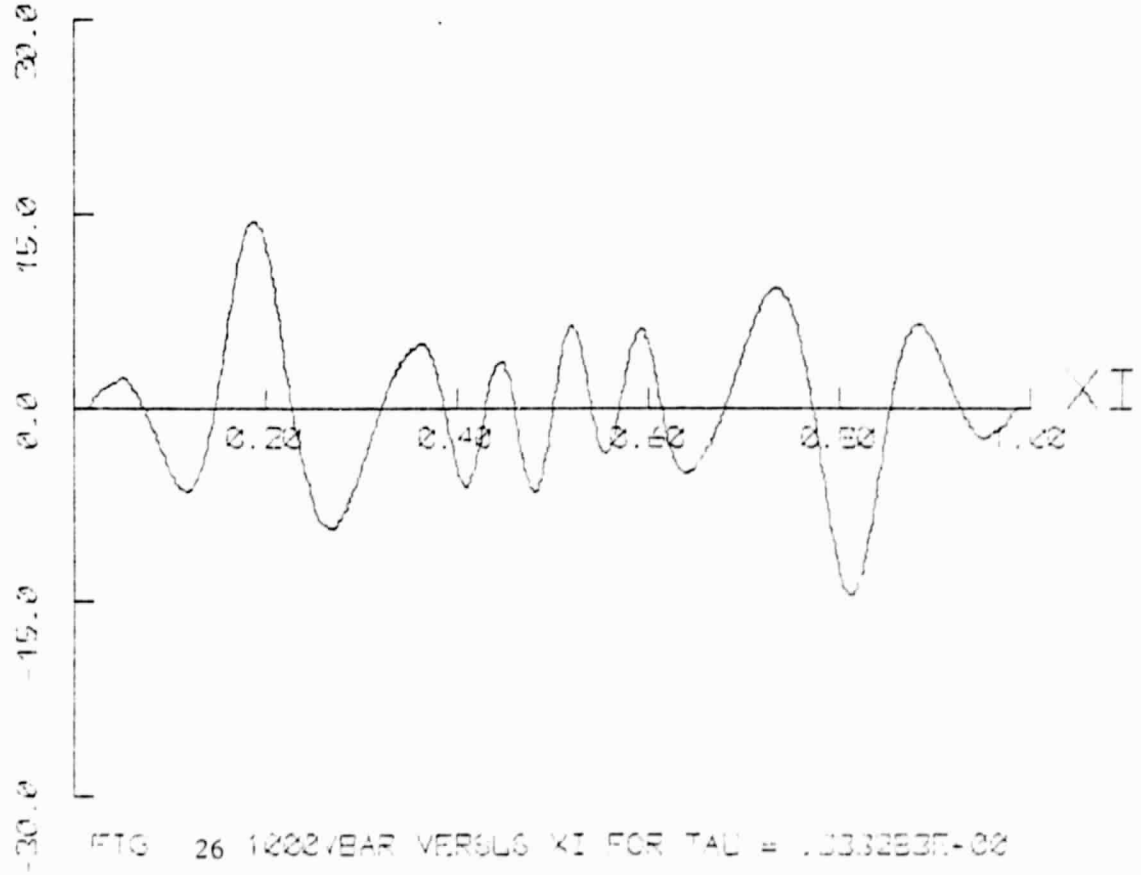

FIG 26 1000VBAR VERSUS XI FOR TAU = .33328E3E-00

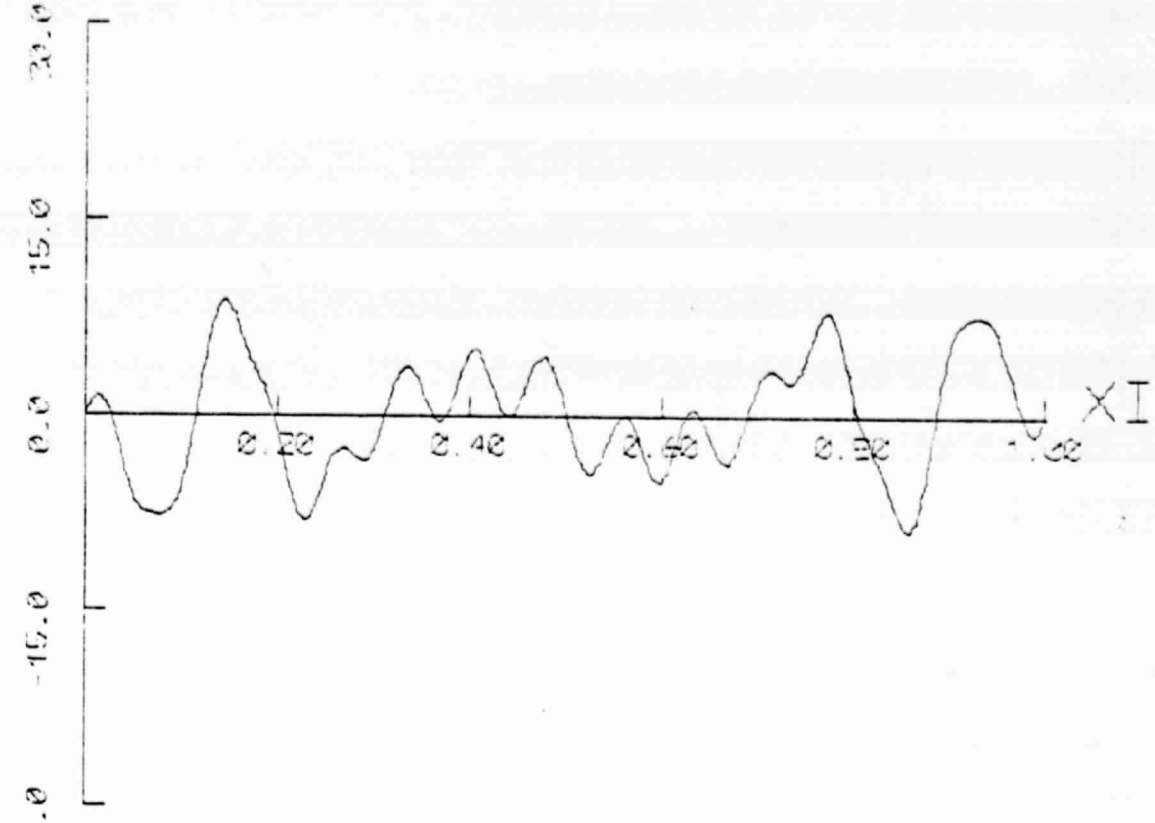

FIG 27 1000√BAR VERSUS XI FOR TAU = .4443750+00

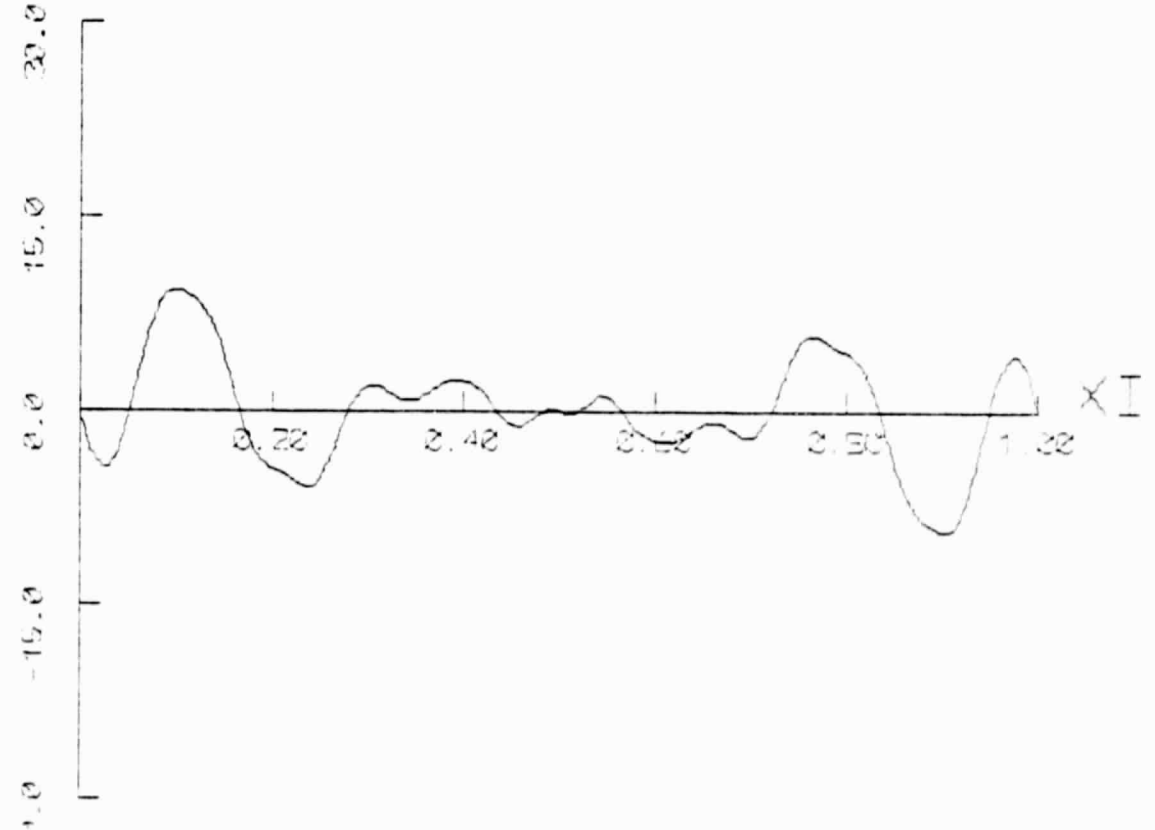

FIG 28 1000√BAR VERSUS XI FOR TAU = .8884725+00

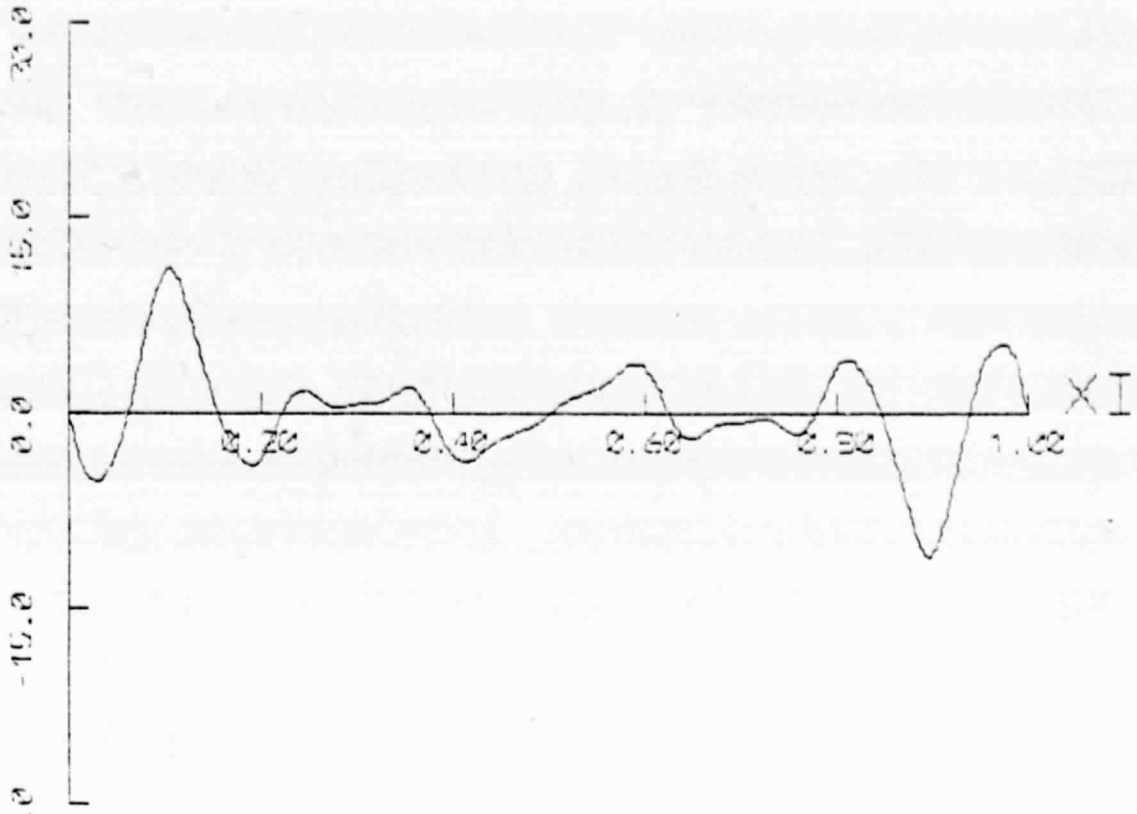

FIG 29 1000/BAR VERSUS XI FOR TAU = .6666670+00

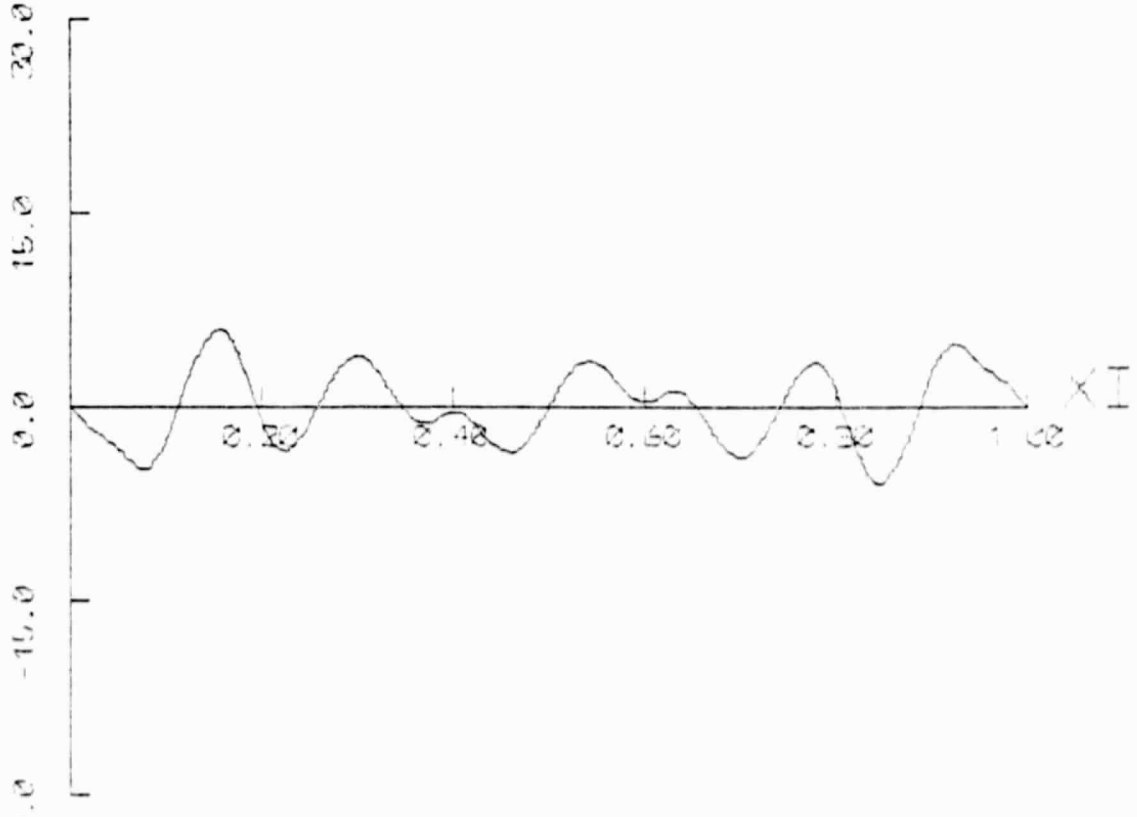

FIG 30 1000/BAR VERSUS XI FOR TAU = .7777ee0+00

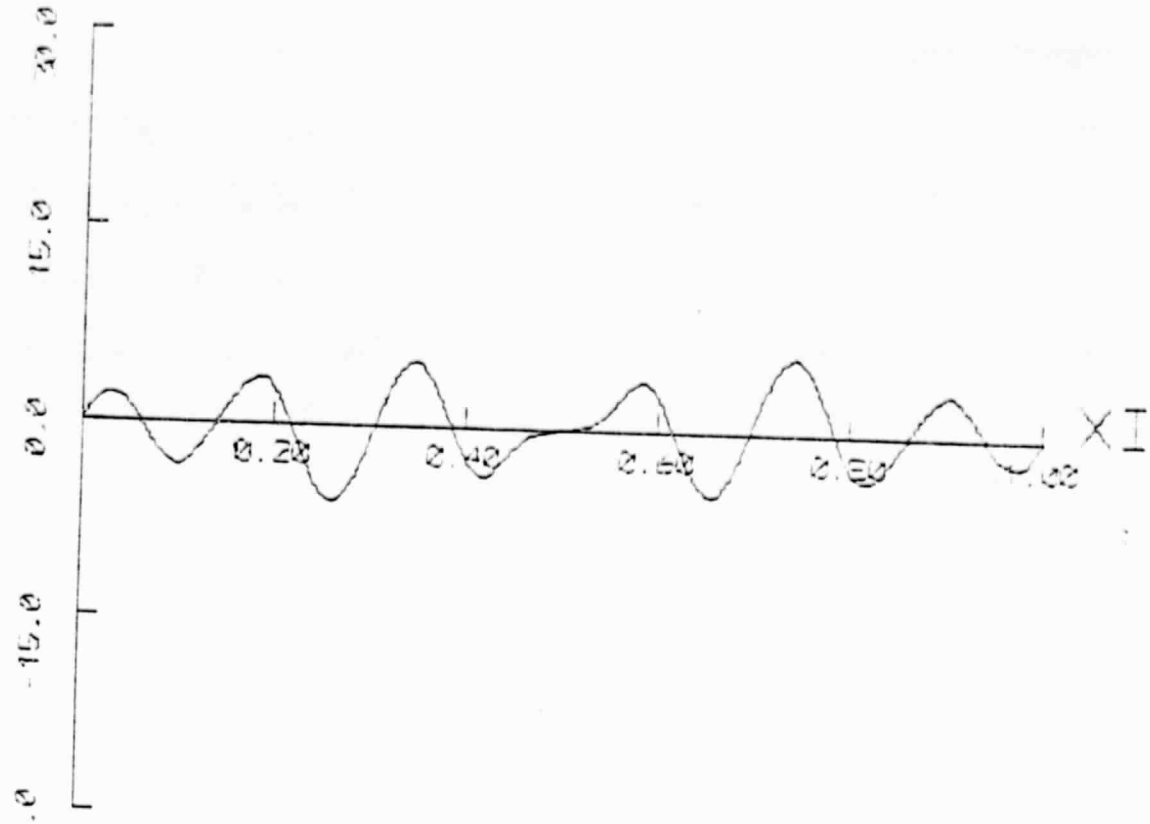

FIG 31 1000VBAR VERSUS XI FOR TAU = .888755E+00

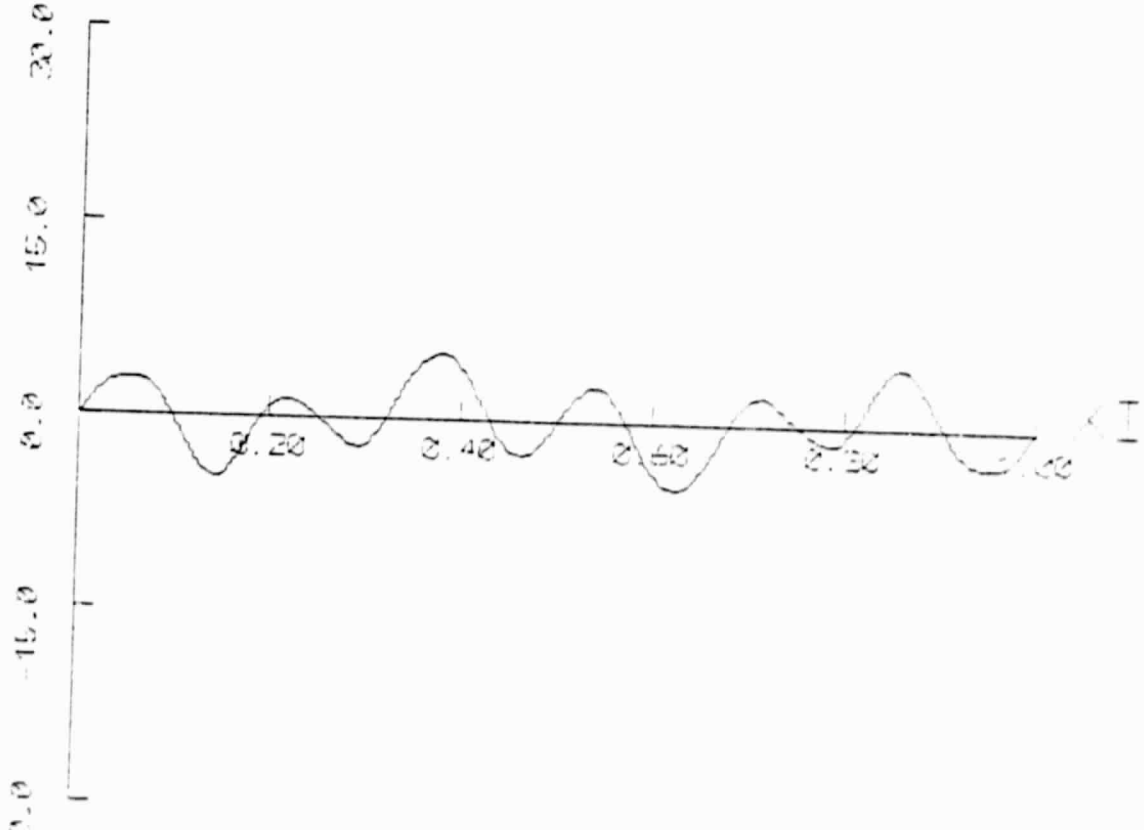

FIG 32 1000VBAR VERSUS XI FOR TAU = .888755E+00

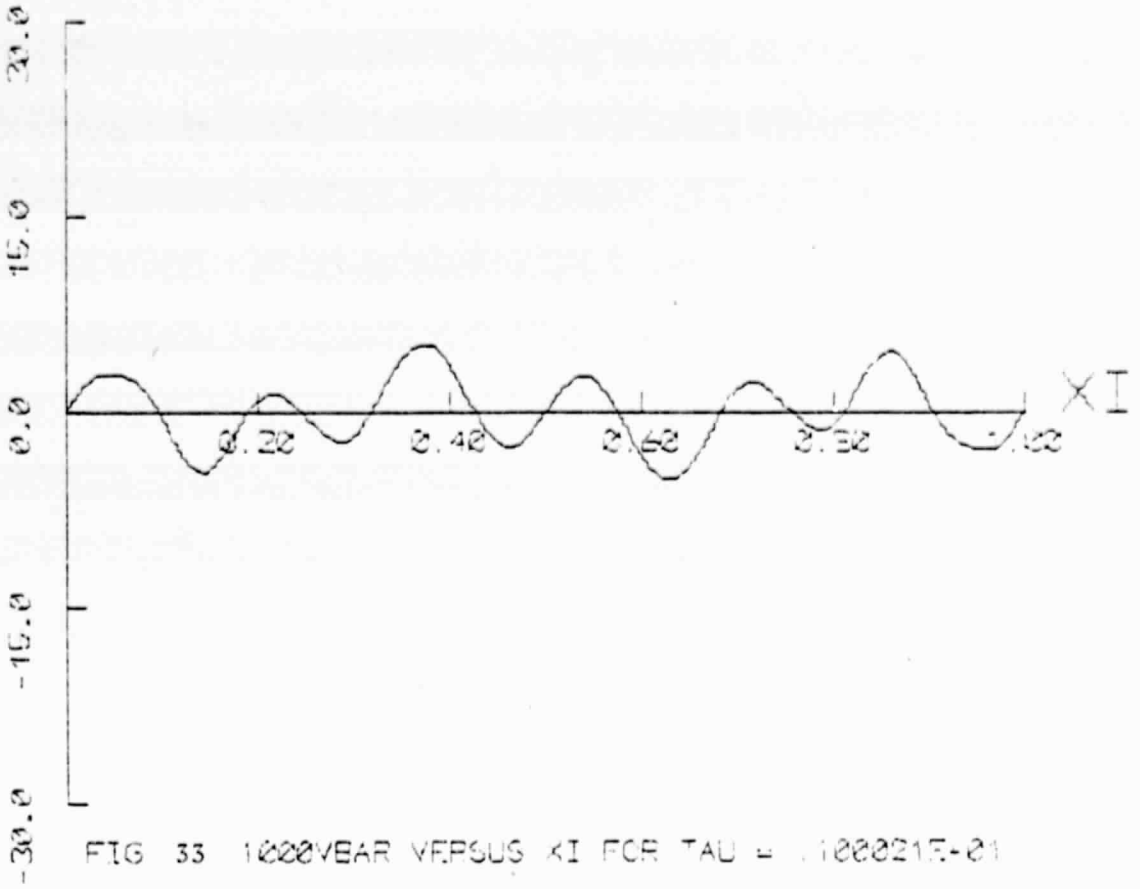

FIG 33 1000VBAR VERSUS XI FOR TAU = .1000213-01

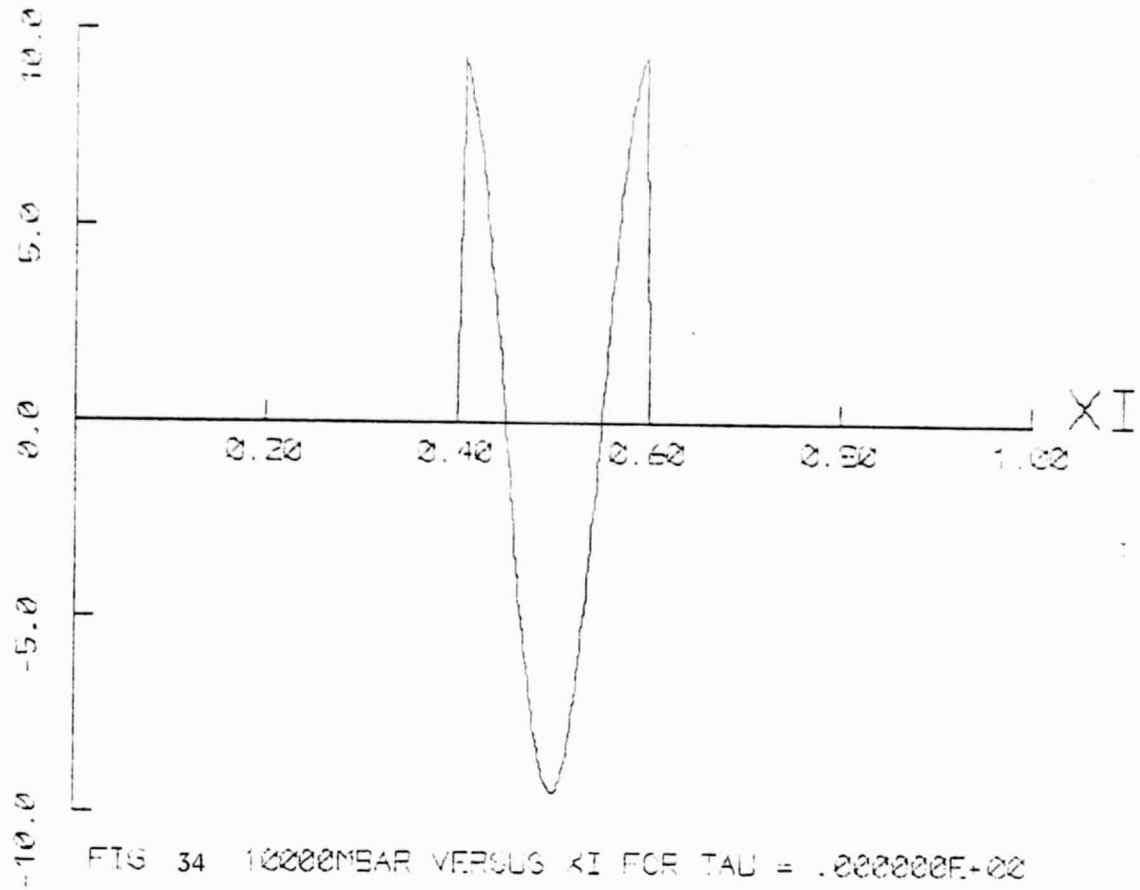

FIG 34 10000MBAR VERSUS XI FOR TAU = .000000E+00

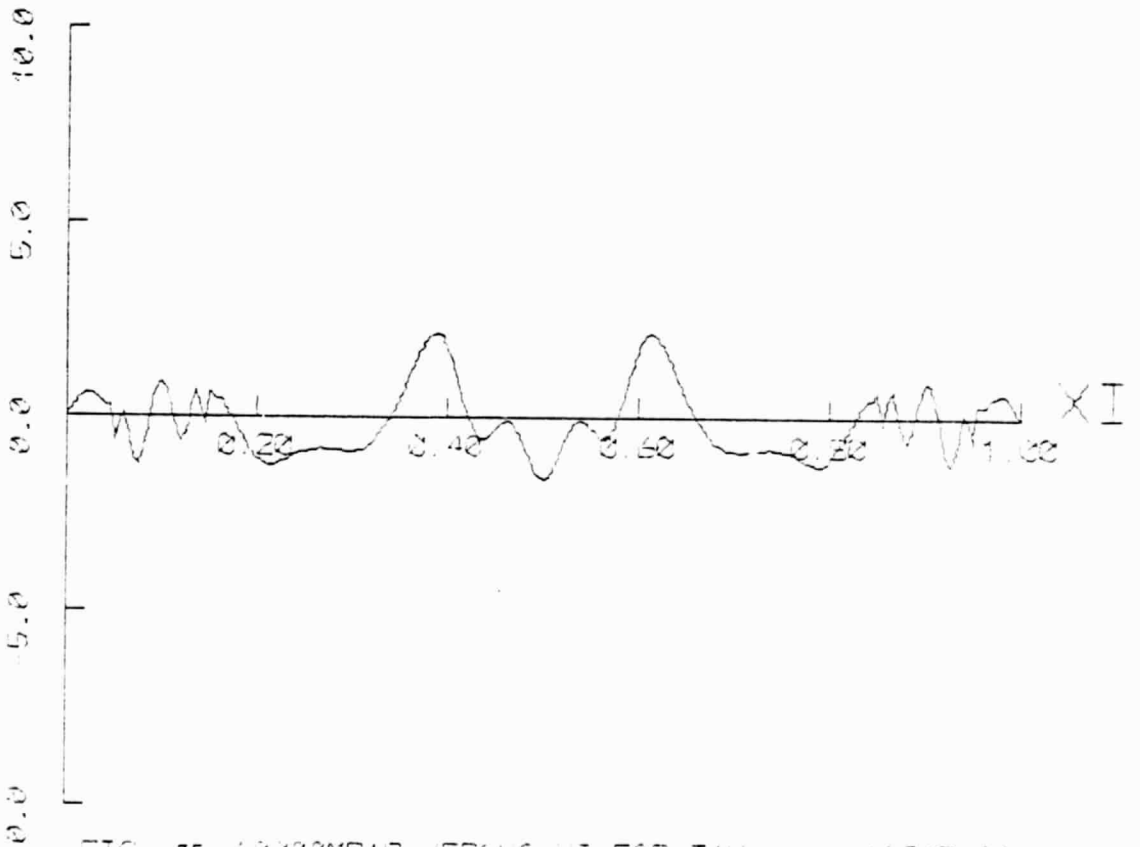

FIG 35 10000MBAR VERSUS XI FOR TAU = .110734E-00

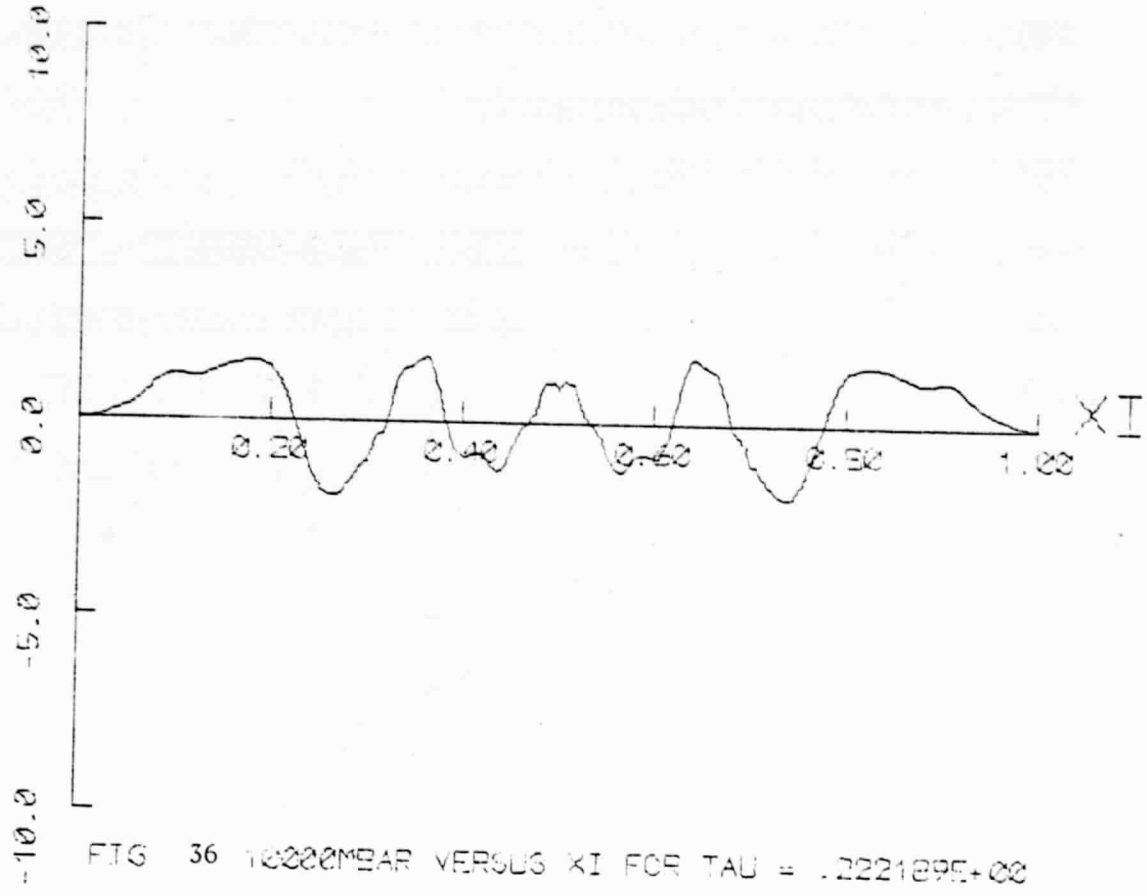

FIG 36 16000MBAR VERSUS XI FOR TAU = .2221095+00

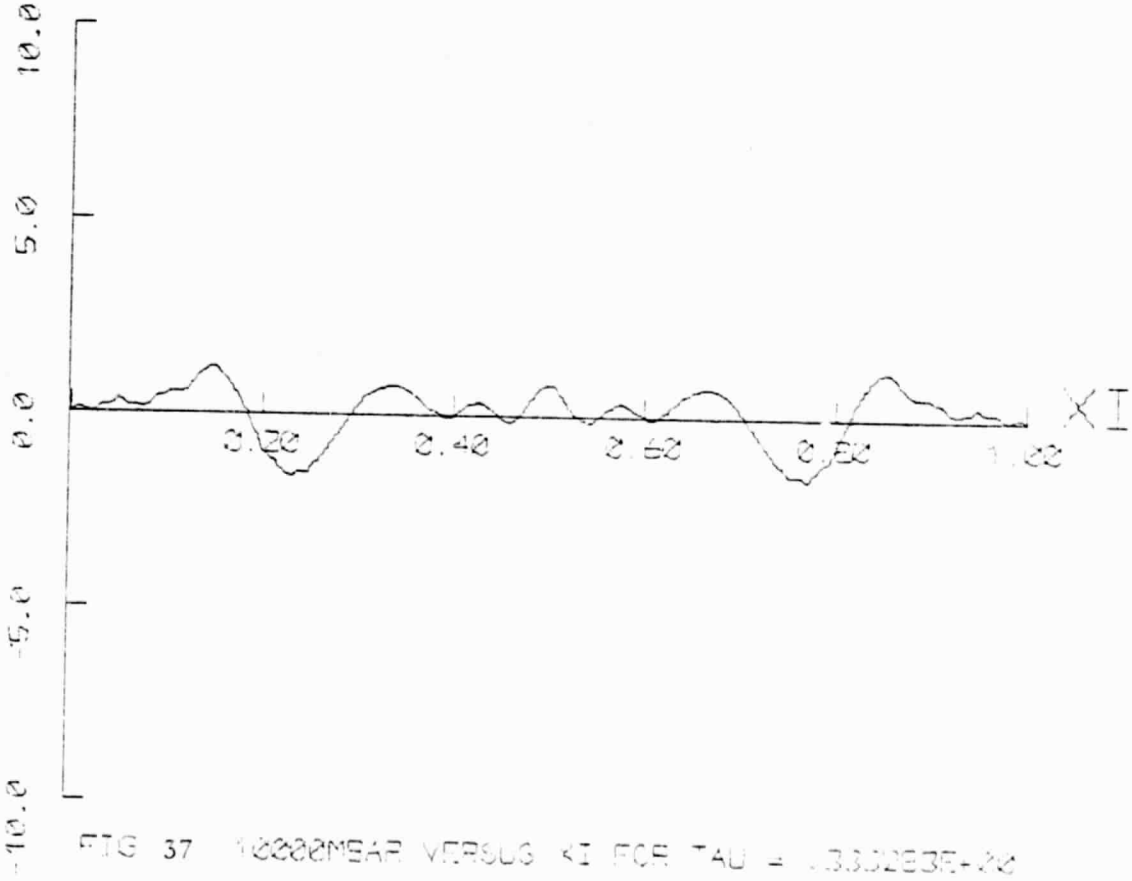

FIG 37 16000MBAR VERSUS XI FOR TAU = .3332835+00

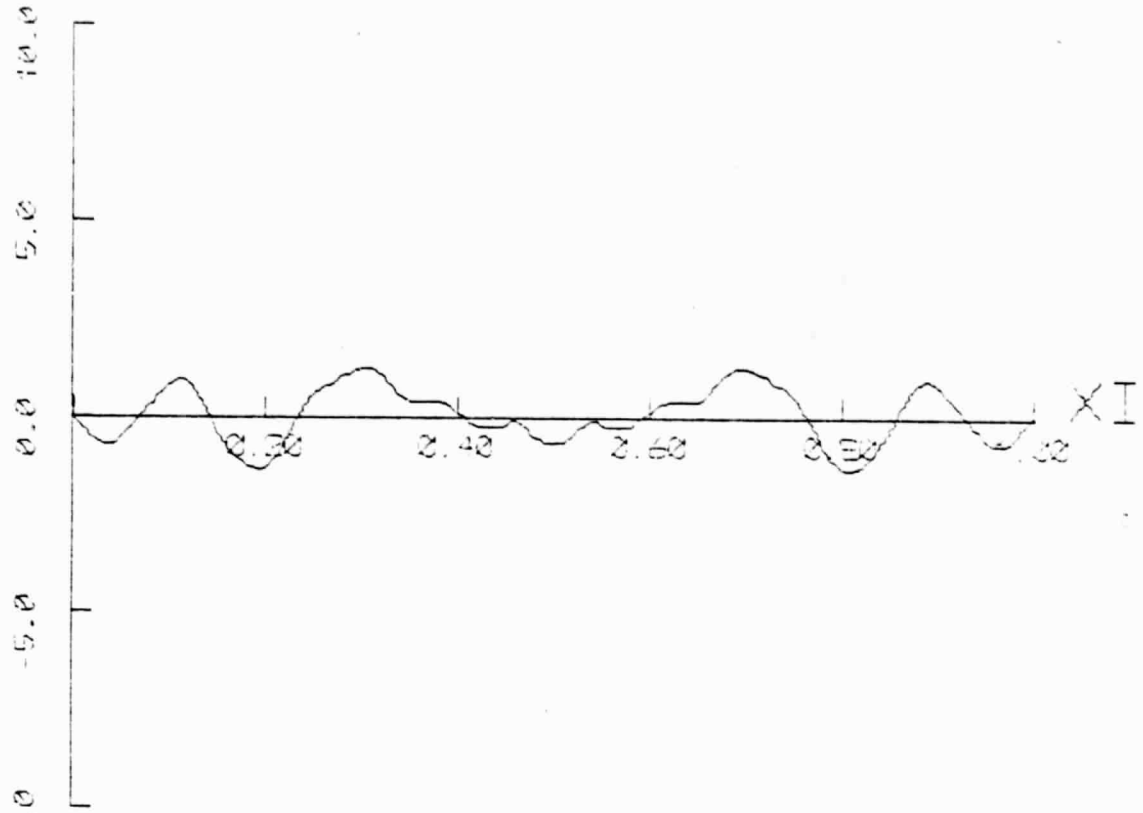

FIG 38 10000MBAR VERSUS XI FOR TAU = .4410738E+00

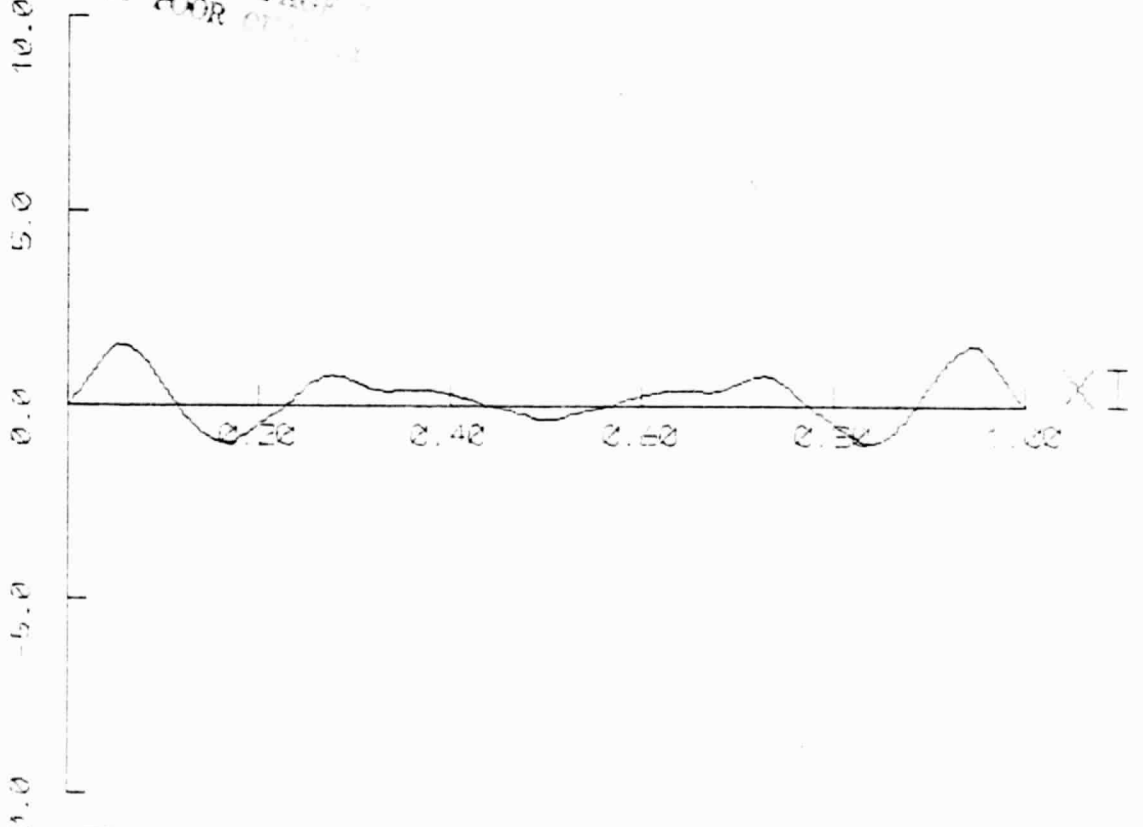

FIG 39 10000MBAR VERSUS XI FOR TAU = .8884726E+00

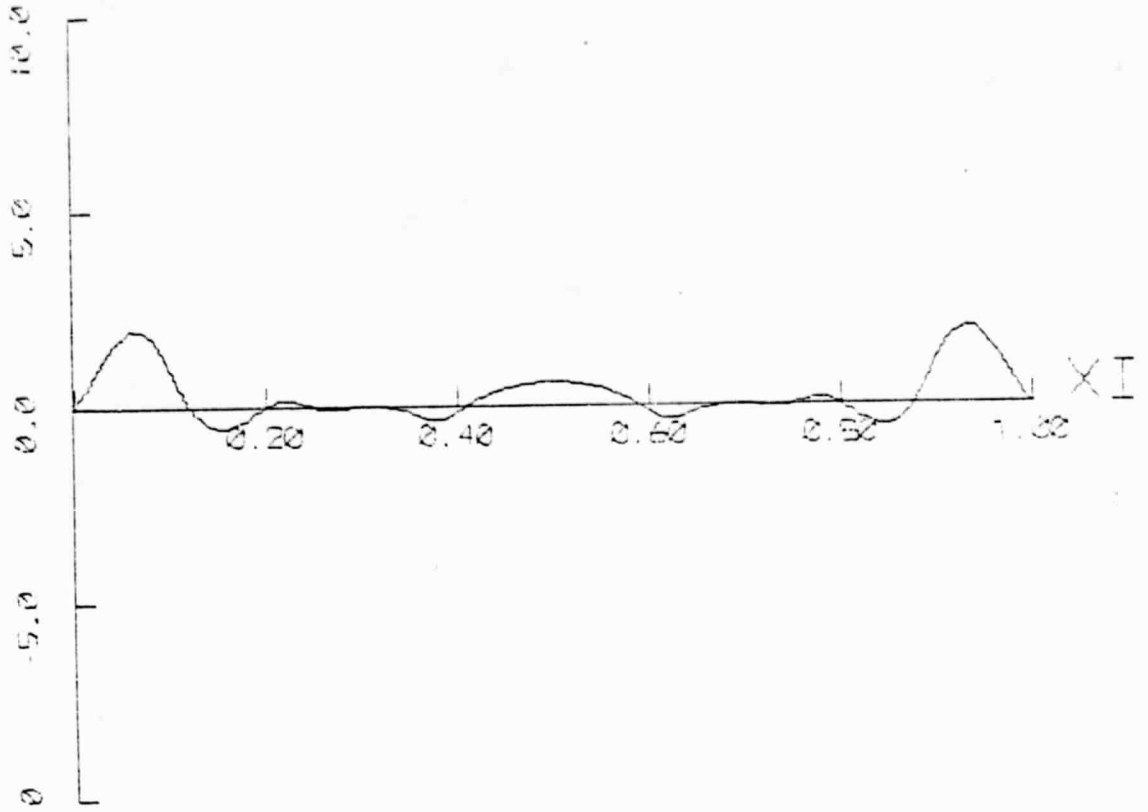

FIG 40 10000MBAR VERSUS XI FOR TAU = .6665675+00

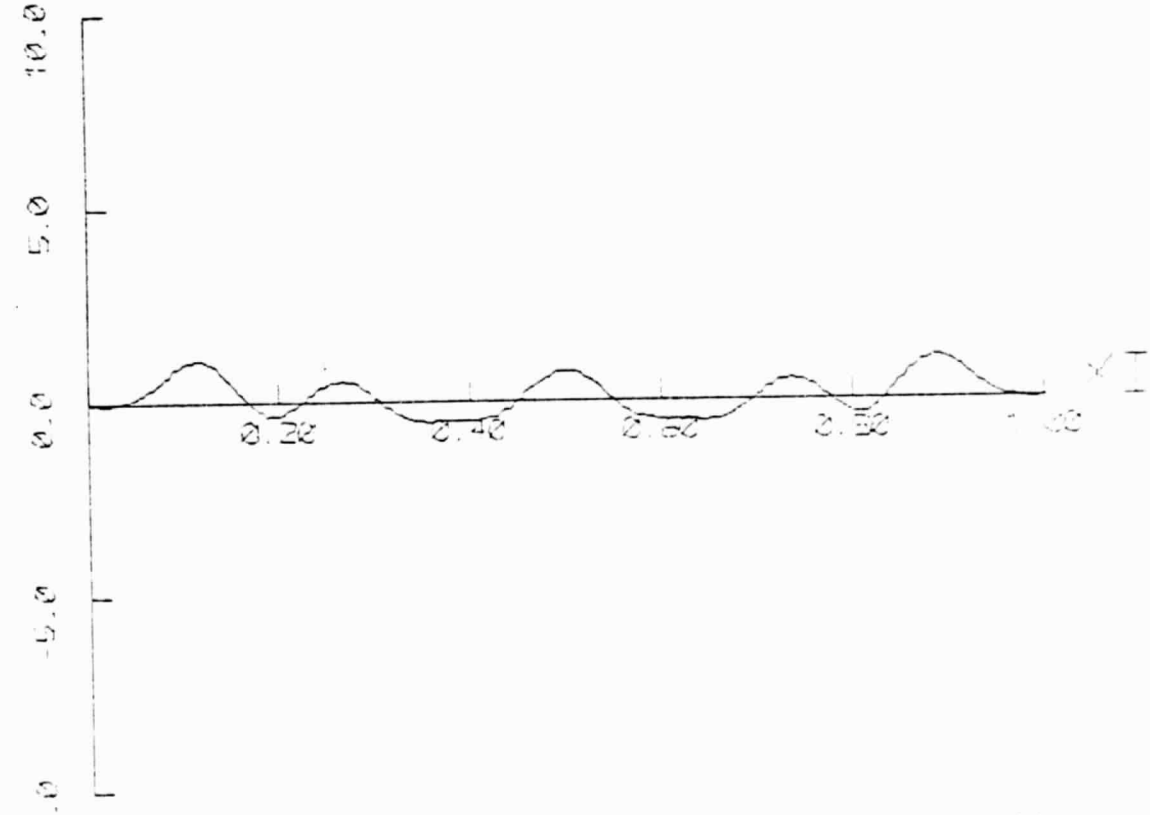

FIG 41 10000MBAR VERSUS XI FOR TAU = .7776875+00

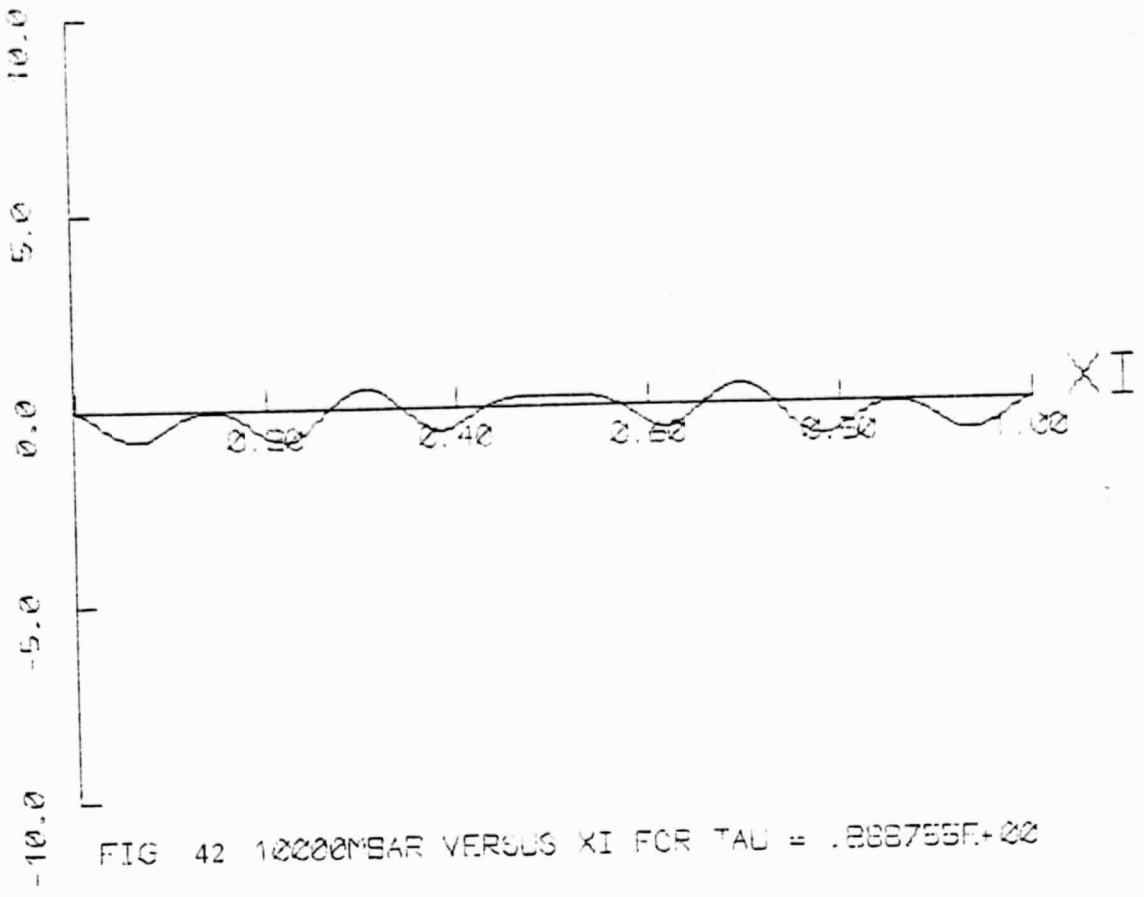

FIG 42 10000MBAR VERSUS XI FOR TAU = .888755E+00

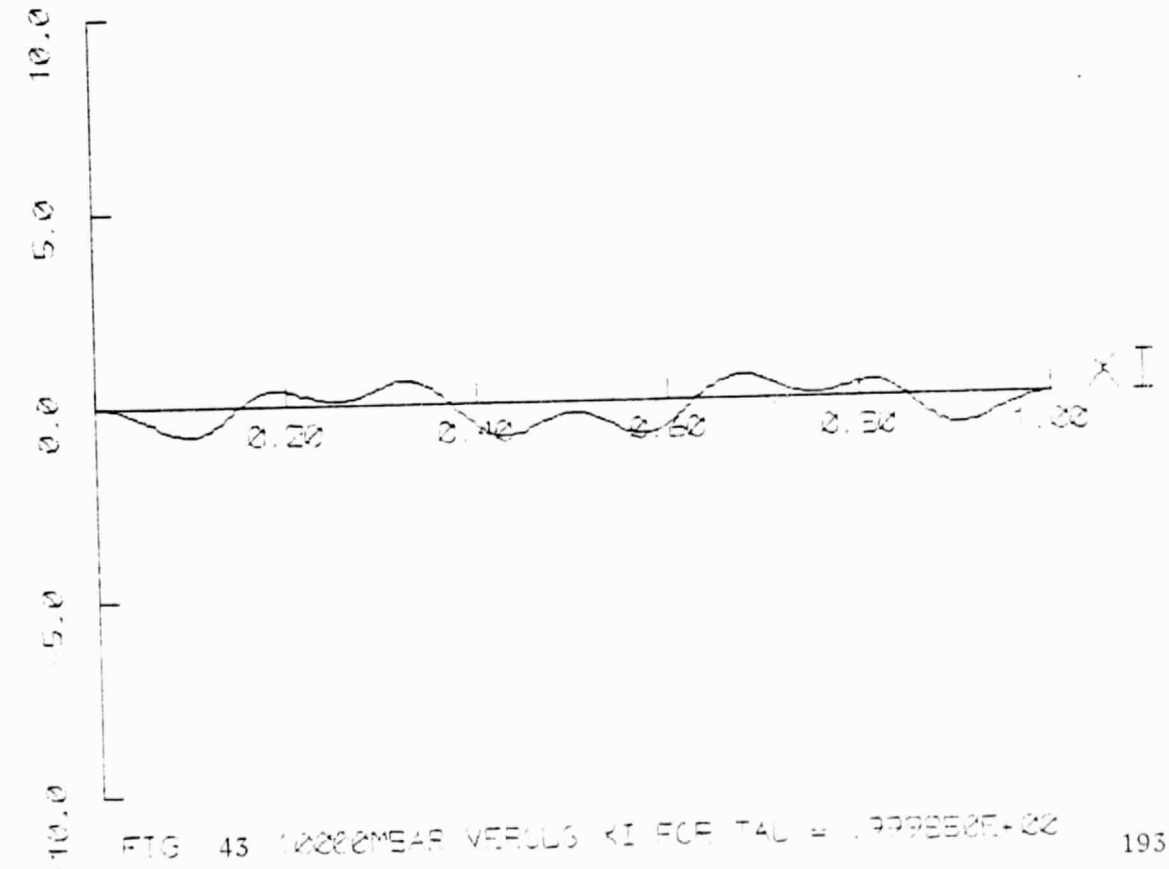

FIG 43 10000MBAR VERSUS XI FOR TAU = .999850E+00

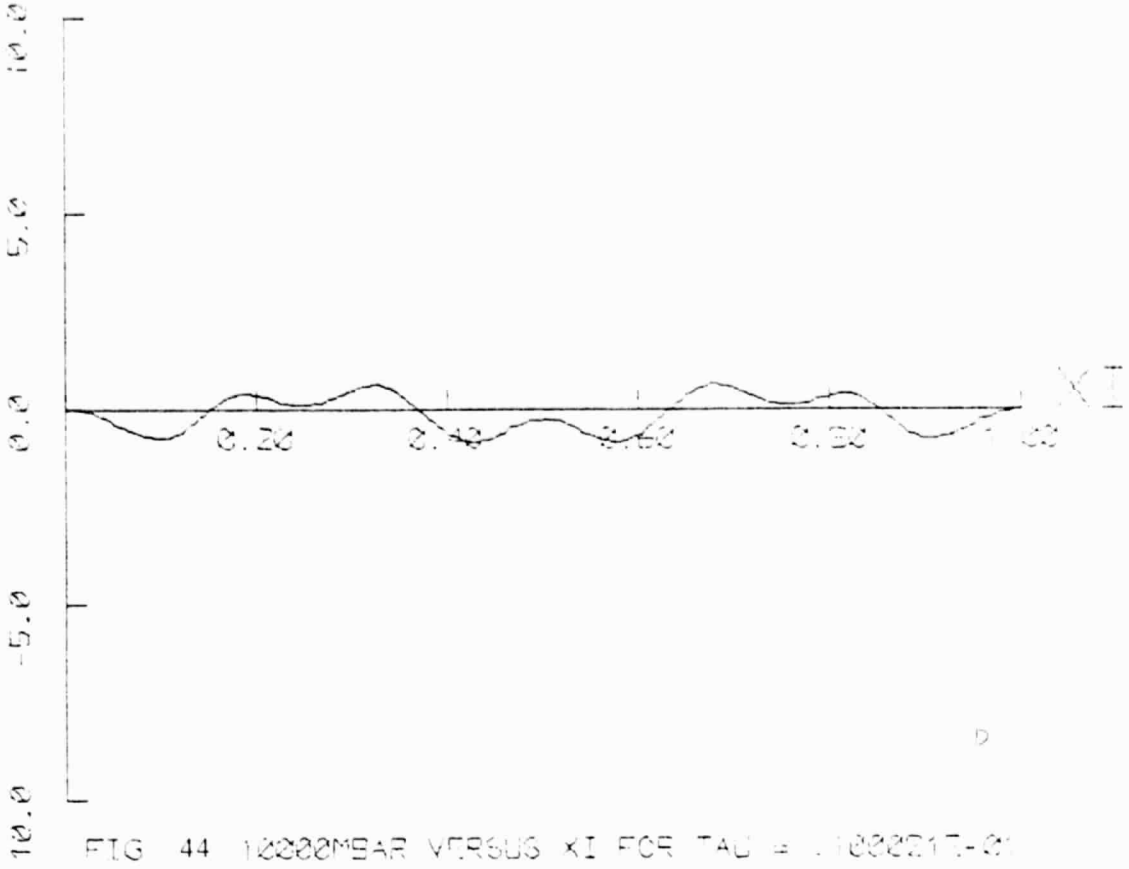

FIG 44 10000MBAR VERSUS XI FOR TAU = .1000217-01